University of Messina

THESIS FOR THE DEGREE OF PHILOSOPHIAE DOCTOR

PHD COURSE IN APPLIED BIOLOGY AND EXPERIMENTAL MEDICINE

CURRICULUM IN BIOLOGICAL AND ENVIRONMENTAL SCIENCES

XXXVI PROGRAM

SSD BIO/05

THE ECOMORPHOLOGICAL ADAPTATION OF MARINE TELEOST FISHES REVEALED BY OTOLITHS

PhD candidate

Claudio D'Iglio

Supervisor

Professor Giorgio Capillo

Coordinator: Professor Nunziacarla Spanò

ACADEMIC YEAR 2022-2023

INDEX

ACKNOWLEDGMENTS

Tante sono le persone alle quali va la mia gratitudine per il sostegno e la guida ricevuti durante questi tre anni.

Innanzitutto, voglio ringraziare la mia famiglia e la mia compagna, Lavinia, per l'affetto e il costante appoggio. Grazie a loro ho avuto la forza che mi ha aiutato nei momenti più faticosi e difficili nonché lo stimolo costante che mi ha spronato nel portare a termine questo percorso di crescita, sia professionale che personale.

Vorrei inoltre ringraziare l'intero Dipartimento di Scienze Chimiche, Biologiche, Farmaceutiche e Ambientali dell'Università di Messina, ed in particolare la prof.ssa Nunziacarla Spanò per le opportunità che mi sono state concesse, per i suoi insegnamenti, il suo costante sostegno e la sua disponibilità.

Al relatore, prof. Gioele Capillo, alla prof.ssa Serena Savoca ed al prof. Marco Albano va tutta la mia gratitudine. Le conoscenze che mi hanno trasmesso, la loro guida ed il loro affetto rappresentano un bagaglio professionale e umano importante, uno stimolo per la mia realizzazione e crescita futura. Ringrazio inoltre tutti i miei colleghi con i quali ho condiviso questi anni di fatiche e soddisfazioni, per la loro amicizia e la stima reciproca.

Un grazie speciale va anche alla prof.ssa Josipa Ferri e a tutta la Facoltà di Scienze Marine di Spalato (Croazia). Lì ho trascorso mesi stupendi, sentendomi a casa, nei quali ho imparato tantissimo, sotto la sua guida preziosa.

Ringrazio inoltre il laboratorio di Scienza della pesca dell'Istituto sperimentale Talassografico dell'IRBIM CNR di Messina, in particolare le ricercatrici e il personale tecnico scientifico. Con loro ho condiviso anni importanti per la mia formazione, avendo la possibilità di avvicinarmi alla scienza della pesca e, in particolare, allo studio degli otoliti.

ABSTRACT

Vertebrate ear is the organ responsible of the sense of hearing and balance, with a high structure and functioning variability inside the group. The semicircular canals of the vestibular part of the inner ears are the structures allowing to the detection of angular acceleration, while the detection and production of sounds is regulated by several structures. In the entire group, the transduction mechanisms for the conversion of sounds (and vestibular stimuli) involves the sensory hair cells, with their cilia, that, once bent due to the pressure component of particle movements related to sound, induce a physiological response of cells. This stimulates the innervating eighth cranial nerve, by the conversions of head movements and sounds into neurochemical signal. Concerning teleost species, their inner ear is characterized by the presence of three semicircular canals, with their end organs (*ampullae*) and sensory *cristae,* and three otolith end organs. These form three pouches (*utricle*, *saccule*, *lagena*), and their rostro-caudal angular orientation (taxon specific) is essential for sound-source location. Otoliths are located inside the otolithic end organs (one for each end organs): *sagitta* in *sacculus, lapillus* in *utricle* and *asteriscus* in *lagena*. These thanks to their strictly connection with the sensory epithelium (*macula*), can convert the particle motion related to sound field in physiologically response resulting in nerve stimulation. Fishes using only the direct stimulation to detect sound (called "hearing generalists") show a lower sensitivity and a narrower band width of hearing, while the so called "hearing specialists" can detect sound with indirect pathways (through the detection of sound pressure) thanks to accessory auditory structures, peripheral to the ear. Otoliths are solid carbonate acellular masses (with a small fraction of proteins), biomineralizing during the entire teleost's life with a daily growth with a metabolic inertia. Any chemical compounds or elements added during the growth process is permanently maintained and, due to the continue growing during the entire animals' lifecycles, otoliths can be the "flight recorder" of fishes. They can preserve several information on environmental conditions experienced by fishes, their life habits, metabolism, and physiology. For this reason, they are widely used to investigate migration pathways and pollution exposure, to validate age and identify stocks, being also used as metabolic indicators, natural tag, and mass marking. Among the interesting features of fish ears, the most striking is for sure the inter specific diversity, ranging from their gross structure to the sensory hair cells' organization. Ear shape can be related both to fishes' size and ear function, but it is almost unknown its significance. Concerning the most studied among otoliths, *sagittae*, they are often the most involved in hearing process, as reported for "hearing specialist" species. The morphological diversity of *sagittae* also involves the sensory epithelia (e.g., shape, size) and its relationship with otolith (e.g., coverage ratio

of otolith on epithelia), with inter specific variation also in sulcus depth. The significance of this high variability at intra and inter specific level is almost completely unknown, but morphology directly influences otoliths' functioning. The peculiar chemistry of otoliths, their growing and deposition dynamics, their intra and inter specific variability in morphology and shape, all these features make otoliths essential tools used, from more than a century, to investigate many aspects of teleost's lifestyle, taxonomy, and population dynamics, as well as to obtain essential information for fisheries management and conservation purposes. Understand the relation between habitats, ecological conditions and otoliths is essential to clarify the dynamics allowing their intra and inter specific diversity, deepening the knowledge on the development dynamics of the entire inner ear, and its relationships with environmental features and different habitat's preferences.

This thesis aims to explore the information that otoliths can provide about the eco-morphological adaptation of Mediterranean teleost fishes to different environments, through the investigation of the intra and inter specific differences of several species characterized by different life habits and exploited habitats. Six cases of study have been provided, obtaining data on the variability of *sagittae* at intra and inter specific level, with useful information on the functional morphology of otoliths in the studied species. The intra specific variability of *sagittae,* in shape, morphology and external textural organization, has been analyzed at inter and intra population level, between different size classes, while the variability at inter specific level has been explored among species belonging to the same genus or family. Moreover, in two of the studied species, for the first time in the Mediterranean Sea, in addition to *sagittae,* they have been analyzed also *lapilli* and *asterisci,* providing a complete description to fill the gap about their intra specific variability. The first, the second and the third cases of study involved respectively the species belonging to *Pagellus* genus (*P. erythrinus, P. bogaraveo, P. acarne*), Mugilidae family (*C. auratus, C. labrosus, O. labeo*) and Macrouridae family (*H. italicus, N. sclerorhynchus, N. aequalis, C. guentheri, C caelorhincus*), exploring the inter and intra specific variability of *sagittae* in phylogenetically close species. The fourth and the fifth cases of study involved *A. hemigymnus* and *B. belone*, respectively, with the analysis of the three otoliths' pairs (*sagittae* and *lapilli* of *A. hemigymnus*, *sagittae, lapilli* and *asterisci* of *B. belone*) at intra specific level to assess their variability in these deeply different species. The inter population variability of *sagittae* has been analyzed in the sixth case of study, involving *S. porcus* specimens, comparing the *sagittae* features of two populations inhabiting completely different environments. They have been also analyzed feeding habits, growth dynamics and age structures, comparing them with literature data from other geographical areas, to find a most clear correlation between environmental conditions and *sagittae* features.

The results provided by the six cases of study have explored the diversity in morphology, mean shape, and morphometry of several Mediterranean teleost species, characterized by different life habits, habitat preferences and phylogenetic relationships. They were also described the inter and intra specific variability occurring between and within the different species, also providing, for the first time, data on the mean *sagittae* shape from shape analysis for many of them. Moreover, for the first time in the Mediterranean Sea, it was provided an accurate description, with data from shape, morphometric analyses, and their intra specific variability, of *lapilli* and *asterisci* belonging to *A. hemigymnus* and *B. belone* specimens. It was also confirmed the reliability for populations discrimination of *sagittae* in *S. porcus*, with the inter population analysis which provided several evidence on the high plasticity in sagittal otoliths features, feeding habits and somatic growth rates under different environmental pressures, experienced by specimens from two totally different habitats. All these data have opened new scenarios for future studies on the eco-morphology of the three otolith pairs from marine teleost species, to better understand the inner ear functioning and detect the mechanisms of population differentiation and speciation processes. Thanks to otoliths, and future advances in otoliths science, it will be possible to understand several aspects of species ecology, difficult to explore directly, and evolution. This will increase our knowledge about the ecological relationships and niche partitioning in marine communities, the dynamics of populations discrimination and the connection between phylogenetic and morphological differentiations.

1. INTRODUCTION

Vertebrates' ear is a complex anatomical structure, essential for sound perception (hearing) and vestibular function (spatial orientation and balance), with a high structure and functioning variability inside the group. In all the vertebrates, the region dealing with the detection of locomotion movements (e.g., head and body movements), and hence equilibrium, is the vestibular part of the inner ear, that, thanks to the presence of semicircular canals (three in gnathostomes), recognizes the angular acceleration, while the linear one is detected by means of *utricle* and *saccule* [1,2]. Concerning the perception and production of sounds in living vertebrates, it is performed by the means of different structures. In tetrapods these differ between non mammalians and mammals; in the first, lagenar recess and stapedial structure are involved in sound transmission, while in the latter are the cochlea and middle ear ossicles [3,4]. In elasmobranchs, the labyrinth and lateral line receptors (thanks to cupulae-like displacement systems with sensory air cells) carry out hearing function [5,6], while in teleost fishes exists different sound transmission systems, always depending on the relationship between gas cavities, or gas-filled organs and vesicles, and ear regions [7,8] (Fig. 1). Indeed, it is

widely reported how, in teleost species which use only the direct stimulation of sensory epithelium to perceive and process sounds, the auditory ability does not allow to detect sounds outside their near-field [9,10].

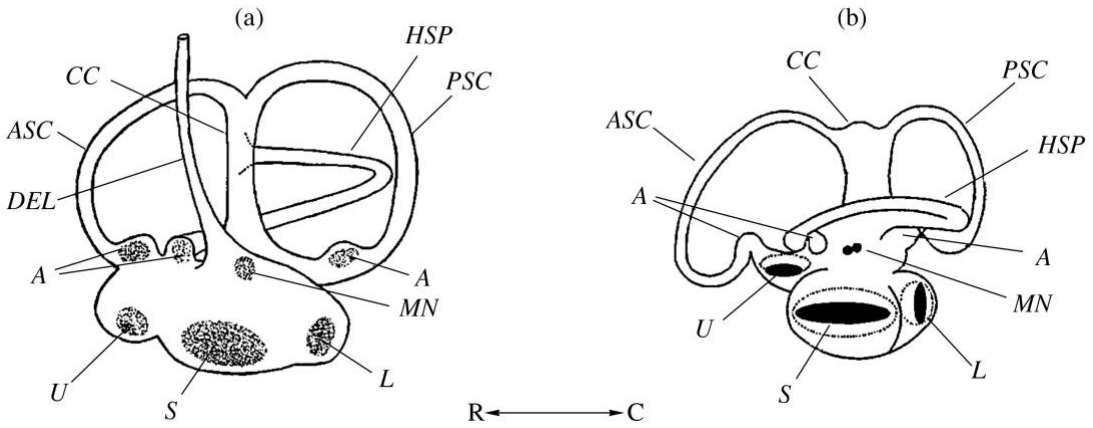

Figure 1. Schematic Inner ear's images of cartilaginous (a) and teleost (b) fish: (HSC) horizontal semicircular canal; (ASC) anterior vertical semicircular canal; (CC) crus; (PSC) posterior vertical semicircular canal; (A) *ampullae*; (MN) *macula neglecta*; (U) *utriculus*; (S) *sacculus*; (L) *lagena*; (DEL) endolymphatic duct; R and C rostral and caudal directions. Image from: *Kasumyan, A. The vestibular system and sense of equilibrium in fish. J. Ichthyol.* ***2004****, 44, S224*.

Accessory auditory structures have been evolved in different taxonomic groups, under the evolutionary pressure, to enhance and expand the frequency (up to several thousand Hertz) detection and sensitivity, improving the overall hearing capability. These structures are (i) gas cavities present at intracranial level (e.g., in mormyrids and anabantids), (ii) gas-filled vesicles extending anteriorly from the swim bladder (e.g., in clupeids, sciaenids, cichlids, holocentrids) and (iii), in otophysans species, a ligaments and ossicles chain linked to the swim bladder, called Weberian apparatus [11,12]. All these structures, thanks to the connection or the closeness with the inner ear, influence the species' hearing ability, improving the detection of spatial hearing and long-distance frequencies.

The transduction mechanisms for the conversion of sounds (and vestibular stimuli) involves the sensory hair cells, as in all the vertebrates. Their cilia, present in the apical ends projecting into the otolithic chamber, once bent due to the pressure component of particle movements related to sound, induce a physiological response of cells, stimulating the innervating eighth cranial nerve. As introduced above, in many teleost species several indirect mechanisms of sound pression detection have been evolved independently, involving structures peripheral to the ear (gas filled cavities or organs) (Figure 2) [13,14]. The gas bubbles present inside them, being of different density and compressibility than water, are set in motion by the pressure of the sound field. Their volume oscillations transmit the signal by particle motion to the otoliths sensory epithelium, thanks to the strict connection between gas filled cavities/organs and inner ears, adding pressure detection to the

simple particle movements once [10]. The swim bladder linked with an otophisic connection (e.g, Weberian ossicles) is the most common mechanism used to permit the detection of pressure, with some limitations related to the distance from the ear. Indeed, species with best hearing sensitivity and very wide hearing bandwidth are those showing a "closer" swim bladder to the inner ear [15,16], or by means of additional gas bubble very closed, or attached to it (as in mormyrids species). Considering the Holocentridae family, it is clear how those species with a swim bladder extension, ending at the *saccule* (as many squirrelfishes), show a most enhanced hearing bandwidth and sensitivity than those holocentrids species without this extension [17]. Similar cases are also founded in many other teleosts' species [15,18], and it is reasonable to think that, according to the presence of swim bladder extension (such as other indirect mechanisms of sound pressure detection), different species are more or less skilled to detect particle motion than pressure, and vice versa, for the detection of sound. Indeed, as suggested by Popper et al. [10], the amount of how auditory stimulation are linked to particle motion or/and pressure could be another hearing related feature varying inter specifically. Among the adaptations allowing to the auditory stimulation through pressure detection, the presence of air bubbles near, and in, the ear (as in many Anabantidae and Mormiridae species) is another specialization showed by teleost with an enhanced hearing sensitivity. According to literature, it has seen how the bubbles removal, or swim bladder deflation, reduce drastically the hearing sensitivity, contrary to those species without an apparent hearing specialization [13,14,19]. While, otophysan fishes (goldfish, catfish, and relatives) with Weberian ossicles have shown an over 3 kHz hearing, thanks to the direct distribution of swim bladder motion, derived by sound pressure, on otoliths [10,20]. Concerning clupeids, them, instead, show a unique inner ear structure among vertebrates, with the presence of a small gas bubble close to *utricle*, that move, transferring the pressure derived by sound to otolith with an increase of sound detection [21]. This peculiar adaptation makes them able to detect up to 4 kHz sounds, with many species, as those in Alosinae group, specialized to arrive to the detection of ultrasounds, to over 180 kHz [22,23].

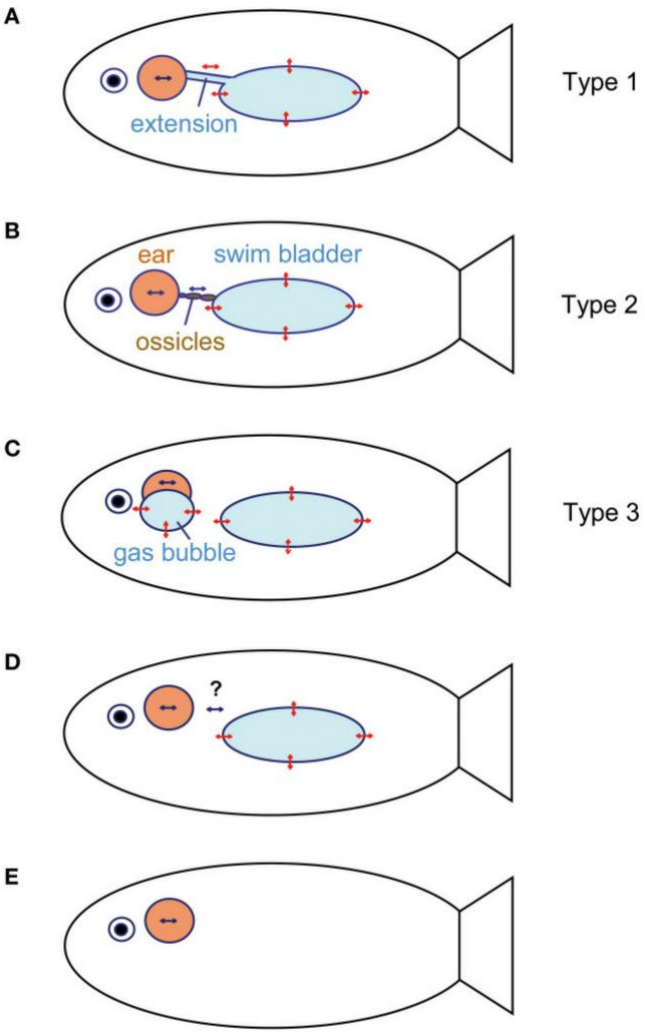

Figure 2. Schematic relationship between the accessory hearing structures and inner ear enhancing hearing ability in fishes. (A) Anterior swim bladder extensions, which may bear an anterior enlargement (e.g., clupeids). (B) A direct connection between inner ear and swim bladder with the Weberian ossicles chain, transmitting swim bladder vibrations to the ear. (C) Air-filled cavities directly connected to the inner ear, with the absence of connection to the swim bladder (e.g., mormyrids). (D) Absence of connection between gas bladder (swim bladder, lungs) and inner ear, with the bladder that could (lungfish, damselfish) or could not (toadfish) have an auditory function (see question marks). (E) No gas-filled cavity, as swim bladder, and no accessory structure to improve hearing (sharks, flatfishes, sculpins). Double-headed red arrows: oscillations of gas bladder walls related to sound pressure fluctuations. Blue arrows: particle motion within the inner ear related to the entire fish movement in the sound field. Image from: *Ladich, F., & Schulz-Mirbach, T. (2016). Diversity in fish auditory systems: one of the riddles of sensory biology. Frontiers in Ecology and Evolution, 4, 28, doi:10.3389/fevo.2016.00028.*

All these different mechanisms, evolved separately in multiple time and in species unrelated each other, could be examples of parallel evolution, mirroring the limited ways used by fish for pressure signals detection and, consequently, to increase the earing sensitivities [12]. Moreover, the high differences in hearing dynamics and inner ear morphology showed by fishes, the largest among vertebrates (as highlighted by the bandwidth variation, from 100 or 200 Hz to 180 kHz, among the few fishes' species for which data are present in literature, larger than those of any other vertebrate group [18]), reflect the high biodiversity and ecomorphological adaptation to marine environments of this vertebrates group.

1.1 ***Teleost inner ear structure and functioning***

Teleost and cartilaginous fishes together represent the largest vertebrate group present in nature (over 30,000 extant species, see www.fishbase.org), with a biodiversity mirroring the wide morpho-functional adaptation which allowed these vertebrates to colonize and inhabit all the marine and freshwater habitats worldwide. The large variability of inner ears' morphology and hearing process among different fishes' taxa is a manifestation of this biodiversity. As argued by Popper et al. [10], this wide ears' structural and functional variability could be a reflection of how sounds detection and processing change among fishes' taxa, being shaped by different evolutionary "experiments" that often can achieve a similar or equal sound detection and processing results, by the meaning of different ways.

It is very difficult to find a unique inner ear structure for fishes, but, despite the extensive variations, an accelerometer-like system is the basis of signal processing and hearing in the large part of teleost and cartilaginous fishes, with a basic inner ear structure shared by all of them. The mechanosensory stimuli at which inner ear is sensitive are oscillations at auditory frequencies and vibrational, gravistatic and acceleratory stimuli [7]. As reported in Figure 3, the shared basic structure of the inner ear is characterized by the presence of three semicircular canals with their end organs (*ampullae*) and sensory *cristae,* and three otolith end organs [24]. In teleost fishes, these form three pouches (*utricle*, *saccule*, *lagena*), and their rostro-caudal angular orientation (taxon specific) is essential for sound-source location [25,26].

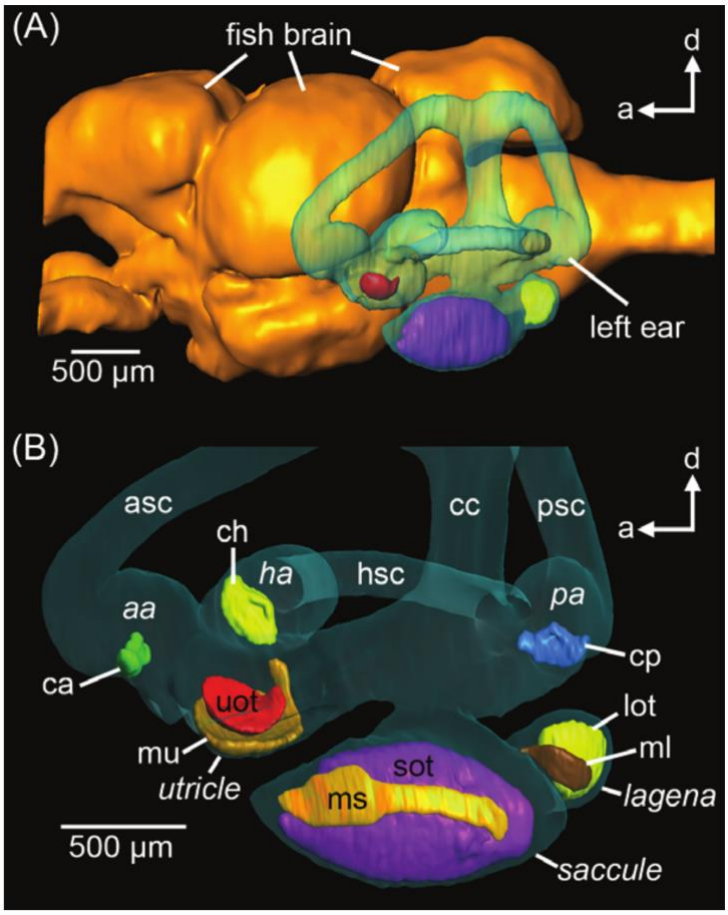

Figure 3. (A) The teleost inner ear position relative to fish's brain. (B) The inner ear components' details through a three-dimensional (3D) reconstruction with micro-computed tomography (microCT) in lateral (A) and medial (B) views, illustrating: anterior (asc), horizontal (hsc), and posterior (psc) semicircular canals; ampulla of the anterior (aa), horizontal (ha), and posterior (pa) canals; cc, common canal (= crus commune); otolith end organs: utricle, saccule, lagena; sensory epithelia: cristae of the anterior (ca), horizontal (ch), posterior (cp) canals; *maculae* of the *utricle* (mu), *saccule* (ms), and *lagena* (ml); otoliths: uot, utricular otolith (*lapillus*), sot, saccular otolith (*sagitta*), and lot, lagenar otolith (*asteriscus*). a, anterior; d, dorsal. Image from: *Schulz-Mirbach, T.; Ladich, F.; Plath, M.; Heß, M. Enigmatic ear stones: what we know about the functional role and evolution of fish otoliths. Biol. Rev. 2019, 94, 457–482, doi:10.1111/brv.12463.*

Inside all the ducts and pouches of the inner ear is present a viscous endolymphatic liquid with peculiar ionic properties. The semicircular canals are three orthogonally situated ducts (anterior, posterior, and lateral or horizontal), with a single dome-shaped sac (*ampulla*) at the origin of each one. Inside each *ampulla* is located the sensory *crista,* characterized by the presence of a gelatinous cupula above of it, which, being deformed by the fluid passage, detect the endolymphatic liquid movement within the canal. The sensory *crista* is composed of hair cells covered by mechanoreceptors called stereocilia. Their deflection, triggered by the angular acceleration of the head during rotation, allow to the release of chemical transmitter to the synapses of nerves present at their base [27]. Indeed, during head rotational movements and turns, the inner ear moves with head, while the endolymphatic fluid inside of it remains inert, exerting a mechanical force against the cupula and leading to the stereocilia deflection, and the consequential chemical transmitter release.

Concerning the otolithic end organs, these pouches-like structures are characterized by the internally presence of dense calcium carbonate masses, called otoliths or statoconia, covering the sensory epithelia (*maculae*). Otoliths and *macula* are embedded in an acellular gelatinous membrane (otolithic membrane), mediating the contact between them. These three structures (otolith, *macula* and otolithic membrane) form the otolithic apparatus, that in teleost fishes represents a physiological and morphological entity [24]. In addition to the three *maculae* present in the three otolithic end organs, in some teleost species there is another macula (*macula neglecta*) located in the common zone at the base of the labyrinth's canals [28]. Despite in elasmobranchs this play a fundamental role in sound perception [29], it is still unknown its function in teleost fishes. Concerning the function of otolith end organs, they play multiple roles in both hearing and vestibular functions [18,30]. *Maculae sacculi* and *utricle* are involved in the detection of linear acceleration and head position in relation to gravity. This is fundamental for the motion perception in both horizontal and vertical planes, thanks to the different orientation of *saccule* and *utricle* (respectively vertical and horizontal) [31]. The otoliths, covering the *maculae* and connected with them by the otolithic membrane*,* acts as a mass that follow the gravity direction, shifting with respect to the *macula*. The otoliths movement, in accordance with gravity, during head inclination, lead to a membrane shift witch allow to the stereocilia deflection in the hair cells, depolarizing them [32,33]. This depolarization seems to be coupled with a neurotransmitters release to the afferent neural fibers' terminals. Otolithic organs are also involved in auditory function [7,34], but it is not still completely clear the specific role of each of them. The relative contribution of *saccule, lagena* and *utricle* to the detection of sounds seems to vary species specifically, also in relation to the presence of accessory auditory structures able to detect and transmit, in the form of particle motion, also pressure component of sound. The otoliths, located inside the otolithic end organs (one for each end organs, called *sagitta* in *sacculus, lapillus* in *utricle* and *asteriscus* in *lagena*), thanks to their strictly connection with the sensory epithelium (*macula*), can convert the particle motion related to sound field in physiologically response resulting in nerve stimulation. Fish body and sensory epithelia, approximately of the same density of water, shift and vibrate as water particle, for phase and amplitude, subjected to a sound field. Differently, otoliths, being denser than body and sensory epithelia, move in a different way. This allows to the banding of ciliary bundles, present in in the hair cells of sensory epithelia, produced by the relative motion between otoliths and sensory epithelia under sound stimulation, allowing to the direct stimulation of the inner ear by a sound source [9]. The hair cells bending leads to the nerve stimulation, with the same physiological mechanism discussed above for sensory *crista* of the *ampulla*, which is the same in the ears of all the vertebrates, also with a virtually same hair cells structure [35]. This indeed represents the most common and ancient hearing mechanism among vertebrates, while the pressure

component detection of sound is relatively new from an evolutionistic point of view. Fishes using only the direct stimulation to detect sound (called “hearing generalist”) show a lower sensitivity and a narrower band width of hearing if compared with those so called “hearing specialists”, able to detect sound with indirect pathways (through the detection of sound pressure) by the meaning of accessory auditory structures, peripheral to the ear [36].

Concerning hair cells’ structure, as showed in Figure 4, they present a ciliary bundle consisting of numerous stereocilia and a kinocilium, eccentrically located. A cuticular plate, extending beneath the cell membrane, enclose the stereocilia, that are organized based on their height, with the longest placed close to the kinocilium. Excitatory of inhibitory response resulting from cilia bending, related to a hyperpolarization and a depolarization mediated by physiochemical receptor potential, depend on the deflection direction of cilia; if it occurs toward the kinocilium will result in an excitatory response (hyperpolarization), otherwise in a maximum inhibition (depolarization) [9,10,37]. These receptor potentials induced inside the cells allow to the stimulation of the eighth nerve neurons by the release of neurotransmitters. Inside the sensory epithelia, the hair cells are organized in orientation groups according with the position of the kinocilium, with the same kinocilium orientation showed by the hair cells belonging to a same orientation group [38]. The hair cells patterns change interspecifically, and this association of morphological and physiological polarization make possible the detection of the direction of a sound source by teleost species. This can happen thanks to the responses of hair cells, that is directionally polarized proportional to the vector component along the axes of the most pronounced physiological sensitivity. According to literature mainly regarding *sacculi* [38,39], each hair cells orientation group is innervated by a different neuron. Once neurological information arrives to the central nervous system, the sound direction is calculated by a comparison of the directional response properties of neurons from sensory cells in the *macula,* especially those of *sacculi,* with different orientations, resulting in the detection of a sound source in three-dimensional space from different angles [40,41].

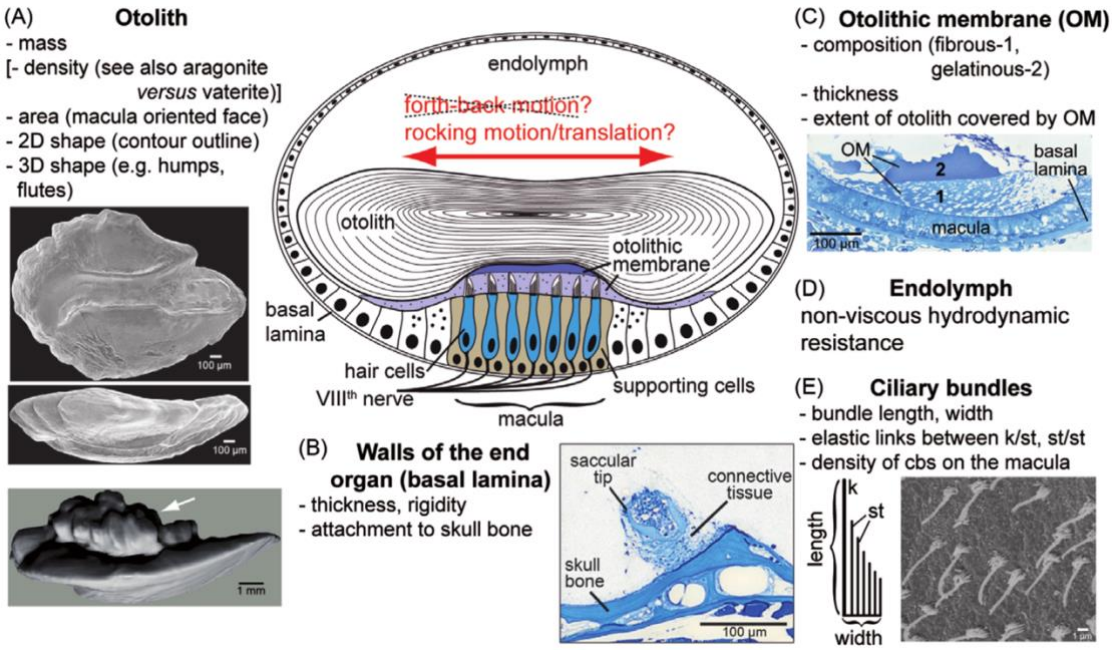

Figure 4. Components of the Inner ear, features influencing otolith movement, including otolith's properties. Scheme of otolith end organ's transverse section showing otolith, otolithic membrane, macula, and their relationships, with its motion described as a rocking-like movement instead of a simple back-and-forth motion. (A) Medial (top) and dorsal view (middle) of the saccular otolith's scanning electron micrograph of *Paratilapia polleni* Bleeker, 1868. The white arrow indicates the saccular otoliths' antisulcal face with protrusions (*Argyrosomus regius* Asso, 1801). (B) Histological section (thickness: 1 µm) illustrating the saccular tip's attachment in *Etroplus maculatus,* Bloch, 1795, to the neurocranium. (C) Histological section (thickness: 1 µm) illustrating the otolithic membrane's components (OM), the fibrous and gelatinous portions. (E) Scanning electron micrograph image of the ciliary bundles on the macula. cb, ciliary bundle; k, kinocilium; st, stereovillus. Image from: *Schulz-Mirbach, T.; Ladich, F.; Plath, M.; Heß, M. Enigmatic ear stones: what we know about the functional role and evolution of fish otoliths. Biol. Rev. 2019, 94, 457–482, doi:10.1111/brv.12463.*

2. WHY OTOLITHS? THEIR PECULIAR FEATURES AND SCIENTIFIC VALUE

2.2 Otoliths chemical composition, growing dynamics and biomineralization process

Otoliths are solid acellular masses (over 90% of their chemical composition consists of inorganic materials [42], with a small fraction of proteins), composed of calcium carbonate which biomineralize during the entire teleost's life, with a daily growth allowing to new material accretion [43]. They are embedded in a non-collagenous organic matrix, and they are metabolically inert. Any chemical compounds or elements added during the growth process is permanently maintained and, due to the continue growing during the entire animals' lifecycles, otoliths can be the "flight recorder" of fishes, in which every moment of their life is recorded [44], with information on environmental temperature history, anadromy, migration pathways, pollution exposure, validation of age, stock identification, being also used as metabolic indicators, natural tag and mass marking [24,45,46]. Due to the massive presence of calcium carbonate in their chemical composition, otoliths are most pure then many other biological structures. Calcium, oxygen, and carbon are the main elements, with many others (e.g., P, Na, K, Sr, N, S and Cl) detected in trace (<100 ppm) or at minor level (>100 ppm).

Concerning biomineralization process, despite it has been widely studied mainly in *sagittae*, it is not yet fully understood ([47,48] and references therein). The description provided below is referred on *sagittae* and *sacculi,* being data on the other otoliths and otolithic end organ almost totally absent. Being otoliths not directly in contact with the calcification region, calcium carbonate deposition is strictly related to the chemical composition of the endolymphatic fluid surrounding them. Its pH seems to be one of the key factor regulating biomineralization, influenced also by the bicarbonate ions concentration in endolymph [42,49,50]. Being otoliths acellular, for the biomineralization process and, consequently, for their growth play a fundamental role the epithelial cells of *sacculum.* All necessary growth components are produced by specialized epithelial cells of the endolymphatic epithelium and secreted in the extracellular space full of endolymph. *Sacculum* epithelium is composed of four areas: the *macula* (sensory zone), two meshwork zones on either *macula* sides (composed of large ionocytes), intermediate zones and patches zone, rich of small ionocytes, facing the *macula* (also called squamous epithelia) [51,52]. Protein production is carried out by the entire epithelium [53], while the ion transport to the endolymph is probably mainly provided by meshwork and patches zones, with different functions (e.g., Ca^{2+}/H^{+} exchange, K^{+} supply to endolymph) according to the differences reported for cell distribution and size between these two zones [54]. Both are rich of carbonic anhydrase isozyme and Na^{+}/K^{+} - ATPase [55]. Connection between *macula* (rich of hair cells) and otoliths occurs through an acellular gelatinous membrane [56], formed by two areas, an unstructured sub-cupular meshwork area and a structured gelatinous layer. This last stretches from the *sulcus acusticus* (a groove presents along the otolith inner face) to the *macula'*s hair cells, covering half of the otolith inner face and following the *sulcus* shape and external structures. The former area is composed of a fibers network extending from the otolith, being incorporated into its organic matrix, to the apical epithelium [57]. The proteins founded in otolith membrane are homologous to those identified in mammals (e.g., Otogelin, Otolin, Alpha- and Beta- tectorin, Otogelin-like), with often differences in expression areas [53,58,59]. The otoliths formation starts at embryo stage with a cluster of precursor particles containing glycogen and glycoproteins (that could form primordia), grounded to the epithelial tissue of *sacculus.* As suggested by otoliths' cores analysis, organic compounds seem to be the mainly constituent of primordia, controlling the verso of mineral precipitation [60]. Biomineralization process starts, after the primordium formation, with the alternating deposition, laid down over daily, of mineral-dominant and organic matrix-rich increments. On otoliths' organic matrix (between 0.1 and 2.3 %, and mainly compose of non-collagenous proteins, collagens and proteoglycans [61,62]) depends the formation of the growth bands, used for age lecture and growth rate reconstructions. Indeed, daily and seasonal variations on the organic matrix concentration create the different colors, detected under reflected light, among zones deposited during

the growth season (“opaque zones”, colored withe, more rich of organic matrix concentrations) and the winter season (“translucent or hyaline zones”, colored dark, more rich of minerals) [63]. The mechanisms allowing increments deposition are poorly understood, indeed ageing techniques still in use are based on otoliths marking studies [64]. The organic matrix included in otoliths (between 0.1 to 2.3 %) [61] is approximately composed for 23% of collagens, 29% proteoglycans and 48 % of other non-collagenous proteins [42,62]. Nowadays, more than 380 matrix proteins have been identified, with the function of many of them that still remains unknown [65]. Generally, the otolith organic matrix is divided in “water soluble” and “insoluble”. This subdivision refers to the capability of molecules to solubilize after EDTA decalcification, with the “water soluble matrix” mainly composed of non-collagenous proteins, proteoglycans and polysaccharides, and the “insoluble” of collagenous molecules [47,59,66]. The main component of these molecules is the Otolin-1, an inner-ear specific collagen essential for the maintenance of otolith position (anchored over the sensory epithelium) and the crystal formation, acting as a nucleation site [58,59,67]. Recently it has been discovered another component of the collagenous matrix, a sialo phosphoprotein (Starmarker) acting as a support for crystal growth by creating other nucleation sites [65]. Concerning the “soluble” fraction of otoliths’ organic matrix, it is mainly composed of glycoproteins, polysaccharides, lipoproteins, and acidic proteins. They are essential for the growing process, as highlighted by the otoliths’ longest growth axes, which show the highest soluble matrix intensity, following and revealing the daily increments of growth. Polysaccharides serve to stabilize the matrix, with glycosaminoglycans (mucopolysaccharides) as mainly component [68]. The glycoproteins play an active role in the calcium carbonate formation process, forming large complexes with others fibrous proteins (as collagen) to facilitate the calcium binding capacity (as Otolith Matrix Protein, OMP-1), regulates increment growth (as Neuroserpin) and bind collagen and calcium (as Secreted protein acidic and rich in cysteine, Sparc) [58,59,65,67,68]. Proteins seem to play an important role on otoliths daily growth, as highlighted by their high concentrations and numbers in endolymph, with values comparable to blood serum [65]. According to literature [50,69,70], it seems clear that there is a connection between the fluctuations of endolymph proteins concentrations and increments formation. However, not all these proteins are involved in the biomineralization process, and it must be considered that all the studies dealing with this topic quantified concentrations of the total protein amount, without focusing on expression changes related to otolith matrix proteins [65]. But there are a lot of evidence on the fluctuation of endolymph proteins concentration between day and night period, with higher proteins levels generally detected in nigh than day. As also highlighted by the high CO_2 concentrations founded during day, and by immunohistochemical studies on proteins of otoliths matrix, the formation of proteinaceous band is believed to start at dusk, continuing for the entire night.

While aragonite precipitation seems to occur mainly during daytime, starting at dawn [67,71,72], with specie specific differences in this day-night alternation on deposition, as highlighted by several examples present in literature of an inverse process [70,73]. Growth, and consequently otoliths symmetry and size, are regulated by key isozymes (Carbonic anhydrase), highly conserved in all the vertebrates, catalyzing the formation of the bicarbonate ion from carbon dioxide.

Two Carbonic anhydrase types have been identified, one in endolymph and saccular epithelium, and another on otoliths surface, confirming the dual role of this isozyme. Indeed, the first type (called CA 1) is involved in the maintenance of a saturated solution in endolymph to enhance the aragonite precipitation, acting as a transport for bicarbonate (Figure 5); the other type (called CA 6) is involved in the maintenance of the local bicarbonate supersaturation on otolith surface to allow the continue aragonitic precipitation [65,74]. There are also mechanisms of pH control, fundamental to maintain chemical condition favorable for aragonite precipitation. These involve energy dependent Na^+/K^+ exchangers and V-type ATPase, which regulate the ionic concentration in endolymph, working together with CA 6 to maintain a bicarbonate concentration useful for aragonitic precipitation [49,65]. Essential for the biomineralization process it is also the Cl^- and HCO_3^- exchanger involved in the transport of carbonate ions from saccular epithelial cells to endolymph [65]. All these information about the mechanisms, and both organic and inorganic substances involved in the biomineralization and otolith growth, highlight how this physiochemical process needs a strictly regulated chemical environment, both in endolymph and on otolith face.

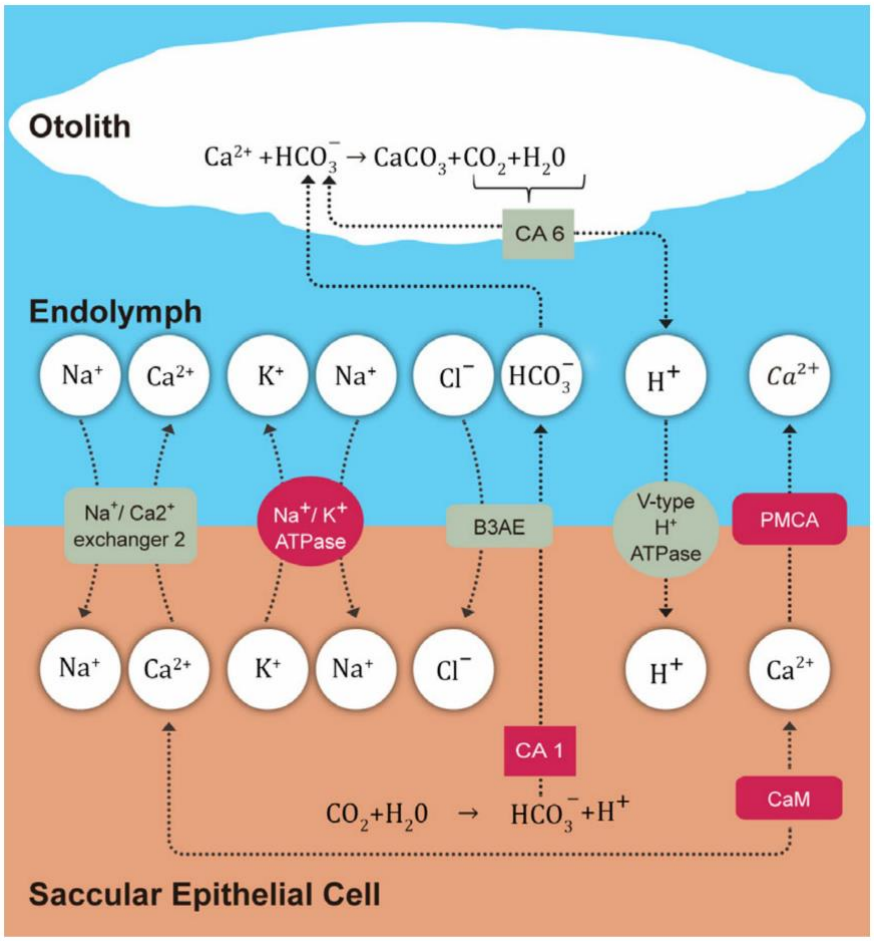

Figure 5. Scheme of ion transport occurring in the inner ear, image from: *Thomas, O.R.B.; Swearer, S.E.; Kapp, E.A.; Peng, P.; Tonkin-Hill, G.Q.; Papenfuss, A.; Roberts, A.; Bernard, P.; Roberts, B.R. The inner ear proteome of fish. FEBS J. 2019, 286, 66–81, doi:10.1111/febs.14715*.

In addition to this, it is widely known how the exposition to different environments, with different physiochemical features, can alter the concentration of minor and trace elements. Fish otoliths are composed by to date 50 elements. These include the majors, as Ca, C, O and N, and minors, as Sr, P, Na, Mg, Cl, K and S. Many of them are required for growth and reproduction processes, and metabolic reactions, with the elemental absorption in marine species occurring mainly across the gut wall. According to literature, which is mainly focused on Sr and Ba [44,45,75], water could be the main source of ions (Figure 6). The mechanism allowing the movement of trace and minor elements from the blood plasma to the endolymph is not completely understood. Calcium, occurring in plasma as ion, moves to endolymph using active transport, assisted by calmodulin, or also by passive transport following the concentration gradient [76]. Data on the other elements is almost absent, except for Sr, which seem to move passively across the endolymphatic epithelium [77]. Concerning other elements, they could occur in plasma as hydrated free ions (e.g., Li^+. Mg^{2+}, Ba^{2+}) and presumably they could enter across the endolymphatic epithelium through passive diffusion along concentration gradient

[44,78]. But the transport of these elements could not be the same for all of them, according to their dimension and chemical behavior. They are involved in the functioning of several enzymes and proteins both in otoliths and endolymph. For instance, magnesium (Mg) is essential for the enzymes' phosphorylation process, as in Starmarker enzymes. Iron (Fe) is a component of Serotransferrin, an endolymph protein, while Copper (Cu) and Selenium (Se) are essential for the well-functioning of several enzymes. Manganese (Mn) is a co-factor of the Extracellular serine threonine protein kinase FAM20C, a biomineralization protein acting on the phosphorylation process of Starmaker homologs, while Zinc (Zn) is a fundamental co-factor for many enzymes (such as metalloproteinases and carbonic anhydrase) involved in the carbon dioxide conversion to bicarbonate ions during the mineralization process [48,65,78]. Trace elements are incorporated into increments following a mechanism does not clear at all. As reported for strontium, they can substitute calcium in aragonite lattice, or they could be trapped both as free ion and with macromolecules interactions, or through interactions with otoliths' organic matrix [44,75]. According to Thomas et al. [79], elements with an ionic radius like Calcium (e.g., Sr, Mn, Ba), appearing with a high enrichment factor, can compete with it for binding sites, interacting with the same proteins and, thus, occurring in the carbonate fraction. Otherwise, elements which appear with no enrichment factors in endolymph and otoliths (e.g., Li, K, Rb, Mg) could be randomly trapped in the crystal lattice. Transitions metals (e.g., Fe, Ni, Zn, Cu) are typically found bounded to soluble fraction of the organic matrix, associated to metalloproteins complexes. As reported by literature [45,78], their incorporation in increments is strongly influenced by physiochemical environmental features, such as concentration gradients, dissolved oxygen, pH, temperature and salinity. This make their concentration in otoliths a way to predict in a consistent way the ambient environmental conditions [44]. The main elements used as environmental tracers are Sr, Ba and Mn, thank to their capability to substitute the Ca [75], but also other elements randomly trapped in the carbonate structure may exhibit environmental sensitivity, serving as geographic markers [47].

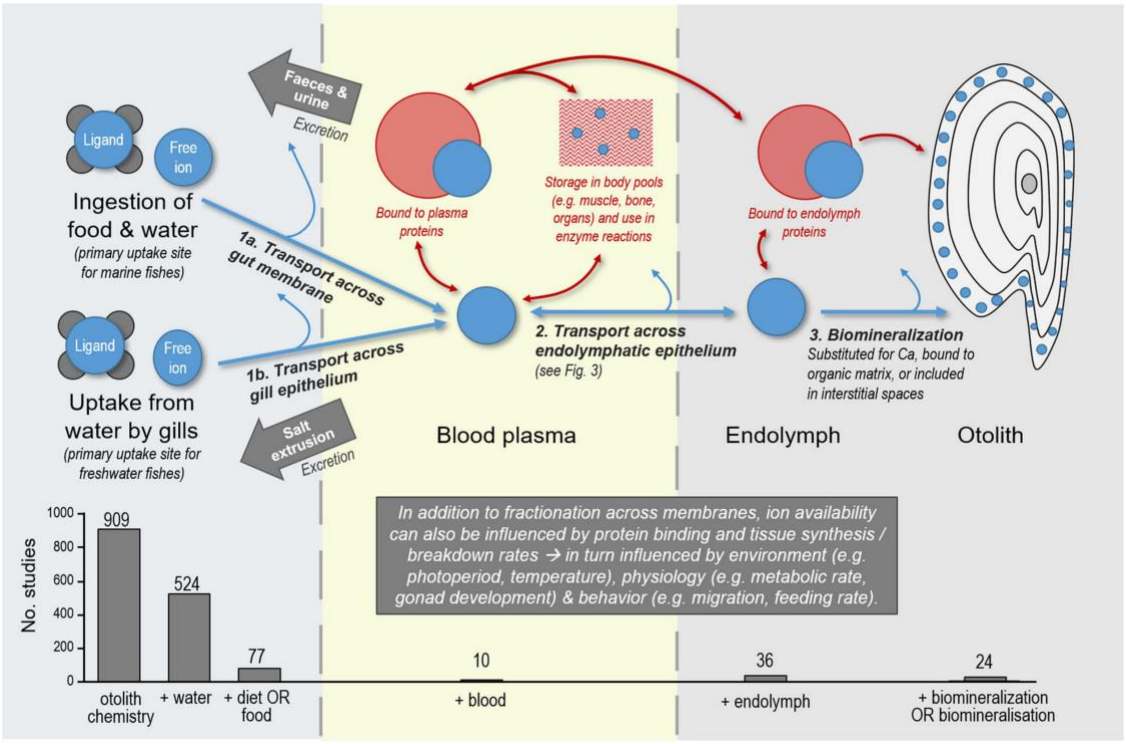

Figure 6. Scheme of the main pathways of ions into an otolith, involving uptake gill and gut membranes uptake into blood plasma, transport across the endolymphatic epithelium into the endolymph, and incorporation into the otolith's growing crystal lattice, image from: *Hüssy, K.; Limburg, K.E.; de Pontual, H.; Thomas, O.R.B.; Cook, P.K.; Heimbrand, Y.; Blass, M.; Sturrock, A.M. Trace Element Patterns in Otoliths: The Role of Biomineralization. Rev. Fish. Sci. Aquac. 2021, 29, 445–477, doi:10.1080/23308249.2020.1760204.*

2.2 Otoliths' variability and the influence of morphology on their motion

Among the interesting features of fish ears, the most striking is for sure the inter specific diversity, ranging from their gross structure to the sensory hair cells' organization. Ear shape can be related both to fishes' size and ear function, but it is almost unknown its significance [80]. Sagittal otoliths perfectly reflect this morphological variability, being their shape and size substantially different at inter specific, and often also at intra specific level. Concerning the other two otoliths' pairs, their intra and inter specific morphological variability has not been investigated deeply as in *sagittae,* except few studies [81–86]. In 'non-otophysan' teleost this could depend to their very smaller dimensions and enhanced fragility respect saccular otoliths, that are considered the only that can provide information about specie-specific morphology, allowing to species delimitation, and intra-population variability [87]. However, in otophysans (Gymnotiformes, Cypriniformes, Siluriformes and Characiformes) including all the taxa with Weberian apparatus [88], *sagittae*, characterized by a needle-like shape, are by far frailer and smaller than *lapilli* and *asterisci.* But, despite this, literature dealing with these otoliths pairs also in otophysans is poor and fragmentary [83,84,89–91]. Contrary to the general belief, Assis [82–84] has provided accurate overviews showing as also these otoliths

types present different specie-specific morphology, while two most recent studies have provided significant evidences of their population-specific morphological variability [81,92].

Concerning the most studied among otoliths, *sagittae*, the otolithic end organ to which they belong (*saccule*) is often the most involved in hearing process, as reported for "hearing specialist" species, that also show specialization in *sagittae* structure and morphology [11]. This is the case of the silver perch (*Bairdiella chrysoura*, Lacepède, 1802), a sound specialist species able to detect sounds up to several kilohertz. It shows a very large *sagitta,* with a deeply grooved *sulcus acusticus,* and a *saccule* located very close to a large *utricle* [80]. The morphological diversity of *sagittae* involves also the sensory epithelia (e.g., shape, size) and its relationship with otolith (e.g., coverage ratio of otolith on epithelia) [18], with inter specific variation also in *sulcus* depth [15,93]. The significance of this high variability at intra and inter specific level is almost completely unknown, but, as suggested by several authors [24,80], morphology influences directly otoliths' functioning. The otoliths' properties relevant to their functionality are density (related to the calcium carbonates' polymorphs composition and influenced by its modifications), mass and thickness (amount of mineralized material), center of gravity and the overall three-dimensional (3D) and two-dimensional (2D) shape [24].

The main polymorphs of calcium carbonate detected in teleosts' otoliths are aragonite (in *sagittae* and *lapilli*) and vaterite (in *asterisci*). Usually, the crystalline forms of calcium carbonate also include calcite in addition to the above mentioned, that generally are the more instable among the three. Differently to mammals, in which otoconia are composed of calcite, polycrystalline aragonite is the main component of almost all sagittal and utricular. Despite it is unclear the reason why there is this strong predominance of aragonite over calcite, organic molecules seem to regulate and control the polymorph selection [94]. This has been proven by research performed on macromolecules extracted from mollusks shells. Aragonitic formation have been induced by macromolecules from aragonitic shell layers, while calcite formation by those from calcitic shell layers, providing evidence for the organic control (mainly of proteins) on crystal formation [95]. Different polymorphs are also present in the different otolithic end organs. As stated above, sagittal and utricular otoliths are mainly composed of aragonite, while almost all the lagenar otoliths are made of vaterite, explaining their glassy appearance. This polymorph is also founded in aberrant (crystalline) otoliths, without a clear and accepted explanation for its formation [96], that are mainly related to the absence of equilibrium in supersaturated solutions [97]. The influence of crystalline polymorphs on otoliths density, vaterite is less dense than aragonite [98], resulting in different patterns of oscillatory movement respect *macula* of vateritic lagenar otoliths compared to aragonitic saccular and utricular ones. Different densities, together with differences in ciliary bundles orientation, could result in differences of the sensory hair cells' stimulation patterns on the *maculae* [24], but it is not clear what triggers the

deposition of one polymorph rather than another. Concerning otoliths size, it is not still clear its influence of vestibular and auditory functions, with conflicting results showed by research dealing with this topic in different species [80,99,100]. It is very difficult to predict also how otoliths shape (both 3D and 2D) and mass can affect ear function. As reported by several authors, otoliths' (especially *sagittae*) 2D (contours) and 3D shape show stock- [101–103], population- [104,105] and specie- specific [82,87,106,107] differences. The ear function could be affected by otoliths' shape in two different ways, according to otoliths movements. If this is a back-and-forth movement induced by tilts, left to right shifts and dorso-ventral axes acceleration of the body, the linear acceleration related to these positional changes could generate an otolith motion more dependent to its mass than shape. If the otolith's movement is a motion/oscillation induced by the particle motion related to a sound source, this could allow to a rather simple back-to-forth movement if the otolith shape is approximately spherical or ellipsoidal, deviating from this simple motion in otoliths with a complex shape, with an increasing influence of mass on motion when this shape is significantly different from a sphere or an ellipse [7,24,108,109]. Several studies, performed on different species or based on mathematical modeling [109–112], have confirmed the frequency- / shape- dependent motion of otoliths, confirming that different frequencies stimulate specific *macula* regions, with the different otoliths' parts (e.g., margin vs center) that move dissimilarly. Also, *sulcus acusticus* (in *sagittae* and *lapilli*) and *fossa acustica* (in *asterisci*) play an essential role in relative motion of otoliths respect their *maculae.* These otoliths' parts represent the zones housing the *maculae,* with their shapes matching that of their respective *maculae* [7]. For this reason, it is assumed that an increased *sulcus* (or *fossa*) *acusticus* (expressed as *sulcus* or *fossa*/*macula* size to otolith size) results in an improved hearing ability [105,113]. Sulcus dimensions have been related by several ecomorphological studies to habitat features (e.g., depth, trophic niche, mobility) and ontogeny [114–116], showing how this otoliths feature could be strictly dependent on the ecology and distribution of the different species. In addition, the others inner ears' structural components (such as the features of the otolithic membrane, the sensory hair cells' number, the length of the ciliary bundle and its stereo villi distribution) can also affect the sensory hair cells' stimulation and the otoliths motion [24], confirming the complexity of the otolithic end organs and the several otoliths' features influencing hearing and vestibular functions.

2.3 Otoliths' science and their importance in ecomorphological analysis

The peculiar chemistry of otoliths, their growing and deposition dynamics, their intra and inter specific variability in morphology and shape, all these features make otoliths essential tools used,

from more than a century, to investigate many aspects of teleost's lifestyle, taxonomy, and population dynamics, as well as to obtain essential information for fisheries management and conservation purposes. The growth bands formation allowed by the biomineralization process (as reported in the first part of this chapter) enables the age estimation through the annual growth increment counting [43,80]. This technique is widely diffused from the 1960s, making possible the longevity estimation of a species and the evaluation of the growth rate of a population. Data about age are also the basis for productivity and mortality rate calculations and, consequently, for population dynamics studies, on which accuracy depend a correct evaluation of stocks and fisheries assessment procedures [117]. , Otoliths' microstructures are used for daily aging to investigate the recruitment and population dynamics of young fishes [118]. The analysis of trace elements, through an evaluation of their concentrations, and stable isotopes composition are used to analyze the migration patterns of teleost species and their movement across area with different salinities [45,119,120], essential information for conservation porpoises and fisheries management. Also, the otoliths mean shape is widely used in fisheries science as tool to discriminate among different stocks [121,122]. Stock assessment is, indeed, essential to improve the evaluation of the fishing effort affecting a population, increasing the fisheries' management policies. In addition to mean shape, also otoliths' overall morphology, thanks to the inter specific variability, is widely used in many scientific fields. First in trophic ecology, where otoliths, thanks to their specie specific morphology, are fundamental for prey identification in stomach content analysis of ichthyophages predators. Indeed, often they are the only preys remains, resilient to the digestion process, useful for preys' identification and the reconstruction of the marine trophic network [123,124]. Moreover, In addition to fisheries science and ecology, otolith morphology is also widely used in archaeological and palaeoichthyological studies, for the analysis of the fossil fish remains applied in the reconstruction of the fossil fish communities and the marine paleo-environments [106,125,126]. Otoliths shape and morphology can be also influenced by the ecological conditions faced by the different species, or by the different populations of a same species, in distinct environments or geographical areas. This process can shape otoliths' diversity and evolution through an imposed ear structures' selection and a phenotypic plasticity induced by the environment [24]. Ecomorphological studies deal with the correlation between otoliths' morphology (and shape) and differences in life-history traits (e.g., slow growth, fast growth), feeding habits and food intakes, lifestyle (e.g., fast-swimming species, bottom dwelling species) and ecological gradients (related for instance to salinity, water depth, temperature) [127–132].

Understanding the relation between habitats, ecological conditions and otoliths is essential to comprehend the dynamics allowing their intra and inter specific diversity, deepening the knowledge on the development dynamics of the entire inner ear, and clarifying how it can be influenced by the

environmental features and different habitat's preferences. According to literature [132,133], water depth and temperature, for instance, seem to affect otoliths' size. Indeed, this seems to increase at higher temperatures and grater depths, despite in abyssal species otoliths size decreases. Concerning lifestyle, otoliths size has been found to be reduced in epipelagic species [134], while shape has been found to be less elongated in benthic species than pelagic fast-swimming once [135,136]. The combination of phylogenetic information and data about species' ecology, eco-acoustic, inner ear physiology, otoliths morphology and life-history traits can clarify the selective force influencing otoliths' morphological features [137–139], also elucidating the impact of the phylogenetic pressure on otoliths development, as well as the relation between otoliths morphology and other components of the inner ear [24]. Tuset et al. [139] have shown the combined effect of environment (habitat depth) and phylogenetic signal on otoliths evolution in the family Sebastidae, joining phylogenetic and shape analysis. Their results confirmed the influence of biogeography, depth distribution, feeding habits and age on otoliths morphological evolution in rockfishes, highlighting the consistence of the sensory drive hypothesis in the studied species and the reliability of the otoliths shape for eco-phylogenetic studies. The so-called sensory drive hypothesis deals with the thesis that sensory interactions between organisms, environment and their diversification may promote speciation [140,141]. In this context, otoliths are the perfect biological structure for the ecomorphological studies, allowing to explore the connections between diversification and sensory processes. Phenotypic, or developmental plasticity, and genetic differences (both at intra and inter specific level) are the two forces triggering to phenotypic divergences founded along ecological gradients and to the taxon-specific morphological differences in otoliths [127,142]. According to Vignon and Morat [127], at intra specific level, contrasting environmental conditions reshape overall otoliths contours, while the locally otolith shape (e.g., *rostrum* and *antirostrum* length) is mainly affected by genetic variations at intra-specific level related to long-time segregations. These direct correlations between otoliths shape, genetic and environmental features have been provided by authors exploring, through shape and phylogenetic analysis, a non-indigenous species (*Lutjanus kasmira*, Forsskål, 1775), introduced by humans in Hawaii archipelagos. Indeed, comparing data between native (inhabiting French Polynesia) and introduced populations, authors have been able to assess that the degrees of phenotypic plasticity are not the same in all the otolith portions. This was highlighted also by others scientists, who have postulated that the shape of *sulcus acusticus* and otoliths mass are mainly controlled by genetic, while overall 3D otoliths shape, margins' sculpture and the presence of humps on the anterior or posterior regions are mainly influenced by environment [143–145]. These evidences confirm the dual regulation controlling otoliths' development, with genetics that influence the general otoliths form,

and environmental factors that, regulating physical constraint and metabolic expression, influence the quantity of deposited material during the otoliths growth [127].

Also diet composition and food quantity can influence otolith features (e.g. shape, morphology, chemical composition) and body morphology, as suggested by several authors [142,146–155]. Food quantity has an indirect impact on otoliths shape affecting its growth, while influence directly the structure of otoliths' margin [147,154,155]. Starvation and food restriction periods can influence otoliths' structure, composition, and growth. Periods of reduced feeding can induce a reduction in the otoliths' increments width, influencing the growth and allowing to an enhanced translucency of the deposited material, through variations in their organic and inorganic compounds' composition [156]. This can lead to structural discontinuities affecting the seasonal alternance of hyaline and opaque annuli, used for teleost fish aging [157]. A reduction of the aragonite precipitation rate, induced by a starvation period, can negatively affect the otoliths' daily growth rate and the biomineralization process [50]. This can be related to variations in blood plasma composition, leading to alterations on chemical equilibrium of the saccular endolymph, and to a concentration decrease of the "factor retarding crystallization" (FRC), a protein precursor for the biomineralization [158]. Concerning energy metabolism, standard metabolic rate and thermogenesis induced by feeding, these strongly regulate otoliths growth and accretion [159]. The energy density of the diet is mainly related to the preys' lipid component, that, consequently, as highlighted in larvae and juveniles, alter otolith growth, influencing the individual condition index which depend to the fish lipid composition [160–162]. In addition to the abundance and the energy content of food, also the diet composition can influence otoliths features, especially regarding their chemical composition [152]. This is the case of *Pomatomus saltatrix* (Linnaeus, 1766), that showed concentrations of Barium (Ba) and Strontium (Sr) in otoliths and preys strictly related. Buckel et al. [153] suggested that diet can influence the concentrations of these two elements in otoliths indirectly, through diet-based changes in otoliths growth rate inducing variations in element incorporation rate, and directly, through the concentrations of these elements in preys. This is also the case of Manganese (Mn), that, according to Sanchez-Jerez et al. [152] showed a clear correlation between its concentration in habitat, preys items and otoliths of *Helotes sexlineatus* (Quoy & Gaimard, 1825). Indeed, despite the 80% of these microelements present in otoliths come from water, trophic transfer can be considered another potential source for metallic element accumulation, as also highlighted by Thorrold et al. for the Mg/Ca ratio [163] in larval and juveniles *Micropogonias undulatus* (Linnaeus, 1766) otoliths. The influence of diet on otoliths chemical composition has been widely confirmed also by stable isotopes analysis [120,164], as showed in reared juveniles of *Fundulus heteroclitus* (Linnaeus, 1766), with a correlation between $\delta^{13}C$ values in muscles and otoliths [165]. This confirm that amino acids in otoliths and muscles co-

varies, suggesting that amino acids found in otoliths proteins come from food items. According to Mille et al. [146], there is also a relationship between *sagittae* shape and diet, with a clear influence of both primary and secondary preys categories on global shape and fine details, that seems to be more enhanced than that of the quantity of ingested food. The intra specific variations, related to taxonomic preys' category consumed, on *sagittae* shape and morphology mainly deal with ellipticity degree, otoliths crenation and *excisura major* width. Indeed, saccular endolymph proteins can be influenced in their quantity and composition by fish diet, affecting the biomineralization process and, consequently, the entire 3D structure of the otoliths, their growth and their 2D shape and morphology. The influence of diet on otoliths shape is also confirmed by the ontogenetic variations reported in several species undergoing feeding habits variations during their growth, as *Odontesthes argentinensis* (Valenciennes, 1835) and *Perca fluviatilis* (Linnaeus, 1758) [151,166], and in larval stages and juvenile of *Gadus morhua* (Linnaeus, 1758) and *Dicentrarchus labrax* (Linnaeus, 1758) [147,150].

3 AIM OF THE THESIS

This thesis aims to explore the information that otoliths (mainly *sagittae*) can provide about the eco-morphological adaptation of Mediterranean teleost fishes to different environments.

The *sagittae* of several Mediterranean species, with different life habits and habitat preferences, have been analyzed using shape, morphometric and Scanning electron microscopy (SEM) analysis to explore their shape, morphology, and external textural organization. The obtained data allowed to deepen the knowledge on the variability of *sagittae* at intra and inter specific level, providing useful information on the functional morphology of otoliths in the studied species. In particular, the intra specific variability of *sagittae,* in shape, morphology and external textural organization, has been analyzed at inter and intra population level, between different ontogenetic classes, while the variability at inter specific level has been explored among species belonging to the same genus or family. Moreover, in two of the studied species, for the first time in the Mediterranean Sea, in addition to *sagittae,* they have been analyzed also *lapilli* and *asterisci,* providing a complete description to fill the gap about their intra specific variability.

In present thesis they have been provided six cases of study (reported in the six following chapters of the thesis), that have led to the drafting of six scientific papers, with the following involved species: *Pagellus erythrinus* (Linnaeus, 1758), *Pagellus bogaraveo* (Brünnich, 1768), *Pagellus acarne* (Risso, 1827), *Chelon auratus* (Risso, 1810), *Chelon labrosus* (Risso, 1827), *Oedalechilus labeo* (Cuvier, 1829), *Hymenocephalus italicus* (Giglioli, 1884), *Nezumia sclerorhynchus* (Valenciennes, 1838), *Nezumia aequalis* (Günther, 1878), *Coryphaenoides guentheri* (Vaillant, 1888), *Coelorinchus*

caelorhincus (Risso, 1810), *Argyropelecus hemigymnus* (Cocco, 1829), *Belone belone* (Linnaeus, 1760) and *Scorpaena porcus* (Linnaeus, 1758).

The first, the second and the third cases of study involved respectively the species belonging to *Pagellus* genus (*P. erythrinus*, *P. bogaraveo*, *P. acarne*), Mugilidae family (*C. auratus*, *C. labrosus*, *O. labeo*) and Macrouridae family (*H. italicus*, *N. sclerorhynchus*, *N. aequalis*, *C. guentheri*, *C caelorhincus*), exploring the inter and intra specific variability of *sagittae* in phylogenetically close species. Concerning Mugilidae and Macrouridae families, their differences in shape and morphology have been applied to confirm the reliability of *sagittae* for taxonomic identification of cryptic species.

The fourth and the fifth cases of study involved *A. hemigymnus* and *B. belone,* respectively. In these two species, completely different for life habits and habitats preferences, the three otoliths' pairs (*sagittae* and *lapilli* in *A. hemigymnus, sagittae, lapilli* and *asterisci* in *B. belone*) have been analyzed to explore their intra specific variability at ontogenetic level, defining the level of variability also *lapilli* and *asterisci*. The obtained data have been also compared to literature from other geographical area, exploring the inter population variability of the three otoliths pairs.

The inter population variability of *sagittae* has been analyzed in the sixth case of study, involving *S. porcus* specimens, comparing the *sagittae* features of two populations inhabiting completely different environments. They have been also analyzed feeding habits, growth dynamics and age structures, comparing them with literature data from other geographical areas, to find a most clear correlation between environmental conditions and *sagittae* features.

Deepen the knowledge on how the otoliths' variability in shape and morphology could be related to different habitats' preferences, life habits and environmental condition experienced by species during their life cycles is fundamental to clarify how the entire inner ear has adapted, under the evolutionary pressure, to different environmental condition.

REFERENCES

1. Pfaff, C.; Schultz, J.A.; Schellhorn, R. The vertebrate middle and inner ear: A short overview. *J. Morphol.* **2019**, *280*, 1098–1105, doi:10.1002/jmor.20880.
2. Breuer, J. Studien Über den Vestibularapparat. *Sitzungsberichte der Akad. der Wissenschaften Math. Klasse* **1903**, *112*, 315–394.
3. Fleischer, G. Evolutionary principles of the mammalian middle ear. In *Advances in anatomy, embryology and cell biology*; Springer-Verlag: New York, 1978; pp. 5–70 ISBN 1545-1542.
4. Clack, J.A.; Anderson, J.S. Early Tetrapods: Experimenting with Form and Function. In; Clack, J.A., Fay, R.R., Popper, A.N., Eds.; Springer International Publishing: Cham, 2016; pp. 71–105 ISBN 978-3-319-46661-3.
5. Dijkgraaf, S. The functioning and significance of the lateral-line organs. *Biol. Rev. Camb. Philos. Soc.* **1963**, *38*, 51–105, doi:10.1111/j.1469-185X.1963.tb00654.x.
6. Harris, G.G.; van Bergeijk, W.A. Evidence that the Lateral Line Organ Responds to Water

Displacements. *J. Acoust. Soc. Am.* **1962**, *34*, 733–733, doi:10.1121/1.1937263.
7. Platt, C.; Popper, A.N. Fine Structure and Function of the Ear. In; 1981; pp. 3–38.
8. Schulz-Mirbach, T.; Heß, M.; Metscher, B.D.; Ladich, F. A unique swim bladder-inner ear connection in a teleost fish revealed by a combined high-resolution microtomographic and three-dimensional histological study. *BMC Biol.* **2013**, *11*, 1–13, doi:10.1186/1741-7007-11-75.
9. Popper, A.N.; Lu, Z. Structure-function relationships in fish otolith organs. *Fish. Res.* **2000**, *46*, 15–25, doi:10.1016/S0165-7836(00)00129-6.
10. Popper, A.N.; Fay, R.R. Rethinking sound detection by fishes. *Hear. Res.* **2011**, *273*, 25–36, doi:10.1016/j.heares.2009.12.023.
11. Ladich, F.; Popper, A.N. Parallel Evolution in Fish Hearing Organs. *Evol. Vertebr. Audit. Syst.* **2004**, 95–127, doi:10.1007/978-1-4419-8957-4_4.
12. Braun, C.B.; Grande, T. Evolution of Peripheral Mechanisms for the Enhancement of Sound Reception. *Fish Bioacoustics* **2008**, 99–144, doi:10.1007/978-0-387-73029-5_4.
13. Fay, R.R.; Popper, A.N. Acoustic stimulation of the ear of the goldfish (Carassius auratus). *J. Exp. Biol.* **1974**, *61*, 243–260, doi:10.1242/jeb.61.1.243.
14. Fay, R.R.; Popper, A.N. Modes of stimulation of the teleost ear. *J. Exp. Biol.* **1975**, *62*, 379–387, doi:10.1242/jeb.62.2.379.
15. Ramcharitar, J.U.; Higgs, D.M.; Popper, A.N. Audition in sciaenid fishes with different swim bladder-inner ear configurations. *J. Acoust. Soc. Am.* **2006**, *119*, 439–443, doi:10.1121/1.2139068.
16. Higgs, D.M.; Souza, M.J.; Wilkins, H.R.; Presson, J.C.; Popper, A.N. Age- and size-related changes in the inner ear and hearing ability of the adult zebrafish (Danio rerio). *JARO - J. Assoc. Res. Otolaryngol.* **2002**, *3*, 174–184, doi:10.1007/s101620020035.
17. Coombs, S.; Popper, A.N. Hearing differences among Hawaiian squirrelfish (family Holocentridae) related to differences in the peripheral auditory system. *J. Comp. Physiol. □ A* **1979**, *132*, 203–207, doi:10.1007/BF00614491.
18. Popper, A.N.; Fay, R.R.; Platt, C.; Sand, O. Sound Detection Mechanisms and Capabilities of Teleost Fishes. *Sens. Process. Aquat. Environ.* **2008**, 3–38, doi:10.1007/978-0-387-22628-6_1.
19. Fletcher, L.B.; Crawford, J.D. Acoustic detection by sound-producing fishes (mormyridae): The role of gas-filled tympanic bladders. *J. Exp. Biol.* **2001**, *204*, 175–183, doi:10.1242/jeb.204.2.175.
20. Fay, R. Behavioral audiogram for the goldfish. *J. Aud. Res.* **1969**, *9*, 112–121.
21. Higgs, D.M.; Plachta, D.T.T.; Rollo, A.K.; Singheiser, M.; Hastings, M.C.; Popper, A.N. Development of ultrasound detection in American shad (Alosa sapidissima). *J. Exp. Biol.* **2004**, *207*, 155–163, doi:10.1242/jeb.00735.
22. Mann, D.A.; Higgs, D.M.; Tavolga, W.N.; Popper, A.N. Ultrasound detection by clupeiform fishes. *Bioacoustics* **2002**, *12*, 188–191, doi:10.1080/09524622.2002.9753691.
23. Mann, D.A.; Lu, Z.; Popper, A.N. A clupeid fish can detect ultrasound [4] (multiple letters). *Nature* **1997**, *389*, 341, doi:10.1038/38636.
24. Schulz-Mirbach, T.; Ladich, F.; Plath, M.; Heß, M. Enigmatic ear stones: what we know about the functional role and evolution of fish otoliths. *Biol. Rev.* **2019**, *94*, 457–482, doi:10.1111/brv.12463.
25. Edds-Walton, P.L.; Fay, R.R. Physiological evidence for binaural directional computations in the brainstem of the oyster toadfish, Opsanus tau (L.). *J. Exp. Biol.* **2009**, *212*, 1483–1493, doi:10.1242/jeb.026898.
26. Schulz-Mirbach, T.; Heß, M.; Plath, M. Inner ear morphology in the atlantic molly Poecilia mexicana-first detailed microanatomical study of the inner ear of a cyprinodontiform species. *PLoS One* **2011**, *6*, doi:10.1371/journal.pone.0027734.
27. Elliott, K.L.; Fritzsch, B.; Duncan, J.S. Evolutionary and developmental biology provide

insights into the regeneration of organ of Corti hair cells. *Front. Cell. Neurosci.* **2018**, *12*, 252, doi:10.3389/fncel.2018.00252.
28. Buran, B.N.; Deng, X.; Popper, A.N. Structural variation in the inner ears of four deep-sea elopomorph fishes. *J. Morphol.* **2005**, *265*, 215–225, doi:10.1002/jmor.10355.
29. Gardiner, J.M.; Hueter, R.E.; Maruska, K.P.; Sisneros, J.A.; Casper, B.M.; Mann, D.A.; Demski, L.S. Sensory Physiology and Behavior of Elasmobranchs. *Biol. Sharks Their Relat.* **2012**, *1*, 365–418, doi:10.1201/b11867-20.
30. Mackowetzky, K.; Yoon, K.H.; Mackowetzky, E.J.; Waskiewicz, A.J. Development and evolution of the vestibular apparatuses of the inner ear. *J. Anat.* **2021**, *239*, 801–828, doi:10.1111/joa.13459.
31. Chagnaud, B.P.; Engelmann, J.; Fritzsch, B.; Glover, J.C.; Straka, H. Sensing External and Self-Motion with Hair Cells: A Comparison of the Lateral Line and Vestibular Systems from a Developmental and Evolutionary Perspective. *Brain. Behav. Evol.* **2017**, *90*, 98–116, doi:10.1159/000456646.
32. Hain, T.; Hekmminski, J. Anatomy and Physiology of the Normal Vestibular System. *Susan J. Herdman Vestib. Rehabil. (3rd Ed)* **2007**, *3*, 2–18.
33. Kasumyan, A. The vestibular system and sense of equilibrium in fish. *J. Ichthyol.* **2004**, *44*, S224.
34. Popper, A.N. Organization of the inner ear and auditory processing. *Fish Neurobiol.* **1983**, *1*, 125–177.
35. Chang, J.S.Y.; Popper, A.N.; Saidel, W.M. Heterogeneity of sensory hair cells in a fish ear. *J. Comp. Neurol.* **1992**, *324*, 621–640, doi:10.1002/cne.903240413.
36. Popper, A.N.; Fay, R.R. The Auditory Periphery in Fishes. *Comp. Hear. fish Amphib.* **1999**, 43–100, doi:10.1007/978-1-4612-0533-3_3.
37. Popper, A.N. Auditory system morphology. In *Encyclopedia of Fish Physiology: from Genome to Environment*; Farrell, A.P., Ed.; Academic Press: San Diego, CA, 2011; pp. 252–261.
38. Popper, A.N.; Schilt, C.R. Hearing and Acoustic Behavior: Basic and Applied Considerations. *Fish Bioacoustics* **2008**, 17–48, doi:10.1007/978-0-387-73029-5_2.
39. Lu, Z.; Popper, A.N. Neural response directionality correlates of hair cell orientation in a teleost fish. *J. Comp. Physiol. - A Sensory, Neural, Behav. Physiol.* **2001**, *187*, 453–465, doi:10.1007/s003590100218.
40. Edds-Walton, P.L. Projections of primary afferents from regions of the saccule in toadfish (Opsanus tau). *Hear. Res.* **1998**, *115*, 45–60, doi:10.1016/S0378-5955(97)00179-2.
41. Rogers, P.H.; Cox, M. Underwater Sound as a Biological Stimulus. In Proceedings of the Sensory Biology of Aquatic Animals; Springer, 1988; pp. 131–149.
42. Borelli, G.; Mayer-Gostan, N.; Merle, P.L.; De Pontual, H.; Boeuf, G.; Allemand, D.; Payan, P. Composition of biomineral organic matrices with special emphasis on turbot (Psetta maxima) otolith and endolymph. *Calcif. Tissue Int.* **2003**, *72*, 717–725, doi:10.1007/s00223-001-2115-6.
43. Campana, S.E.; Thorrold, S.R. Otoliths, increments, and elements: Keys to a comprehensive understanding of fish populations? *Can. J. Fish. Aquat. Sci.* **2001**, *58*, 30–38, doi:10.1139/f00-177.
44. Campana, S.E. Chemistry and composition of fish otoliths: Pathways, mechanisms and applications. *Mar. Ecol. Prog. Ser.* 1999, *188*, 263–297.
45. Izzo, C.; Doubleday, Z.A.; Schultz, A.G.; Woodcock, S.H.; Gillanders, B.M. Contribution of water chemistry and fish condition to otolith chemistry: Comparisons across salinity environments. *J. Fish Biol.* **2015**, *86*, 1680–1698, doi:10.1111/jfb.12672.
46. McGowan, N.; Fowler, A.M.; Parkinson, K.; Bishop, D.P.; Ganio, K.; Doble, P.A.; Booth, D.J.; Hare, D.J. Beyond the transect: An alternative microchemical imaging method for fine scale analysis of trace elements in fish otoliths during early life. *Sci. Total Environ.* **2014**,

494–495, 177–186, doi:10.1016/j.scitotenv.2014.05.115.
47. Hüssy, K.; Limburg, K.E.; de Pontual, H.; Thomas, O.R.B.; Cook, P.K.; Heimbrand, Y.; Blass, M.; Sturrock, A.M. Trace Element Patterns in Otoliths: The Role of Biomineralization. *Rev. Fish. Sci. Aquac.* **2021**, *29*, 445–477, doi:10.1080/23308249.2020.1760204.
48. Thomas, O.R.B.; Swearer, S.E. Otolith biochemistry—a review. *Rev. Fish. Sci. Aquac.* **2019**, *27*, 458–489.
49. Payan, P.; Kossmann, H.; Watrin, A.; Mayer-Gostan, N.; Boeuf, G. Ionic composition of endolymph in teleosts: Origin and importance of endolymph alkalinity. *J. Exp. Biol.* **1997**, *200*, 1905–1912, doi:10.1242/jeb.200.13.1905.
50. Payan, P.; Borelli, G.; Boeuf, G.; Mayer-Gostan, N. Relationship between otolith and somatic growth: Consequence of starvation on acid-base balance in plasma and endolymph in the rainbow trout Oncorhynchus mykiss. *Fish Physiol. Biochem.* **1998**, *19*, 35–41, doi:10.1023/A:1016064813517.
51. Weigele, J.; Franz-Odendaal, T.A.; Hilbig, R. Formation of the inner ear during embryonic and larval development of the cichlid fish (Oreochromis mossambicus). *Connect. Tissue Res.* **2017**, *58*, 172–195, doi:10.1080/03008207.2016.1198337.
52. Takagi, Y.; Takahashi, A. Characterization of ootolith soluble-matrix producing cells in the saccular epithelium of rainbow trout (Oncorhynchus mykiss) inner ear. *Anat. Rec. An Off. Publ. Am. Assoc. Anat.* **1999**, *254*, 322–329.
53. Stooke-Vaughan, G.A.; Obholzer, N.D.; Baxendale, S.; Megason, S.G.; Whitfield, T.T. Otolith tethering in the zebrafish otic vesicle requires otogelin and α-Tectorin. *Dev.* **2015**, *142*, 1137–1145, doi:10.1242/dev.116632.
54. Mayer-Gostan, N.; Kossmann, H.; Watrin, A.; Payan, P.; Boeuf, G. Distribution of ionocytes in the saccular epithelium of the inner ear of two teleosts (Oncorhynchus mykiss and Scophthalmus maximus). *Cell Tissue Res.* **1997**, *289*, 53–61, doi:10.1007/s004410050851.
55. Takagi, Y. Meshwork arrangement of mitochondria-rich, Na+,K+-ATPase-rich cells in the saccular epithelium of rainbow trout (Oncorhynchus mykiss) inner ear. *Anat. Rec.* **1997**, *248*, 483–489, doi:10.1002/(SICI)1097-0185(199708)248:4<483::AID-AR1>3.0.CO;2-N.
56. Hughes, I.; Blasiole, B.; Huss, D.; Warchol, M.E.; Rath, N.P.; Hurle, B.; Ignatova, E.; David Dickman, J.; Thalmann, R.; Levenson, R.; et al. Otopetrin 1 is required for otolith formation in the zebrafish Danio rerio. *Dev. Biol.* **2004**, *276*, 391–402, doi:10.1016/j.ydbio.2004.09.001.
57. Dunkelberger, D.G.; Dean, J.M.; Watabe, N. The ultrastructure of the otolithic membrane and otolith in the juvenile mummichog, Fundulus heteroclitus. *J. Morphol.* **1980**, *163*, 367–377, doi:10.1002/jmor.1051630309.
58. Murayama, E.; Herbomel, P.; Kawakami, A.; Takeda, H.; Nagasawa, H. Otolith matrix proteins OMP-1 and Otolin-1 are necessary for normal otolith growth and their correct anchoring onto the sensory maculae. *Mech. Dev.* **2005**, *122*, 791–803, doi:10.1016/j.mod.2005.03.002.
59. Murayama, E.; Takagi, Y.; Nagasawa, H. Immunohistochemical localization of two otolith matrix proteins in the otolith and inner ear of the rainbow trout, Qncorhynchus mykiss: Comparative aspects between the adult inner ear and embryonic otocysts. *Histochem. Cell Biol.* **2004**, *121*, 155–166, doi:10.1007/s00418-003-0605-5.
60. Jolivet, A.; Bardeau, J.F.; Fablet, R.; Paulet, Y.M.; De Pontual, H. Understanding otolith biomineralization processes: New insights into microscale spatial distribution of organic and mineral fractions from Raman microspectrometry. *Anal. Bioanal. Chem.* **2008**, *392*, 551–560, doi:10.1007/s00216-008-2273-8.
61. Hüssy, K.; Mosegaard, H.; Jessen, F. Effect of age and temperature on amino acid composition and the content of different protein types of juvenile Atlantic cod (Gadus morhua) otoliths. *Can. J. Fish. Aquat. Sci.* **2004**, *61*, 1012–1020, doi:10.1139/F04-037.

62. Payan, P.; De Pontual, H.; Bœuf, G.; Mayer-Gostan, N. Endolymph chemistry and otolith growth in fish. *Comptes Rendus Palevol* **2004**, *3*, 535–547.
63. Beckman, D.; Wilson, C. Seasonal timing of opaque zone formation in fish otoliths. *Recent Dev. Fish Otolith Res.* **1995**, 27–43.
64. Campana, S.E. Accuracy, precision and quality control in age determination, including a review of the use and abuse of age validation methods. *J. Fish Biol.* **2001**, *59*, 197–242, doi:10.1006/jfbi.2001.1668.
65. Thomas, O.R.B.; Swearer, S.E.; Kapp, E.A.; Peng, P.; Tonkin-Hill, G.Q.; Papenfuss, A.; Roberts, A.; Bernard, P.; Roberts, B.R. The inner ear proteome of fish. *FEBS J.* **2019**, *286*, 66–81, doi:10.1111/febs.14715.
66. Kang, Y.J.; Stevenson, A.K.; Yau, P.M.; Kollmar, R. Sparc protein is required for normal growth of zebrafish otoliths. *JARO - J. Assoc. Res. Otolaryngol.* **2008**, *9*, 436–451, doi:10.1007/s10162-008-0137-8.
67. Takagi, Y.; Tohse, H.; Murayama, E.; Ohira, T.; Nagasawa, H. Diel changes in endolymph aragonite saturation rate and mRNA expression of otolith matrix proteins in the trout otolith organ. *Mar. Ecol. Prog. Ser.* **2005**, *294*, 249–256, doi:10.3354/meps294249.
68. Asano, M.; Mugiya, Y. Biochemical and calcium-binding properties of water-soluble proteins isolated from otoliths of the tilapia, Orecchromis niloticus. *Comp. Biochem. Physiol. -- Part B Biochem.* **1993**, *104*, 201–205, doi:10.1016/0305-0491(93)90359-D.
69. Kalish, J.M. Pseudophycis barbatus. *Mar. Ecol. Prog. Ser* **1991**, *74*, 137–159.
70. Edeyer, A.; De Pontual, H.; Payan, P.; Troadec, H.; Sévère, A.; Mayer-Gostan, N. Daily variations of the saccular endolymph and plasma compositions in the turbot Psetta maxima: Relationship with the diurnal rhythm in otolith formation. *Mar. Ecol. Prog. Ser.* **2000**, *192*, 287–294, doi:10.3354/meps192287.
71. Tohse, H.; Murayama, E.; Ohira, T.; Takagi, Y.; Nagasawa, H. Localization and diurnal variations of carbonic anhydrase mRNA expression in the inner ear of the rainbow trout Oncorhynchus mykiss. *Comp. Biochem. Physiol. - B Biochem. Mol. Biol.* **2006**, *145*, 257–264, doi:10.1016/j.cbpb.2006.06.011.
72. Borelli, G.; Guibbolini, M.E.; Mayer-Gostan, N.; Priouzeau, F.; De Pontual, H.; Allemand, D.; Puverel, S.; Tambutte, E.; Payan, P. Daily variations of endolymph composition: Relationship with the otolith calcification process in trout. *J. Exp. Biol.* **2003**, *206*, 2685–2692, doi:10.1242/jeb.00479.
73. Parmentier, E.; Cloots, R.; Warin, R.; Henrist, C. Otolith crystals (in Carapidae): Growth and habit. *J. Struct. Biol.* **2007**, *159*, 462–473, doi:10.1016/j.jsb.2007.05.006.
74. Tohse, H.; Mugiya, Y. Effects of acidity and a metabolic inhibitor on incorporation of calcium and inorganic carbon into endolymph and otoliths in salmon Oncorhynchus masou. *Fish. Sci.* **2004**, *70*, 595–600, doi:10.1111/j.1444-2906.2004.00846.x.
75. Doubleday, Z.A.; Harris, H.H.; Izzo, C.; Gillanders, B.M. Strontium randomly substituting for calcium in fish otolith aragonite. *Anal. Chem.* **2014**, *86*, 865–869, doi:10.1021/ac4034278.
76. Funamoto, T.; Mugiya, Y. Binding of Strontium vs Calcium to 17β-Estradiol-Induced Proteins in the Plasma of the Goldfish Carassius auratus. *Fish. Sci.* **1998**, *64*, 325–328, doi:10.2331/fishsci.64.325.
77. Payan, P.; Borelli, G.; Priouzeau, F.; De Pontual, H.; Boeuf, G.; Mayer-Gostan, N. Otolith growth in trout Oncorhynchus mykiss: Supply of Ca2+ and Sr2+ to the saccular endolymph. *J. Exp. Biol.* **2002**, *205*, 2687–2695, doi:10.1242/jeb.205.17.2687.
78. Sturrock, A.M.; Trueman, C.N.; Darnaude, A.M.; Hunter, E. Can otolith elemental chemistry retrospectively track migrations in fully marine fishes? *J. Fish Biol.* **2012**, *81*, 766–795, doi:10.1111/j.1095-8649.2012.03372.x.
79. Thomas, O.R.B.; Ganio, K.; Roberts, B.R.; Swearer, S.E. Trace element-protein interactions in endolymph from the inner ear of fish: implications for environmental reconstructions using

fish otolith chemistry. *Metallomics* **2017**, *9*, 239–249, doi:10.1039/c6mt00189k.
80. Popper, A.N.; Ramcharitar, J.; Campana, S.E. Why otoliths? Insights from inner ear physiology and fisheries biology. *Mar. Freshw. Res.* **2005**, *56*, 497–504, doi:10.1071/MF04267.
81. Schulz-Mirbach, T.; Riesch, R.; García de León, F.J.; Plath, M. Effects of extreme habitat conditions on otolith morphology - a case study on extremophile livebearing fishes (Poecilia mexicana, P. sulphuraria). *Zoology* **2011**, *114*, 321–334, doi:10.1016/j.zool.2011.07.004.
82. Assis, C.A. Estudo morfológico dos otólitos sagitta, asteriscus e lapillus de Teleóstei (Actinopterygii, Teleostei) de Portugal continental. Sua aplicação em estudos de filogenia, sistematica e ecologia. *Ecologia* 2000, 1005.
83. Assis, C.A. The utricular otoliths, lapilli, of teleosts: Their morphology and relevance for species identification and systematics studies. *Sci. Mar.* **2005**, *69*, 259–273, doi:10.3989/scimar.2005.69n2259.
84. Assis, C.A. The lagenar otoliths of teleosts: Their morphology and its application in species identification, phylogeny and systematics. *J. Fish Biol.* **2003**, *62*, 1268–1295, doi:10.1046/j.1095-8649.2003.00106.x.
85. Schulz-Mirbach, T.; Plath, M. All good things come in threes–species delimitation through shape analysis of saccular, lagenar and utricular otoliths. *Mar. Freshw. Res.* **2012**, *63*, 934–940.
86. D'Iglio, C.; Famulari, S.; Albano, M.; Carnevale, A.; Di Fresco, D.; Costanzo, M.; Lanteri, G.; Spanò, N.; Savoca, S.; Capillo, G. Intraspecific variability of the saccular and utricular otoliths of the hatchetfish Argyropelecus hemigymnus (Cocco, 1829) from the Strait of Messina (Central Mediterranean Sea). *PLoS One* **2023**, *18*, 1–31, doi:10.1371/journal.pone.0281621.
87. Nolf, D. *Otolithi Piscium. Handbook of Paleoichthyology, Vol. 10.*; Fischer, G., Ed.; Stuttgart, New York, 1985;
88. Bonde, N.; Greenwood, P.H.; Patterson, C. *Interrelationships of Fishes.*; Academic Press, 1974; Vol. 23; ISBN 0080534929.
89. Schulz-Mirbach, T.; Reichenbacher, B. Reconstruction of Oligocene and Neogene freshwater fish faunas - An actualistic study on cypriniform otoliths. *Acta Palaeontol. Pol.* **2006**, *51*, 283–304.
90. Frost, G.A. XIX.— A Comparative study of the otoliths of the Neopterygian fishes . *Ann. Mag. Nat. Hist.* **1930**, *5*, 231–239, doi:10.1080/00222933008673124.
91. Adams, L.A. Some characteristic otoliths of American ostariophysi. *J. Morphol.* **1940**, *66*, 497–527, doi:10.1002/jmor.1050660307.
92. Schulz-Mirbach, T.; Ladich, F.; Riesch, R.; Plath, M. Otolith morphology and hearing abilities in cave- and surface-dwelling ecotypes of the Atlantic molly, Poecilia mexicana (Teleostei: Poeciliidae). *Hear. Res.* **2010**, *267*, 137–148, doi:10.1016/j.heares.2010.04.001.
93. Ramcharitar, J.; Gannon, D.P.; Popper, A.N. Bioacoustics of Fishes of the Family Sciaenidae (Croakers and Drums). *Trans. Am. Fish. Soc.* **2006**, *135*, 1409–1431, doi:10.1577/t05-207.1.
94. Falini, G.; Fermani, S.; Vanzo, S.; Miletic, M.; Zaffino, G. Influence on the formation of aragonite or vaterite by otolith macromolecules. *Eur. J. Inorg. Chem.* **2005**, *2005*, 162–167, doi:10.1002/ejic.200400419.
95. Falini, G.; Albeck, S.; Weiner, S.; Addadi, L. Control of aragonite or calcite polymorphism by mollusk shell macromolecules. *Science (80-.).* **1996**, *271*, 67–69, doi:10.1126/science.271.5245.67.
96. Gauldie, R.W.; Sharma, S.K.; Volk, E. Micro-Raman spectral study of vaterite and aragonite otoliths of the coho salmon, Oncorhynchus kisutch. *Comp. Biochem. Physiol. - A Physiol.* **1997**, *118*, 753–757, doi:10.1016/S0300-9629(97)00059-5.
97. CARLSTRÖM, D. a Crystallographic Study of Vertebrate Otoliths. *Biol. Bull.* **1963**, *125*, 441–463, doi:10.2307/1539358.

98. Tomas, J.; Geffen, A.J. Morphometry and composition of aragonite and vaterite otoliths of deformed laboratory reared juvenile herring from two populations. *J. Fish Biol.* **2003**, *63*, 1383–1401, doi:10.1111/j.1095-8649.2003.00245.x.
99. Kéver, L.; Colleye, O.; Herrel, A.; Romans, P.; Parmentier, E. Hearing capacities and otolith size in two ophidiiform species (Ophidion rochei and Carapus acus). *J. Exp. Biol.* **2014**, *217*, 2517–2525, doi:10.1242/jeb.105254.
100. Inoue, M.; Tanimoto, M.; Oda, Y. The role of ear stone size in hair cell acoustic sensory transduction. *Sci. Rep.* **2013**, *3*, 2114, doi:10.1038/srep02114.
101. Soeth, M.; Daros, F.A.; Correia, A.T.; Fabré, N.N.; Medeiros, R.; Feitosa, C.V.; de Sousa Duarte, O.; Lenz, T.M.; Spach, H.L. Otolith phenotypic variation as an indicator of stock structure of Scomberomorus brasiliensis from the southwestern Atlantic Ocean. *Fish. Res.* **2022**, *252*, 106357, doi:10.1016/j.fishres.2022.106357.
102. Benzinou, A.; Carbini, S.; Nasreddine, K.; Elleboode, R.; Mahé, K. Discriminating stocks of striped red mullet (Mullus surmuletus) in the Northwest European seas using three automatic shape classification methods. *Fish. Res.* **2013**, *143*, 153–160, doi:10.1016/j.fishres.2013.01.015.
103. Neves, J.; Silva, A.A.; Moreno, A.; Veríssimo, A.; Santos, A.M.; Garrido, S. Population structure of the European sardine Sardina pilchardus from Atlantic and Mediterranean waters based on otolith shape analysis. *Fish. Res.* **2021**, *243*, 106050, doi:10.1016/j.fishres.2021.106050.
104. Teimori, A.; Schulz-Mirbach, T.; Esmaeili, H.R.; Reichenbacher, B. Geographical differentiation of Aphanius dispar (Teleostei: Cyprinodontidae) from Southern Iran. *J. Zool. Syst. Evol. Res.* **2012**, *50*, 289–304, doi:10.1111/j.1439-0469.2012.00667.x.
105. Schulz-Mirbach, T.; Ladich, F.; Riesch, R.; Plath, M. Otolith morphology and hearing abilities in cave- and surface-dwelling ecotypes of the Atlantic molly, Poecilia mexicana (Teleostei: Poeciliidae). *Hear. Res.* **2010**, *267*, 137–148, doi:10.1016/j.heares.2010.04.001.
106. Nolf, D. Studies on fossil otoliths - The state of the art. *Recent Dev. Fish Otolith Res.* **1995**, *19*, 513–544.
107. Tuset, V.M.; Lombarte, A.; Assis, C.A. Otolith atlas for the western Mediterranean, north and central eastern Atlantic. *Sci. Mar.* **2008**, *72*, 7–198.
108. Schellart, N.A.M.; Popper, A.N. Functional Aspects of the Evolution of the Auditory System of Actinopterygian Fish. In *The Evolutionary Biology of Hearing*; Springer, 1992; pp. 295–322.
109. Krysl, P.; Hawkins, A.D.; Schilt, C.; Cranford, T.W. Angular oscillation of solid scatterers in response to progressive planar acoustic waves: Do fish otoliths rock? *PLoS One* **2012**, *7*, doi:10.1371/journal.pone.0042591.
110. Enger, P.S. Frequency discrimination in teleosts—central or peripheral? In *Hearing and sound communication in fishes*; Springer, 1981; pp. 243–255.
111. Smith, M.E.; Schuck, J.B.; Gilley, R.R.; Rogers, B.D. Structural and functional effects of acoustic exposure in goldfish: Evidence for tonotopy in the teleost saccule. *BMC Neurosci.* **2011**, *12*, 1–17, doi:10.1186/1471-2202-12-19.
112. Lychakov, D. V.; Rebane, Y.T. Otolith regularities. *Hear. Res.* **2000**, *143*, 83–102, doi:10.1016/S0378-5955(00)00026-5.
113. Ramcharitar, J.U.; Deng, X.; Ketten, D.; Popper, A.N. Form and function in the unique inner ear of a teleost: The silver perch (Bairdiella chrysoura). *J. Comp. Neurol.* **2004**, *475*, 531–539, doi:10.1002/cne.20192.
114. Tuset, V.M.; Piretti, S.; Lombarte, A.; González, J.A. Using sagittal otoliths and eye diameter for ecological characterization of deep-sea fish: *Aphanopus carbo* and *A. intermedius* from NE Atlantic waters. *Sci. Mar.* **2010**, *74*, 807–814, doi:10.3989/scimar.2010.74n4807.
115. Lombarte, A.; Fortuño, J.M. Differences in morphological features of the sacculus of the

inner ear of two hakes (Merluccius capensis and M. paradoxus, gadiformes) inhabits from different depth of sea. *J. Morphol.* **1992**, *214*, 97–107, doi:10.1002/jmor.1052140107.
116. Aguirre, H.; Lombarte, A. Ecomorphological comparisons of sagittae in Mullus barbatus and M. surmuletus. *J. Fish Biol.* **1999**, *55*, 105–114, doi:10.1006/jfbi.1999.0974.
117. Hilborn, C.R.; Walters, J. *Quantitative Fisheries Stock Assessment: Choice, Dynamics and Uncertainty*; Springer Science & Business Media, 1992; Vol. 67; ISBN 1461535980.
118. Campana, S.E.; Neilson, J.D. Microstructure of Fish Otoliths. *Can. J. Fish. Aquat. Sci.* **1985**, *42*, 1014–1032, doi:10.1139/f85-127.
119. Limburg, K.E.; Elfman, M. Insights from two-dimensional mapping of otolith chemistry. In Proceedings of the Journal of Fish Biology; 2017; Vol. 90, pp. 480–491.
120. Radtke, R.L.; Showers, W.; Moksness, E.; Lenz, P. Environmental information stored in otoliths: Insights from stable isotopes. *Mar. Biol.* **1996**, *127*, 161–170, doi:10.1007/BF00993656.
121. Stransky, C.; Murta, A.G.; Schlickeisen, J.; Zimmermann, C. Otolith shape analysis as a tool for stock separation of horse mackerel (Trachurus trachurus) in the Northeast Atlantic and Mediterranean. *Fish. Res.* **2008**, *89*, 159–166, doi:10.1016/j.fishres.2007.09.017.
122. Campana, S.E.; Casselman, J.M. Stock discrimination using otolith shape analysis. *Can. J. Fish. Aquat. Sci.* **1993**, *50*, 1062–1083, doi:10.1139/f93-123.
123. Giménez, J.; Marçalo, A.; Ramírez, F.; Verborgh, P.; Gauffier, P.; Esteban, R.; Nicolau, L.; González-Ortegón, E.; Baldó, F.; Vilas, C.; et al. Diet of bottlenose dolphins (Tursiops truncatus) from the Gulf of Cadiz: Insights from stomach content and stable isotope analyses. *PLoS One* **2017**, *12*, e0184673, doi:10.1371/journal.pone.0184673.
124. Giménez, J.; Marçalo, A.; García-Polo, M.; García-Barón, I.; Castillo, J.J.; Fernández-Maldonado, C.; Saavedra, C.; Santos, M.B.; de Stephanis, R. Feeding ecology of Mediterranean common dolphins: The importance of mesopelagic fish in the diet of an endangered subpopulation. *Mar. Mammal Sci.* **2018**, *34*, 136–154, doi:10.1111/mms.12442.
125. Lin, C.H.; Girone, A.; Nolf, D. Fish otolith assemblages from Recent NE Atlantic sea bottoms: A comparative study of palaeoecology. *Palaeogeogr. Palaeoclimatol. Palaeoecol.* **2016**, *446*, 98–107, doi:10.1016/j.palaeo.2016.01.022.
126. Girone, A.; Nolf, D.; Cappetta, H. Pleistocene fish otoliths from the Mediterranean Basin: a synthesis. *Geobios* **2006**, *39*, 651–671, doi:10.1016/j.geobios.2005.05.004.
127. Vignon, M.; Morat, F. Environmental and genetic determinant of otolith shape revealed by a non-indigenous tropical fish. *Mar. Ecol. Prog. Ser.* **2010**, *411*, 231–241, doi:10.3354/meps08651.
128. Vignon, M. Disentangling and quantifying sources of otolith shape variation across multiple scales using a new hierarchical partitioning approach. *Mar. Ecol. Prog. Ser.* **2015**, *534*, 163–177, doi:10.3354/meps11376.
129. Volpedo, A.; Diana Echeverría, D. Ecomorphological patterns of the sagitta in fish on the continental shelf off Argentine. *Fish. Res.* **2003**, *60*, 551–560, doi:10.1016/S0165-7836(02)00170-4.
130. Volpedo, A. V.; Fuchs, D. V. Ecomorphological patterns of the lapilli of Paranoplatense Siluriforms (South America). *Fish. Res.* **2010**, *102*, 160–165, doi:10.1016/j.fishres.2009.11.007.
131. Aguirre, H.; Lombarte, A. Ecomorphological comparisons of sagittae in Mullus barbatus and M. surmuletus. *J. Fish Biol.* **1999**, *55*, 105–114, doi:10.1006/jfbi.1999.0974.
132. Lombarte, A.; Cruz, A. Otolith size trends in marine fish communities from different depth strata. *J. Fish Biol.* **2007**, *71*, 53–76, doi:10.1111/j.1095-8649.2007.01465.x.
133. Lombarte, A.; Lleonart, J. Otolith size changes related with body growth, habitat depth and temperature. *Environ. Biol. Fishes* **1993**, *37*, 297–306, doi:10.1007/BF00004637.
134. Paxton, J.R. Fish otoliths: Do sizes correlate with taxonomic group, habitat and/or luminescence? *Philos. Trans. R. Soc. B Biol. Sci.* **2000**, *355*, 1299–1303,

doi:10.1098/rstb.2000.0688.
135. Volpedo, A. V.; Tombari, A.D.; Echeverría, D.D. Eco-morphological patterns of the sagitta of Antarctic fish. *Polar Biol.* **2008**, *31*, 635–640, doi:10.1007/s00300-007-0400-1.
136. Tuset, V.M.; Imondi, R.; Aguado, G.; Otero-Ferrer, J.L.; Santschi, L.; Lombarte, A.; Love, M. Otolith patterns of rockfishes from the northeastern pacific. *J. Morphol.* **2015**, *276*, 458–469, doi:10.1002/jmor.20353.
137. Wainwright, P.C.; Smith, W.L.; Price, S.A.; Tang, K.L.; Sparks, J.S.; Ferry, L.A.; Kuhn, K.L.; Eytan, R.I.; Near, T.J. The Evolution of Pharyngognathy: A Phylogenetic and Functional Appraisal of the Pharyngeal Jaw Key Innovation in Labroid Fishes and beyond. *Syst. Biol.* **2012**, *61*, 1001–1027, doi:10.1093/sysbio/sys060.
138. Tsuboi, M.; Gonzalez-Voyer, A.; Kolm, N. Phenotypic integration of brain size and head morphology in Lake Tanganyika Cichlids. *BMC Evol. Biol.* **2014**, *14*, 1–10, doi:10.1186/1471-2148-14-39.
139. Tuset, V.M.; Otero-Ferrer, J.L.; Gómez-Zurita, J.; Venerus, L.A.; Stransky, C.; Imondi, R.; Orlov, A.M.; Ye, Z.; Santschi, L.; Afanasiev, P.K.; et al. Otolith shape lends support to the sensory drive hypothesis in rockfishes. *J. Evol. Biol.* **2016**, *29*, 2083–2097, doi:10.1111/jeb.12932.
140. Endler, J.A. Signals, signal conditions, and the direction of evolution. *Am. Nat.* **1992**, *139*, S125–S153, doi:10.1086/285308.
141. Endler, J.A. Some general comments on the evolution and design of animal communication systems. *Philos. Trans. - R. Soc. London, B* **1993**, *340*, 215–225, doi:10.1098/rstb.1993.0060.
142. Abaad, M.; Tuset, V.M.; Montero, D.; Lombarte, A.; Otero-Ferrer, J.L.; Haroun, R. Phenotypic plasticity in wild marine fishes associated with fish-cage aquaculture. *Hydrobiologia* **2016**, *765*, 343–358, doi:10.1007/s10750-015-2428-5.
143. Lombarte, A.; Morales-Nin, B. Morphology and ultrastructure of saccular otoliths from five species of the genus Coelorinchus (Gadiformes: Macrouridae) from the Southeast Atlantic. *J. Morphol.* **1995**, *225*, 179–192, doi:10.1002/jmor.1052250204.
144. Gauldie, R.W. Function, form and time-keeping properties of fish otoliths. *Comp. Biochem. Physiol. -- Part A Physiol.* **1988**, *91*, 395–402, doi:10.1016/0300-9629(88)90436-7.
145. Schwarzhans, W. A review of Jurassic and Early Cretaceous otoliths and the development of early morphological diversity in otoliths. *Neues Jahrb. fur Geol. und Palaontologie - Abhandlungen* **2018**, *287*, 75–121, doi:10.1127/njgpa/2018/0707.
146. Mille, T.; Mahé, K.; Cachera, M.; Villanueva, M.C.; De Pontual, H.; Ernande, B. Diet is correlated with otolith shape in marine fish. *Mar. Ecol. Prog. Ser.* **2016**, *555*, 167–184, doi:10.3354/meps11784.
147. Hüssy, K. Otolith shape in juvenile cod (Gadus morhua): Ontogenetic and environmental effects. *J. Exp. Mar. Bio. Ecol.* **2008**, *364*, 35–41, doi:10.1016/j.jembe.2008.06.026.
148. Mille, T.; Ernande, B.; Pontual, H. de; Villanueva, C.; Mahé, K. Sources of otolith morphology variation at the intra-population level : directional asymmetry and diet marine fishes. In Proceedings of the SFI Days; 2016; p. 2016.
149. Third, G.M. Morphological and diet variation in Chrysophrys auratus populations 2022.
150. Mahé, K.; Gourtay, C.; Defruit, G.B.; Chantre, C.; de Pontual, H.; Amara, R.; Claireaux, G.; Audet, C.; Zambonino-Infante, J.L.; Ernande, B. Do environmental conditions (temperature and food composition) affect otolith shape during fish early-juvenile phase? An experimental approach applied to European Seabass (Dicentrarchus labrax). *J. Exp. Mar. Bio. Ecol.* **2019**, *521*, 151239, doi:10.1016/j.jembe.2019.151239.
151. Çöl, O.; Yilmaz, S. The effect of ontogenetic diet shifts on sagittal otolith shape of European perch, Perca fluviatilis (Actinopterygii: Percidae) from Lake Ladik, Turkey. *Turkish J. Zool.* **2022**, *46*, 385–396, doi:10.55730/1300-0179.3090.
152. Sanchez-Jerez, P.; Gillanders, B.M.; Kingsford, M.J. Spatial variability of trace elements in fish otoliths: Comparison with dietary items and habitat constituents in seagrass meadows. *J.*

Fish Biol. **2002**, *61*, 801–821, doi:10.1006/jfbi.2002.2109.
153. Buckel, J.A.; Sharack, B.L.; Zdanowicz, V.S. Effect of diet on otolith composition in Pomatomus saltatrix, an estuarine piscivore. *J. Fish Biol.* **2004**, *64*, 1469–1484, doi:10.1111/j.0022-1112.2004.00393.x.
154. Gagliano, M.; McCormick, M.I. Feeding history influences otolith shape in tropical fish. *Mar. Ecol. Prog. Ser.* **2004**, *278*, 291–296, doi:10.3354/meps278291.
155. Cardinale, M.; Doering-Arjes, P.; Kastowsky, M.; Mosegaard, H. Effects of sex, stock, and environment on the shape of known-age Atlantic cod (Gadus morhua) otoliths. *Can. J. Fish. Aquat. Sci.* **2004**, *61*, 158–167, doi:10.1139/f03-151.
156. Massou, A.M.; Panfili, J.; Laë, R.; Baroiller, J.F.; Mikolasek, O.; Fontenelle, G.; Le Bail, P.Y. Effects of different food restrictions on somatic and otolith growth in Nile tilapia reared under controlled conditions. *J. Fish Biol.* **2002**, *60*, 1093–1104, doi:10.1006/jfbi.2002.1917.
157. Høie, H.; Folkvord, A.; Mosegaard, H.; Li, L.; Clausen, L.A.W.; Norberg, B.; Geffen, A.J. Restricted fish feeding reduces cod otolith opacity. *J. Appl. Ichthyol.* **2008**, *24*, 138–143, doi:10.1111/j.1439-0426.2007.01014.x.
158. Guibbolini, M.; Borelli, G.; Mayer-Gostan, N.; Priouzeau, F.; De Pontual, H.; Allemand, D.; Payan, P. Characterization and variations of organic parameters in teleost fish endolymph during day-night cycle, starvation and stress conditions. *Comp. Biochem. Physiol. - A Mol. Integr. Physiol.* **2006**, *145*, 99–107, doi:10.1016/j.cbpa.2006.05.003.
159. Fablet, R.; Pecquerie, L.; de Pontual, H.; Høie, H.; Millner, R.; Mosegaard, H.; Kooijman, S.A.L.M. Shedding Light on Fish Otolith Biomineralization Using a Bioenergetic Approach. *PLoS One* **2011**, *6*, e27055, doi:10.1371/journal.pone.0027055.
160. Anthony, J.A.; Roby, D.D.; Turco, K.R. Lipid content and energy density of forage fishes from the northern Gulf of Alaska. *J. Exp. Mar. Bio. Ecol.* **2000**, *248*, 53–78, doi:10.1016/S0022-0981(00)00159-3.
161. Spitz, J.; Mourocq, E.; Schoen, V.; Ridoux, V. Proximate composition and energy content of forage species from the Bay of Biscay: High- or low-quality food? *ICES J. Mar. Sci.* **2010**, *67*, 909–915, doi:10.1093/icesjms/fsq008.
162. Amara, R.; Meziane, T.; Gilliers, C.; Hermel, G.; Laffargue, P. Growth and condition indices in juvenile sole Solea solea measured to assess the quality of essential fish habitat. *Mar. Ecol. Prog. Ser.* **2007**, *351*, 201–208, doi:10.3354/meps07154.
163. Thorrold, S.R.; Jones, C.M.; Campana, S.E. Response of otolith microchemistry to environmental variations experienced by larval and juvenile Atlantic croaker (Micropogonias undulatus). *Limnol. Oceanogr.* **1997**, *42*, 102–111, doi:10.4319/lo.1997.42.1.0102.
164. McMahon, K.W.; Fogel, M.L.; Johnson, B.J.; Houghton, L.A.; Thorrold, S.R. A new method to reconstruct fish diet and movement patterns from δ 13C values in otolith amino acids. *Can. J. Fish. Aquat. Sci.* **2011**, *68*, 1330–1340, doi:10.1139/f2011-070.
165. Elsdon, T.S.; Ayvazian, S.; McMahon, K.W.; Thorrold, S.R. Experimental evaluation of stable isotope fractionation in fish muscle and otoliths. *Mar. Ecol. Prog. Ser.* **2010**, *408*, 195–205, doi:10.3354/meps08518.
166. Biolé, F.G.; Callicó Fortunato, R.; Thompson, G.A.; Volpedo, A.V. Application of otolith morphometry for the study of ontogenetic variations of Odontesthes argentinensis. *Environ. Biol. Fishes* **2019**, *102*, 1301–1310, doi:10.1007/s10641-019-00908-0.
167. D'Iglio, C.; Savoca, S.; Rinelli, P.; Spanò, N. Diet of the Deep-Sea Shark Galeus melastomus Rafinesque , 1810 , in the Mediterranean Sea : What We Know and What We Should Know. *Sustainability* **2021**, *13*, doi:https:// doi.org/10.3390/su13073962.

scientific reports

Check for updates

OPEN

Intra- and interspecific variability among congeneric *Pagellus* otoliths

Claudio D'Iglio[1,2,5], Marco Albano[1,5], Sergio Famulari[1], Serena Savoca[1]✉, Giuseppe Panarello[1], Davide Di Paola[1], Anna Perdichizzi[2], Paola Rinelli[2], Giovanni Lanteri[3], Nunziacarla Spanò[4] & Gioele Capillo[2,3]

Otolith features are useful tools for studying taxonomy, ecology, paleontology, and fish biology since they represent a permanent record of life history. Nevertheless, the functional morphology of otoliths remains an open research question that is useful to completely understand their eco-morphology. This study aims to deepen the knowledge of intra- and interspecific variation in *sagitta* morphology in three congeneric seabreams, to understand how such variability could be related to the lifestyles of each species. Therefore, the *sagittae* (n = 161) of 24 *Pagellus bogaraveo*, 24 *Pagellus acarne*, and 37 *Pagellus erythrinus* specimens, collected from the south Tyrrhenian Sea, were analyzed using scanning electron microscopy and a stereomicroscope to assess morphometric features, variability between otolith pairs and the external crystalline structure the of *sulcus acusticus*. Statistical analysis demonstrated that, between the species, variability in sagittal otolith rostral length growth and *sulcus acusticus* features, correlated with increased fish total length and body weight. Moreover, slight differences between otolith pairs were detected in *P. acarne* and *P. erythrinus* ($P < 0.05$). The results confirm changes in otolith morphometry and morphology between different congeneric species and populations of the same species from different habitats.

The inner ear is fundamental for vestibular and acoustic functions (balance and hearing) in teleost fishes. Its structure comprises three semicircular canals and their end organs, the ampullae, and three otolith organs (the *sacculus, utriculus,* and *lagena*). These organs contain three pairs of otoliths (three on each side), known as the *sagitta, lapillus,* and *asteriscus*[1,2].

The main chemical component of otoliths is calcium carbonate. This is normally in form of aragonite, and other inorganic salts, associated with a protein matrix from which the otoliths develop[3].

Otoliths are one of the most studied elements of teleost fish anatomy because they represent a permanent record of life history. Due to their species-specific morphology, otoliths are especially important in taxonomy and are a useful tool for distinguishing species among large numbers of bony fishes[1,4–10]. Several factors affect the morphology, morphometry, and microstructure of otoliths. These include environmental factors (e.g., water depth, temperature, salinity, and substrate)[11], feeding habits[12,13], ontogeny[14], physiology (e.g., hearing capabilities associated with acoustic communication)[2,15] and phylogeny[16]. In recent decades, otolith shape analysis has become fundamental in fisheries management for differentiating between fish stock, populations and their migration[17,18], and eco-geochemistry[19].

The *sagitta* (or saccular otolith) is usually the largest otolith and displays the highest inter-specific morphological diversity (exceptions include some otophysan species, in which the utricular otoliths are much larger than the *sagitta*, e.g., *Arius felis* (Linnaeus, 1766)[20]). Therefore, it is the most studied otolith. It is linked to the *macula sacculi* by a depression (called the *sulcus acusticus*) on the mesial face. The *macula sacculi* are indirectly attached to the complete *sulcus acusticus* via the otolithic membrane. The *sulcus acusticus* is composed of two areas, the *ostium* (anterior, generally in the rostral position) and the *cauda* (posterior), which are connected by the *collum*. Morphological features, shape, and the crystalline structure of the *sulcus* are occasionally used to differentiate between different fish stock, species, and size relationships within populations, regarding the environmental, biological, and ecological behavior of the species[21–23]. Conversely, otolith morphology has long been

[1]Department of Chemical, Biological, Pharmaceutical and Environmental Sciences, University of Messina, Viale F. Stagno d'Alcontres 31, 98166 Messina, Italy. [2]Institute for Marine Biological Resources and Biotechnology (IRBIM), National Research Council (CNR), Section of Messina, Messina, Italy. [3]Department of Veterinary Sciences, University of Messina, Messina, Italy. [4]Department of Biomedical, Dental and Morphological and Functional Imaging, University of Messina, Messina, Italy. [5]These authors contributed equally: Claudio D'Iglio and Marco Albano. ✉email: ssavoca@unime.it

used to distinguish between species, and in stomach contents analysis for prey identification, since otoliths are often the only identifiable components.

The Sparidae family (seabreams) is a ubiquitous taxon found in waters worldwide, especially in coastal ecosystems. Several important recreational and commercial fisheries are sustained by this teleost family. Sparidae are hosted by many marine habitats, from rocky to sandy substrates, at depths ranging from 0 to 500 m.

Among seabreams, species belonging to the *Pagellus* genus exhibit a wider geographical distribution. Blackspot seabream, *Pagellus bogaraveo* (Brünnich, 1768), axillary seabream, *Pagellus acarne* (Risso, 1826), and common pandora, *Pagellus erythrinus* (Linneus, 1758) are the most significant *Pagellus* species due to their high commercial value in the East Atlantic and the Mediterranean. Consequently, different fisheries target them.

These fishes demonstrate a cosmopolitan distribution in both hemispheres, with differences in relative abundance and frequency in Mediterranean areas, especially between western and eastern regions. Seabreams have different biological and ecological features. *P. acarne* and the *P. erythrinus* predominantly inhabit the continental shelf floor, while the continental slope is inhabited by *P. bogaraveo*[24].

The *P. acarne* is commonly found in muddy and sandy substrates at depths between 40 and 500 m, with the highest frequency of occurrence between 40 and 100 m[25]. It is a carnivorous, euryphagous, and zooplanktivorous fish[26]. *P. acarne* exhibit protandric hermaphroditism; they are initially male with an immature ovarian zone, which subsequently becomes mature and functional as testicular regression occurs[25]. In most Atlantic fisheries (the northern Atlantic Algarve, Azores, and the Canary Islands), the *P. acarne* is a target species, especially among small-scale commercial fisheries[27]. In the Mediterranean, however, it is one of the principal by-catch species of artisanal vessels and trawlers. Little information exists about the status of stocks in Mediterranean regions, where the minimum landing size (17 cm) is the only management measure for the species.

Pagellus erythrinus is a demersal species with gregarious habits. It largely inhabits rocky and muddy-sandy substrates, exhibiting a high frequency of occurrence at depths between 20 and 300 m. *Pagellus erythrinus* is a generalist predator and a benthic feeder. It displays protogynous hermaphroditism[28,29]. *Pagellus erythrinus* has a high commercial value worldwide and is targeted by many commercial and artisanal fisheries, especially in the Atlantic and Mediterranean, where signs of overexploitation have been reported in many sub-regions[28].

Pagellus bogaraveo is ubiquitous throughout the Mediterranean Sea, common in the western Mediterranean Sea, less common in the eastern Mediterranean Sea, and absent from the Black Sea[24]. It is also a species with high commercial value. *Pagellus bogaraveo* forms small schools above all substrata, near offshore banks, on seamounts[27,30], and in cold-water reefs. *Pagellus bogaraveo* is a benthopelagic predator and a protandrous hermaphrodite (late first maturity as females). Juveniles live near the coast, whereas adults live on the continental slope at depths reaching 800 m. Adults reproduce all year round, with maximum reproduction varying according to region. This biological feature makes the species more sensitive to fisheries efforts[27,31].

Although otoliths, particularly *sagittae,* are commonly used in several disciplines (e.g., systematics, auditory neuroscience, bioacoustics, fisheries biology, and ecology) to investigate fish biology and assess stocks, it is not yet fully understood how *sagitta* morphology varies inter- and intra-specifically regarding several ecological features of species.

Therefore, we investigate the intra- and inter-specific differences among *P. bogaraveo, P. acarne,* and *P. erythrinus* otoliths, to add to the knowledge base regarding the eco-morphology of *sagittae*.

To achieve an accurate description of the *sagittae* for each species, we first investigated existing differences in morphology and morphometry between juvenile and adult specimens and left and right *sagittae*. Moreover, it is of fundamental importance to answer still open questions, "What are the differences in *sagittae* between these congeneric species?" and "how these differences could be related to the eco-functional features and ecology of each seabream species by considering similarities and differences in lifestyle (e.g., feeding, bathymetric distribution, habitat, and locomotion)".

Therefore, we examined a representative sample of *sagittae* from three congeneric seabreams, carefully analyzing the morphology, morphometry, and microstructure of the otoliths, and highlighting possible changes at different life stages and between left and right *sagittae*.

This study provides an accurate description of the *sagittae* of these seabream species, providing new data regarding the shape, using R software, and microstructure, using SEM imaging, of the *Pagellus* genus *sagittae*.

Moreover, deepening the knowledge about variations in *sagitta* eco-morphology and morphometry between and within these three congeneric species will lay the foundations for further studies concerning the functional-morphological aspects of fish otoliths. Concerning fisheries management, deeper knowledge about *sagittae* and their changes during fish growth can aid understanding of the stock structure, population connectivity, and dynamics of these species. This is essential for developing improved strategies for managing stocks with high commercial value.

Comparing the morphological features and morphometry of the *Pagellus* genus *sagittae* in the study area with data from other geographical areas could improve understanding of variations in *sagittae* morphology and morphometry in different geographical areas and habitats since these changes could be related to both genetic differentiation between populations and ecomorphological adaptation to different environments.

Results

Morphometric and shape analysis. The otoliths extracted from each specimen of the three studied species were examined and divided into juveniles and adults (when applicable). The 24 *P. bogaraveo* individuals were divided into seven juveniles (14 otoliths) and 17 adults (30 otoliths). The 37 *P. erythrinus* individuals were divided into eight juveniles (13 otoliths) and 29 adults (57 otoliths). All 24 *P. acarne* individuals belonged to adults (46 otoliths). The means and standard deviations of the measured morphometries are summarized in Table 1 (juveniles) and Table 2 (adults).

Otolith morphological characters (mm-mm²)	*P. bogaraveo* Mean ± SD	*P. bogaraveo* Min.–Max	*P. erythrinus* Mean ± SD (R otoliths)	*P. erythrinus* Min.–Max (Rotoliths)	*P. erythrinus* Mean ± SD (L otoliths)	*P. erythrinus* Min.–Max (L otoliths)
OL	5.75 ± 0.091	5.26–6.67	5.75 ± 0.198	5.44–5.96	5.41 ± 0.136	5.26–5.58
OW	3.77 ± 0.078	3.44–4.58	4.35 ± 0.394	3.85–4.88	3.93 ± 0.222	3.74–4.25
OP	17.97 ± 0.58	15.81–24.96	18.71 ± 2.409	15.98–22.44	17.53 ± 0.918	16.67–18.94
OS	15 ± 0.61	13.05–22.17	17.37 ± 2.070	14.54–19.8	15.38 ± 1.277	13.76–16.69
SP	11.66 ± 0.211	9.47–12.61	12.41 ± 0.189	12.14–12.64	12.14 ± 0.575	11.23–12.80
SS	2.46 ± 0.088	1.52–2.92	3.44 ± 0.036	3.40–3.49	3.49 ± 0.493	2.77–3.97
SL	4.60 ± 0.115	3.66–5.15	4.80 ± 0.217	4.62–5.16	4.82 ± 0.208	4.57–5.02
CL	2.44 ± 0.073	1.71–2.88	2.60 ± 0.228	2.29–2.92	2.44 ± 0.232	2.15–2.66
CW	0.90 ± 0.065	0.53–1.49	1.08 ± 0.255	0.85–1.42	0.97 ± 0.100	0.87–1.09
CP	5.81 ± 0.17	3.91–6.61	6.51 ± 0.300	6.13–6.97	6.08 ± 0.417	5.72–6.67
CS	1.15 ± 0.052	0.62–1.40	1.56 ± 0.117	1.35–1.64	1.47 ± 0.187	1.26–1.75
OSL	2.15 ± 0.093	1.68–2.67	2.20 ± 0.119	2.04–2.33	2.38 ± 0.034	2.34–2.43
OSW	1.19 ± 0.064	0.83–1.62	1.32 ± 0.128	1.22–1.54	1.28 ± 0.294	0.91–1.68
OSP	5.84 ± 0.121	5.23–6.72	5.90 ± 0.379	5.57–6.50	6.06 ± 0.350	5.57–6.50
OSS	1.31 ± 0.064	0.90–1.73	1.89 ± 0.141	1.79–2.13	2.02 ± 0.382	1.51–2.52
RW	2.21 ± 0.064	1.82–2.82	5.88 ± 0.486	5.56–6.72	2.32 ± 0.349	1.98–2.85
RL	1.36 ± 0.064	0.93–1.97	1.59 ± 0.286	1.35–2.07	1.02 ± 0.213	0.77–1.28
OP^2/OS	21.57 ± 0.618	18.89–28.10	20.18 ± 3.057	17.57–25.44	20.14 ± 2.677	17.42–24.13
OS/(OLxOW)	0.68 ± 0.004	0.65–0.72	0.69 ± 0.007	0.68–0.7	0.71 ± 0.012	0.67–0.73
OW/OL %	65.73 ± 1.001	61.05–74.55	75.60 ± 4.46	70.81–81.92	73.53 ± 2.62	71.02–77.44
OL/TL	0.05 ± 0.000	0.05–0.06	0.058 ± 0.002	0.054–0.0038	0.054 ± 0.002	0.053–0.056
SS/OS %	1.6 ± 0.8	9.9–19	20.03 ± 2.47	17.29–23.49	22.59 ± 1.68	20.15–24.54
CL/SL %	53.3 ± 1.3	46.7–60.3	54.04 ± 2.96	49.56–56.64	50.56 ± 2.69	46.95–53.26
OSL/SL %	46.6 ± 1.38	39.6–53.2	45.96 ± 2.96	43.36–50.44	49.44 ± 2.69	46.72–53.05
RW/RL %	165 ± 5	131–194	233.58 ± 24.58	197.40–256.63	229.78 ± 23.61	198.01–257.33
RL/OL %	23.4 ± 1.15	15.8–34.9	17.73 ± 1.99	14.94–19.28	18.93 ± 3.94	14.04–22.97

Table 1. Morphometric mean values with standard deviation (SD) and range of *P. bogaraveo* and *P. erythrinus* juvenile group individuals: OL (otolith length), OW (otolith width), OP (otolith perimeter), OS (otolith surface), SP (sulcus perimeter), SS (sulcus surface), SL (sulcus length), SW (sulcus width), CL (cauda length), CW (cauda width), OSL, (ostium length), OSW (ostial width), RW (rostrum width), RL (rostrum length), CI (circularity), RE (rectangularity), aspect ratio (OW/OL %), the ratio of otolith length to total fish length (OL/TL), percentage of the otolith surface occupied by the sulcus (SS/OS%), percentage of the sulcus length occupied by the cauda length (CL/SL%), percentage of the sulcus length occupied by the ostium length (OSL/SL%), rostrum aspect ratio (RW/RL%) and percentage of the rostrum length occupied by the otolith length (RL/OL%). The morphometric data of *Pagellus bogaraveo* shown in the table relate only to the left otolith since no significant difference was found between the left (L) and right (R) sides.

The *P. bogaraveo* specimens exhibited an elliptical otolith shape with crenate margins, developmentally increasing margin regularity, notch depth, and antirostrum length. The t-test performed on otolith morphometrical parameters did not reveal differences between the right and left *sagittae* in the two size groups analyzed (Supplementary Table S1).

The differences between adults and juveniles were observed in the shape and size of the rostrum, the shape and borders of the ventral and dorsal margins, and the proportions of otolith length to fish length and otolith width to otolith length. In the otoliths of juveniles, dorsal and ventral margins were lobed, and the rostrum was shorter, broader, and rounder. The *sulcus acusticus* occupied a greater sagittal area compared to adult otoliths, with the *cauda* larger than the ostium. In adult specimens, the sulcus penetrated deeper into the sagitta's carbonate structure compared to juveniles. Significant differences were detected in *sagitta* aspect ratio (OW/OL %), *sagitta* length to total fish length ratio (OL/TL), and rostrum aspect ratio (RW/RL %) between juveniles and adults (Supplementary Table S1).

As in *P. bogaraveo,* in *P. acarne* adult specimens, the *sulcus acusticus* penetrated deeper into the *sagitta* structure (Figs. 2d–e; 4e–f). In the *P. acarne* specimens, significant differences in rostrum aspect ratio (RW/RL %) were detected between right and left *sagittae* (Supplementary Table S1). A significant negative correlation was found between *sagitta* aspect ratio (OW/OL %) and fish total length (TL), while a positive correlation was observed between relative sulcus area percentage (SS/OS %) and fish weight (Supplementary Table S2).

The *P. erythrinus* specimens displayed a pentagonal otolith shape, highlighted by high rectangularity, with a high circularity value. In juvenile specimens, the rostrum and sagittal width increased in relation to fish length and weight, while the *sagitta* length values did not varied significantly between juveniles and adults, highlighting an exponential increase in fish length compared to sagittal length. In adult *P. erythrinus* specimens, the sulcus

Otolith morphological characters (mm-mm²)	*P. bogaraveo* Mean ± SD	*P. bogaraveo* Min.–Max	*P. erythrinus* Mean ± SD (R otoliths)	*P. erythrinus* Min.–Max (R otoliths)	*P. erythrinus* Mean ± SD (L otoliths)	*P. erythrinus* Min.–Max (L otoliths)	*P. acarne* Mean ± SD (R otoliths)	*P. acarne* Min.–Max (R otoliths)	*P. acarne* Mean ± SD (L otoliths)	*P. acarne* Min.–Max (L otoliths)
OL	9.81 ± 0.34	7.40–13.90	10.04 ± 1.092	7.37–11.95	9.83 ± 1.175	7.46–12.16	9.67 ± 0.875	8.11–11.25	9.81 ± 1.332	4.98–11.24
OW	6.06 ± 0.19	4.57–8.29	7.76 ± 0.865	5.89–9.14	7.21 ± 0. 894	5.44–8.76	4.99 ± 0.500	4.09–5.70	5.21 ± 0.901	4.38–9.10
OP	29.37 ± 1.06	21.64–43.63	31.10 ± 3.628	24.56–11.95	31.19 ± 3.273	26–37.94	28.77 ± 3.69	21.85–38.22	30.12 ± 3.390	23.10–35.84
OS	41.4 ± 2.85	24.23–76.71	52.59 ± 10.56	31.25–72.21	49.40 ± 10.943	27.50–69.45	32.79 ± 5.381	22.47–41.49	34.66 ± 4.682	26.37–41.54
SP	19.83 ± 0.51	14.01–25.24	21.61 ± 3.507	12.26–26.47	21.91 ± 2.750	16.30–27.27	20.06 ± 2.605	15,01–25,12	20.52 ± 2.535	16.49–25.21
SS	6.12 ± 0.27	3.61–9.49	11.72 ± 3.201	5.58–18.42	10.56 ± 2.750	5.77–15.81	7.38 ± 1.562	4.95–9.98	7.87 ± 1.608	5.55–10.41
SL	8.01 ± 0.20	5.95–9.69	8.43 ± 1.129	5.95–11.18	8.71 ± 1.101	6.33–10.85	7.49 ± 1.739	3.05–10.22	7.98 ± 1.874	3.13–10.47
CL	4.189 ± 0.131	3.03–5.59	4.51 ± 0.580	3.26–5.47	4.70 ± 0.613	3.52–5.74	4.03 ± 1.042	1.38–5.61	4.55 ± 1.203	1.26–5.96
CW	1.50 ± 0.063	0.77–2.13	2.370 ± 0.584	1.41–3.94	1.73 ± 0.255	1.25–2.40	2.19 ± 0.997	1.30–5.44	1.91 ± 0.940	1.25–5.00
CP	9.93 ± 0.29	7.32–12.74	11.20 ± 2.730	2.34–14.97	11.66 ± 1.454	9.03–14.03	10.69 ± 1.565	8.12–13.47	11.33 ± 1.369	13.37–8.60
CS	2.95 ± 0.14	1.46–4.35	5.41 ± 1.524	2.85–8.28	4.74 ± 1.181	2.78–7.25	4.07 ± 1.080	2.15–5.76	4.39 ± 0.890	3.08–5.97
OSL	3.82 ± 0.10	2.61–4.92	3.913–0.685	2.69–6.29	4.01 ± 0.610	2.81–5.26	3.46 ± 0.795	1.48–4.68	3.43 ± 0.756	1.87–4.80
OSW	1.70 ± 0.080	1.03–3.26	3.053 ± 2.191	1.30–12.86	2.10 ± 0.391	1.45–2.93	2.06 ± 0.611	1.43–3.89	2.19 ± 0.460	3.40–1.40
OSP	9.89 ± 0.29	6.46–14.24	10.41 ± 1.401	7.20–12.71	10.26 ± 1.545	7.27–13.23	9.37 ± 1.437	6.88–12.25	9.19 ± 1.362	6.71–11,93
OSS	3.16 ± 0.15	1.88–5.65	6.31 ± 1.800	2.51–10.14	5.82 ± 1.708	2.93–9.55	3.31 ± 0.793	2.14–4.76	3.48 ± 0.837	5.20–1.96
RW	3.26 ± 0.08	2.31–4.42	9.83 ± 1.805	6.20–13.30	3.67 ± 0.537	2.87–5.04	3.17 ± 0.520	2.25–4.05	3.42 ± 0.510	2.57–4.34
RL	2.29 ± 0.080	1.61–3.18	4.37 ± 1.748	1.41–8.23	1.73 ± 0.380	1.13–2.77	2.58 ± 0.400	1.77–3.22	2.97 ± 0.049	2.29–4.33
OP^2/OS	21.39 ± 0.26	19.07–25.16	18.57 ± 1.271	16.61–22.65	20.21 ± 3.27	17.54–33.28	25.46 ± 3.917	19.94–36.90	26.35 ± 3.892	20.24–34.67
OS/(Ol × OW)	0.67 ± 0.006	0.55–0.73	0.67 ± 0.023	0.62–0.72	0.69 ± 0.66	0.42–0.80	0.67 ± 0.025	0.64–0.73	0.69 ± 0.021	0.63–0.72
OW/OL%	62 ± 0.5	57–69	77.45 ± 5.06	69.38–91.22	73.41 ± 2.53	68.53 -80.04	51.71 ± 3.49	47.01–59.43	56.02 ±27.21	44.27–182.66
OL/TL	0.04 ± 0.001	0.04–0.06	0.054 ± 0.0038	0.048–0.062	0.053 ± 0.005	0.04–0.06	0.047 ± 0.005	0.035–0.054	0.047 ± 0.006	0.024–0.055
SS/OS%	15 ± 0.5	9.4–18.9	22.15 ± 2.34	16.10–25.52	21.44 ± 3.86	16.03–38.36	22.50 ± 2.80	16.39–27.08	22.59 ± 2.60	16.57–27.78
CL/SL%	52 ± 0.6	47–63	53.69 ± 3.22	43.76–58.86	54.05 ± 2.98	44.30–60.72	53.44 ± 4.38	41.09–58.09	56.28 ± 5.82	39.22–63.82
OSL/SL%	47 ± 0.6	36–52	46.31 ± 3.22	56.24–41.14	45.95 ± 2.98	39.28–55.70	46.56 ± 4.38	41.91–58.91	43.73 ± 5.82	36.18–60.78
RW/RL%	144 ± 2.8	120–186	230.51 ± 38.28	91.43–317.81	215.95 ± 23.33	161.49–254.20	125.15 ± 22.76	79.47–152.30	115.85 ± 12.44	87.70–132.92
RL/OL%	23.7 ± 0.6	18–30	17.42 ± 3.80	9.31–30.07	17.60 ± 3.02	10.97–24.80	26.78 ± 4.23	20.39–36.57	30.87 ± 6.78	22.07–57.14

Table 2. Morphometric mean values with standard deviation (SD) and range of *P. acarne*, *P. bogaraveo,* and *P. erythrinus* adult group individuals: OL (otolith length), OW (otolith width), OP (otolith perimeter), OS (otolith surface), SP (sulcus perimeter), SS (sulcus surface), SL (sulcus length), SW (sulcus width), CL (cauda length), CW (cauda width), OSL (ostium length), OSW (ostium width), RW (rostrum width), RL (rostrum length), CI (circularity), RE (rectangularity), aspect ratio (OW/OL%), the ratio of otolith length to total fish length (OL/TL), percentage of otolith surface occupied by the sulcus (SS/OS%), percentage of the sulcus length occupied by the cauda length (CL/SL%), percentage of the sulcus length occupied by the ostium length (OSL/SL%), rostrum aspect ratio (RW/RL%) and percentage of the rostrum length occupied by the otolith length (RL/OL%). (R = right, L = left).

did not penetrate as deeply as in the other two seabreams species (Fig. 3d–f). *Pagellus erythrinus* individuals did not display significant differences between juveniles and adults, although significant differences in circularity (OP^2/OS), rectangularity ($OS/(OL \times OW)$), and *sagitta* aspect ratio (OW/OL %) were detected between right and left *sagittae* (Supplementary Table S1).

In the juvenile group, a negative correlation between *sagitta* length to total fish length ratio (OL/TL), fish weight, and total length was highlighted. A statistically significant positive correlation was observed between rostrum aspect ratio (RW/RL %) and fish weight, *sagitta* aspect ratio (OW/OL%) and fish weight, and *sagitta* aspect ratio (OW/OL%) and fish total length (Supplementary Table S2).

The negative correlation between *sagitta* length to total fish length ratio (OL/TL), fish weight, and total length was also observed in the adult group, whereas a significant positive correlation was detected for relative sulcus area percentage (SS/OS %) and fish weight, and relative sulcus area percentage (SS/OS%) and fish total length (Supplementary Table S2).

The t-test performed on juvenile specimens of *P. bogaraveo* and *P. erythrinus* did not show significant differences only for percentage of the sulcus length occupied by the cauda length (CL/SL%), percentage of the sulcus length occupied by the ostium length (OSL/SL%), and percentage of *sagitta* length to total fish length ratio (OL/TL %). A one-way ANOVA performed on the morphometrical parameters of adult samples, showed the following significant differences: circularity (OP^2/OS), *sagitta* length to total fish length ratio (OL/TL), *sagitta* aspect ratio (OW/OL%), relative sulcus area percentage (SS/OS%), percentage of the otolith length occupied by rostrum length (RL/OL%), and rostrum aspect ratio (RW/RL%) between *P. bogaraveo* and *P. erythrinus*; circularity (OP^2/OS), *sagitta* length to total fish length ratio (OL/TL), *sagitta* aspect ratio (OW/OL%), relative sulcus area percentage (SS/OS%), percentage of the otolith length occupied by rostrum length (RL/OL%), rostrum aspect

ratio (RW/RL%), percentage of the sulcus length occupied by the cauda length (CL/SL%) and percentage of the sulcus length occupied by the ostium length (OSL/SL%) between *P. bogaraveo* and *P. acarne*; and circularity (OP^2/OS), *sagitta* length to total fish length ratio (OL/TL), *sagitta* aspect ratio (OW/OL%), percentage of the otolith length occupied by rostrum length (RL/OL %) and rostrum aspect ratio (RW/RL %) between *P. erythrinus* and *P. acarne* (Supplementary Table S1).

Interestingly, the first two axes (PC1 and PC2) of the PCA plot showed slight separation in the *sulcus acusticus* parameters between the fish species analyzed. In particular, PC1 (74%) separated *P. erythrinus* sulcus acusticus parameters from *P. bogaraveo* and *P. acarne* parameters, which overlapped on the left side of the diagram along PC2 (26%). As shown in the LDA plot, *Pagellus* spp. resulted well separated (Supplementary Figure S1a, b).

The mean shape of otoliths differed significantly between *P. bogaraveo*, *P. erythrinus*, and *P. acarne* ($P < 0.001$), although minor differences were observed between *P. bogaraveo* and *P. acarne*. The otolith contours are shown in Fig. 1a. The first two axes (PC1 and PC2) of the PCA plot showed a separation of otoliths contours between the three fish species. In particular, PC1 (80%) separated *P. erythrinus* otolith shape from that of *P. bogaraveo* and *P. acarne*, which overlapped on the left side of the diagram along PC2 (20%) (Fig. 1b). Marked differences in the otoliths shape have also been confirmed by LDA. From the LDA plot of the first two discriminant functions, we can see that *Pagellus* species were quite well separated (Fig. 1c).

Scanning electron microscopy (SEM) analysis. Among the otoliths in all the examined species, SEM showed clear changes in the shape, size, and direction of the external textural organization of the *sulcus acusticus* and differences in the surface of the *crista* superior and inferior between juvenile and adult individuals at the intra-specific level.

In juveniles, the *crista* superior and inferior sloped gently toward the *sulcus acusticus* depression, with an almost flat surface (Figs. 2a, 3a). The *sulcus* surface appeared smoother than in adults, with several tips distributed over the entire sulcal surface (Figs. 2b, c, 3c). In juveniles, the external textural organization of the sulcus was composed of smaller and thin crystals sometimes melted together or embedded in organic materials. In comparison, however, the crystals in adult specimens had become larger and thicker (Figs. 2b, f, 5a–h). The crystals of juveniles were grouped, with rounded edges, and slightly orientated in the vertical and oblique planes, with the long axis of crystals following the incremental growth direction of the otoliths (from the nucleus to the outer edge of the growth) (Fig. 5a, b, e, f). Not all the crystals had the same shape and external 3D organization as in the adults; they had a smoother surface with a more compact structure.

Regarding adult specimens, the *crista* surface steeply declined towards the *sulcus*, with a hollow preceding the sulcal depression (Figs. 2d, 3d, 4a–d). The external sulcal structure was more complex with a more textured, rougher surface than in juveniles. The crystals were narrowed, with a prismatic shape. They had sharp edges, were almost equally sized, longer, and had a more chaotic orientation than in juvenile individuals (Fig. 5c, d, g, h).

Our results showed that the sulcus of *Pagellus* individuals from the south Tyrrhenian Sea was heterosulcoid. Furthermore, a greater size difference in the ostium and cauda was observed in adult *P. erythrinus* and *P. bogaraveo* compared to juveniles. Generally, the cauda was larger than the ostium and markedly different in shape. Despite the ostium, cauda growth during fish development indicated a most pronounced heterosulcoid character in adult individuals than in juveniles.

The macroscopic structure and shape of *sulcus acusticus* displayed in the SEM images exhibited inter-specific differences between the three congeneric seabreams. The *ostium* of *P. acarne* otoliths was deeper than that in the other congeneric species, and it displayed, with those of *P. bogaraveo,* according to with the *ostium* and *cauda* shape classification[1], a funnel-like shape with concave *ostium* walls that expand and broaden anteriorly from the region of confluence with the *cauda*. Unlike the other seabreams examined in this study, the shape of the *ostium* in the *P. erythrinus sulcus acusticus* was more rectangular, with a markedly tubular shape, and the cauda was distinctly curved, especially in juvenile specimens.

Discussion

Intra- and interspecific differences: comparison with former studies on *Pagellus* species and other fish species. To understand the relationship between function, shape, and the environment, it is essential to include the morphological variability of otoliths, considering biological and environmental variability leads to otolith shape heterogeneity through morpho-functional adaptation to different habitats. Several authors have highlighted changes in otolith shape between species and, in many cases, among populations of the same species (e.g., herrings, salmonids, and lutjanids). The intra-specific variability of otolith morphology and shape are the basis of stock separation and assessment and is related, especially in *sagittae*, with environmental (e.g., water temperature, salinity, and depth) and biological factors (e.g., sex, ontogeny, and genetic variability)[20].

The analysis of the three *Pagellus* species revealed that otolith morphology and morphometry did not follow those described in a previous study[1] conducted in the western Mediterranean Sea and the Atlantic Ocean in term of rectangularity, circularity, *sagitta* aspect ratio and *sagitta* length to total fish length ratio. Although the images provided in our study closely resembled those from research in other geographical areas, the morphometric measures (obtained according to the procedures and methods described in the previous literature[1,20,23,32]) exhibited several differences. Considering the scale of our study compared to previous studies, it is difficult to provide an entirely valid comparison; the differences in *sagitta* morphology and morphometry could have been triggered by biotic and abiotic parameters (e.g., temperature, salinity, genotype, habitat type, differences in food quality and quantity)[13,33–35]. Such environmental and genetic factors may be primary drivers of otolith morphometry and morphology among fishes in different habitats. Therefore, detected shape differences are at the basis of fish stock differentiation[36].

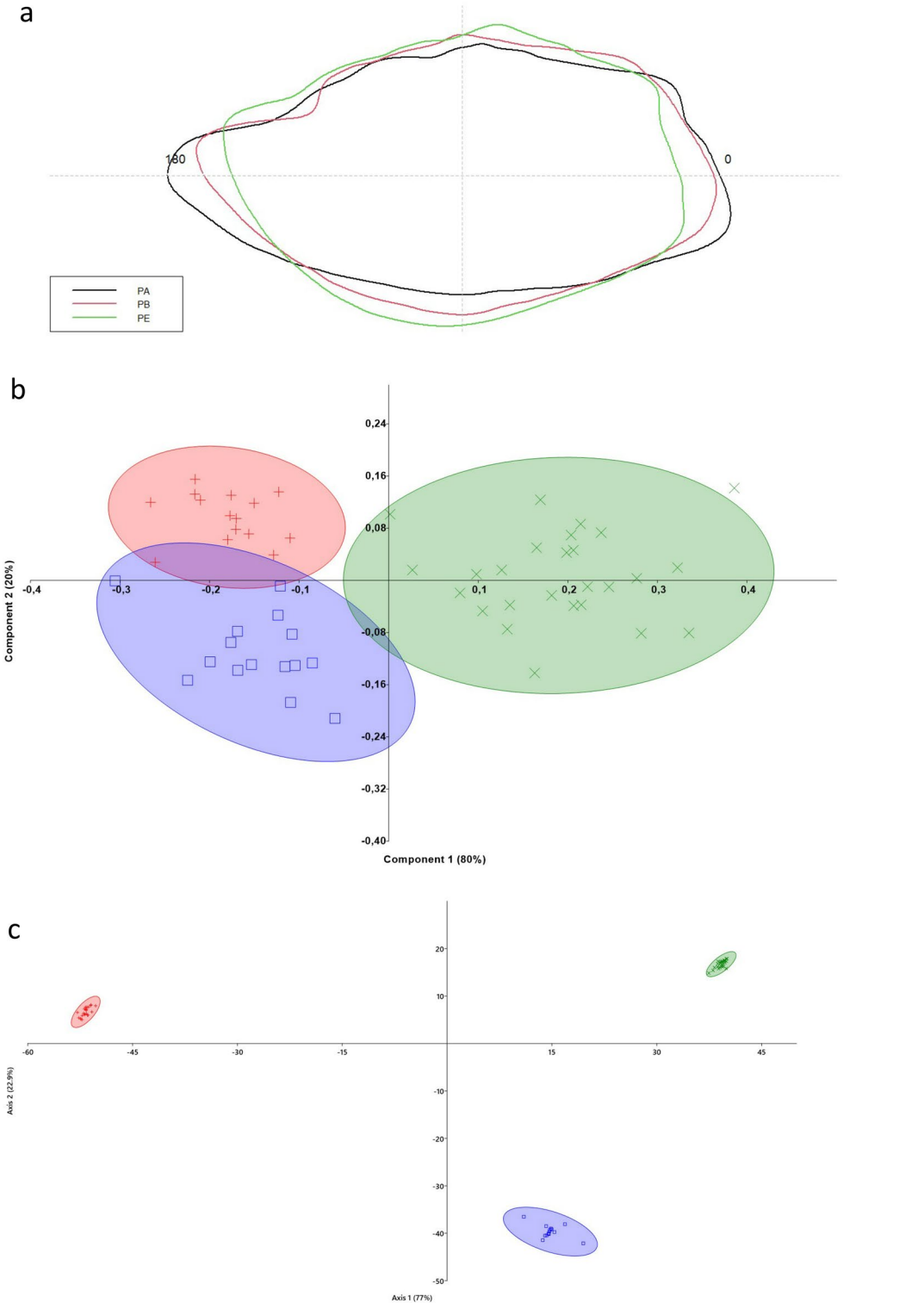

Figure 1. (**a**) Mean shapes of otolith contours. PA is *Pagellus acarne*, PB is *Pagellus bogaraveo*, and PE is *Pagellus erythrinus*. (**b**) Principal component analysis plot (PC1 versus PC2) of the otolith contours computed between the species analyzed. The PCA was based on wavelet Fourier descriptors, with 95% probability ellipses shown. (**c**) Linear Discriminant Analysis between species, calculated on elliptic Fourier descriptors. Ellipses include 95% confidence interval.

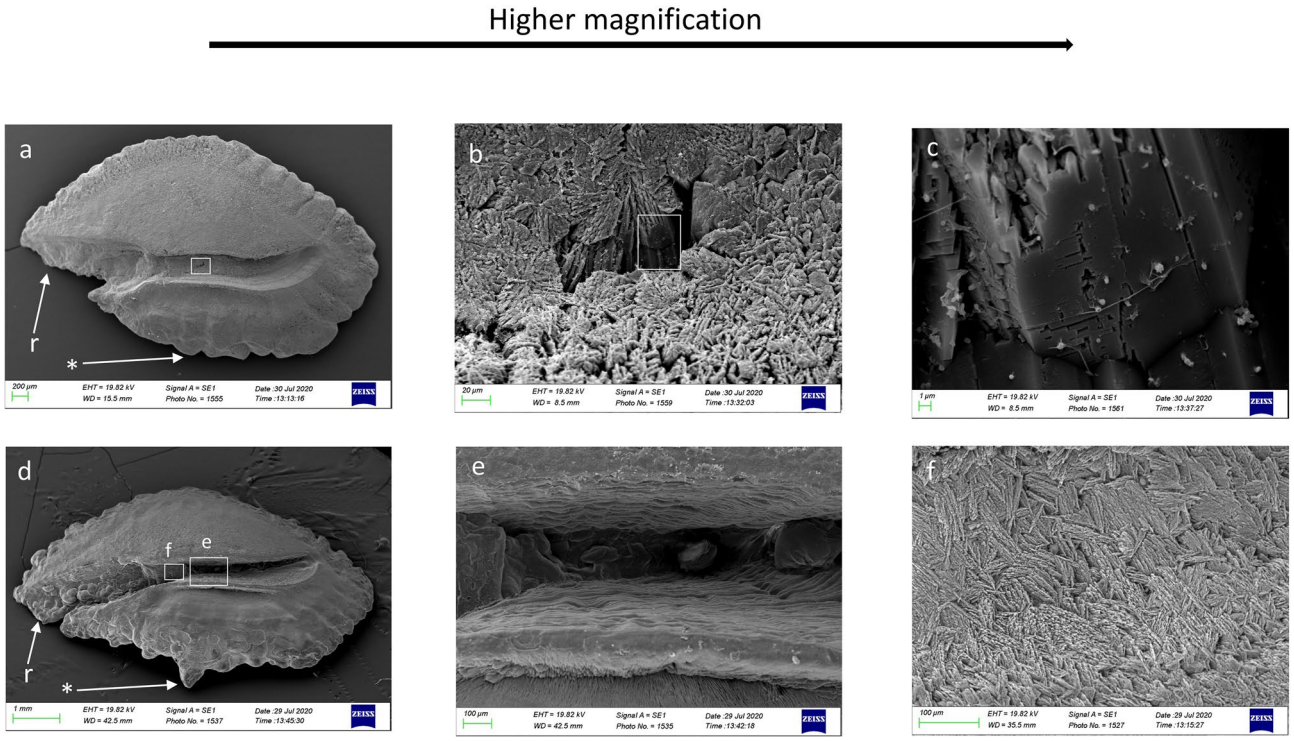

Figure 2. SEM images of the proximal surface of *P. bogaraveo*: juvenile (**a**) and adult (**d**) right *sagitta*, with details of a tip on sulcus acusticus surface (**b**–**c**), and details of external textural organization and crystalline structure (**f**) of caudal surface (**e**). (r) Indicates the rostrum and (*) indicates the dorsal rim.

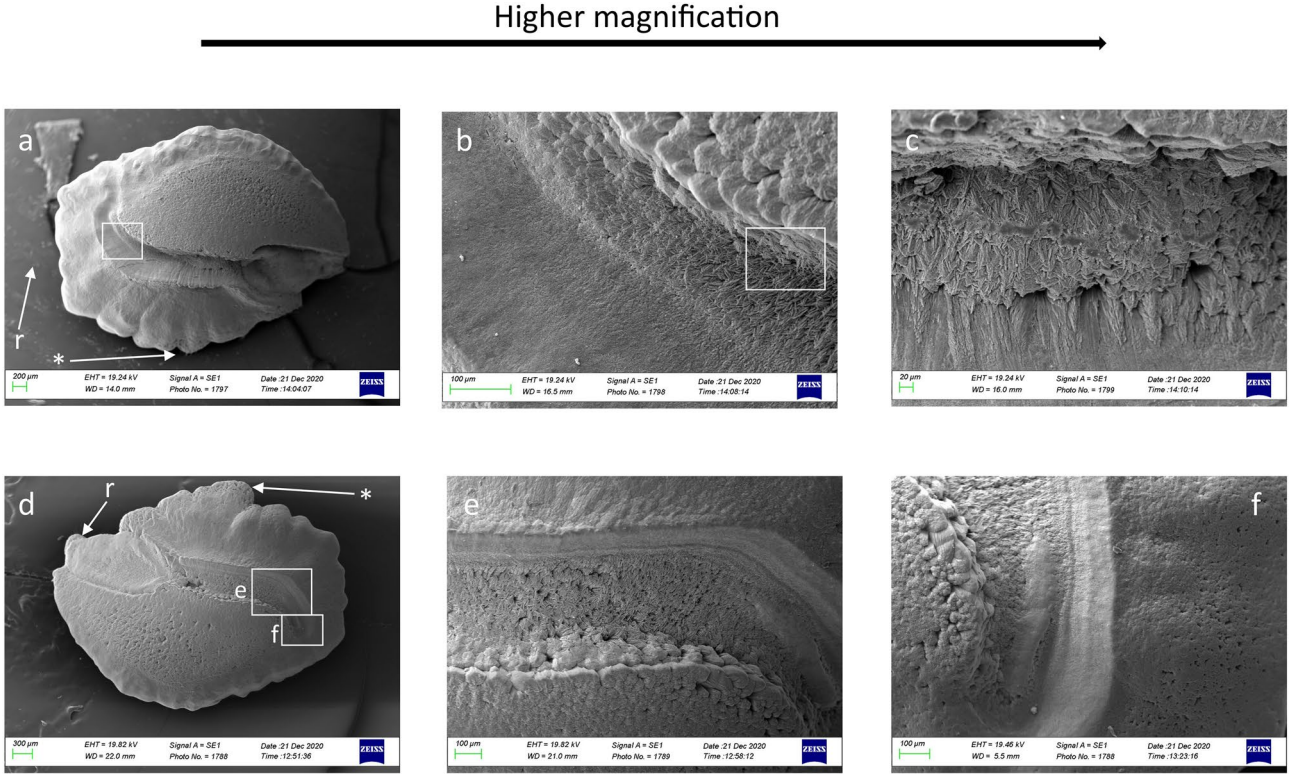

Figure 3. SEM images of the proximal surface of *P. erythrinus*: adults (**d**) and juveniles (**a**) otoliths left sagittae, with details of sulcus acusticus (**b**, **c**, **e**, **f**). (r) indicates the rostrum and (*) indicates the dorsal rim.

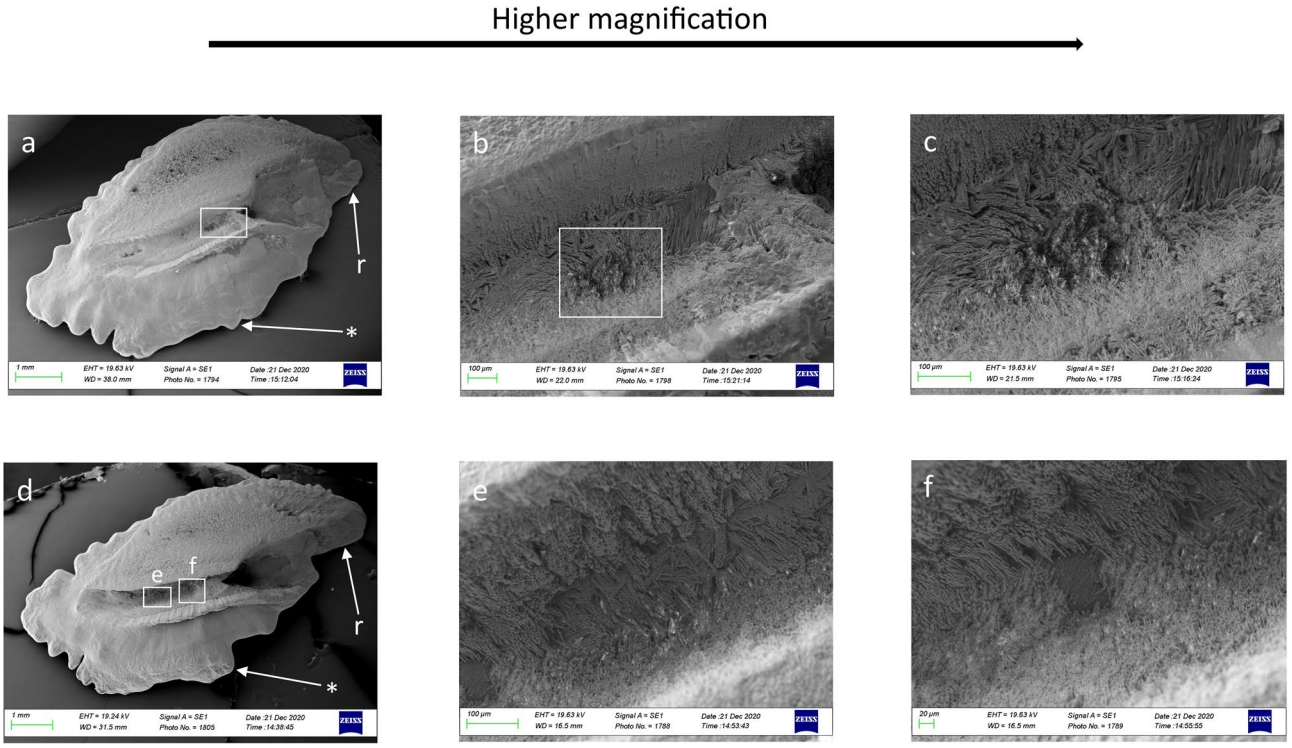

Figure 4. SEM images of the proximal surface of *P. acarne*: adult otoliths left sagitta (**a**–**d**), with details of sulcus acusticus (**b**–**e**), and external textural organization (**c**–**f**). (r) indicates the rostrum and (*) indicates the dorsal rim.

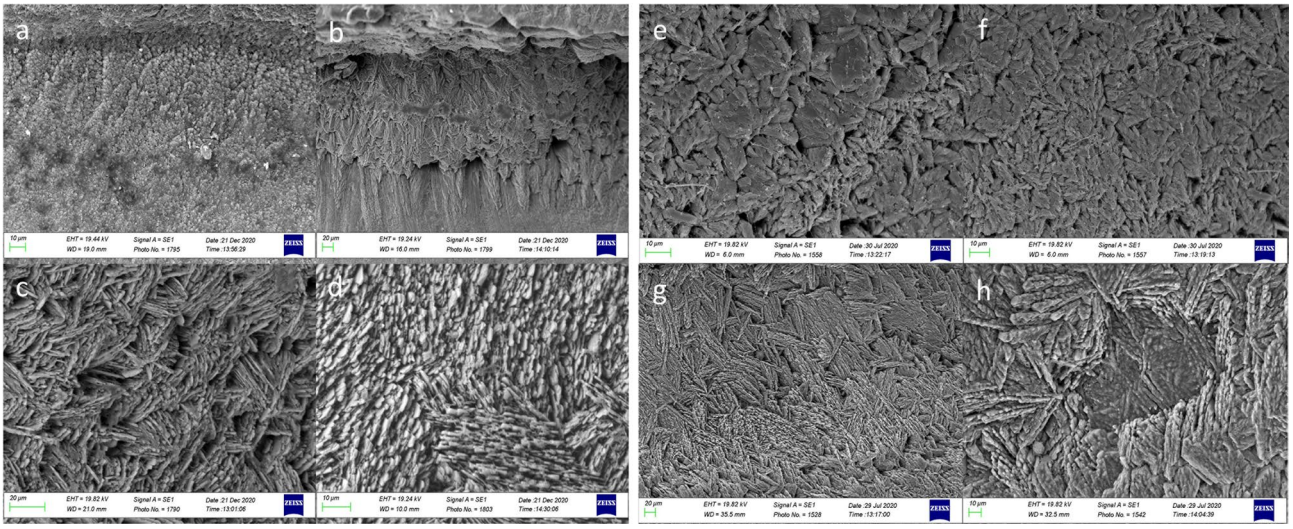

Figure 5. SEM images of the crystalline structure of *P. bogaraveo*, juveniles (**a**, **b**) and adults (**c**, **d**), and *P. erythrinus*, juveniles (**e**, **f**) and adults (**g**, **h**) *sagittae.*

Our results indicate that the min–max circularity and rectangularity of *P. bogaraveo* from the Southern Tyrrhenian Sea differ from those calculated in a previous study[1] in the western Mediterranean Sea, and the north and central-eastern Atlantic ocean. Moreover, the increase in circularity in larger specimens, confirms a greater tendency toward circular than elliptical otolith shape in southern Tyrrhenian Sea species compared to those in other Mediterranean and Atlantic areas.

Despite statistical differences and correlations in this study supported the hypothesis that some changes in *sagitta* morphology are related to fish size differences, several aspects and studies should be performed to better understand this relation. The negative correlation between the ratio of *sulcus acusticus* surface to the entire *sagitta*, rostral morphology, and the increase in specimen's size was related to the expansion in the length and surface of the entire sagitta and rostral area in larger specimens. These features, with no statistical relevant increment

in *sulcus acusticus* surface and increased *rostrum* length, could be correlated with more pronounced peripheral *sagitta* growth in this species. *Sagitta*, in fact, after fish pelagic phase, might increases its surface in the rostral area and the margins. Since the present study did not take into account ontogenetic stages and specimens age, it is hard to relate this result with *sagitta* and *sulcus acusticus* growth. But reading this increase by an ecological point of view, it could be related to the lifecycle of the species. During the juvenile stage, in the early stage of pelagic life, the species inhabits shallow water. Adults inhabit deep-water environments, migrating down the continental slope to a depth of 800 m after the juvenile stage. These changes in habitat might be the cause of morphological variations in the *sagittae,* highlighting the relationship between *sagitta* features and environmental and biological factors.

The *P. acarne* specimens demonstrated the highest number of morphometrical parameters that did not follow those of the same species described in a previous study (i.e., circularity, rectangularity, sagitta length to total fish length ratio, and *sagitta* aspect ratio)[1]. These morphometrical changes are reflected in otolith shape. The otoliths from specimens in our study were largely circular, with highly irregular margins and a *rostrum* that varied in length and width through the left and right *sagitta*, as indicated by the significant differences in rostrum aspect ratio values.

The morphometrical results in *P. erythrinus* revealed differences in circularity, rectangularity, *sagitta* length to total fish length ratio and *sagitta* aspect ratio compared to a previous study[1] in the western Mediterranean Sea and north-central eastern Atlantic ocean.

The *P. erythrinus* specimens were characterized by a pentagonal otoliths shape, and increased circularity compared to the same species from other areas. The results also indicated small differences between the left and right *sagitta*. This small differences were previously described in other Mediterranean sub-areas, for example, otolith width values in *P. erythrinus* specimens collected in the Gulf of Tunisia[37,38].

As said above for *P. bogaraveo*, it is hard to relate the differences between juveniles and adults with fish growth due to the absence in present paper of ontogenetic and age analysis. The higher width than length, demonstrated by min–max width values in Tables 1 and 2, in *sagittae* of adults *P. erythrinus* specimens could be correlated with an exponential increment in fish size compared to the sagittal length. Further analyses on ontogenetic development of this species are required to better define the *sagitta* growth related to fish growth.

The increase in *sulcus acusticus* surface exhibited in the adult specimens could be correlated with feeding habits; during its adult life, this species is a benthic feeder and inhabits deeper environments than juveniles[28,29].

Although meaningful lateral dimorphism of the *sagittae* was detected only in flatfish, statistical analysis revealed several small differences between the left and right *sagitta* in *P. erythrinus* and *P. acarne*, as previously described in other round fish species, such as *Chelon ramada* (Risso, 1827)[40], *Diplodus annularis* (Linnaeus, 1758)[41], *Diplodus puntazzo* (Walbaum, 1792)[42], *Clupea harengus (*Linnaeus, 1758)[43], and *Scomberomorus niphonius* (Cuvier, 1832)[44].

Our study confirmed slight differences between width values in left and right *sagitta* previously described in *P. erythrinus* and extend the differences to other parameters, such as circularity and rectangularity (Tables 1, 2). Concerning *P. acarne,* however, marginal differences between the left and right *sagittae* were observed for the first time.

This slight differences are supported by the literature concerning genetic and environmental stressors[41]. Since the functional morphology of otoliths is not completely understood, it is difficult to find a direct link between these small differences and the ecology of the species. However, several eco-functional factors, such as feeding behavior, deserve attention as fundamental for a better understanding of the relationship between otolith features and species habitat. For example, *P. erythrinus* largely preys on strictly benthic organisms, such as polychaetes, brachyuran crabs, and benthic crustaceans. Most of these species frequently escape predators by hiding under the sandy substrate. Other Sparidae (*Lythognathus mormyrus,* Linnaeus, 1758) feed on benthic fauna, engulfing sediment and filtering it in the buccal cavity, demonstrated by the high percentage of detritus and benthic remains (e.g., scales, urchin spines, and benthic foraminifers) in the gut and stomach contents[29]. To engulf sediment, *P. erythrinus* performs a particular movement with the head and body, laterally shifting and pushing forward, to dig the bottom sand and reach prey. This kind of behavior, common in all benthopelagic species with the same feeding habits, could influence the *sagitta* growth and morphology, triggering small differences between the left and right *sagitta*. Further studies on this and other species with this behavior (e.g., *L. mormyrus*) are necessary to confirm this hypothesis.

Concerning inter-specific differences in *sagitta* morphology among the three species, it is difficult to read the results obtained in this study eco-morphologically since an insufficient understanding of the functional morphology and physiology of otoliths prohibits a direct relationship, valid for all the species, between eco-functional features and otolith morphology. Nevertheless, as expected, the shape analysis (Fig. 1) revealed clear differences between the three congeneric species. Considering several ecological, functional, and biological features in each species, the results have demonstrated a *sagitta* morphology that could be in accordance with the ecology and lifestyle of these three congeneric seabreams.

Relationship between otolith morphology and ecology/lifestyle. The *sagittae* of *P. acarne* exhibited a shape resembling those in other pelagic species, with a long *rostrum* and the entire *sagitta* elongated and narrower than those in other two seabream species. The species that show the most pelagic habits, with largely planktivorous feeding at a small size, adapt also to benthopelagic feeding activity in adult life. The statistically relevant similarity found in *P. bogaraveo* could be proof of the ecomorphological adaptation of *sagittae* to pelagic and demersal environments. This hypothesis may be confirmed by marked differences in shape compared to those in *P. erythrinus,* which is the most benthic among the three species.

Pagellus erythrinus was the species with the shortest *rostrum*. It also has the most benthic habits, largely preying on epibenthic and infaunal species. Moreover, its ecology and life cycle differ among the three species under study since they are strictly related to the benthic environment. This lifestyle could be in accordance with the differences observed in the shape analysis results. The *sagitta* contours appeared more circular and wider than those in the other two species. The PCA and LDA also confirmed the most difference in shape among the three species.

The species with the most marked antirostrum and *sagitta* shape was *P. bogaraveo*, which is a cross between the other two congeneric species. *Pagellus bogaraveo* is a demersal species, which inhabits the deep biocenosis and feeds in both benthic and mesopelagic environments. Furthermore, the ecology of this species could support the *sagitta* shape described in our study[27,30].

Otolith morphology and morphometry in congeneric *Pagellus* species described in this study has followed the relationship between sagittal parameters, habitat, and depth described in previous literature[15]. According to several authors, the percentage of species with large otoliths increases with depth, except for abyssal depth. The specimens of *P. bogaraveo* analyzed in this paper (especially adult individuals) had larger otoliths than the other two *Pagellus* species due to their demersal habits (they inhabit the continental slope to a depth of 800 m). A larger sagitta is essential in demersal environments to compensate for light reduction by providing improved acoustic communication, sound perception[15,45], and a sense of equilibrium[46].

Sulcus shape. Considering the *sulcus acusticus,* in the otolith atlas for the western Mediterranean Sea and Atlantic ocean[1], studies describing and comparing otoliths[10] and the diversity and variability of otoliths in teleost fishes[9], the sulcus in *P. bogaraveo, P. acarne* and *P. erythrinus* was described as heterosulcoid, with an ostium shorter than the cauda and a long, narrowed rostrum, especially in adult *P. bogaraveo* and *P. acarne* individuals. Heterosulcoid otoliths were also observed in south Tyrrhenian Sea *Pagellus* individuals, with marked differences between juvenile and adult specimens. In a demersal species, such as *P. bogaraveo,* juveniles live in shallow, coastal water. Once adults, they inhabit deeper water (to a depth of 800 m). Changes in the crystalline and morphological structure of *sulcus acusticus* between juveniles and adults reflect this species' need to adapt to deeper environments with less light.

The results indicate that in *P. bogaraveo,* the *sulcus acusticus* does not differ in surface between juvenile and adult specimens. This feature could be correlated with earlier *sulcus acusticus* development in this species, compared to *P. erythrinus* and *P. acarne,* emphasizing the role of the *sulcus acusticus* in this demersal species[48,49]. This might also confirm the strict correlation between biological and environmental factors and *sagitta* morphology in studied seabreams species.

Another morphological feature of the *sulcus acusticus,* which might support the ecology of the species, is the deep ostium and cauda. In adult specimens of *P. bogaraveo* and *P. acarne,* the *sulcus* structure deeply penetrated in the *sagitta* carbonate structure. Conversely, in adult *P. erythrinus* specimens, the sulcus did not penetrate as deeply as in the other two seabream species. This sulcal feature could correspond with the ecology and feeding behavior of *P. erythrinus*, which specializes in benthic strategies, including small differences between left and right *sagitta* and the absence of the notch and antirostrum in *sagittae*.

Although the deeper *sulcus acusticus* in *P. bogaraveo* and *P. acarne* might be linked to depth distribution, as in *P. bogaraveo,* it may also correspond with high mobility related to feeding behavior, as in both *P. bogaraveo* and *P. acarne.* The different depths of *sulcus acusticus* can change the thickness of the otolithic membrane, by varying the relative motion of otoliths with the *macula sacculi*[2]. As previously demonstrated[50], the different thicknesses of the otolithic membrane induce differences in mechanical resistance between the otolith and sensory epithelium.

The differences in *sulcus acusticus* and otolith ratio between *P. bogaraveo* specimens and the other congeneric species, demonstrated by the results, might be also correlated to the differences in habitat, feeding habits, and soundscape.

Despite the lack of information concerning the physiological ear response related to variations in *macula* or *sulcus* size, the sensory hair cells in *macula sacculi* are likely to be affected by changes in *sulcus* depth, shape, 3D structure (planar vs. curved), and surface.

The significant difference in relative sulcus area may be due to typical alteration in this parameter concerning differences in the mobility patterns, food, feeding behavior, and spatial niche.

Higher relative sulcus area ratios have been observed in the deepest species or those with high mobility[49]. In our study, the morphometry results concerning the sulcus did not follow those in the previous literature, displaying higher values in *P. erythrinus* and *P. acarne* compared to *P. bogaraveo*, although the latter inhabits a deeper environment than the other congeneric species.

This higher relative *sulcus acusticus* surface and the larger, curved *sulcus acusticus* of *P. acarne* and *P. erythrinus* could be correlated with higher mobility in these species (especially *P. acarne*). In *P. erythrinus,* however, these features might be related to its benthic lifestyle.

As demonstrated by the PCA and LDA of *sulcus acusticus* parameters, *P. erythrinus* and *P. acarne*, which share similar depths and habitats, revealed marked similarities, whereas *P. bogaraveo,* which lives in the deepest strata of the water column, displayed the most different *sulcus acusticus*. However, PCA and LDA indicated that the otolith shape in the entire *P. erythrinus sagitta* was significantly different compared to those in *P. acarne* and *P. bogaraveo.*

These features could provide a reading key for *sagitta* and *sulcus acusticus* eco-morphology in the life cycle and environmental adaptation of fish.

The connection between the otoliths and the *macula sacculi* is fundamental for transducing environmental acoustic signals and for the relative motion of fish (balance). The *sulcus acusticus* is the area of the otoliths in which this connection occurs.

Features of the texture. Furthermore, the external textural organization[23] changes between juveniles and adults or when environmental changes occur. The differences in the external textural organization found in juveniles and adults support those reported in the literature concerning other species[39]. Figures 3b, c and 5a–h, demonstrate that our study supported this prediction. However, *P. bogaraveo* and *P. erythrinus* juveniles, compared with other species (such as gurnards)[23] displayed a more uniform, mineralized, external textural organization.

According to previous literature[8], improved hearing capabilities in a species are closely related to a higher value of relative sulcus area ratio. Habitat features, such as depth, feeding strategies, mobility, trophic distribution, and ontogeny, could also influence this ratio.

Hence, it may be concluded that morphological differences in *sulcus acusticus* shape and surface among species are important for comprehending the ecomorphological and eco-functional role of *sagitta* [2,48].

Comparing the intra-specific differences indicated by our results with those in the literature, discussing other populations, we cannot determine whether site-differences observed in *sagitta* shape are related to genetic evolution and/or adaptative response to environment. To make this distinction it would require a specific experiment in which offspring from different populations are raised in a controlled environment.

Furthermore, the knowledge about physiology and functional morphology is insufficient to provide a clear correlation between inter-specific differences among the three congeneric *Pagellus* species and their ecological and functional features. However, differences in *sagitta* morphology and morphometry among these three *Pagellus* species may be related to differences in lifestyle, ecology, and biology since they follow the ecomorphological features of *sagittae* and species ecology described in the literature.

Concluding remarks

This study has considered a wide range of morphometric and morphological characteristics in *Pagellus* species otoliths. Despite excellent and detailed photographs provided in previous studies[9,10], this paper provides, to our best knowledge, the first shape analyses, using R software of *P. bogaraveo* and *P. acarne* otoliths, and the first accurate SEM analyses of *P. bogaraveo, P. acarne,* and *P. erythrinus* from the study area and other regions.

An overall image of *P. bogaraveo sagitta* and its morphometrical features was created. Due to SEM imaging, we obtained, for the first time, the most accurate image of otoliths in these species and their external textural organization. This preliminary study provides grounding for an improved understanding of the structure and eco-morphological role of the *sagitta* in the life cycle of this species. Other methodologies (e.g., X-ray diffraction, auditory sensitive measurement, CT scan) are needed to deeply investigate the physiology of the *sagitta* and its ecological adaptation to the environment. The results could aid stock identification and improve understanding of the distribution of different Mediterranean populations and their differences. Improved understanding of the phenotypic plasticity and ecomorphological role of otoliths could also serve to compare the structure, morphometry, and crystalline composition of otoliths in congeneric species of *Pagellus* from different populations, to evaluate how the sagittal structures and features change according to different environments and habitats. This approach is essential to evaluate how the morphometry and shape of different sagittal areas, such as the *sulcus acusticus*, change under different environmental pressures.

It is essential to deepen the knowledge about the later asymmetry between *sagitta* pairs in *P. erythrinus* and *P. acarne* since this may affect stock differentiation based on shape analysis between populations from different sub-areas. This feature of otolith morphometry and shape could be another response to environmental pressure, which may clarify the role of phenotypic plasticity in *sagitta* development.

Materials and methods

A total of 44 *P. bogaraveo* otoliths (n = 24), 46 *P. acarne* otoliths (n = 24), and 71 *P. erythrinus* otoliths (n = 37) were collected from trawled specimens in the southern Tyrrhenian Sea (GSA10) between March and October 2019. Fish specimen collection was authorized by the CAMP.BIOL.19 project[52,53]. Fish otoliths were collected as part of annual research surveys, all involving lethal sampling. No experiments were conducted, nor were surgical procedures performed. No procedures caused lasting harm to sentient fish, nor were sentient fish subjected to chemical agents. The care and use of collected animals complied with animal welfare guidelines, laws, and regulations set by the Italian Government.

Before otolith extraction, each specimen was measured (TL to the nearest mm), weighed (body weight (BW) to the nearest g), and dissected to evaluate the sex and the maturity stage, according to the codes of sexual maturity in fish (MEDITS, freely available at http://archimer.ifremer.fr/doc/00002/11321/). For accurate morphometric analysis and statistical comparison of the data, specimens of each species were divided into two groups, according to the sexual maturity codes (i.e., juvenile and adult individuals).

The *sagittae* were removed from the otic capsule and cleaned of tissue using 3% H_2O_2 for 15 min, followed by Milli-Q water. The dry otoliths were stored inside an Eppendorf microtube.

A Leica M205C stereomicroscope with a built-in LEICA IC80 digital camera was used to collect digital images of the otolith samples (Supplementary Figures S2, S3, S4).

Each sagitta was photographed twice, once with the *sulcus acusticus* facing upwards and once with the annuli side facing up.

Before being converted into binary format for contour extraction using ImageJ 1.48p software[53] (freely available at http://rsb.info.nih.gov/ij/), the longest axis was used to orientate the images horizontally and vertically to capture clear *sulcus acusticus* images, according to the literature[20].

Morphometry. According to the literature[1,20,23,32], ImageJ was used to recorded several otolith measurements: otolith length (OL, mm), otolith width (OW, mm), otolith perimeter (OP, mm), otolith surface (OS, mm^2), sulcus perimeter (SP, mm), sulcus surface (SS, mm^2), sulcus length (SL, mm), cauda length (CL, mm),

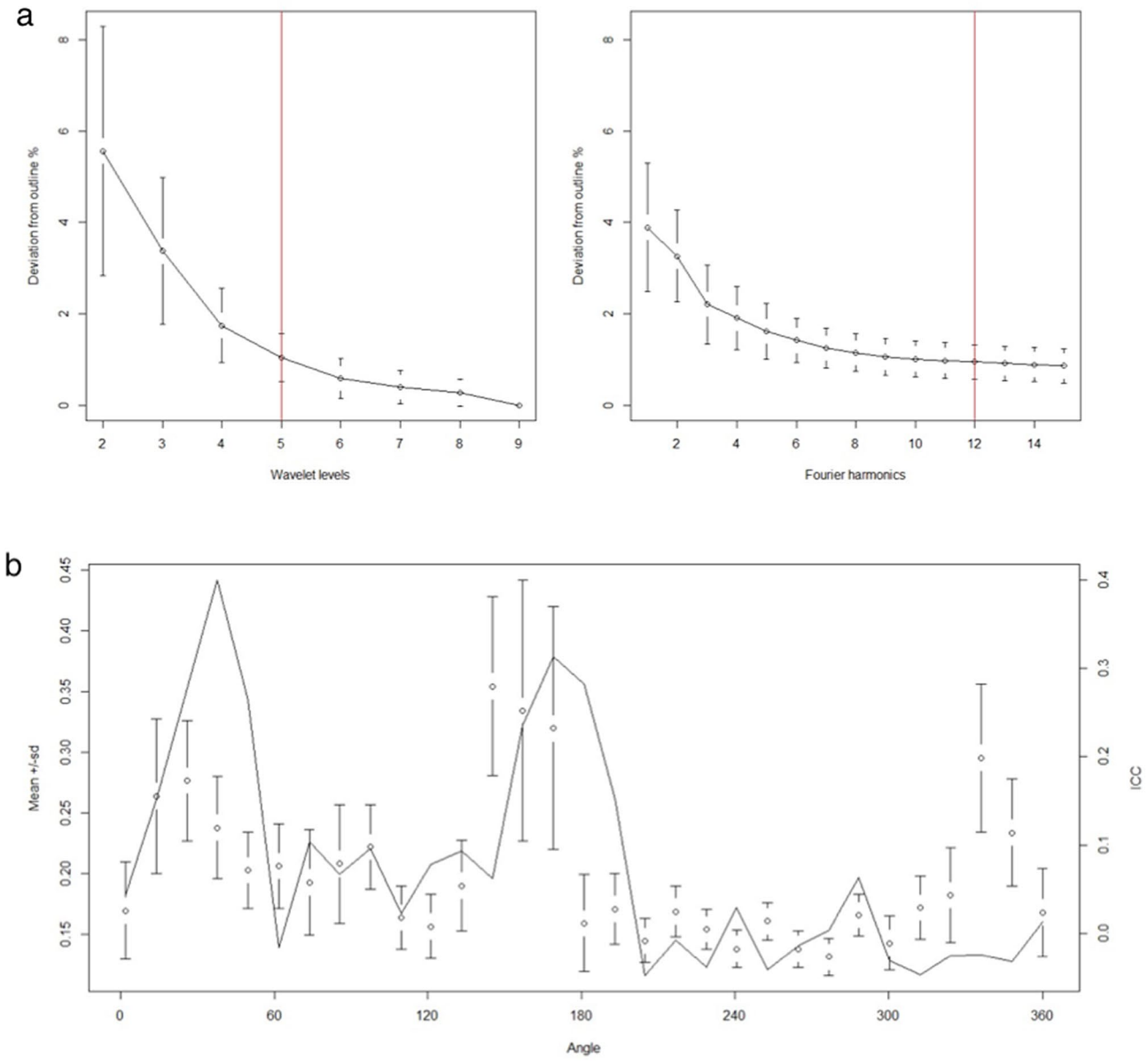

Figure 6. (**a**) Quality of the wavelet and Fourier outline reconstruction of left adult *sagittae* of studied species. The red vertical lines show the level of wavelet and number of Fourier harmonics needed for a 98.5% accuracy of the reconstruction. (**b**) Mean and standard deviation (SD) of the wavelet coefficients for all combined left adult *sagittae* of studied species and the proportion of variance among species or the intraclass correlation (ICC, black solid line). The horizontal axis shows an angle in degrees (°) based on the same polar coordinates of Fig. 1a, in which the centroid of the otolith is the center point of the polar coordinates.

cauda width (CW, mm), ostium length (OSL, mm), ostium width (OSW, mm), rostrum width (RW, mm) and rostrum length (RL, mm). Afterward, other otolith shape indices were calculated: circularity (OP^2/OS), rectangularity ($OS/[OL \times OW]$), aspect ratio (OW/OL%), the ratio of otolith length to the total fish length (OL/TL), the percentage of the otolith surface occupied by the sulcus (SS/OS%), the percentage of the sulcus length occupied by the cauda length (CL/SL%), the percentage of the sulcus length occupied by the ostium length (OSL/SL%), the rostrum aspect ratio (RW/RL%) and percentage of the otolith length occupied by rostrum length (RL/OL%). Supplementary Figure S5 provides a schematic diagram of the measured features.

Otolith shape analysis. Analysis of otolith shape was performed using shape R, an open-source software package that runs on the R platform (R version 4.0.5). This package was specifically designed to study otolith shape variation among fish populations or species[54]. First, the stereoscope captured otolith images were binarized using a threshold pixel value of 0.05 (intensity threshold). Once the outline of each image was detected, the master file containing the analyzed specimen information (e.g., fish length, weight, origin, maturity, and sex) was linked to each extracted outline. Wavelet and Fourier coefficients, required for statistical analysis, were extracted and adjusted for allometric relationships with the fish lengths. The wavelet coefficient was also used to

obtain the graph shown in Fig. 1a, which compares the mean otolith shapes of the analyzed species. The quality of the wavelet and Fourier reconstruction was estimated by comparing how it deviated from the otolith outline (Fig. 6a). The maximum number of Fourier harmonics to be displayed was set at 15. Finally, the graph presented in Fig. 6b was produced by running a specific function of the g-plots R package, to investigate how the variation in wavelet coefficients is dependent on the position along the outline.

SEM analysis. A total of four *P. bogaraveo* otoliths, three *P. acarne* otoliths, and four *P. erythrinus* otoliths underwent SEM analysis as described in previous studies[55]. The samples were fixed in 70% alcohol for 48 h and subsequently dehydrated using a graded series of alcohol from 70 to 100% (1 h in each solution). To avoid the critical drying point, samples were placed on a stub (SEM-PT-F-12) using conductive adhesive tables (G3347) and left for 12 h at 28 °C. Finally, the samples were sputter-coated with 20 nm gold–palladium. The samples were examined using a Zeiss EVO MA10 operating at an acceleration voltage of 20 kV.

Data analysis. All statistical analyses were conducted using the following software: Prism V.8.2.1 (Graphpad Software Ltd., La Jolla, CA 92037, USA), R vegan package V.2.5, and PAST V. 2.7[56].

Selected morphological parameters (OP^2/OS, OS/[OL × OW], OL/TL, OW/OL%, SS/OS%, RW/RL%, and RL/OL%) were analysed using an unpaired *t* test to highlight any significant differences between the right and left sides of the otoliths and between juvenile and adult specimens. Differences in morphological parameters between specimens of different species (at the same maturity stage) were analyzed using a one-way analysis of variance (one-way ANOVA). Additionally, *sulcus acusticus* parameters were subjected to a principal component analysis (PCA) based on a variance–covariance matrix and Linear Discriminant Analysis (LDA) to show differences between all the analyzed species.

Finally, the correlation between the measured parameters and fish weight and total length was tested using the Pearson correlation coefficient.

To determine differences in otolith contours, wavelet coefficients were used to analyze shape variation among species using an ANOVA-like permutation test. Moreover, shape coefficients were subjected to a PCA, based on a variance–covariance matrix, and LDA to obtain an overview of the differences in otolith shape between the congeneric species examined. The significance level was set at $P < 0.05$.

Received: 7 May 2021; Accepted: 29 July 2021
Published online: 11 August 2021

References

1. Tuset, V. M., Lombarte, A. & Assis, C. A. Otolith atlas for the western Mediterranean, north and central eastern Atlantic. *Sci. Mar.* **72**, 7–198 (2008).
2. Schulz-Mirbach, T., Ladich, F., Plath, M. & Heß, M. Enigmatic ear stones: What we know about the functional role and evolution of fish otoliths. *Biol. Rev.* **94**, 457–482 (2019).
3. Cermeño, P., Morales-Nin, B. & Uriarte, A. Juvenile European anchovy otolith microstructure. *Sci. Mar.* **70**, 553–557 (2006).
4. Chaine, J. & Duvergier, J. Recherches sur les otolithes des poisons. Etude déscriptive et comparative de la sagitta des téléostéens. *Act Soc Linn* **86**, 1–254 (1934).
5. Chaine, J. & Duvergier, J. Recherches sur les otolithes des poisons. Etude déscriptive et comparative de la sagitta des téléostéens. *Act Soc Linn* **92**, 3–133 (1942).
6. Nolf, D. *Otolithi Piscium. Handbook of Paleoichthyology, Vol. 10.* (1985).
7. Volpedo, A. & Echeverría, D. D. *Catálogo y claves de otolitos para la identificación de peces del mar Argentino.* (2000).
8. Tuset, V. M. *et al.* Testing otolith morphology for measuring marine fish biodiversity. *Mar. Freshw. Res.* **67**, 1037–1048 (2016).
9. Nolf, D., de Potter, H. & Lafond-Grellety, J. *Hommage à Joseph Chaine et Jean Duvergier: Diversité et variabilité des otolithes des poissons. Palaeo Publishing and Library vzw*. (Palaeo Publishing and Library vzw, 2009).
10. Chaine, J. Recherches sur les otolithes des poisons. Étude descriptive et comparative de la sagitta des Téléostéens. *Actes Soc. Linn. Bord* **89**, 5–252 (1937).
11. Volpedo, A. & DianaEcheverría, D. Ecomorphological patterns of the sagitta in fish on the continental shelf off Argentine. *Fish. Res.* **60**, 551–560 (2003).
12. Amorim, M. C. P., Stratoudakis, Y. & Hawkins, A. D. Sound production during competitive feeding in the grey gurnard. *J. Fish Biol.* **65**, 182–194 (2004).
13. Cardinale, M., Doering-Arjes, P., Kastowsky, M. & Mosegaard, H. Effects of sex, stock, and environment on the shape of known-age Atlantic cod (*Gadus morhua*) otoliths. *Can. J. Fish. Aquat. Sci.* **61**, 158–167 (2004).
14. Capoccioni, F. *et al.* Ontogenetic and environmental effects on otolith shape variability in three Mediterranean European eel (*Anguilla anguilla*, L.) local stocks. *J. Exp. Mar. Biol. Ecol.* **397**, 1–7 (2011).
15. Lombarte, A. & Cruz, A. Otolith size trends in marine fish communities from different depth strata. *J. Fish Biol.* **71**, 53–76 (2007).
16. Torres, G. J., Lombarte, A. & Morales-Nin, B. Sagittal otolith size and shape variability to identify geographical intraspecific differences in three species of the genus Merluccius. *J. Mar. Biol. Assoc. U. K.* **80**, 333–342 (2000).
17. Mahé, K., Evano, H., Mille, T., Muths, D. & Bourjea, J. Otolith shape as a valuable tool to evaluate the stock structure of swordfish *Xiphias gladius* in the Indian Ocean. *Afr. J. Mar. Sci.* **38**, 457–464 (2016).
18. Morat, F., Letourneur, Y., Nérini, D., Banaru, D. & Batjakas, I. E. Discrimination of red mullet populations (Teleostean, Mullidae) along multi-spatial and ontogenetic scales within the Mediterranean basin on the basis of otolith shape analysis. *Aquat. Living Resour.* **25**, 27–39 (2012).
19. Truman, C. N., Chung, M. T. & Shores, D. Ecogeochemistry potential in deep time biodiversity illustrated using a modern deep-water case study. *Philos. Trans. R. Soc. B Biol. Sci.* **371**, 20150223 (2016).
20. Lombarte, A. & Tuset, V. M. Chapter3- Morfometría de otolitos. in *Métodos de estudios con otolitos: principios y aplicaciones/ Métodos de estudos com otólitos: princípios e aplicações* (eds. Volpedo, A. V. & Vaz-dos-Santos, A. M.) 31 (2015).
21. Murta, A. G. Morphological variation of horse mackerel (*Trachurus trachurus*) in the Iberian and North African Atlantic: Implications for stock identification. *ICES J. Mar. Sci.* **57**, 1240–1248 (2000).
22. Bolles, K. L. & Begg, G. A. Distinction between silver hake (*Merluccius bilinearis*) stocks in U.S. waters of the northwest Atlantic based on whole otolith morphometrics. *Fish. Bull.* **98**, 451–462 (2000).

23. Montanini, S., Stagioni, M., Valdrè, G., Tommasini, S. & Vallisneri, M. Intra-specific and inter-specific variability of the sulcus acusticus of sagittal otoliths in two gurnard species (Scorpaeniformes, Triglidae). *Fish. Res.* **161**, 93–101 (2015).
24. Spedicato, M. T. *et al.* Geographical distribution, abundance and some population characteristics of the species of the genus *Pagellus* (Osteichthyes: Perciformes) in different areas of the Mediterranean. *Sci. Mar.* **66**, 65–82 (2002).
25. Di Maio, F. *et al.* Age structure of spawners of the axillary seabream, *Pagellus acarne* (Risso, 1827), in the central Mediterranean Sea (Strait of Sicily). *Reg. Stud. Mar. Sci.* **34**, 101082 (2020).
26. İlhan, D. Age, growth, and diet of axillary seabream, *Pagellus Acarne* (Actinopterygii: Perciformes: Sparidae), in the central Aegean sea. *Acta Ichthyol. Piscat.* **48**, 329–339 (2018).
27. Morato, T., Solà, E., Grós, M. P. & Menezes, G. Feeding habits of two congener species of seabreams, *Pagellus bogaraveo* and *Pagellus acarne*, off the Azores (northeastern Atlantic) during spring of 1996 and 1997. *Bull. Mar. Sci.* https://doi.org/10.1016/j.yhbeh.2011.02.016 (2001).
28. Busalacchi, B., Bottari, T., Giordano, D., Profeta, A. & Rinelli, P. Distribution and biological features of the common pandora, *Pagellus erythrinus* (Linnaeus, 1758), in the southern Tyrrhenian Sea (Central Mediterranean). *Helgol. Mar. Res.* **68**, 491–501 (2014).
29. Fanelli, E. *et al.* Food partitioning and diet temporal variation in two coexisting sparids, *Pagellus erythrinus* and *Pagellus acarne*. *J. Fish Biol.* **78**, 869–900 (2011).
30. Savoca, S. *et al.* Microplastics occurrence in the Tyrrhenian waters and in the gastrointestinal tract of two congener species of seabreams. *Environ. Toxicol. Pharmacol.* **67**, 35–41 (2019).
31. Lorance, P. History and dynamics of the overexploitation of the blackspot sea bream (*Pagellus bogaraveo*) in the Bay of Biscay. *ICES J. Mar. Sci.* **68**, 290–301 (2011).
32. Jawad, L. A., Sabatino, G., Ibáñez, A. L., Andaloro, F. & Battaglia, P. Morphology and ontogenetic changes in otoliths of the mesopelagic fishes *Ceratoscopelus maderensis* (Myctophidae), *Vinciguerria attenuata* and *V. poweriae* (Phosichthyidae) from the Strait of Messina (Mediterranean Sea). *Acta Zool.* https://doi.org/10.1111/azo.12197 (2018).
33. Swan, S. C. *et al.* Otolith chemistry: An aid to stock separation of *Helicolenus dactylopterus* (bluemouth) and *Merluccius merluccius* (European hake) in the Northeast Atlantic and Mediterranean. *ICES J. Mar. Sci.* **63**, 504–513 (2006).
34. Vignon, M. & Morat, F. Environmental and genetic determinant of otolith shape revealed by a non-indigenous tropical fish. *Mar. Ecol. Prog. Ser.* **411**, 231–241 (2010).
35. Gagliano, M. & McCormick, M. I. Feeding history influences otolith shape in tropical fish. *Mar. Ecol. Prog. Ser.* https://doi.org/10.3354/meps278291 (2004).
36. Stransky, C., Murta, A. G., Schlickeisen, J. & Zimmermann, C. Otolith shape analysis as a tool for stock separation of horse mackerel (*Trachurus trachurus*) in the Northeast Atlantic and Mediterranean. *Fish. Res.* **89**, 159–166 (2008).
37. Mejri, M. *et al.* Use of otolith shape to differentiate two lagoon populations of *Pagellus erythrinus* (Actinopterygii: Perciformes: Sparidae) in Tunisian waters. *Acta Ichthyol. Piscat.* **48**, 153–161 (2018).
38. Mejri, M. *et al.* Fluctuating asymmetry in the otolith shape, length, width and area of *Pagellus erythrinus* collected from the Gulf of Tunis. *Cah. Biol.* **60**, 1–7 (2020).
39. Volpedo, A. V. & Cirelli, A. F. Otolith chemical composition as a useful tool for sciaenid stock discrimination in the south-western Atlantic. *Sci. Mar.* https://doi.org/10.3989/scimar.2006.70n2325 (2006).
40. Rebaya, M. *et al.* Otolith shape discrimination of *Liza ramada* (Actinopterygii: Mugiliformes: Mugilidae) from marine and estuarine populations in Tunisia. *Acta Ichthyol. Piscat.* **47**, 13–21 (2017).
41. Trojette, M. *et al.* Stock discrimination of two insular populations of diplodus annularis (Actinopterygii: Perciformes: Sparidae) along the coast of tunisia by analysis of otolith shape. *Acta Ichthyol. Piscat.* **45**, 363–372 (2015).
42. Bostanci, D. *et al.* Sagittal Otolith Morphology of Sharpsnout Seabream *Diplodus puntazzo* (Walbaum, 1792) in the Aegean Sea. *Int. J. Morphol.* https://doi.org/10.4067/s0717-95022016000200012 (2016).
43. Bird, J. L., Eppler, D. T. & Checkley, D. M. Comparisons of herring otoliths using Fourier series shape analysis. *Can. J. Fish. Aquat. Sci.* https://doi.org/10.1139/f86-152 (1986).
44. Zhang, C. *et al.* Population structure of Japanese Spanish mackerel *Scomberomorus niphonius* in the Bohai Sea, the Yellow Sea and the East China Sea: evidence from random forests based on otolith features. *Fish. Sci.* https://doi.org/10.1007/s12562-016-0968-x (2016).
45. Buran, B. N., Deng, X. & Popper, A. N. Structural variation in the inner ears of four deep-sea elopomorph fishes. *J. Morphol.* https://doi.org/10.1002/jmor.10355 (2005).
46. Kéver, L., Colleye, O., Herrel, A., Romans, P. & Parmentier, E. Hearing capacities and otolith size in two ophidiiform species (*Ophidion rochei* and *Carapus acus*). *J. Exp. Biol.* https://doi.org/10.1242/jeb.105254 (2014).
47. Paxton, J. R. Fish otoliths: Do sizes correlate with taxonomic group, habitat and/or luminescence?. *Philos. Trans. R. Soc. B Biol. Sci.* https://doi.org/10.1098/rstb.2000.0688 (2000).
48. Torres, G. J., Lombarte, A. & Morales-Nin, B. Variability of the sulcus acusticus in the sagittal otolith of the genus Merluccius (Merlucciidae). *Fish. Res.* **46**, 5–13 (2000).
49. Tuset, V. M., Lombarte, A., González, J. A., Pertusa, J. F. & Lorente, M. J. Comparative morphology of the sagittal otolith in *Serranus* spp. *J. Fish Biol.* **63**, 1491–1504 (2003).
50. Popper, A. N., Ramcharitar, J. & Campana, S. E. Why otoliths? Insights from inner ear physiology and fisheries biology. *Mar. Freshw. Res.* **56**, 497–504 (2005).
51. Capillo, G. *et al.* Quali-quantive analysis of plastics and microfibers found in demersal species from Southern Tyrrhenian Sea (Central Mediterranean). *Mar. Poll. Bull.* **150**, 110596 (2020)
52. Schneider, C. A., Rasband, W. S. & Eliceiri, K. W. NIH Image to ImageJ: 25 years of image analysis. *Nat. Methods* **9**, 671–675 (2012).
53. Mangano, M. C., Kaiser, M. J., Porporato, E. M. D., Lambert, G. I. & Spanò, N. Trawling disturbance effects on the trophic ecology of two co-generic Astropectinid species. *Mediterr. Mar. Sci.* **16**, 538–549 (2015).
54. Libungan, L. A. & Pálsson, S. ShapeR: An R package to study otolith shape variation among fish populations. *PLoS ONE* **10**, 1–12 (2015).
55. Savoca, S. *et al.* Plastics occurrence in juveniles of *Engraulis encrasicolus* and *Sardina pilchardus* in the Southern Tyrrhenian Sea. *Sci. Total Environ.* **718**, 137457 (2020).
56. Hammer, Ø., Harper, D. A. T. & Ryan, P. D. Past: Paleontological statistics software package for education and data analysis. *Palaeontol. Electron.* **4**, 9 (2001).

Author contributions

C.D. procedure design, investigation, writing; M. A. investigation, formal analysis, data curation, writing; S.F. Formal analysis, data curation; S.S. writing, data analysis, review and editing; G.P. investigation, data collection, visualization; D.D.P. formal analysis, data curation, visualization, ; A.P. formal analysis, visualization, data curation; P.R. project administration, conceptualization, resources; G.L. resources, formal analysis and supervision; N.S. project administration, supervision, review and editing; G.C. project supervision, conceptualization, writing, review and editing .

Competing interests
The authors declare no competing interests.

Additional information
Supplementary Information The online version contains supplementary material available at https://doi.org/10.1038/s41598-021-95814-w.

Correspondence and requests for materials should be addressed to S.S.

Reprints and permissions information is available at www.nature.com/reprints.

Publisher's note Springer Nature remains neutral with regard to jurisdictional claims in published maps and institutional affiliations.

Terms and Conditions

Springer Nature journal content, brought to you courtesy of Springer Nature Customer Service Center GmbH (“Springer Nature”).
Springer Nature supports a reasonable amount of sharing of research papers by authors, subscribers and authorised users (“Users”), for small-scale personal, non-commercial use provided that all copyright, trade and service marks and other proprietary notices are maintained. By accessing, sharing, receiving or otherwise using the Springer Nature journal content you agree to these terms of use (“Terms”). For these purposes, Springer Nature considers academic use (by researchers and students) to be non-commercial.
These Terms are supplementary and will apply in addition to any applicable website terms and conditions, a relevant site licence or a personal subscription. These Terms will prevail over any conflict or ambiguity with regards to the relevant terms, a site licence or a personal subscription (to the extent of the conflict or ambiguity only). For Creative Commons-licensed articles, the terms of the Creative Commons license used will apply.
We collect and use personal data to provide access to the Springer Nature journal content. We may also use these personal data internally within ResearchGate and Springer Nature and as agreed share it, in an anonymised way, for purposes of tracking, analysis and reporting. We will not otherwise disclose your personal data outside the ResearchGate or the Springer Nature group of companies unless we have your permission as detailed in the Privacy Policy.
While Users may use the Springer Nature journal content for small scale, personal non-commercial use, it is important to note that Users may not:

1. use such content for the purpose of providing other users with access on a regular or large scale basis or as a means to circumvent access control;
2. use such content where to do so would be considered a criminal or statutory offence in any jurisdiction, or gives rise to civil liability, or is otherwise unlawful;
3. falsely or misleadingly imply or suggest endorsement, approval , sponsorship, or association unless explicitly agreed to by Springer Nature in writing;
4. use bots or other automated methods to access the content or redirect messages
5. override any security feature or exclusionary protocol; or
6. share the content in order to create substitute for Springer Nature products or services or a systematic database of Springer Nature journal content.

In line with the restriction against commercial use, Springer Nature does not permit the creation of a product or service that creates revenue, royalties, rent or income from our content or its inclusion as part of a paid for service or for other commercial gain. Springer Nature journal content cannot be used for inter-library loans and librarians may not upload Springer Nature journal content on a large scale into their, or any other, institutional repository.
These terms of use are reviewed regularly and may be amended at any time. Springer Nature is not obligated to publish any information or content on this website and may remove it or features or functionality at our sole discretion, at any time with or without notice. Springer Nature may revoke this licence to you at any time and remove access to any copies of the Springer Nature journal content which have been saved.
To the fullest extent permitted by law, Springer Nature makes no warranties, representations or guarantees to Users, either express or implied with respect to the Springer nature journal content and all parties disclaim and waive any implied warranties or warranties imposed by law, including merchantability or fitness for any particular purpose.
Please note that these rights do not automatically extend to content, data or other material published by Springer Nature that may be licensed from third parties.
If you would like to use or distribute our Springer Nature journal content to a wider audience or on a regular basis or in any other manner not expressly permitted by these Terms, please contact Springer Nature at

onlineservice@springernature.com

sustainability

MDPI

Article

Otolith Analyses Highlight Morpho-Functional Differences of Three Species of Mullet (Mugilidae) from Transitional Water

Claudio D'Iglio [1,2,†], Sabrina Natale [1,†], Marco Albano [1], Serena Savoca [3,*], Sergio Famulari [1], Claudio Gervasi [1], Giovanni Lanteri [1], Giuseppe Panarello [1], Nunziacarla Spanò [2,3] and Gioele Capillo [2,4]

1 Department of Chemical, Biological, Pharmaceutical and Environmental Sciences, University of Messina, Viale F. Stagno d'Alcontres 31, 98166 Messina, Italy; cladiglio@unime.it (C.D.); snatale@unime.it (S.N.); malbano@unime.it (M.A.); serfamulari@unime.it (S.F.); claudio.gervasi@unime.it (C.G.); giovanni.lanteri@unime.it (G.L.); gpanarello@unime.it (G.P.)
2 Institute for Marine Biological Resources and Biotechnology (IRBIM), National Research Council, 98122 Messina, Italy; spano@unime.it (N.S.); gcapillo@unime.it (G.C.)
3 Department of Biomedical, Dental and Morphological and Functional Imaging, University of Messina, Via Consolare Valeria, 98166 Messina, Italy
4 Department of Veterinary Sciences, University of Messina, Viale Dell'annunziata, 98168 Messina, Italy
* Correspondence: ssavoca@unime.it
† These authors contributed equally to this work.

Abstract: Otoliths are used in taxonomy and ichthyology as they can provide a wide range of information about specimens. They are an essential tool to monitor the most sensitive species for a sustainable exploitation level. Despite the increasing use of sagittae in research, their inter- and intra-specific variability and eco-functionality are still poorly explored. This paper aims to investigate the inter- and intra-specific variability of Mugilidae sagittae using morphological and morphometrical analysis, as well as scanning electron microscopy and shape analysis. The sagittae of 74 specimens belonging to three different Mugilidae species, collected from a coastal lagoon, were analyzed to give an accurate description of their morphology, morphometry, shape and crystalline habits. The results highlighted the intra- and inter-specific variability of sagittae, showing morphometrical differences among species and slight differences between left and right sagittae in *C. labrosus* individuals. Moreover, SEM images showed a peculiar crystal organization, with several different crystal habits and polymorphs. This study provides an accurate description of sagittae in the studied species, deepening the knowledge on inter- and intra-specific variations and crystal habits and providingdata which will be useful for future studies on otoliths. With this data, it will be possible to improve conservation and exploitation sustainability in sensitive habitats.

Keywords: sagittae; Mugilidae otoliths; fish biology; SEM imaging; shape analysis

Citation: D'Iglio, C.; Natale, S.; Albano, M.; Savoca, S.; Famulari, S.; Gervasi, C.; Lanteri, G.; Panarello, G.; Spanò, N.; Capillo, G. Otolith Analyses Highlight Morpho-Functional Differences of Three Species of Mullet (Mugilidae) from Transitional Water. *Sustainability* **2022**, *14*, 398. https://doi.org/10.3390/su14010398

Academic Editor: Mario D'Amico

Received: 15 November 2021
Accepted: 18 December 2021
Published: 31 December 2021

1. Introduction

Otoliths are acellular biomineralized concretions of calcium carbonate and other minor elements (Na, Sr, K, S, N, Cl and P), generated on a protein matrix in vertebrates' inner ears. In teleosts, inner ears are multi-sensory, stato-acoustic organs [1] with basic vestibular and acoustic functions (e.g., balance and hearing). They are essential in the perception of angular acceleration (derived from head/body rotation), linear acceleration and sound [1–7]. Each inner ear is composed of three semicircular canals, three end organs, named ampullae, and three otolith organs (sacculus, utriculus and lagena). Inside these are located three otoliths (or ear stones): sagitta, lapillus and asteriscus. Each otolith is surrounded by an otolithic membrane. The latter mediates the connection between the sensory epithelia (macula sacculi) and otoliths. The otolithic membrane, the macula sacculi and the otolith are considered the "otolithic apparatus", a single physiological and morphological entity. Once perceived, sound occurs in the lower part of inner ear (sacculus

and lagena), which is specialized in sound reception, while the upper part (consisting of the utricle and semicircular canals) controls equilibrium. The otolith acts as a transducer of acoustic and vestibular signals to the fish's nervous system, through the macula sacculi. In bony fish, it consists of a solid calcium carbonate concretion, normally in form of aragonite crystals, with a small percentage (from 0.2% to 10% of the entire otolith) of organic matter (otoline) and other inorganic salts, secreted by the labyrinth walls and associated with a protein matrix on which they are developed [8,9].

Otolith growth is continuous over the fish's entire life, showing a daily deposition of new materials [10] and a high purity. They are metabolically inert [11,12] and represent a source of information about an individual's life history and age, thus possessing a high time-keeping properties [12].

They are one of the most useful anatomical structures for various studies of fish, leading to many practical applications [1,13,14]. These are not limited to ichthyology, but include ecological studies of predator fish, and some aspects of paleontology, stratigraphy, archeology and zoogeography. The otolith's morphology, due to its high inter-specific variability, is used in taxonomy for species discrimination and, since it is one of the main fossil fish remains, in palaeoichthyology for the evaluation of the biodiversity and species composition of past teleosts [9,13–18]. The otolith's morphometry, shape and chemical composition are also essential in ecological studies for prey identification during stomach content analysis [19,20], in fisheries science for stock discrimination [21–26] and population age structures [27,28], in fisheries management for migration pattern evaluations [29,30] and also in defining the morphofunctional adaptations of teleosts to different environmental conditions.

Among otoliths, sagittae, or saccular otoliths, are the most studied, due to their dimensions and their high inter-specific morphological variability. They are usually the largest otolith, except in some otophysan species, such as *Arius felis* (Linnaeus, 1766) [31]. Therefore, the saccular otolith is widely used for age determination in most bony fish species. In the mesial face of the sagitta, there is a depression called the *sulcus acusticus*, by which it is linked to macula sacculi. The sulcus acusticus is made up of two areas, ostium (anterior) and cauda (posterior), connected to each other by the collum. The morphological features, shape and crystalline structure of the sulcus acusticus have increasingly been used as a tool in stock assessment, species identification and ecological studies, analyzing their intra- and inter-specific variability in relation to environmental factors and ecological behavior of the species [32]. In fish, the size, shape and structure of sagittae vary ontogenetically, as well as from species to species and even between different populations of the same species. For this reason, it can be used in species discrimination and population studies [33–36].

The Mugilidae family, to which the species generally known as mullets belong, represents a large taxon of coastal marine fish, with a worldwide distribution that includes temperate, subtropical and tropical seas. Due to their tolerance to a wide range of salinities, they not only inhabit coastal marine waters, but also spend part of their life cycle in coastal lagoons, lakes and/or rivers. Mullets, after their periods of rest and maturation in transitional environments (coastal lagoons, estuaries), perform a reproductive migration towards the sea; after spawning, some of them return to estuaries while others remain in marine waters [37–40]. The Mugilidae family includes 17 genera and approximately 72 species [41]. The Mediterranean Sea is inhabited only by eight of these species, all of which originally belonged to the same Genus: *Mugil*. Later, these were subdivided into four Genera: *Mugil*, *Liza*, *Chelon* and *Oedalechilus* [42]. Taxonomical discrimination among these species can be complex due to their complicated internal anatomy and external morphology. They are of great importance for professional and artisanal fishing, being species of high commercial value, especially for their gonads. Mugilidae are fished both for food purposes (and also often for bait) [38,39,43–45] over almost the entire planet, and for aquaculture production [43,44]. They are farmed both in extensive systems, and in semi-intensive and intensive systems, often in polyculture with other species; however, the latter production system is still based on the collection of wild fries, as induced spawning it is not practiced commercially.

Despite otoliths (especially sagittae) being increasingly used in many research fields, it is not yet fully understood how differences detected in sagittae among several fish species and populations are related to ecological, environmental or habitat variations. For this reason, the present study aimed to investigate inter- and intra-specific variability within Mugilidae sagittae, analyzing and comparing their morphology, morphometry, shape and external textural organization among three selected species: golden grey mullet, *Chelon auratus* (Risso, 1810), thicklip grey mullet, *Chelon labrosus* (Risso, 1827) and boxlip mullet, *Oedalechilus labeo* (Cuvier, 1829). These three species are euryhaline and share similar habitats. They inhabit neritic environments, forming inshore schools and frequently entering brackish lagoons and estuaries. In freshwater, it is also common to find *C. labrosus* and less common to find *C. auratus* [45–47]. *O. labeo* is the least euryhaline species among them. It mainly inhabits marine environments; but, occasionally, it is found in coastal lagoons [48,49]. All three species also share a similar trophic position, with *C. auratus* exhibiting the most pronounced predatory feeding habit. It mainly feeds on small zoobenthic organisms and detritus and, occasionally, on insects and plankton, while the other two species alternate a vegetarian diet (e.g., benthic diatoms, epiphytic algae) with the consumption of small invertebrates [50–53].

Individuals belonging to the aforementioned species were collected from a peculiar Sicilian transitional basin (Ganzirri lagoon) in order to add new information about the eco-morphological adaptation of marine species to brackish and transitional environments, especially in a constantly monitored area such as the Ganzirri lagoon. This is a sensitive environment, exploited by human activities since ancient times, and it is very important for the biodiversity it hosts, being a nursery and a shelter area for many marine species.

Investigating the sagitta features of individuals collected from this area, this study aimed to monitor and improve the knowledge of these species for a sustainable exploitation level of habitats and stocks and in order to better manage conservation. In order to give an accurate description of the sagittae in the studied species, with morphometrical measurements and comparisons between the left and right sagitta, a shape analysis was performed with R software, and an SEM imaging evaluation of their microcrystalline structure, between and within the species, was also performed. This research fills a gap in the literature regarding the considered mullet species, highlighting intra- and inter-specific otolith variability. Moreover, variability in microcrystalline organization, detected through SEM imaging, provides useful reference data for future studies on the microchemical and crystal organization of otoliths, which are essential for population studies and for environmental variation monitoring in natural conditions. This research adds new information regarding sagitta eco-morphology, laying the foundations for further studies concerning their functionality, morphology and adaptative role in the lives of teleosts. Deepening this knowledge is also essential for conservation purposes—both for brackish habitats, which are very vulnerable, and, by adding new shape analysis data, for Mullets stocks, which are exploited worldwide.

2. Materials and Methods

2.1. Study Area

The study area is located in the north-eastern area of Sicily, Italy (38°15′57″ N, 15°37′50″ E) (Figure 1a), between the Tyrrhenian and the Ionian Sea [49,50]. This area is of particular ecological importance, being part of the extremely peculiar and characteris- tic habitats of the area around the Strait of Messina [51–53].

In particular, the sampling location, Ganzirri Lagoon, is a brackish pond continuously in communication with the Strait of Messina through the “Due Torri” and “Carmine” Channels and with Faro Lake through the Margi Channel [54,55] (Figure 1b). The water level of this basin is not stable, as it is affected daily by the Strait of Messina tidal currents that change every 6h regularly, raising and lowering the level of the lagoon water [53].

This basin covers a 0.33 km^2 area (maximum depth: ~7 m; water volume: ~106 m^3). It extends parallel to the coast of the Strait of Messina for 1670 m in length, and it is 282 m at its maximum width, with an elongated form oriented in the SW-NE direction [50].

Ganzirri and Faro lagoons are "Assets of ethno-anthropological interest" (declaratory measure 1342/88) since they are seats of traditional working and productive activities related to shellfish farming (mussel and cockle farming). The Lagoon of Capo Peloro is also an Oriented Natural Reserve (ONR), established by the Sicilian Region [56], as well as a Site of Community Importance (SIC) [57] and a Special Protection Zone (ZPS) [58–63].

In Ganzirri lagoon, shellfish farming took place from the first half of the 1700s up to 1995. Subsequently, due to sporadic events of anthropogenic pollution and contamination by pathogenic prokaryotes from the nearby town, this activity was interrupted by competent authorities [59].

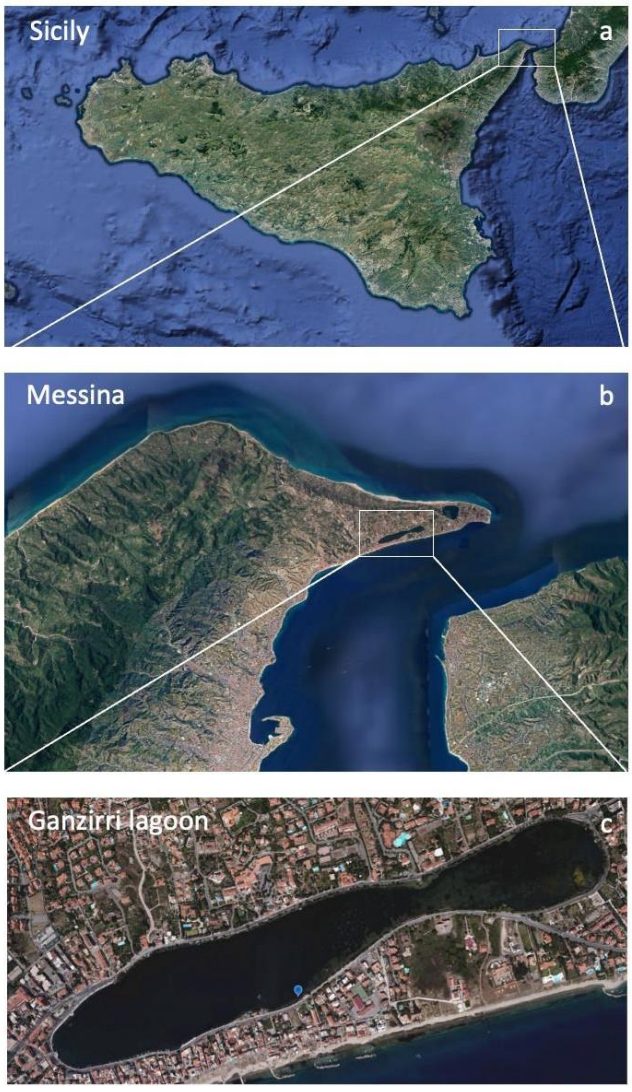

Figure 1. Location of the studied area (**a**,**b**); image of Ganzirri lake (**c**) with sampling point in blue.

2.2. Sampling

Samples were collected between March 2021 and June 2021, in Ganzirri Lagoon (38°15′33″ N; 15° 36′ 58″ E) (Figure 1c). A total of 74 Mugilidae (31 *C. auratus,* 32 *C. labrosus* and 11 *O. labeo*) were caught using throwing nets, also known as sparrow hawks or "rezzaglio" (Autorizzazione n.1138/A del 15.03.2021). This is an ancient circular fishingnet, tied to a rope in the center of the circle. Fish were sampled and transported to the

Experimental Fish Pathology Center (Centro di Ittiopatologia Sperimentale della Sicilia–CISS), Department of Veterinary Sciences University of Messina, Italy. The fish included in this paper were not part of an experiment; all samples were used for diagnostic purposes commissioned by fish farmers, aiming at fish disease control. For that reason, no ethical committee approval was needed, even though all animal handling was performed under the European and Italian guidelines on animal welfare. The conducted analysis does not fall within the provisions of Legislative Decree No. 26/2014, implementation of the European Directive 2010/63/EU of the European Parliament, as waste material was used for diagnostic purposes and was, therefore, not regulated by laws on animal testing.

Next, each specimen was identified using dichotomous keys [50,51,64,65], weighed and measured [60]. For species identification, the head morphology, which is the most useful anatomical part from a taxonomic point of view and is normally employed in any identification key of the mullet, was evaluated (Table 1) [50,51,64–66]. Although the head is often broad and flattened or slightly dorsally convex in mullets, a wide variation in relative shape and size can be observed among Mugilidae species. The positional relationships between different anatomical elements such as jaws, nostrils, lips, eyes, opercular and preorbital bones and jugular space and their shape and size generate a variety of information useful for taxonomic identification [50,51,64–66]. For a precise identification of the species, the number of spines and rays of paired and unpaired fins and the number of scales in the lateral series were also evaluated. These features can be observed on the left side of the specimens, from the scales located just behind the head. The number of spines varied from approximately 24 to nearly 63, although sometimes different species had the same number. To have a greater confirmation of the species, at the time of necropsy, the pyloric blinds were collected and counted. Normally the number varies within a certain range in specimens belonging to the same species. Pyloric blinds can vary from 3 to 48 but more commonly from 5 to 10, although it is common to find several species of the same genus with the same number of pyloric blinds.

Finally, pairs of sagittae were manually removed by auditory capsule dissection, cleaned from tissue with 3% H_2O_2 for 15 min and then washed with Milli-Q water and stored dry inside Eppendorf microtubes. Images of left and right sagittae were captured for each individual specimen by a Leica M205C stereomicroscope with a LEICA IC80 digital camera. Each sagitta was photographed twice, once with the inner face facing up and once with the external face facing up, using the longest axis to orient the images horizontally for external face photos and vertically for inner face photos, in accordance with the literature [31].

Table 1. Morphological characters of studied species used for taxonomical identification.

Chelon auratus	*Chelon labrosus*	*Oedalechilus labeo*
Presence of pure gold stain on theoperculum	Absence of pure gold stain on the operculum	Absence of pure gold stain on the operculum
Oval jugular space	Jugular space very short, straight, delimiting a very narrow oval space	Jugular space very narrow and linear
Anal fin with 8–9 rays, without spiny rays closetogether	Anal fin with 8–9 rays, without spiny rays closetogether	First anal fin with 3 spiny rays closetogether and 11 soft rays
Scales on head not extending beyond eyes	Scales on head extending beyond the eyes	Scales on head extendingbeyond the eyes
Upper lip not deep, shorter than pupil	Upper lip very deep, larger than pupil, with 3–4 sets of papillae	Upper lip deeper than pupil with finelabial fold
Rudimentary adipose eyelid	Rudimentary adipose eyelid	Rudimentary adipose eyelid
Dorsal scales with a dimple	Dorsal scales with a short dimple	Dorsal scales without dimple
Space between the two nostrils devoid of scales	Space between the twonostrils with scales	Space between the twonostrils devoid of scales

2.3. Morphometrical Analysis

Using ImageJ (ImageJ 1.48p software, freely available at https://imagej.nih.gov/ij/) (accessed on 21 September 2021) [61], in accordance with the literature [17,32,35,67–69], otolith measurements were recorded: otolith length (OL, mm), otolith width (OW, mm), otolith perimeter (OP, mm), otolith surface (OS, mm^2), sulcus perimeter (SP, mm), sulcus surface (SS, mm^2), sulcus length (SL, mm), cauda length (CL, mm), cauda width (CW, mm), cauda perimeter (CP, mm), cauda surface (CS), ostium length (OSL, mm), ostium width (OSW, mm), ostium perimeter (OSP) and ostium surface (OSS). Afterwards, other otolith shape indices were calculated: circularity (P^2/A), rectangularity (OS/(OL × OW)), aspect ratio (OW/OL; %), the ratio of the otolith length to the total fish length (OL/TL), the percentage of the otolith surface occupied by the sulcus (SS/OS, %), the percentage of the sulcus length occupied by the cauda length (CL/SL, %) and the percentage of the sulcus length occupied by the ostium length (OSL/SL, %) (Tables 2 and 3).

Table 2. Morphometric mean values with standard deviation (SD) and range of *Chelon auratus* and *Oedalechilus labeo* individuals: OL (otolith length), OW (otolith width), OP (otolith perimeter), OS (otolith surface), SP (sulcus perimeter), SS (sulcus surface), SL (sulcus length), CL (cauda length), CW (cauda width), CP (cauda perimeter), CS (cauda surface), OSL (ostium length), OSW (ostial width), OSP (ostium perimeter), OSS (ostium surface), CI (circularity), RE (rectangularity), aspect ratio (OW/OL %), the ratio of otolith length to total fish length (OL/TL), percentage of the otolith surface occupied by the sulcus (SS/OS %), percentage of the sulcus length occupied by the cauda length (CL/SL %) and percentage of the sulcus length occupied by the ostium length (OSL/SL %).

Otolith Morphological Characters (mm-mm^2)	*Chelon auratus* Mean ± SD	*Chelon auratus* Min.–Max.	*Oedalechilus labeo* Mean ± SD	*Oedalechilus labeo* Min.–Max.
OL	6.82 ± 0.78	5.56–9.60	6.27 ± 0.81	5.27–7.43
OW	3.38 ± 0.27	2.97–4.24	3.27 ± 0.28	2.83–3.62
OP	17.32 ± 1.44	14.21–22.05	16.38 ± 2.39	13.46–20.45
OS	17.06 ± 2.38	12.71–26.01	15.48 ± 3.18	11.65–20.05
SP	14.72 ± 1.89	10.62–19.28	14.24 ± 2.18	10.54–16.95
SS	0.12 ± 0.01	0.08–0.16	0.11 ± 0.02	0.08–0.13
SL	6.35 ± 0.89	4.31–8.41	6.05 ± 1.09	4.15–7.36
CL	4.12 ± 0.71	2.47–5.92	3.72 ± 0.83	2.27–4.63
CW	1.08 ± 0.24	0.50–1.60	0.98 ± 0.23	0.57–1.40
CP	9.04 ± 1.54	5.69–12.34	8.29 ± 1.53	5.77–10.30
CS	0.07 ± 0.01	0.04–0.09	0.06 ± 0.01	0.04–0.08
OSL	2.23 ± 0.38	1.54–3.20	2.34 ± 0.47	1.69–3.16
OSW	1.24 ± 0.29	0.80–2.09	1.24 ± 0.17	1.00–1.45
OSP	5.69 ± 0.83	4.02–7.60	5.95 ± 1.01	4.75–7.93
OSS	0.04 ± 0.01	0.03–0.06	0.04 ± 0.01	0.04–0.06
OP^2/OS	17.65 ± 1.10	15.89–19.99	17.41 ± 1.73	15.55–20.93
OS/(OL × OW)	0.74 ± 0.04	0.52–0.78	0.75 ± 0.03	0.71–0.79
OW/OL %	49.88% ± 0.04	38.11%–57.50%	52.44% ± 0.03	46.97%–56.48%
OL/TL	0.04 ± 0.01	0.03–0.06	0.04 ± 0.01	0.02–0.05
SS/OS %	0.66% ± 0.001	0.42%–1.12%	0.72% ± 0.00	0.47%–1.02%
CL/SL %	64.76% ± 0.05	52.00%–71.66%	0.61 ± 0.06	0.53–0.69
OSL/SL %	35.24% ± 0.05	28.34%–48.00%	0.39 ± 0.06	0.31–0.47

Table 3. Morphometric mean values with standard deviation (SD) and range of right (R) and left (L) sagittae in *Chelon labrosus* individuals: OL (otolith length), OW (otolith width), OP (otolith perimeter), OS (otolith surface), SP (sulcus perimeter), SS (sulcus surface), SL (sulcus length), SW (sulcus width), CL (cauda length), CW (cauda width), CP (cauda perimeter), CS (cauda surface), OSL (ostium length), OSW (ostium width), OSP (ostium perimeter), OSS (ostium surface), CI (circularity), RE (rectangularity), aspect ratio (OW/OL %), the ratio of otolith length to total fish length (OL/TL), percentage of otolith surface occupied by the sulcus (SS/OS %), percentage of the sulcus length occupied by the cauda length (CL/SL %) and percentage of the sulcus length occupied by the ostium length (OSL/SL %). (R = right, L = left).

Otolith Morphological Characters (mm-mm^2)	*Chelon labrosus* Mean ± SD. (L. otoliths)	*Chelon labrosus* Min.–Max (L. otoliths)	*Chelon labrosus* Mean ± SD (R. otoliths)	*Chelon labrosus* Min.–Max. (R. otoliths)
OL	6.73 ± 0.33	5.97–7.54	6.71 ± 0.33	6.04–7.45
OW	3.52 ± 0.19	3.24–4.00	3.48 ± 0.15	3.21–3.88
OP	17.36 ± 0.79	15.88–19.62	17.24 ± 0.72	15.93–18.89
OS	18.21 ± 1.44	15.98–21.64	17.91 ± 1.47	15.67–22.05
SP	15.57 ± 1.22	13.19–18.13	14.72 ± 1.51	12.31–19.30
SS	0.12 ± 0.01	0.10–0.13	0.11 ± 0.01	0.09–0.14
SL	6.29 ± 0.41	5.45–7.25	2.43 ± 0.77	0.93–5.75
CL	4.21 ± 0.39	3.39–4.80	1.18 ± 0.52	0.84–3.67
CW	1.20 ± 0.19	0.65–1.58	4.15 ± 0.68	1.04–5.13
CP	9.78 ± 1.05	7.58–11.68	9.51 ± 1.15	6.99–13.44
CS	0.07 ± 0.01	0.06–0.09	0.07 ± 0.01	0.05–0.10
OSL	2.09 ± 0.31	1.64–2.90	1.26 ± 0.37	0.09–2.07
OSW	1.43 ± 0.25	0.97–2.00	1.90 ± 0.34	0.94–2.37
OSP	5.79 ± 0.65	4.82–7.20	5.21 ± 0.76	3.79–6.98
OSS	0.04 ± 0.005	0.04–0.05	0.04 ± 0.01	0.03–0.05
OP^2/OS	16.58 ± 0.61	15.71–18.48	16.62 ± 0.60	15.59–18.69
OS/(OL × OW)	0.77 ± 0.02	0.71–0.81	0.77 ± 0.02	0.72–0.81
OW/OL %	52.43% ± 0.03	48.43–59.70%	51.95% ± 0.02	46.58%–55.80%
OL/TL	0.03 ± 0.003	0.03–0.04	0.03 ± 0.003	0.03–0.04
SS/OS %	0.64% ± 0.001	0.48%–0.78%	0.61% ± 0.00	0.46%–0.85%
CL/SL %	66.84% ± 0.04	56.98%–74.49%	48.51% ± 0.10	34.29%–90.46%
OSL/SL %	33.16% ± 0.04	25.51%–43.02%	51.49% ± 0.10	9.53%–65.71%

2.4. Otolith Shape Analysis

Analysis of otolith shapes was performed using shape R, an open-source software package that runs on the R platform (R Gui 4.0.5), globally used to study otolith shape variation among teleost populations and species [62]. A threshold pixel value of 0.05 (intensity threshold) was used to binarize sagittae images. Each extracted outline was coupled to a master list file enclosing information on analyzed specimens (e.g., fish length, weight and origin). Wavelet and Fourier coefficients were extracted and adjusted to define the allometric relationships with fish lengths. The graph shown in Figure 2 was obtained through wavelet coefficient, with a mean otolith shape comparison among analyzed species. Deviation from the otolith outline was used to estimate the quality of obtained wavelet and Fourier reconstruction. The value 15 was set as the maximum number of Fourier harmonics to be shown. Finally, a g-plots R package was used to obtain the graph shown in Figure 3, to evaluate how variation in the wavelet coefficients is dependent on the position along the outline.

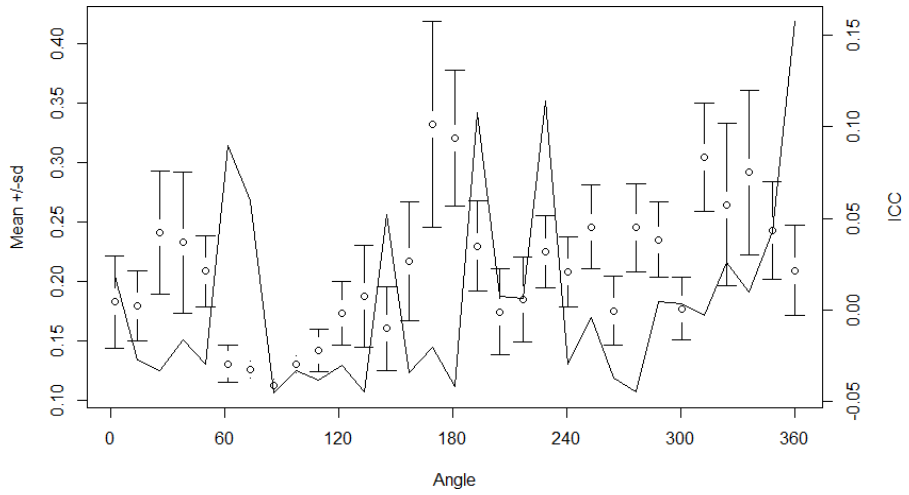

Figure 2. Mean and standard deviation (SD) of wavelet coefficients for all combined otoliths and the proportion of variance among species (black line). The horizontal axis shows angle in degrees (°) based on the polar coordinates of mean shapes of left otolith contours. The centroid of the otolith is the centre point of polar coordinates.

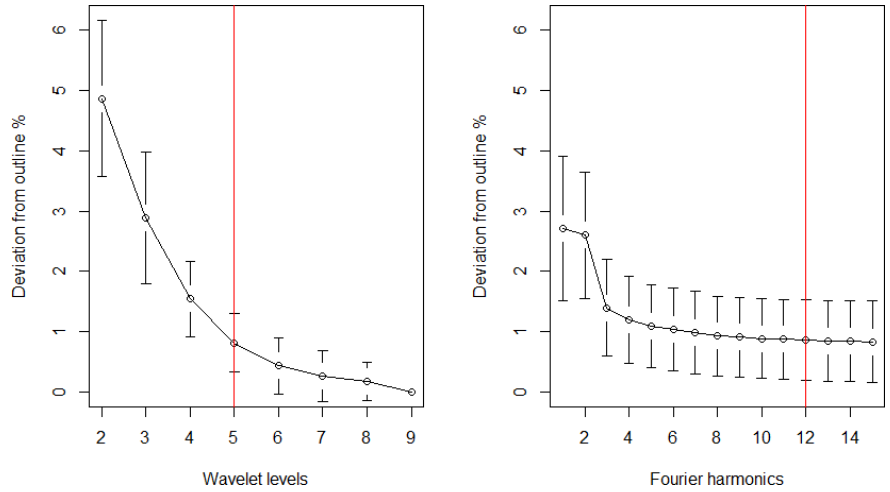

Figure 3. Plotting the quality of wavelet and Fourier outline reconstruction. The red lines indicate the level of wavelet and number of Fourier harmonics needed for a 98.5% accuracy of the remodelling.

2.5. SEM Analysis

A total of 9 otoliths were observed using SEM analysis, including 3 of *C. auratus,* 3 of *C. labrosus* and 3 of *O. labeo*. They were fixed for 48 h in 70% alcohol. Subsequently, samples were dehydrated in a graded series of alcohol from 70 to 100%, for 1 h in each solution. To avoid the critical drying point, samples were placed on a stub (SEM-PT-F-12) using conductive adhesive tables (G3347) and left for 12 h at 28 °C. Finally, the samples were sputter coated with 20 nm gold palladium. The samples were examined using a Zeiss EVO MA10 operating at the acceleration voltage of 20 Kv.

2.6. Data Analyses

All statistical analyses were conducted using Sigmaplot V.14, R vegan package V.2.5, and PAST V. 2.756 software.

Specific morphological parameters (OP2/OS, OS/[OL OW], OL/TL, OW/OL %, SS/OS %) were analyzed using a one-way analysis of variance (One-Way ANOVA) or Kruskal–Wallis one-way ANOVA to highlight any significant differences between the right and left sides of the otolith specimens within the same species. Differences in morphological

parameters between specimens of different species were also analyzed using one-way ANOVA or Kruskal–Wallis one-way ANOVA. Additionally, sulcus acusticus parameters were subjected to a linear discriminant analysis (LDA) to show differences between all the analyzed species.

Finally, the correlation between the measured parameters and fish weight and total length was tested using the Pearson correlation coefficient.

To determine differences in otolith contours, wavelet coefficients were used to analyze shape variation among species using an ANOVA-like permutation test. Moreover, shape coefficients were subjected to an LDA to obtain an overview of the differences in otolith shape between the species examined. The significance level was set at $p < 0.05$.

3. Results

3.1. Morphometric and Shape Analysis

As shown in Figures 4 and S1, the *C. auratus* specimens had a sagitta with rectangular or oblong shape, with an entire margin in the dorsal rim and lobed to the entire margins in the ventral rim. The anterior region was angled-round, with a short and pointed rostrumand an almost entirely absent anti-rostrum. The posterior region was flattened-round.

As shown in Figures 5 and S2, the *C. labrosus* specimens had a rectangular shaped sagitta, with crenate to irregular margins and irregular protuberances. The anterior region was angled-irregular, with a short and broad rostrum. The dorsal rim showed a marked plateau tilting towards the anterior rim. The anti-rostrum was absent or, in some specimens, poorly marked with a wide and small excisura. The posterior region was slightly irregular to round.

As shown in Figures 6 and S3, the *O. labeo* specimens' sagitta had a rectangular shape, with irregular margins in the dorsal and ventral rims. The anterior region was round to irregular, with a short and broad rostrum, and a short and pointed anti-rostrum.

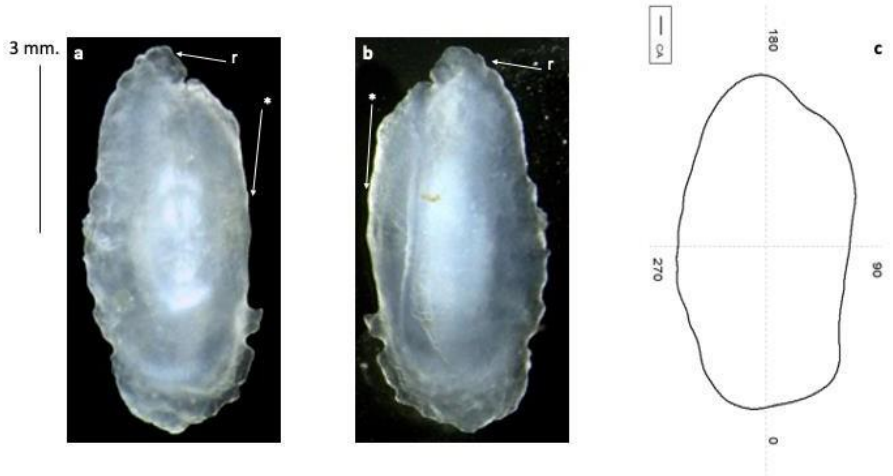

Figure 4. Left sagittae of *Chelon auratus* with scale bar. (**a**) Medial view; (**b**) lateral view; (**c**) mean shape; (r) indicates the rostrum, and (*) indicates the dorsal rim.

Concerning intra-specific differences (Table 4) among sagitta morphometrical parameters, in the specimens belonging to the *C. auratus* species, the correlation analysis revealed a moderate significant correlation between TL and SS/OS % ($\rho = 0.416$; $p = 0.001$). *C. labrosus* was the only species that showed differences between the right and left side of the otoliths, for the parameters CL/SL % ($H = 38.48$, df 1, $p < 0.001$) and OSL/SL % ($H = 38.48$, df 1, $p < 0.001$). Moreover, a significantly positive correlation was detected between TL and OW/OL ($\rho = 0.411$; $p = 0.001$), while a negative correlation was noted between TL and OL/TL ($\rho = 0.366$; $p = 0.0029$) and between BW and OL/TL ($\rho = 0.392$; $p = 0.001$). In *O. labeo* specimens a strong negative correlation was observed between TL and OL/TL ($\rho = -0.729$; $p = 0.001$) and between BW and OL/TL ($\rho = -0.658$; $p = 0.001$). A significant

positive correlation was recorded between TL and SS/OS % (ρ = 0.561; p = 0.008) and between BW and SS/OS % (ρ = 0.499; p = 0.02).

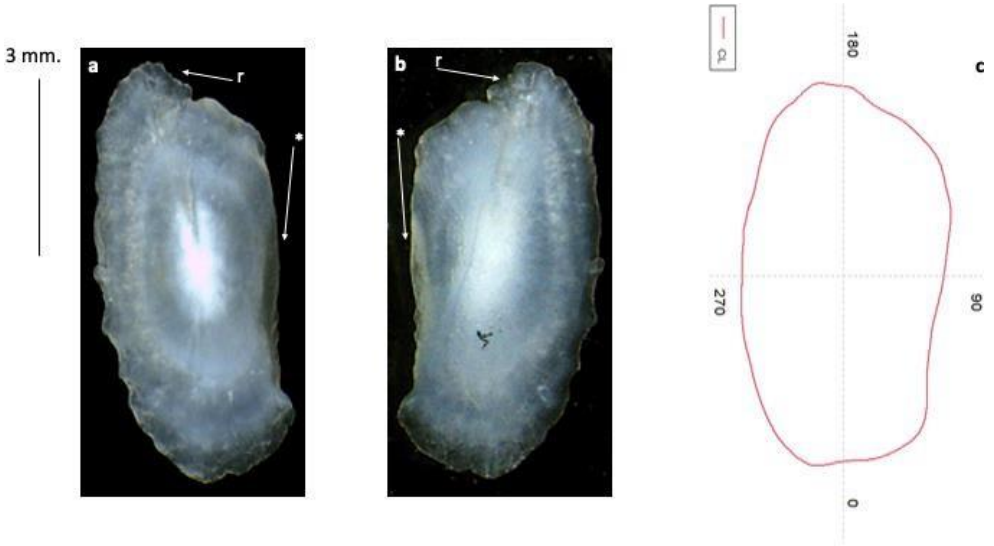

Figure 5. Left sagittae of *Chelon labrosus* with scale bar. (**a**) Medial view; (**b**) lateral view; (**c**) mean shape; (r) indicates the rostrum, and (*) indicates the dorsal rim.

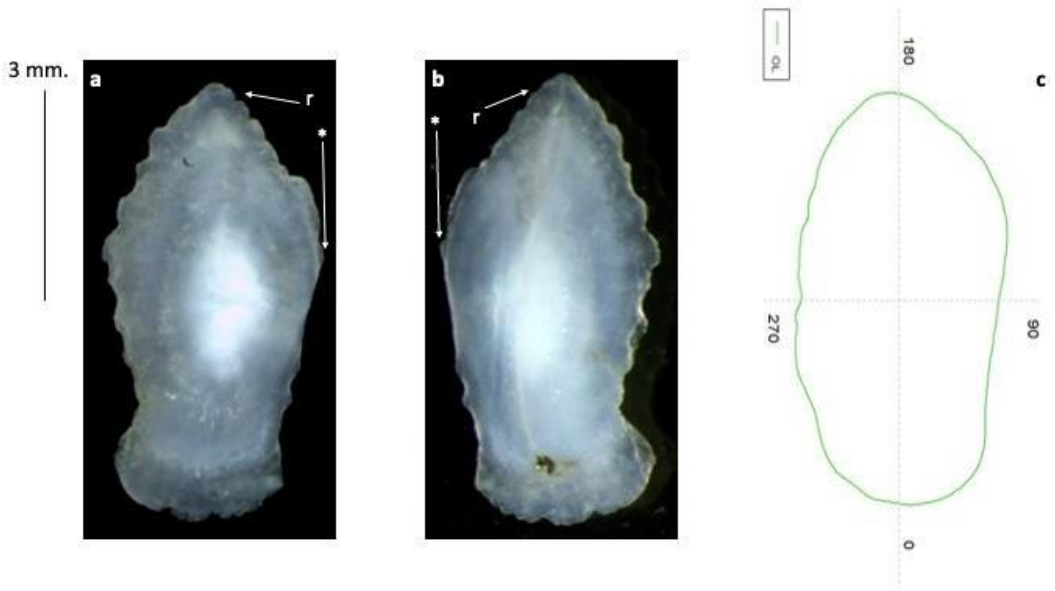

Figure 6. Left sagittae of *Oedalechius labeo* with scale bar. (**a**) Medial view; (**b**) lateral view; (**c**) mean shape; (r) indicates the rostrum, and (*) indicates the dorsal rim.

Concerning inter-specific differences among sagitta morphometrical parameters (Table 5), the investigated species showed significant differences in some parameters. *C. auratus* and *C. labrosus* showed differences in OP^2/OS (H = 20.802, df2, $p < 0.001$), OS/[OLXOW] (p = 0.001), OW/OL % ($p < 0.002$) and OL/TL (H = 12.477, df 2, p = 0.002). *C. auratus* and *O. labeo* showed significant differences only in OW/OL % (p = 0.014). Finally, *C. labrosus* and *O. labeo* showed differences in OS/[OLXOW] (p = 0.012).

As shown in the LDA plot (Figure 7), the first two axes showed a slight separation in the sulcus acusticus parameters between the three fish species analyzed.

The mean shape of otoliths differed significantly between the *C. auratus*, *C. labrosus* and *O. labeo* specimens ($p < 0.001$). The otolith contours are shown in Figure 8a. Marked differences in otolith shape have also been confirmed by LDA. From the LDA plot of the

first two discriminant functions, we can see that the three species were quite well separated (Figure 8b).

Table 4. Pearson Correlation results between total length, weight and selected morphometric parameters of *Chelon auratus, Chelon labrosus* and *Oedalechilus labeo*. Significant result was set at $p = 0.05$. OS (circularity), OS/(OL × OW) (rectangularity), aspect ratio (OW/OL; %), the ratio of the otolith length to the total fish length (OL/TL), percentage of the otolith surface occupied by the sulcus (SS/OS, %), percentage of the sulcus length occupied by the cauda length (CL/SL, %) and percentage of the sulcus length occupied by the ostium length (OSL/SL, %). ns = not significant.

Fish Species	Morphometric Parameters	Weight		Total Length	
		ρ	*p* Value	ρ	*p* Value
Chelon auratus	OP^2/OS	ns	ns	ns	ns
	OS/(OL × OW)	ns	ns	ns	ns
	OW/OL %	ns	ns	ns	ns
	OL/TL	ns	ns	ns	ns
	SS/OS %	ns	ns	0.416	0.001
	CL/SL %	ns	ns	ns	ns
	OSL/SL %	ns	ns	ns	ns
Chelon labrosus	OP^2/OS	ns	ns	ns	ns
	OS/(OL × OW)	ns	ns	ns	ns
	OW/OL %	ns	ns	0.411	0.001
	OL/TL	−0.392	0.001	−0.366	0.0029
	SS/OS %	ns	ns	ns	ns
	CL/SL %	ns	ns	ns	ns
	OSL/SL %	ns	ns	ns	ns
Oedalechilus labeo	OP^2/OS	ns	ns	ns	ns
	OS/(OL × OW)	ns	ns	ns	ns
	OW/OL %	ns	ns	ns	ns
	OL/TL	−0.658	0.001	−0.729	0.001
	SS/OS %	0.499	0.02	0.561	0.008
	CL/SL %	ns	ns	ns	ns
	OSL/SL %	ns	ns	ns	ns

Table 5. Results of t-test and ANOVA carried out on selected morphometric parameters between left and wright sagitta and among left sagittae of Chelon auratus, Chelon labrosus and Oedalechilus labeo. Significant result was set at $p = 0.05$. OP2/OS (circularity), OS/(OL × OW) (rectangularity), aspect ratio (OW/OL; %), the ratio of the otolith length to the total fish length (OL/TL), percentage of the otolith surface occupied by the sulcus (SS/OS, %), percentage of the sulcus length occupied by the cauda length (CL/SL, %) and percentage of the sulcus length occupied by the ostium length (OSL/SL, %). ns = not significant.

	OP^2/OS	OS/(OL × OW)	OW/OL %	OL/TL	SS/OS %	CL/SL %	OSL/SL %
Comparison between L and R otoliths:							
Chelon auratus	ns	ns	ns	ns	ns	ns	ns
Chelon labrosus	ns	ns	ns	ns	ns	$p < 0.001$	$p < 0.001$
Oedalechilus labeo	ns	ns	ns	ns	ns	ns	ns
Comparison between species:							
Chelon auratus vs. *Chelon labrosus*	$p < 0.001$	$p = 0.001$	$p < 0.002$	$p = 0.002$	ns	ns	ns
Chelon auratus vs. *Oedalechilus labeo*	ns	ns	$p = 0.014$	ns	ns	ns	ns
Chelon labrosus vs. *Oedalechilus labeo*	ns	$p = 0.012$	ns	ns	ns	ns	ns

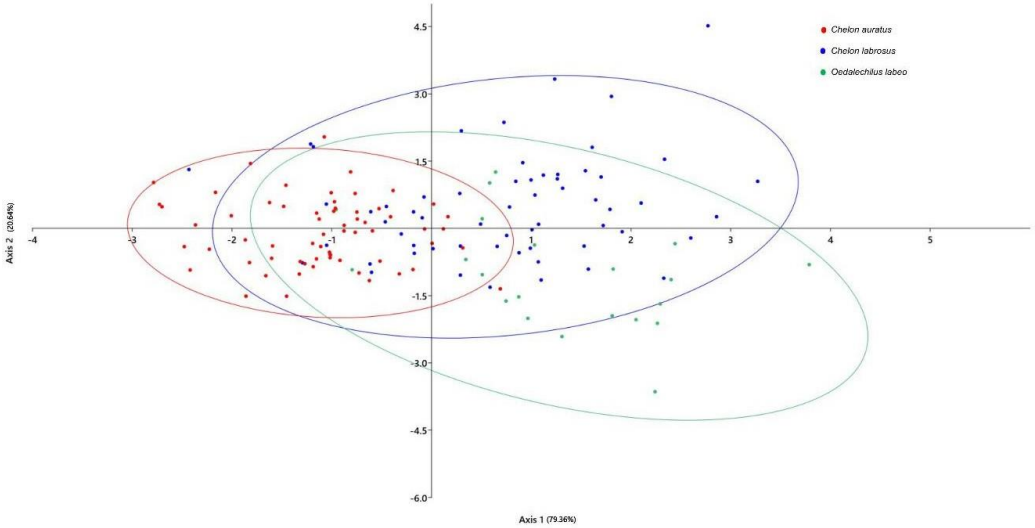

Figure 7. Linear Discriminant Analysis (LDA) of the sulcus acusticus computed between the species *Chelon auratus*, *Chelon labrosus* and *Oedalechilus labeo*. The LDA was based on selected sulcus acusticus parameters: sulcus acusticus area, sulcus acusticus perimeter, sulcus acusticus length, ostium area, ostium perimeter, ostium length, ostium width, cauda area, cauda perimeter, cauda length, cauda width, percentage of the otolith surface occupied by the sulcus (SS/OS, %), percentage of the sulcus length occupied by the cauda length (CL/SL, %) and percentage of the sulcus length occupied by the ostium length (OSL/SL, %). 95% probability ellipses are shown.

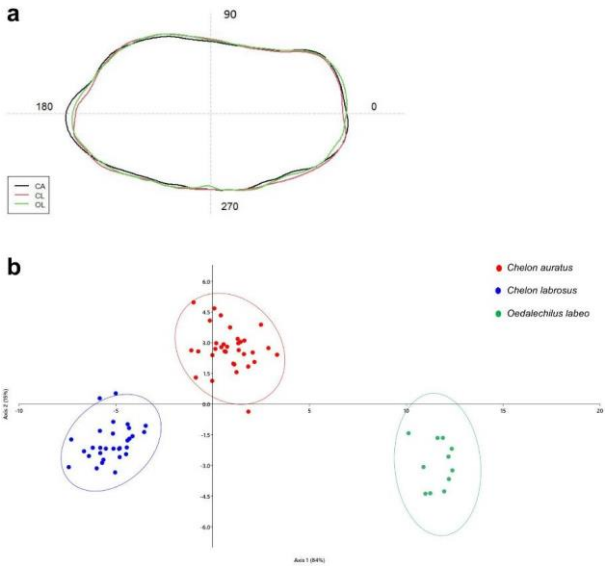

Figure 8. (**a**) Mean shapes of left otolith contours. CA is *Chelon auratus*, CL is *Chelon labrosus* and OE is *Oedalechilus labeo.* (**b**) Linear discriminant analysis plot between the species *Chelon auratus*, *Chelon labrosus* and *Oedalechilus labeo*, calculated on elliptic Fourier descriptors. Ellipses include 95% confidence interval.

3.2. Scanning Electron Microscopy (SEM) Analysis

Figure 9 gives an accurate sagittae view via SEM of the studied species. The sulcus acusticus was heterosulcoid with a supramedian position and flat colliculi (homomorph) in all three species. The ostium was opened wide in the anterior margin and the cauda was distinctly closed away from the posterior margin (ostial mode opening). The ostium was tubular and curved in all the three species, with a more markedly curved shape in *C. labrosus* and *O. labeo* than *C. auratus* (Figure 9a–d). In this last species, the ostium was

funnel-like (Figure 9a), while in the other two species, it was more rectangular (Figure 9e,f). The anterior regions of the sagittae were peaked in all the studied species, with an absent or poorly developed anti-rostrum and a short and poorly pronounced rostrum, while the posterior regions were flattened and slightly oblique in some *C. auratus* specimens.

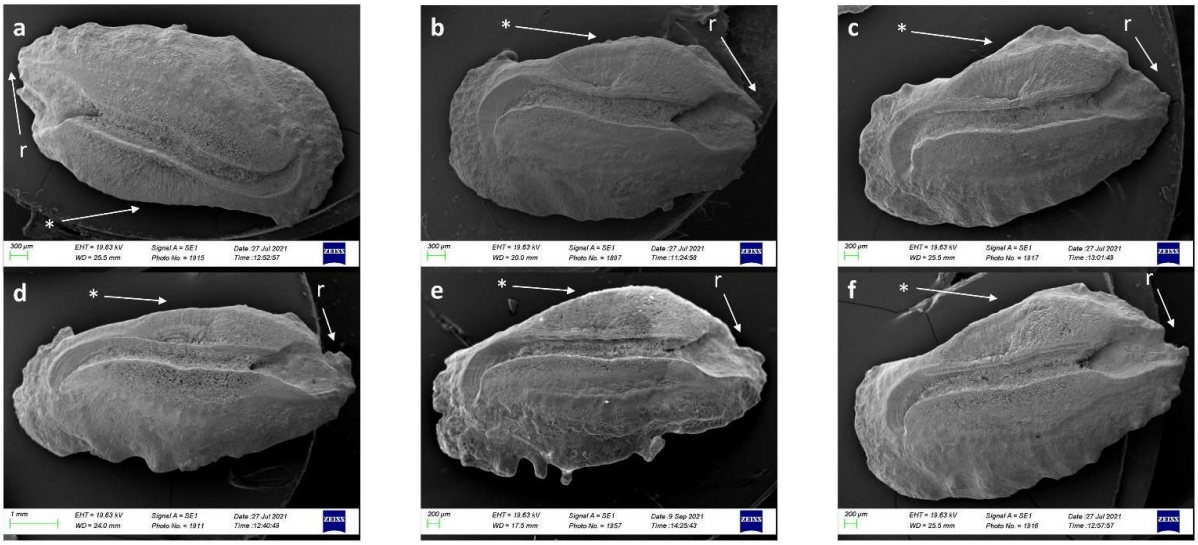

Figure 9. SEM imaging of the left sagittae proximal surface; (**a**–**d**) *Chelon auratus*; (**b**–**e**) *Chelon labrosus*; (**c**–**f**) *Oedalechilus labeo;* (r) indicates the rostrum, and (*) indicates the dorsal rim.

Concerning the external textural organization, SEM analysis highlighted a polymorph transformation, strictly related to the otoliths' mineralization process. All the analyzed sagittae showed radial oriented crystalline units, which had a chaotic orientation and were not equally sized (Figures 10a–e, 11a–c and 12a–c), probably due to the polymorph composition of the crystals. In all the studied species, the aragonite was found in two crystal habits (columnar habits and distinct plate habits) on the cauda surface with bigger, longer and narrower crystals (Figures 10d,e, 11b and 12c–e), while in the ostium, they were smaller and shorter than in the cauda, with a smooth surface (Figures 10b, 11d and 12b).

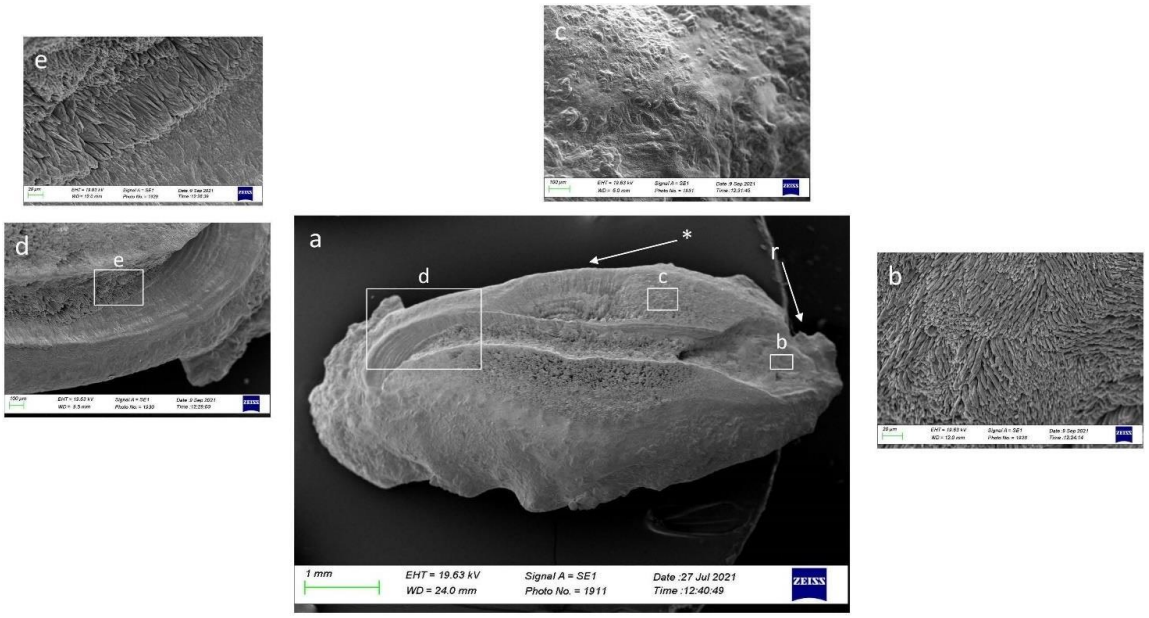

Figure 10. SEM imaging of left sagitta proximal surface in *Chelon auratus* (**a**), with details of external textural organization of ostium (**b**), area between cauda and dorsal rim (**c**) and cauda (**d**,**e**); (r) indicates the rostrum, and (*) indicates the dorsal rim.

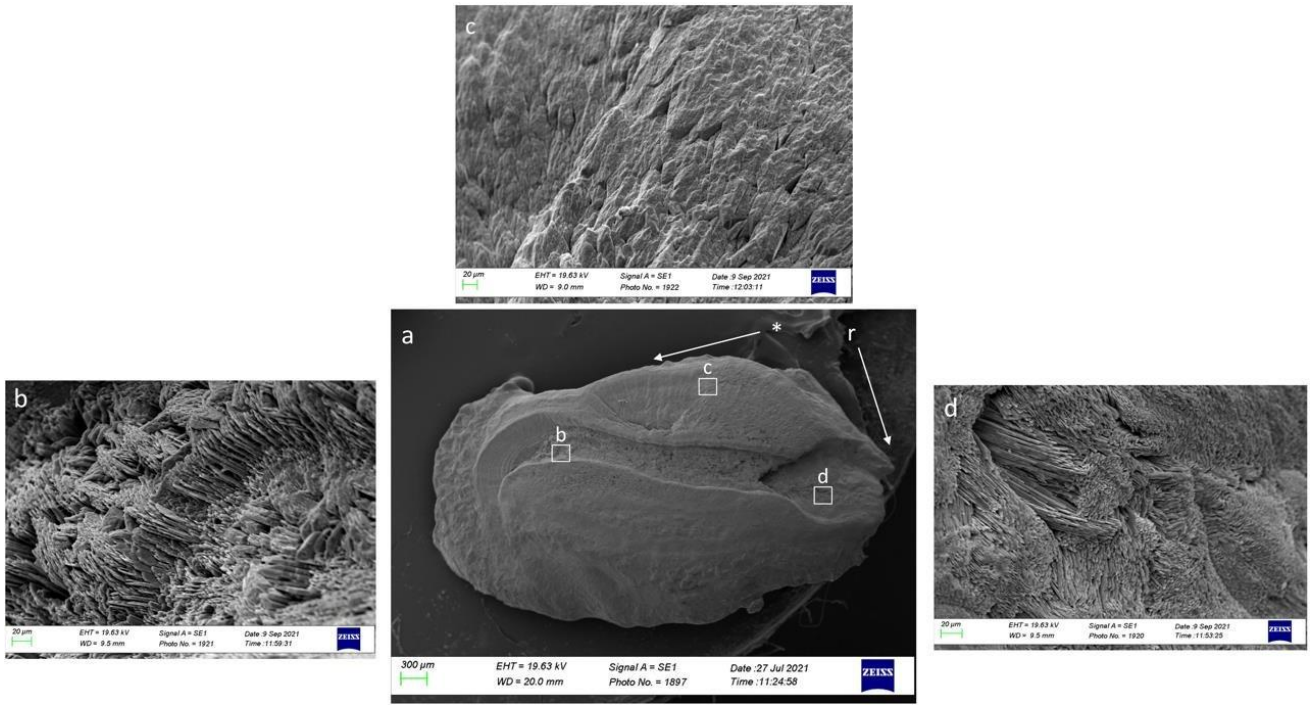

Figure 11. SEM imaging of left sagitta proximal surface in *Chelon labrosus* (**a**) with details of external textural organization of cauda (**b**), dorsal area (**c**) and ostium (**d**); (r) indicates the rostrum, and (*) indicates the dorsal rim.

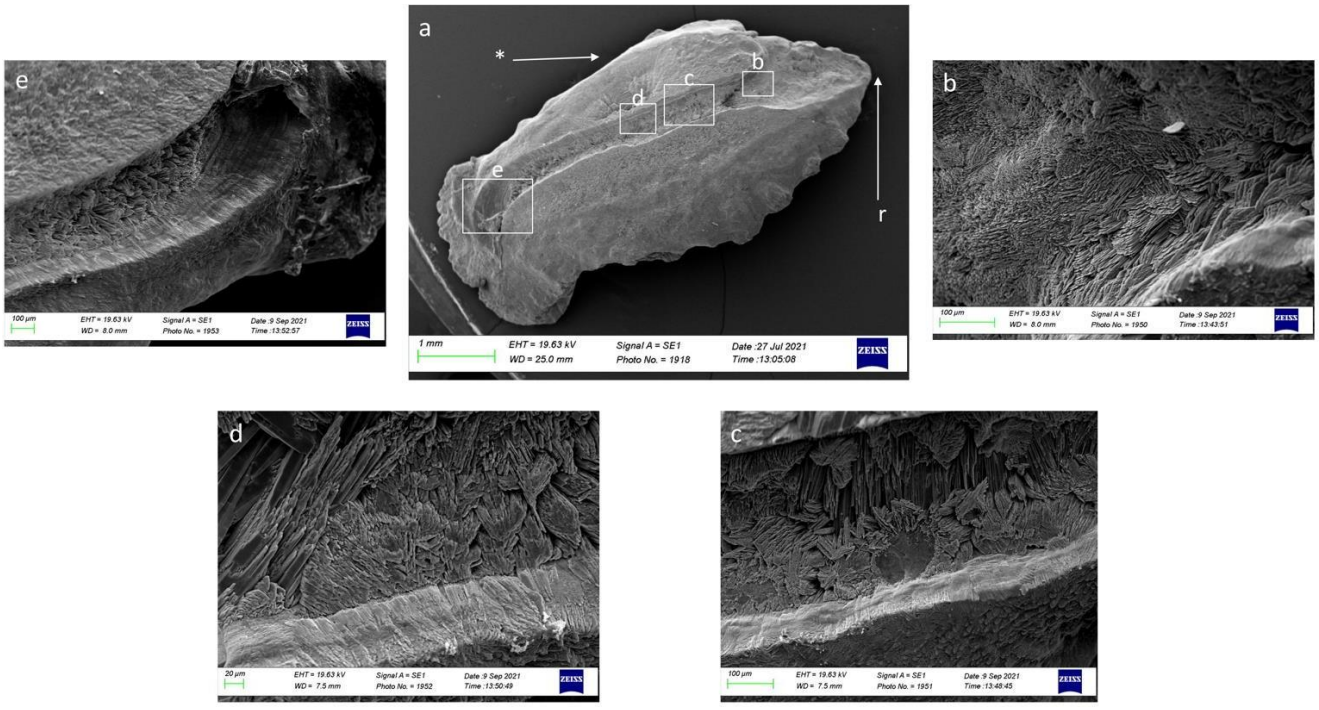

Figure 12. SEM imaging of left sagitta proximal surface in *Oedalechilus labeo* (**a**) with details of external textural organization of ostium (**b**) and cauda (**c**–**e**); (r) indicates the rostrum, and (*) indicates the dorsal rim.

Moreover, several polymorphs and habits of calcium carbonates were detected in many otoliths, especially of *C. labrosus*. These crystalline habits showed different shapes and organizations including small, locally oriented needles, long prisms and large rhombohedral

crystals. This last kind was detected on the *C. labrosus* sagitta surface (Figure 13a–h); the long prism shaped crystals (Figure 14a,c,e) and small, locally oriented needles (Figure 14b,d)were detected on the cauda surface of *O. labeo* and of *C. auratus*. SEM imaging also showed carbonate formations similar to "globular secretion" on the sagitta surface of *C. labrosus* (Figure 15a–c), along with evidence of large prismatic crystals (Figure 16a–d).

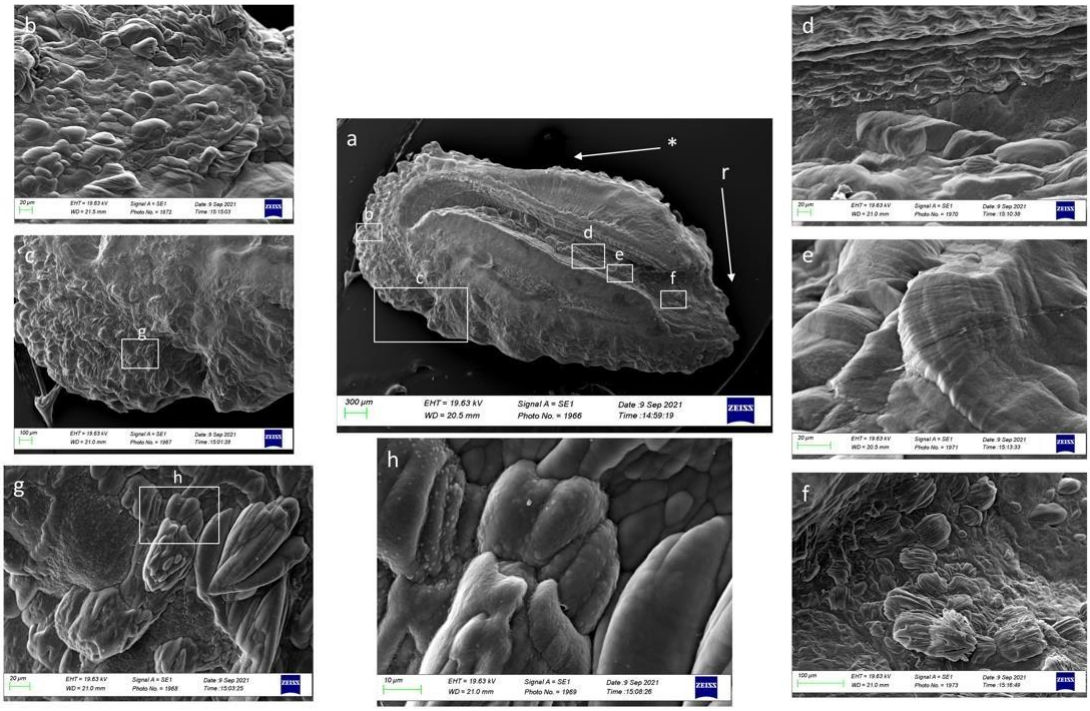

Figure 13. SEM imaging of left sagitta proximal surface in *Chelon labrosus* (**a**) with details of several calcium carbonate habits in posterior area (**b**), ventral area (**c**–**h**), cauda (**d**,**e**) and ostium (**f**); (r) indicates the rostrum, and (*) indicates the dorsal rim.

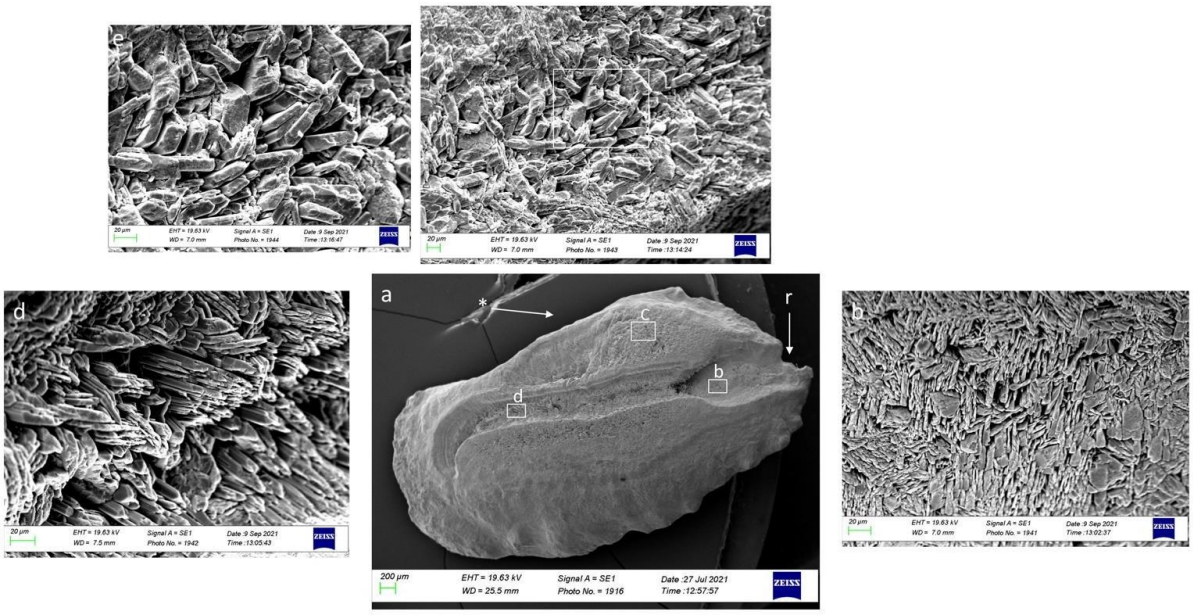

Figure 14. SEM imaging of left sagitta proximal surface in *Oedalechilus labeo* (**a**) with details of several calcium carbonate habits in ostium (**b**), dorsal area (**c**–**e**) and cauda (**d**); (r) indicates the rostrum, and (*) indicates the dorsal rim.

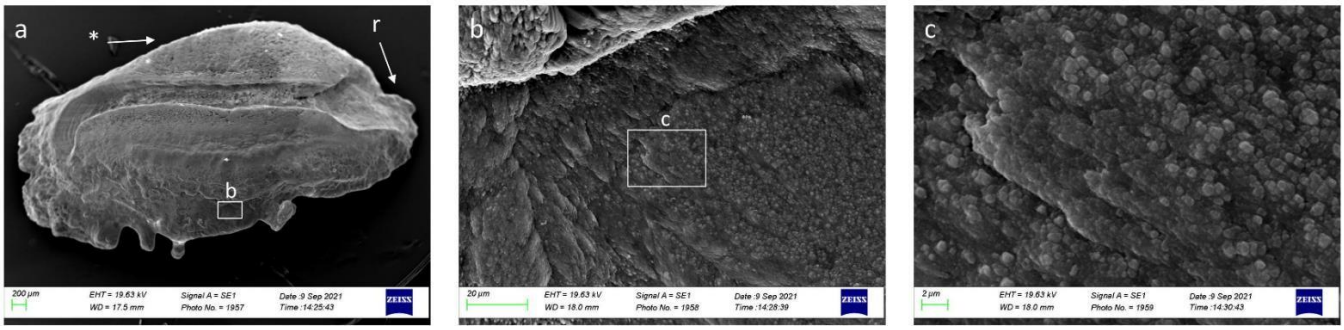

Figure 15. SEM imaging of left sagitta proximal surface in *Chelon labrosus* (**a**) with details of granular crystalline habit in ventral area (**b**,**c**); (r) indicates the rostrum, and (*) indicates the dorsal rim.

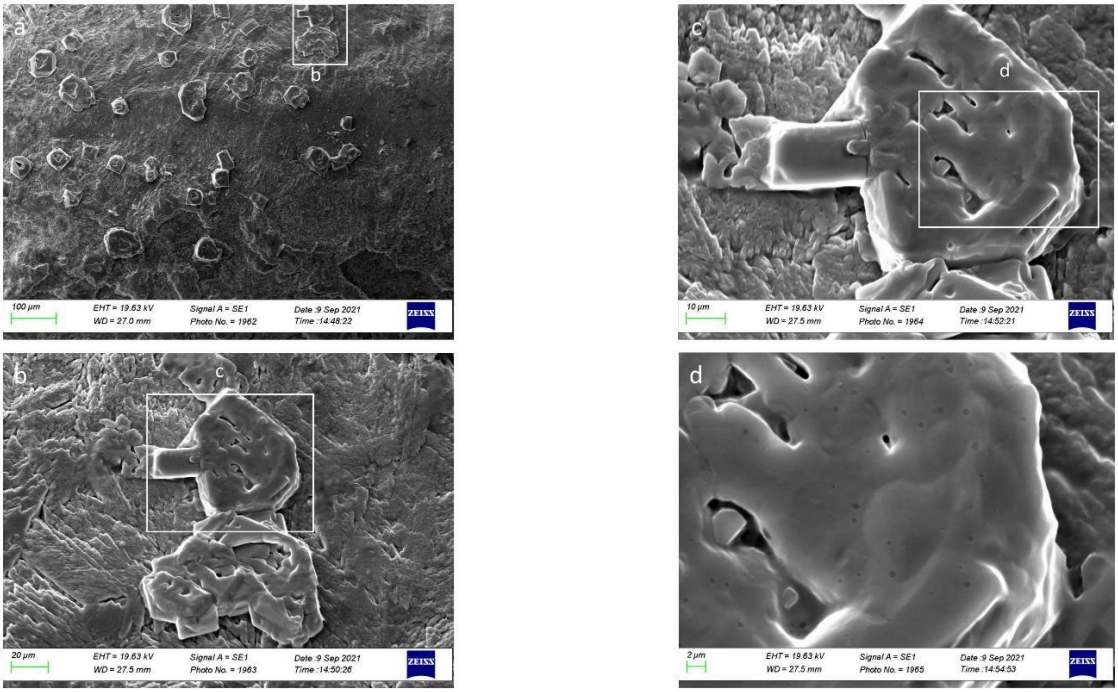

Figure 16. SEM imaging of large prismatic crystals in *Chelon labrosus* (**a**–**d**).

4. Discussion

The evaluation of intra-specific morphological differences among sagittae is essential to better understand otolith variability in relation to environmental factors and habitats. The morphological and shape variability of sagittae among populations from different geographical areas is at the base of stock assessment, and it has been demonstrated and thoroughly investigated by several authors [31,63–70]. Although the application of shape and morphological studies on wild populations are not enough to explain all the adaptative response of sagittae to environmental conditions or habitats, and common garden experiments are generally required, studies on otolith morphometry and morphology and the comparison among otoliths of different populations are essential to broaden knowledge on these differences and to help in detecting them.

Morphometrical results reported in the present study showed slightly morphological differences between the sagittae of Mugilidae species from the investigated area and those, described in the literature, from western Mediterranean Sea, northeastern Mediterranean Sea and Atlantic Ocean populations [17,42,71–80]. The *C. auratus* specimens from Ganzirri lagoon showed a more rectangular sagitta, with pronounced sagitta length to total fish length ratio and rectangularity values, and a lower circularity and sagitta aspect ratio than

those, reported by previous literature, from others geographical areas [17,42,79,80]. The margins of anterior region showed an accentuated regularity in the studied specimens compared to those from the northeastern Mediterranean Sea [71], while the rostrum was more pointed than those from the western Mediterranean Sea [15,72]. The positive correlation shown by statistical analysis confirmed the most pronounced sagitta dimension in the studied specimens. The positive correlation between ratio of sulcus acusticus surface to the entire sagitta and the increase in specimen size was probably related to an accentuated sulcus acusticus growth, which could depend on species ecology and its adaptation to the sampling area.

In addition, for *C. labrosus,* the morphology of the sagittae was different compared to those, shown by the literature, from the western Mediterranean and Atlantic Ocean [15]. The rectangularity was higher, while circularity was lower than data reported by previous literature [15], while the sagitta aspect ratio was the same, and the sagitta length to total fish length ratio was slightly higher. The irregular margins of the anterior region were similar to those observed in specimens from the northeastern Mediterranean Sea, western Mediterranean Sea and north Atlantic [17,71–80]. By contrast, the posterior region was flattened. Statistical analysis showed an accentuated increase in sagitta width, related to total fish length increase. This condition was also confirmed by the negative correlation observed between total fish length and the sagitta length to total fish length ratio. This was also the only species to show slight differences between left and right sagittae, especially on sulcus acusticus proportions (the cauda length to sulcus acusticus length ratio and the ostium length to sulcus acusticus length ratio). To the best of our knowledge, this is the first description of these differences in *C. labrosus* otoliths, confirming the peculiarity of specimens inhabiting Ganzirri lagoon. The detection of directional bilateral asymmetry is essential for stock assessment studies since it can affect otolith shape enough to be a potential new accurate method for stock identification [73,74]. Slight changes between left and right sagittae could be related to ecology (e.g., feeding strategy), and it is possible that the *C. labrosus* population from the studied area could show ecological features, related to habitat peculiarity, not found in other populations. Further analysis on specimens from Ganzirri lagoon are required to confirm this hypothesis.

To the best of our knowledge, this is also the first time in which *O. labeo* morphometrical parameters have been described. Regarding morphological aspects, the *O. labeo* specimens from the investigated area showed a rectangular sagitta, with regular rims in dorsal and ventral margins and an irregular anterior region different than those shown in the literature regarding the northeastern Atlantic and Mediterranean Sea [41]. The strong negative correlation observed between sagitta length and total fish length and weight showed an otolith dimension not directly related to those of the specimens. In contrast, the positive correlation between the sulcus acusticus surface to sagitta surface ratio and total fish length and weight confirmed a more accentuated increase in sulcus area than in the entire sagitta. These morphometrical features of the sagitta could be related to species lifestyle and life history. Further analysis of its ecology, migration patterns and key lifetime habitats are required to understand what might be related to these correlations.

All these differences in morphology detected between the studied fish species and populations from other geographical areas could lead to changes in sagittae between different stocks and they could be related to transitional environment peculiarities. It is difficult to find a direct correlation between environmental factors and variations in morphology and the morphometrical parameters of sagittae, but this kind of study broadens knowledge of the morphofunctionality of Mugilidae sagittae and their adaptation to different environ- mental factors. The results reported in the present paper confirm the great value of research on sagitta morphology in exploring the differences between different populations of the same species inhabiting different environments, highlighting the adaptation of teleosts to various habitats, as well as their features. Regarding Ganzirri lagoon, the particular water circulation affecting this transitional basin often generates a vertical gradient of nutrient stratifications, which determines consequences for the biogeochemical cycling of

nutrients and the anaerobic decomposition of organic matter [75]. Moreover, these also influence a vertical zonation of the planktonic microbial community of the basins. Water exchanges with the sea and underground springs, as well as meteorological and climatic conditions, influence the environmental characteristics of Ganzirri lagoon across seasons through large fluctuations in chemical-physical parameters, especially salinity, temperature and dissolved oxygen [76]. This kind of environmental factor fluctuation leads to adaptative behavioral and morphological responses, especially influencing otolith structure and composition [12,27,77–79], to a greater extent in fish that inhabit transitional waters than in fish that inhabit the open sea. According to the literature, salinity and temperature variations can influence the deposition rate of calcium carbonate, causing variations in sagitta polymorph percentage, crystal habits and, at the macroscopical level, morphological and shape variations too [80–83]. For this reason, Ganzirri lagoon features could lead to several variations among the sagittae of investigated species [12,32,34,73,84–92], confirming the importance of otoliths for eco-morphological and morphofunctional studies. Further analysis on feeding behavior and population dynamics is required to better understand the ecology of these three species in peculiar environments, such as the brackish lagoon considered in the present study.

The relatively few interspecific differences detected among the morphometrical parameters could be strictly related to the closeness at the taxonomic level of the studied species, since these belong to the same family and, in the case of *C. auratus* and *C. labrosus*, to the same genus [43]. Interspecific differences among otoliths, reported between the studied species, primarily concerned circularity, rectangularity, sagitta aspect ratio and the ratio of the sagitta length to the total fish length. All these differences were confirmed by the shape analysis. Indeed, *O. labeo* sagitta contours have clearly shown a stronger circularity than in those of the other species. A marked rectangular shape and longer sagitta were detected in *C. auratus*, which showed the highest otolith width compared with the other species analysed. This result have been confirmed by the highest values of sagitta aspect ratio and otolith length to total fish length ratio, compared to the other two species,

The *C. labrosus* specimens showed an intermediate sagitta morphology compared with the other two species, with a more pronounced rectangularity than *O. labeo* and a marked circularity compared to *C. auratus*. Concerning the sulcus acusticus parameters, the three Mugilidae species showed a similar morphology, as confirmed by LDA, with few differ-ences. Indeed, the species share the same habitats and a similar ecological niche. Ecological differences with regard to the feeding habits—which in *C. auratus* are mainly those of a pelagic predator, while the other two species are herbivorous and benthic predators—could lead to the variation, although small, in sagittae morphology and shape between species, as reported by the previous literature on different species [32,33,35,73,88,93,94]. Further analysis of the feeding habits and diet of the studied species is required to confirm this hypothesis. Regarding the life cycles of the analyzed fish species, *O. labeo* has some differences compared to the other two. It is mainly a marine species; but it is common to find it in Ganzirri lagoon as well. It probably enters the brackish lagoon during the spawning period. The lagoon is a transition zone with high water trophism and low hydrodynamism, especially compared to the Strait of Messina waters. Because of these features, the study site represents a nursery area for many marine species and an optimal environment for feeding and protection against predators and the strong Strait of Messina currents. Further analysis of the ecology and life history traits of the studied species are required to better understand what drives the interspecific shape variations shown by the results. As reported in the previous literature on different species [28,34,64,84–89], the factors influencing sagittae shape diversity among species are manifold. They are mainly related to life history traits and ecological differences, highlighting how otoliths can reflect eco-morphological and morphofunctional adaptation to several habitats and lifestyles.

Moreover, our results have confirmed the effectiveness of interspecific variation among sagittae shape and morphology as a useful tool for discrimination among congeneric species, especially in a cryptic family such as Mugilidae. Indeed, discrimination of species

through taxonomic identification in this family is very difficult, due to high morphological similarities [40]. For this reason, molecular phylogenetic analysis provides essential information to understand the speciation mechanism of the Mugilidae family, as reported in the literature [42,90–92]. Interspecific morphological, morphometrical and shape differences among sagittae are another useful tool with which to discriminate among Mugilidae species. However, it is essential to consider the dual regulation which influence otolith growth and shape. Indeed, several studies have shown how environmental factors (e.g., water temperature and depth), species biology (e.g., year class, age, sex and stock) and genetics could influence the differences in otolith shape and morphology between stocks and species [23,93–96]. Further genetic analysis is required to understand the systematic relationship among studied species from Ganzirri lagoon and to evaluate the influence of genetics and environmental factors on otolith shape and morphology. This is essential for proper fisheries management and for all studies that involve such species with high commercial and ecological value.

The SEM imaging, performed in this study for the first time to investigate the sagittae external textural organization of *C. auratus, C. labrosus* and *O. labeo,* showed a very peculiar crystal organization.

SEM imaging analysis showed the presence of aragonitic crystals with various shapes (circular, hexagonal and lamellar forms) as described by previous research for other species [97]. As reported by a previous study on *Poecilia mexicana* (Steindachner, 1863) [98],large hexagonal crystals were detected in the sulcus acusticus of some *O. labeo* specimens (see Figure 12c,d). This peculiar crystalline habit was related to populations living in well-lit surface environments. Despite Ganzirri lagoon being a typical transitional environment,it is characterized by well-lit and oxygenated water for most of the year. In the *Acipenser brevirostrum* (Lesueur, 1818) specimens, these hexagonal crystals were described as calcite-like crystals [97]. The large rhombohedral crystals found in some *C. labrosus* specimens resembled those described in *Macruronus novaezelandiae* (Hector, 1871) as static calcitic crystals. Similar prismatic calcite crystals were also found in *Cilus gilberti,* (Abbott, 1899) and *Sciaena deliciosa* (Tschudi, 1846) specimens [99]. This carbonate habit was found in sulcus acusticus and near the posterior margin of *C. labrosus* specimens (see Figure 13b,d,e). Moreover, near the sagitta ventral margin, another peculiar crystal habit was detected (see Figure 13c,g,h), similar to those described in *Hoplostethus atlanticus* (Collett, 1889) as small granular vateritic crystals [97]. The large crystals found in *C. labrosus* (see Figure 16a–d) were like the calcium carbonate overgrowth observed by previous investigation on the otolith surface and in vitro crystallization experiments [100]. Moreover, the presence of on the sagitta surface of some specimens was also detected (see Figures 13h and 15b,c). These spherules, composed of several subunits, seemed to be similar to those described in *Encheliophis boraborensis* (Kaup, 1856) [101]. The spherules could be the layer of carbonate deposition, which give otoliths their globular surface. This globular carbonate deposition was similar to the calcium carbonate precipitate found on extracellular globules secreted by *Desulfonatronum lacustre* [102,103]. The endolymph proteins in teleosts' inner ears could induce carbonate precipitation, as seen in this bacterium [104], triggering the globular surface of otoliths with the presence of spherules, as shown in SEM images of the specimens analyzed in our study.

The presence of different crystal habits and of polymorphs with small locally oriented needles, long prism shapes, large rhombohedral crystals and globular secretion, especially in *C. labrosus* specimens, may be related to several environmental factors. Considering the Ganzirri lagoon, this is indeed a highly unstable environment close to the sea, with salinity fluctuation, which could influence the carbonate precipitation triggered by endolymph proteins and consequently the crystalline orientation and composition of otoliths, as reported in previous literature on other geographical area and species [1,11,12,31,34,105–115]. The presence of calcite and vaterite crystals and the several habits of different carbonate polymorphs are strictly related not only to environmental parameters, but also to individ- ual pathological conditions and the species' ecological features, such as feeding habits,

as demonstrated by several authors [76,107,109,110,115]. Further analysis on the microchemical composition of sagittae is required to confirm the presence and the percentage of different carbonate polymorphs, investigating also how their occurrence is related to the environmental conditions and parameters of Ganzirri lagoon, or to species ecology or physiology. The continuous environmental parameter monitoring of this brackish lagoon offers a unique opportunity to find a correlation between crystalline variations in sagittae and the physico-chemical parameters of a natural environment. Understanding the morphological, morphometrical and microcrystalline structure variations in relation to transitional environmental conditions is essential to increase knowledge about teleost adaptation to several environmental factors and habitats and to the investigation of how sagittae variations are related to environmental parameters or anthropogenic activities. Indeed, the changes between populations might be caused by both ecomorphological adaptation to different environments and genetic differentiation.

This study has also created data that will be useful as reference data for future studies by means of which it will be possible to improve conservation and sustainable exploitation in sensitive habitats such as transitional water. An improved analysis and study of Mugilidae sagitta microchemistry and crystal composition will aid the comprehension of the coastal lagoon's role in stock maintenance as an essential environment associated with recruitment, settlement and spawning [82,105–108]. Therefore, improving the conservation of these sensitive environments, with sustainable stock and habitat exploitation, is essential for species protection and for the good functioning of the entire marine ecosystem [91,116–121].

5. Conclusions

The present study provides an accurate description of sagitta morphology, morphometry, shape and crystal habits in *C. labrosus, C. auratus* and *O. labeo*, deepening our knowledge of inter- and intra-specific variations. This kind of study is essential for a correct evaluation and subdivision of several species and stocks, especially for cryptic species, such as those belonging to the Mugilidae family, which are of high commercial value. Proper fisheries management is essential for their conservation, to guarantee a sustainable exploitation level in compliance with the environmental history and ecology of the species; for this purpose, thorough and accurate studies of the otoliths of each Mugilidae species are needed. To the best of our knowledge, this study reports the first description of the external textural organization of *C. labrosus, C. auratus* and *O. labeo* investigated using SEM imaging, and the first otolith shape and contour analysis performed with R software. Morphometrical analysis on *O. labeo* sagittae has never been carried out before, and this study adds new and important information to the knowledge base.

SEM images of the crystalline structure showed peculiar crystalline habits and polymorphs which could be related to several factors, such as environmental parameters and chemical features of Ganzirri lagoon, individuals' physiological conditions and species ecological features. This study confirmed that otolith capacity reflects environmental and other parameters; this should be reconfirmed by further analyses of the same and similar areas.

Supplementary Materials: The following are available online at https://www.mdpi.com/article/10.3390/su14010398/s1, Figure S1: Representative stereomicroscope pictures of left Sagittal otoliths of Chelon auratus examined in the study. Scale bar: 3 mm; Figure S2: Representative stereomicroscope pictures of left Sagittal otoliths of Chelon labrosus examined in the study. Scale bar: 3 mm; Figure S3: Representative stereomicroscope pictures of left Sagittal otoliths of Oedalechilus labeo examined in the study. Scale bar: 3 mm. Table S4: Chemical parameter of Ganzirri lagoon during the sampling periods.

Author Contributions: Conceptualization, C.D. and G.C.; methodology, S.N., S.F. and M.A.; software, S.F. and S.S.; validation, S.N., C.G. and C.D.; formal analysis, S.S. and S.F.; investigation, C.D. and M.A.; resources, N.S.; data curation, G.L.; writing—original draft preparation, C.D. and S.N.; writing—review and editing, G.C., S.S. and M.A.; visualization, G.P.; supervision, N.S. and G.C.; project administration, N.S. and G.C.; funding acquisition, N.S. and G.C. All authors have read and agreed to the published version of the manuscript.

Funding: This research received no external funding.

Institutional Review Board Statement: Not applicable.

Informed Consent Statement: Not applicable.

Data Availability Statement: Not applicable.

Conflicts of Interest: The authors declare no conflict of interest.

References

1. Schulz-Mirbach, T.; Ladich, F.; Plath, M.; Heß, M. Enigmatic ear stones: What we know about the functional role and evolution of fish otoliths. *Biol. Rev.* **2019**, *94*, 457–482. [CrossRef] [PubMed]
2. Flock, Å.; Goldstein, M.H. Cupular movement and nerve impulse response in the isolated semicircular canal. *Brain Res.* **1978**, *157*, 11–19. [CrossRef]
3. Lowenstein, O.; Roberts, T.D.M. The equilibrium function of the otolith organs of the thornback ray (*Raja clavata*). *J. Physiol.* **1949**, *110*, 392–415. [CrossRef] [PubMed]
4. Anken, R.H.; Baur, U.; Hilbig, R. Clinorotation increases the growth of utricular otoliths of developing cichlid fish. *Microgravity Sci. Technol.* **2010**, *22*, 151–154. [CrossRef]
5. Hawkins, A.D. Underwater sound and fish behaviour. In *Behaviour of Teleost Fishes*; Springer: Boston, MA, USA, 1993; pp. 129–169.
6. v. Frisch, K. Über den Sitz des Geruchsinnes bei Insekten. *Naturwissenschaften* **1922**, *10*, 454–455. [CrossRef]
7. Fay, R.R. The goldfish ear codes the axis of acoustic particle motion in three dimensions. *Science* **1984**, *225*, 951–954. [CrossRef]
8. Cermeño, P.; Morales-Nin, B.; Uriarte, A. Juvenile European anchovy otolith microstructure. *Sci. Mar.* **2006**, *70*, 553–557. [CrossRef]
9. Nolf, D. *Otolithi Piscium. Handbook of Paleoichthyology*; Fischer, G., Ed.; Lubrecht & Cramer Ltd.: Port Jervis, NY, USA, 1985; Volume 10.
10. Pannella, G. Fish otoliths: Daily growth layers and periodical patterns. *Science* **1971**, *173*, 1124–1127. [CrossRef]
11. Campana, S.E. Chemistry and composition of fish otoliths: Pathways, mechanisms and applications. *Mar. Ecol. Prog. Ser.* **1999**, *188*, 263–297. [CrossRef]
12. Campana, S.E.; Thorrold, S.R. Otoliths, increments, and elements: Keys to a comprehensive understanding of fish populations? *Can. J. Fish. Aquat. Sci.* **2001**, *58*, 30–38. [CrossRef]
13. Kerr, L.A.; Campana, S.E. Chemical Composition of Fish Hard Parts as a Natural Marker of Fish Stocks. In *Stock Identification Methods: Applications in Fishery Science*, 2nd ed.; Elsevier: San Diego, CA, USA, 2013; pp. 205–234. ISBN 9780123970039.
14. Morales-Nin, B. Review of the growth regulation processes of otolith daily increment formation. *Fish. Res.* **2000**, *46*, 53–67. [CrossRef]
15. Nolf, D.; de Potter, H.; Lafond-Grellety, J. *Hommage à Joseph Chaine et Jean Duvergier: Diversité et Variabilité des Otolithes des Poissons*; Palaeo Publishing and Library vzw: Mortsel, Belgium, 2009.
16. Tuset, V.M.; Farré, M.; Otero-Ferrer, J.L.; Vilar, A.; Morales-Nin, B.; Lombarte, A. Testing otolith morphology for measuring marine fish biodiversity. *Mar. Freshw. Res.* **2016**, *67*, 1037–1048. [CrossRef]
17. Tuset, V.M.; Lombarte, A.; Assis, C.A. Otolith atlas for the western Mediterranean, north and central eastern Atlantic. *Sci. Mar.* **2008**, *72*, 7–198. [CrossRef]
18. Nolf, D. Studies on fossil otoliths—The state of the art. *Recent Dev. Fish. Otolith Res.* **1995**, *19*, 513–544.
19. Lin, C.H.; Girone, A.; Nolf, D. Fish otolith assemblages from Recent NE Atlantic sea bottoms: A comparative study of palaeoecology. *Palaeogeogr. Palaeoclimatol. Palaeoecol.* **2016**, *446*, 98–107. [CrossRef]
20. Disspain, M.C.F.; Ulm, S.; Gillanders, B.M. Otoliths in archaeology: Methods, applications and future prospects. *J. Archaeol. Sci. Rep.* **2016**, *6*, 623–632. [CrossRef]
21. D'Iglio, C.; Savoca, S.; Rinelli, P.; Spanò, N. Diet of the Deep-Sea Shark Galeus melastomus Rafinesque, 1810, in the Mediterranean Sea: What We Know and What We Should Know. *Sustainability* **2021**, *13*, 3962. [CrossRef]
22. D'Iglio, C.; Albano, M.; Tiralongo, F.; Famulari, S.; Rinelli, P.; Savoca, S.; Spanò, N.; Capillo, G. Biological and Ecological Aspects of the Blackmouth Catshark (Galeus melastomus Rafinesque, 1810) in the Southern Tyrrhenian Sea. *J. Mar. Sci. Eng.* **2021**, *9*, 967. [CrossRef]
23. Mahé, K.; Evano, H.; Mille, T.; Muths, D.; Bourjea, J. Otolith shape as a valuable tool to evaluate the stock structure of swordfish Xiphias gladius in the Indian Ocean. *African J. Mar. Sci.* **2016**, *38*, 457–464. [CrossRef]
24. Morat, F.; Letourneur, Y.; Nérini, D.; Banaru, D.; Batjakas, I.E. Discrimination of red mullet populations (Teleostean, Mullidae) along multi-spatial and ontogenetic scales within the Mediterranean basin on the basis of otolith shape analysis. *Aquat. Living Resour.* **2012**, *25*, 27–39. [CrossRef]
25. Vignon, M.; Morat, F. Environmental and genetic determinant of otolith shape revealed by a non-indigenous tropical fish. *Mar. Ecol. Prog. Ser.* **2010**, *411*, 231–241. [CrossRef]
26. Ramírez-Pérez, J.S.; Quiñónez-Velazquez, C.; García-Rodríguez, F.J.; Félix-Uraga, R.; Melo-Barrera, F.N. Using the shape of Sagitta Otoliths in the discrimination of phenotypic stocks in Scomberomorus sierra (Jordan and Starks, 1895). *J. Fish. Aquat. Sci.* **2010**, *5*, 82–93. [CrossRef]

27. Marengo, M.; Baudouin, M.; Viret, A.; Laporte, M.; Berrebi, P.; Vignon, M.; Marchand, B.; Durieux, E.D.H. Combining microsatellite, otolith shape and parasites community analyses as a holistic approach to assess population structure of Dentex dentex. *J. Sea Res.* **2017**, *128*, 1–14. [CrossRef]
28. Rebaya, M.; Ben Faleh, A.; Allaya, H.; Khedher, M.; Trojette, M.; Marsaoui, B.; Fatnassi, M.; Chalh, A.; Quignard, J.P.; Trabelsi, M. Otolith shape discrimination of Liza ramada (Actinopterygii: Mugiliformes: Mugilidae) from marine and estuarine populations in Tunisia. *Acta Ichthyol. Piscat.* **2017**, *47*, 13–21. [CrossRef]
29. Starrs, D.; Ebner, B.C.; Fulton, C.J. All in the ears: Unlocking the early life history biology and spatial ecology of fishes. *Biol. Rev.* **2016**, *91*, 86–105. [CrossRef] [PubMed]
30. McGowan, N.; Fowler, A.M.; Parkinson, K.; Bishop, D.P.; Ganio, K.; Doble, P.A.; Booth, D.J.; Hare, D.J. Beyond the transect: An alternative microchemical imaging method for fine scale analysis of trace elements in fish otoliths during early life. *Sci. Total Environ.* **2014**, *494–495*, 177–186. [CrossRef] [PubMed]
31. Izzo, C.; Doubleday, Z.A.; Schultz, A.G.; Woodcock, S.H.; Gillanders, B.M. Contribution of water chemistry and fish condition to otolith chemistry: Comparisons across salinity environments. *J. Fish. Biol.* **2015**, *86*, 1680–1698. [CrossRef]
32. Lombarte, A.; Tuset, V.M. Chapter3-Morfometría de otolitos. In *Métodos de Estudios con Otolitos: Principios y Aplicaciones/ Métodos de Estudos com Otólitos: Princípios e Aplicações*; Volpedo, A.V., Vaz-dos-Santos, A.M., Eds.; PIESCE-SPU: Buenos Aires, Argentina, 2015; p. 31.
33. D'Iglio, C.; Albano, M.; Famulari, S.; Savoca, S.; Panarello, G.; Di Paola, D.; Perdichizzi, A.; Rinelli, P.; Lanteri, G.; Spanò, N.; et al. Intra- and interspecific variability among congeneric Pagellus otoliths. *Sci. Rep.* **2021**, *11*, 16315. [CrossRef]
34. Popper, A.N.; Ramcharitar, J.; Campana, S.E. Why otoliths? Insights from inner ear physiology and fisheries biology. *Mar. Freshw. Res.* **2005**, *56*, 497–504. [CrossRef]
35. Montanini, S.; Stagioni, M.; Valdrè, G.; Tommasini, S.; Vallisneri, M. Intra-specific and inter-specific variability of the sulcus acusticus of sagittal otoliths in two gurnard species (Scorpaeniformes, Triglidae). *Fish. Res.* **2015**, *161*, 93–101. [CrossRef]
36. Bolles, K.L.; Begg, G.A. Distinction between silver hake (Merluccius bilinearis) stocks in U.S. waters of the northwest Atlantic based on whole otolith morphometrics. *Fish. Bull.* **2000**, *98*, 451–462.
37. Murta, A.G. Morphological variation of horse mackerel (Trachurus trachurus) in the Iberian and North African Atlantic: Implications for stock identification. *ICES J. Mar. Sci.* **2000**, *57*, 1240–1248. [CrossRef]
38. González Castro, M.; Abachian, V.; Perrotta, R.G. Age and growth of the striped mullet, Mugil platanus (Actinopterygii, Mugilidae), in a southwestern Atlantic coastal lagoon (37°32'S-57°19'W): A proposal for a life-history model. *J. Appl. Ichthyol.* **2009**, *25*, 61–66. [CrossRef]
39. González-Castro, M.; Macchi, G.J.; Cousseau, M.B. Studies on reproduction of the mullet Mugil platanus Günther, 1880 (Actinopterygii, Mugilidae) from the Mar Chiquita coastal lagoon, Argentina: Similarities and differences with related species. *Ital. J. Zool.* **2011**, *78*, 343–353. [CrossRef]
40. Whitfield, A.K. Ecological Role of Mugilidae in the Coastal Zone. In *Biology, Ecology and Culture of Grey Mullets*; CRC Press: Boca Raton, FL, USA, 2015; pp. 334–358. [CrossRef]
41. Whitfield, A.K.; Panfili, J.; Durand, J.D. A global review of the cosmopolitan flathead mullet Mugil cephalus Linnaeus 1758 (Teleostei: Mugilidae), with emphasis on the biology, genetics, ecology and fisheries aspects of this apparent species complex. *Rev. Fish. Biol. Fish.* **2012**, *22*, 641–681. [CrossRef]
42. Callicó Fortunato, R.; Benedito Durà, V.; Volpedo, A. The morphology of saccular otoliths as a tool to identify different mugilid species from the Northeastern Atlantic and Mediterranean Sea. *Estuar. Coast. Shelf Sci.* **2014**, *146*, 95–101. [CrossRef]
43. Turan, C.; Gürlek, M.; Ergüden, D.; Yağlioğlu, D.; Öztürk, B. Systematic status of nine mullet species (mugilidae) in the Mediterranean sea. *Turk. J. Fish. Aquat. Sci.* **2011**, *11*, 315–321. [CrossRef]
44. Gallardo-Cabello, M.; Espino-Barr, E.; Cabral-Solís, E.G.; Puente-Gómez, M.; García-Boa, A. Study of the otoliths of stripped mullet Mugil cephalus Linnaeus, 1758 in Mexican Central Pacific. *J. Fish. Aquat. Sci.* **2012**, *7*, 346–363. [CrossRef]
45. Marin, E.; Baumar, J.; Quintero, A.; Bussière, D.; Dodson, J.J. Reproduction and recruitment of white mullet (Mugil curema) to a tropical lagoon (Margarita Island, Venezuela) as revealed by otolith microstructure. *Fish. Bull.* **2003**, *101*, 809–821.
46. Thomson, J.M. The Mugilidae of the world. *Mem. Queensl. Museum* **1997**, *41*, 547–562.
47. Bacheler, N.M.; Wong, R.A.; Buckel, J.A. Movements and Mortality Rates of Striped Mullet in North Carolina. *N. Am. J. Fish. Manag.* **2005**, *25*, 361–373. [CrossRef]
48. Greenwood, P.H.; Daget, J.; Gosse, J.P.; Thys van den Audenaerde, D.F.E. Check-List of the Freshwater Fishes of Africa. CLOFFA. ORSTOM Paris, MARC Tervuren. 1984. Available online: https://horizon.documentation.ird.fr/exl-doc/pleins_textes/divers13-06/15357.pdf (accessed on 26 December 2021).
49. Cardona, L. Habitat selection by grey mullets (Osteichthytes: Mugilidae) in Mediterranean estuaries: The role of salinity. *Sci. Mar.* **2006**, *70*, 443–455. [CrossRef]
50. Wheeler, A.; Whitehead, P.J.P.; Bauchot, M.-L.; Hureau, J.-C.; Nielsen, J.; Tortonese, E. Fishes of the North-Eastern Atlantic and the Mediterranean. Vol. 1. *Copeia* **1986**, *1986*, 266. [CrossRef]
51. Costa, F. *Atlante dei Pesci dei Mari Italiani*; Biblioteca del mare; Ugo Mursia Editore: Milan, Italy, 1991; ISBN 9788842522591.
52. Koutsidi, M.; Moukas, C.; Tzanatos, E. Trait-based life strategies, ecological niches, and niche overlap in the nekton of the data-poor Mediterranean Sea. *Ecol. Evol.* **2020**, *10*, 7129–7144. [CrossRef]

53. Blanco, S.; Romo, S.; Villena, M.J.; Martínez, S. Fish communities and food web interactions in some shallow Mediterranean lakes. *Hydrobiologia* **2003**, *506–509*, 473–480. [CrossRef]
54. Manganaro, A.; Pulicanò, G.; Sanfilippo, M. Temporal evolution of the area of Capo Peloro (Sicily, Italy) from pristine site into urbanized area. *Transit. Waters Bull.* **2011**, *5*, 23–31. [CrossRef]
55. Bottari, A.; Bottari, C.; Carveni, P.; Giacobbe, S.; Spanò, N. Genesis and geomorphologic and ecological evolution of the Ganzirri salt marsh (Messina, Italy). *Quat. Int.* **2005**, *140–141*, 150–158. [CrossRef]
56. Albano, M.; Panarello, G.; Di Paola, D.; D'Angelo, G.; Granata, A.; Savoca, S.; Capillo, G. The mauve stinger Pelagia noctiluca (Cnidaria, Scyphozoa) plastics contamination, the Strait of Messina case. *Int. J. Environ. Stud.* **2021**, *78*, 977–982. [CrossRef]
57. Savoca, S.; Grifó, G.; Panarello, G.; Albano, M.; Giacobbe, S.; Capillo, G.; Spanó, N.; Consolo, G. Modelling prey-predator interactions in Messina beachrock pools. *Ecol. Modell.* **2020**, *434*, 109206. [CrossRef]
58. Capillo, G.; Panarello, G.; Savoca, S.; Sanfilippo, M.; Albano, M.; Volsi, R.L.; Consolo, G.; Spanò, N. Intertidal ponds of messina's beachrock faunal assemblage, evaluation of ecosystem dynamics and communities' interactions. *AAPP Atti Accad. Pelorit. Pericol. Cl. Sci. Fis. Mat. Nat.* **2018**, *96*, A41–A416. [CrossRef]
59. Mazzola, A.; Bergamasco, A.; Calvo, S.; Caruso, G.; Chemello, R.; Colombo, F.; Giaccone, G.; Gianguzza, P.; Guglielmo, L.;Leonardi, M.; et al. Sicilian transitional waters: Current status and future development. *Chem. Ecol.* **2010**, *26*, 267–283. [CrossRef]
60. Sanfilippo, M. La Componente Organica del Seston nel Lago di Ganzirri: Qualità e Valore Nutrizionale come Risorsa Ambientale. Ph.D. Thesis, University of Messina, Messina, Italy, 2000.
61. Regione Sicilia. *Istituzione della Riserva Naturale Laguna di Capo Peloro, Ricadente nel Comune di Messina*; Regione Sicilia: Messina, Italy, 21 June 2011.
62. Ec. *Council Directive 92/43/EEC on the Conservation of Natural Habitats and of Wild Fauna and Flora*; European Commission: Bruxelles, Belgium, 1992; Volume L269, pp. 1–15.
63. European Community. *Council Directive of 2 April 1979 on the Conservation of Wild Birds (79/409/EEC)*; European Community: Bruxelles, Belgium, 1979; Volume 94, p. 18.
64. Fischer, W. Fiches FAO d'identification des especes pour les besoins de la peche. (Revision 1). In *Mediterranee et mer Noire. Zone de Peche 37. Vertebres*; FAO: Rome, Italy, 1987.
65. Bauchot, M.-L. Poissons osseux. Fiches FAO d'identification des espèces pour les besoins la pêche. (Révision 1). In *Méditerranée mer Noire. rZone Pêche 37. Vol. II. Vertébrés*; FAO: Rome, Italy, 1987.
66. Spanò, N.; Di Paola, D.; Albano, M.; Manganaro, A.; Sanfilippo, M.; D'Iglio, C.; Capillo, G.; Savoca, S. Growth performanceand bioremediation potential of Gracilaria gracilis (Steentoft, L.M. Irvine & Farnham, 1995). *Int. J. Environ. Stud.* **2021**, 1–13. [CrossRef]
67. Follesa, M.C.; Carbonara, P. *Atlas of the Maturity Stages of Mediterranean Fishery Resources. Studies and Reviews N. 99*; FAO: Rome, Italy, 2019; ISBN 9789251319758.
68. Schneider, C.A.; Rasband, W.S.; Eliceiri, K.W. NIH Image to ImageJ: 25 years of image analysis. *Nat. Methods* **2012**, *9*, 671–675. [CrossRef] [PubMed]
69. Jawad, L.A.; Sabatino, G.; Ibáñez, A.L.; Andaloro, F.; Battaglia, P. Morphology and ontogenetic changes in otoliths of the mesopelagic fishes Ceratoscopelus maderensis (Myctophidae), Vinciguerria attenuata and V. poweriae (Phosichthyidae) from the Strait of Messina (Mediterranean Sea). *Acta Zool.* **2018**, *99*, 126–142. [CrossRef]
70. Libungan, L.A.; Pálsson, S. ShapeR: An R package to study otolith shape variation among fish populations. *PLoS ONE* **2015**, *10*, 1–12. [CrossRef] [PubMed]
71. Zhuang, L.; Ye, Z.; Zhang, C.; Ye, Z.; Li, Z.; Wan, R.; Ren, Y.; Dou, S.; Wheeler, A.; Whitehead, P.J.P.; et al. Stock discrimination of two insular populations of diplodus annularis (Actinopterygii: Perciformes: Sparidae) along the coast of tunisia by analysis of otolith shape. *J. Fish. Biol.* **2015**, *46*, 1–14. [CrossRef]
72. Bose, A.P.H.; Zimmermann, H.; Winkler, G.; Kaufmann, A.; Strohmeier, T.; Koblmüller, S.; Sefc, K.M. Congruent geographic variation in saccular otolith shape across multiple species of African cichlids. *Sci. Rep.* **2020**, *10*, 1–14. [CrossRef]
73. Abaad, M.; Tuset, V.M.; Montero, D.; Lombarte, A.; Otero-Ferrer, J.L.; Haroun, R. Phenotypic plasticity in wild marine fishes associated with fish-cage aquaculture. *Hydrobiologia* **2016**, *765*, 343–358. [CrossRef]
74. Sadighzadeh, Z.; Tuset, V.M.; Valinassab, T.; Dadpour, M.R.; Lombarte, A. Comparison of different otolith shape descriptors and morphometrics for the identification of closely related species of Lutjanus spp. from the Persian Gulf. *Mar. Biol. Res.* **2012**, *8*, 802–814. [CrossRef]
75. Torres, G.J.; Lombarte, A.; Morales-Nin, B. Sagittal otolith size and shape variability to identify geographical intraspecific differences in three species of the genus Merluccius. *J. Mar. Biol. Assoc. U. K.* **2000**, *80*, 333–342. [CrossRef]
76. Gauldie, R.W.; Crampton, J.S. An eco-morphological explanation of individual variability in the shape of the fish otolith: Comparison of the otolith of Hoplostethus atlanticus with other species by depth. *J. Fish. Biol.* **2002**, *60*, 1204–1221. [CrossRef]
77. Sadeghi, R.; Esmaeili, H.R.; Zarei, F.; Reichenbacher, B. Population structure of the ornate goby, Istigobius ornatus (Teleostei: Gobiidae), in the Persian Gulf and Oman Sea as determined by otolith shape variation using ShapeR. *Environ. Biol. Fishes* **2020**, *103*, 1217–1230. [CrossRef]
78. Bose, A.P.H.; Adragna, J.B.; Balshine, S. Otolith morphology varies between populations, sexes and male alternative reproductive tactics in a vocal toadfish Porichthys notatus. *J. Fish. Biol.* **2017**, *90*, 311–325. [CrossRef]

79. Çiçek, E.; Avşar, D.; Yeldan, H.; Manaşirli, M. Comparative morphology of the sagittal otolith of mullet species (Mugilidae) from the Iskenderun Bay, north-eastern Mediterranean. *Acta Biol. Turc.* **2020**, *33*, 219–226.
80. Bauzà Rullan, J. Nueva contribución al conocimiento de los otolitos de peces actuales. *Bolletí Soc. d'Història Nat. Balear.* **1960**, *6*, 49–69.
81. Mahé, K.; MacKenzie, K.; Ider, D.; Massaro, A.; Hamed, O.; Jurado-Ruzafa, A.; Gonçalves, P.; Anastasopoulou, A.; Jadaud, A.; Mytilineou, C.; et al. Directional Bilateral Asymmetry in Fish Otolith: A Potential Tool to Evaluate Stock Boundaries? *Symmetry* **2021**, *13*, 987. [CrossRef]
82. Mahé, K.; Ider, D.; Massaro, A.; Hamed, O.; Jurado-Ruzafa, A.; Gonçalves, P.; Anastasopoulou, A.; Jadaud, A.; Mytilineou, C.; Elleboode, R.; et al. Directional bilateral asymmetry in otolith morphology may affect fish stock discrimination based on otolith shape analysis. *ICES J. Mar. Sci.* **2019**, *76*, 232–243. [CrossRef]
83. Raffa, C.; Rizzo, C.; Strous, M.; De Domenico, E.; Sanfilippo, M.; Michaud, L.; Lo Giudice, A. Prokaryotic dynamics in the meromictic coastal Lake Faro (Sicily, Italy). *Diversity* **2019**, *11*, 37. [CrossRef]
84. Giordani, G.; Viaroli, P.; Swaney, D.P.; Murray, N.C. *Nutrient Fluxes in Transitional Zones of the Italian Coast*; LOICZ: Texel, The Netherlands, 2005.
85. Elsdon, T.S.; Wells, B.K.; Campana, S.E.; Gillanders, B.M.; Jones, C.M.; Limburg, K.E.; Secor, D.H.; Thorrold, S.R.; Walther, B.D. Otolith chemistry to describe movements and life-history parameters of fishes: Hypotheses, assumptions, limitations and inferences. In *Oceanography and Marine Biology*; CRC Press: Boca Raton, FL, USA, 2008; Volume 46, pp. 297–330. ISBN 0429137257.
86. Campana, S.E.; Gagne, J.A.; McLaren, J.W. Elemental fingerprinting of fish otoliths using ID-ICPMS. *Mar. Ecol. Prog. Ser.* **1995**, *122*, 115–120. [CrossRef]
87. Vrdoljak, D.; Matić-Skoko, S.; Peharda, M.; Uvanović, H.; Markulin, K.; Mertz-Kraus, R. Otolith fingerprints reveals potential pollution exposure of newly settled juvenile Sparus aurata. *Mar. Pollut. Bull.* **2020**, *160*, 111695. [CrossRef]
88. Capoccioni, F.; Costa, C.; Aguzzi, J.; Menesatti, P.; Lombarte, A.; Ciccotti, E. Ontogenetic and environmental effects on otolith shape variability in three Mediterranean European eel (*Anguilla anguilla*, L.) local stocks. *J. Exp. Mar. Bio. Ecol.* **2011**, *397*, 1–7. [CrossRef]
89. Loeppky, A.R.; Belding, L.D.; Quijada-Rodriguez, A.R.; Morgan, J.D.; Pracheil, B.M.; Chakoumakos, B.C.; Anderson, W.G. Influence of ontogenetic development, temperature, and pCO2 on otolith calcium carbonate polymorph composition in sturgeons. *Sci. Rep.* **2021**, *11*, 1–10. [CrossRef] [PubMed]
90. Matić-Skoko, S.; Peharda, M.; Vrdoljak, D.; Uvanović, H.; Markulin, K. Fish and Sclerochronology Research in the Mediterranean: Challenges and Opportunities for Reconstructing Environmental Changes. *Front. Mar. Sci.* **2020**, *7*, 195. [CrossRef]
91. Matić-Skoko, S.; Vrdoljak, D.; Uvanović, H.; Pavičić, M.; Tutman, P.; Bojanić Varezić, D. Early evidence of a shift in juvenile fish communities in response to conditions in nursery areas. *Sci. Rep.* **2020**, *10*, 1–16. [CrossRef]
92. Lombarte, A.; Lleonart, J. Otolith size changes related with body growth, habitat depth and temperature. *Environ. Biol. Fishes* **1993**, *37*, 297–306. [CrossRef]
93. Aguirre, H.; Lombarte, A. Ecomorphological comparisons of sagittae in Mullus barbatus and M. surmuletus. *J. Fish. Biol.* **1999**, *55*, 105–114. [CrossRef]
94. Torres, G.J.; Lombarte, A.; Morales-Nin, B. Variability of the sulcus acusticus in the sagittal otolith of the genus Merluccius (Merlucciidae). *Fish. Res.* **2000**, *46*, 5–13. [CrossRef]
95. Volpedo, A.; Diana Echeverría, D. Ecomorphological patterns of the sagitta in fish on the continental shelf off Argentine. *Fish. Res.* **2003**, *60*, 551–560. [CrossRef]
96. Cruz, A.; Lombarte, A. Otolith size and its relationship with colour patterns and sound production. *J. Fish. Biol.* **2004**, *65*, 1512–1525. [CrossRef]
97. Stransky, C.; Murta, A.G.; Schlickeisen, J.; Zimmermann, C. Otolith shape analysis as a tool for stock separation of horse mackerel (*Trachurus trachurus*) in the Northeast Atlantic and Mediterranean. *Fish. Res.* **2008**, *89*, 159–166. [CrossRef]
98. Popper, A.N.; Lu, Z. Structure-function relationships in fish otolith organs. *Fish. Res.* **2000**, *46*, 15–25. [CrossRef]
99. Jaramilo, A.M.; Tombari, A.D.; Benedito Dura, V.; Eugeni Rodrigo, M.; Volpedo, A.V. Otolith eco-morphological patterns of benthic fishes from the coast of Valencia (Spain). *Thalassas* **2014**, *30*, 57–66.
100. Turan, C.; Caliskan, M.; Kucuktas, H. Phylogenetic relationships of nine mullet species (Mugilidae) in the Mediterranean Sea. *Hydrobiologia* **2005**, *532*, 45–51. [CrossRef]
101. Durand, J.D.; Shen, K.N.; Chen, W.J.; Jamandre, B.W.; Blel, H.; Diop, K.; Nirchio, M.; Garcia de León, F.J.; Whitfield, A.K.; Chang, C.W.; et al. Systematics of the grey mullets (Teleostei: Mugiliformes: Mugilidae): Molecular phylogenetic evidence challenges two centuries of morphology-based taxonomy. *Mol. Phylogenet. Evol.* **2012**, *64*, 73–92. [CrossRef] [PubMed]
102. Papasotiropoulos, V.; Klossa-Kilia, E.; Kilias, G.; Alahiotis, S. Genetic divergence and phylogenetic relationships in grey mullets (Teleostei: Mugilidae) based on PCR-RFLP analysis of mtDNA segments. *Biochem. Genet.* **2002**, *40*, 71–86. [CrossRef] [PubMed]
103. Cardinale, M.; Doering-Arjes, P.; Kastowsky, M.; Mosegaard, H. Effects of sex, stock, and environment on the shape of known-age Atlantic cod (Gadus morhua) otoliths. *Can. J. Fish. Aquat. Sci.* **2004**, *61*, 158–167. [CrossRef]
104. Simoneau, M.; Casselman, J.M.; Fortin, R. Determining the effect of negative allometry (length/height relationship) on variation in otolith shape in lake trout (Salvelinus namaycush), using Fourier-series analysis. *Can. J. Zool.* **2000**, *78*, 1597–1603. [CrossRef]
105. Monteiro, L.R.; Di Beneditto, A.P.M.; Guillermo, L.H.; Rivera, L.A. Allometric changes and shape differentiation of sagitta otoliths in sciaenid fishes. *Fish. Res.* **2005**, *74*, 288–299. [CrossRef]

106. Hüssy, K. Otolith shape in juvenile cod (Gadus morhua): Ontogenetic and environmental effects. *J. Exp. Mar. Bio. Ecol.* **2008**, *364*, 35–41. [CrossRef]
107. Gauldie, R.W. Polymorphic crystalline structure of fish otoliths. *J. Morphol.* **1993**, *218*, 1–28. [CrossRef]
108. Schulz-Mirbach, T.; Riesch, R.; García de León, F.J.; Plath, M. Effects of extreme habitat conditions on otolith morphology—a case study on extremophile livebearing fishes (Poecilia mexicana, P. sulphuraria). *Zoology* **2011**, *114*, 321–334. [CrossRef]
109. Béarez, P.; Carlier, G.; Lorand, J.P.; Parodi, G.C. Destructive and non-destructive microanalysis of biocarbonates applied to anomalous otoliths of archaeological and modern sciaenids (Teleostei) from Peru and Chile. *Comptes Rendus-Biol.* **2005**, *328*, 243–252. [CrossRef]
110. Falini, G.; Fermani, S.; Vanzo, S.; Miletic, M.; Zaffino, G. Influence on the formation of aragonite or vaterite by otolith macromolecules. *Eur. J. Inorg. Chem.* **2005**, *2005*, 162–167. [CrossRef]
111. Parmentier, E.; Cloots, R.; Warin, R.; Henrist, C. Otolith crystals (in Carapidae): Growth and habit. *J. Struct. Biol.* **2007**, *159*, 462–473. [CrossRef]
112. Wilcox Freeburg, E.D. Exploring the Link between Otolith Growth and Function along the Biological Continuum in the Context of Ocean. Acidification. Ph.D. Thesis, University of Massachusetts Boston, Boston, MA, USA, 2014.
113. Pikuta, E.V. Desulfonatronum lacustre gen. nov., sp. nov.: A new alkaliphilic sulfate-reducing bacterium utilizing ethanol. *Mikrobiologiya* **1998**, *67*, 123–131.
114. Aloisi, G.; Gloter, A.; Krüger, M.; Wallman, K.; Guyot, F.; Zuddas, P. Nucleation of calcium carbonate on bacterial nanoglobules. *Geology* **2006**, *34*, 1017–1020. [CrossRef]
115. Schulz-Mirbach, T.; Götz, A.; Griesshaber, E.; Plath, M.; Schmahl, W.W. Texture and nano-scale internal microstructure of otoliths in the atlantic molly, poecilia mexicana: A high-resolution EBSD study. *Micron* **2013**, *51*, 60–69. [CrossRef] [PubMed]
116. Beck, M.; Heck, K.; Able, K.; Bioscience, D.C.-; 2001, U. The identification, conservation, and management of estuarine and marine nurseries for fish and invertebrates: A better understanding of the habitats that serve as. *Bioscience* **2001**, *51*, 633–641. [CrossRef]
117. Cowen, R.K.; Lwiza, K.M.M.; Sponaugle, S.; Paris, C.B.; Olson, D.B. Connectivity of marine populations: Open or closed? *Science* **2000**, *287*, 857–859. [CrossRef] [PubMed]
118. Houde, E.D. Comparative growth, mortality, and energetics of marine fish larvae: Temperature and implied latitudinal effects. *Fish. Bull.* **1989**, *87*, 471–495.
119. Matić-Skoko, S.; Peharda, M.; Pallaoro, A.; Franičević, M. Species composition, seasonal fluctuations, and residency of inshore fish assemblages in the Pantan estuary of the eastern middle Adriatic. *Acta Adriat.* **2005**, *46*, 201–212.
120. Dulčić, J.; Matić-Skoko, S.; Kraljević, M.; Fencil, M.; Glamuzina, B. Seasonality of a fish assemblage in shallow waters of Duće-Glava, eastern middle Adriatic. *Cybium* **2005**, *29*, 57–63.
121. Dulčić, J.; Matić, S.; Kraljević, M. Shallow coves as nurseries for non-resident fish: A case study in the eastern middle Adriatic. *J. Mar. Biol. Assoc. U. K.* **2002**, *82*, 991–993. [CrossRef]

Eco-morphology of sagittal otoliths in five Macrouridae species from Central Mediterranean Sea

ABSTRACT

The increase of deep environments exploitation and depletion related to fisheries activities have enhanced the needing to improve the knowledge base about demersal and abyssal species. Macrourids are an ecologically essential component of bathyal community, and among the most abundant species in the deep environments world-wide. Present paper aims to investigate the *sagittae* morphology, morphometry, and shape of five Mediterranean's Macrouridae species, investigating their intra and inter specific relationships, also comparing data with literature from other geographical areas. Result showed the absence of directional bilateral asymmetry in all the studied species, with clear differences in morphometry and shape at inter specific level. They were detected statistically significant similarity patterns between *Coelorinchus caelorhincus* and *Coryphaenoides guentheri* specimens (*Coelorhynchus*/*Coryphaenoides* group), and even between *Nezumia aequalis* and *Nezumia sclerorhynchus* specimens (*Nezumia* sp group). *Hymenocephalus italicus* showed the most marked differences in otoliths features compared to the other investigated species. Results confirmed the similarity in shape and morphometry of *sagittae* belonging to phylogenetically close species, sharing several aspects of their life habits. Furter analysis on the genetics, growth dynamics, feeding habits and environmental conditions experienced by specimens are required to confirm the environmental influence on *sagittae*, also comparing data from different Macruridae populations.

Keywords: Macrouridae, sagittae, otolith analysis, Shape analysis, Tyrrhenian Sea

1. INTRODUCTION

Concerning marine demersal domain, species belonging to Macrouridae family, also called grenadiers or rattails, are among the most globally abundant for biomass (Shi et al., 2016) and species numbers (405 of valid species) (Eschmeyer and Fong, 2014). These benthopelagic global distributed species inhabit a wide range of environments, from the continental shelves and slopes between 200 and 2000 m (Dunn et al., 1992; Marshall, 1979; Weitzman, 1997), to the abyssal plains between 2000 and 6000 m (Gaither et al., 2016; Linley et al., 2016). In the Mediterranean Sea, this family represents an essential component of the bathyal community in continental slope environments (García-Ruiz et

al., 2019; Sobrino et al., 2012), and a dominant component for abundance below the 1000 m of depth (Danovaro et al., 2010), with temporal and spatial trends in abundance and distribution which vary geographically for the different species (García-Ruiz et al., 2019). Grenadiers, despite their low commercial value in Mediterranean basin, are caught by trawling fisheries, being one of the major components of by-catch in deep-seas shrimps fisheries (D'Onghia et al., 2000, 1998; Matarrese et al., 1996). The increases of deep environments exploitation and depletion related to fisheries activities (Devine et al., 2012; Kuemlangan and Sanders, 2008; Norse et al., 2012), together with the essential role of species belonging to Macrouridae family for meso- and bathypelagic ecological dynamics (Drazen, 2002; Stergiou and Karpouzi, 2002), have led to an improving attention of scientific community on grenadiers species to monitor the effects of over-exploitation on Mediterranean demersal fish assemblage and deep habitats.

In the Mediterranean basin, the Macrouridae family is composed by eight species, belonging to five genera (*Coelorinchus*, Giorna, 1809, *Coryphaenoides*, Gunnerus, 1765, *Hymenocephalus*, Giglioli, 1884, *Nezumia*, Jordan, 1904, *Trachyrincus*, Giorna, 1809) (Bauchot, 1987; Lloris, 2015). Present paper aims to investigate the intra and inter specific sagittal otoliths variability in five species of grenadiers (*Hymenocephalus italicus*, Giglioli, 1884, *Nezumia sclerorhynchus*, Valenciennes, 1838, *Nezumia aequalis*, Günther, 1878, *Coryphaenoides guentheri*, Vaillant, 1888, *Coelorinchus caelorhincus*, Risso, 1810) by comparing otoliths weight and data obtained from shape and morphometrical analysis.

Otoliths are calcareous structures contained in teleost's inner ears. Both organs (one for side), fundamental in balance and hearing, are composed by three semicircular canals, three end organs (*ampullae*) and three otoliths' organs (*sacculus, utriculus* and *lagena*). These last contains otoliths, respectively *sagitta, lapillus* and *asteriscus*. *Sagittae*, or sagittal otoliths, are the largest among them in non-ostariophysian fishes (Lombarte and Tuset, 2015; Popper and Lu, 2000), and they are widely used in many research fields: in paleontology and palaeoecology, to asses past marine teleost biodiversity and populations (Lin et al., 2016; Nolf, 1995, 1985; Nolf et al., 2009); in fisheries science, to identify stocks, species and populations through otoliths shape analysis (Begg and Brown, 2000; Lord et al., 2012; Morat et al., 2012; Stransky et al., 2008; Torres et al., 2000a; Tuset et al., 2003b; Zhuang et al., 2015); in ecology, being used for prey identification in stomach content analysis, and in ecomorphological studies for their intra-specific variability (Battaglia et al., 2013; Bose et al., 2020; D'Iglio et al., 2022c, 2021c, 2021b; Jaramilo et al., 2014; Karachle and Stergiou, 2010; Lombarte et al., 2010; Lombarte and Cruz, 2007; Mangano et al., 2017; Montanini et al., 2015; Neves et al., 2021; Tiralongo et al., 2020; Torres et al., 2000b; Tuset et al., 2020, 2018; Volpedo and Diana Echeverría, 2003; Volpedo et al., 2008); in taxonomy, for their species-specific morphology (D'iglio et al., 2022;

D'Iglio et al., 2021a; Lombarte et al., 2018; Moore et al., 2022; Ponton, 2006; Reichenbacher et al., 2007; Teimori et al., 2019; Tuset et al., 2016a, 2008, 2003a; Zischke et al., 2016) and in migratory and life cycle studies through microchemical analysis (Dulčić et al., 2005; Matić-Skoko et al., 2020b, 2020a, 2005).

Concerning the Macrouridae family, several studies have been performed on otoliths of these species worldwide (Draganik et al., 1998; Labropoulou and Papaconstantinou, 2000; Lombarte and Morales-Nin, 1995; Schwarzhans, 2014; Wilson, 1988). In the Mediterranean Sea, studies on grenadiers' otoliths were mainly focused on their populations structure and growth dynamics (Massutí et al., 1995; Sion et al., 2012; Swan et al., 2003). On our best knowledge, present paper represents the first intra and inter specific comparison among sagittal otoliths morphology, morphometry, and shape of five species belonging to the Macrouridae family from the Southern Tyrrhenian Sea. Data provided, for each studied species, by the analysis on intra specific sagittal otoliths variability were valuable to assess: (i) the efficiency of shape analysis for stock discrimination in Macrouridae species, (ii) the presence of directional bilateral asymmetry, (iii) the relationships between sagittal otoliths morphometries, and (iv) changes in sagittal otoliths mass, morphology and morphometry related to fish length and weight. Inter specifically, it has been possible to assess the taxonomy of grenadiers' species through sagittal otoliths' morphology, morphometry, and shape, also investigating the differences of the analyzed specimens with those from other geographical areas, through a literature comparison. These data are essential to improve the knowledge base on the ecology and taxonomy of these species, for a better management and conservation of marine environment and resources, being grenadiers' species important for the well-functioning of the deep Mediterranean ecosystems.

2. MATHERIALS AND METHODS

2.1 Samples collection

A total of 144 individuals (35 *C. guentheri,* 20 *C. caelorhincus*, 24 *H. italicus,* 24 *N. aequalis*, 40 *N. sclerorhynchus*) collected from Tyrrhenian Sea were obtained by professional fisherman.

After landings, they were transferred in the laboratory, where each specimen was measured (total length, TL) and weighted (total weight, TW), sampling the left and right sagittal otoliths. After sampling, each left and right sagittal otolith was polished from tissues remains using 3% H_2O_2 for 15 minutes, and Milli-Q water. Once dried, they were weighted and stored in plastic Eppendorf microtubes.

Each left and right sagittal otolith was photographed twice (one photo for each otolith face) under a Axiocam 208 colour camera (Carl Zeiss, Jena, Germany), installed on a stereomicroscope Zeiss Discovery V8 equipped. According to literature (Lombarte and Tuset, 2015), the photos of the macular surface were acquired with the otoliths orientated vertically with respect to the longest axis to obtain *sulcus acusticus* images as clear as possible.

2.2 Images elaboration and morphometric analysis

ImageJ 1.48p software (Schneider et al., 2012) was used to perform several otoliths measurements and to convert images into binary format for contour extraction.
The performed otoliths measurements have been otolith length (OL, mm), otolith height (OH, mm), otolith perimeter (OP, mm), otolith surface (OS, mm^2), otolith weight (OW, g), sulcus perimeter (SP, mm), sulcus surface (SS, mm^2), sulcus length (SL, mm), cauda length (CL, mm), cauda width (CW, mm), ostium length (OSL, mm), ostium width (OSW, mm). Several shape indices were also calculated according to literature (Jawad et al., 2018; Pavlov, 2021, 2016; Tuset et al., 2016a, 2003a, 2003b): circularity (OP^2/OS), rectangularity (OS/[OL×OW]), ellipticity (OL–OW/OL+OW), aspect ratio (OW/OL%), form factor ($4\pi OS/OP^2$), roundness ($4OS/\pi OL^2$), the ratio of otolith length to the total fish length (OL/TL), the percentage of the otolith surface occupied by the sulcus (SS/OS%), the percentage of the sulcus length occupied by the cauda length (CL/SL%), the percentage of the sulcus length occupied by the ostium length (OSL/SL%). The *ostium* and *cauda* measurements were not performed in sagittal otoliths of *H. italicus* specimens due to the peculiar *sulcus acusticus* structure showed by this species. Indeed, this is characterized by the absence of separation between *ostium* and *cauda* which make it impossible to measure separately their length and width (Schwarzhans, 2014).

2.3 Otolith shape analysis

Shaper R (open-source software package running on R version 4.0.5, RStudio 2022.07.1 Build 554; R Gui 4.1.3 2022.03.10) was used to perform the otolith shape analysis, with a specific package for the investigation of the intra and inter specific otoliths shape variability (Libungan and Pálsson, 2015). ImageJ software (version 1.53k freely available at https://imagej.nih.gov/ij/) was used to binarized each image of *sagittae*, with an intensity threshold value of 0.05, classifying the extracted outlines according to the individuals and otoliths information (e.g., species, otolith side). The getMeasurements function was applied to calculate the otoliths measurements, using the previously detected outlines. The extraction of Wavelet and Fourier coefficients were performed for the

statistical analysis, adjusting them for the analysis of the allometric relationships between otolith shape and fish length. The comparison between the mean *sagittae* shape of the analyzed species were obtained using the Wavelet coefficients. The deviation of the coefficients reconstruction from the otolith outline was analyzed to estimate the quality of the reconstruction (Supplementary materials 1_Figure). Finally, a g-plots R package's specific function was used to investigate how the position along the outline can influence the wavelet coefficients variation (Supplementary materials 2_Figure).

2.4 Data analysis

Univariate and multivariate statistical methods were applied to conduct investigations on *sagittae* using Prism V.8.2.1 (Graph- pad Software Ltd., La Jolla, CA 92037, USA), R vegan package V.2.5, and PAST V.4.

An unpaired t-test was used as a tool to investigate the occurrence of differences in morphometric parameters between right and left otoliths. Any otolith morphometric variations between the different species investigated were detected using a one-way analysis of variance (one-way ANOVA) and Linear Discriminant Analysis (LDA). Additionally, the correlation between the measured parameters and fish body weight (BW) and total length (TL) was tested using the Pearson correlation coefficient. To explore the variation of otolith contours between the specimens, the shape indices were extrapolated and analyzed through an ANOVA-like permutation test and a Linear Discriminant Analysis (LDA) to obtain an overview of the differences in otolith shape between the species examined. The significance level of p-value was set at < 0.05.

3. RESULTS

3.1. Morphometric and shape analysis

All the analyzed *sagittae* have been described according to the terminology of Assis, Nolf, and Tuset et al. (Assis, 2000; Nolf, 1985; Tuset et al., 2008).

H. italicus specimens showed an overall elliptical and lobed shape of *sagittae*, with irregular margins slightly lobed anterodorsally, and generally equals length and heigh (Figure 1 a-c).

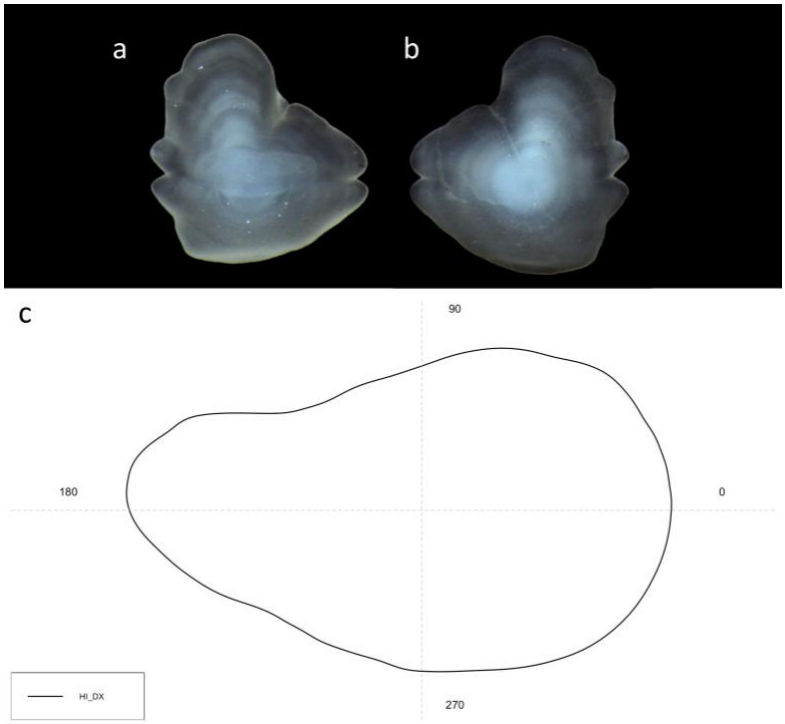

Figure 1. Lateral view (a) and medial view (b) of right *sagitta* of *H. italicus*, with mean otoliths' shape (c)

The maximum length was infra median, while the maximum heigh was pre median. Both the dorsal and ventral margins were deeply asymmetric and convex. The dorsal one was crenate and slightly lobed, while the ventral was flat and smooth. The posterior region was bifid and slightly sharp, while the anterior was irregular to double-peacked. The external face was concave, while the internal was convex. *Rostrum* and *antirostrum* were both triangular, small, and almost of the same size. *Rostrum* was generally longer than the *antirostrum*, antero-dorsally oriented. The *excisura ostii* was asymmetric, pointed and generally small. *Excisura caudalis* was deeper or deep as the *excisura ostii. Pseudorostrum* and *pseudoantirostrum* were triangular and almost of the same size, more dorsally oriented and pointed than *rostrum* and *antirostrum. Sulcus acusticus* was archaeosulcoid, median, with indistinct *cauda* and *ostium*, and a horizontal orientation.

The morphometrical parameters of *sagittae* calculated for *H. ialicus* specimens are summarized in Table 1. The unpaired t-test did not detect the presence of bilateral asymmetry.

Table 1. Morphometric mean values of right *sagittae* of *H. italicus* individuals with standard deviation (SD) and minimum (Min.) and maximum (Max.) range: OL (otolith length), OH (otolith height), OP (otolith perimeter), OS (otolith surface), OW (otolith weight), SP (sulcus perimeter), SS (sulcus surface), SL (sulcus length), SH (sulcus height), C (circularity), Re (rectangularity), E (ellepticity), AR (OW/OL %), FF (form factor), Ro (roundness), OL/TL (the ratio of otolith length to total fish length), SS/OS % (percentage of otolith surface occupied by the sulcus), CL/SL % (percentage of the sulcus length occupied by the cauda length) and OSL/SL % (percentage of the sulcus length occupied by the ostium length)

	Mean	**s.d.**	**Min. - Max.**

OL	3.66	0.6	2.58 - 4.77
OH	3.88	0.58	2.76 - 4.81
OP	14.48	2.45	9.97 - 18.88
OS	9.81	2.80	5.15 - 14.8
OW	0.02	0.01	0.01 - 0.04
SP	5.15	0.97	3.61 - 6.92
SS	1.33	0.45	0.76 - 2.2
SL	2.25	0.46	1.49 -- 3.13
SH	0.76	0.14	0.53 - 1.01
C	21.75	1.94	18.36 - 25.24
Re	0.68	0.02	0.65 - 0.71
E	-0.03	0.02	-0.07 - 0
AR	1.07	0.05	0.99 - 1.16
FF	0.58	0.05	0.5 - 0.69
Ro	0.92	0.06	0.83 - 1.04
OL/TL	0.04	0.01	0.03 - 0.05
SS/OS%	0.14	0.02	0.1 - 0.17

Concerning *N. sclerorhynchus* specimens, they showed longer than higher *sagittae*, with an approximately oval overall shape. The general morphology of irregular polygon was characterized by a visible different angulation of the five sides (Figure 2).

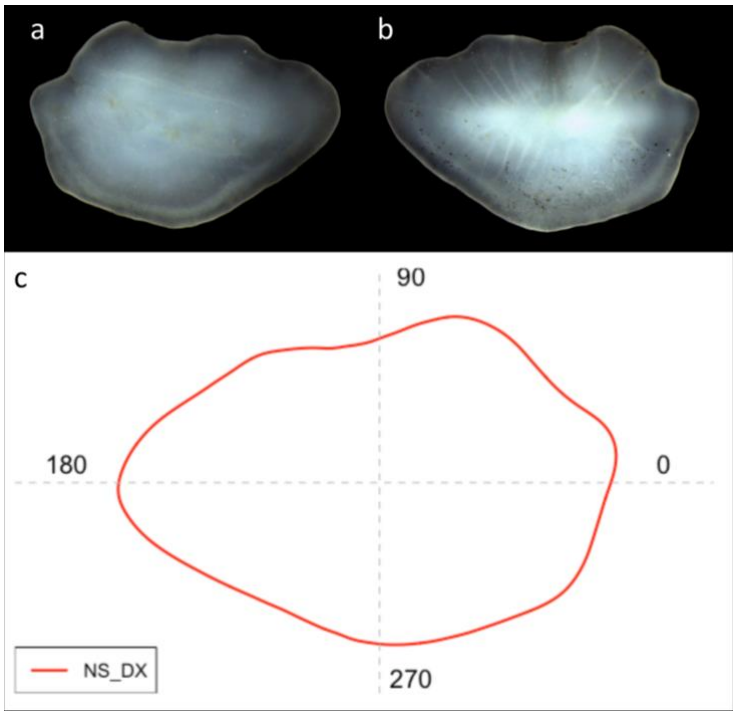

Figure 2. Lateral view (a) and medial view (b) of right *sagittae* of *N. sclerorhynchus*, with mean otoliths' shape (c)

The maximum *sagittae* length was not perfectly median in all the specimens, and the maximum heigh was always pre medial. The posterior region was more pointed than the anterior, that was characterized by a bilobed antero-dorsal part. The dorsal and the ventral regions of the *sagittae* were both convex, with an evident crenulation in the anterior one. The *rostrum* was rounded and not clearly defined, with the general not differentiation of an *antirostrum* and an *excisura ostii. Sulcus acusticus* was generally homosulcoid and median, with *cauda* and *ostium* both oval, straight, almost equal in length and heigh. The *cauda* was characterized by a visible distance of its ending part from the posterior otolith's margin.

The morphometrical parameters of *sagittae* calculated for *N. sclerorhynchus* specimens are summarized in Table 2. The unpaired t-test did not detect the presence of a marked bilateral asymmetry, despite SS/OS% parameter varied significantly between the right and left side ($p<0.001$).

Table 2. Morphometric mean values of right *sagittae* of *N. sclerorhynchus* individuals with standard deviation (SD) and minimum (Min.) and maximum (Max.) range: OL (otolith length), OH (otolith height), OP (otolith perimeter), OS (otolith surface), OW (otolith weight), SP (sulcus perimeter), SS (sulcus surface), SL (sulcus length), SH (sulcus height), CL (cauda length), CW (cauda width), CP (cauda perimeter), CS (cauda surface), OSL (ostium length), OSW (ostium width), OSP (ostium perimeter), OSS (ostium surface), C (circularity), Re (rectangularity), E (ellepticity), AR (OW/OL %), FF (form factor), Ro (roundness), OL/TL (the ratio of otolith length to total fish length), SS/OS % (percentage of otolith surface occupied by the sulcus), CL/SL % (percentage of the sulcus length occupied by the cauda length) and OSL/SL % (percentage of the sulcus length occupied by the ostium length)

	Mean	**s.d.**	**Min. - Max.**
OL	5.42	1.18	3.65 - 7.78
OH	3.45	0.69	2.25 - 5.06
OP	17.12	4.16	10.98 - 28.81
OS	13.75	5.73	5.92 - 28.52
OW	0.02	0.01	0.01 - 0.06
SP	7.63	2.39	2.82 - 13.12
SS	2.22	1.65	0.28 - 7.09
SL	3.40	1.04	1.29 - 5.61
CL	1.48	0.44	0.63 - 2.4
CH	0.67	0.27	0.27 - 1.49
CP	3.6	1.1	1.44 - 6.08
CS	0.77	0.55	0.1 - 2.6
OSL	1.71	0.54	0.65 - 2.80
OSH	0.75	0.33	0.22 - 1.55
OSP	4.09	1.34	1.48 - 6.89
OSS	1.01	0.73	0.08 - 3
C	22.36	5.35	17.93 - 52.51
Re	0.71	0.02	0.68 - 0.75
E	0.22	0.03	0.18 - 0.31
AR	0.64	0.04	0.53 - 0.7
FF	0.58	0.08	0.24 - 0.7
Ro	0.57	0.04	0.47 - 0.62

OL/TL	0.04	0.004	0.03 - 0.05
SS/OS%	15.05	5.86	4.71 - 28.64
CL/SL%	43.9	4.23	35.35 - 52.88
OSL/SL%	50.19	3.95	41.59 - 59.54

N. aequalis specimens showed an approximately oval *sagitta*, with a slightly polygonal morphology, characterized by lobed margins, more irregulars in the dorsal region than in the ventral one. The polygonal morphology was highlighted by the presence of five differently angled sides (Figure 3).

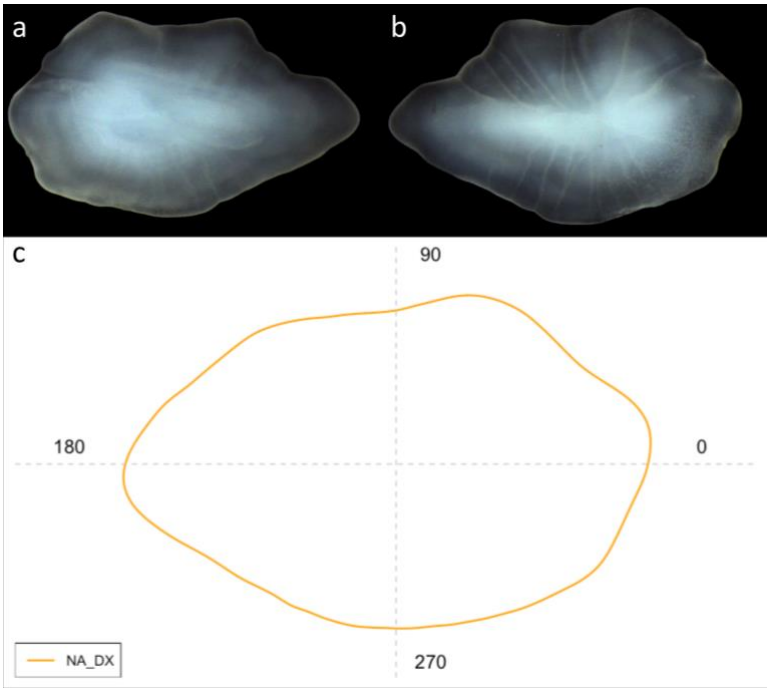

Figure 3. Lateral view (a) and medial view (b) of right *sagittae* of *N. aequalis*, with mean otoliths' shape (c)

The maximum *sagittae* length was not perfectly median in all the specimens, and the maximum heigh was always pre medial. The ventral region was pointed, while the anterior one was rounded and asymmetric. The dorsolateral part of the dorsal region was bilobed, while the ventral part was curved to deeply irregular. *Rostrum* and *antirostrum* were not differentiated, such as, consequently, the *excisura ostii.* The mesial *sulcus acusticus* was slightly heterosulcoid, with larger cauda than the *ostium*, located in a median position.

The morphometrical parameters of *sagittae* calculated for *N. aequalis* specimens are summarized in Table 3. The unpaired t-test did not detect the presence of bilateral asymmetry.

Table 3. Morphometric mean values of right *sagittae* of *N. aequalis* individuals with standard deviation (SD) and minimum (Min.) and maximum (Max.) range: OL (otolith length), OH (otolith height), OP (otolith perimeter), OS (otolith surface), OW (otolith weight), SP (sulcus perimeter), SS (sulcus surface), SL (sulcus length), SH (sulcus height), CL (cauda length), CW (cauda width), CP (cauda perimeter), CS (cauda surface), OSL (ostium length), OSW (ostium width), OSP (ostium perimeter), OSS (ostium surface), C (circularity), Re (rectangularity), E (ellepticity), AR (OW/OL %), FF (form factor), Ro (roundness), OL/TL (the ratio of otolith length to total fish

length), SS/OS % (percentage of otolith surface occupied by the sulcus), CL/SL % (percentage of the sulcus length occupied by the cauda length) and OSL/SL % (percentage of the sulcus length occupied by the ostium length)

	Mean	s.d.	Min. - Max.
OL	5.37	1.22	3.62 - 7.28
OH	3.46	0.8	2.25 - 4.8
OP	15.93	3.34	10.61 - 21.33
OS	13.6	5.93	5.66 - 24.42
OW	0.02	0.01	0.01 - 0.06
SP	6.91	2.36	3.97 - 12.20
SS	1.71	1.22	0.44 - 4.97
SL	3.02	1	1.71 - 5.17
CL	1.3	0.43	0.68 - 2.09
CH	0.68	0.26	0.25 - 1.31
CP	3.16	1.04	1.83 - 5.04
CS	0.6	0.4	0.14 - 1.53
OSL	1.59	0.54	0.93 - 2.66
OSH	0.72	0.32	0.3 - 1.44
OSP	3.77	1.27	2.09 - 6.65
OSS	0.82	0.64	0.19 - 2.69
C	19.82	1.79	17.44 - 27.12
Re	0.7	0.02	0.66 - 0.72
E	0.22	0.03	0.15 - 0.28
AR	0.65	0.04	0.56 - 0.74
FF	0.64	0.05	0.46 - 0.72
Ro	0.57	0.04	0.49 - 0.66
OL/TL	0.04	0.004	0.03 - 0.05
SS/OS%	0.11	0.04	0.06 - 0.2
CL/SL%	0.43	0.05	0.36 - 0.51
OSL/SL%	0.53	0.09	0.4 - 0.82

C. guentheri specimens showed a pentagonal shape, characterized by a triangular dorsal region and a trapezoidal ventral one (Figure 4).

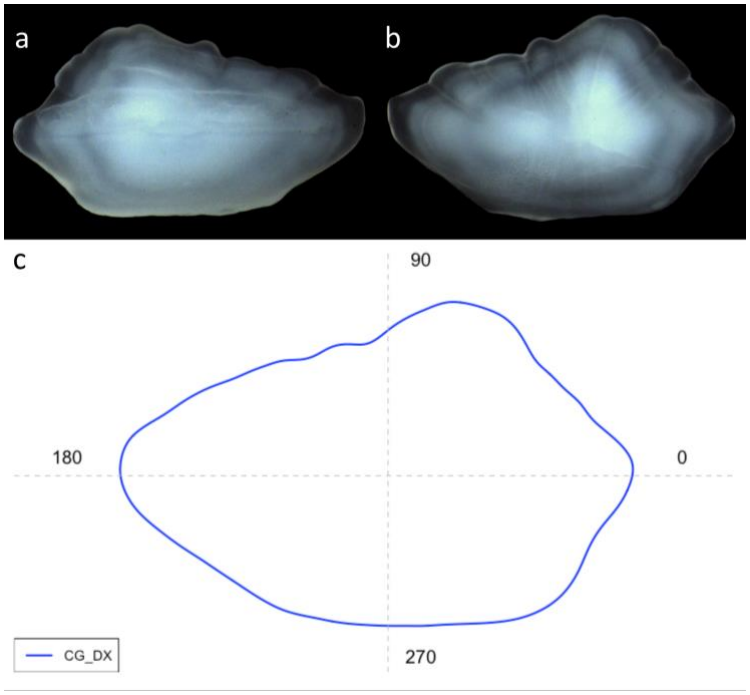

Figure 4. Lateral view (a) and medial view (b) of right *sagittae* of *C. guentheri*, with mean otoliths' shape (c)

The maximum otolith length was median, while the maximum heigh was pre median. The dorsal margin was irregular and slightly crenulated, while the ventral one was smooth. Both the posterior and the anterior regions were pointed. The *rostrum* was small, rounded and anteriorly directed, not always clearly differentiated. *Extremo posterior* was slightly pointed, median and horizontal. *Sulcus acusticus* was very large, pseudo-ostiocaudal, medial and horizontal. *Cauda* and *ostium* were approximatively of the same shape, with *Ostium* slightly longer than *cauda.* It was detected the presence of a *canalis postcaudalis*, a *colliculum* heteromorphico and a medial *pseudocolliculum.*
The morphometrical parameters of *sagittae* calculated for *C. guentheri* specimens are summarized in Table 4. The unpaired t-test did not detect the presence of bilateral asymmetry.

Table 4. Morphometric mean values of right *sagittae* of *C. guentheri* individuals with standard deviation (SD) and minimum (Min.) and maximum (Max.) range: OL (otolith length), OH (otolith height), OP (otolith perimeter), OS (otolith surface), OW (otolith weight), SP (sulcus perimeter), SS (sulcus surface), SL (sulcus length), SH (sulcus height), CL (cauda length), CW (cauda width), CP (cauda perimeter), CS (cauda surface), OSL (ostium length), OSW (ostium width), OSP (ostium perimeter), OSS (ostium surface), C (circularity), Re (rectangularity), E (ellepticity), AR (OW/OL %), FF (form factor), Ro (roundness), OL/TL (the ratio of otolith length to total fish length), SS/OS % (percentage of otolith surface occupied by the sulcus), CL/SL % (percentage of the sulcus length occupied by the cauda length) and OSL/SL % (percentage of the sulcus length occupied by the ostium length)

	Mean	**s.d.**	**Min. - Max.**
OL	8.29	1.10	5.26 - 10.21
OH	5.27	0.55	3.79 - 6.18
OP	24.87	3.05	16.52 - 28.69
OS	30.05	6.71	13.24 - 40.81
OW	0.08	0.03	0.02 - 0.14
SP	13.87	2.62	8.1 - 17.8

SS	5.97	2.36	1.18 - 10.63
SL	6.41	1.2	3.85 - 8.34
CL	2.57	0.7	0.87 - 3.53
CH	0.96	0.34	0.3 - 1.44
CP	5.86	1.62	2.09 - 8.31
CS	1.78	0.9	0.18 - 3.66
OSL	3.11	0.77	1.33 - 4.5
OSH	1	0.33	0.26 - 1.94
OSP	6.96	1.74	2.93 - 10.55
OSS	2.35	1.2	0.31 - 5.87
C	20.86	1.05	19.02 - 23.3
Re	0.68	0.02	0.63 - 0.72
E	0.22	0.03	0.16 - 0.27
AR	0.64	0.04	0.57 - 0.72
FF	0.6	0.03	0.54 - 0.66
Ro	0.55	0.04	0.48 - 0.63
OL/TL	0.05	0.004	0.04 - 0.06
SS/OS%	0.19	0.05	0.07 - 0.3
CL/SL%	0.4	0.06	0.19 - 0.53
OSL/SL%	0.48	0.06	0.3 - 0.56

Concerning *C. caelorhincus* specimens, they showed *sagittae* longer than higher, with a pentagonal shape, characterized by sides differently angled, a triangular dorsal region and a trapezoidal ventral one. The posterior and anterior region were pointed, with the posterior longer and more pointed than the anterior one (Figure 5).

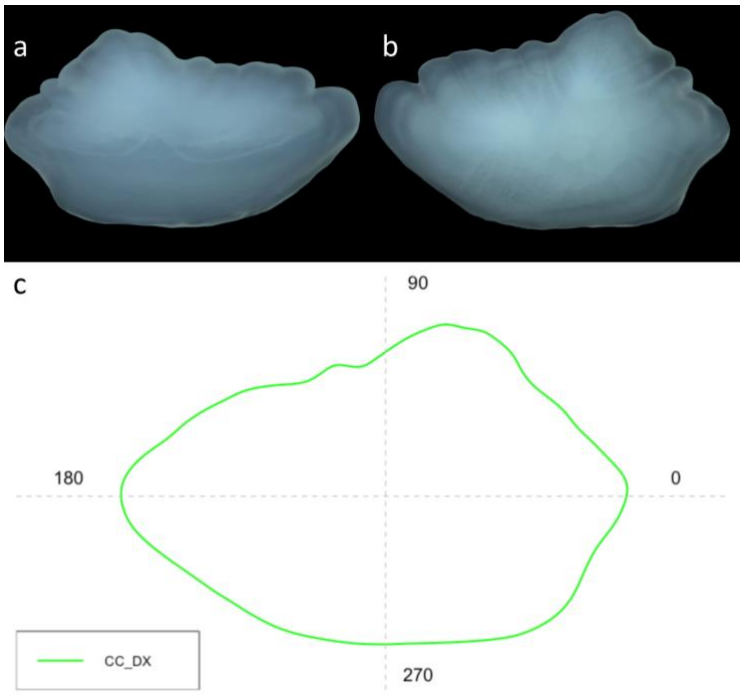

Figure 5. Lateral view (a) and medial view (b) of right *sagittae* of *C. caelorhincus*, with mean otoliths' shape (c)

The maximum otolith length was median, while the maximum heigh was pre median. Dorsal and ventral margins were not symmetric and both convex. The margins were crenulated, with crenulations more evident in smaller otoliths. While larger otoliths were smoother than the smaller ones. The *rostrum* was short, rounded in median position, while *antirostrum* and excisura *ostia* were not differentiated. *Extremo posterior* was rounded, median and horizontal. The *sulcus acusticus* was superficial, heterosulcoid, horizontal and median. *Cauda* was longer than *ostium*, and both were rectangular and with the same height.

The morphometrical parameters of *sagittae* calculated for *C caelorhincus* specimens are summarized in Table 5. The unpaired t-test did not detect the presence of bilateral asymmetry, despite CL/SL% varied significantly between the right and left side ($p<0.001$).

Table 5. Morphometric mean values of right *sagittae* of *C. caelorhincus* individuals with standard deviation (SD) and minimum (Min.) and maximum (Max.) range: OL (otolith length), OH (otolith height), OP (otolith perimeter), OS (otolith surface), OW (otolith weight), SP (sulcus perimeter), SS (sulcus surface), SL (sulcus length), SH (sulcus height), CL (cauda length), CW (cauda width), CP (cauda perimeter), CS (cauda surface), OSL (ostium length), OSW (ostium width), OSP (ostium perimeter), OSS (ostium surface), C (circularity), Re (rectangularity), E (ellepticity), AR (OW/OL %), FF (form factor), Ro (roundness), OL/TL (the ratio of otolith length to total fish length), SS/OS % (percentage of otolith surface occupied by the sulcus), CL/SL % (percentage of the sulcus length occupied by the cauda length) and OSL/SL % (percentage of the sulcus length occupied by the ostium length)

	Mean	**s.d.**	**Min. - Max.**
OL	7.76	0.83	6.38 - 9.4
OH	5.1	0.37	4.5 - 5.9
OP	23.85	1.95	19.41 - 27.25
OS	27.25	4.74	18.85 - 35.88
OW	0.07	0.02	0.04 - 0.11
SP	15.1	2.79	11.78 - 20.23
SS	7.38	3.25	3.84 - 13.51
SL	6.7	1.23	4.5 - 8.99
CL	3.07	0.57	2.32 - 3.99
CH	1.02	0.33	0.6 - 1.81
CP	7.14	1.51	5.05 - 9.98
CS	2.57	1.2	1.07 - 5.17
OSL	3.47	0.82	2.3 - 4.77
OSH	1.05	0.3	0.7 - 1.68
OSP	8.04	2.09	5.4 - 11.97
OSS	3.19	1.66	1.44 - 6.87
C	21.11	1.75	19.2 - 26.89
Re	0.68	0.02	0.65 - 0.72
E	0.21	0.03	0.17 - 0.27
AR	0.66	0.04	0.57 - 0.7
FF	0.6	0.04	0.47 - 0.66
Ro	0.57	0.03	0.52 - 0.62

OL/TL	0.05	0.01	0.03 - 0.06
SS/OS%	26.11	7.63	16.51 - 38.5
CL/SL%	46.39	9.01	39.92 - 81.21
OSL/SL%	52.22	12.27	43.2 - 101.22

3.2 Inter-specific differences in morphology and shape

Since no striking differences in the morphometry of the *sagittae* were detected between the right and left sides, only the morphometric parameters of the right otoliths were used and subjected to ANOVA to evaluate the interspecific variations. The morphometric measurements of the right otoliths belonging to the investigated species are summarized in Table 6.

Table 6. Morphometric mean values of right *sagittae* of the investigated species with standard deviation (SD) and minimum (Min.) and maximum (Max.) range: OL (otolith length), OH (otolith height), OP (otolith perimeter), OS (otolith surface), OW (otolith weight), SP (sulcus perimeter), SS (sulcus surface), SL (sulcus length), SH (sulcus height), CL (cauda length), CW (cauda width), CP (cauda perimeter), CS (cauda surface), OSL (ostium length), OSW (ostium width), OSP (ostium perimeter), OSS (ostium surface), C (circularity), Re (rectangularity), E (ellepticity), AR (OW/OL %), FF (form factor), Ro (roundness), OL/TL (the ratio of otolith length to total fish length), SS/OS % (percentage of otolith surface occupied by the sulcus), CL/SL % (percentage of the sulcus length occupied by the cauda length) and OSL/SL % (percentage of the sulcus length occupied by the ostium length)

	H. italicus			***N. sclerorhynchus***			***N. aequalis***			***C. guentheri***			***C. caelorinchus***		
	Mean	**s.d.**	**Min. - Max.**	**Mean**	**s.d.**	**Min. - Max.**	**Mean**	**s.d.**	**Min. - Max.**	**Mean**	**s.d.**	**Min. - Max.**	**Mean**	**s.d.**	**Min. - Max.**
OL	3.66	0.6	2.58 - 4.77	5.42	1.18	3.65 - 7.78	5.37	1.22	3.62 - 7.28	8.29	1.10	5.26 - 10.21	7.76	0.83	6.38 - 9.4
OH	3.88	0.58	2.76 - 4.81	3.45	0.69	2.25 - 5.06	3.46	0.8	2.25 - 4.8	5.27	0.55	3.79 - 6.18	5.1	0.37	4.5 - 5.9
OP	14.48	2.45	9.97 - 18.88	17.12	4.16	10.98 - 28.81	15.93	3.34	10.61 - 21.33	24.87	3.05	16.52 - 28.69	23.85	1.95	19.41 - 27.25
OS	9.81	2.80	5.15 - 14.8	13.75	5.73	5.92 - 28.52	13.6	5.93	5.66 - 24.42	30.05	6.71	13.24 - 40.81	27.25	4.74	18.85 - 35.88
OW	0.02	0.01	0.01 - 0.04	0.02	0.01	0.01 - 0.06	0.02	0.01	0.01 - 0.06	0.08	0.03	0.02 - 0.14	0.07	0.02	0.04 - 0.11
SP	5.15	0.97	3.61 - 6.92	7.63	2.39	2.82 - 13.12	6.91	2.36	3.97 - 12.20	13.87	2.62	8.1 - 17.8	15.1	2.79	11.78 - 20.23
SS	1.33	0.45	0.76 - 2.2	2.22	1.65	0.28 - 7.09	1.71	1.22	0.44 - 4.97	5.97	2.36	1.18 - 10.63	7.38	3.25	3.84 - 13.51
SL	2.25	0.46	1.49 -- 3.13	3.40	1.04	1.29 - 5.61	3.02	1	1.71 - 5.17	6.41	1.2	3.85 - 8.34	6.7	1.23	4.5 - 8.99
SH	0.76	0.14	0.53 - 1.01	-	-	-	-	-	-	-	-	-	-	-	-
CL	-	-	-	1.48	0.44	0.63 - 2.4	1.3	0.43	0.68 - 2.09	2.57	0.7	0.87 - 3.53	3.07	0.57	2.32 - 3.99
CH	-	-	-	0.67	0.27	0.27 - 1.49	0.68	0.26	0.25 - 1.31	0.96	0.34	0.3 - 1.44	1.02	0.33	0.6 - 1.81
CP	-	-	-	3.6	1.1	1.44 - 6.08	3.16	1.04	1.83 - 5.04	5.86	1.62	2.09 - 8.31	7.14	1.51	5.05 - 9.98
CS	-	-	-	0.77	0.55	0.1 - 2.6	0.6	0.4	0.14 - 1.53	1.78	0.9	0.18 - 3.66	2.57	1.2	1.07 - 5.17
OSL	-	-	-	1.71	0.54	0.65 - 2.80	1.59	0.54	0.93 - 2.66	3.11	0.77	1.33 - 4.5	3.47	0.82	2.3 - 4.77
OSH	-	-	-	0.75	0.33	0.22 - 1.55	0.72	0.32	0.3 - 1.44	1	0.33	0.26 - 1.94	1.05	0.3	0.7 - 1.68
OSP	-	-	-	4.09	1.34	1.48 - 6.89	3.77	1.27	2.09 - 6.65	6.96	1.74	2.93 - 10.55	8.04	2.09	5.4 - 11.97
OSS	-	-	-	1.01	0.73	0.08 - 3	0.82	0.64	0.19 - 2.69	2.35	1.2	0.31 - 5.87	3.19	1.66	1.44 - 6.87
C	21.75	1.94	18.36 - 25.24	22.36	5.35	17.93 - 52.51	19.82	1.79	17.44 - 27.12	20.86	1.05	19.02 - 23.3	21.11	1.75	19.2 - 26.89
Re	0.68	0.02	0.65 - 0.71	0.71	0.02	0.68 - 0.75	0.7	0.02	0.66 - 0.72	0.68	0.02	0.63 - 0.72	0.68	0.02	0.65 - 0.72
E	-0.03	0.02	-0.07 - 0	0.22	0.03	0.18 - 0.31	0.22	0.03	0.15 - 0.28	0.22	0.03	0.16 - 0.27	0.21	0.03	0.17 - 0.27
AR	1.07	0.05	0.99 - 1.16	0.64	0.04	0.53 - 0.7	0.65	0.04	0.56 - 0.74	0.64	0.04	0.57 - 0.72	0.66	0.04	0.57 - 0.7

FF	0.58	0.05	0.5 - 0.69	0.58	0.08	0.24 - 0.7	0.64	0.05	0.46 - 0.72	0.6	0.03	0.54 - 0.66	0.6	0.04	0.47 - 0.66
Ro	0.92	0.06	0.83 - 1.04	0.57	0.04	0.47 - 0.62	0.57	0.04	0.49 - 0.66	0.55	0.04	0.48 - 0.63	0.57	0.03	0.52 - 0.62
OL/TL	0.04	0.01	0.03 - 0.05	0.04	0.004	0.03 - 0.05	0.04	0.004	0.03 - 0.05	0.05	0.004	0.04 - 0.06	0.05	0.01	0.03 - 0.06
SS/OS%	0.14	0.02	0.1 - 0.17	15.05	5.86	4.71 - 28.64	0.11	0.04	0.06 - 0.2	0.19	0.05	0.07 - 0.3	26.11	7.63	16.51 - 38.5
CL/SL%	-	-	-	43.9	4.23	35.35 - 52.88	0.43	0.05	0.36 - 0.51	0.4	0.06	0.19 - 0.53	46.39	9.01	39.92 - 81.21
OSL/SL%	-	-	-	50.19	3.95	41.59 - 59.54	0.53	0.09	0.4 - 0.82	0.48	0.06	0.3 - 0.56	52.22	12.27	43.2 - 101.22

Generalizing, some species have shown similar characteristics, for example *C. caelorhincus* and *C. guentheri*, or even the congeneric species *N. aequalis* and *N. sclerorhynchus*. *H. italicus*, on the other hand, appeared more dissimilar from the other species investigated. This was already evident from the comparison of fish parameters, such as total length and body weight. The detailed results obtained through the ANOVA are reported in Table 7.

Table 7. Results of ANOVA carried out on the investigated species between morphometric parameters of right *sagittae,* with significant results setted at $p<0.05$ (OL: otolith length, OH: otolith height, OP: otolith perimeter, OS: otolith surface, OW: otolith weight, SP: sulcus perimeter, SS: sulcus surface, SL: sulcus length, SH: sulcus height, CL: cauda length, CW: cauda width, CP: cauda perimeter, CS: cauda surface, OSL: ostium length, OSW: ostium width, OSP: ostium perimeter, OSS: ostium surface, C: circularity, Re: rectangularity, E: ellipticity, AR: OW/OL %, FF: form factor, Ro: roundness, OL/TL: the ratio of otolith length to total fish length, SS/OS %: percentage of otolith surface occupied by the sulcus, CL/SL %: percentage of the sulcus length occupied by the cauda length, and OSL/SL %: percentage of the sulcus length occupied by the ostium length).

	C. caelorhincus* vs *C. guentheri	***C. caelorhincus* vs *N. aequalis***	***C. caelorhincus* vs *N. sclerorhyncus***	***C. caelorhincus* vs *H. italicus***	***C. guentheri* vs *N. aequalis***	***C. guentheri* vs *N.sclerorhyncus***	***C. guentheri* vs *H. italicus***	***N. aequalis vs N. sclerorhyncus***	***N. aequalis* vs *H. italicus***	***N. sclerorhyncus* vs *H. italicus***
	p value	*p value*	*p value*	*p value*	*p value*	*p value*	*p value*	*p value*	*p value*	*p value*
OW	0.1323	<0.0001*	<0.0001*	<0.0001*	<0.0001*	<0.0001*	<0.0001*	>0.9999	0.9649	0.9437
OS	0.3744	<0.0001*	<0.0001*	<0.0001*	<0.0001*	<0.0001*	<0.0001*	>0.9999	0.1285	0.051
OP	0.7999	<0.0001*	<0.0001*	<0.0001*	<0.0001*	<0.0001*	<0.0001*	0.6132	0.5354	0.0168*
OL	0.3828	<0.0001*	<0.0001*	<0.0001*	<0.0001*	<0.0001*	<0.0001*	0.9998	<0.0001*	<0.0001*
OH	0.863	<0.0001*	<0.0001*	<0.0001*	<0.0001*	<0.0001*	<0.0001*	>0.9999	0.1412	0.0658
Ro	0.3395	>0.9999	>0.9999	<0.0001*	0.3519	0.1383	<0.0001*	0.9996	<0.0001*	<0.0001*
FF	0.3562	0.9997	>0.9999	<0.0001*	0.4177	0.1892	<0.0001*	0.9997	<0.0001*	<0.0001*
E	0.5478	0.8241	0.4618	<0.0001*	0.9947	>0.9999	<0.0001*	0.986	<0.0001*	<0.0001*
C	0.9986	0.6618	0.6025	0.9624	0.7284	0.2486	0.8231	0.0191*	0.2187	0.9463
Re	0.8184	0.1241	0.0001*	0.8325	0.0016*	<0.0001*	>0.9999	0.2825	0.0039*	<0.0001*
AR	0.4613	0.8082	0.4975	<0.0001*	0.9868	>0.9999	<0.0001*	0.9937	<0.0001*	<0.0001*
OL/TL	0.3775	0.0006*	<0.0001*	0.0061*	0.0472*	<0.0001*	0.2426	0.7119	0.9636	0.2667
SS	0.0832	<0.0001*	<0.0001*	<0.0001*	<0.0001*	<0.0001*	<0.0001*	0.8527	0.9629	0.4061
SP	0.3386	<0.0001*	<0.0001*	<0.0001*	<0.0001*	<0.0001*	<0.0001*	0.7553	0.0746	0.0006*
SL	0.8392	<0.0001*	<0.0001*	<0.0001*	<0.0001*	<0.0001*	<0.0001*	0.6038	0.0811	0.0003*
OS	0.0295	<0.0001*	<0.0001*		<0.0001*	<0.0001*		0.9057		
OP	0.0813	<0.0001*	<0.0001*		<0.0001*	<0.0001*		0.8592		
OL	0.2232	<0.0001*	<0.0001*		<0.0001*	<0.0001*		0.9		
OH	0.9402	0.0059*	0.0053*		0.0088*	0.0066*		0.9864		
CS	0.0023*	<0.0001*	<0.0001*		<0.0001*	<0.0001*		0.8409		
CP	0.005*	<0.0001*	<0.0001*		<0.0001*	<0.0001*		0.5673		

CL	0.0079*	<0.0001*	<0.0001*		<0.0001*	<0.0001*		0.5469		
CH	0.8948	0.0021*	0.0003*		0.0043*	0.0004*		0.9983		
SS/OS %	<0.0001*	<0.0001*	<0.0001*	<0.0001*	<0.0001*	0.0083*	0.0008*	0.0518	0.603	0.7848
CL/SL %	0.0006*	0.2639	0.4308		0.1369	0.0132*		0.9493		
OSL/SL %	0.2256	0.9453	0.7521		0.0433*	0.6615		0.3255		

The investigated species show clear differences in the parameters of the otoliths, *sulcus acusticus*, *ostium* and *cauda*. The most recurrent pattern is the similarity between *C. caelorhincus* and *C. guentheri*, between *N. aequalis* and *N. sclerorhynchus* and finally *H. italicus* which distances itself from the other two groups, as highlighted by the LDA (Figure 6).

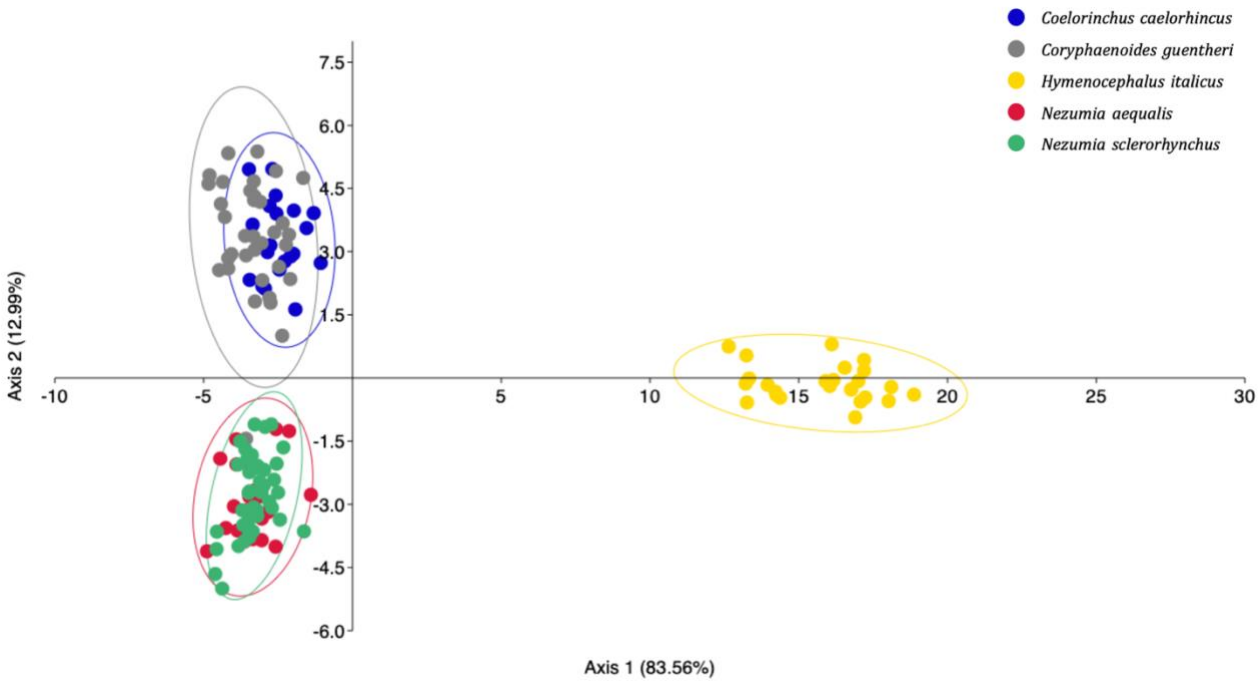

Figure 6. Linear Discriminant Analysis (LDA) between morphometric parameters of the investigated species.

Results from Pearson correlation, are reported in Supplementary materials 3_Table.

A comparison among the mean contours of the studied species, obtained from the shape analysis performed at inter specific level, is provided in Figure 7. The shape *H. italicus* specimens showed the most different shape of the *sagittae*, with a peculiar oval contour and prominent dorsal al posterior

region, visibly lobed. *C. caelorinchus* and *C. guentheri* showed a similar contour, characterized by a pentagonal shape, with differences in the prominence of the *rostrum*. Conversely, both *N. aequalis* and *N. sclerorhynchus* showed an approximately overall oval shape, with differences in the irregularity of the margins.

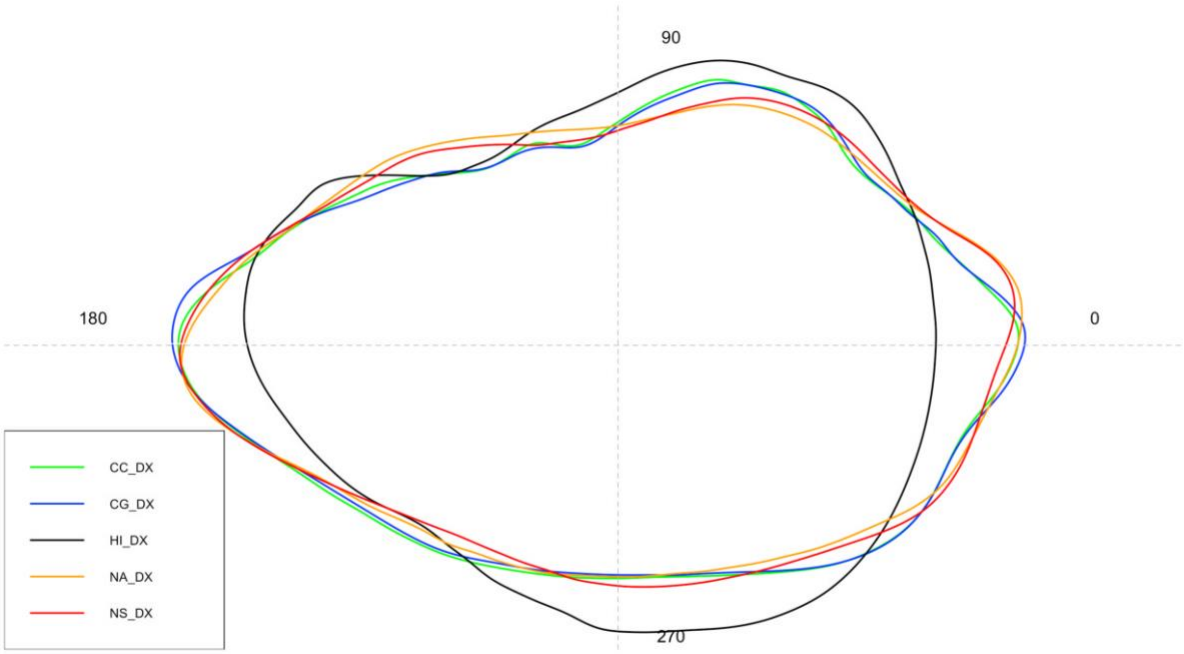

Figure 7. Mean shape of *sagittae* contours of the investigated species. CC is *C. coelorhiincus,* CG is *C. guentheri,* HI is *H. italicus,* NA is *N. aequalis,* NS is *N. sclerorhynchus*

The results of the ANOVA performed on the shape indices highlighted the differences between the investigated species, showing the same pattern observed for the measurements of the *sagittae* previously mentioned. The results were also confirmed by LDA (Figure 8), showing a greater distance for the *H. italicus* species.

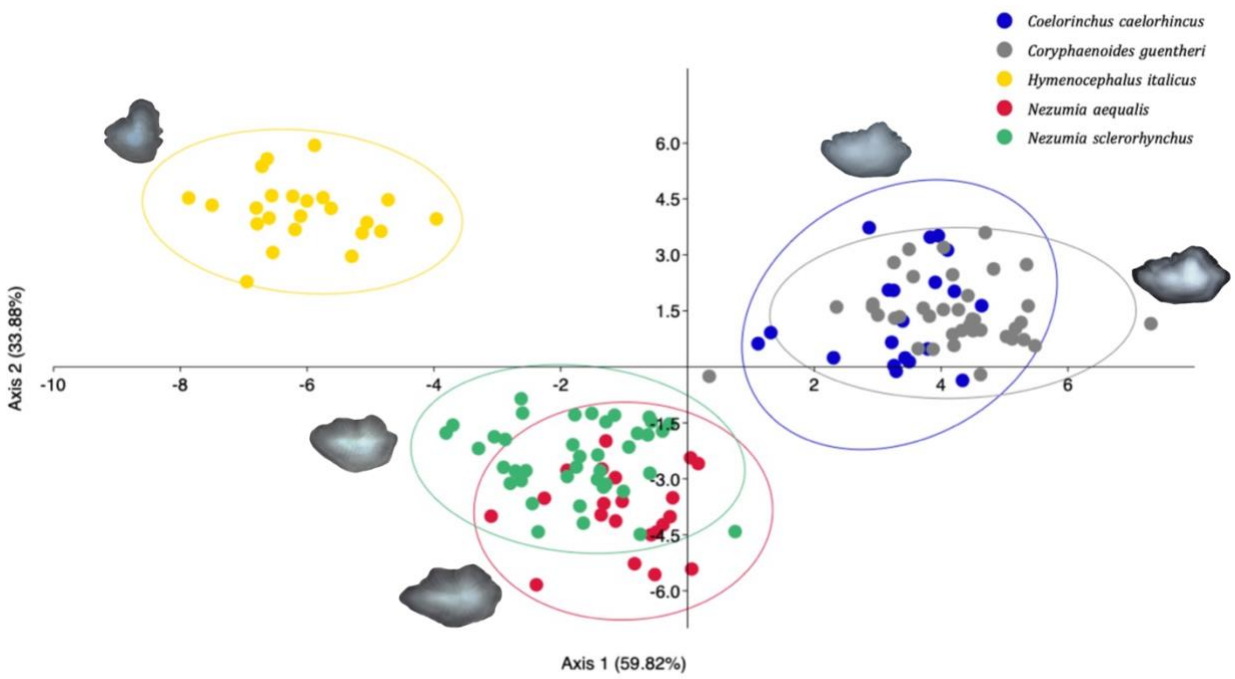

Figure 8. Linear Discriminant Analysis (LDA) between elliptic Fourier descriptors calculated for the investigated species. Ellipses include 95% confidence interval.

DISCUSSION

Findings from present paper reported and overall morphology of the investigated *sagittae* not in line with data from literature for the studied species, with differences detected between morphometrical parameters and morphological features. While, concerning the shape analysis, results confirmed its reliability for the discrimination of the main otolith contour in the studied species.

H. italicus specimens from the western and central Mediterranean Sea show smaller values of aspect ratio, circularity and rectangularity (Tuset et al., 2008) than those reported by results. These differences resulted in longer *sagittae*, with higher surface and perimeter values, and a more oval overall shape, in *H. italicus* population from the studied area. This was also characterized by a smaller *rostrum*, less pointed, with a most prominent *antirostrum*, *pseudorostrum* and *pseudoantirostrum*, than those reported in literature from western and central Mediterranean Sea, and from the Atlantic Portuguese waters (Assis, 2000). The descriptions provided by Schwarzans (Schwarzhans, 2014) highlight a marked variability in *sagittae* compression and margins regularity between eastern, western Atlantic Ocean and Indian Ocean. Concerning analyzed specimens, they showed dorsal and ventral margins generally smooth, in line with those from western Atlantic Ocean, described by Schwarzans (Schwarzhans, 2014).

Regarding *N. sclerorhynchus*, specimens showed morphometrical values of aspect ratio, circularity, and rectangularity much higher than those reported from Western and central Mediterranean Sea, resulting in a more oval and less polygonal *sagittae* shape described in literature than those reported by results (Tuset et al., 2008). Otherwise, specimens from the off Portuguese West coast (Marques and Almeida, 2001) present longer and heavier otoliths, resulting in more lanceolate to oval *sagittae*, with a very pointed *rostrum*, as confirmed also by description of Assis from Atlantic Portuguese waters (Assis, 2000). Differently, specimens form Northwest Atlantic Ocean, described by Campana (Campana, 2004), are characterized by *sagittae* with a more regular oval shape and smoother margins than those from the studied area. Also *N. aequalis* specimens showed much higher values for aspect ratio, circularity and rectangularity than those reported in literature from the western and central Mediterranean Sea (Tuset et al., 2008), resulting in oval and high *sagittae*. Differently, specimens from Portuguese waters (Assis, 2000; Marques and Almeida, 2001) described in literature have longer *sagittae*, characterized by a more pointed posterior region and a more lanceolate shape.

C. guentheri individuals showed aspect ratio values similar to those reported from western and central Mediterranean Sea (Tuset et al., 2008), with marked differences in circularity and rectangularity. These differences in shape indexes result in a different shape, with specimens from the studied area that exhibited a pentagonal shape, very distant from the oval one reported by Tuset et al. (Tuset et al., 2008) and by Campana from the Northwest Atlantic Ocean (Campana, 2004). Also *C. coelorhincus* specimens showed similar values of aspect ratio and highly different values of circularity and rectangularity than those reported in literature from the western and central Mediterranean Sea (Tuset et al., 2008). The overall shape showed also an evident variability, with specimens from the studied area that exhibited a pentagonal shape, clearly different from the elliptic to trapezoidal one reported in literature by Tuset et al. (Tuset et al., 2008). Otherwise, comparing results to data from the Portuguese Atlantic waters (Assis, 2000), it appears evident a similarity between the *sagittae* of the two populations. Both are characterized by a polygonal shape, with differences in the organization of *rostrum* and *antirostrum.*

These discrepancies between literature data on *sagittae* morphology and morphometry, and those showed by results could be related to the genetic variability among the populations of the studied species, and to the differences in environmental conditions experienced by individuals inhabiting different geographical areas. Indeed, it is widely reported how otolith are influenced by both genetic and environmental habitats' conditions (Vignon and Morat, 2010). The overall otoliths' form is regulated by genetics, while the quantity of deposited calcium carbonate during otolith formation is under environmental control. Indeed, somatic and otolith growth (which deeply influence otoliths' shape, morphology and morphometry) are deeply related to metabolic expression and physical

constrain, which in turn are sensitive to environmental conditions, such as water temperature, food availability and composition, depth and soundscape organization and complexity (Gagliano and McCormick, 2004; Hüssy, 2008; Lombarte and Lleonart, 1993; Schulz-Mirbach et al., 2010, 2008). The interactions between genetic and environment could act as a driver, resulting in shape and morphometry changes of *sagittae* between populations, as highlighted by the phenotypic variations that allow to the better adaptability of individuals to different habitats (Vasconcelos et al., 2021). As stated by Vignon and Morat (Vignon and Morat, 2010), several otoliths morphometrical features (such as the presence of *antirostrum* and the morphology of the *rostrum*) are under the genetic control, while overall otolith contour can be shaped by contrasting environmental features. The absence of literature data regarding shape analyses performed on different Macrourids' populations make difficult to quantify and identify the contour differences allowing to the inter population variability in the studied species. Data from literature deal with the general otolith's morphology and morphometry (Assis, 2000; Campana, 2004; Marques and Almeida, 2001; Schwarzhans, 2014; Tuset et al., 2008), but, according to several authors (Colura et al., 1995; Friedland and Reddin, 1994; Tuset et al., 2003b), shape indexes can be considered as good indicators for stock and populations separation in several species. For this reason, the variability reported by results for many shape indexes could suggest a high separation at population level for the studied species. Moreover, concerning their life habits, Macrourids species show a high plasticity in feeding habits and depth distribution between different geographical area (Carrassón and Matallanas, 2002; Drazen et al., 2008; García-Ruiz et al., 2019; Massutí et al., 1995). They are considered as generalist feeders which can adapt their diet to the preys' availability experienced in the different areas, an essential adaptation to the low productive deep environment inhabited by these species. Also concerning their genetic structure, species belonging to Macrouridae family can exhibit significant degrees of genetic divergence between different geographic areas (Catarino et al., 2017; Olson, 2017). The possible presence of genetic and life habits differences, added to the detected variability in *sagittae* morphology and morphometry, and to the different environmental conditions experienced by individuals in different geographical areas, could suggest the presence of different populations and stocks of the studied species within the Mediterranean Sea and the Atlantic Ocean. This high inter population variability it was also reported for other Macrouridae species between the Atlantic and Pacific Oceans (Wilson, 1985), with species from the Atlantic Ocean which showed larger *sagittae* than the Pacific one. This differences in size it was related to environmental factors, and specifically with depth, being the Pacific populations distributed at grater depths than the Atlantic ones, and being Atlantic waters warmer than the Pacific ones. This was related to differences in growth rates between shallow and deep populations. Indeed, it is well known as fast growth is reported for teleost species and populations inhabiting warmer,

more eutrophic, superficial waters (KUDERSKAYA, 1979; Templeman and Squires, 1956; Yefanov and Khorevin, 1979). Somatic growth rate strongly influences the otoliths growth, resulting in larger *sagittae* reported for species characterized by a fast growth (Lombarte and Lleonart, 1993). Improve the knowledge base on the populations structure of these species within the Mediterranean basin, elucidating their growth dynamics and *sagittae* features, is essential for conservation porpoises, being Macrourids fundamental for the well-being of the deep marine ecosystems worldwide.

At inter specific level, present paper confirmed the reliability of *sagittae* to discriminate between the different Macruridae species, assessing the high variability in morphology, morphometry, and shape between the investigated species. These findings were in line with those reported by Moore et al. (Moore et al., 2022), which demonstrated, in the geographical area of Ross and Amundsen Sea, the accuracy of otolith shape as a rapid, simple, and reliable tool for species differentiation between two grenadiers species, *Macrourus caml*, McMillan, Iwamoto, Stewart & Smith, 2012, and *Macrourus whitsoni*, Regan, 1913. Other authors successfully applied *sagittae* shape analysis and otolith morphometry to identify cryptic species, such as Tuset et al (Tuset et al., 2016b) for rockfishes (Sebastidae family), Sadighzadeh et al. (Sadighzadeh et al., 2012) for snapper species (Lutjanidae family) and Lombarte et al (Lombarte et al., 2018) for Mediterranean Sea gobies (Gobidae family). A correct identification at species level is fundamental, especially for the main harvested teleost with a high ecological value and diversity, such as Macruridae family. For instance, in the fisheries sampling programs, the accuracy of species identification can affect the reported catch and landings by vessels, the biological data collection and, consequently, the efficiency of the entire management design (see Moore et al. (Moore et al., 2022), and references therein). The taxonomic identification of the studied species, and of all those belonging to the Macruridae family, is very challenging and time consuming, and otoliths can improve this process, giving a reliable tool for a correct species discrimination. This is essential for the validity of fisheries programs dealing with grenadiers' species conservation, being their fisheries widely diffused, either as target species or as by-catch, world-wide (Devine et al., 2012; García-Ruiz et al., 2019). Moreover, these species play a vital role in several deep marine communities, being close to the top predator in the food chain, controlling preys populations, being among the main preys of several demersal predators (D'Iglio et al., 2022b, 2022a, 2021b), and influencing the dynamics of the entire communities (Drazen, 2002). For all these reasons the conservation and discrimination of Macrourids' populations is fundamental for the well-being of the deep communities and, consequently, for the entire marine ecosystem.

The main inter specific differences between the investigated species were related to the *sulcus acusticus*, the general otolith morphology and the mean contours. The similarity detected between congeneric species (*N. aequalis* and *N. sclerorhynchus*) or phylogenetically close genus

(*Coelorhynchis* and *Coryphaenoides*) (Endo, 2002; Han et al., 2021; Roa-Varón and Ortí, 2009), which constituted two statistically significant and clearly detectable patterns of similarity, was in line with literature. It is widely reported for several teleost groups (e.g., gobies, rockfishes, Scianidae species) (Lombarte et al., 2018; Tuset et al., 2016b, 2015; Verocai et al., 2023) how both phylogenetic divergence, together with environmental factors and life habits, have a strong effect on otoliths' shape and their morphological/morphometrical features. Concerning *C. coelorhynchis* and *C. guentheri*, in addition to be phylogenetically close, they share several aspect of their life habits, such as the feeding strategy, being both benthic predators (Carrassón and Matallanas, 2002; McLellan, 1977), and the distribution depth, being both mainly distributed, and with highest abundance values, between 400 and 500 m in the Mediterranean basin (García-Ruiz et al., 2019). Abundance and biomass of *N. sclerorhynchus* and *N. aequalis* increase with depth, with a maximum depth of distribution until 1600 m reported in the Tyrrhenian and in the Ionian Sea (D'Onghia et al., 2004; Follesa et al., 2011). Also, they mainly feed on benthic preys, with *N. sclerorhynchus* which occasionally show some benthopelagic habits (Madurell and Cartes, 2006, 2005; Saldanha et al., 1995), according to their generalist opportunistic predator behavior. According to results, *C. coelorhynchis, C. guentheri, N. sclerorhynchus* and *N. aequalis* specimens showed general oval contours of the *sagittae,* which could be strictly related to their benthic feeding habits. Indeed, the foraging techniques, together with feeding habits and diet composition experienced by the species, can shape the feature of *sagittae*, such as biochemistry, growth, mean contour, morphology and morphometry (Mille et al., 2016; Tuset et al., 2016b, 2015). The absence of data on the diet composition of the studied species from the investigated area make impossible to find direct correlations between feeding strategies and otoliths features to confirm this hypothesis. Conversely, the differences, resulting in a pentagonal shape, more lanceolate, in *C. coelorhynchus* and *C. guentheri,* and a more oval shape, with a marked irregularity of the margins in species belonging to *Nezumia* genus, could be influenced by the differences in their depth distribution. Moreover, morphometrical parameters of *sulcus acusticus* and *sagittae* showed significant differences between *Nezumia* species and, *Coryphaenoides* and *Coelorhynchus* species. Specimens belonging to the last two species showed markedly higher values of otoliths surface, length, weight, and *sulcus acusticus* surface and length, than those belonging to *Nezumia* genus. According to literature (Lombarte and Cruz, 2007), species belonging to abyssal communities (between 1000 and 2000 m) show a decrease in otoliths size, if compared with the belonging to demersal communities, until the 750 m of depth. *N. sclerorhynchus* and *N. aequalis* inhabit deeper habitats than *C. coelorhynchus* and *C. guentheri*, with a close relation with the abyssal environment that could influenced the detected differences in morphometry and mean contours. The decrease in *sagittae* size related to the increase of habitats depths it was also reported for others Macruridae species from the

Atlantic and Pacific Ocean (Wilson, 1985), with the similarity in otoliths length assessed for species with a similar depth distribution. Authors suggested that environment can control otoliths' size, being temperature and carbonate solubility strictly influenced by depth. Concerning *H. italicus*, it shows the highest abundance values between 400 and 500 m of depth, with a decrease in abundance below the 600 m (Massutí et al., 1995), and a maximum distribution depth reported in some Mediterranean areas at 1200 m (Follesa et al., 2011). It shows pelagic habits, preying mainly on copepods, planktonic amphipods and pelagic crustaceans (García-Ruiz et al., 2019; Madurell and Cartes, 2006, 2005; Saldanha et al., 1995). It performs wide vertical movement, following the prey along the water column, and being capable to inhabit also deep environments (Aguzzi et al., 2015; Madurell and Cartes, 2006). This differences in life habits could be reflected in *sagittae* features. Indeed, otoliths belonging to this species showed the higher distance to the other two groups (*Nezumia* sp group and *Coelorhynchus*/*Coryphaenoides* group) in LDA and PCA analysis performed on morphometric and shape indexes.

CONCLUSION

Present paper has provided the first accurate description of *sagittae* belonging to Macruridae species from the studied areas. On our best knowledge, it was the first time in which shape analysis was applied on the studied species, providing evidence on the reliability of mean contours to discriminate the between species and, eventually, different populations. Moreover, findings reported the absence of directional bilateral asymmetry in all the investigated species, showing several differences in morphometry and morphology with literature data from other geographical areas. At inter specific level, it was stated the statistically significant distance among *Nezumia* sp group, *Coelorhynchus*/*Coryphaenoides* group and *H. italicus* group regarding data from both morphometrical and shape analysis. This confirmed the dual influence of phylogenetic and environment on otoliths development and features, being the three groups of species characterized by similarity in life habits and phylogenetically closeness.

Further analyses are required to understand and detect the direct correlations between genetics, life habits, environment and *sagittae* features at intra and inter specific level. It will be essential to provide information on the genetics, feeding habits and depth distribution of the studied species from the investigated area to understand their influence on *sagittae* shape and morphometry. Moreover, it will be interesting to compare growth dynamics, environmental and genetical data of different populations to add valuable information and new insights on the otoliths' eco-morphology and inter-population

differences. This is of the utmost importance to better understand the dynamics allowing to the stocks and populations separation in demersal and abyssal teleost fishes.

Improve the knowledge base on Macrouridae inter specific and inter populations differences, and on the dynamics allowing to these variations, is fundamental to understand at all their life habits and improve their conservation for the well-being of the entire Mediterranean ecosystem.

Authors contribution

Claudio D'Iglio, Investigation, Data curation, Writing-Original draft; Sergio Famulari, Formal analysis, Software, Data curation; Dario Di Fresco, Mariachiara Costanzo and Alex Carnevale, Methodology and Investigation; Marco Albano, Data curation, Writing - review & editing; Nunziacarla Spanò, Supervision, Validation; Serena Savoca, Data curation, Formal analysis, Software, Writing - review & editing; Gioele Capillo Conceptualization, Supervision, Visualization, Writing-review and editing.

BIBLIOGRAPHY

Aguzzi, J., Sbragaglia, V., Tecchio, S., Navarro, J., Company, J.B., 2015. Rhythmic behaviour of marine benthopelagic species and the synchronous dynamics of benthic communities. Deep. Res. Part I Oceanogr. Res. Pap. 95, 1–11. https://doi.org/10.1016/j.dsr.2014.10.003

Assis, C.A., 2000. Estudo morfológico dos otólitos sagitta, asteriscus e lapillus de Teleóstei (Actinopterygii, Teleostei) de Portugal continental. Sua aplicação em estudos de filogenia, sistematica e ecologia. Ecologia.

Battaglia, P., Andaloro, F., Consoli, P., Esposito, V., Malara, D., Musolino, S., Pedà, C., Romeo, T., 2013. Feeding habits of the Atlantic bluefin tuna, Thunnus thynnus (L. 1758), in the central Mediterranean Sea (Strait of Messina). Helgol. Mar. Res. 67, 97–107. https://doi.org/10.1007/s10152-012-0307-2

Bauchot, M.-L., 1987. Poissons osseux. Fiches FAO d'identification des espèces pour les besoins la pêche. (Révision 1). Méditerranée mer Noire.\rZone pêche 37. Vol. II. Vertébrés.

Begg, G.A., Brown, R.W., 2000. Stock Identification of Haddock Melanogrammus aeglefinus on Georges Bank Based on Otolith Shape Analysis . Trans. Am. Fish. Soc. 129, 935–945. https://doi.org/10.1577/1548-8659(2000)129<0935:siohma>2.3.co;2

Bose, A.P.H., Zimmermann, H., Winkler, G., Kaufmann, A., Strohmeier, T., Koblmüller, S., Sefc, K.M., 2020. Congruent geographic variation in saccular otolith shape across multiple species of African cichlids. Sci. Rep. 10, 1–14. https://doi.org/10.1038/s41598-020-69701-9

Campana, S.E., 2004. Photographic Atlas of Fish Otoliths of the Northwest Atlantic Ocean, Photographic Atlas of Fish Otoliths of the Northwest Atlantic Ocean. NRC Research Press. https://doi.org/10.1139/9780660191089

Carrassón, M., Matallanas, J., 2002. Diets of deep-sea macrourid fishes in the western Mediterranean. Mar. Ecol. Prog. Ser. 234, 215–228. https://doi.org/10.3354/meps234215

Catarino, D., Stefanni, S., Jorde, P.E., Menezes, G.M., Company, J.B., Neat, F., Knutsen, H., 2017. The role of the Strait of Gibraltar in shaping the genetic structure of the Mediterranean Grenadier, Coryphaenoides mediterraneus, between the Atlantic and Mediterranean Sea. PLoS One 12, e0174988. https://doi.org/10.1371/journal.pone.0174988

Colura, R.L., King, T.L., Secor, D.H., Dean, J.M., Campana, 1995. Using scale and otolith Morphologies to Separate spotted Seatrout collected from two areas within Galveston Bay. Recent Dev. fish otolith Res. 617–628.

D'Iglio, C., Albano, M., Famulari, S., Savoca, S., Panarello, G., Di Paola, D., Perdichizzi, A., Rinelli, P., Lanteri, G., Spanò, N., Capillo, G., 2021a. Intra- and interspecific variability among congeneric Pagellus otoliths. Sci. Rep. 11, 16315. https://doi.org/10.1038/s41598-021-95814-w

D'Iglio, C., Albano, M., Tiralongo, F., Famulari, S., Rinelli, P., Savoca, S., Spanò, N., Capillo, G., 2021b. Biological and Ecological Aspects of the Blackmouth Catshark (Galeus melastomus Rafinesque, 1810) in the Southern Tyrrhenian Sea. J. Mar. Sci. Eng. 9, 967. https://doi.org/10.3390/jmse9090967

D'Iglio, C., Famulari, S., Albano, M., Giordano, D., Rinelli, P., Capillo, G., Spanò, N., Savoca, S., 2022a. Time-Scale Analysis of Prey Preferences and Ontogenetic Shift in the Diet of European Hake Merluccius merluccius (Linnaeus, 1758) in Southern and Central Tyrrhenian Sea. Fishes 7. https://doi.org/10.3390/fishes7040167

D'iglio, C., Natale, S., Albano, M., Savoca, S., Famulari, S., Gervasi, C., Lanteri, G., Panarello, G., Spanò, N., Capillo, G., 2022. Otolith Analyses Highlight Morpho-Functional Differences of Three Species of Mullet (Mugilidae) from Transitional Water. Sustain. https://doi.org/10.3390/su14010398

D'Iglio, C., Porcino, N., Savoca, S., Profeta, A., Perdichizzi, A., Armeli, E., Davide, M., Francesco, S., Rinelli, P., Giordano, D., 2022b. Ontogenetic shift and feeding habits of the European hake (Merluccius merluccius L ., 1758) in Central and Southern Tyrrhenian Sea (Western Mediterranean Sea): A comparison between past and present data. Ecol. Evol. 12. https://doi.org/10.1002/ece3.8634

D'Iglio, C., Porcino, N., Savoca, S., Profeta, A., Perdichizzi, A., Armeli Minicante, E., Salvati, D.,

Soraci, F., Rinelli, P., Giordano, D., 2022c. Ontogenetic shift and feeding habits of the European hake (Merluccius merluccius L., 1758) in Central and Southern Tyrrhenian Sea (Western Mediterranean Sea): A comparison between past and present data . Ecol. Evol. 12, e8634. https://doi.org/10.1002/ece3.8634

D'Iglio, C., Savoca, S., Rinelli, P., Spanò, N., 2021c. Diet of the Deep-Sea Shark Galeus melastomus Rafinesque , 1810 , in the Mediterranean Sea : What We Know and What We Should Know. Sustainability 13. https://doi.org/https:// doi.org/10.3390/su13073962

D'Onghia, G., Basanisi, M., Tursi, A., 2000. Population structure, age and growth of macrourid fish from the upper slope of the Eastern-Central Mediterranean. J. Fish Biol. 56, 1217–1238. https://doi.org/10.1006/jfbi.2000.1243

D'Onghia, G., Politou, C.Y., Bozzano, A., LLoris, D., Rotllant, G., Sion, L., Mastrototaro, F., 2004. Deep-water fish assemblages in the Mediterranean Sea. Sci. Mar. 68, 87–99. https://doi.org/10.3989/scimar.2004.68s387

D'Onghia, G., Tursi, A., Maiorano, P., Matarrese, A., Panza, M., 1998. Demersal fish assemblages from the bathyal grounds of the Ionian sea (middle-eastern mediterranean). Ital. J. Zool. 65, 287–292. https://doi.org/10.1080/11250009809386834

Danovaro, R., Company, J.B., Corinaldesi, C., D'Onghia, G., Galil, B., Gambi, C., Gooday, A.J., Lampadariou, N., Luna, G.M., Morigi, C., Olu, K., Polymenakou, P., Ramirez-Llodra, E., Sabbatini, A., Sardá, F., Sibuet, M., Tselepides, A., 2010. Deep-sea biodiversity in the Mediterranean Sea: The known, the unknown, and the unknowable. PLoS One 5, e11832. https://doi.org/10.1371/journal.pone.0011832

Devine, J.A., Watling, L., Cailliet, G., Drazen, J., Durán Muñoz, P., Orlov, A.M., Bezaury, J., 2012. Evaluation of potential sustainability of deep-sea fisheries for grenadiers (Macrouridae). J. Ichthyol. 52, 709–721. https://doi.org/10.1134/S0032945212100062

Draganik, B., Psuty-Lipska, I., Janusz, J., 1998. Ageing of roundnose grenadier (Coryphaenoides rupestris Gunn.) from otoliths. ICES C.

Drazen, J.C., 2002. Energy budgets and feeding rates of Coryphaenoides acrolepis and C. armatus. Mar. Biol. 140, 677–686. https://doi.org/10.1007/s00227-001-0747-8

Drazen, J.C., Popp, B.N., Choy, C.A., Clemente, T., De Forest, L., Smith, K.L., 2008. Bypassing the abyssal benthic food web: Macrourid diet in the eastern North Pacific inferred from stomach content and stable isotopes analyses. Limnol. Oceanogr. 53, 2644–2654. https://doi.org/10.4319/lo.2008.53.6.2644

Dulčić, J., Matić-Skoko, S., Kraljević, M., Fencil, M., Glamuzina, B., 2005. Seasonality of a fish assemblage in shallow waters of Duće-Glava, eastern middle Adriatic. Cybium 29, 57–63.

Dunn, J.R., Cohen, D.M., Inada, T., Iwamoto, T., Scialabba, N., 1992. Gadiform Fishes of the World (Order Gadiformes). An Annotated and Illustrated Catalogue of Cods, Hakes, Grenadiers and Other Gadiform Fishes Known to Date, Copeia. FAO. https://doi.org/10.2307/1446232

Endo, H., 2002. Phylogeny of the Order Gadiformes (Teleostei, Paracanthopterygii). Mem. Grad. Sch. Fish. Sci. Hokkaido Univ. 49, 75–149.

Eschmeyer, W.N., Fong, J.D., 2014. Catalog of fishes: species by family/sub-family [WWW Document]. Cat. Fishes. URL http://research.calacademy.org/redirect?url=http://researcharchive.calacademy.org/research/Ichthyology/catalog/SpeciesByFamily.asp

Follesa, M.C., Porcu, C., Cabiddu, S., Mulas, A., Deiana, A.M., Cau, A., 2011. Deep-water fish assemblages in the central-western Mediterranean (south Sardinian deep-waters). J. Appl. Ichthyol. 27, 129–135.

Friedland, K.D., Reddin, D.G., 1994. Use of otolith morphology in stock discriminations of Atlantic salmon (Salmo salar). Can. J. Fish. Aquat. Sci. 51, 91–98. https://doi.org/10.1139/f94-011

Gagliano, M., McCormick, M.I., 2004. Feeding history influences otolith shape in tropical fish. Mar. Ecol. Prog. Ser. 278, 291–296. https://doi.org/10.3354/meps278291

Gaither, M.R., Violi, B., Gray, H.W.I., Neat, F., Drazen, J.C., Grubbs, R.D., Roa-Varón, A., Sutton, T., Hoelzel, A.R., 2016. Depth as a driver of evolution in the deep sea: Insights from grenadiers (Gadiformes: Macrouridae) of the genus Coryphaenoides. Mol. Phylogenet. Evol. 104, 73–82. https://doi.org/10.1016/j.ympev.2016.07.027

García-Ruiz, C., Hidalgo, M., Carpentieri, P., Fernandez-Arcaya, U., Gaudio, P., González, M., Jadaud, A., Mulas, A., Peristeraki, P., Rueda, J.L., Vitale, S., D'onghia, G., 2019. Spatio-temporal patterns of macrourid fish species in the northern Mediterranean sea. Sci. Mar. 83, 117–127. https://doi.org/10.3989/scimar.04889.11A

Han, Z., Shou, C., Liu, M., Gao, T., 2021. Large-scale phylogenomic analysis provides new insights into the phylogeny of the order Gadiformes and evolution of freshwater gadiform species burbot (Lota lota).

Hüssy, K., 2008. Otolith shape in juvenile cod (Gadus morhua): Ontogenetic and environmental effects. J. Exp. Mar. Bio. Ecol. 364, 35–41. https://doi.org/10.1016/j.jembe.2008.06.026

Jaramilo, A.M., Tombari, A.D., Benedito Dura, V., Eugeni Rodrigo, M., Volpedo, A. V., 2014. Otolith eco-morphological patterns of benthic fishes from the coast of Valencia (Spain). Thalassas 30, 57–66.

Jawad, L.A., Sabatino, G., Ibáñez, A.L., Andaloro, F., Battaglia, P., 2018. Morphology and

ontogenetic changes in otoliths of the mesopelagic fishes Ceratoscopelus maderensis (Myctophidae), Vinciguerria attenuata and V. poweriae (Phosichthyidae) from the Strait of Messina (Mediterranean Sea). Acta Zool. https://doi.org/10.1111/azo.12197

Karachle, P. k, Stergiou, K. i, 2010. Food and feeding habits of nine elasmobranch species in the N. Aegeans Sea. Rapp. Comm. int. Mer Médit. 39.

KUDERSKAYA, R.A., 1979. PARTICULARITES MORPHO-ECOLOGIQUES D'HELICOLENUS MACULATUS (CUVIER) DE LA COTE ATLANTIQUE DE L'AFRIQUE DU SUD (FAMILLE DES SCORPAENIDAE).

Kuemlangan, B., Sanders, J., 2008. International guidelines: Management of deep-sea fisheries in the high seas, Environmental Policy and Law. FAO.

Labropoulou, M., Papaconstantinou, C., 2000. Comparison of otolith growth and somatic growth in two macrourid fishes. Fish. Res. 46, 177–188. https://doi.org/10.1016/S0165-7836(00)00144-2

Libungan, L.A., Pálsson, S., 2015. ShapeR: An R package to study otolith shape variation among fish populations. PLoS One 10, 1–12. https://doi.org/10.1371/journal.pone.0121102

Lin, C.H., Girone, A., Nolf, D., 2016. Fish otolith assemblages from Recent NE Atlantic sea bottoms: A comparative study of palaeoecology. Palaeogeogr. Palaeoclimatol. Palaeoecol. 446, 98–107. https://doi.org/10.1016/j.palaeo.2016.01.022

Linley, T.D., Gerringer, M.E., Yancey, P.H., Drazen, J.C., Weinstock, C.L., Jamieson, A.J., 2016. Fishes of the hadal zone including new species, in situ observations and depth records of Liparidae. Deep. Res. Part I Oceanogr. Res. Pap. 114, 99–110. https://doi.org/10.1016/j.dsr.2016.05.003

Lloris, D., 2015. Ictiofauna marina: manual de identificación de los peces marinos de la Península Ibérica y Balears. 954 especies. Omega.

Lombarte, A., Cruz, A., 2007. Otolith size trends in marine fish communities from different depth strata. J. Fish Biol. 71, 53–76. https://doi.org/10.1111/j.1095-8649.2007.01465.x

Lombarte, A., Lleonart, J., 1993. Otolith size changes related with body growth, habitat depth and temperature. Environ. Biol. Fishes 37, 297–306. https://doi.org/10.1007/BF00004637

Lombarte, A., Miletić, M., Kovačić, M., Otero-Ferrer, J.L., Tuset, V.M., 2018. Identifying sagittal otoliths of Mediterranean Sea gobies: variability among phylogenetic lineages. J. Fish Biol. 92, 1768–1787. https://doi.org/10.1111/jfb.13615

Lombarte, A., Morales-Nin, B., 1995. Morphology and ultrastructure of saccular otoliths from five species of the genus Coelorinchus (Gadiformes: Macrouridae) from the Southeast Atlantic. J. Morphol. 225, 179–192. https://doi.org/10.1002/jmor.1052250204

Lombarte, A., Palmer, M., Matallanas, J., Gómez-Zurita, J., Morales-Nin, B., 2010.

Ecomorphological trends and phylogenetic inertia of otolith sagittae in Nototheniidae. Environ. Biol. Fishes 89, 607–618. https://doi.org/10.1007/s10641-010-9673-2

Lombarte, A., Tuset, V.M., 2015. Chapter3- Morfometría de otolitos, in: Volpedo, A.V., Vaz-dos-Santos, A.M. (Eds.), Métodos de Estudios Con Otolitos: Principios y Aplicaciones/ Métodos de Estudos Com Otólitos: Princípios e Aplicações. Ciudad Autónoma de Buenos Aires, p. 31.

Lord, C., Morat, F., Lecomte-Finiger, R., Keith, P., 2012. Otolith shape analysis for three Sicyopterus (Teleostei: Gobioidei: Sicydiinae) species from New Caledonia and Vanuatu. Environ. Biol. Fishes 93, 209–222. https://doi.org/10.1007/s10641-011-9907-y

Madurell, T., Cartes, J.E., 2006. Trophic relationships and food consumption of slope dwelling macrourids from the bathyal Ionian Sea (eastern Mediterranean). Mar. Biol. 148, 1325–1338. https://doi.org/10.1007/s00227-005-0158-3

Madurell, T., Cartes, J.E., 2005. Trophodynamics of a deep-sea demersal fish assemblage from the bathyal eastern Ionian Sea (Mediterranean Sea). Deep. Res. Part I Oceanogr. Res. Pap. 52, 2049–2064. https://doi.org/10.1016/j.dsr.2005.06.013

Mangano, M.C., Bottari, T., Caridi, F., Porporato, E.M.D., Rinelli, P., Spanò, N., Johnson, M., Sarà, G., 2017. The effectiveness of fish feeding behaviour in mirroring trawling-induced patterns. Mar. Environ. Res. 131, 195–204. https://doi.org/https://doi.org/10.1016/j.marenvres.2017.09.004

Marques, A., Almeida, A.J., 2001. Otolith morphology of Nezumia sclerorhynchus and Nezumia aequalis (Macrouridae): A useful tool to species identification and ecologycal studies. Bol. Mus. Mun. Funchal, Sup. N.º 6, 205–212.

Marshall, N.B., 1979. Developments in deep-sea biology.

Massutí, E., Morales-Nin, B., Stefanescu, C., 1995. Distribution and biology of five grenadier fish (Pisces: Macrouridae) from the upper and middle slope of the northwestern Mediterranean. Deep. Res. Part I 42, 307–330. https://doi.org/10.1016/0967-0637(95)00003-O

Matarrese, A., D'Onghia, G., Tursi, A., Basanisi, M., 1996. New information on the ichthyofauna of the south-eastern Italian coasts (Ionian Sea). Cybium 20, 197–211.

Matić-Skoko, S., Peharda, M., Pallaoro, A., Franiçević, M., 2005. Species composition, seasonal fluctuations, and residency of inshore fish assemblages in the Pantan estuary of the eastern middle Adriatic. Acta Adriat. 46, 201–212.

Matić-Skoko, S., Peharda, M., Vrdoljak, D., Uvanović, H., Markulin, K., 2020a. Fish and Sclerochronology Research in the Mediterranean: Challenges and Opportunities for Reconstructing Environmental Changes. Front. Mar. Sci. 7, 195. https://doi.org/10.3389/fmars.2020.00195

Matić-Skoko, S., Vrdoljak, D., Uvanović, H., Pavičić, M., Tutman, P., Bojanić Varezić, D., 2020b. Early evidence of a shift in juvenile fish communities in response to conditions in nursery areas. Sci. Rep. 10, 1–16. https://doi.org/10.1038/s41598-020-78181-w

McLellan, T., 1977. Feeding strategies of the macrourids. Deep. Res. 24, 1019–1036. https://doi.org/10.1016/0146-6291(77)90572-0

Mille, T., Mahé, K., Cachera, M., Villanueva, M.C., De Pontual, H., Ernande, B., 2016. Diet is correlated with otolith shape in marine fish. Mar. Ecol. Prog. Ser. 555, 167–184. https://doi.org/10.3354/meps11784

Montanini, S., Stagioni, M., Valdrè, G., Tommasini, S., Vallisneri, M., 2015. Intra-specific and inter-specific variability of the sulcus acusticus of sagittal otoliths in two gurnard species (Scorpaeniformes, Triglidae). Fish. Res. 161, 93–101. https://doi.org/10.1016/j.fishres.2014.07.003

Moore, B.R., Parker, S.J., Pinkerton, M.H., 2022. Otolith shape as a tool for species identification of the grenadiers Macrourus caml and M. whitsoni. Fish. Res. 253, 106370.

Morat, F., Letourneur, Y., Nérini, D., Banaru, D., Batjakas, I.E., 2012. Discrimination of red mullet populations (Teleostean, Mullidae) along multi-spatial and ontogenetic scales within the Mediterranean basin on the basis of otolith shape analysis. Aquat. Living Resour. 25, 27–39. https://doi.org/10.1051/alr/2011151

Neves, J., Giacomello, E., Menezes, G.M., Fontes, J., Tanner, S.E., 2021. Temperature-Driven Growth Variation in a Deep-Sea Fish: The Case of Pagellus bogaraveo (Brünnich, 1768) in the Azores Archipelago. Front. Mar. Sci. https://doi.org/10.3389/fmars.2021.703820

Nolf, D., 1995. Studies on fossil otoliths - The state of the art. Recent Dev. Fish Otolith Res. 19, 513–544.

Nolf, D., 1985. Otolithi Piscium. Handbook of Paleoichthyology, Vol. 10. Stuttgart, New York.

Nolf, D., de Potter, H., Lafond-Grellety, J., 2009. Hommage à Joseph Chaine et Jean Duvergier: Diversité et variabilité des otolithes des poissons. Palaeo Publishing and Library vzw. Palaeo Publishing and Library vzw, Belgium.

Norse, E.A., Brooke, S., Cheung, W.W.L., Clark, M.R., Ekeland, I., Froese, R., Gjerde, K.M., Haedrich, R.L., Heppell, S.S., Morato, T., 2012. Sustainability of deep-sea fisheries. Mar. policy 36, 307–320.

Olson, C.R., 2017. Population genetic structure of two abyssal grenadiers of the north Atlantic and northeastern Pacific oceans. California State University, Long Beach.

Pavlov, D.A., 2021. Otolith Morphology and Relationships of Several Fish Species of the Suborder Scorpaenoidei. J. Ichthyol. 61, 33–47. https://doi.org/10.1134/S0032945221010100

Pavlov, D.A., 2016. Differentiation of three species of the genus Upeneus (Mullidae) based on otolith shape analysis. J. Ichthyol. 56, 37–51. https://doi.org/10.1134/S0032945216010094

Ponton, D., 2006. Is geometric morphometrics efficient for comparing otolith shape of different fish species? J. Morphol. 267, 750–757. https://doi.org/10.1002/jmor.10439

Popper, A.N., Lu, Z., 2000. Structure-function relationships in fish otolith organs. Fish. Res. 46, 15–25. https://doi.org/10.1016/S0165-7836(00)00129-6

Reichenbacher, B., Sienknecht, U., Küchenhoff, H., Fenske, N., 2007. Combined otolith morphology and morphometry for assessing taxonomy and diversity in fossil and extant killifish (Aphanius, †Prolebias). J. Morphol. 268, 898–915. https://doi.org/10.1002/jmor.10561

Roa-Varón, A., Ortí, G., 2009. Phylogenetic relationships among families of Gadiformes (Teleostei, Paracanthopterygii) based on nuclear and mitochondrial data. Mol. Phylogenet. Evol. 52, 688–704. https://doi.org/10.1016/j.ympev.2009.03.020

Sadighzadeh, Z., Tuset, V.M., Valinassab, T., Dadpour, M.R., Lombarte, A., 2012. Comparison of different otolith shape descriptors and morphometrics for the identification of closely related species of Lutjanus spp. from the Persian Gulf. Mar. Biol. Res. 8, 802–814. https://doi.org/10.1080/17451000.2012.692163

Saldanha, L., Almeida, A.J., Andrade, F., Guerreiro, J., 1995. Observations on the Diet of Some Slope Dwelling Fishes of Southern Portugal. Int. Rev. der gesamten Hydrobiol. und Hydrogr. 80, 217–234. https://doi.org/10.1002/iroh.19950800210

Schneider, C.A., Rasband, W.S., Eliceiri, K.W., 2012. NIH Image to ImageJ: 25 years of image analysis. Nat. Methods 9, 671–675. https://doi.org/10.1038/nmeth.2089

Schulz-Mirbach, T., Ladich, F., Riesch, R., Plath, M., 2010. Otolith morphology and hearing abilities in cave- and surface-dwelling ecotypes of the Atlantic molly, Poecilia mexicana (Teleostei: Poeciliidae). Hear. Res. 267, 137–148. https://doi.org/10.1016/j.heares.2010.04.001

Schulz-Mirbach, T., Stransky, C., Schlickeisen, J., Reichenbacher, B., 2008. Differences in otolith morphologies between surface- and cave-dwelling populations of Poecilia mexicana (Teleostei, Poeciliidae) reflect adaptations to life in an extreme habitat. Evol. Ecol. Res. 10, 537–558.

Schwarzhans, W., 2014. Head and otolith morphology of the genera Hymenocephalus, Hymenogadus and Spicomacrurus (Macrouridae), with the description of three new species. Zootaxa 3888, 1–73. https://doi.org/10.11646/zootaxa.3888.1.1

Shi, X., Tian, P., Lin, R., Huang, D., Wang, J., 2016. Characterization of the complete mitochondrial genome sequence of the globose head whiptail Cetonurus globiceps (Gadiformes: Macrouridae) and its phylogenetic analysis. PLoS One 11, e0153666.

https://doi.org/10.1371/journal.pone.0153666

Sion, L., Maiorano, P., Carlucci, R., Capezzuto, F., Indennidate, A., Tursi, A., D'Onghia, G., 2012. Review of the literature on age and growth of grenadiers in the Mediterranean and new data on age of Trachyrincus scabrus (Macrouridae) in the Ionian Sea. J. Ichthyol. 52, 740–749. https://doi.org/10.1134/S0032945212100116

Sobrino, I., González, J., Hernández-González, C.L., Balguerias, E., 2012. Distribution and relative abundance of main species of grenadiers (Macrouridae, Gadiformes) from the African Atlantic Coast. J. Ichthyol. 52, 690–699. https://doi.org/10.1134/S0032945212100128

Stergiou, K.I., Karpouzi, V.S., 2002. Feeding habits and trophic levels of Mediterranean fish. Rev. Fish Biol. Fish. 11, 217–254. https://doi.org/10.1023/A:1020556722822

Stransky, C., Murta, A.G., Schlickeisen, J., Zimmermann, C., 2008. Otolith shape analysis as a tool for stock separation of horse mackerel (Trachurus trachurus) in the Northeast Atlantic and Mediterranean. Fish. Res. 89, 159–166. https://doi.org/10.1016/j.fishres.2007.09.017

Swan, S.C., Gordon, J.D.M., Morales-Nin, B., Shimmield, T., Sawyer, T., Geffen, A.J., 2003. Otolith microchemistry of Nezumia aequalis (Pisces: Macrouridae) from widely different habitats in the Atlantic and Mediterranean. J. Mar. Biol. Assoc. United Kingdom 83, 883–886. https://doi.org/10.1017/S0025315403007987h

Teimori, A., Khajooei, A., Motamedi, M., Hesni, M.A., 2019. Characteristics of sagittae morphology in sixteen marine fish species collected from the Persian Gulf: Demonstration of the phylogenetic influence on otolith shape. Reg. Stud. Mar. Sci. 29, 100661. https://doi.org/10.1016/j.rsma.2019.100661

Templeman, W., Squires, H.J., 1956. Relationship of Otolith Lengths and Weights in the Haddock Melanogrammus aeglefinus (L.) to the Rate of Growth of the Fish . J. Fish. Res. Board Canada 13, 467–487. https://doi.org/10.1139/f56-029

Tiralongo, F., Messina, G., Lombardo, B.M., 2020. Biological Aspects of Juveniles of the Common Stingray , Dasyatis pastinaca (Linnaeus , 1758) (Elasmobranchii , Dasyatidae), from the Central Mediterranean Sea. J. Mar. Sci. Eng. 8, 269. https://doi.org/doi:10.3390/jmse8040269

Torres, G.J., Lombarte, A., Morales-Nin, B., 2000a. Sagittal otolith size and shape variability to identify geographical intraspecific differences in three species of the genus Merluccius. J. Mar. Biol. Assoc. United Kingdom 80, 333–342. https://doi.org/10.1017/S0025315499001915

Torres, G.J., Lombarte, A., Morales-Nin, B., 2000b. Variability of the sulcus acusticus in the sagittal otolith of the genus Merluccius (Merlucciidae). Fish. Res. 46, 5–13. https://doi.org/10.1016/S0165-7836(00)00128-4

Tuset, V.M., Farré, M., Otero-Ferrer, J.L., Vilar, A., Morales-Nin, B., Lombarte, A., 2016a. Testing

otolith morphology for measuring marine fish biodiversity. Mar. Freshw. Res. 67, 1037–1048. https://doi.org/10.1071/MF15052

Tuset, V.M., Imondi, R., Aguado, G., Otero-Ferrer, J.L., Santschi, L., Lombarte, A., Love, M., 2015. Otolith patterns of rockfishes from the northeastern pacific. J. Morphol. 276, 458–469. https://doi.org/10.1002/jmor.20353

Tuset, V.M., Lombarte, A., Assis, C.A., 2008. Otolith atlas for the western Mediterranean, north and central eastern Atlantic. Sci. Mar. 72, 7–198.

Tuset, V.M., Lombarte, A., Bariche, M., Maynou, F., Azzurro, E., 2020. Otolith morphological divergences of successful Lessepsian fishes on the Mediterranean coastal waters. Estuar. Coast. Shelf Sci. 236, 106631. https://doi.org/10.1016/j.ecss.2020.106631

Tuset, V.M., Lombarte, A., González, J.A., Pertusa, J.F., Lorente, M.J., 2003a. Comparative morphology of the sagittal otolith in Serranus spp. J. Fish Biol. 63, 1491–1504. https://doi.org/10.1111/j.1095-8649.2003.00262.x

Tuset, V.M., Lozano, I.J., GonzÍez, J.A., Pertusa, J.F., García-Díaz, M.M., 2003b. Shape indices to identify regional differences in otolith morphology of comber, Serranus cabrilla (L., 1758). J. Appl. Ichthyol. 19, 88–93. https://doi.org/10.1046/j.1439-0426.2003.00344.x

Tuset, V.M., Olivar, M.P., Otero-Ferrer, J.L., López-Pérez, C., Hulley, P.A., Lombarte, A., 2018. Morpho-functional diversity in Diaphus spp. (Pisces: Myctophidae) from the central Atlantic Ocean: Ecological and evolutionary implications. Deep. Res. Part I Oceanogr. Res. Pap. 138, 46–59. https://doi.org/10.1016/j.dsr.2018.07.005

Tuset, V.M., Otero-Ferrer, J.L., Gómez-Zurita, J., Venerus, L.A., Stransky, C., Imondi, R., Orlov, A.M., Ye, Z., Santschi, L., Afanasiev, P.K., Zhuang, L., Farré, M., Love, M.S., Lombarte, A., 2016b. Otolith shape lends support to the sensory drive hypothesis in rockfishes. J. Evol. Biol. 29, 2083–2097. https://doi.org/10.1111/jeb.12932

Vasconcelos, J., Jurado-Ruzafa, A., Otero-Ferrer, J.L., Lombarte, A., Riera, R., Tuset, V.M., 2021. Thinking of Fish Population Discrimination: Population Average Phenotype vs. Population Phenotypes. Front. Mar. Sci. 8. https://doi.org/10.3389/fmars.2021.740296

Verocai, J.E., Cabrera, F., Lombarte, A., Norbis, W., 2023. Form function of sulcus acusticus of the sagittal otolith in seven Sciaenidae (Acanthuriformes) species using geometric morphometrics (southwestern Atlantic). J. Fish Biol. https://doi.org/10.1111/jfb.15521

Vignon, M., Morat, F., 2010. Environmental and genetic determinant of otolith shape revealed by a non-indigenous tropical fish. Mar. Ecol. Prog. Ser. 411, 231–241. https://doi.org/10.3354/meps08651

Volpedo, A., Diana Echeverría, D., 2003. Ecomorphological patterns of the sagitta in fish on the

continental shelf off Argentine. Fish. Res. 60, 551–560. https://doi.org/10.1016/S0165-7836(02)00170-4

Volpedo, A. V., Tombari, A.D., Echeverría, D.D., 2008. Eco-morphological patterns of the sagitta of Antarctic fish. Polar Biol. 31, 635–640. https://doi.org/10.1007/s00300-007-0400-1

Weitzman, S.H., 1997. 2 Systematics of Deep-Sea Fishes, in: Fish Physiology. Elsevier, pp. 43–77. https://doi.org/10.1016/S1546-5098(08)60227-7

Wilson, R.R., 1988. Analysis of growth zones and microstructure in otoliths of two macrourids from the North Pacific abyss. Environ. Biol. Fishes 21, 251–261. https://doi.org/10.1007/BF00000374

Wilson, R.R., 1985. Depth-Related Changes in Sagitta Morphology in Six Macrourid Fishes of the Pacific and Atlantic Oceans. Copeia 1985, 1011. https://doi.org/10.2307/1445256

Yefanov, V.N., Khorevin, L.D., 1979. Distinguishing populations of pink salmon, Oncorhynchus gorbuscha , by the size of their otoliths. J. Ichthyol. 19, 142–145.

Zhuang, L., Ye, Z., Zhang, C., 2015. Application of otolith shape analysis to species separation in Sebastes spp. from the Bohai Sea and the Yellow Sea, northwest Pacific. Environ. Biol. Fishes 98, 547–558. https://doi.org/10.1007/s10641-014-0286-z

Zischke, M.T., Litherland, L., Tilyard, B.R., Stratford, N.J., Jones, E.L., Wang, Y.G., 2016. Otolith morphology of four mackerel species (Scomberomorus spp.) in Australia: Species differentiation and prediction for fisheries monitoring and assessment. Fish. Res. 176, 39–47. https://doi.org/10.1016/j.fishres.2015.12.003

PLOS ONE

RESEARCH ARTICLE

Intraspecific variability of the saccular and utricular otoliths of the hatchetfish *Argyropelecus hemigymnus* (Cocco, 1829) from the Strait of Messina (Central Mediterranean Sea)

Claudio D'Iglio[1], Sergio Famulari[1], Marco Albano[1], Alex Carnevale[1], Dario Di Fresco[1], Mariachiara Costanzo[1], Giovanni Lanteri[1], Nunziacarla Spanò[2], Serena Savoca[2☯*], Gioele Capillo[3☯]

1 Department of Chemical, Biological, Pharmaceutical and Environmental Sciences, University of Messina, Messina, Italy, **2** Department of Biomedical, Dental and Morphological and Functional Imaging, University of Messina, Messina, Italy, **3** Department of Veterinary Sciences, University of Messina, Messina, Italy

☯ These authors contributed equally to this work.
* ssavoca@unime.it

Citation: D'Iglio C, Famulari S, Albano M, Carnevale A, Di Fresco D, Costanzo M, et al. (2023) Intraspecific variability of the saccular and utricular otoliths of the hatchetfish *Argyropelecus hemigymnus* (Cocco, 1829) from the Strait of Messina (Central Mediterranean Sea). PLoS ONE 18(2): e0281621. https://doi.org/10.1371/journal.pone.0281621

Editor: Sanja Puljas, University of Split, Faculty of science, CROATIA

Received: October 7, 2022

Accepted: January 27, 2023

Published: February 14, 2023

Data Availability Statement: All relevant data are within the paper and its Supporting information files.

Funding: The funders had no role in study design, data collection and analysis, decision to publish, or preparation of the manuscript.

Competing interests: The authors have declared that no competing interests exist.

Abstract

Mesopelagic species are enjoining increasing attention due to the growing impact of fisheries activities on deep marine biocenosis. Improving the knowledge base on mesopelagic species is required to enhance their conservation due to the knowledge gaps regarding many species and families. In this context, otoliths can be fundamental to assessing their life history, ecomorphological adaptation to the deep environment and stock composition. The present paper aims to explore the saccular and utricular otoliths morphology and intraspecific variability of the hatchetfish, *Argyropelecus hemigymnus*, from the Strait of Messina. *Lapilli* and *sagittae* were collected from 70 specimens and separated into four size classes. Morphometric, shape and SEM investigations were performed to describe their morphology, contours, and external structural organization, also studying their intraspecific variability related to sample sizes and differences between otolith pairs. Results showed an otolith morphology different from those reported in the literature with fluctuating asymmetry in *sagittae* and *lapilli* belonging to Class IV, and a high otolith variability between all the size classes. Data herein described confirm the otoliths singularity of the population from the Strait of Messina, shaped by a unique marine environment for oceanographic and ecological features.

Introduction

The vertebrates' inner ear represents a highly specialized organ for sound detection, motion/position measuring, and equilibrium regulation [1, 2]. All the vertebrates (except for the jawless) share a similar inner ear morphology, with one ear for side, each characterized by three

semicircular canals. In most non-mammalian vertebrates, these canals present three otolithic end organs (*utricle*, *saccule*, *lagena*). Within each of these are calcium carbonate crystals that in teleost fishes solidify in single acellular masses, called otoliths (respectively *lapillus*, *sagitta*, *asteriscus*) [3]. These are characterized by continued growing during the entire fish's lifetime, with a daily deposition of new material [4, 5]. Their isolation from the external environment and their capability to be metabolically inert make them an essential tool for fish life history studies [4, 6]. Especially *sagittae* (the largest among otoliths in non-otophysan species [7]) have been extensively used in many research fields (e.g., fisheries science [8–12], ecology [13–20], taxonomy [21–25], palaeontology [26–28] and eco-geochemistry [29]) due to their species-specific morphology [25, 30, 31], their persistence in ancient sediments [32] and stomach contents of ichthyophages predators [13–16], and their inter-specific variability in morphology, microstructure and microchemical composition [33, 34]. Despite *lapilli* and *asterisci* being widely described in many species [35–37], there is relatively less information, if compared with *sagittae*, regarding their morphology and diversity, especially in marine teleost [38]. *Lapilli* has been broadly used for the identification of otophysan fishes (being larger than *sagittae*) [39, 40], but due to their generally small size, their low persistence in geological layers and predators' stomach contents, and their almost completely unknown intra and interspecific diversity, the knowledge base on these otoliths is still limited, especially regarding Mediterranean bony fishes.

The Mediterranean Sea is a semi-enclosed basin characterized by enhanced biodiversity and a high anthropogenic impact related to pollution, fisheries activities, and urbanization. The growing impact of human activities (especially fisheries [41–44]) on Mediterranean deep environments has led the scientific community to focus on meso- and bathypelagic communities. Due to their vertical migrations and trophic relationships, these play a fundamental ecological role in the energy flowing and carbon transport between different marine domains [45–54]. Mesopelagic fishes show a great abundance in biomass, being the main component of the deep scattering layer (DSL) and mesopelagic zone, and the most abundant vertebrates on earth for their density and diffusion in all the Oceans [55, 56]. Several studies have been focused worldwide on these species' distribution, biology, biodiversity and ecology [51, 56–59], also investigating morphology, microstructures and growth of *sagittae* [57, 60–65]. Despite this, the knowledge base on mesopelagic fishes remains scarce, with several gaps regarding the biology and eco morphology of many species and families. Due to their deep distribution, these teleosts are mainly sampled with expensive methods, such as trawling (being large specimens abundant in trawling discards and by-catch) or other nets for micronekton sampling (e.g., Isaacs-Kidd Midwater Trawl Net, Environmental Sensing System, young fish trawl) [58, 66]. However, the small dimensions of these fishes (often smaller than large trawl mashes), added to their high mobility and patchy distribution (which often is related to specimens' ontogenetic stage, time of the day and season), increase the difficulties in obtaining representative fresh samples useful to investigate their life histories, biodiversity, and population dynamics without bias.

In this context, the Strait of Messina takes on great importance. It is characterized by an intense hydrodynamism, with very strong upwelling currents strictly related to tidal phases [67–69]. These moon-related phenomena, combined with the strong winds blowing in the area and the daily vertical movements performed by mesopelagic micronekton, cause a natural stranding, sometimes even massive, of deep fauna along the Sicilian and Calabrian coasts [70, 71]. These peculiar events were well documented and studied from the end of the 800' century, making the Strait of Messina one of the main Mediterranean geographical areas to study and investigate the mesopelagic fauna [71–81].

The current paper aims to examinae the morphology, morphometry, shape, and external textural organization of saccular (*sagittae*) and utricular (*lapilli*) otoliths of the half-naked

hatchetfish, *Argyropelecus hemigymnus*, Cocco, 1829, from the Strait of Messina, also investigating the occurrence of bilateral asymmetry and their intraspecific variability related to specimens' total length and weight. The family Sternoptychidae (hatchetfishes) belongs to the order Stomiiformes and represents one of the most abundant teleost's family in biomass and abundance of the mesopelagic zone worldwide [82–84]. It includes 73 valid species distributed in all the Oceans, characterized by bodies usually smaller than 100 mm (total length, TL), with several photophores species specifically distributed on their surface, and great intergeneric morphological variability [85]. In the Mediterranean Sea, this family includes three genera (*Argyropelecus*, *Maurolicus* and *Valenciennellus*), with the *Argyropelecus* genus (deep-bodied hatchetfishes) composed of three species (*A. hemigymnus*, *Argyropelecus olfersii*, Cuvier, 1829, and *Argyropelecus aculeatus*, Valenciennes, 1850) [86]. *A. hemigymnus* is distributed worldwide and, like the other deep-bodied hatchetfishes species, inhabits deep marine environments (up to 1000 m of depth), forming shoals and aggregations [87]. They generally stay in the deep during the day to avoid predation (being preyed on by a large number of predators belonging to several taxa [47, 79, 88–91]), performing vertical migrations for trophic porpoises at night, following their preys (mainly euphausiids for larger specimens, and copepods for smaller specimens) [47, 92].

According to previous studies performed in the Strait of Messina [70, 71], *A. hemigymnus* is among the most numerically relevant species for abundance and frequency of stranding during the entire year. This large number of available specimens is useful to obtain information on the eco-morphological adaptations and life history of this species due to the high inter-regional variability of life histories in mesopelagic teleost [59, 93]. Therefore, obtaining new data on hathcetfishes' saccular and utricular otoliths' morphology and intra-specific variability, applying techniques never applied before on this species, such as SEM and shape analysis, is essential to improve the knowledge base on this rare and still poorly studied mesopelagic teleost, exploring ecomorphological adaptation to deep marine habitats. This represents a fundamental step to fully understanding the teleosts' inner ear functioning and how its morphology change in relation to the environmental and fishes' life cycle. The data obtained in the present study increase the information on the inner ear of a cosmopolitan and ecologically essential species, investigating its intra-specific variability, which can be an expression of environmental biophysical effects or an indicator for environmental stress, nutritional condition and water column seasonal variations (such as Fluctuating asymmetry) [61, 94], also adding new data on the poorly understood, but not the less important for being so, utricular otoliths [95, 96]. Moreover, all this information can pave the way to further comparisons with other populations of the same species from different geographical areas, clarifying the effects of environmental (such as currents and physiochemical water features) and ecological conditions on mesopelagic fishes' otoliths.

Materials and methods

Sampling area

A total of 70 individuals of *A. hemigymnus* were sampled before the sunshine (to avoid the action of scavenger predators, such as bees, rats, cats, and seagulls) on the Sicilian coast of the Strait of Messina in March 2022. Specimens were stranded on the shore due to the high hydrodynamism and strong winds acting in the area.

Indeed, the Strait of Messina (central Mediterranean Sea) is located at the junction between Tyrrhenian and Ionian Seas, separating the Italian peninsula from Sicily (Fig 1). This peculiar position makes it a meeting and colliding area between two water masses with different physic-chemical properties [68, 69]. The narrow passage of the Strait (only around 3 km

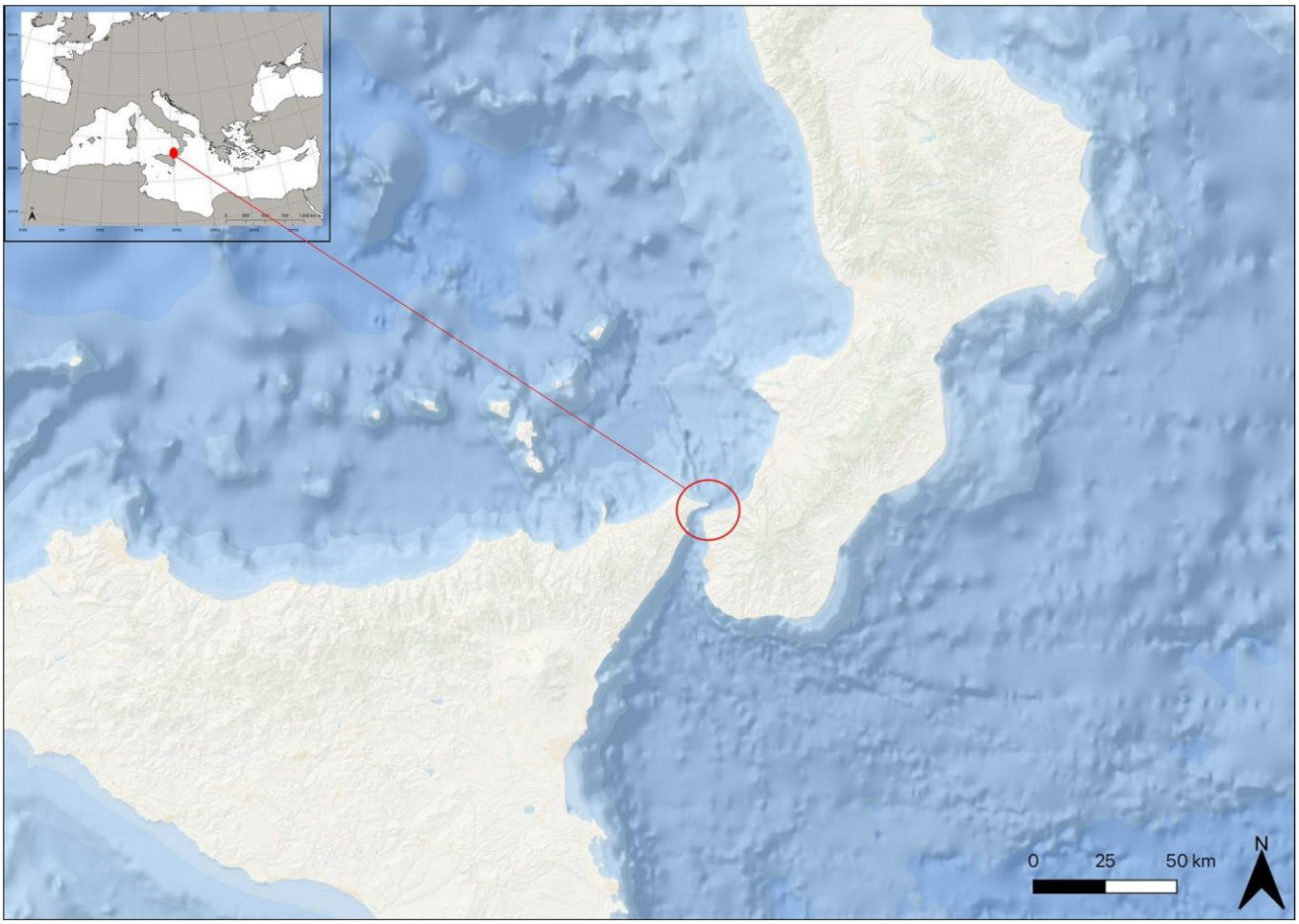

Fig 1. Maps of the studied area with the Strait of Messina reported in the red circle and the Mediterranean Sea in the insert. Data source: QGIS Development Team. QGIS Geographic Information System (version 3.26). https://qgis.org/en/site/.

https://doi.org/10.1371/journal.pone.0281621.g001

separates the Italian and Sicilian coast at the nearest point) enlarges toward the Tyrrhenian Sea at the north and the Ionian Sea at the south, with an enhanced morpho-bathymetrical irregularity of the bottom. A shallower central area (the saddle, -70/-90 m of depth) divides the Strait into two deeper zones: one toward the Tyrrhenian Sea (the northern Strait's exit, -100/-400 m of depth) and one toward the Ionian Sea (the southern Strait's exit, until -1000 m of depth). The narrowest and shallowest Strait zone amplifies the water's volume from the two basins, producing strong currents acting in the area (with velocity until 3 m s^{-1}) [97, 98]. The water masses get mixed, flowing one on the other, with dynamics regulated by tidal phases, according to their physic-chemical properties. The semi-diurnal currents inversions cause a difference in elevation between the Ionian and Tyrrhenians Seas (when one is in high tide, the other is in low tide, and vice versa). This gradient drives a large volume of water to pass across the Strait's saddle from South to North and vice versa, in alternating phases with opposite directions, every 5–6 hours.

This intense hydrodynamism results from the upwelling of deep water from the Ionian Sea, which is one of the main causes of marine organisms' stranding. The intense flowing of waters from the deep, added to the Straits physiography, allows a quick transport of deep fauna toward the surface. This rapid bathymetric change causes shock or even death in the organisms that, moved by wave, wind and current, strain on the shore [62, 70, 71]. This natural

phenomenon is also influenced by seasonality, wind direction, moon phases and different ecological and biological features of the species, which regulate their movement along the water column. Indeed, the vertical daily migrations of several mesopelagic species toward the shallower marine strata enhance the risk of being swept by the current and transported too quickly on the surface.

Samples processing, images elaboration and morphometric analysis

Once sampled, all the specimens were transferred still fresh in the laboratory, where each one was measured (total length, TL) and weighed (total weight, TW). The individuals were assigned to four size classes, according to their TL. Class I comprised all those with a TL between 10 and 20 mm, Class II between 20 and 30 mm, Class III between 30 and 40 mm and Class IV greater than 40 mm. Each left and right sagittal and utricular otolith was sampled and polished from tissue remains using 3% H_2O_2 for 15 minutes and Milli-Q water. Once dried, they were photographed twice (one photo for each otolith face) under a stereomicroscope Zeiss Discovery V8 equipped with Axiocam 208 colour camera (Carl Zeiss, Jena, Germany), being later stored in Eppendorf microtubes. One *sagitta* and one *lapillus* for each size class were chosen for SEM analysis.

ImageJ 1.48p software [99] was used to perform several measurements on otoliths images and convert them into binary format for contour extraction. For each *sagitta* and *lapillus*, it was measured the maximum otolith length (OL, mm), the maximum otolith width (OW, mm), the otolith perimeter (OP, mm) and the otolith surface (OS, mm^2). It was also calculated the ratio of otolith length to the total fish length (OL/TL) to investigate how otoliths increase in length in relation to fish total length. In order to evaluate how the shape of *sagittae* and *lapilli* varied in the different size classes, several shapes indices were calculated for each otolith according to the literature [57, 100–104]: circularity ($C = OP^2/OS$), rectangularity ($Re = OS/[OL \times OW]$), ellipticity ($E = (OL–OW)/(OL+OW)$), aspect ratio ($AR = OW/OL\%$), form factor ($FF = 4\pi OS/OP^2$) and roundness ($Ro = 4OS/\pi OL^2$). Circularity and roundness show how the otolith's shape resembles a perfect circle, considering minimum values 1 and 4π, respectively. Rectangularity gives information on how otolith length and width vary in relation to the surface, with the value of 1 assumed by a perfect square. Ellipticity indicates if changes in the otolith's axis are proportional, giving information on how it is similar to an ellipse, resulting in 0 for a perfect circle. Aspect ratio, the ratio between width and length, gives information on how the otolith is elongated; the larger aspect ratio value, the more elongated the otolith. The form factor indicates how the otolith's contour is similar to a circle, with values ranging between 0 and 1, where 1 indicates a perfect circle.

Shape analysis

Shape analysis based on the outlines of the collected otoliths was performed using shape R, an open-access package that runs on R software (RStudio 2022.07.1 Build 554; R Gui 4.1.3 2022.03.10). This R package was specially designed to study otolith shape variation among bony fishes populations or species [105]. Each taken picture of *sagittae* and *lapilli* was first binarized using ImageJ software (version 1.53k freely available at https://imagej.nih.gov/ij/) and subsequently classified based on fish size class and otolith side. The outlines were detected through a specific function of shape R, with the grayscale threshold value set at 0.05 (intensity threshold). The contours thus extracted were linked to a data file containing information about the specimens analyzed (e.g., fish length and body weight). Otolith measurements (i.e., length, width, perimeter, and area) for each size class were calculated using the getMeasurements function based on outlines previously detected. Wavelet and Fourier coefficients were

extracted and adjusted through proper functions of the shape R package to define the allometric relationships between otolith shapes and fish lengths.

SEM analysis

A total of four *sagittae* and four *lapilli* (one *sagitta* and one *lapillus* for size classes) were investigated through SEM analysis with a Zeiss EVO MA10 at the acceleration voltage of 20Kv. Firstly 70% alcohol for 48 hours was used to fix the samples. After this, they were soaked in a series of alcohol (from 70% to 100%, one hour for each passage) to dehydrate them. One stub (SEM-PT-F-12) covered by conductive adhesive tables (G3347) was used to place otoliths, avoiding the critical drying point. They were left at 28˚ for 12h, and finally, before the observation at SEM, a layer of 20 nm gold palladium was deposited to sputter coated them.

Data analysis

Univariate and multivariate statistical analyses were conducted using Prism V.8.2.1 (Graphpad Software Ltd., La Jolla, CA 92037, USA), R vegan package V.2.5, and PAST V. 2.756.

Morphological parameters were analyzed using an unpaired t-test to highlight any significant differences between the right and left sides of the otoliths.

Differences in morphological parameters between specimens of different ontogenetic classes were analyzed using a one-way analysis of variance (one-way ANOVA). The correlation between the measured parameters and fish weight and total length was also tested using the Pearson correlation coefficient.

Additionally, wavelet coefficients were used to analyze shape variation among the left and right sides of *lapilli* and *sagittae* and between ontogenetic classes using an ANOVA-like permutation test, to determine differences in otolith contours. Moreover, shape coefficients were subjected to a Linear Discriminant Analysis (LDA) to obtain an overview of the differences in otolith shape between the size classes examined. All analyses were conducted on *lapilli* and *sagittae*. The significance level was set at $P < 0.05$.

Results

Morphometric and shape analysis

Sagittae. According to the terminology used by Tuset, Nolf and Assis [21, 25, 38], *A. hemigymnus* specimens showed tall *sagittae*, higher than wider, characterized by an oval to angled shape and a vertical axis longer than the horizontal one. The dorsal region was tapered, with an asymmetrical shape and a rounded extremity. The ventral region was globular with a symmetrical shape. Dorsal and ventral rims were smooth and convex. The external face was smooth and convex-shaped, while the internal face was also smooth but concave. *Rostrum* and *antirostrum* were inconspicuous, very short and round. In Table 1 there were reported the morphometric mean values obtained for *sagittae*, divided into investigated size classes.

Concerning morphological differences between size classes (Fig 2a–2h), *sagittae* of specimens belonging to Class I showed a marked asymmetry between dorsal and ventral regions, with a very enhanced globular shape, especially in the ventral one, and a marked *excisura ostii*, which became gradually most inconspicuous in the other size Classes. The dorsal region became increasingly tapered in Classes II, III and IV, with a slightly triangular shape in Classes III and IV, characterized by crenate margins and a most increased otoliths' width than length. In Class IV, the ventral region became less globular, with an angled shape characterized by an irregular angular rim and a most enhanced symmetry with the dorsal region. The traits that

Table 1. Morphometric mean values of *sagittae*, standard deviation (s.d.) and minimums (Min.) and maximus (Max.) values divided for the size classes investigated: Maximum otolith length (OL, mm), the maximum otolith width (OW, mm), otolith perimeter (OP, mm) and otolith surface (OS, mm²), the ratio of otolith length to the total fish length (OL/TL), circularity (C = OP²/OS), rectangularity (Re = OS/[OL×OW]), ellipticity (E = OL–OW/OL+OW), aspect ratio (AR = OW/OL%), form factor (FF = 4πOS/OP²) and roundness (Ro = 4OS/πOL²).

	CLASS I			CLASS II			CLASS III			CLASS IV		
	Mean	s.d.	Min.—Max.	Mean	s.d.	Min.—Max.	Mean	s.d.	Min.—Max.	Mean	s.d.	Min.—Max.
OL	0.309	0.029	0.237–0.347	0.394	0.035	0.333–0.476	0.718	0.056	0.631–0.872	0.846	0.044	0.754–0.923
OW	0.379	0.032	0.316–0.434	0.518	0.051	0.424–0.600	0.519	0.043	0.437–0.610	0.570	0.032	0.531–0.636
OP	1.260	0.117	0.989–1.474	1.755	0.190	1.408–2.129	2.167	0.154	1.946–2.497	2.573	0.160	2.289–2.917
OS	0.091	0.015	0.059–0.116	0.161	0.028	0.122–0.215	0.284	0.039	0.234–0.385	0.374	0.037	0.310–0.444
OL / TL	0.022	0.004	0.015–0.030	0.017	0.002	0.012–0.022	0.021	0.002	0.017–0.028	0.020	0.001	0.018–0.022
C	17.597	1.235	16.227–20.486	19.229	2.091	16.048–23.779	16.591	0.547	15.661–18.089	17.731	0.938	15.482–19.889
Re	0.771	0.015	0.745–0.798	0.786	0.015	0.764–0.814	0.760	0.018	0.723–0.794	0.772	0.021	0.735–0.816
E	-0.541	0.091	-0.782—0.432	-0.400	0.097	-0.579—0.167	0.513	0.103	0.344–0.785	0.742	0.078	0.580–0.872
AR	1.229	0.051	1.157–1.336	1.312	0.071	1.161–1.497	0.724	0.047	0.614–0.795	0.675	0.039	0.621–0.748
FF	0.718	0.048	0.614–0.775	0.661	0.071	0.529–0.784	0.759	0.024	0.695–0.803	0.711	0.037	0.632–0.812
Ro	0.798	0.028	0.750–0.833	0.763	0.038	0.678–0.881	1.340	0.107	1.160–1.599	1.460	0.095	1.272–1.598

https://doi.org/10.1371/journal.pone.0281621.t001

have remained constant among the size classes were *rostrum* and *antirostrum* (short and round in all the size classes) and the heterosulcoid *sulcus acusticus*.

ANOVA showed significant differences for almost all the morphometric measurements of the *sagittae* between the four size classes examined ($p < 0.05$) (S1 Table). A significant correlation between the body weight and total length of the specimens and the morphometries of the *sagittae* was observed for all parameters except for A/(OLxOH) ($P > 0.05$) (S2 and S3 Tables).

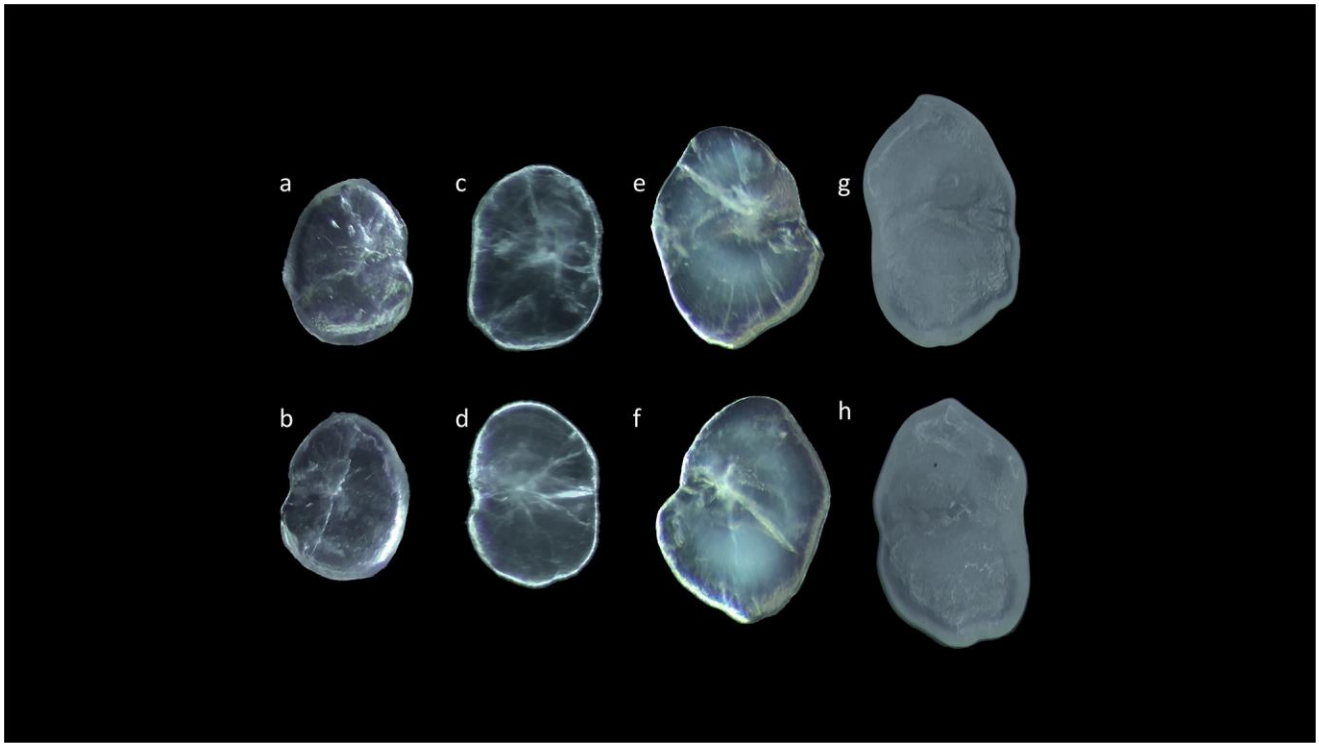

Fig 2. Stereoscope images of left (a,c,e,g) and right (b,d,,f,h) *sagittae* inner surfaces belonging to size Classes I (a,b), II (c,d), III (e,f) and IV (g,h).

https://doi.org/10.1371/journal.pone.0281621.g002

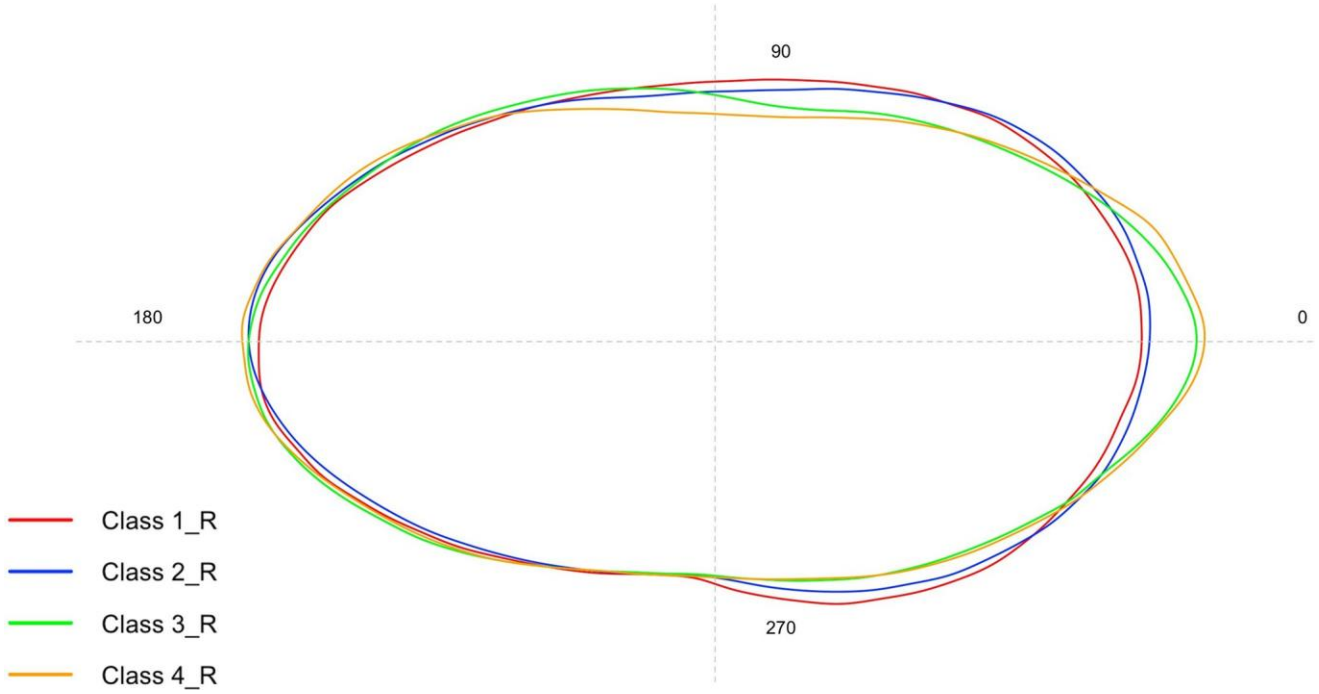

Fig 3. Mean shape of right *sagittae* contours belonging to the four investigated size classes.

https://doi.org/10.1371/journal.pone.0281621.g003

The morphometrical parameters did not show significant differences between the right and left *sagittae* for each size class investigated ($p > 0.05$).

The graph in Fig 3 represents the mean otolith shape comparison among different size classes for right *sagittae* obtained through standardized Wavelet coefficients. The quality of both Wavelet and Fourier reconstruction was estimated by comparing the deviations from the otolith outlines, with the value 15 sets as the maximum number of Fourier harmonics to be shown (S1 Fig). The mean and standard deviation of calculated coefficients was plotted using the gplots R package to assess how the variation of Wavelet coefficients depends on the position along the outline (S2 Fig).

The shape analysis showed a significant difference between the right and left side of the *sagittae* for all sizes classes (S4 Table) except for Class II ($p = 0.18$) (Fig 4a–4d). Furthermore, significant variability of the boundaries was observed between size classes for both the right and left sides ($p = 0.001$). LDA highlighted how the contours of the class IV sagittas are markedly separated from the left and right contours obtained for the other size classes, as shown in Fig 5 (Axis 1 71.13% and 90.6%, respectively).

Lapilli. According to the terminology used by Assis [35, 38], the *lapilli* of *A. hemigymnus* showed a non-clupeiform type morphology, with a globular anterior region and a slender posterior region. The internal and external margins were smooth, convex shaped and asymmetrical, with curved rims with different degrees of bending. The *Extremum posterior* was tapered with a triangular shape and oriented horizontally, while the *extremum anterior* was rounded. *Prominentia marginalis* was large and rounded, and *gibbus maculae* was slender and small. *Sulcus lapilli* was superficial and very thin. Table 2 reported the morphometric mean values obtained for *lapilli*, divided into the investigated size classes.

Concerning the morphological differences between size classes (Fig 6a–6h), specimens belonging to Class I showed *lapilli* with a globular shape characterized by an enhanced

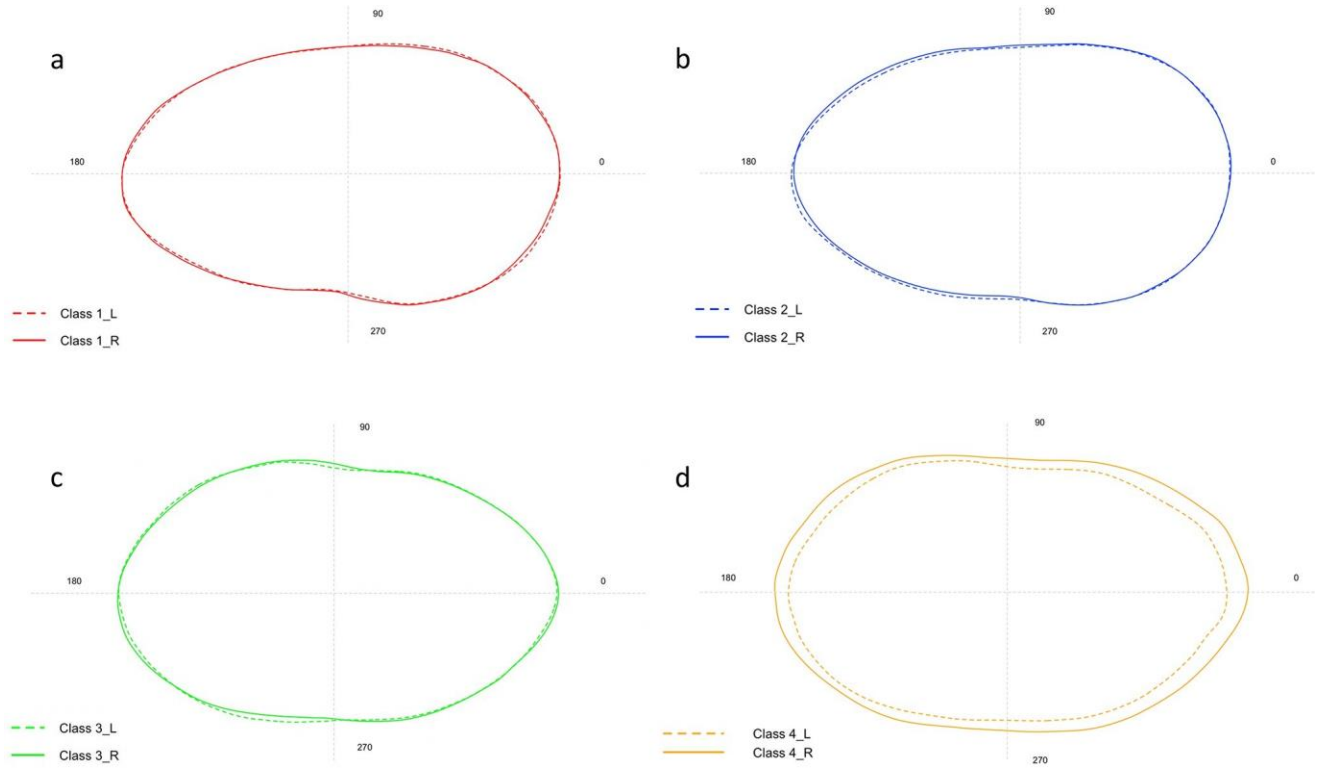

Fig 4. Comparison between the mean shape of left and right *sagittae* contours belonging to Class I (a), Class II (b), Class III (c) and Class (IV).

https://doi.org/10.1371/journal.pone.0281621.g004

asymmetry between internal and external zones. Class II showed a most ovoidal shape with an increased symmetry between internal and external zones. The *extremum posterior* was less triangular in Classes I and II than in Classes III and IV. In Classes III and IV, *lapilli* showed the most irregular shapes, with very prominent *prominentia marginalis* and *extremum posterior*, as also highlighted by the increase of ellipticity (E) value and the decrease of circularity (C) values (Table 2).

ANOVA showed significant differences for almost all the morphometric measurements of the *lapilli* between the four size classes examined ($p < 0.05$). Some exceptions were found for roundness and OW/OL%, which did not show any significance among any size class ($P > 0.05$). Form-Factor, Ellipticity and P^2/A showed no significant changes between Class I and II ($p > 0.05$). Finally, A/(OLxOH) showed no variability between Classes I, II and III ($p > 0.05$) (S5 Table). A significant correlation between the body weight and total length of the specimens and the *lapilli* morphometries was observed for all parameters except for OW/OL% ($P > 0.05$) (S6 and S7 Tables). The morphometrical parameters did not show significant differences between the right and left side *lapilli* for each size class investigated ($p > 0.05$).

The graph in Fig 7 represents the mean otolith shape comparison among different size classes for right *sagittae* obtained through standardized Wavelet coefficients. The quality of both Wavelet and Fourier reconstruction was estimated by comparing the deviations from the otolith outlines, with the value 15 sets as the maximum number of Fourier harmonics to be shown (S1 Fig). The mean and standard deviation of calculated coefficients was plotted using the gplots R package to assess how the variation of Wavelet coefficients depends on the position along the outline (S2 Fig).

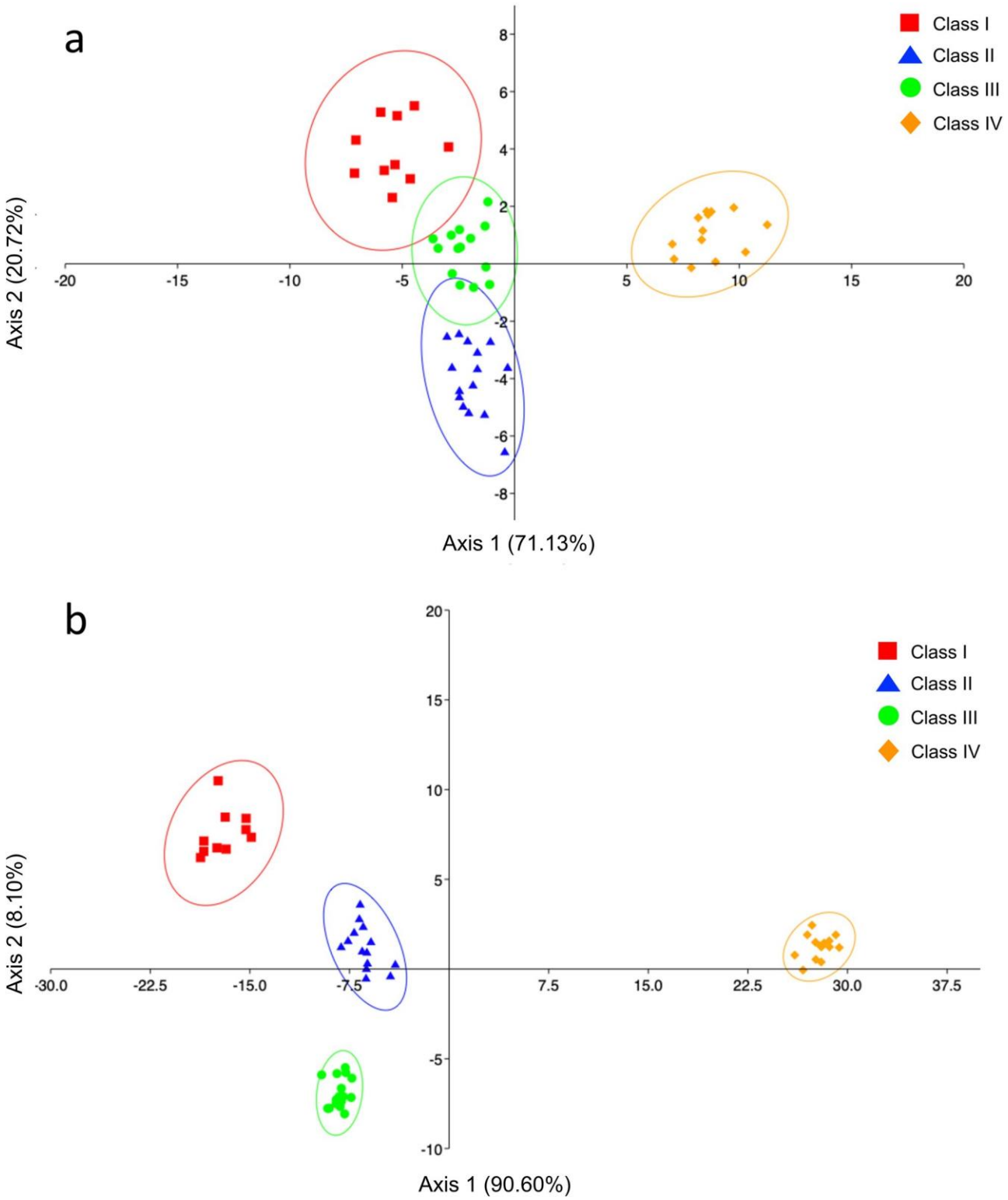

Fig 5. Linear Discriminant Analysis (LDA) computed between the size classes analyzed, calculated on Wavelet Fourier descriptors obtained by the left side (a) and right (b) of *sagittae*. Ellipses includes 95% confidence interval.

https://doi.org/10.1371/journal.pone.0281621.g005

Table 2. Morphometric mean values of *lapilli*, standard deviation (s.d.) and minimums (Min.) and maximus (Max.) values divided for the size classes investigated: Maximum otolith length (OL, mm), the maximum otolith width (OW, mm), otolith perimeter (OP, mm) and otolith surface (OS, mm²), the ratio of otolith length to the total fish length (OL/TL), circularity (C = OP²/OS), rectangularity (Re = OS/[OL×OW]), ellipticity (E = OL–OW/OL+OW), aspect ratio (AR = OW/OL%), form factor (FF = 4πOS/OP²) and roundness (Ro = 4OS/πOL²).

	CLASS I			CLASS II			CLASS III			CLASS IV		
	Mean	s.d.	Min.—Max.	Mean	s.d.	Min.—Max.	Mean	s.d.	Min.—Max.	Mean	s.d.	Min.—Max.
OL	0.178	0.014	0.158–0.204	0.224	0.012	0.193–0.249	0.285	0.026	0.250–0.318	0.325	0.022	0.293–0.347
OW	0.169	0.013	0.146–0.190	0.222	0.019	0.192–0.261	0.292	0.019	0.254–0.326	0.321	0.013	0.303–0.342
OP	0.554	0.029	0.489–0.597	0.715	0.045	0.624–0.817	0.935	0.077	0.824–1.048	1.035	0.027	0.992–1.070
OS	0.024	0.002	0.018–0.027	0.040	0.004	0.030–0.050	0.065	0.009	0.051–0.081	0.078	0.004	0.073–0.084
OL / TL	0.010	0.002	0.009–0.017	0.01	0.001	0.006–0.008	0.008	0.001	0.006–0.010	0.007	0.001	0.006–0.008
C	12.975	0.133	12.751–13.176	12.989	0.104	12.827–13.180	13.361	0.363	12.899–14.020	13.633	0.243	13.427–14.243
Re	0.783	0.019	0.736–0.807	0.790	0.018	0.748–0.824	0.785	0.032	0.728–0.841	0.754	0.017	0.718–0.781
E	-0.607	0.120	-0.803—0.409	-0.547	0.077	-0.703—0.439	-0.451	0.088	-0.563—0.307	-0.344	0.113	-0.526—0.235
AR	0.955	0.118	0.772–1.158	0.994	0.086	0.871–1.182	1.029	0.060	0.903–1.105	0.991	0.102	0.893–1.160
FF	0.969	0.009	0.954–0.986	0.968	0.007	0.954–0.980	0.942	0.025	0.897–0.975	0.923	0.015	0.883–0.937
Ro	1.058	0.135	0.808–1.298	1.018	0.097	0.804–1.167	0.974	0.082	0.888–1.183	0.975	0.090	0.820–1.074

https://doi.org/10.1371/journal.pone.0281621.t002

The investigations carried out on the shape analysis showed a significant difference between the right and left sides of the *lapilli* only for Class IV ($p = 0.017$, $df = 1$, $F = 4.12$) (Fig 8a–8d). Furthermore, significant variability was observed between size classes for the left side ($p = 0.01$). This result was confirmed by the LDA, also in agreement with what was obtained from the analysis of variance, highlighting how classes I and II are markedly separated from classes III and IV, as shown in Fig 9 (Axis 1 89.18%).

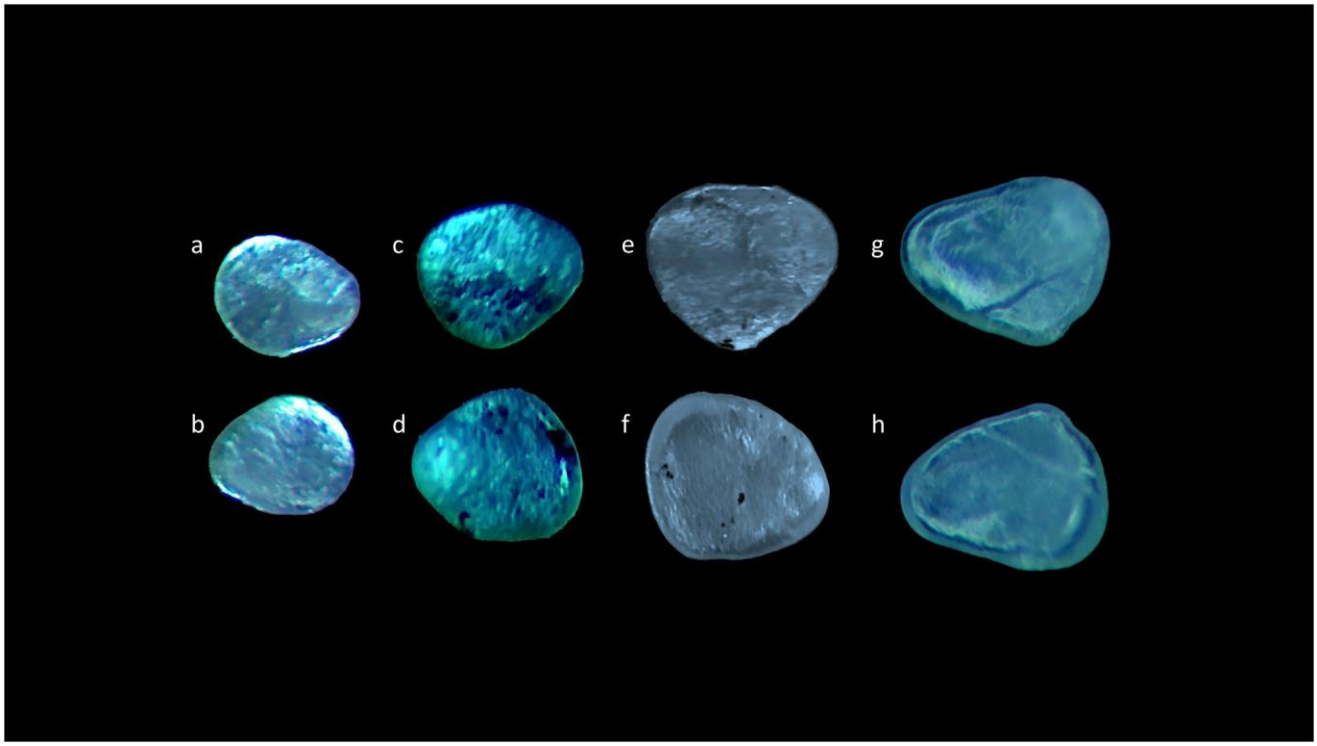

Fig 6. Stereoscope images of left (a,c,e,g) and right (b,d,,f,h) *lapilli* dorsal surfaces belonging to size Classes I (a,b), II (c,d), III (e,f) and IV (g,h).

https://doi.org/10.1371/journal.pone.0281621.g006

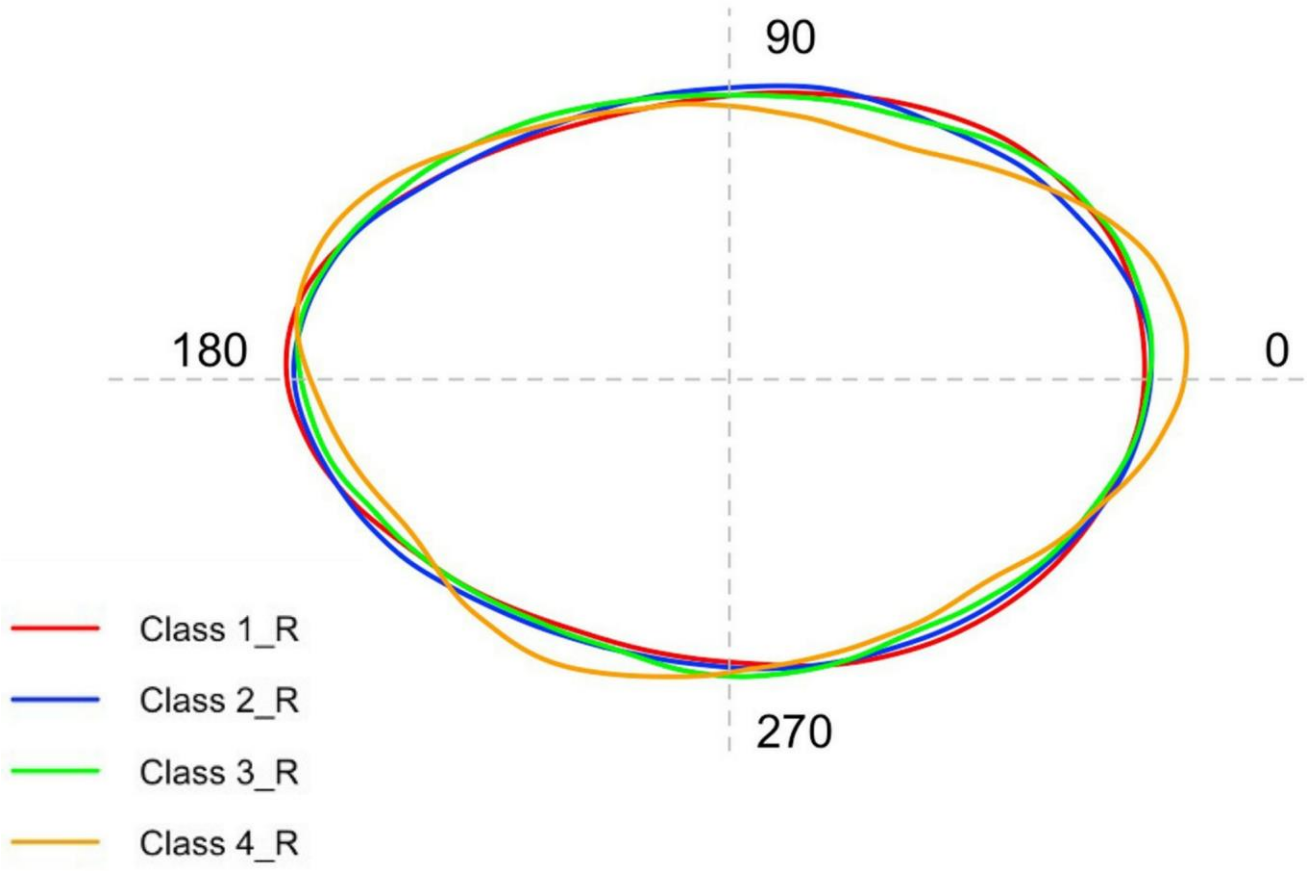

Fig 7. Mean shape of right *lapilli* contours belonging to the four investigated size classes.

https://doi.org/10.1371/journal.pone.0281621.g007

Scanning Electron Microscopy (SEM) analysis

As shown by Fig 10a–10g, the external textural organization of *sagittae* was uniform, with a granular surface and an almost completely homogeneous dimension and orientation of crystals. The *sulcus acusticus* was heterosulcoid, located on the longitudinal midline of the *sagitta* with a bi-ostial opening (Fig 10a–10c and 10e). The *ostium* was deep with a rectangular to funnel-like shape, while the *cauda* was very different, superficial and with a not well-defined ventral limit.

In Class I, it was visible, at a superficial view, the carbonate daily increments on a concentric deposition plane (Fig 11a, 11c and 11d), which made the ventral margins jagged and irregular. The superficial crystalline habit was uniform, characterized by the presence of small aragonitic crystals with an irregular granular shape, organized in overlapping successive concentric thin layers that made the orange skin-like surface rough (Fig 12a and 12c). As highlighted in Figs 11b, 12b and 12d, crystal regions of various sizes and shapes in the *sulcus* were also detected. The presence of large crystals was detected near the ventral margins and the *crista superior*.

In Class II, the surface became smoother than in Class I and fine-pored, with the characteristic small aragonitic prismatic crystals with a regular shape and organization (Fig 13a, 13c and 13d). *Sulcus acusticus* became larger without carbonate sculpturing organized in growing units (Fig 13b, 13e and 13f). Some carbonate crystals were associated in lamellae in the posterior otoliths area, forming large superficial wave-like structures (Fig 13g).

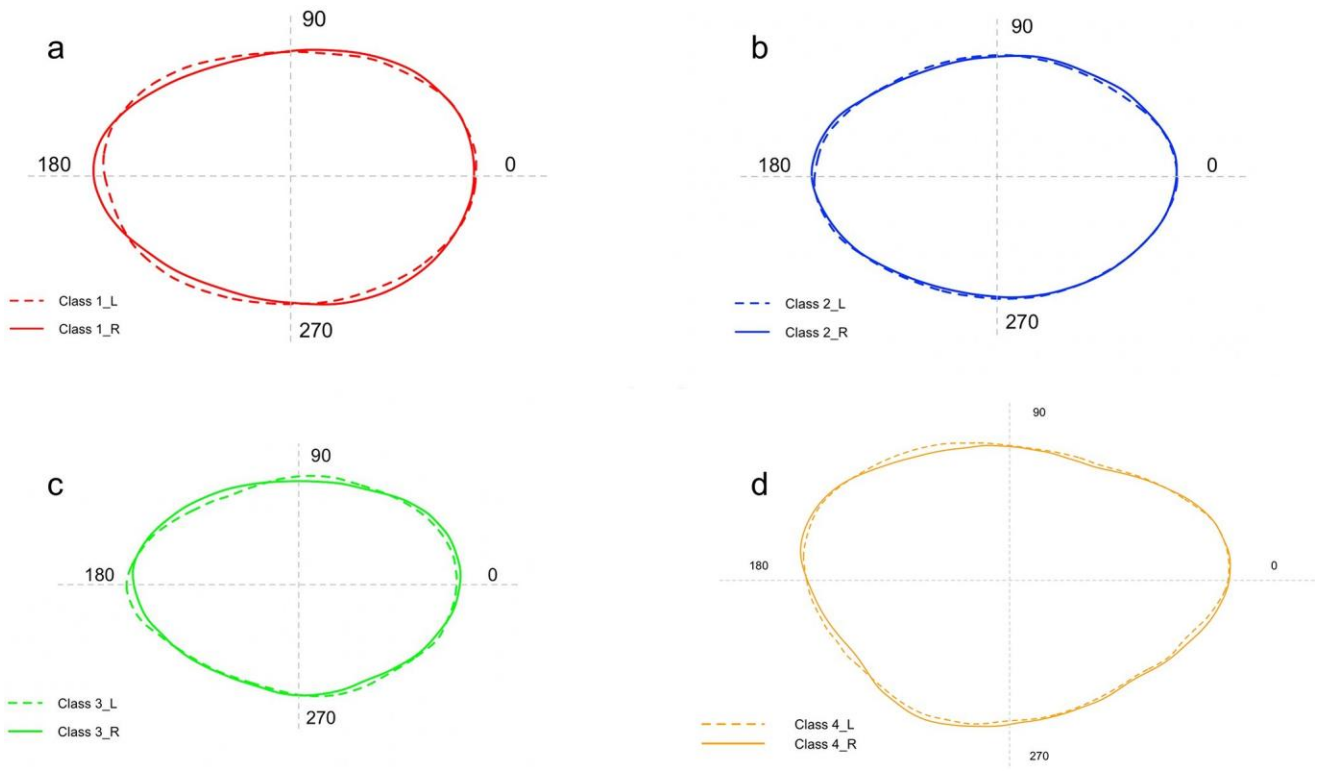

Fig 8. Comparison between the mean shape of left and right *lapilli* contours belonging to Class I (a), Class II (b), Class III (c) and Class (IV).

https://doi.org/10.1371/journal.pone.0281621.g008

In Class III, the surface became more irregular than in the last two classes, with different carbonate polymorphs, characterized by large botryoidal to hexagonal prisms crystals, in the internal surface near the *excisura ostii* (Fig 14a–14c). In the internal face was visible a circular groove (Fig 14a) representing the core of the *sagitta*, characterized by an external crystalline organization uniformly composed of small regular crystals.

In Class IV, the external textural organization was uniformly characterized by globular secretions widely distributed on the whole otolith surface (Fig 15a and 15b). As shown by Fig 16b, the presence of aragonitic crystals forming superficial wave-like lamellae was also reported. The carbonate crystal habit was mainly composed of aragonitic crystals organized in distinct uniform plates, with large carbonate sculpturing inside the circular groove of the core (Figs 15a and 16a). These made the central *sagitta* zone most irregular than the peripherical ones.

As shown in Fig 17a–17d, the external textural organization of *lapilli* was irregular, with different carbonate polymorphs and crystals with different orientations and sizes. The surface was granular to fine-pored, with edges on the ventral and posterior faces, especially near *confluentia gibbus maculae*. The ventral face was characterized by large crystals, especially on the *gibbus maculae*. *Sulcus lapillus* was thin and superficial, characterized by a uniform orientation of crystals and a regular external textural organization.

In Class I, the ventral face was characterized by different carbonate polymorphs with different orientations. Large rhombohedral and hexagonal crystals were detected on *gibbus maculae* and near the margins of the inner and anterior otoliths (Fig 18a, 18b and 18d). *Sulcus lapillus* showed a different external textural organization and a uniform surface, with small aragonitic crystals with a regular shape and orientation (Fig 18c).

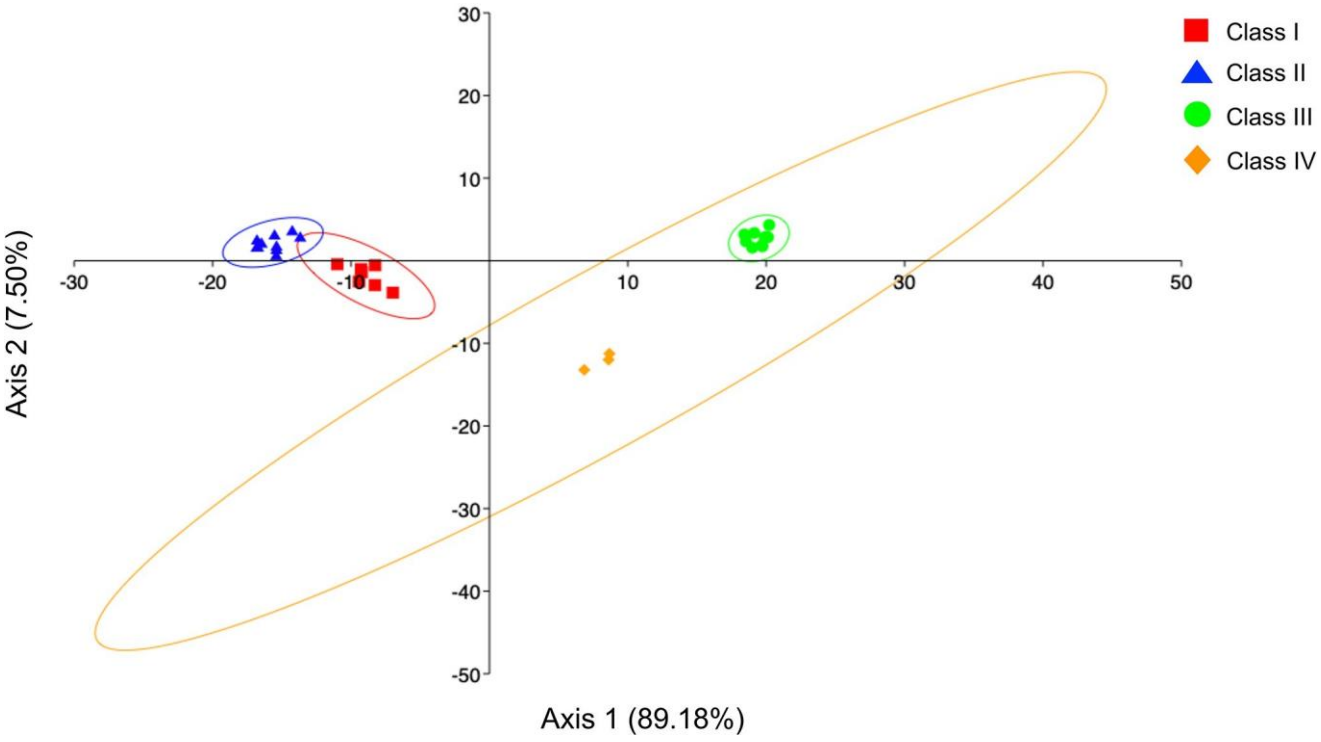

Fig 9. Linear Discriminant Analysis (LDA) computed between the size class analyzed, calculated on Wavelet Fourier descriptors obtained by the left side of *lapilli*. Ellipses includes 95% confidence interval.

https://doi.org/10.1371/journal.pone.0281621.g009

From a lateral view (Fig 19a–19c), the *lapillus* of Class II showed an irregular external textural organization, with large rhombohedral crystals on *gibbus maculae* and the *confluentia gibbi maculae*. It was also reported the presence of several edges on the *confluentia gibbi maculae* and the ventral face, separating the large prismatic crystals with a discontinuity in their orientation (Fig 19c).

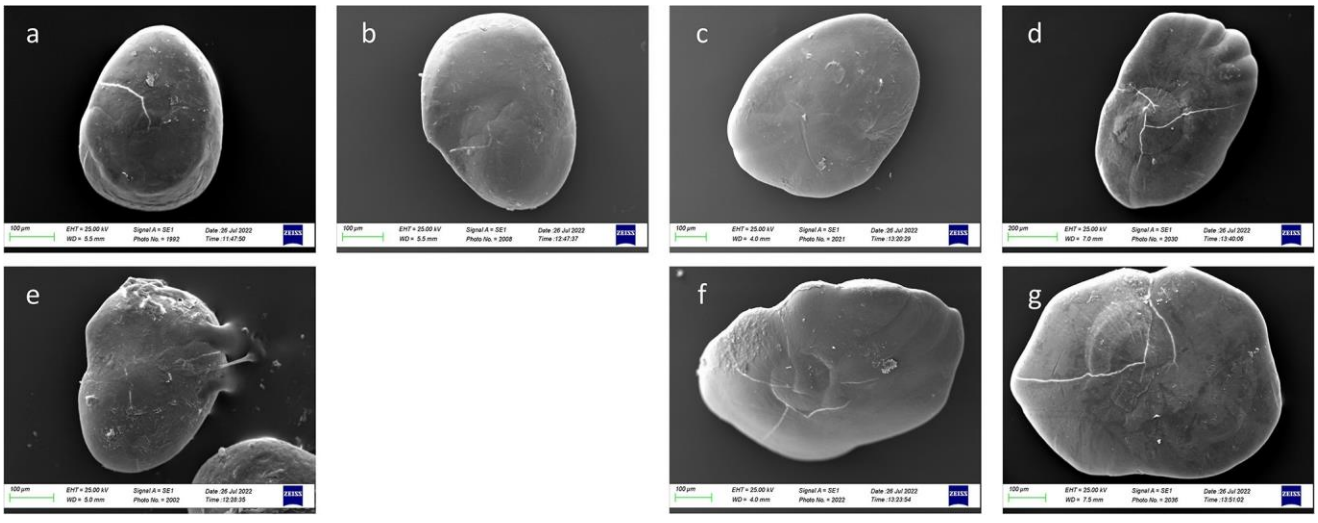

Fig 10. SEM images of *A. hemigymnus' sagittae* inners (a, b, c, e) and external (d, f, g) surfaces separated for size classes: Class I (a, e), Class II (b), Class III (c, f) and Class IV (d, g).

https://doi.org/10.1371/journal.pone.0281621.g010

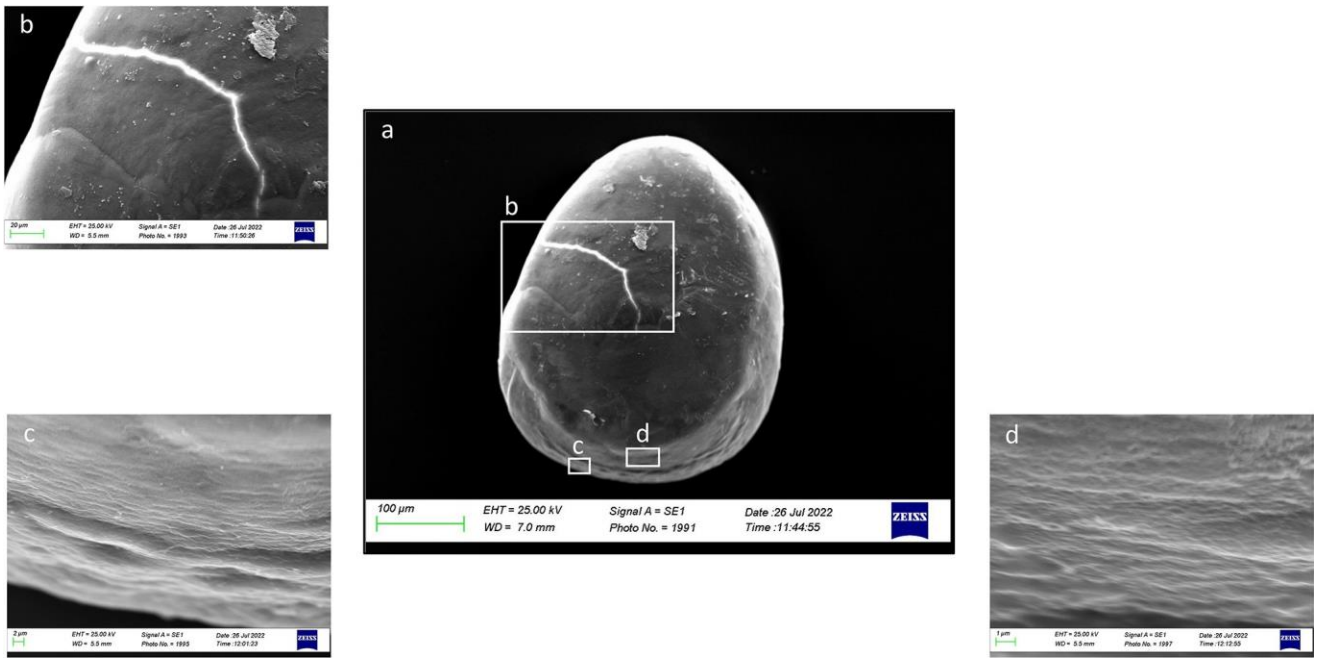

Fig 11. SEM images of a right *sagitta* inner surface belonging to size Class I (a) with details of the external textural organization of *sulcus acusticus* (b) and concentric deposition planes of carbonate detected in ventral margin (c and d).

https://doi.org/10.1371/journal.pone.0281621.g011

In Class III, the dorsal face was characterized by large prismatic and hexagonal crystals that alternated with small aragonitic crystals, making the surface irregular (Fig 20a–20c). The presence of globular secretion was also reported often absorbed in the growing otoliths matrix (Fig 20d). Several deep pores were reported near the external margin, separating the large prismatic and hexagonal crystals with different orientations.

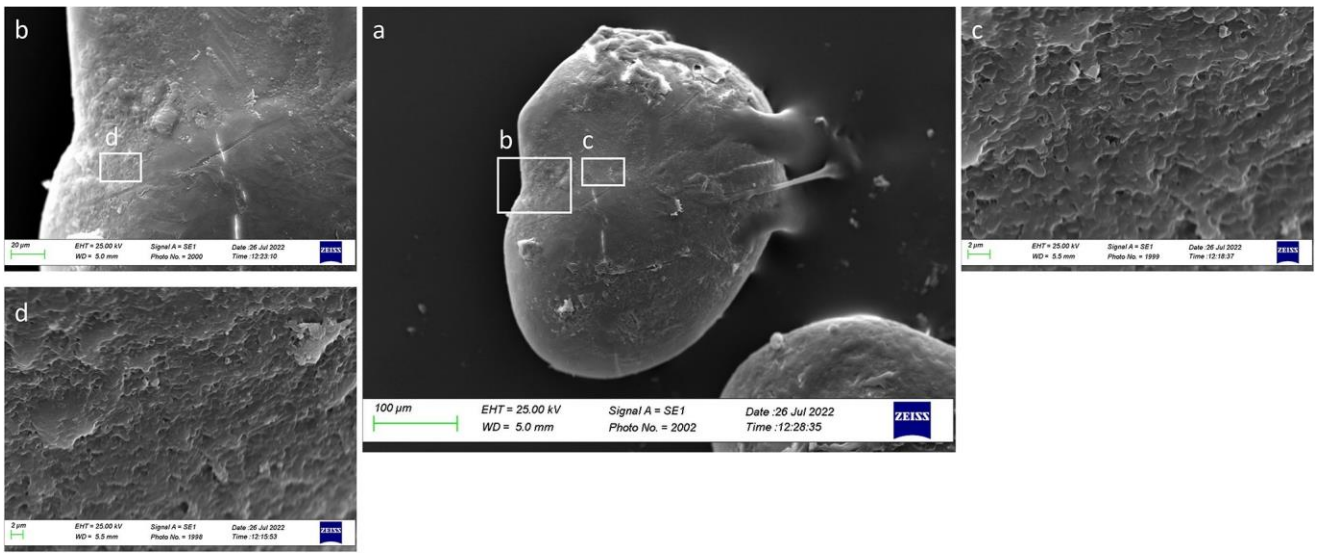

Fig 12. SEM images of a left *sagitta* inner surface belonging to size Class I (a) with detail of *sulcus acusticus* (b), *ostium* (c) and *crista superior* (d) external textural organization.

https://doi.org/10.1371/journal.pone.0281621.g012

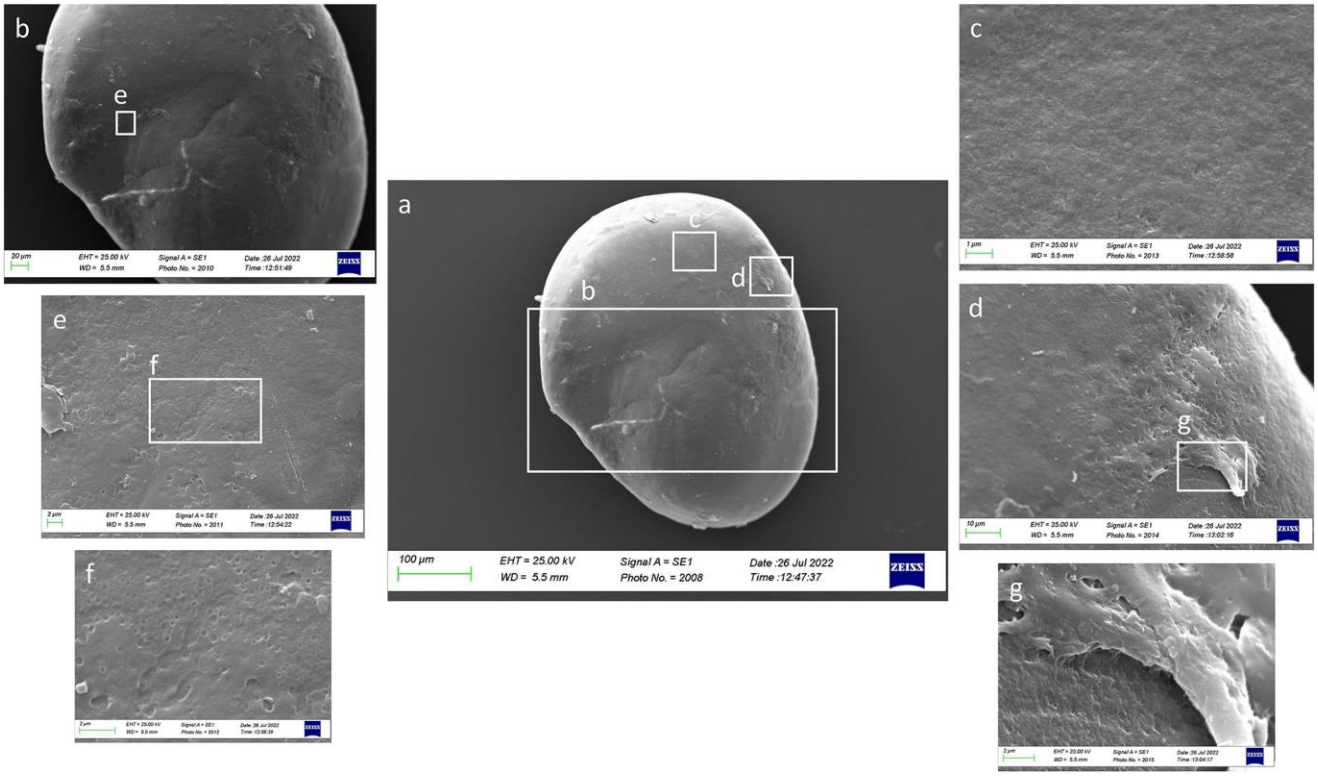

Fig 13. SEM images of a left *sagitta* inner surface belonging to size Class II (a) with details of *sulcus acusticus* (b), with its external textural organization (e, f), and crystalline habits of the posterior otoliths zone (c,d,g).

https://doi.org/10.1371/journal.pone.0281621.g013

As reported in Fig 21a–21c, in Class IV, the external textural organization was regular, with the presence of prismatic aragonite crystals organized in plates in almost all the otolith's surface except on the *gibbus maculae* and *prominentia marginalis*, characterized by the presence of large rhombohedral crystals. It was also reported the presence of deep pores separating large plates aggregations of crystals, located on an upper superficial level, from small prismatic carbonates association located on a lower level (Fig 21c).

Discussion

Improving the knowledge base on otoliths of mesopelagic species is essential to understand their eco-morphological adaptation to deep environments. Indeed, the variability of inner ear morphology among individuals of the same species inhabiting different geographical areas reflects the adaptation capability of marine organisms to environments under different evolutionary pressures. Despite the physiological processes allowing otoliths' shapes and morphological intraspecific variations at a geographical scale are still now largely unknown, it is widely reported how diet [106], temperature [107], genetic lineage [108], soundscape [109] and physicochemical features of water masses [61] can lead to these differences, impacting hearing ability (in addition to otoliths mass, endolymph viscosity and *sulcus acusticus* dimensions) and shaping otoliths' contours and morphology. According to this, the present paper confirmed the otoliths variability in populations of the studied species inhabiting different environments in both *lapilli* and *sagittae*. Results showed a morphology of *sagittae* different than those reported in the literature on the same species from other geographical areas [25, 27, 32, 38, 110, 111]. *A. hemigymnus* specimens inhabiting the Strait of Messina had larger *sagittae* than

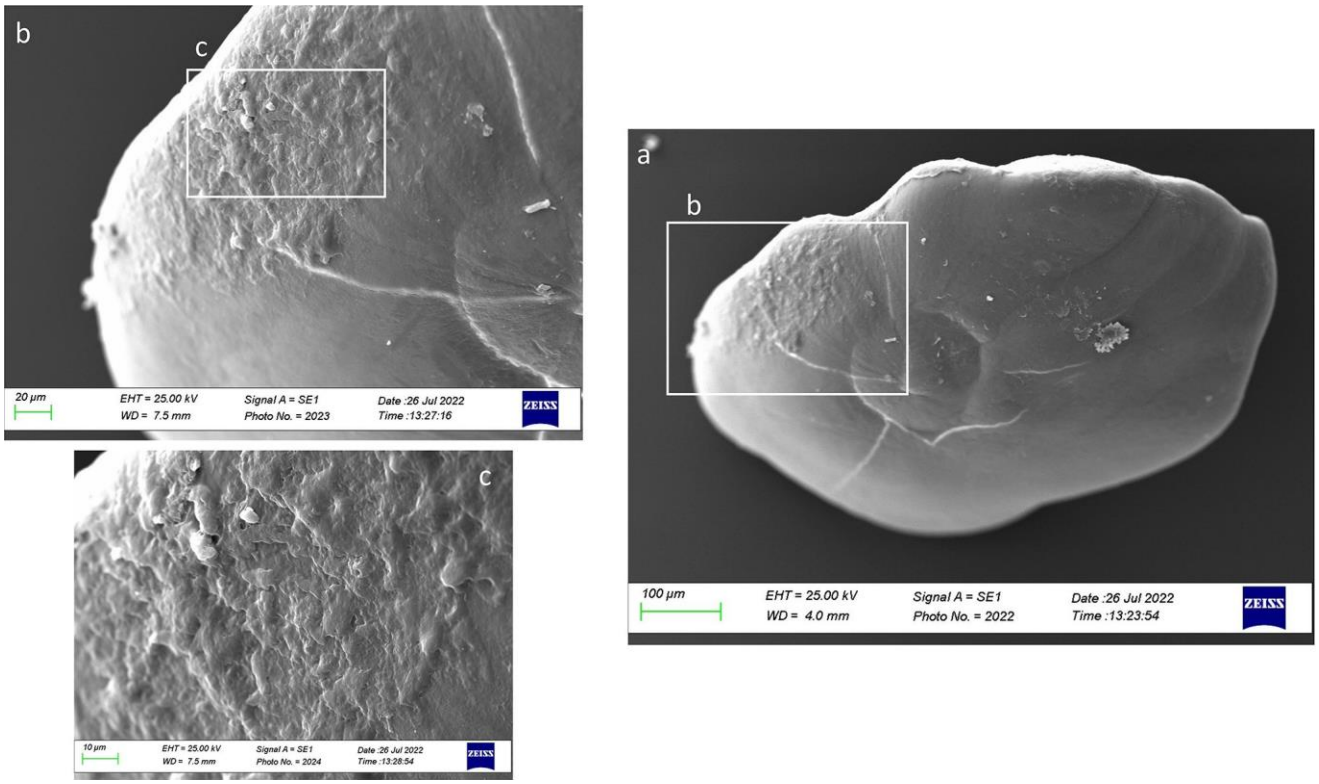

Fig 14. SEM images of a right *sagitta* external surface belonging to size Class III (a) with detail of the external textural organization near the *excisura ostii* (b, c).

https://doi.org/10.1371/journal.pone.0281621.g014

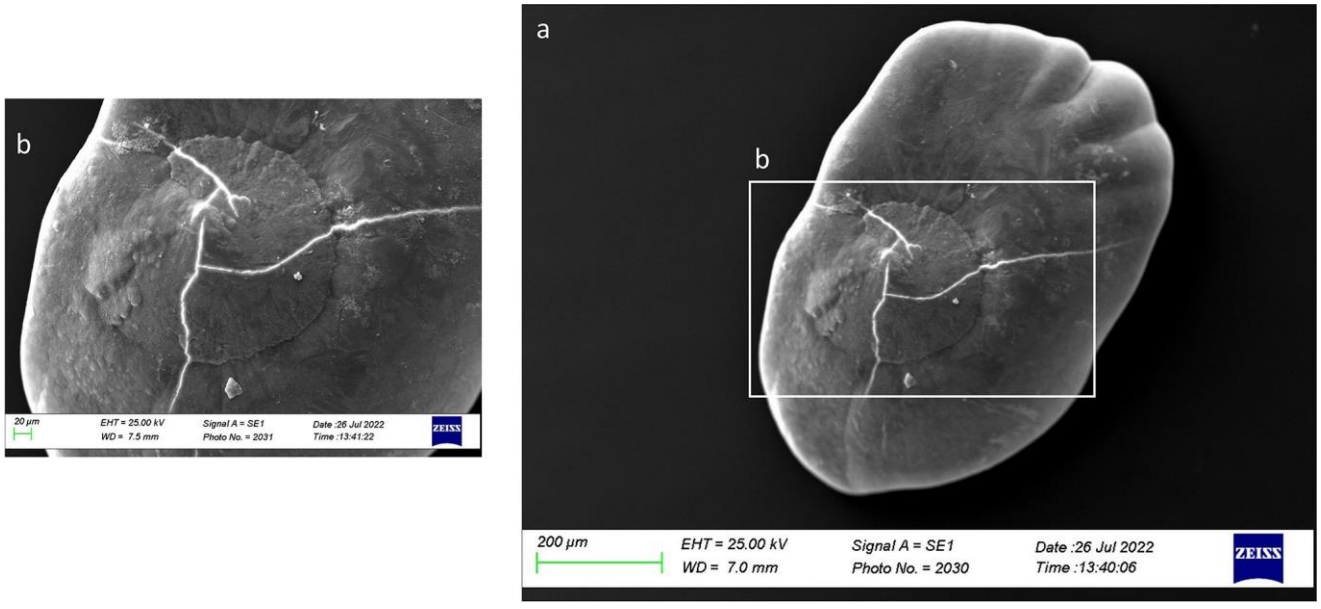

Fig 15. SEM images of a right *sagitta* external surface belonging to size Class IV (a) with details of the external textural organization of the *core* zone (b).

https://doi.org/10.1371/journal.pone.0281621.g015

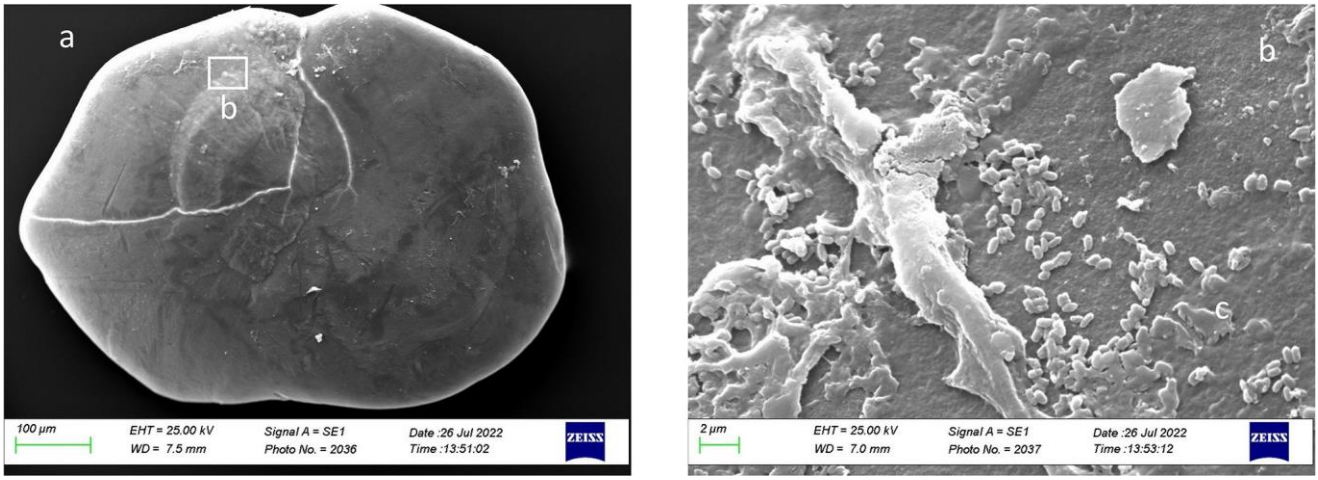

Fig 16. SEM images of a right *sagitta* external surface belonging to size Class IV (a) with details of the crystalline habits and external textural organization (b).

https://doi.org/10.1371/journal.pone.0281621.g016

those from the western Mediterranean Sea and Atlantic Ocean. This was highlighted by higher OL/TL values, Re and C, than those reported by Tuset in 2008 [25] for individuals with a total length between 30 and 40 mm. The larger surface and perimeter, together with a conformation most squared (than round) of posterior and anterior regions, and most angled to peaked of dorsal and ventral regions, markedly different than those reported in the literature, could be strictly related to the peculiarity of the studied area. The Stait of Messina is characterized by unique oceanographic features [97, 98] that inevitably influence habitats and inhabiting species. The morphological features of *sagittae* shown by results, more similar to those described

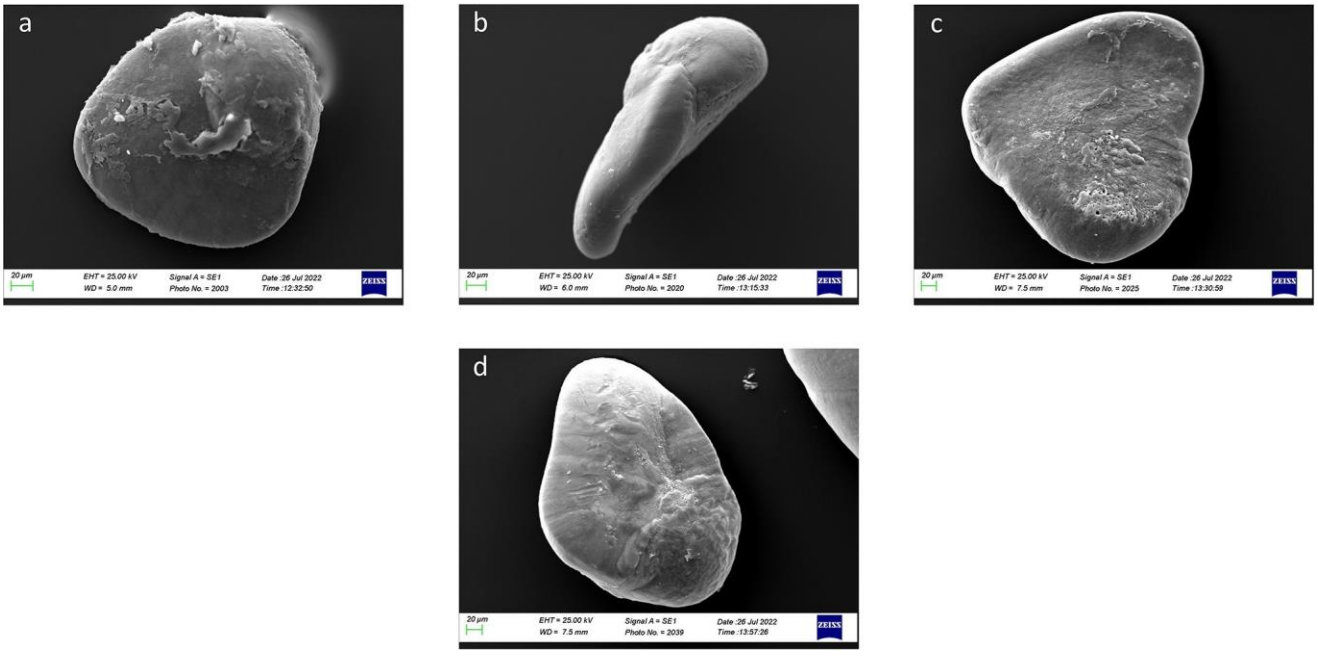

Fig 17. SEM images of ventral (a, d), lateral (b) and dorsal (c) surfaces of *A. hemigymnus' lapilli* separated for size classes: Class I (a), Class II (b), Class III (c) and Class IV (d).

https://doi.org/10.1371/journal.pone.0281621.g017

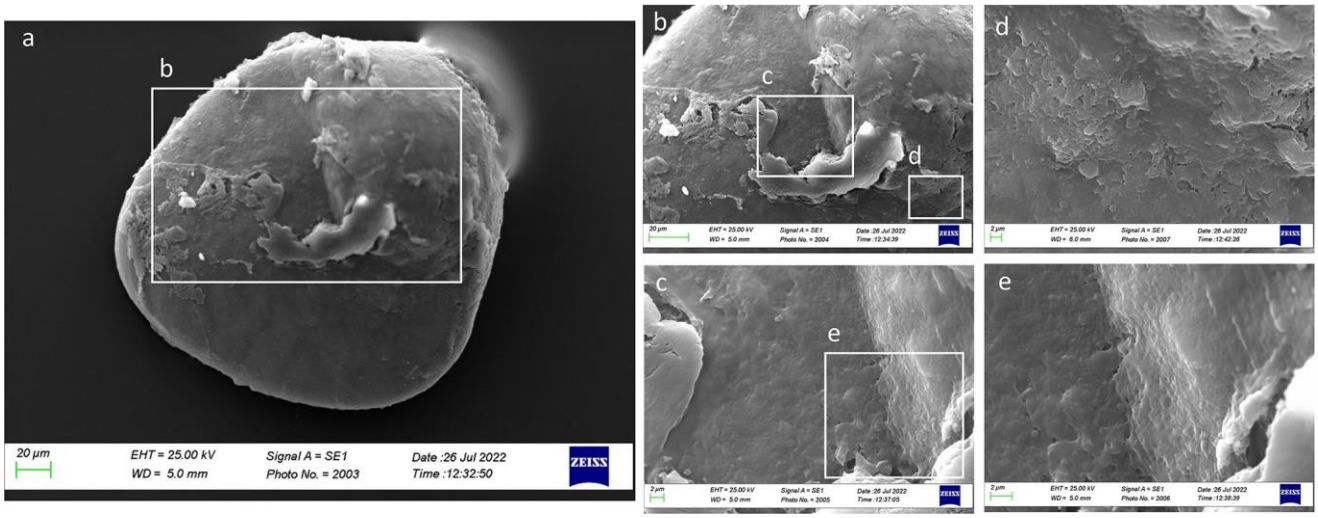

Fig 18. SEM images of a *lapillus* ventral surface belonging to size Class I (a) with details of *sulcus lapillus* (b, c) and *gibbus maculae* (d, e) external textural organization.

https://doi.org/10.1371/journal.pone.0281621.g018

in specimens from the Portuguese Atlantic Ocean and Northwestern Atlantic Ocean [38, 111] than Mediterranean ones, could be indeed connected with the environmental features of the Strait of Messina. Several external factors, such as those related to the environment (e.g., temperature, pH, salinity, depth) [96, 112–117] or food availability [106], could influence otoliths

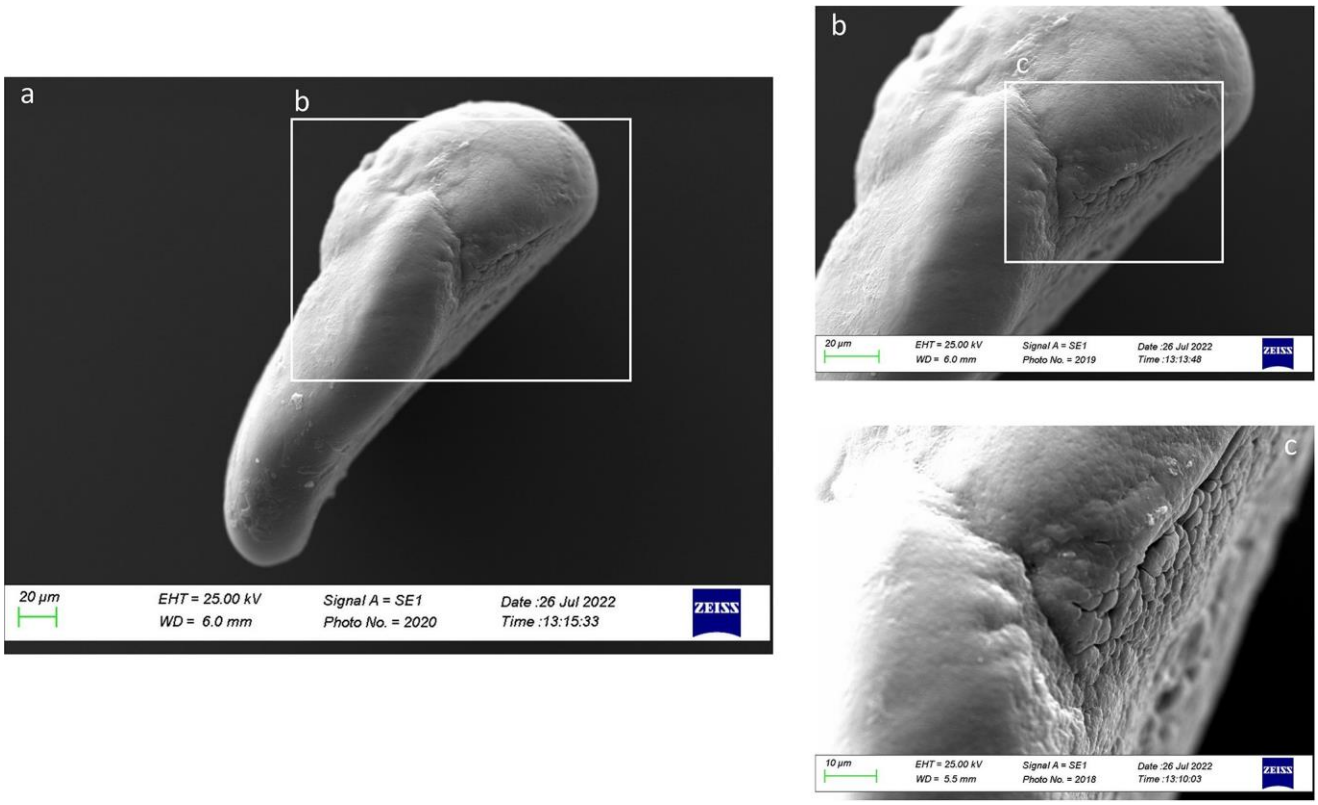

Fig 19. SEM images of a *lapillus* lateral surface belonging to size Class II (a) with details of *gibbus maculae* (b) and *confluentia gibbi maculae* (c) crystalline habits.

https://doi.org/10.1371/journal.pone.0281621.g019

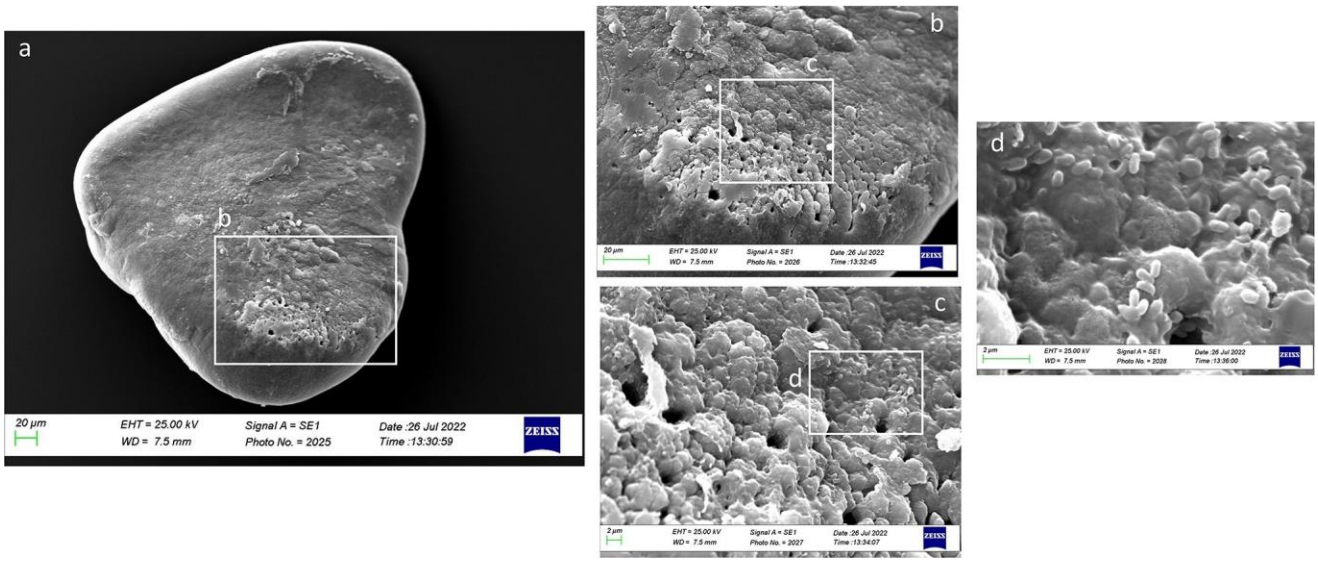

Fig 20. SEM images of a *lapillus* dorsal surface belonging to size Class III (a) with details of the external textural organization near the external margin (b, c).

https://doi.org/10.1371/journal.pone.0281621.g020

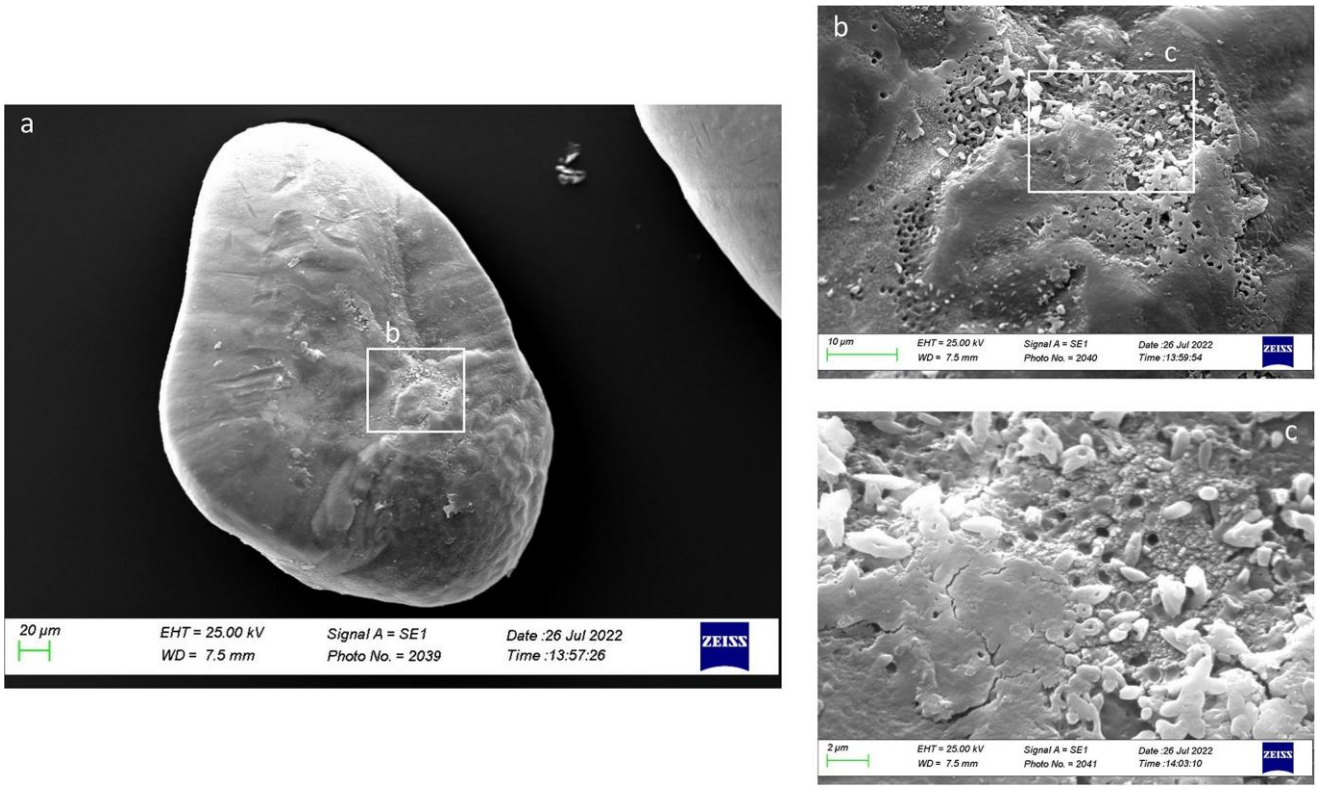

Fig 21. SEM images of a *lapillus* ventral surface belonging to size Class IV (a) with detail of the *gibbus maculae* and *prominentia marginalis* external textural organization and crystalline habits (b, c).

https://doi.org/10.1371/journal.pone.0281621.g021

morphology, shape and morphometry. In this context, the strong tidal currents regime acting in the Strait of Messina, together with the peculiar chemical features of the sea masses, similar in temperature, nutrients, and oxygen concentrations to the Atlantic waters, could induce an otoliths morphology and shape different to those exhibited in species inhabiting other Mediterranean areas. Also, *lapilli* described in the present paper showed a similarity in morphology and morphometry with those described in Atlantic populations by Assis [38], currently the only descriptions reference of *A. hemigymnus lapilli* in literature.

For this reason, it was not possible to compare with Mediterranean Sea data. According to the literature [6, 34], otoltihs' shape, size and morphology, in addition to the dimension and shape of sensory epithelia and ear structure, are intimately related to sound detection, discrimination between sounds with differences in frequencies and/or intensities, determination of sounds' direction in a three-dimensional space and detecting of sound signals in the presence of unwanted sounds. At the interspecific level, otoliths' differences in teleosts' fishes reflect the different hearing abilities that are strictly related to the different life habits, ecology and life history traits of the species. From an intra-specific point of view, otoliths' shape and morphological differences between the different populations of the same species can be allowed by several factors. Diet influences the composition and quantity of endolymph proteins, which are fundamental for otoliths' biomineralization processes [118]. For this reason, diet variations between populations of the same species from different geographical areas may induce differences in otolith morphology and shape. Water masses' physicochemical differences between geographical areas and genetic differences between population lineages can also induce these differences. For example, the temperature can drive growth and morphological variations in deep-sea fishes, as reported for the black spot sea beam *Pagellus bogaraveo*, Brünnich, 1768 [119], while the overall contrasting environmental conditions between different marine areas can influence the overall otoliths morphological and outlines differences, as highlighted for the populations of coral reef snapper *Lutjanus kasmira*, Forsskål, 1775 from the Pacific Ocean [108]. Otherwise, genetic variations at the intra-specific level, such as those derived from long-time separation events among populations, only affect otolith locally, mainly in the rostrum and antirostrum parts [108]. Concerning the present paper, further analysis of the inner ears of species inhabiting the Strait of Messina, comparing the populations from this area with those from others, are required to confirm and better understand the influence of these peculiar environments on marine organisms deepening the knowledge on their eco morphological adaptation.

Concerning the variation in otolith morphology and shape related to specimens' total length and weight, results showed clear differences between the size classes in both *sagittae* and *lapilli*. The absence of literature data on size-related otoliths variations from other geographical areas on the studied species makes it challenging to investigate the environmental influence on the variation among different size classes. *A. hemigymnus* showed an overall morphology and shape of *sagittae*, often widespread in fish inhabiting deep environments which perform simple movements in the water column [6, 120]. Unlike other mesopelagic species, which show elongate *sagittae* with a pronounced *rostrum*, the studied species showed tall *sagittae*, small, with a not pronounced short *rostrum*, like those reported for other Stomiiformes species (e.g., *Chauliodus sloani*, Bloch & Schneider, 1801) [25, 111, 121].

The significant difference in shape, morphometry and morphology showed by results for both *lapilli* and *sagittae* between size classes could be strictly related to the life history and biology of the studied species. Indeed, *A. hemigymnus* is a mesopelagic predator with a relatively high trophic level, mainly hunting on zooplankton (e.g., chaetognaths, euphausiids, copepods), fish and gelatinous plankton. The feeding habits of this species varies geographically according to prey availability and distribution, showing a niche and resource partitioning with the other

mesopelagic predators [47, 89, 92, 93]. The vertical distribution of this species also shows geographical variations mainly related to water temperature, with the deepest distribution reported in oceanic populations than in the Mediterranean ones, which show mostly enhanced migratory behaviour. Indeed, the daily vertical migrations performed by this species are widely reported in the Mediterranean Sea [47, 93, 122]. Also, individuals' size and ontogenetic stages influence their vertical distribution, migratory behaviour and diet, with small specimens that do not perform large vertical movements, inhabit shallower depths than larger ones, and mainly prey on small copepods [123, 124]. These differences in life and feeding habits could influence the inner ear structures and morphology in the different size classes. Indeed, *lapilli* and *sagittae* showed significant differences for all the morphometrical indices between all the size Classes. The larger *sagittae*, with a bigger surface and increased rectangularity and roundness, reported for individuals belonging to size Classes III and IV, could be related to the variation in life habits and ecology during their growing process. Indeed, as widely reported in the literature, many free and fast swimming fishes, which perform large movements, are characterized by large sagittal otoliths, with enhanced dorsal and ventral regions characterized by large *crista superior* and *inferior* [114, 115, 120, 125, 126]. The variations reported by results for *sagittae* between the different size Classes could be in line with these ecomorphological features. Concerning *lapilli*, they also showed clear differences in shape, morphology, and morphometry between size Classes. According to the literature [35, 38], *lapilli* have a most regular intra and inter-specific morphology if compared to *sagittae*. As shown by the results, the *lapilli* of *A. hemigymnus* had a circular morphology and shape maintained in all the size classes. The pointed and most pronounced *extremum posterior*, with a triangular shape, in individuals belonging to Class III and IV than those of other classes has led to significant differences reported for morphology and shape. The lack of reference data from the literature on utricular otoliths did not allow for an ecomorphological interpretation of the differences related to specimens' size. However, as reported for *sagittae*, the variation among size classes could also be related to the studied species' life history. Further analysis on ontogenetic and size-related variations on sagittal and utricular otoliths features, biology and ecology of mesopelagic species are required to understand the relation between inner ears eco morphological adaptation and life history traits of these species.

Regarding the differences between left and right sagittal and utricular otoliths, results showed significant differences only regarding otoliths contours. *A. hemigymnus* population from the Strait of Messina showed a fluctuating asymmetry [94, 127] in *sagittae*, considered as the presence of random deviations from the perfect symmetry between left and right otoliths. *Lapilli* showed a more marked bilateral symmetry, with the asymmetry reported only for Class IV, confirming their most enhanced intraspecific stability than *sagittae*. The fluctuating asymmetry between otolith pairs can be related to environmental heterogeneity or stress [128, 129]. The studied area is characterized by large fluctuations of oceanographic features related to the strong tidal currents' regime acting in the entire area. Moreover, the vertical movements performed by the studied species can increase the environmental factors' heterogeneity to which individuals can be exposed. This strong oceanographic instability could allow the asymmetry shown by the results. Indeed, several authors have related the fluctuating asymmetry to a suboptimally fish growing under stressful conditions or environmental stressors [130]. Concerning the studied area, its oceanographic features allow a substantial water column variability which could induce the fluctuating asymmetry showed by results, as reported in other mesopelagic species (e.g., larvae of *Maurolicus parvipinnis*, Vailliant, 1888 from southern Patagonia) [61]. Further analyses comparing population of *A. hemigymnus* from the studied area with others from other habitats are required to confirm the relationship between asymmetry and environmental heterogeneity of the studied area.

The overall uniform external textural organization of *sagittae* showed by SEM analysis, characterized by the presence of regular small aragonitic crystals with a uniform orientation that made the surface granular, was different from those reported in the literature for other species inhabiting shallower environments [23, 24]. This difference could be related to the stability of mesopelagic strata. Indeed, deep marine environments did not show large fluctuations in chemical and oceanographic features. According to the literature, large crystals with chaotic orientation can be associated with physiological stress and environmental instability [131–134]. Moreover, as reported for a particular ecotype of *Poecilia mexicana*, Steindachner, 1863, inhabiting low-light environments [117], the presence of crystal regions in the *sulcus acusticus* characterized by various sizes and shapes could be related to the low light arriving in the mesopelagic environment. Comparing results from the present paper with those of literature on other mesopelagic species, *A. hemigymnus* specimens showed a more uniform crystals organization in the *sulcus acusticus* than those reported by Lombarte et al. for species belonging to *Coelorinchus* genus from the Southeast Atlantic [135]. The presence of large-size crystal aggregates characterized these last. In contrast, in the studied species, the large crystals in the *sulcus* were isolated and surrounded by small aragonitic crystals with the same orientation. This difference could be related to the different feeding habits of the two species (both predators, but the first is specialized in fishes hunting while the second is a zoo-planktivorous species), added to the different environments with different chemical features inhabited by them (Atlantic Ocean and Strait of Messina). Also, the large crystals detected in other *sagittae* areas (near the ventral margin and the *crista superior*) were isolated, with botryoidal habits, similar to the vateritic crystals showed in literature for *Macruronus novaezelandiae*, Hector, 1871 [1313]. Also, the complex crystalline habits, with a peculiar wave-like macrostructure, showed in some specimens belonging to class II and IV, were reported in vateritic otoliths belonging to *Notothenia microlepidota*, Hutton, 1875 [131]. The presence of botryoidal crystals increased of Class III and IV large specimens, characterized by the entire otoliths zone of the inner face. The formation of vateritic crystals could be strictly related to transient ambient events. As stated by Pach et al. [136], temperature shocks and variations of endolymphatic fluid viscosity can induce vaterite deposition. In this context, the vertical migrations performed by large *A. hemigymnus* specimens could induce the variations in carbonate polymorphs detected by SEM analysis. Indeed, the movements towards superficial marine strata of this species cause the transition from deep water masses to surficial ones, characterized by different chemical features (e.g., temperature, salinity, oxygen concentration), allowing the possible incidence of transient ambient events. The *lapilli's* external textural organization showed a more pronounced irregularity than *sagittae* in all the analyzed size classes, with large crystals on *gibbus maculae* and *prominentia marginalis* characterized by shapes from rhombohedral to botryoidal and deep pores and edges on both dorsal and ventral faces. The lack of literature regarding crystal habits and external textural organization of *lapilli* makes it challenging to compare with other species to understand the possible reasons for their crystalline peculiarity. Despite this, results on *lapilli* were in line with those shown by *sagittae*, with an external textural organization which became most complex, with several carbonate polymorphs and textural irregularities, in specimens belonging to class III and IV than in the others. As stated above for *sagittae*, *lapilli's* external textural organization and crystalline habits could also confirm the influence of migratory habits on carbonate deposition and otoliths' crystalline structure. Further analyses of the crystalline habits and carbonate polymorphs of otoliths, both utricular and sagittal, of *A. hemigymnus* and other mesopelagic species are required to confirm the influence of life habits on the external textural organization of *sagittae*, performing x-ray diffraction and other techniques to detect their polymorphs percentage composition.

Conclusion

To our best knowledge, concerning *A. hemigymnus*, the present paper represents: (i) the first description of *lapilli* from a Mediterranean area, (ii) the first description of otoliths (both utricular and saccular) using shape and SEM analysis and (iii) the first investigation on their intraspecific variability. Results showed a different morphology of *sagittae* compared to data present in literature from other Mediterranean geographical areas, confirming the high intraspecific variability of saccular otoliths between individuals inhabiting different habitats. SEM analysis has provided the first investigation of external textural organization and crystalline habits in *sagittae* and *lapilli* of the studied species, giving information on their superficial structure and morphology, useful to improve the knowledge base on mesopelagic teleost's adaptation to deep marine environments. Indeed, these new data added to those on otoliths variation related to fish size and fluctuating asymmetry of *sagittae* give a pool of information essential to understand how a peculiar environment, such as the Strait of Messina, can shape the organisms that inhabit it. Further analyses comparing populations from the studied area with those from other geographical areas are required to understand the ecomorphological adaptation of *A. hemigymnus* inner ears, showing how different environments and habitats can shape otoliths' features.

Supporting information

S1 Table. Results of the ANOVA conducted on the morphometric parameters of *sagittae* extracted from specimens of *Argyropelecus hemigymnus* belonging to 4 size classes.
(DOCX)

S2 Table. Results of correlation analysis between *sagittae* parameters and sample body weight.
(DOCX)

S3 Table. Results of correlation analysis between sagittae parameters and sample total length.
(DOCX)

S4 Table. Results of the ANOVA conducted on Wavelet Fourier descriptors obtained by the right side of *sagittae* extracted from specimens of *Argyropelecus hemigymnus* belonging to 4 size classes.
(DOCX)

S5 Table. Results of the ANOVA conducted on the morphometric parameters of *lapilli* extracted from specimens of *Argyropelecus hemigymnus* belonging to 4 size classes.
(DOCX)

S6 Table. Results of correlation analysis between l*apilli* parameters and sample body weight.
(DOCX)

S7 Table. Results of correlation analysis between *lapilli* parameters and sample total length.
(DOCX)

S1 Fig. Plotting the quality of *sagittae* (a) and l*apilli* (b) outline reconstruction based on Wavelet and Fourier coefficients. The red lines indicate the level of Wavelet and number of Fourier harmonics needed for a 98.5% accuracy of the remodelling.
(TIF)

S2 Fig. Mean and standard deviation (sd) of Wavelet coefficients for all combined *sagittae* (a) and *lapilli* (b) and the proportion of variance among size classes (black line). The horizontal axis shows angle in degrees (˚) based on the polar coordinates of the mean otoliths shape plot. The centroid of the otolith is the center point of polar coordinates.
(TIF)

Author Contributions

Conceptualization: Marco Albano.

Data curation: Marco Albano, Serena Savoca, Gioele Capillo.

Formal analysis: Sergio Famulari, Dario Di Fresco, Mariachiara Costanzo, Giovanni Lanteri, Serena Savoca.

Funding acquisition: Nunziacarla Spanò.

Investigation: Claudio D'Iglio, Alex Carnevale, Giovanni Lanteri.

Methodology: Sergio Famulari, Marco Albano, Dario Di Fresco, Mariachiara Costanzo.

Project administration: Nunziacarla Spanò.

Resources: Nunziacarla Spanò.

Software: Sergio Famulari, Alex Carnevale, Giovanni Lanteri, Serena Savoca.

Supervision: Nunziacarla Spanò, Gioele Capillo.

Validation: Nunziacarla Spanò, Serena Savoca, Gioele Capillo.

Visualization: Nunziacarla Spanò.

Writing – original draft: Claudio D'Iglio.

Writing – review & editing: Serena Savoca, Gioele Capillo.

References

1. van Bergeijk WA. The evolution of vertebrate hearing. Academic P. In: Neff WD, editor. Contributions to sensory physiology. Academic P. New York: Elsevier; 1967. pp. 1–49.
2. Manley GA, Clack JA. An Outline of the Evolution of Vertebrate Hearing Organs. Evolution of the vertebrate auditory system. Springer; 2004. pp. 1–26.
3. Popper AN. Auditory system morphology. In: Farrell AP, editor. Encyclopedia of Fish Physiology: from Genome to Environment. San Diego, CA: Academic Press; 2011. pp. 252–261.
4. Campana SE, Thorrold SR. Otoliths, increments, and elements: Keys to a comprehensive understanding of fish populations? Can J Fish Aquat Sci. 2001; 58: 30–38. https://doi.org/10.1139/f00-177
5. Campana SE, Neilson JD. Microstructure of Fish Otoliths. Can J Fish Aquat Sci. 1985; 42: 1014–1032. https://doi.org/10.1139/f85-127
6. Schulz-Mirbach T, Ladich F, Plath M, Heß M. Enigmatic ear stones: what we know about the functional role and evolution of fish otoliths. Biol Rev. 2019; 94: 457–482. https://doi.org/10.1111/brv.12463 PMID: 30239135
7. Lombarte A, Tuset VM. Chapter3- Morfometr´ıa de otolitos. 1a ed. edi. In: Volpedo AV, Vaz-dos-Santos AM, editors. Me´todos de estudios con otolitos: principios y aplicaciones/ Me´todos de estudos com oto´litos: princ´ıpios e aplicac¸ões. 1a ed. edi. Ciudad Auto´noma de Buenos Aires; 2015. p. 31.
8. Campana SE, Casselman JM. Stock discrimination using otolith shape analysis. Can J Fish Aquat Sci. 1993; 50: 1062–1083. https://doi.org/10.1139/f93-123
9. Zhuang L, Ye Z, Zhang C, Ye Z, Li Z, Wan R, et al. Stock discrimination of two insular populations of *Diplodus annularis* (Actinopterygii: Perciformes: Sparidae) along the coast of tunisia by analysis of otolith shape. J Fish Biol. 2015; 46: 1–14. https://doi.org/10.3750/AIP2015.45.4.04

10. Newman SJ, Dunk IJ. Growth, age validation, mortality, and other population characteristics of the red emperor snapper, *Lutjanus sebae* (Cuvier, 1828), off the Kimberley coast of north-western Australia. Estuar Coast Shelf Sci. 2002. https://doi.org/10.1006/ecss.2001.0887

11. Mejri M, Trojette M, Allaya H, Ben Faleh A, Jmil I, Chalh A, et al. Use of otolith shape to differentiate two lagoon populations of *Pagellus erythrinus* (Actinopterygii: Perciformes: Sparidae) in Tunisian waters. Acta Ichthyol Piscat. 2018; 48: 153–161. https://doi.org/10.3750/AIEP/02376

12. Kerr LA, Campana SE. Chapter Eleven—Chemical Composition of Fish Hard Parts as a Natural Marker of Fish Stocks. In: Cadrin SX, Kerr LA, Mariani SBT-SIM (Second E, editors. San Diego: Academic Press; 2014. pp. 205–234.

13. D'Iglio C, Savoca S, Rinelli P, Spanò N. Diet of the Deep-Sea Shark *Galeus melastomus* Rafinesque, 1810, in the Mediterranean Sea: What We Know and What We Should Know. Sustainability. 2021; 13. https://doi.org/10.3390/su13073962

14. D'Iglio C, Albano M, Tiralongo F, Famulari S, Rinelli P, Savoca S, et al. Biological and Ecological Aspects of the Blackmouth Catshark (*Galeus melastomus* Rafinesque, 1810) in the Southern Tyrrhenian Sea. J Mar Sci Eng. 2021; 9: 967. https://doi.org/10.3390/jmse9090967

15. D'Iglio C, Porcino N, Savoca S, Profeta A, Perdichizzi A, Armeli Minicante E, et al. Ontogenetic shift and feeding habits of the European hake (*Merluccius merluccius* L., 1758) in Central and Southern Tyrrhenian Sea (Western Mediterranean Sea): A comparison between past and present data. Ecol Evol. 2022; 12: e8634. https://doi.org/10.1002/ece3.8634 PMID: 35356562

16. D'Iglio C, Famulari S, Albano M, Giordano D, Rinelli P, Capillo G, et al. Time-Scale Analysis of Prey Preferences and Ontogenetic Shift in the Diet of European Hake *Merluccius merluccius* (Linnaeus, 1758) in Southern and Central Tyrrhenian Sea. Fishes. 2022; 7. https://doi.org/10.3390/fishes7040167

17. Murie DJ, Lavigne DM. A Technique for the Recovery of Otoliths from Stomach Contents of Piscivorous Pinnipeds. J Wildl Manage. 1985; 49: 910. https://doi.org/10.2307/3801368

18. Murie DJ, Lavigne DM. Interpretation of otoliths in stomach content analyses of phocid seals: quantifying fish consumption. Can J Zool. 1986; 64: 1152–1157. https://doi.org/10.1139/z86-174

19. Polito MJ, Trivelpiece WZ, Karnovsky NJ, Ng E, Patterson WP, Emslie SD. Integrating stomach content and stable isotope analyses to quantify the diets of pygoscelid penguins. PLoS One. 2011; 6: e26642. https://doi.org/10.1371/journal.pone.0026642 PMID: 22053199

20. Christiansen JS, Gamst Moen AG, Hansen TH, Nilssen KT. Digestion of capelin, *Mallotus villosus* (Mu¨ller), herring, *Clupea harengus* L., and polar cod, *Boreogadus saida* (Lepechin), otoliths in a simulated seal stomach. ICES J Mar Sci. 2005; 62: 86–92. https://doi.org/10.1016/j.icesjms.2004.06.022

21. Nolf D. Otolithi Piscium. Handbook of Paleoichthyology, Vol. 10. Fischer G, editor. Stuttgart, New York; 1985.

22. Nolf D, de Potter H, Lafond-Grellety J. Hommage à Joseph Chaine et Jean Duvergier: Diversite´ et variabilite´ des otolithes des poissons. Palaeo Publishing and Library vzw. Belgium: Palaeo Publishing and Library vzw; 2009.

23. D'Iglio C, Albano M, Famulari S, Savoca S, Panarello G, Di Paola D, et al. Intra- and interspecific variability among congeneric Pagellus otoliths. Sci Rep. 2021; 11: 16315. https://doi.org/10.1038/s41598-021-95814-w PMID: 34381131

24. D'iglio C, Natale S, Albano M, Savoca S, Famulari S, Gervasi C, et al. Otolith Analyses Highlight Morpho-Functional Differences of Three Species of Mullet (Mugilidae) from Transitional Water. Sustainability (Switzerland). 2022. https://doi.org/10.3390/su14010398

25. Tuset VM, Lombarte A, Assis CA. Otolith atlas for the western Mediterranean, north and central eastern Atlantic. Sci Mar. 2008; 72: 7–198.

26. Nolf D. Studies on fossil otoliths—The state of the art. Recent Dev Fish Otolith Res. 1995; 19: 513–544.

27. Lin CH, Girone A, Nolf D. Fish otolith assemblages from Recent NE Atlantic sea bottoms: A comparative study of palaeoecology. Palaeogeogr Palaeoclimatol Palaeoecol. 2016; 446: 98–107. https://doi.org/10.1016/j.palaeo.2016.01.022

28. Reichenbacher B, Sienknecht U, Ku¨chenhoff H, Fenske N. Combined otolith morphology and morphometry for assessing taxonomy and diversity in fossil and extant killifish (Aphanius, †Prolebias). J Morphol. 2007; 268: 898–915. https://doi.org/10.1002/jmor.10561 PMID: 17674357

29. Trueman CN, Chung MT, Shores D. Ecogeochemistry potential in deep time biodiversity illustrated using a modern deep-water case study. Philos Trans R Soc B Biol Sci. 2016; 371. https://doi.org/10.1098/rstb.2015.0223 PMID: 26977063

30. Smale MJ, Watson G, Hecht T. Otolith atlas of Southern African marine fishes. Ichthyol Monogr JLB Smith Inst Ichthyol. 1995; 1.

31. Kasapoglu N, Duzgunes E. Otolith atlas for the black sea. J Environ Prot Ecol. 2015; 16: 133–144.

32. Girone A, Nolf D, Cappetta H. Pleistocene fish otoliths from the Mediterranean Basin: a synthesis. Geobios. 2006; 39: 651–671. https://doi.org/10.1016/j.geobios.2005.05.004

33. Kerr LA, Campana SE. Chemical Composition of Fish Hard Parts as a Natural Marker of Fish Stocks. Stock Identification Methods: Applications in Fishery Science: Second Edition. Elsevier; 2013. pp. 205–234.

34. Popper AN, Ramcharitar J, Campana SE. Why otoliths? Insights from inner ear physiology and fisheries biology. Mar Freshw Res. 2005; 56: 497–504. https://doi.org/10.1071/MF04267

35. Assis CA. The utricular otoliths, lapilli, of teleosts: Their morphology and relevance for species identification and systematics studies. Sci Mar. 2005; 69: 259–273. https://doi.org/10.3989/scimar.2005.69n2259

36. Assis CA. The lagenar otoliths of teleosts: Their morphology and its application in species identification, phylogeny and systematics. J Fish Biol. 2003; 62: 1268–1295. https://doi.org/10.1046/j.1095-8649.2003.00106.x

37. Hecht T. A descriptive systematic study of the otoliths of the neopterygean marine fishes of South Africa part i introduction. Trans R Soc South Africa. 1978; 43: 191–197. https://doi.org/10.1080/00359197809520236

38. Assis CA. Estudo morfolo´gico dos oto´litos sagitta, asteriscus e lapillus de Teleo´stei (Actinopterygii, Teleostei) de Portugal continental. Sua aplicac¸ão em estudos de filogenia, sistematica e ecologia. Ecologia. Universidade de Lisboa (Portugal); 2000. p. 1005.

39. Mart´ınez V, Monasterio de Gonzo G. Clave de Identificacio´n de Algunos Peces Siluriformes en Base al Estudio de sus Otolitos. Nat Neotrop. 2005; 2: 95–118. https://doi.org/10.14409/natura.v2i22.3624

40. Volpedo A V., Fuchs D V. Ecomorphological patterns of the lapilli of Paranoplatense Siluriforms (South America). Fish Res. 2010; 102: 160–165. https://doi.org/10.1016/j.fishres.2009.11.007

41. Norse EA, Brooke S, Cheung WWL, Clark MR, Ekeland I, Froese R, et al. Sustainability of deep-sea fisheries. Mar policy. 2012; 36: 307–320.

42. Oanta GA. International organizations and deep-sea fisheries: Current status and future prospects. Mar Policy. 2018; 87: 51–59. https://doi.org/10.1016/j.marpol.2017.09.009

43. Devine JA, Watling L, Cailliet G, Drazen J, Dura´n Muñoz P, Orlov AM, et al. Evaluation of potential sustainability of deep-sea fisheries for grenadiers (Macrouridae). J Ichthyol. 2012; 52: 709–721. https://doi.org/10.1134/S0032945212100062

44. Hidalgo M, Browman HI. Developing the knowledge base needed to sustainably manage mesopelagic resources. ICES Journal of Marine Science. Oxford University Press; 2019. pp. 609–615. https://doi.org/10.1093/icesjms/fsz067

45. Modica L, Cartes JE, Velasco F, Bozzano A. Juvenile hake predation on Myctophidae and Sternoptychidae: Quantifying an energy transfer between mesopelagic and neritic communities. J Sea Res. 2015. https://doi.org/10.1016/j.seares.2014.05.004

46. Agnetta D, Badalamenti F, Colloca F, D'Anna G, Di Lorenzo M, Fiorentino F, et al. Benthic-pelagic coupling mediates interactions in Mediterranean mixed fisheries: An ecosystem modeling approach. PLoS One. 2019; 14: 1–24. https://doi.org/10.1371/journal.pone.0210659 PMID: 30645620

47. Granata A, Brancato G, Sidoti O, Guglielmo L. Energy Flux in the South Tyrrhenian Deep-sea Ecosystem: Role of Mesopelagic Fishes and Squids. Mediterranean Ecosystems. Springer; 2001. pp. 197–207.

48. Gime´nez J, Marc¸alo A, Garc´ıa-Polo M, Garc´ıa-Baro´n I, Castillo JJ, Ferna´ndez-Maldonado C, et al. Feeding ecology of Mediterranean common dolphins: The importance of mesopelagic fish in the diet of an endangered subpopulation. Mar Mammal Sci. 2018; 34: 136–154. https://doi.org/10.1111/mms.12442

49. Geoffroy M, Daase M, Cusa M, Darnis G, Graeve M, Herna´ndez NS, et al. Mesopelagic sound scattering layers of the high Arctic: Seasonal variations in biomass, species assemblage, and trophic relationships. Front Mar Sci. 2019; 6: 364. https://doi.org/10.3389/fmars.2019.00364

50. McMahon CR, Hindell MA, Charrassin JB, Corney S, Guinet C, Harcourt R, et al. Finding mesopelagic prey in a changing Southern Ocean. Sci Rep. 2019; 9: 1–11. https://doi.org/10.1038/s41598-019-55152-4 PMID: 31831763

51. Catul V, Gauns M, Karuppasamy PK. A review on mesopelagic fishes belonging to family Myctophidae. Rev Fish Biol Fish. 2011; 21: 339–354. https://doi.org/10.1007/s11160-010-9176-4

52. Robinson C, Steinberg DK, Anderson TR, Ar´ıstegui J, Carlson CA, Frost JR, et al. Mesopelagic zone ecology and biogeochemistry—A synthesis. Deep Res Part II Top Stud Oceanogr. 2010; 57: 1504–1518. https://doi.org/10.1016/j.dsr2.2010.02.018

53. Albano M, D'Iglio C, Spanò N, Fernandes JM de O, Savoca S, Capillo G. Distribution of the Order Lampriformes in the Mediterranean Sea with Notes on Their Biology, Morphology, and Taxonomy. Biology. 2022. https://doi.org/10.3390/biology11101534 PMID: 36290437

54. Albano M, D'Iglio C, Spanò N, Di Paola D, Alesci A, Savoca S, et al. New Report of *Zu cristatus* (Bonelli, 1819) in the Ionian Sea with an In-Depth Morphometrical Comparison with All Mediterranean Records. Fishes. 2022. p. 305. https://doi.org/10.3390/fishes7060305

55. Mann KH. Fish Production in Open Ocean Ecosystems. Flows of Energy and Materials in Marine Ecosystems. Springer; 1984. pp. 435–458.

56. Irigoien X, Klevjer TA, Røstad A, Martinez U, Boyra G, Acuña JL, et al. Large mesopelagic fishes biomass and trophic efficiency in the open ocean. Nat Commun. 2014; 5: 3271. https://doi.org/10.1038/ncomms4271 PMID: 24509953

57. Jawad LA, Sabatino G, Iba´ñez AL, Andaloro F, Battaglia P. Morphology and ontogenetic changes in otoliths of the mesopelagic fishes *Ceratoscopelus maderensis* (Myctophidae), *Vinciguerria attenuata* and *V. poweriae* (Phosichthyidae) from the Strait of Messina (Mediterranean Sea). Acta Zool. 2018. https://doi.org/10.1111/azo.12197

58. Pauly D, Piroddi C, Hood L, Bailly N, Chu E, Lam V, et al. The biology of mesopelagic fishes and their catches (1950–2018) by commercial and experimental fisheries. J Mar Sci Eng. 2021; 9: 1057. https://doi.org/10.3390/jmse9101057

59. Caiger PE, Lefebve LS, Llopiz JK. Growth and reproduction in mesopelagic fishes: A literature synthesis. ICES J Mar Sci. 2021; 78: 765–781. https://doi.org/10.1093/icesjms/fsaa247

60. Battaglia P, Malara D, Ammendolia G, Romeo T, Andaloro F. Relationships between otolith size and fish length in some mesopelagic teleosts (Myctophidae, Paralepididae, Phosichthyidae and Stomiidae). J Fish Biol. 2015; 87: 774–782. https://doi.org/10.1111/jfb.12744 PMID: 26242808

61. Zenteno JI, Bustos CA, Landaeta MF. Larval growth, condition and fluctuating asymmetry in the otoliths of a mesopelagic fish in an area influenced by a large Patagonian glacier. Mar Biol Res. 2014; 10: 504–514. https://doi.org/10.1080/17451000.2013.831176

62. Battaglia P, Malara D, Romeo T, Andaloro F. Relationships between otolith size and fish size in some mesopelagic and bathypelagic species from the Mediterranean Sea (strait of messina, Italy). Sci Mar. 2010; 74: 605–612. https://doi.org/10.3989/scimar.2010.74n3605

63. Molina-Valdivia V, Bustos CA, Castillo MI, Search F V., Plaza G, Landaeta MF. Oceanographic influences on the early life stages of a mesopelagic fish across the Chilean Patagonia. Prog Oceanogr. 2021; 195: 102572. https://doi.org/10.1016/j.pocean.2021.102572

64. Liu C, Zhang C, Liu Y, Ye Z, Zhang J, Duan M, et al. Age and growth of Antarctic deep-sea smelt (Bathylagus antarcticus), an important mesopelagic fish in the Southern Ocean. Deep Res Part II Top Stud Oceanogr. 2022; 201: 105122. https://doi.org/10.1016/j.dsr2.2022.105122

65. Jones WA, Checkley DM. Mesopelagic fishes dominate otolith record of past two millennia in the Santa Barbara Basin. Nat Commun. 2019; 10: 1–8. https://doi.org/10.1038/s41467-019-12600-z PMID: 31594950

66. Pakhomov EA, Yamamura O, Domokos R, Suntsov A V, Brodeur RD, Seki M. Report of the Advisory Panel on Micronekton Sampling Inter-calibration Experiment. PICES Scientific Report. North Pacific Marine Science Organization (PICES); 2010.

67. Massi M, Salusti E, Stocchino C. On the currents in the strait of Messina. Il Nuovo Cimento C. Osservatorio Geofisico Sperimentale; 1979. https://doi.org/10.1007/BF02557754

68. Cortese G, De Domenico E. Some considerations on the levantine intermediate water distribution in the Straits of Messina. Boll Ocean Teor Appl. 1990; 8: 197–207.

69. De Domenico E. Caratteristiche fisiche e chimiche delle acque nello Stretto di Messina. Doc Trav IGAL. 1987; 11: 225–235.

70. Battaglia P, Ammendolia G, Cavallaro M, Consoli P, Esposito V, Malara D, et al. Influence of lunar phases, winds and seasonality on the stranding of mesopelagic fish in the Strait of Messina (Central Mediterranean Sea). Mar Ecol. 2017; 38: e12459. https://doi.org/10.1111/maec.12459

71. Cavallaro M, Ammendolia G, Rao I, Villari A, Battaglia P. Variazioni pluriennali del fenomeno dello spiaggiamento di specie ittiche nello Stretto di Messina, con particolare attenzione alle specie mesopelagiche. Annales: Series Historia Naturalis. Scientific and Research Center of the Republic of Slovenia; 2021. pp. 69–84.

72. Ammendolia G, Rao I, Cavallaro M. Anastasio Cocco: naturalista messinese dell'Ottocento. Messina, Italy: EDAS; 2014.

73. Mazzarelli G. Gli animali abissali e le correnti sottomarine dello Stretto di Messina. Riv Mens di Pesca e Idrobiol. 1909; 11: 177–218.

74. Sanzo L. Comparsa degli organi luminosi in una serie di larve di *Gonostoma denudatum* Raf. R. Mem R Com Talassog Ital. 1912;9.

75. Sanzo L. Larva di *Ichthyococcus ovatus*, Cocco. Real Com Talassogr Ital Venezia XXVII. 1913.

76. Sanzo L. Stadi post-embrionali di *Vinciguerria attenuata* (Cocco) e *V. poweriae* (Cocco) Jordan ed Evermann. R Com Talassogr Ital Mem. 1913;35.

77. Sanzo L. Uova e larve di *Trachypterus cristatus* Bp. R Com Talassogr Ital—Mem. 1918; 64: 1–16 + 1pl.

78. Genovese S, Berdar A, Guglielmo L. Spiaggiamenti di fauna abissale nello Stretto di Messina. Atti Soc Pelor Sci Fis Mat Nat. 1971; XVII: 331–370.

79. Guglielmo L, Marabello F, Vanucci S. The role of the mesopelagic fishes in the pelagic food web of the Strait of Messina. Straits Messin Ecosyst Proc Symp Messin. 1995; 223–246.

80. Longo F. Il canale di Messina e le sue correnti: con appendice sui pesci che lo popolano. Ribera; 1882.

81. Marini L. Le correnti dello Stretto di Messina e la distribuzione del plancton in esso. Riv mens Pesca Idrobiol. 1910; 12: 41–47.

82. Gjøsaeter J, Kawaguchi K. A review of the world resources of mesopelagic fish. FAO Fish Tech Pap. 1980; 193: 123–134. Available: https://ia600301.us.archive.org/7/items/reviewoftheworld034721mbp/reviewoftheworld034721mbp.pdf

83. Olivar MP, Bernal A, Mol´ı B, Peña M, Balb´ın R, Castello´n A, et al. Vertical distribution, diversity and assemblages of mesopelagic fishes in the western Mediterranean. Deep Res Part I Oceanogr Res Pap. 2012; 62: 53–69. https://doi.org/10.1016/j.dsr.2011.12.014

84. Olivar MP, Hulley PA, Castello´n A, Emelianov M, Lo´pez C, Tuset VM, et al. Mesopelagic fishes across the tropical and equatorial Atlantic: Biogeographical and vertical patterns. Prog Oceanogr. 2017; 151: 116–137. https://doi.org/10.1016/j.pocean.2016.12.001

85. Hubbs CL, Nelson JS. Fishes of the World. Systematic Zoology. John Wiley & Sons; 1978.

86. Goren M. The fishes of the mediterranean: A biota under siege. The Mediterranean Sea: Its History and Present Challenges. 2014. pp. 385–400. https://doi.org/10.1007/978-94-007-6704-1_22

87. Genovese S, Guglielmo L, Ianora A, Scotto di Carlo B. Osservazioni biologiche con il mesoscafo «Forel» nello Stretto di Messina. Archivio di Oceanografia e Limnologia. Istituto di Biologia del Mare del Consiglio Nazionale delle Ricerche; 1985.

88. Spitz J, Mourocq E, Leaute´ JP, Que´ro JC, Ridoux V. Prey selection by the common dolphin: Fulfilling high energy requirements with high quality food. J Exp Mar Bio Ecol. 2010; 390: 73–77. https://doi.org/10.1016/j.jembe.2010.05.010

89. Carmo V, Sutton T, Menezes G, Falkenhaug T, Bergstad OA. Feeding ecology of the Stomiiformes (Pisces) of the northern Mid-Atlantic Ridge. 1. The Sternoptychidae and Phosichthyidae. Prog Oceanogr. 2015; 130: 172–187. https://doi.org/10.1016/j.pocean.2014.11.003

90. Miyazaki N, Kusaka T, Nishiwaki M. Food of *Stenella caeruleoalba*. Sci Rep Whales Res Inst. 1973; 25: 265–275.

91. Lordan C, Burnell GM, Cross TF. The diet and ecological importance of *Illex coindetii* and *Todaropsis eblanae* (Cephalopoda: Ommastrephidae) in Irish waters. South African J Mar Sci. 1998; 20: 153–163. https://doi.org/10.2989/025776198784126214

92. Kinzer J, Schulz K. Vertical distribution and feeding patterns of midwater fish in the central equatorial Atlantic II. Sternoptychidae. Mar Biol. 1988; 99: 261–269. https://doi.org/10.1007/BF00391989

93. Eduardo LN, Bertrand A, Mincarone MM, Santos L V., Fre´dou T, Assunc¸ão R V., et al. Hatchetfishes (Stomiiformes: Sternoptychidae) biodiversity, trophic ecology, vertical niche partitioning and functional roles in the western Tropical Atlantic. Prog Oceanogr. 2020; 187: 102389. https://doi.org/10.1016/j.pocean.2020.102389

94. D´ıaz-Gil C, Palmer M, Catala´n IA, Alo´s J, Fuiman LA, Garc´ıa E, et al. Otolith fluctuating asymmetry: A misconception of its biological relevance? ICES J Mar Sci. 2015; 72: 2079–2089. https://doi.org/10.1093/icesjms/fsv067

95. Schulz-Mirbach T, Plath M. All good things come in threes–species delimitation through shape analysis of saccular, lagenar and utricular otoliths. Mar Freshw Res. 2012; 63: 934–940.

96. Schulz-Mirbach T, Ladich F, Riesch R, Plath M. Otolith morphology and hearing abilities in cave- and surface-dwelling ecotypes of the Atlantic molly, *Poecilia mexicana* (Teleostei: Poeciliidae). Hear Res. 2010; 267: 137–148. https://doi.org/10.1016/j.heares.2010.04.001 PMID: 20430090

97. Longhitano SG. Between Scylla and Charybdis (part 2): The sedimentary dynamics of the ancient, Early Pleistocene Messina Strait (central Mediterranean) based on its modern analogue. Earth-Science Rev. 2018; 179: 248–286. https://doi.org/10.1016/j.earscirev.2018.01.017

98. Cucco A, Quattrocchi G, Olita A, Fazioli L, Ribotti A, Sinerchia M, et al. Hydrodynamic modelling of coastal seas: The role of tidal dynamics in the Messina Strait, Western Mediterranean Sea. Nat Hazards Earth Syst Sci. 2016; 16: 1553–1569. https://doi.org/10.5194/nhess-16-1553-2016

99. Schneider CA, Rasband WS, Eliceiri KW. NIH Image to ImageJ: 25 years of image analysis. Nat Methods. 2012; 9: 671–675. https://doi.org/10.1038/nmeth.2089 PMID: 22930834

100. Pavlov DA. Differentiation of three species of the genus Upeneus (Mullidae) based on otolith shape analysis. J Ichthyol. 2016; 56: 37–51. https://doi.org/10.1134/S0032945216010094

101. Pavlov DA. Otolith Morphology and Relationships of Several Fish Species of the Suborder Scorpaenoidei. J Ichthyol. 2021; 61: 33–47. https://doi.org/10.1134/S0032945221010100

102. Tuset VM, Farre´ M, Otero-Ferrer JL, Vilar A, Morales-Nin B, Lombarte A. Testing otolith morphology for measuring marine fish biodiversity. Mar Freshw Res. 2016; 67: 1037–1048. https://doi.org/10.1071/MF15052

103. Tuset VM, Lombarte A, Gonza´lez JA, Pertusa JF, Lorente MJ. Comparative morphology of the sagittal otolith in *Serranus spp*. J Fish Biol. 2003; 63: 1491–1504. https://doi.org/10.1111/j.1095-8649.2003.00262.x

104. Tuset VM, Lozano IJ, Gonz´lez JA, Pertusa JF, Garc´ıa-D´ıaz MM. Shape indices to identify regional differences in otolith morphology of comber, *Serranus cabrilla* (L., 1758). J Appl Ichthyol. 2003; 19: 88–93. https://doi.org/10.1046/j.1439-0426.2003.00344.x

105. Libungan LA, Pa´lsson S. ShapeR: An R package to study otolith shape variation among fish populations. PLoS One. 2015; 10: 1–12. https://doi.org/10.1371/journal.pone.0121102 PMID: 25803855

106. Gagliano M, McCormick MI. Feeding history influences otolith shape in tropical fish. Mar Ecol Prog Ser. 2004; 278: 291–296. https://doi.org/10.3354/meps278291

107. Hoff GR, Fuiman LA. Morphometry and composition of red drum otoliths: Changes associated with temperature, somatic growth rate, and age. Comp Biochem Physiol—Part A Physiol. 1993; 106: 209–219. https://doi.org/10.1016/0300-9629(93)90502-U

108. Vignon M, Morat F. Environmental and genetic determinant of otolith shape revealed by a non-indigenous tropical fish. Mar Ecol Prog Ser. 2010; 411: 231–241. https://doi.org/10.3354/meps08651

109. Bose APH, Zimmermann H, Winkler G, Kaufmann A, Strohmeier T, Koblmu¨ller S, et al. Congruent geographic variation in saccular otolith shape across multiple species of African cichlids. Sci Rep. 2020; 10: 1–14. https://doi.org/10.1038/s41598-020-69701-9 PMID: 32733082

110. Lin CH, Chiang YP, Tuset VM, Lombarte A, Girone A. Late Quaternary to Recent diversity of fish otoliths from the Red Sea, central Mediterranean, and NE Atlantic sea bottoms. Geobios. 2018; 51: 335–358. https://doi.org/10.1016/j.geobios.2018.06.002

111. Campana SE. Photographic Atlas of Fish Otoliths of the Northwest Atlantic Ocean. Photographic Atlas of Fish Otoliths of the Northwest Atlantic Ocean. NRC Research Press; 2004.

112. Volpedo A V, Echeverria D. Morfolog´ıa de los otolitos sagittae de juveniles y adultos de *Micropogonias furnieri* (Demarest, 1823) (Scianidae). Thalassas. 1999; 15: 19–24.

113. Torres GJ, Lombarte A, Morales-Nin B. Variability of the sulcus acusticus in the sagittal otolith of the genus Merluccius (Merlucciidae). Fish Res. 2000; 46: 5–13. https://doi.org/10.1016/S0165-7836(00)00128-4

114. Lombarte A, Cruz A. Otolith size trends in marine fish communities from different depth strata. J Fish Biol. 2007; 71: 53–76. https://doi.org/10.1111/j.1095-8649.2007.01465.x

115. Lombarte A, Lleonart J. Otolith size changes related with body growth, habitat depth and temperature. Environ Biol Fishes. 1993; 37: 297–306. https://doi.org/10.1007/BF00004637

116. Schulz-Mirbach T, Riesch R, Garc´ıa de Leo´n FJ, Plath M. Effects of extreme habitat conditions on otolith morphology—a case study on extremophile livebearing fishes (*Poecilia mexicana*, *P. sulphuraria*). Zoology. 2011; 114: 321–334. https://doi.org/10.1016/j.zool.2011.07.004 PMID: 22000528

117. Schulz-Mirbach T, Go¨tz A, Griesshaber E, Plath M, Schmahl WW. Texture and nano-scale internal microstructure of otoliths in the atlantic molly, *Poecilia mexicana*: A high-resolution EBSD study. Micron. 2013; 51: 60–69. https://doi.org/10.1016/j.micron.2013.07.001 PMID: 23891259

118. Mille T, Mahe´ K, Cachera M, Villanueva MC, De Pontual H, Ernande B. Diet is correlated with otolith shape in marine fish. Mar Ecol Prog Ser. 2016; 555: 167–184. https://doi.org/10.3354/meps11784

119. Neves J, Giacomello E, Menezes GM, Fontes J, Tanner SE. Temperature-Driven Growth Variation in a Deep-Sea Fish: The Case of *Pagellus bogaraveo* (Bru¨nnich, 1768) in the Azores Archipelago. Frontiers in Marine Science. 2021. https://doi.org/10.3389/fmars.2021.703820

120. Assis IO, da Silva VEL, Souto-Vieira D, Lozano AP, Volpedo A V., Fabre´ NN. Ecomorphological patterns in otoliths of tropical fishes: assessing trophic groups and depth strata preference by shape. Environ Biol Fishes. 2020; 103: 349–361. https://doi.org/10.1007/s10641-020-00961-0

121. Lombarte A, Chic O` , Parisi-Baradad V, Olivella R, Piera J, Garc´ıa-Ladona E. A web-based environment for shape analysis of fish otoliths. The AFORO database. Sci Mar. 2006; 70: 147–152. https://doi.org/10.3989/scimar.2006.70n1147

122. Andersen V, Sardou J, Nival P. The diel migrations and vertical distributions of zooplankton and micronekton in the Northwestern Mediterranean Sea. 2. Siphonophores, hydromedusae and pyrosomids. J Plankton Res. 1992; 14: 1155–1169. https://doi.org/10.1093/plankt/14.8.1155

123. Contreras T, Olivar MP, Bernal A, Sabate´s A. Comparative feeding patterns of early stages of mesopelagic fishes with vertical habitat partitioning. Mar Biol. 2015; 162: 2265–2277. https://doi.org/10.1007/s00227-015-2749-y

124. Olivar MP, Sabate´s A, Alemany F, Balb´ın R, de Puelles MLF, Torres AP. Diel-depth distributions of fish larvae off the Balearic Islands (western Mediterranean) under two environmental scenarios. J Mar Syst. 2014; 138: 127–138.

125. Volpedo A, Diana Echeverr´ıa D. Ecomorphological patterns of the sagitta in fish on the continental shelf off Argentine. Fish Res. 2003; 60: 551–560. https://doi.org/10.1016/S0165-7836(02)00170-4

126. Tuset VM, Olivar MP, Otero-Ferrer JL, Lo´pez-Pe´rez C, Hulley PA, Lombarte A. Morpho-functional diversity in *Diaphus spp*. (Pisces: Myctophidae) from the central Atlantic Ocean: Ecological and evolutionary implications. Deep Res Part I Oceanogr Res Pap. 2018; 138: 46–59. https://doi.org/10.1016/j.dsr.2018.07.005

127. Mahe´ K, Ider D, Massaro A, Hamed O, Jurado-Ruzafa A, Gonc¸alves P, et al. Directional bilateral asymmetry in otolith morphology may affect fish stock discrimination based on otolith shape analysis. ICES J Mar Sci. 2019; 76: 232–243. https://doi.org/10.1093/icesjms/fsy163

128. Downhower JF, Blumer LS, Lejeune P, Gaudin P. Otolith asymmetry in *Cottus bairdi* and *C. gobio*. Pol Arcghiwum Hydrobiol. 1990; 37: 209–220.

129. Green AA, Mosaliganti KR, Swinburne IA, Obholzer ND, Megason SG. Recovery of shape and size in a developing organ pair. Dev Dyn. 2017; 246: 451–465. https://doi.org/10.1002/dvdy.24498 PMID: 28295855

130. Franco A, Malavasi S, Pranovi F, Nasci C, Torricelli P. Ethoxyresorufin O-deethylase (EROD) activity and fluctuating asymmetry (FA) in *Zosterisessor ophiocephalus* (Teleostei, Gobiidae) as indicators of environmental stress in the Venice lagoon. J Aquat Ecosyst Stress Recover. 2002; 9: 239–247. https://doi.org/10.1023/A:1024010813669

131. Gauldie RW. Polymorphic crystalline structure of fish otoliths. J Morphol. 1993; 218: 1–28. https://doi.org/10.1002/jmor.1052180102 PMID: 29865482

132. Reimer T, Dempster T, Warren-Myers F, Jensen AJ, Swearer SE. High prevalence of vaterite in sagittal otoliths causes hearing impairment in farmed fish. Sci Rep. 2016; 6: 1–8. https://doi.org/10.1038/srep25249 PMID: 27121086

133. Oxman DS, Barnett-Johnson R, Smith ME, Coffin A, Miller DL, Josephson R, et al. The effect of vaterite deposition on sound reception, otolith morphology, and inner ear sensory epithelia in hatchery-reared *Chinook salmon* (Oncorhynchus tshawytscha). Can J Fish Aquat Sci. 2007; 64: 1469–1478. https://doi.org/10.1139/F07-106

134. Falini G, Fermani S, Vanzo S, Miletic M, Zaffino G. Influence on the formation of aragonite or vaterite by otolith macromolecules. Eur J Inorg Chem. 2005; 2005: 162–167. https://doi.org/10.1002/ejic.200400419

135. Lombarte A, Morales-Nin B. Morphology and ultrastructure of saccular otoliths from five species of the genus Coelorinchus (Gadiformes: Macrouridae) from the Southeast Atlantic. J Morphol. 1995; 225: 179–192. https://doi.org/10.1002/jmor.1052250204 PMID: 29865328

136. Pach L, Hrabe Z, Komarneni S, Roy R. Controlled crystallization of vaterite from viscous solutions of organic colloids. J Mater Res. 2011/01/31. 1990; 5: 2928–2932. https://doi.org/10.1557/JMR.1990.2928

Intra-specific variability of the saccular, utricular and lagenar otoliths of the garfish *Belone belone* (Linnaeus, 1760) from South-Western Ionian Sea (Central Mediterranean Sea)

ABSTRACT

The garfish *Belone belone* represents the only valid endemic *Belone* species for the Mediterranean Sea and the eastern Atlantic Ocean. It shows a wide global distribution range, with a high commercial value and ecological relevance in the pelagic domain. Despite this, there needs to be more knowledge regarding the otoliths of this species, with the total absence of descriptions regarding *asterisci* and *lapilli* from Mediterranean populations and a lack of studies on the reliability of shape analysis on its *sagittae.* The present paper aims to provide the first main contours description of the three otoliths pairs from a Mediterranean population, providing an accurate investigation of morphology, morphometry, and intra-specific variability of *sagittae, lapilli,* and *asterisci*. Results showed (i) the absence of directional bilateral asymmetry and sexual asymmetry for the three otoliths pairs, (ii) a different morphology and morphometry of *sagittae, lapilli* and *asterisci* than those described in the literature, and (iii) an enhanced variability between *sagittae* morphometry and shape between the three investigated size classes. All these data confirmed the reliability of the studied species of shape analysis, showing a geographical and size-related variability of otoliths features probably related to genetics, environmental conditions, and life habits variations.

1. INTRODUCTION

The family Belonidae, order Beloniformes, includes ten genera and 34 species of freshwater and marine teleost known as needlefishes [1,2]. They are characterized by an elongated body and long upper and lower jaws, resulting in a beak with a large mouth opening equipped with sharp needle-like teeth. Small cycloid scales are distributed along their lateral lines. A separation in the third pair of the upper pharyngeal bones is typical of this family, together with the absence of spines in the fins, no finlets behind the anal and the dorsal fins, and the nostrils placed in a pit anteriorly to the eyes [3,4]. All needlefishes' species are oviparous and live close to the surface. They are ichthyophage predators, hunting on small fishes using their beaks. In the Mediterranean Sea, they have been recognized six species of needlefishes belonging to three genera: *Ablennes hians*, Valenciennes, 1846, *Belone belone,* Linnaeus, 1761, *Belone svetovidovi*, Collette & Parin, 1970, *Tylosurus acus acus*, Lacépède, 1803, and *Tylosurus acus imperialis*, Rafinesque, 1810 [4–6].

Concerning *B. belone*, in 1970 [7], they were acknowledged three subspecies according to their global distribution (*B. b. belone*, Linnaeus, 1761, *B. b. euxini*, Günther, 1866, *B. b. gracilis*, Lowe, 1839),

but recently the garfish *B. belone* was accepted as the only valid endemic species for the Mediterranean Sea and the eastern Atlantic Ocean [8]. This species shows a wide distribution range, inhabiting brackish and marine environments from Norway to the Canaries, in addition to the Mediterranean and Black Seas. Like other pelagic teleosts, it is an oceanodromous species. It inhabits the offshore areas, moving near the coast during spawning season. It is during this migratory pattern that garfish populations are more susceptible to fisheries activities [9,10], being mainly caught using floating gill nets and pelagic trawling. In the Adriatic Sea and Turkish Mediterranean waters, garfish is the principal target species of seine nets, representing also a by-catch species in purse seine fisheries [3,11–13]. In the Mediterranean Sea, the *B. belone* capture production has been growing since 2016, stationing at 621 tons in 2018, with Turkey, Tunisia, Greece, and Spain as the leading countries for its harvesting and consumption [14]. This species is among the most important pelagic commercial species of Turkey, especially for the Black Sea's Turkish artisanal fisheries and Tunisia, representing the main belonids species for catch in the entire Mediterranean basin [15–17]. In addition to its commercial value, garfish plays a fundamental ecological role in the pelagic domain. It is an opportunistic predator that switches its prey preferences from crustaceans (e.g., copepods, decapods larvae, amphipods) to teleost fishes (e.g., clupeids, engraulids, horse mackerels), according to its size and the preys' availability [18–21]. Additionally, it is among the principal preys of larger pelagic fishes and marine mammals [22–24]. Due to its high commercial and ecological value, many studies have been performed on the biology of this species. These provided essential information for accurate stock assessments, exploring its population dynamics (e.g., age structure, growth, mortality, reproductive cycle), metazoan parasites communities, and trophic ecology in the different Mediterranean geographical areas [12,15,17,21,25–30]. However, relatively few researches have been performed on garfish otoliths, another fundamental tool for stock assessment and population studies [31–36].

Otoliths are paired carbonate structures in the vertebrates' inner ears, close to the midbrain, with auditory and vestibular functions [37]. Teleost's inner ear (one for each side) is characterized by a great morphological variability among different taxa [38]. Its basic structure, common in bony and cartilaginous fishes, is characterized by three semicircular canals, with their end organs (*ampullae*) and three otoliths end organs (*saccule, utricle, lagena)*. Otoliths are located inside these lasts (one otolith in each organ: respectively, *sagitta, lapillus,* and *asteriscus*), which, according to their taxon-specific orientation related to the fish's rostrocaudal axis, are essential for the localization of sound sources [37]. They are composed of calcium carbonate and non-collagenous organic matrix, depositing daily for the entire fishes' lifetime [39,40], and, among the three otoliths pairs, *sagittae* have long been the most studied. Due to their species-specific morphology, timekeeping and chemical

properties, and variability at intra and interspecific levels, *sagittae* long been widely used in many research fields, including taxonomy and paleoethology, to trophic ecology and fisheries science [33,41–52]. Data on *lapilli* and *asterisci* are very few and fragmentary, especially concerning the marine teleost species; this is attributable to their dimension, smaller than *sagittae* in non-ostariophysian fishes [53–55], and, especially for *asterisci,* mainly composed of vaterite, to their low resistance to the extraction process. It has also been claimed that *lapilli* and *asterisci* show a low intra and inter-specific variability, considerably less evident than *sagittae* [56,57]. Conversely, recent findings by several authors have assessed, also in otophysans species, a substantial inter-specific diversity valuable for species identification and evident intra-specific variations between different populations related to environmental factors, as also confirmed in not-otophysans species [56–60]. Indeed, according to T. Schulz-Mirbach et al. [58], providing new information on *lapilli* and *asterisci* of the different teleost's species, also applying shape analysis, is required to evaluate the additional data provided by the investigations on all the otoliths pairs, improving species identification processes, stock assessment, and fisheries management.

Concerning *B. belone* otoliths, literature data are scarce, with few studies on *sagittae,* describing their gross morphology, the relations between fish length and otolith size, and some morphometrical features [61–65]. Only three studies describe *lapilli* and *asterisci* in populations inhabiting the Mediterranean Sea and Portuguese Atlantic waters [56,57,66]. In this context, the present paper aims to analyze the three otoliths pairs of garfish from the Ionian Sea (the Italian Sea with the highest values of capture production for this species in 2020 [67]) through morphological, morphometrical, and shape analysis, in order to investigate the intra specific variability of *sagittae, lapilli* and *asterisci* between different size classes, otoliths pairs and populations, comparing data from present paper to those from literature. The present paper can allow (i) to investigate the presence of otoliths' bilateral asymmetry and sexual variability inside the analyzed population, (ii) to compare otoliths' morphology and morphometry between the Ionian Sea and other geographical areas through a comparison with literature data and (iii) to give an accurate otoliths' contours description, essential for stock assessment.

All this information is fundamental to improving the knowledge base on the eco-morphological adaptation of this species to the pelagic environment, filling the gap in the morphology, shape, and intra-specific variability of *sagittae, lapilli,* and *asterisci.* Indeed, there needs to be more data on *sagittae* from the Ionian Sea and an almost total absence of studies on *lapilli* and *asterisci,* especially from the Mediterranean Sea, regarding the studied species [56,57,66]. Moreover, taking into account the difficulties in assessing the stock composition and discriminating among populations of medium-large size pelagic fishes due to their broad geographical range and the absence of biogeographical

barriers [68,69], the present paper can improve the capability to distinguish separated fish groups of *B. belone,* providing the first accurate shape analysis on the three otoliths pairs. This is fundamental to correctly distinguishing populations and stocks for better conservation and improved fisheries management.

2. MATERIALS AND METHODS

2.1 Sample collection, processing, and image analysis

Seventy-five specimens of *B. belone* were obtained from a market in Catania (Italy, Sicily) supplied by local artisanal fisheries operating in the Ionian Sea (FAO statistical division 37.2.2-Ionian Sea) (Figure 1).

Figure 1. Map of the Mediterranean Sea with sampling area of B. belone specimens analyzed in this study highlighted by the red circle.

Samples were transported still frozen in the laboratory, where each specimen was weighted (Total Weight: TW, g), measured (Total Length: TL, mm), and assigned to three size classes according to its TL (Class I: TL ≤ 240 mm; Class II: 240 mm < TL ≤ 290 mm; Class III: TL > 290 mm), also assessing the sex. Each otolith (*sagitta, lapillus,* and *asteriscus* of each inner ear) was extracted and gently washed in 3 % H_2O_2 and Milli-Q water to remove tissue remains. Once dried, each *sagitta, lapillus,* and *asteriscus* face was photographed twice using the Axiocam 208 color camera (Carl Zeiss, Jena, Germany) under a stereomicroscope Zeiss Discovery V8. Otolith images were processed and converted into binary format for shape analysis using ImageJ 1.48p software [70]. Once obtained

from shape analysis, data on maximum otolith length, OL mm, maximum otolith width, OW mm, otolith perimeter, OP mm and otolith surface, OS, mm^2 for each analyzed otolith, investigated the relation between otolith and fish length calculating the ratio of otolith length to the total fish length (OL/TL). Moreover, in order to evaluate how otoliths' morphometric relationships and morphology features change intra-specifically, they were calculated several shape indices, according to literature [71–76]: circularity ($C = OP^2/OS$), rectangularity ($Re = OS/[OL \times OW]$), ellipticity ($E = OL–OW/OL+OW$), aspect ratio ($AR = OW/OL\%$), form factor ($FF = 4\pi OS/OP^2$) and roundness ($Ro = 4OS/\pi OL^2$).

2.2 Shape analysis

The otoliths outlines were used to perform the Shape analysis using the open-assess package shape R on R software (RStudio 2022.07.1 Build 554; R Gui 4.1.3 2022.03.10). This package was designed for the otolith shape studies, widely used to analyze the intra and inter-specific variations in teleost species and populations [77]. ImageJ software (version 1.53k freely available at https://imagej.nih.gov/ij/) was used to binarize each *sagitta, lapilli* and *asterisci* picture, which, subsequently, was classified according to fish size classes, sex, and otoliths' side. The greyscale threshold was set at 0.05 (intensity threshold) to detect the outlines using a specific shape R function. The data file with analyzed specimens' information (e.g., body weight and fish length) was linked to the extracted contours. The getMeasurements function was applied to calculate the otoliths' length, width, area, and perimeter for each specimen on the previously detected outlines. The allometric relationships were assessed between fish lengths and otolith shapes, extracting Wavelet and Fourier coefficients, adequately adjusted, through proper functions of Shape R. The intra-specific comparison between the mean otolith shapes was obtained using the Wavelet coefficients, estimating the quality of the reconstruction through the analysis of the deviation of the coefficients' reconstruction from the otolith outline (S1 Fig). A specific function of the g-plots R package was applied to investigate the influence of the position along the outline on the wavelet coefficients' variation (S2 Fig).

2.3 Data analysis

Univariate and multivariate statistical methods were applied to conduct investigations on *asterisci*, *lapilli,* and *sagittae* using Prism V.8.2.1 (Graph-pad Software Ltd., La Jolla, CA 92037, USA), R vegan package V.2.5, and PAST V.4.

An unpaired t-test was used as a tool to investigate the occurrence of differences in morphometric parameters between sexes and between right and left otoliths. Any otolith morphometric variations between the different size classes investigated were detected using a one-way analysis of variance (one-way ANOVA) and Linear Discriminant Analysis (LDA). Additionally, the correlation between the measured parameters and fish body weight (BW) and total length (TL) was tested using the Pearson correlation coefficient.

To explore the variation of otolith contours between specimens, the shape indices were extrapolated and analyzed through an ANOVA-like permutation test and a Linear Discriminant Analysis (LDA) to obtain an overview of the differences in otolith shape between right and left side, gender, and size classes examined. The significance level of the p-value was set at < 0.05.

3. RESULTS

A total of 65 individuals (20 males and 45 females) were examined, with 18 specimens classified as Class I, 35 as Class II, and 12 as Class III.

3.1 Morphometric and Shape analysis of Sagittae

According to the terminology proposed by Tuset et al., Nolf and Assis [65,66,78], *B. belone* showed overall elliptic-lanceolate *sagittae* (Fig 2 a-c), characterized by peaked anterior region, with a short *rostrum*, pointed and broad, and a round posterior region. The *antirostrum* was generally absent, except in some specimens, in which it was very short, broad, and pointed. The *excisura ostii* was absent or wide, changing in the different individuals according to the size class of belonging.

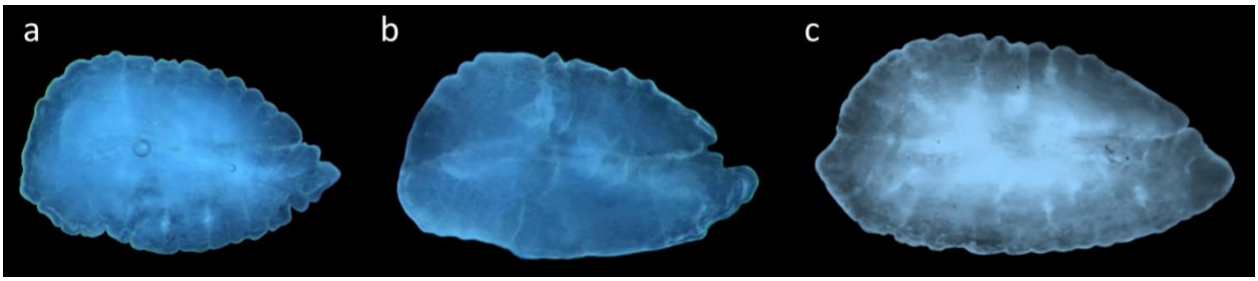

Figure 2. Stereoscope images of left sagittae belonging to size class I (a), II (b) and III (c).

In Table 1 they were reported the morphometric parameters assessed for the studied specimens.

Table 1. Sagittae morphometric mean values, with standard deviation (s.d.), maximum (Max.), and minimum (Min.) values, for each investigated size class: maximum otolith length (OL, mm) and otolith width (OW, mm), otolith perimeter (OP, mm), otolith surface

(OS, mm²), otolith length to the total fish length ratio (OL/TL), circularity (C), rectangularity (Re), ellipticity (E), aspect ratio (AR), form factor (FF) and roundness (Ro).

	Class I			Class II			Class II		
	Mean	s.d.	Min - Max	Mean	s.d.	Min - Max	Mean	s.d.	Min - Max
OL	2.16	0.23	1.7 - 2.67	2.36	0.21	2.02 - 2.88	2.64	0.27	2.05 - 3.33
OW	1.29	0.13	1.01 - 1.55	1.37	0.1	1.64 - 1.15	1.54	0.11	1.31 - 1.79
OP	6.46	0.71	4.93 - 7.88	7	0.57	5.85 - 8.25	7.8	0.74	6.3 - 9.34
OS	2.08	0.41	1.29 - 2.97	2.34	0.35	1.75 - 3.28	2.97	0.45	2.12 - 4.1
OL/TL %	0.95	0.1	0.79 - 1.21	0.9	0.08	0.71 - 1.09	0.82	0.11	0.67 - 1.11
C	20.28	1.5	17.65 - 24.75	21.02	1.26	18.86 - 23.7	20.6	1.28	18.58 - 23.37
Re	0.74	0.02	0.7 - 0.79	0.72	0.02	0.67 - 0.79	0.73	0.02	0.69 - 0.77
E	0.25	0.03	0.19 - 0.33	0.26	0.03	0.19 - 0.32	0.26	0.03	0.2 - 0.32
AR	0.6	0.04	0.5 - 0.69	0.58	0.03	0.51 - 0.68	0.58	0.04	0.52 - 0.66
FF	0.62	0.04	0.51 - 0.71	0.6	0.03	0.53 - 0.66	0.61	0.04	0.54 - 0.67
Ro	0.56	0.05	0.47 - 0.68	0.54	0.04	0.47 - 0.64	0.54	0.04	0.47 - 0.64

The examination showed no significant variation between the right and left *sagittae* ($p>0.05$).

Gender represented a discriminating factor only for 3 of the morphometric parameters investigated, namely OS ($p=0.014$) and OL ($p=0.025$).

Finally, the size class strongly influenced the morphometric variability observed between the samples, as confirmed by LDA (Figure 3). Results, reported in Table 2, highlighted how AR was the only parameter that did not vary between size classes ($p>0.05$).

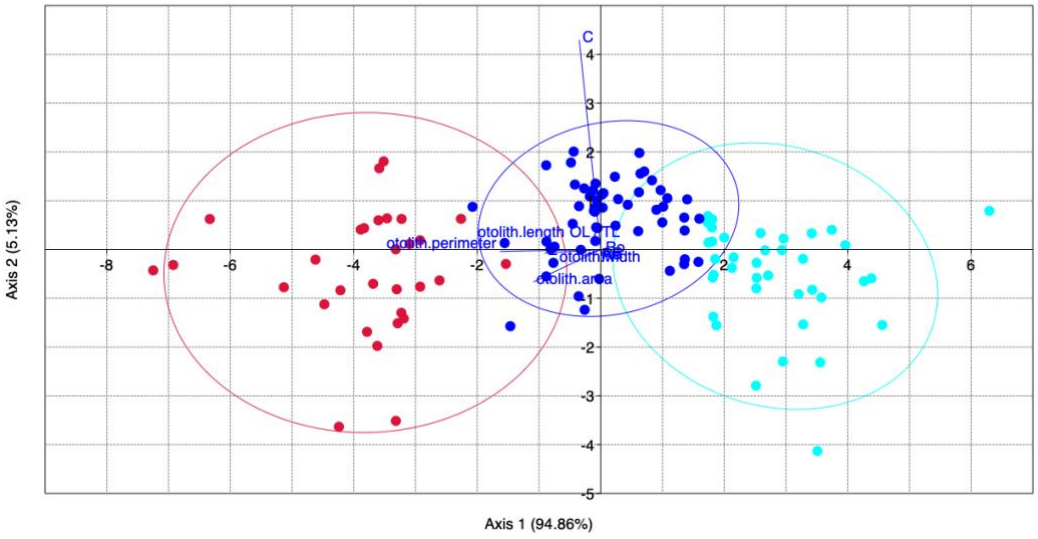

Figure 3. Linear Discriminant Analysis (LDA) between sagittae morphometric parameters from the three investigated size classes.

Table 2. Results of ANOVA carried out between biometric data (total fish length, TL, and body weight, BW) morphometric sagittal parameters of the investigated specimens belonging to the three size classes, with significant results set at $p<0.05$: maximum otolith

length (OL, mm) and otolith width (OW, mm), otolith perimeter (OP, mm), otolith surface (OS, mm^2), otolith length to the total fish length ratio (OL/TL), circularity (C), rectangularity (Re), ellipticity (E), aspect ratio (AR), form factor (FF) and roundness (Ro)

Tukey's multiple comparisons test	95,00% CI of diff,	Summary	P Value
TL_mm I vs. TL _mm II	-42,88 to -26,68	****	<0.0001
TL _mm I vs. TL _mm III	-106,9 to -88,19	****	<0.0001
TL _mm II vs. TL_mm III	-71,50 to -54,07	****	<0.0001
BW_g I vs. BW_g II	-1036 to 57,77	ns	0.0896
BW_g I vs. BW_g III	-2252 to -986,3	****	<0.0001
BW_g II vs. BW_g III	-1718 to -542,1	****	<0.0001
OS I vs. OS II	-0,4661 to -0,07006	**	0.0048
OS I vs. OS III	-1,122 to -0,6634	****	<0.0001
OS II vs. OS III	-0,8377 to -0,4115	****	<0.0001
OL I vs. OL II	-0,3109 to -0,07977	***	0.0003
OL I vs. OL III	-0,6152 to -0,3476	****	<0.0001
OL II vs. OL III	-0,4104 to -0,1618	****	<0.0001
OW I vs. OW II	-0,1401 to -0,02504	**	0.0026
OW I vs. OW III	-0,3183 to -0,1852	****	<0.0001
OW II vs. OW III	-0,2311 to -0,1073	****	<0.0001
OP I vs. OP II	-0,8692 to -0,2118	***	0.0005
OP I vs. OP III	-1,723 to -0,9623	****	<0.0001
OP II vs. OP III	-1,156 to -0,4487	****	<0.0001
OL / TL I vs. OL / TL II	5,377e-005 to 0,0009866	*	0.0248
OL / TL I vs. OL / TL III	0,0007877 to 0,001868	****	<0.0001
OL / TL II vs. OL / TL III	0,0003057 to 0,001309	***	0.0006
C I vs. C II	-1,417 to -0,07310	*	0.0259
C I vs. C III	-1,103 to 0,4529	ns	0.5838
C II vs. C III	-0,3028 to 1,143	ns	0.3552
Re I vs. Re II	0,006217 to 0,02819	***	0.0009
Re I vs. Re III	0,001084 to 0,02653	*	0.03
Re II vs. Re III	-0,01522 to 0,008423	ns	0.7742
E I vs. E II	-0,02559 to 0,003630	ns	0,1795
E I vs. E III	-0,02631 to 0,007517	ns	0,3877
E II vs. E III	-0,01414 to 0,01730	ns	0,9691
AR I vs. AR II	-0,004328 to 0,03268	ns	0.1681
AR I vs. AR III	-0,009358 to 0,03349	ns	0.3778
AR II vs. AR III	-0,02202 to 0,01780	ns	0.9657
FF I vs. FF II	0,003775 to 0,04212	*	0.0145
FF I vs. FF III	-0,01156 to 0,03283	ns	0.493
FF II vs. FF III	-0,03294 to 0,008320	ns	0.3359
Ro I vs. Ro II	0,003644 to 0,04910	*	0.0185
Ro I vs. Ro III	-0,004466 to 0,04816	ns	0.124
Ro II vs. Ro III	-0,02898 to 0,01993	ns	0.8993

Some morphometric parameters showed a strong positive correlation with the biometric data of the examined specimens (total length, TL, and body weight, BW), except for the OL/TL variable, which,

on the contrary, exhibited a negative correlation with the body weight and the total length of the examined species. The Pearson correlation results are shown in Table 3.

Table 3. Pearson correlation results between biometric data (total fish length, TL, and body weight, BW) of the investigated species and morphometric sagittal parameters

	Pearson Correlation			
	r	95% confidence interval	P value	P value summary
TL (mm) vs OS	0.6358	0.5169 to 0.7306	<0.0001	****
TL (mm) vs OL	0.5933	0.4651 to 0.6971	<0.0001	****
TL (mm) vs OW	0.6313	0.5114 to 0.7271	<0.0001	****
TL (mm) vs OP	0.5874	0.4580 to 0.6925	<0.0001	****
TL (mm) vs OL / TL	-0.5716	-0.6798 to -0.4390	<0.0001	****
TL (mm) vs C	0.03367	-0.1442 to 0.2095	0.7116	ns
TL (mm) vs Re	-0.1669	-0.3341 to 0.01043	0.065	ns
TL (mm) vs E	0.0798	-0.0986 to 0.2533	0.380	ns
TL (mm) vs AR	-0.08159	-0.2549 to 0.09684	0.3696	ns
TL (mm) vs FF	-0.04425	-0.2196 to 0.1338	0.627	ns
TL (mm) vs Ro	-0.1244	-0.2950 to 0.05380	0.1703	ns
BW (g) vs OS	0.3184	0.1498 to 0.4690	0.0003	***
BW (g) vs OL	0.2752	0.1032 to 0.4312	0.0021	**
BW (g) vs OW	0.3428	0.1765 to 0.4901	0.0001	***

BW (g) vs OP	0.26	0.08697 to 0.4178	0.0037	**
BW (g) vs OL / TL	-0.378	-0.5203 to -0.2154	<0.0001	****
BW (g) vs C	-0.1007	-0.2729 to 0.07770	0.2677	ns
BW (g) vs Re	-0.07778	-0.2513 to 0.1006	0.3925	ns
BW (g) vs E	-0.0255	-0.2017 to 0.1522	0.7789	ns
BW (g) vs AR	0.02288	-0.1548 to 0.1991	0.8017	ns
BW (g) vs FF	0.08955	-0.08890 to 0.2624	0.3246	ns
BW (g) vs Ro	-0.01331	-0.1899 to 0.1641	0.8838	ns

As reported in Figure 4a, the shape analysis showed a marked *excisura ostii* in *sagittae* belonging to Class I, with regular posterior, slightly lobed margins. Dorsal and ventral margins were crenate, with sculptures that become evident in size classes II and III. Specimens belonging to these last size classes showed a most enhanced *rostrum*, and a most marked irregularity of the margins, then the first. Concerning the differences between male and female specimens (Figure 4b), the mean contours evidenced only a slight variation in margin crenation, more marked in males than females, especially in the dorsal margins.

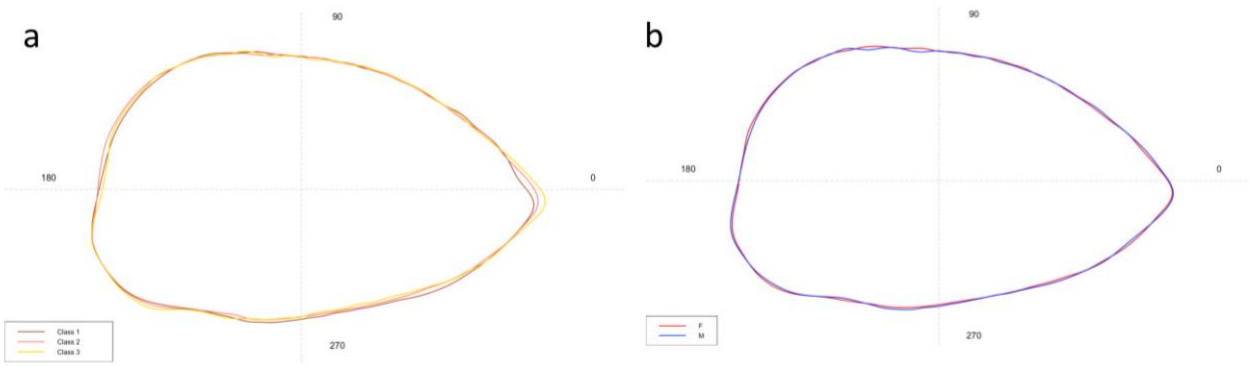

Figure 4. Mean shape of the left sagittae contours belonging to the three size classes (a) and to males (M) and females (F) (b).

Given the low significance of the differences observed between the right and left sides, these data were excluded from subsequent analyses. ANOVA and LDA analyzed the wavelet coefficients obtained by the shape analysis to provide an overview of the diversity of sagittal contours between specimens of the opposite sex and between the size classes investigated in the present study. ANOVA showed significant differences between sagittal contours of different size classes ($p<0.05$), as confirmed by LDA (Figure 5). Shape indexes did not show significant variation between sexes ($p<0.05$).

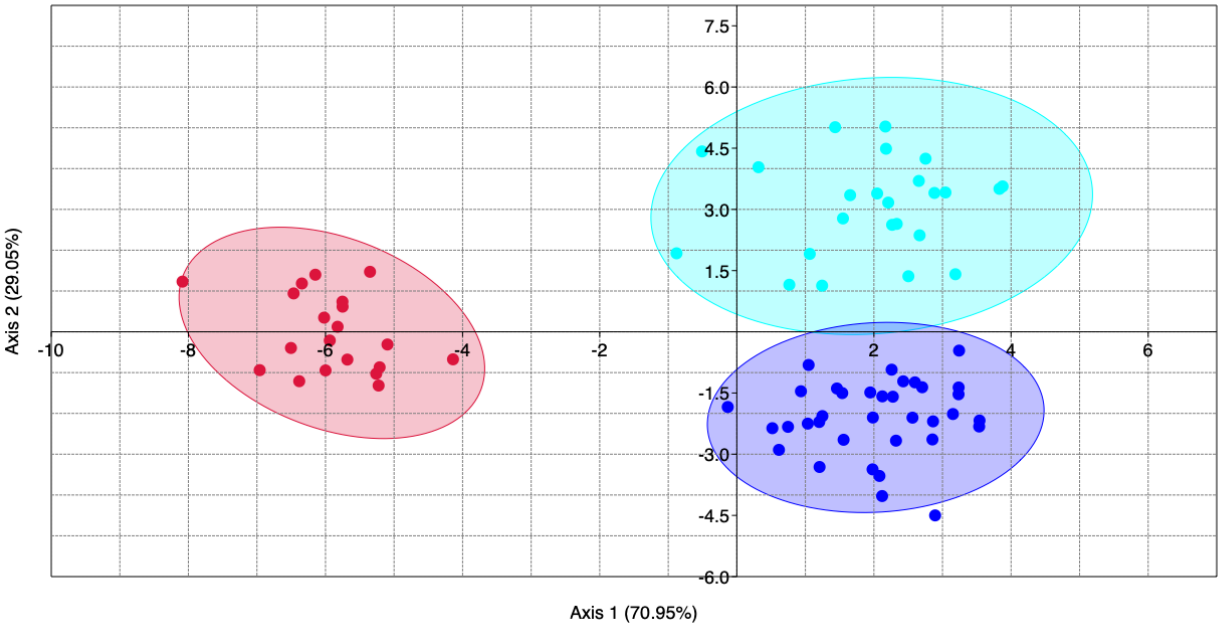

Figure 5. Linear Discriminant Analysis (LDA) between elliptic Fourier descriptors calculated for the different size classes. Ellipses include a 95% confidence interval.

3.2 Morphometric and Shape analysis of Lapilli

Following the terminology of Assis [56,66], the studied species showed triangular *lapilli* with a non-clupeiform-type morphology, longer than wider (Figure 6 a-b). They showed a convex ventral face with a rounded, symmetrical junction between the ventral and dorsal faces. The dorsal face was generally smooth, with a not clearly lobed medial part. The *Extremum posterior* was lobed and smooth. At the same time, the *extremum anterior* was sharp and blunt pointed. *Prominentia marginalis* was little, triangular with a blunt apex, while *gibbus maculae* was large, with a slightly rough surface and an asymmetric, rounded outline, covering almost entirely the ventral otolith's face. It did not cover completely *prominentia marginalis* on the ventral face, while from the dorsal one, it

was clearly visible the *regio apicale gibbi*, almost entirely covering the dorsal outline of the *prominentia marginalis.* Anteriorly, the *sulcus lapillus* was clearly visible, sunken along the entire outline of the *gibbus maculae.*

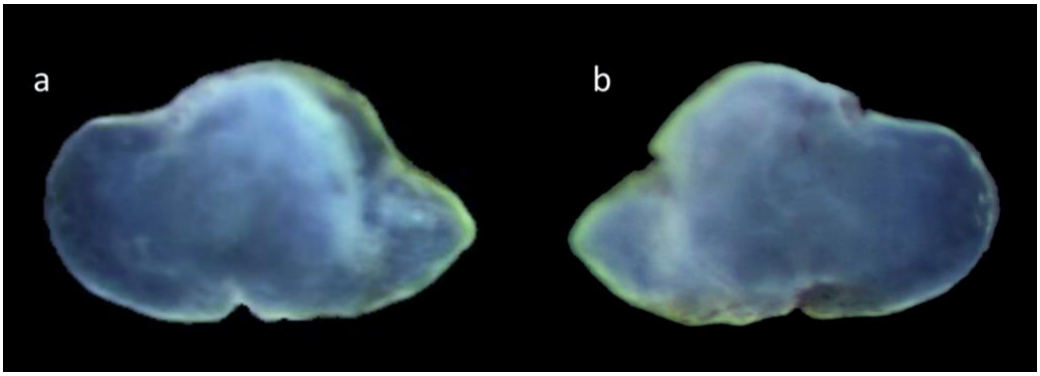

Figure 6. Stereoscope images of the dorsal (a) and ventral (b) sides of left lapillus.

In Table 4 they were reported the morphometric parameters calculated for the studied specimens for each side.

Table 4. Lapilli morphometric mean values, with standard deviation (s.d.), maximum (Max.), and minimum (Min.) values, for each investigated size class: maximum otolith length (OL, mm) and otolith width (OW, mm), otolith perimeter (OP, mm), otolith surface (OS, mm^2), otolith length to the total fish length ratio (OL/TL), circularity ($C = OP^2/OS$), rectangularity ($Re = OS/[OL \times OW]$), ellipticity ($E = OL–OW/OL+OW$), aspect ratio ($AR = OW/OL\%$), form factor ($FF = 4\pi OS/OP^2$) and roundness ($Ro = 4OS/\pi OL^2$).

	R			L		
	Mean	**s.d.**	**Min. - Max.**	**Mean**	**s.d.**	**Min. - Max.**
OL	0.53	0.06	0.37 - 0.62	0.52	0.04	0.43 - 0.6
OW	0.38	0.06	0.31 - 0.51	0.35	0.05	0.31 - 0.47
OP	1.61	0.2	1.29 - 1.95	1.56	0.15	1.3 - 1.84
OS	0.14	0.03	0.1 - 0.2	0.13	0.02	0.09 - 0.18
OL/TL %	0.2	0.04	0.13 - 0.24	0.2	0.04	0.14 - 0.26
C	18.32	0.65	17.28 - 19.63	18.7	0.69	17.77 - 20.11
Re	0.7	0.02	0.67 - 0.74	0.7	0.01	0.68 - 0.72
E	0.16	0.07	0.02 - 0.24	0.19	0.05	0.08 - 0.26
AR	0.73	0.11	0.61 - 0.95	0.68	0.07	0.58 - 0.86
FF	0.69	0.02	0.64 - 0.73	0.67	0.02	0.62 - 0.71
Ro	0.65	0.1	0.54 - 0.9	0.61	0.06	0.52 - 0.76

Eleven pairs of *Lapilli* were analyzed, and no significant variations of the morphometric parameters between the right and left sides were identified. It was not possible to perform comparative analyses between males and females as it was not possible to extract an equal number of *lapilli* from both sexes. For the same reason, the analysis was inaccurate for size class investigations.

Strong positive correlations were found between TL and BW of the specimens' *vs* OL/TL (see Figure 7).

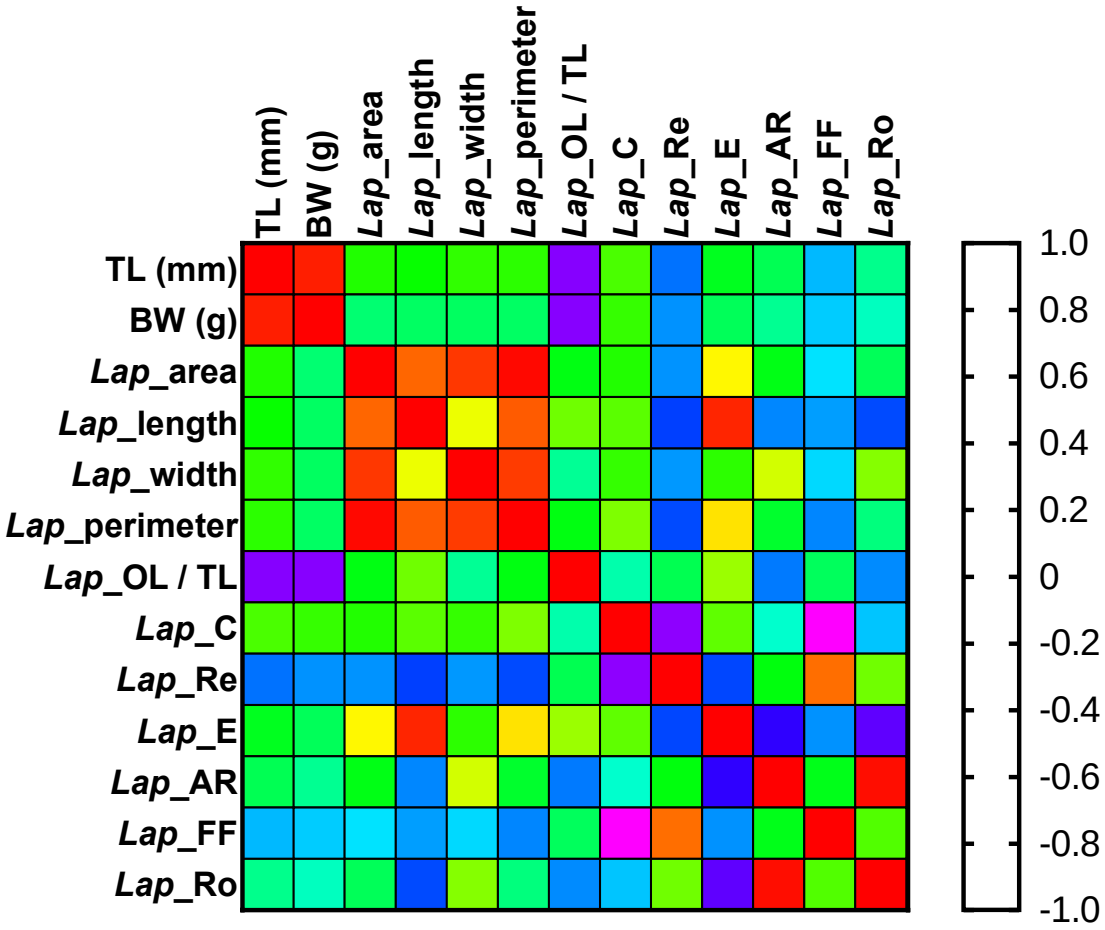

Figure 7. Pearson correlation matrix assessed between biometric specimens' data (total fish length, TL, and body weight, BW) of the investigated species and morphometric lapilli parameters.

Concerning the shape analysis, it showed a rhomboidal to oval mean contour of *lapilli* (Figure 8). The medial edge was regular, without the presence of distinct lobes. There was no incision between the *extremum posterior* and the lateral base of the *gibbus maculae*. The edge of the *extremum anterior* was also regular, not lobed. ANOVA reported no significant differences between the shape indices of left and right *lapilli.*

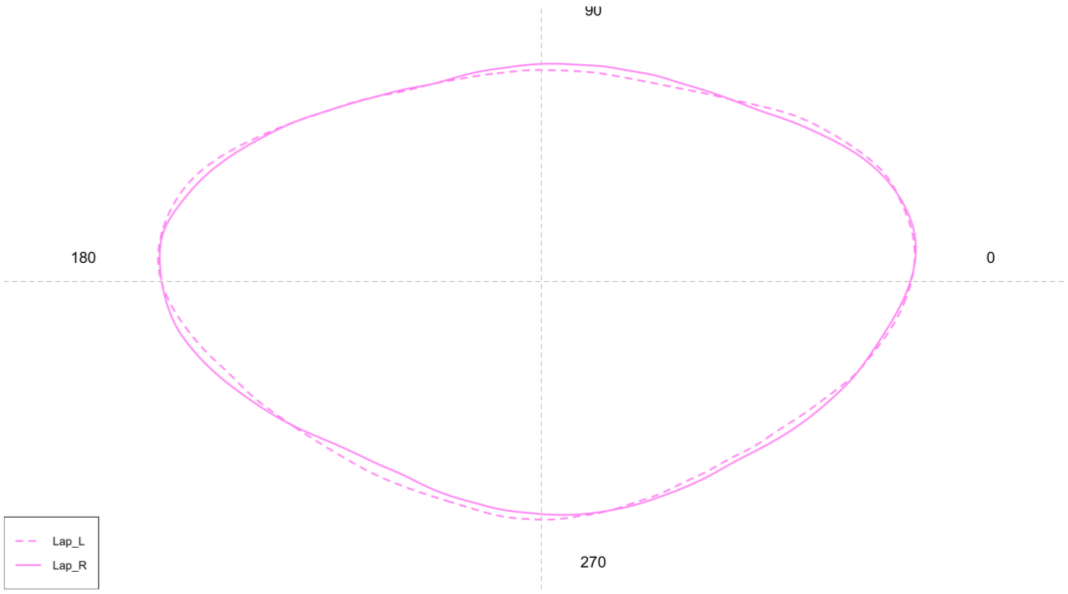

Figura 8. Mean shape of the left (L) and right (R) lapilli contours.

3.3 Morphometric and Shape analysis of Asterisci

According to the terminology adopted by Assis [57,66], the studied species showed vertical-type *asterisci* with a globular dorsal region and a pointed ventral one (Figure 9 a-b). The external face was dorsally flat and ventrally concave, with a slightly rough surface, while the inner face was markedly convex. *Lobi* were almost completely merged, not always clearly recognizable, with a furrow delimitating *lobus minor* and *lobus major.* This last was semi-oval, with a vertical axis much longer than the *lobus minor.* This was semi-circular, slightly anteriorly angled. *Rostrum* was short but always identifiable as a short, angled protuberance in the anterior otolith's margin.

Conversely, *antirostrum* was large, globular, and very evident. It was placed in the anterior margin of the antero-dorsal part of the *lobus major*. *Excisura major* was wide, and not deep and the *fossa acustica* was antero-ventrally located, superficial, and very long. *Colliculumu* was very evident, covering a large part of the *fossa acustica.*

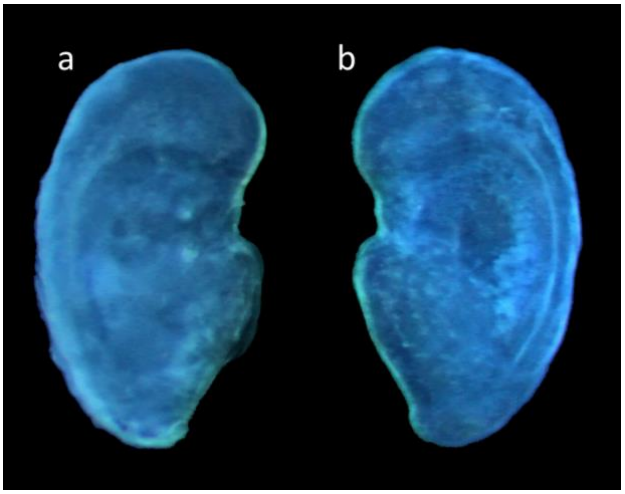

Figura 9. Stereoscope images of the external (a) and internal (b) faces of the right asteriscus.

Table 5 reported the morphometric parameters calculated for the left and right otoliths of the studied specimens.

Table 5. Asterisci morphometric mean values, with standard deviation (s.d.), maximum (Max.), and minimum (Min.) values, for each investigated size class: maximum otolith length (OL, mm) and otolith width (OW, mm), otolith perimeter (OP, mm), otolith surface (OS mm^2), otolith length to the total fish length ratio (OL/TL), circularity (C = OP^2/OS), rectangularity (Re = OS/[OL×OW]), ellipticity (E = OL–OW/OL+OW), aspect ratio (AR = OW/OL%), form factor (FF = 4πOS/OP^2) and roundness (Ro = 4OS/πOL^2).

	R			L		
	Mean	**s.d.**	**Min. - Max.**	**Mean**	**s.d.**	**Min. - Max.**
OL	0.44	0.07	0.3 - 0.57	0.45	0.07	0.32 - 0.56
OW	0.74	0.09	0.58 - 0.9	0.71	0.08	0.54 - 0.85
OP	2.18	0.25	1.64 - 2.71	2.31	0.37	1.62 - 2.95
OS	0.24	0.06	0.13 - 0.38	0.24	0.06	0.14 - 0.35
OL/TL %	0.16	0.03	0.12 - 0.22	0.16	0.02	0.13 - 0.21
C	20.07	1.09	18.54 - 22.63	22.15	1.76	18.42 - 24.58
Re	0.73	0.03	0.69 - 0.77	0.75	0.02	0.71 - 0.78
E (-)	0.25	0.06	0.15 - 0.36	0.22	0.05	0.17 - 0.36
AR	1.69	0.22	1.38 - 2.13	1.59	0.17	1.4 - 2.1
FF	0.63	0.03	0.55 - 0.68	0.57	0.05	0.51 - 0.68
Ro	1.57	0.21	1.24 - 1.93	1.51	0.17	1.3 - 2.01

Fourteen pairs of *asterisci* were analyzed, and no significant variations of the morphometric parameters between the right and left sides were identified. It was not possible to perform comparative analyses between males and females as it was not possible to extract an equal number of otoliths from both sexes. For the same reason, the analysis was inaccurate for size class investigations.

Strong positive correlations were found between TL and BW of specimens vs. *Asterisci* area, length, width, and perimeter (see Figure 10).

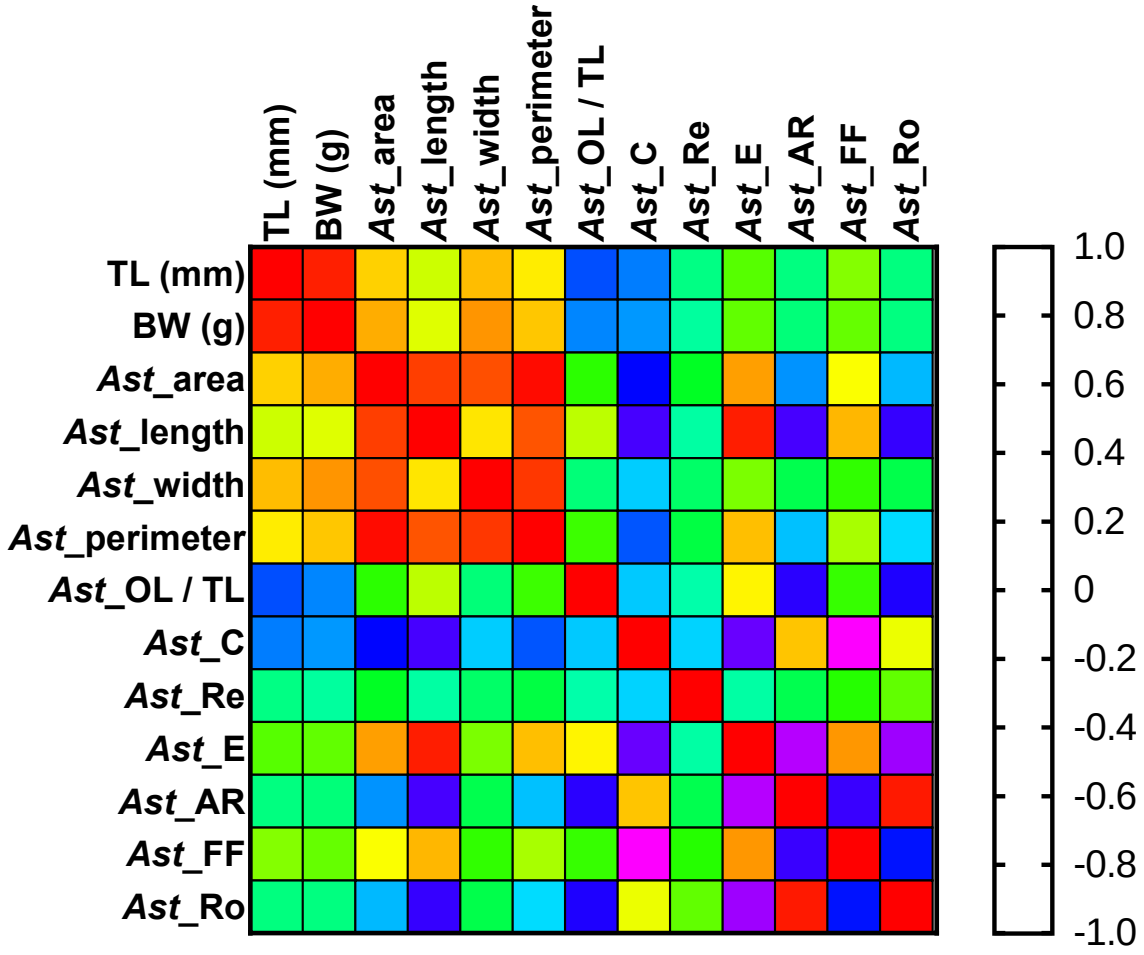

Figure 10. Pearson correlation matrix assessed between biometric specimens' data (total fish length, TL, and body weight, BW) of the investigated species and morphometric asterisci parameters.

Concerning the shape analysis, the mean *asterisci* contours showed an overall oval shape of the otoliths (Figure 11). The dorsal region contour was globular, while the ventral was tapered and more pointed in the right *asterisci* than in the left ones. The *excisura major* was large, with a short and rounded *rostrum* and a large and globular *antirostrum.* ANOVA reported no significant differences between the shape indices of left and right *asterisci.*

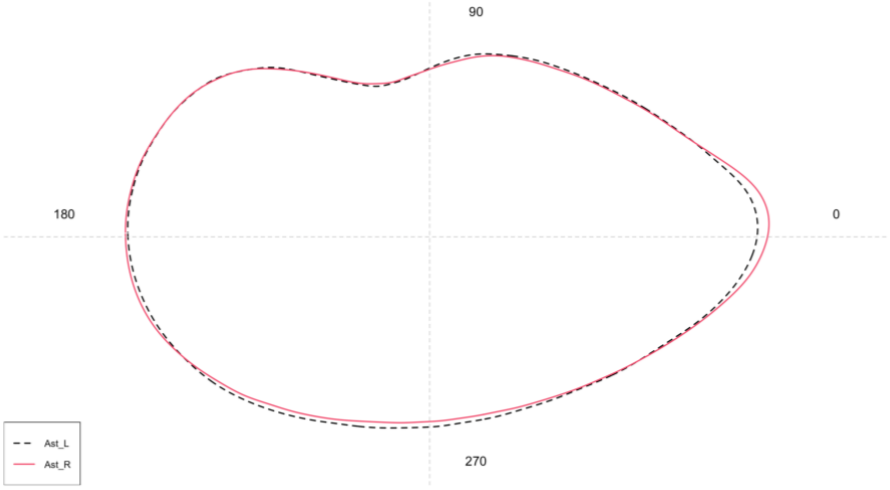

Figure 11. Mean shape of the left (L) and right (R) asterisci contours.

4. DISCUSSION

The results from present study provided the first complete description of the three otoliths pairs of *B. belone* through morphometric, morphological and shape analysis, useful to understand their intra specific variability and how this could be influenced by the epipelagic habits of this species. It is important to explore the information stored inside these carbonate structures, able to provide reliable data on the life habits, large- or small-scale migrations, populations structure and habitats switches. Indeed, especially regarding the high migratory epipelagic species, it is often difficult to discriminate between populations, understanding their movements, life habit, and ecomorphological adaptation to epipelagic environment. These kinds of information are essential for conservation porpoises (for a correct fisheries management and resource conservation) and to improve the knowledge base on the ecological dynamics occurring in the pelagic domain. The studied species is an epipelagic species characterized by a migratory pattern, from the off-shore to the near-shore waters, related to spawning. Moreover, it shows a habitat switch during its growth, inhabiting the near-shore coastal environment, often close to freshwater streams, in the first part of the life, moving in the off-shore epipelagic environment during the adult life. The description of the mean otoliths shape and morphometry, and their intra specific variability, provided by results fill the gap present in literature (especially regarding utricular and lagenar otoliths) about the *B. belone* from the studied area, trying to analyze how its life habit can influence the three otoliths' pairs morphology, morphometry, and shape.

Concerning *sagittae,* morphological data showed an overall morphology in line with literature from the western and central Mediterranean Sea and the Black Sea [63,65]. Shape indexes presented differences in aspect ratio and rectangularity, with markedly higher values in the studied population than that from the western and central Mediterranean Sea [65]. Differences were evident for both

morphometric parameters (OL, OW, OP) and shape indexes (C, AR, Ro), also comparing data with those reported in the literature from the Aegean Sea [62,79] and the Adriatic Sea [61]. These differences in shape indexes could suggest the reliability, in the studied species, of shape and overall contours for stock assessment and population discrimination, but, unfortunately, no literature data on shape analysis performed on *B. belone* from other geographical areas are available to confirm this. It is widely reported how morphometric and shape data on *sagittae* are reliable and useful to understand the population structure of migratory epipelagic species. This is the case of *Sardina pilchardus,* Walbaum, 1792. The population structure if this species in the Mediterranean Sea and Atlantic Ocean has been reconstructed successfully using otoliths shape descriptors, also elucidating the connectivity between Mediterranean and Oceanic individuals groups [80]. This is also the case of *Scomberomorus brasiliensis* Collette, Russo & Zavala-Camin, 1978, in which the *sagittae* phenotypic variation has been used as a stock structure's indicator [68]. Otolith features' variations between different geographical areas could be related to environmental and genetic differences between the areas and the populations, being otoliths under the dual regulation of environmental conditions and genetics [81,82]. The main environmental factors influencing otolith morphometry, morphology, and shape are depth, temperature, salinity, diet composition, and food availability. These can alter somatic growth, fish metabolism, and otoliths features [51,52,83–85] under strong genetic control [80,81,86–88]. According to the literature, *B. belone* populations show substantial geographical variability in age at first maturity, growth rates, size ranges, sexes portions, age structures, and length distribution [12,15,17,28]. This high geographical variability in population dynamics could reflect a strong sensitivity of the studied species to environmental conditions and fisheries activities. Indeed, many population descriptors, such as growth rates, abundance, length distribution, and age composition, are strongly affected by water masses, physiochemical and biological features, and fishing pressure [36,89,90]. Concerning feeding habits, studied species show a generally stable diet composition within the Mediterranean Sea and the Atlantic Ocean [18,20,21], with crustaceans as the main prey category and main differences related to crustaceans' species contribution and minor preys items composition. The variability in diet composition, with the different environmental conditions experienced by the populations, and the inter-population genetic variability, could shape the variations between the different geographical areas in otolith features. Further analyses of the *sagittae* at inter-population level are required to understand and confirm the strong shape, morphological, and morphometrical differences between specimens of *B. belone* from different geographical areas. This is essential to assess the reliability of shape analysis for the stock assessment and population discrimination of the species, an essential tool to improve its conservation in the entire Mediterranean basin.

As highlighted by statistical analyses on shape data, the mean sagittal contour of the specimens from the Ionian Sea was not affected by bias related to intra-specific differences between otoliths' sides and sexes. This, indeed, is one of the main factors that could affect the accuracy of shape analysis for stock assessment, being this strongly altered by choice of *sagittae* from one side rather than the other, or from one sex rather than the other, in the presence of directional bilateral asymmetry or sexual asymmetry [91–93]. Statistical analysis has detected significant differences between the three size classes in morphometry and shape. This strong relation between *sagittae* morphometry and morphology and specimens' biometry (total length and body weight); Pearson correlation results also confirmed it. This finding was in line with literature from the Adriatic and Aegean Seas [61,62], which reported a strong correlation between total fish length and otolith morphometry for *B. belone*, the strongest among several investigated pelagic species, essential for the back calculation of fish length from the otolith one. The high variability in shape between the *sagittae* belonging to the three investigated size classes could be related to the life habits of the species. For instance, according to Dorman [18], smaller specimens of *B. belone* seem to feed more frequently at nearshore surface waters than larger ones, resulting in differences in diet composition. In addition to the contribution of different prey items, the variations in environmental conditions are experienced by smaller and adult specimens, being nearshore water characterized by different physiochemical properties and oceanographic features than the offshore ones. This environmental variability could allow the differences detected between size classes in sagittal shape, but further analysis of the life habits of the studied species in the Ionian Sea are required to confirm this thesis.

Concerning *lapilli,* results showed a different morphology than those reported literature from the Atlantic coast of Portugal [56,66]. As stated by Assis, the variability was mainly related to the general otolith's shape and the *gibbus maculae* dimensions. Indeed, specimens from the Ionian Sea showed a more oval and rhomboidal than triangular shape, with less bulky *gibbus maculae* than those shown by specimens from the Portugal coast. These differences between shape and morphological results and literature data could indicate an inter population variability of *lapilli*, not investigated at all in literature. Unfortunately, no references with comparable data are present in literature to assess the morphometrical distance of *lapilli* at inter-population level. The detected differences with the literature in morphology and shape confirm the need to improve the knowledge base on the intra-population variability of these otoliths, which nowadays are deeply underestimated [58].

Concerning *asterisci,* results showed a morphology in line with that reported in the literature from the Atlantic Portuguese coast [57]. Some differences were detected regarding the general shape, more oblong in the studied population and the *rostrum,* less evident in the studied population, than those from the literature. As stated above, for *lapilli,* these differences could indicate a variability at the

inter-population level, until now not investigated at all in *asterisci*. The absence of literature on morphometrical data made it impossible to compare the morphometry of *B. belone asterisci* from the Ionian Sea with that from other geographical areas. As highlighted by the detected differences in morphology and shape with literature data, it is essential to improve the knowledge base on the intra-population variability of these otoliths, until now deeply underestimated [58].

At the intra-population level, statistical analyses on *lapilli* and *asterisci* did not show significant differences between left and right otoliths. Concerning size classes, especially *asterisci,* showed a strong correlation between otoliths morphometries (e.g., OS, OL, OW, and OP) and specimen biometrics (TL and BW), as stated by Pearson correlation results. This could introduce a substantial variability between small and large individuals in the studied species from the Ionian Sea. This may be related to the life habit differences between life stages of *B. belone*, stated above, to discuss the size class differences detected in *sagittae.* It was widely stated that *saccule* and *lagena* are mainly involved in the perception of sound, while the *utricle* seems to have an important role in vestibular sense [58,94,95].

For this reason, *sagittae, asterisci,* and their end organs could be influenced by the same selective forces, explaining the more enhanced correlation of morphometries to fish total length and body weight shown by these otoliths than *lapilli.* These last have always been considered the most conservative of the three [56], despite Schulz-Mirbach et al. [58] having shown their variability at the inter-specific level, assessing differences also in the development of vestibular sense. Further analysis on *lapilli* and *asterisci* from different populations of the studied species, and with a vast number of samples, are required to confirm the reliability of shape, morphology, and morphometry for population discrimination and to assess the variability at intra-population between sexes and size classes.

5. CONCLUSION

Results provided the first accurate description of the three otoliths pairs of the studied species from the Ionian Sea, with the first-ever description of *lapilli* and *asterisci* from the Mediterranean Sea.

These data have confirmed the heterogeneity of sagittal morphology and morphometry between the present paper and literature, also highlighting the presence of differences in mean contour and morphometry between size classes. The absence of directional bilateral asymmetry and sexual asymmetry lets us hope for a reliable and straightforward application of shape analysis for the stock assessment on this species, which is essential for its conservation and correct management of its commercial exploitation.

Concerning *lapilli* and *asterisci,* results have confirmed the need to deepen the knowledge of these two otoliths pairs, not studied at all in the Mediterranean teleost species. They showed differences in morphometry and shape with literature data, which could indicate an intra-specific variability between specimens belonging to different populations. Improving the knowledge base on this is essential to understanding how different environments can influence the inner ear development and morphology and how the vestibular and hearing senses change between species and populations according to their life habits and adaptation to environments. Moreover, for both otolith pairs, it was not possible to investigate the variability between size classes and sexes in the studied population for lack of samples. Further analyses on a broader number of lagenar and utricular otoliths are required to analyze their variability between size classes and sexes.

Future research on the three otoliths pairs of the studied species shall investigate the reliability of shape analysis for stock assessment and population discrimination, adding data on genetics, somatic growth dynamics, and feeding habits on specimens from different geographical areas. This will be essential to find direct correlations to elucidate the dynamics influencing the inter-population differences in *sagittae, lapilli,* and *asterisci,* improving the information about the connections between inner ears, species and population genetics, and environment. This is the base of the phenotypic plasticity and the ecomorphological adaptation of teleost species, allowing the shape differences between *sagittae,* so crucial for stock assessments and conservation porpoises. Moreover, by deepening the knowledge base on the intra and inter-specific variability of lagenar and utricular otoliths, elucidating their variations related to genetic and environmental conditions, it will be possible to improve the information about teleost inner ear functioning and eco-morphology, opening new ways for species population discrimination.

REFERENCES

1. Van Der Laan, R.; Eschmeyer, W.N.; Fricke, R. Family-group names of recent fishes. *Zootaxa* **2014**, *3882*, 1–230, doi:10.11646/zootaxa.3882.1.1.
2. Nelson, J.S.; Grande, T.C.; Wilson, M.V.H. *Fishes of the World: Fifth Edition*; 2016; ISBN 9781119174844.
3. Collette, B.B. Family Belonidae Bonaparte 1832 - needlfishes. *Calif. Acad. Sci. Annot. Checklists Fishes.* **2003**, 1–22.
4. Poutiers, J.M. FICHES FAO D'IDENTIFICATION DES ESPECES POUR LES BESOINS DE LA PECHE. MEDITERRANEE ET MER NOIRE ZONE DE PECHE 37 Révision 1 Volume 1 VEGETAUX ET INVERTEBRES. *Vertebres* **1987**, *2*.

5. Deidun, A.; Zava, B.; Corsini-Foka, M.; Galdies, J.; Di Natale, A.; Collette, B.B. First record of the flat needlefish, ablennes hians (Belonidae) in central mediterranean waters (western ionian sea). *Ann. Ser. Hist. Nat.* **2021**, *31*, 9–16, doi:10.19233/ASHN.2021.02.
6. Alshawy, F.; Ibrahim, A.; Hussein, C.; Lahlah, M. First record of the flat needlefish Ablennes hians (Valenciennes, 1846) from Syrian marine waters (eastern Mediterranean). *Mar. Biodivers. Rec.* **2019**, *12*, 410–412, doi:10.1186/s41200-019-0174-5.
7. Collette, B.B.; Parin, N. V *Needlefishes (Belonidae) of the Eastern Atlantic-Ocean...*; Danish Science Press, 1970;
8. Froese, R.; Pauly, D. Belone belone (Linnaeus, 1760) Available online: https://www.marinespecies.org/aphia.php?p=taxdetails&id=126375 on 2022-11-21 (accessed on Nov 21, 2022).
9. Jardas, I. *Jadranska ihtiofauna*; Školska knjiga, 1996; ISBN 9530615019.
10. Riede, K. *Global Register of Migratory Species - from Global to Regional Scales. Final Report of the R&D-Project 808 05 081. Federal Agency for Nature Conservation, Bonn, Germany*; Federal Agency for Nature Conservation, 2004; ISBN 3784338453.
11. Nedelec, C. *FAO Catalogue of small scale fishing gear*; Fishing News (Books) Ltd., 1975; ISBN 0-85238-077-1.
12. Zorica, B.; Keč, V.Č. Age, growth and mortality of the garfish, Belone belone (L. 1761) in the Adriatic Sea. *J. Mar. Biol. Assoc. United Kingdom* **2013**, *93*, 365–372, doi:10.1017/S002531541200149X.
13. Elsdon, T.S.; Wells, B.K.; Campana, S.E.; Gillanders, B.M.; Jones, C.M.; Limburg, K.E.; Secor, D.H.; Thorrold, S.R.; Walther, B.D. Otolith chemistry to describe movements and life-history parameters of fishes: Hypotheses, assumptions, limitations and inferences. In *Oceanography and Marine Biology*; CRC Press, 2008; Vol. 46, pp. 297–330 ISBN 0429137257.
14. FAO *Fishery and Aquaculture Statistics (Capture productoin)*; 2018;
15. Bilgin, S.; Taşçi, B.; Bal, H. Population dynamics of the garfish, Belone euxini (Belonidae: Belone) from the south-east Black Sea. *J. Mar. Biol. Assoc. United Kingdom* **2014**, *94*, 1687–1700, doi:10.1017/S0025315414000769.
16. Ouannes Ghorbel, A.; Bradai, M.N.; Bouain, A. Période de reproduction et maturité sexuelle de Symphodus (Crenilabrus) tinca (Labridae), des côtes de Sfax (Tunisie). *Cybium* **2002**, *26*, 89–92.
17. Châari, M.; Boudaya, L.; Gancitano, S.; Gancitano, V.; Neifar, L. Age, Growth and Reproductive Biology of the Garfish, Belone belone (Linnaeus, 1760) (Teleostei: Belonidae)

in the Central Mediterranean Sea. *Turkish J. Fish. Aquat. Sci.* **2022**, *22*, doi:10.4194/TRJFAS21161.

18. Dorman, J.A. Diet of the garfish, Belone belone (L.), from Courtmacsherry Bay, Ireland. *J. Fish Biol.* **1988**, *33*, 339–346, doi:10.1111/j.1095-8649.1988.tb05476.x.
19. Dorman, J.A. Investigations into the biology of the garfish, Belone belone (L.), in Swedish waters. *J. Fish Biol.* **1991**, *39*, 59–69, doi:10.1111/j.1095-8649.1991.tb04341.x.
20. Sever, T.M.; Bayhan, B.; Bilge, G.; Taşkavak, E. Diet composition of belone belone (Linnaeus, 1761) (Pisces: Belonidae) in the Aegean Sea. *J. Appl. Ichthyol.* **2009**, *25*, 702–706, doi:10.1111/j.1439-0426.2009.01368.x.
21. Zorica, B.; Cikes Kec, V. Preliminary observations on feeding habits of Garfish Belone belone (L., 1761) in the Adriatic Sea. *Croat. J. Fish.* **2012**, *70*, 53–60.
22. Wurtz, M.; Marrale, D. Food of striped dolphin, stenella coeruleoalba, in the ligurian sea. *J. Mar. Biol. Assoc. United Kingdom* **1993**, *73*, 571–578, doi:10.1017/S0025315400033117.
23. Albano, M.; D'Iglio, C.; Spanò, N.; Fernandes, J.M. de O.; Savoca, S.; Capillo, G. Distribution of the Order Lampriformes in the Mediterranean Sea with Notes on Their Biology, Morphology, and Taxonomy. *Biology (Basel).* 2022, *11*.
24. Albano, M.; D'Iglio, C.; Spanò, N.; Di Paola, D.; Alesci, A.; Savoca, S.; Capillo, G. New Report of Zu cristatus (Bonelli, 1819) in the Ionian Sea with an In-Depth Morphometrical Comparison with All Mediterranean Records. *Fishes* 2022, *7*, 305.
25. Samsun, O.; Özdamar, E.; Erkoyuncu, İ. Sinop yöresinde avlanan zargana (Belone belone euxini, Günther, 1866) balığının bazı balıkçılık biyolojisi parametreleri ile et veriminin araştırılması. *Doğu Anadolu Bölgesi II. Su Ürünleri Sempozyumu, Atatürk Üniversitesi, Ziraat Fakültesi, Su Ürünleri Bölümü, Erzurum* **1995**, 14–16.
26. Bilgin, S.; Taşçı, B.; Bal, H. Reproduction biology of the garfish, Belone euxini Günther, 1866 (Belonidae: Belone) in the southeast Black Sea. *Turkish J. Fish. Aquat. Sci.* **2014**, *14*, 623–631, doi:10.4194/1303-2712-v14_3_04.
27. Ceyhan, T.; Samsun, O.; Akyol, O. Age, growth and mortality of Garfish, Belone euxini Günther, 1866 in the Central Black Sea, Turkey. *Pak. J. Zool.* **2019**, *51*, 273–278, doi:10.17582/journal.pjz/2019.51.1.273.278.
28. Uçkun, D.; Akalin, S.; Taşkavak, E.; Toğulga, M. Some biological characteristics of the garfish (Belone belone L., 1761) in Izmir Bay, Aegean Sea. *J. Appl. Ichthyol.* **2004**, *20*, 413–416, doi:10.1111/j.1439-0426.2004.00592.x.
29. Fehri-Bedoui, R.; Gharbi, K. Contribution a l'etude de la croissance et l'age de Belone belone (Belonidae) des cotes Est de la Tunisie. *Rapp. la Comm. Int. pour la Mer Mediterr.*

2004, *37*, 352.

30. Châari, M.; Feki, M.; Neifar, L. Metazoan Parasites of the Mediterranean Garfish <i>Belone belone gracilis</i> (Teleostei: Belonidae) as a Tool for Stock Discrimination. *Open J. Mar. Sci.* **2015**, *05*, 324–334, doi:10.4236/ojms.2015.53027.
31. Ramírez-Pérez, J.S.; Quiñónez-Velazquez, C.; García-Rodríguez, F.J.; Félix-Uraga, R.; Melo-Barrera, F.N. Using the shape of Sagitta Otoliths in the discrimination of phenotypic stocks in Scomberomorus sierra (Jordan and Starks, 1895). *J. Fish. Aquat. Sci.* **2010**, doi:10.3923/jfas.2010.82.93.
32. DeVries, D.A.; Grimes, C.B.; Prager, M.H. Using otolith shape analysis to distinguish eastern Gulf of Mexico and Atlantic Ocean stocks of king mackerel. *Fish. Res.* **2002**, *57*, 51–62, doi:10.1016/S0165-7836(01)00332-0.
33. Benzinou, A.; Carbini, S.; Nasreddine, K.; Elleboode, R.; Mahé, K. Discriminating stocks of striped red mullet (Mullus surmuletus) in the Northwest European seas using three automatic shape classification methods. *Fish. Res.* **2013**, *143*, 153–160, doi:10.1016/j.fishres.2013.01.015.
34. Zhuang, L.; Ye, Z.; Zhang, C.; Ye, Z.; Li, Z.; Wan, R.; Ren, Y.; Dou, S.; Wheeler, A.; Whitehead, P.J.P.; et al. Stock discrimination of two insular populations of diplodus annularis (Actinopterygii: Perciformes: Sparidae) along the coast of tunisia by analysis of otolith shape. *J. Fish Biol.* **2015**, *46*, 1–14, doi:10.3750/AIP2015.45.4.04.
35. Mahé, K.; Evano, H.; Mille, T.; Muths, D.; Bourjea, J. Otolith shape as a valuable tool to evaluate the stock structure of swordfish Xiphias gladius in the Indian Ocean. *African J. Mar. Sci.* **2016**, *38*, 457–464, doi:10.2989/1814232X.2016.1224205.
36. Perdichizzi, A.; D'Iglio, C.; Giordano, D.; Profeta, A.; Ragonese, S.; Rinelli, P. Comparing life-history traits in two contiguous stocks of the deep-water rose shrimp Parapenaeus longirostris (H. Lucas, 1846) (Crustacea: Decapoda) in the Southern Tyrrhenian Sea (Central Mediterranean Sea). *Fish. Res.* **2022**, *248*, 106206, doi:10.1016/j.fishres.2021.106206.
37. Schulz-Mirbach, T.; Ladich, F.; Plath, M.; Heß, M. Enigmatic ear stones: what we know about the functional role and evolution of fish otoliths. *Biol. Rev.* **2019**, *94*, 457–482, doi:10.1111/brv.12463.
38. Ladich, F.; Schulz-Mirbach, T. Diversity in fish auditory systems: One of the riddles of sensory biology. *Front. Ecol. Evol.* **2016**, *4*, 28, doi:10.3389/fevo.2016.00028.
39. Campana, S.E. Chemistry and composition of fish otoliths: Pathways, mechanisms and applications. *Mar. Ecol. Prog. Ser.* 1999, *188*, 263–297.
40. Popper, A.N.; Ramcharitar, J.; Campana, S.E. Why otoliths? Insights from inner ear

physiology and fisheries biology. *Mar. Freshw. Res.* **2005**, *56*, 497–504, doi:10.1071/MF04267.

41. D'iglio, C.; Natale, S.; Albano, M.; Savoca, S.; Famulari, S.; Gervasi, C.; Lanteri, G.; Panarello, G.; Spanò, N.; Capillo, G. Otolith Analyses Highlight Morpho-Functional Differences of Three Species of Mullet (Mugilidae) from Transitional Water. *Sustain.* 2022, *14*.
42. Lombarte, A.; Miletić, M.; Kovačić, M.; Otero-Ferrer, J.L.; Tuset, V.M. Identifying sagittal otoliths of Mediterranean Sea gobies: variability among phylogenetic lineages. *J. Fish Biol.* **2018**, *92*, 1768–1787, doi:10.1111/jfb.13615.
43. Lin, C.H.; Girone, A.; Nolf, D. Fish otolith assemblages from Recent NE Atlantic sea bottoms: A comparative study of palaeoecology. *Palaeogeogr. Palaeoclimatol. Palaeoecol.* **2016**, *446*, 98–107, doi:10.1016/j.palaeo.2016.01.022.
44. Nolf, D. Studies on fossil otoliths - The state of the art. *Recent Dev. Fish Otolith Res.* **1995**, *19*, 513–544.
45. D'Iglio, C.; Porcino, N.; Savoca, S.; Profeta, A.; Perdichizzi, A.; Armeli Minicante, E.; Salvati, D.; Soraci, F.; Rinelli, P.; Giordano, D. Ontogenetic shift and feeding habits of the European hake (Merluccius merluccius L., 1758) in Central and Southern Tyrrhenian Sea (Western Mediterranean Sea): A comparison between past and present data . *Ecol. Evol.* **2022**, *12*, e8634, doi:10.1002/ece3.8634.
46. D'Iglio, C.; Albano, M.; Famulari, S.; Savoca, S.; Panarello, G.; Di Paola, D.; Perdichizzi, A.; Rinelli, P.; Lanteri, G.; Spanò, N.; et al. Intra- and interspecific variability among congeneric Pagellus otoliths. *Sci. Rep.* **2021**, *11*, 16315, doi:10.1038/s41598-021-95814-w.
47. Bostanci, D.; Yilmaz, M.; Yedier, S.; Kurucu, G.; Kontas, S.; Darçin, M.; Polat, N. Sagittal Otolith Morphology of Sharpsnout Seabream Diplodus puntazzo (Walbaum, 1792) in the Aegean Sea. *Int. J. Morphol.* **2016**, doi:10.4067/s0717-95022016000200012.
48. Montanini, S.; Stagioni, M.; Valdrè, G.; Tommasini, S.; Vallisneri, M. Intra-specific and inter-specific variability of the sulcus acusticus of sagittal otoliths in two gurnard species (Scorpaeniformes, Triglidae). *Fish. Res.* **2015**, *161*, 93–101, doi:10.1016/j.fishres.2014.07.003.
49. Tuset, V.M.; Rosin, P.L.; Lombarte, A. Sagittal otolith shape used in the identification of fishes of the genus Serranus. *Fish. Res.* **2006**, *81*, 316–325, doi:10.1016/j.fishres.2006.06.020.
50. Campana, S.E.; Thorrold, S.R. Otoliths, increments, and elements: Keys to a comprehensive understanding of fish populations? *Can. J. Fish. Aquat. Sci.* **2001**, *58*, 30–38,

doi:10.1139/f00-177.

51. Neves, J.; Giacomello, E.; Menezes, G.M.; Fontes, J.; Tanner, S.E. Temperature-Driven Growth Variation in a Deep-Sea Fish: The Case of Pagellus bogaraveo (Brünnich, 1768) in the Azores Archipelago. *Front. Mar. Sci.* 2021, *8*.
52. Abaad, M.; Tuset, V.M.; Montero, D.; Lombarte, A.; Otero-Ferrer, J.L.; Haroun, R. Phenotypic plasticity in wild marine fishes associated with fish-cage aquaculture. *Hydrobiologia* **2016**, *765*, 343–358, doi:10.1007/s10750-015-2428-5.
53. Lombarte, A.; Tuset, V.M. Chapter3- Morfometría de otolitos. In *Métodos de estudios con otolitos: principios y aplicaciones/ Métodos de estudos com otólitos: princípios e aplicações*; Volpedo, A.V., Vaz-dos-Santos, A.M., Eds.; Ciudad Autónoma de Buenos Aires, 2015; p. 31.
54. Popper, A.N.; Lu, Z. Structure-function relationships in fish otolith organs. *Fish. Res.* **2000**, *46*, 15–25, doi:10.1016/S0165-7836(00)00129-6.
55. D'Iglio, C.; Famulari, S.; Albano, M.; Carnevale, A.; Di Fresco, D.; Costanzo, M.; Lanteri, G.; Spanò, N.; Savoca, S.; Capillo, G. Intraspecific variability of the saccular and utricular otoliths of the hatchetfish Argyropelecus hemigymnus (Cocco, 1829) from the Strait of Messina (Central Mediterranean Sea). *PLoS One* **2023**, *18*, 1–31, doi:10.1371/journal.pone.0281621.
56. Assis, C.A. The utricular otoliths, lapilli, of teleosts: Their morphology and relevance for species identification and systematics studies. *Sci. Mar.* **2005**, *69*, 259–273, doi:10.3989/scimar.2005.69n2259.
57. Assis, C.A. The lagenar otoliths of teleosts: Their morphology and its application in species identification, phylogeny and systematics. *J. Fish Biol.* **2003**, *62*, 1268–1295, doi:10.1046/j.1095-8649.2003.00106.x.
58. Schulz-Mirbach, T.; Plath, M. All good things come in threes–species delimitation through shape analysis of saccular, lagenar and utricular otoliths. *Mar. Freshw. Res.* **2012**, *63*, 934–940.
59. Schulz-Mirbach, T.; Riesch, R.; García de León, F.J.; Plath, M. Effects of extreme habitat conditions on otolith morphology - a case study on extremophile livebearing fishes (Poecilia mexicana, P. sulphuraria). *Zoology* **2011**, *114*, 321–334, doi:10.1016/j.zool.2011.07.004.
60. Schulz-Mirbach, T.; Ladich, F.; Riesch, R.; Plath, M. Otolith morphology and hearing abilities in cave- and surface-dwelling ecotypes of the Atlantic molly, Poecilia mexicana (Teleostei: Poeciliidae). *Hear. Res.* **2010**, *267*, 137–148, doi:10.1016/j.heares.2010.04.001.
61. Zorica, B.; Sinovčić, G.; Keč, V.Č. Preliminary data on the study of otolith morphology of

five pelagic fish species from the Adriatic Sea (Croatia). *Acta Adriat.* **2010**, *51*, 89–96.

62. Bal, H.; Türker, D.; Zengin, K. Morphological characteristics of otolith for four fish species in the Edremit Gulf, Aegean Sea, Turkey. *Iran. J. Ichthyol.* **2018**, *5*, 303–311, doi:10.22034/iji.v5i4.312.
63. Kasapoglu, N.; Duzgunes, E. Otolith atlas for the black sea. *J. Environ. Prot. Ecol.* **2015**, *16*, 133–144.
64. Altin, A.; Ayyildiz, H. Relationships between total length and otolith measurements for 36 fish species from Gökçeada Island, Turkey. *J. Appl. Ichthyol.* **2018**, *34*, 136–141, doi:10.1111/jai.13509.
65. Tuset, V.M.; Lombarte, A.; Assis, C.A. Otolith atlas for the western Mediterranean, north and central eastern Atlantic. *Sci. Mar.* **2008**, *72*, 7–198.
66. Assis, C.A. Estudo morfológico dos otólitos sagitta, asteriscus e lapillus de Teleóstei (Actinopterygii, Teleostei) de Portugal continental. Sua aplicação em estudos de filogenia, sistematica e ecologia. *Ecologia* 2000, 1005.
67. FAO Fishery and Aquaculture Statistics. (Global capture production 1950-2020) (FishStatJ). *FAO Fish. Aquac. Dep.* 2022.
68. Soeth, M.; Daros, F.A.; Correia, A.T.; Fabré, N.N.; Medeiros, R.; Feitosa, C.V.; de Sousa Duarte, O.; Lenz, T.M.; Spach, H.L. Otolith phenotypic variation as an indicator of stock structure of Scomberomorus brasiliensis from the southwestern Atlantic Ocean. *Fish. Res.* **2022**, *252*, 106357, doi:10.1016/j.fishres.2022.106357.
69. Lennox, R.J.; Paukert, C.P.; Aarestrup, K.; Auger-Méthé, M.; Baumgartner, L.; Birnie-Gauvin, K.; Bøe, K.; Brink, K.; Brownscombe, J.W.; Chen, Y.; et al. One hundred pressing questions on the future of global fish migration science, conservation, and policy. *Front. Ecol. Evol.* **2019**, *7*, 286, doi:10.3389/fevo.2019.00286.
70. Schneider, C.A.; Rasband, W.S.; Eliceiri, K.W. NIH Image to ImageJ: 25 years of image analysis. *Nat. Methods* **2012**, *9*, 671–675, doi:10.1038/nmeth.2089.
71. Jawad, L.A.; Sabatino, G.; Ibáñez, A.L.; Andaloro, F.; Battaglia, P. Morphology and ontogenetic changes in otoliths of the mesopelagic fishes Ceratoscopelus maderensis (Myctophidae), Vinciguerria attenuata and V. poweriae (Phosichthyidae) from the Strait of Messina (Mediterranean Sea). *Acta Zool.* **2018**, doi:10.1111/azo.12197.
72. Pavlov, D.A. Differentiation of three species of the genus Upeneus (Mullidae) based on otolith shape analysis. *J. Ichthyol.* **2016**, *56*, 37–51, doi:10.1134/S0032945216010094.
73. Pavlov, D.A. Otolith Morphology and Relationships of Several Fish Species of the Suborder Scorpaenoidei. *J. Ichthyol.* **2021**, *61*, 33–47, doi:10.1134/S0032945221010100.

74. Tuset, V.M.; Lozano, I.J.; GonzÍez, J.A.; Pertusa, J.F.; García-Díaz, M.M. Shape indices to identify regional differences in otolith morphology of comber, Serranus cabrilla (L., 1758). *J. Appl. Ichthyol.* **2003**, *19*, 88–93, doi:10.1046/j.1439-0426.2003.00344.x.
75. Tuset, V.M.; Lombarte, A.; González, J.A.; Pertusa, J.F.; Lorente, M.J. Comparative morphology of the sagittal otolith in Serranus spp. *J. Fish Biol.* **2003**, *63*, 1491–1504, doi:10.1111/j.1095-8649.2003.00262.x.
76. Tuset, V.M.; Farré, M.; Otero-Ferrer, J.L.; Vilar, A.; Morales-Nin, B.; Lombarte, A. Testing otolith morphology for measuring marine fish biodiversity. *Mar. Freshw. Res.* **2016**, *67*, 1037–1048, doi:10.1071/MF15052.
77. Libungan, L.A.; Pálsson, S. ShapeR: An R package to study otolith shape variation among fish populations. *PLoS One* **2015**, *10*, 1–12, doi:10.1371/journal.pone.0121102.
78. Nolf, D. *Otolithi Piscium. Handbook of Paleoichthyology, Vol. 10.*; Fischer, G., Ed.; Stuttgart, New York, 1985;
79. Altin, A.; Ayyildiz, H. Relationships between total length and otolith measurements for 36 fish species from Gökçeada Island, Turkey. *J. Appl. Ichthyol.* **2018**, *34*, 136–141, doi:10.1111/jai.13509.
80. Neves, J.; Silva, A.A.; Moreno, A.; Veríssimo, A.; Santos, A.M.; Garrido, S. Population structure of the European sardine Sardina pilchardus from Atlantic and Mediterranean waters based on otolith shape analysis. *Fish. Res.* **2021**, *243*, 106050, doi:10.1016/j.fishres.2021.106050.
81. Vignon, M.; Morat, F. Environmental and genetic determinant of otolith shape revealed by a non-indigenous tropical fish. *Mar. Ecol. Prog. Ser.* **2010**, *411*, 231–241, doi:10.3354/meps08651.
82. Tuset, V.M.; Otero-Ferrer, J.L.; Gómez-Zurita, J.; Venerus, L.A.; Stransky, C.; Imondi, R.; Orlov, A.M.; Ye, Z.; Santschi, L.; Afanasiev, P.K.; et al. Otolith shape lends support to the sensory drive hypothesis in rockfishes. *J. Evol. Biol.* **2016**, *29*, 2083–2097, doi:10.1111/jeb.12932.
83. Assis, I.O.; da Silva, V.E.L.; Souto-Vieira, D.; Lozano, A.P.; Volpedo, A. V.; Fabré, N.N. Ecomorphological patterns in otoliths of tropical fishes: assessing trophic groups and depth strata preference by shape. *Environ. Biol. Fishes* **2020**, *103*, 349–361, doi:10.1007/s10641-020-00961-0.
84. Lombarte, A.; Cruz, A. Otolith size trends in marine fish communities from different depth strata. *J. Fish Biol.* **2007**, *71*, 53–76, doi:10.1111/j.1095-8649.2007.01465.x.
85. Zhuang, L.; Ye, Z.; Zhang, C. Application of otolith shape analysis to species separation in

Sebastes spp. from the Bohai Sea and the Yellow Sea, northwest Pacific. *Environ. Biol. Fishes* **2015**, *98*, 547–558, doi:10.1007/s10641-014-0286-z.

86. Nazir, A.; Khan, M.A. Using otoliths for fish stock discrimination: Status and challenges. *Acta Ichthyol. Piscat.* **2021**, *51*, 199–218, doi:10.3897/aiep.51.64166.
87. Barnes, T.C.; Gillanders, B.M. Combined effects of extrinsic and intrinsic factors on otolith chemistry: Implications for environmental reconstructions. *Can. J. Fish. Aquat. Sci.* **2013**, *70*, 1159–1166, doi:10.1139/cjfas-2012-0442.
88. Clarke, L.M.; Conover, D.O.; Thorrold, S.R. Population differences in otolith chemistry have a genetic basis in menidia menidia. *Can. J. Fish. Aquat. Sci.* **2011**, *68*, 105–114, doi:10.1139/F10-147.
89. Howarth, L.M.; Waggitt, J.J.; Bolam, S.G.; Eggleton, J.; Somerfield, P.J.; Hiddink, J.G. Effects of bottom trawling and primary production on the composition of biological traits in benthic assemblages. *Mar. Ecol. Prog. Ser.* **2018**, *602*, 31–48, doi:10.3354/meps12690.
90. Jobling, M. Temperature and growth: modulation of growth rate via temperature change. *Glob. Warm.* **2011**, 225–254, doi:10.1017/cbo9780511983375.010.
91. Mahé, K.; Ider, D.; Massaro, A.; Hamed, O.; Jurado-Ruzafa, A.; Gonçalves, P.; Anastasopoulou, A.; Jadaud, A.; Mytilineou, C.; Elleboode, R.; et al. Directional bilateral asymmetry in otolith morphology may affect fish stock discrimination based on otolith shape analysis. *ICES J. Mar. Sci.* **2019**, *76*, 232–243, doi:10.1093/icesjms/fsy163.
92. Díaz-Gil, C.; Palmer, M.; Catalán, I.A.; Alós, J.; Fuiman, L.A.; García, E.; Del Mar Gil, M.; Grau, A.; Kang, A.; Maneja, R.H.; et al. Otolith fluctuating asymmetry: A misconception of its biological relevance? *ICES J. Mar. Sci.* **2015**, *72*, 2079–2089, doi:10.1093/icesjms/fsv067.
93. Mille, T.; Ernande, B.; Pontual, H. de; Villanueva, C.; Mahé, K. Sources of otolith morphology variation at the intra-population level : directional asymmetry and diet marine fishes. In Proceedings of the SFI Days; 2016; p. 2016.
94. Popper, A.N. Auditory system morphology. In *Encyclopedia of Fish Physiology: from Genome to Environment*; Farrell, A.P., Ed.; Academic Press: San Diego, CA, 2011; pp. 252–261.
95. Popper, A.N.; Schilt, C.R. Hearing and Acoustic Behavior: Basic and Applied Considerations. *Fish Bioacoustics* **2008**, 17–48, doi:10.1007/978-0-387-73029-5_2.

Ecomorphological adaptation of *Scorpaena porcus* (Linnaeus, 1758): evidence from two different environments revealed by *sagittae* features and somatic growth rates

ABSTRACT

Improve the knowledge base on the ecomorphological adaptation of teleost species to different environments, trying to reconstruct how habitat can shape *sagittae,* is essential for conservational porpoises, evolutionary evaluations, and population dynamics' studies. Here is provided a comparative study between *sagittae* features, growth rates and age structures of two *Scorpaena porcus* populations, both the Mediterranean Sea, one from the Strait of Messina (Central Mediterranean Sea) and one from Split area (Adriatic Sea). A total of ninety individuals, half from Messina (Italy) and half from Split (Croatia) have been collected from two totally different environments in terms of depths and physiochemical features. Results showed an overall different morphology, shape, and morphometry of *sagittae* among the three size classes of the two investigated populations. Samples from Messina were characterized by a most elliptical and slender shape, and a most regular serration of margins than those from Split, that exhibited a wider *sagitta,* with a most enhanced *anti-rostrum* and longer *rostrum*. Split population showed also a significantly slower growth, with a deeply different age structure than Messina's one. Results have confirmed the reliability of *sagittae* to detect the inter population variability of *S. porcus* from different geographical area, an essential tool for stock assessment, population studies and investigation on ecomorphological adaptation of teleost species to different habitats.

1. INTRODUCTION

The family Scorpaenidae counts more than 1400 species and represents one of the most diverse fish groups worldwide. It includes species adapted to live in many different environments, from the coastal shallow waters to the deep seas. Within the family, species belonging to *Scorpaena* genus are among the most abundant in all the temperate marine environments, and in several tropical seas, around the world. They are benthic species, living in sandy rocky bottoms, with 61 valid species included belonging to the genus [1,2].

Among these, the black scorpionfish, *Scorpaena porcus* (Linnaeus, 1758), is one of the most common in the entire Mediterranean basin, Black Sea, and the Eastern Atlantic Ocean, from the British Islands to the Atlantic Moroccan coasts [3,4]. It dwells rocky, or mixed rocky-sandy, benthic habitats, from the shallow water to the bathyal plan, up to 800 m of depth [2]. It is very common also on seagrass

beds, showing a sedentary lifestyle with nocturnal feeding habits [5,6]. According to literature [7–12], this species is a small-body benthic predator, with a preference for small fishes and crustaceans. It is considered, together with the other scorpionfishes species, an essential predator for the well-functioning of the rocky-reefs ecosystems worldwide, both in temperate and tropical areas. Unlike other congeneric species, *S. porcus* is characterized by a slow-growth and a relatively short life, with 12 years as maximum recorded age [13], and an enhanced geographical heterogeneity in life span and growth rates within the distribution areas. This high inter population variability has been related to the influence of the different fishing pressures and environmental factors experienced by the populations within the distribution range [7,13–18]. Many authors [19–22] have also suggested *S. porcus* as indicator species for biomonitoring and environmental conditions' assessments. In the Black Sea, this species showed a significant negative trend in body size related to several factors, as pollution, and temperature rise, being negative affected by anthropogenetic pressure [20–22]. While, in the Adriatic Sea, analyses on historical trammel catch data have shown variations in population dynamics, biological traits and biomass, related to fishing pressure, confirming the sensitivity of the species to fisheries activities [7,19,23–26]. It represents one of the main target species of Mediterranean artisanal fisheries (especially in the eastern and western parts of the basin), being a large portion of the total catch and, consequently, a large source of income [14,19,24,27–31] thanks to its relatively high commercial value in Croatia, Spain, and Italy. Improve the knowledge base on the intra-specific variability of *S. porcus*, analyzing the different growth dynamics and eco-morphological adaptations of populations inhabiting different geographical areas, is essential to enhance its conservation. In addition, in fishery biology, a proper assessment of fishes' populations dynamics and stocks' structure is a fundamental step to establish good management measures, monitoring species and communities' response to management actions and different exploitation levels [32–35]. Moreover, being *S. porcus* a benthic species with a low home-range, a high spatial heterogeneity, and an enhanced ecological value, investigate how different habitats can influence its otoliths' features (such as shape, morphology, and morphometry) and growth rates acquires great relevance and scientific interest, also in terms of taxonomical studies and evolution.

Otoliths are pairs of calcium carbonate masses located in the fishes' inner ear. This is composed of three semicircular canals, with their end organs (*ampullae*), and three otolithic end organs (*saccule*, *utricle* and *lagena*) [36]. In each of this is located an otolith mass (respectively, *sagitta*, *lapillus* and *asteriscus*) connected through an otolithic membrane to the sensory epithelium (*macula*) [37]. Ciliary bundles of mechanoreceptive hair cells, extending from this area, convert mechanical stimuli to electrochemical energy, resulting in the neurotransmitters release, which allow the nerve stimulation [38,39]. This physiological process, present in all the vertebrates, lies at the basis of sound perception

and vestibular functions, with the inner ear serving as multi-sensory statoacustic organ [40,41]. Semicircular canals detect angular acceleration (e.g., head-body rotation), while otolithic end organs detect linear acceleration (resulting from movement and body tilts), gravitational force and sounds [38,42,43]. According to the mixed function hypothesis [38,44], each otolithic end organ is involved in both vestibular and auditory functions, with a different involvement degree for each of them, changing specie-specifically. Several scientific evidences, provided by otolith-removal experiments and microphonic potential evaluations, have shown a major involving in the vestibular function for the *utricle* (e.g., in gravitational force detection), than *saccule* and *lagena*, which seem to have a most enhanced sound perception function [45–49]. Indeed, *saccule* is increasingly considered as the main auditory end organ, as also highlighted by the anatomy of the peripheral structures (e.g., anterior swim bladder extensions) involved in the hearing process of sound specialist teleost species, and usually connected to *saccule*, and rarely to *lagena* or *utricle* [50]. Inside *saccule*, *sagitta* acts as the mass of an accelerometer, moving with different phase and amplitude than sensory epithelia and fish body, when exposed to the water particle motion induced by a sound field [41]. This relative motion of *sagittae* respect sensory epithelia (related to the density differences between otolith masses and fishes tissues) induces the hair cells' deflection and the consequential physiological response to sounds [51].

Sagittae, as the other otoliths, growth for the entire fishes' life, with a daily metabolically-inert deposition of calcium carbonate [52,53]. Their peculiar physiology and growing mechanism have made otoliths (mainly *sagittae*, for their larger dimension, in non-otophysan species, and most enhanced intra and inter specific variability, than *lapilli* and *asterisci* [54–56]) an essential tool to study fish ages and growth dynamics [57,58]. Thanks to their microelements (being several elements, as Sr, Na, K, Cu, Ba, Cd, Pb, Fe, Li, present as a very small fraction [59]) and isotopic composition, *sagittae* can help to understand several aspects of fishes' life history, as migration patterns [60,61], population structure [62,63], nursery areas [64,65], trophic ecology [66,67] and environmental variability experienced by species during their life [68]. Moreover, thanks to their high variability in morphology and shape between and within species [69–74], they have been widely used also in taxonomy [75–79], paleontological studies [80–82], stomach content analysis [83,84], and stocks assessment in fisheries studies [85–88]. Concerning the intra-specific variations in shape and morphology, they can be related to many factors, ranging from those genetically-driven [89], to environmental conditions and diet [86,90]. For this reason, *sagittae* are considered a good phenotypic marker, reliable to investigate the ecomorphological adaptation of teleost species to different environmental conditions and ecological dynamics [91,92], as highlighted by the shape and morphological differences between stocks and populations [85–88].

The present paper aims to investigate the intra specific differences in age structures, growth dynamics, diet composition, and *sagittae* shape and morphology, between two populations of *S. porcus* inhabiting, respectively, the tidal ponds in the beach rock formations, along the Strait of Messina coast (Central Mediterranean Sea), and the coastal environment near the Split Area (Eastern Adriatic Sea). The stomach content analysis has been performed only on the specimens from Messina, using the obtained data to make a comparison with the data present in literature for the diet composition of the studied species in the Split area [7]. The main purposes were (i) to assess how *sagittae* contours, morphology and morphometry change among size classes in the two studied populations, (ii) to evaluate the reliability of shape and morphometrical analysis in the assessment of different *S. porcus* populations, (iii) to investigate the differences in growth dynamics and age classes composition showed between the studied areas, and (iv) how much this differences can be related to geographical differences in diet composition and/or environmental conditions. These information are important to improve the knowledge base on the influences of environment on inner ear morphology, otoliths and somatic growth.

2. MATERIALS AND METHODS

2.1 Sample collection and studied areas.

A total number of 90 *S. porcus* specimens were sampled in two different localities of the Mediterranean Sea: 45 specimens from the tidal ponds occurring toward the Sicilian coast of the Messina's Strait (Central Mediterranean Sea, 38°15'25.76"N, 15°36'51.37"E), and 45 specimens from the coastal environment near the Split Area (Eastern Adriatic Sea, 43°26'0.93"N, 16°26'55.44"E) (Figure 1). Both sampling, in Messina and Split, were carried out during the Winter season of the 2023.

Figure 1. Map of the central Mediterranean Sea with the two studied areas highlighted in the boxes (Strait of Messina in green and Split area in red).

Thanks to the limited depth (ranging from 0,2 to 1,2 m) of the tidal ponds occurring in the "beach rock" formations toward the Sicilian coast of the Strait of Messina, specimens were caught manually, using a sampling net from the rocky bench present in the beach front. The sampling was authorized by local authorities.

"Beach rock" is a coastal biotope extending in the north-eastern Messina coast, between two villages: Ganzirri and Torre Faro. This sedimentary formation represents a rocky bench (2 kilometers long) that arrive from the beachfront, in the intertidal zone, to a depth of 2-3 meters, at the beginning of the infralittoral zone. It is considered an area of high interest, being part of the Oriented Natural Reserve of "Capo Peloro Lagoon", from an anthropological (used in the past as a quarry for milestones), geological (proof of Tyrrhenian age) and ecological point of view [93]. This biotope hosts very peculiar benthic communities, with a substantially different species composition and richness to those founded in other similar Mediterranean environments [94]. It also houses extended *Vermetus* formations (protected by European Community) with an unique arrangement, being on the substrate surface, and not in the typical *trottoir* formation, as in the rest of the Mediterranean Sea [95]. Thanks to its irregular shape, this area is characterized by several tidal ponds, with different surface and connection dynamics to the sea, hosting very complex ecological communities. These are essential nursery areas for several teleost species and a shelter zone for numerous taxa [96,97]. Indeed, beach rock represents the only natural substrate for benthic species present at these depths [94], and a shelter

from the strong currents that make the coastal areas of the Strait of Messina a difficult environment for habitat exploitation [97]. Indeed, the Strait of Messina is located at the junction area between Ionian and Tyrrhenian Sea. The meet of these two water masses, different in physiochemical properties, occurs in an area with an enhanced morpho-bathymetrical irregularity of the bottom, resulting in a very intense hydro dynamism. This generates a mixing process of the water masses, with strong currents regulated by tidal phases [98,99]. This intense hydro dynamism, and the peculiar waters' physio chemistry, has meant that this area has become a hot spot of biodiversity, with the presence of unique biological communities [94,100].

Concerning specimens from Split area (Figure 1), they were collected using sets of trammel nets; 1.5 m high and 32 m long trammel nets with inner layer mesh size of 28 mm and 150 mm mesh size of outer layers. Fish samples were captured in the nearshore, coastal waters in the Split area (43.5°N), in the eastern Adriatic, at depths ranging between 10 and 40 m (20 m in average). The biotope is characterized mainly by rocky substrata covered by photophilic algae alternating with patches of sand and *Posidonia oceanica* seagrass beds [7,19]. The ecological condition of the coastal waters in the Split area is assessed as very good [101], with a relatively high biodiversity, and up to 27 different recorded fish species. Such high biodiversity is characteristic for coastal waters, especially protected coves, and bays, and for more complex habitats that are overgrown with the seagrass beds. Almost all widespread fish families of the Adriatic were represented in the sampled area, namely: Sparidae, Mullidae, Mugilidae, Centracanthidae, Labridae and Gobiidae [102]. The eastern Adriatic Sea, to which belong the Split area, is outflowed by the East Adriatic current, bringing Levantine Intermediate Water from the Ionian Sea [103,104]. In all the Adriatic, the water column is characterized by a high homogeneity during winter, thanks to wind mixing processes and surface cooling. While, during Summer it becomes more stratified, due to the drop of wind mixing processes [105].

2.2 Samples processing, stomachs sampling, otolith extraction and age reading

All sampled specimens were transported in the laboratory, where they were weighed (TL, cm) and measured (TW, g). *Sagittae* were collected from each specimen, cleaned (15 min in 3% H_2O_2, followed by Milli-Q water) and, once dried, stored in Eppendorf microtubes. Concerning stomachs, they were sampled only from Messina's specimens, and stored in ethanol 70% + glycerin 5% for stomach content analysis. To assess the intra specific difference in *sagittae* features (shape and morphology), samples from both areas were divided in three size classes, according to TL. Class I included specimens smaller than 120 mm, Class II those with a TL ranging from 120 mm to 180 mm,

and Class III larger than 180 mm. Left *sagittae* of both populations were photographed on the annuli side using a stereomicroscope (Olympus SZX10) equipped with an Olympus DP-25 digital camera,. Images were converted in binary format for shape analysis, using the ImageJ 1.48p free software, available at http://rsb.info.nih.gov/ij/.

After images collection, left *sagittae* were used for age reading. Reading process was carried out by two different operators, without data on fish length. Both readers performed two different readings, with one month of distance one from the other. If readings were different for one or two years, it was performed a third reading, with the otolith discarding in the case of persisting differences. Specimens age was assessed under reflection light, using the stereomicroscope. The pattern of opaque and translucent zone was used for annuli counting. Indeed, according to literature on studied species [7,14], an annulus is the combination of an opaque and a translucent (or hyaline) ring, appearing, under the reflecting light respectively light and dark. When this pattern was not clear, *sagittae* were grinded to facilitate the rings' counting. It was not necessary the otoliths sectioning, being grinding enough to reveal the opaque and translucent zones' pattern for those samples in which this was not clear from the whole otoliths viewing. The count was performed in the axis from nucleus (appearing as a light ring under the reflecting light) to the rostrum tip, detected as the area with the most unambiguous annulation pattern.

2.3 Stomach content analysis

Each stomach content was analyzed under the stereomicroscope, to identify, at the lowest taxonomic level possible, each prey. Each preys' items were counted and weighted, also detecting the digestion degree (1 = undamaged; 2 = almost digested; 3 = highly digested). The anatomical undigested preys' parts (e.g., otoliths, telsons, carapaces, mouth parts, heads capsules, fish columns) were counted to assess the contribution of each prey taxon to the diet, grouping the unidentifiable preys' items, due to the advanced state of digestion, into undetermined taxa. According to their presence in the stomachs, only one type of anatomical remains was counted for each prey group to avoid the double-counting.

Following indexes were calculated to evaluate the contribution of each preys' taxa to the diet: the percentage of biomass composition (%W), the percentage of abundance composition (%*N*), and the frequency of occurrence (%F) [106]. The Relative Importance Index was also calculated (IRI = %F (%N + %P)) expressing it also as percentage ($\%\,\mathrm{IRI} = \left(\mathrm{IRI}_i\, \Sigma_i^N\, \mathrm{IRI}_i\right) \times 100$) [107–109]. Concerning the empty stomachs, it was calculated the Vacuity Index, VC = (Ne/N) × 100, as the percentage of empty stomachs (Ne) on the total stomach number (N).

2.4 Shape and morphometric analysis

Shape R (R software package, RStudio 2022.07.1 Build 554; R Gui 4.1.3 2022.03.10) was used to perform the Shape analysis from the otoliths' outlines. This package has been developed for inter and inter specific analysis on shape variability in teleost's otoliths [110]. Each binarized *sagitta* photo was analyzed for the outlines' detection using a shape R specific function, with 0.05 as value for intensity threshold greyscale. A data file with studied specimens' information (as body weight and fish length) was linked to extracted contours. These was used for each size classes to perform several otoliths' measurements (maximum width, OW, mm, maximum length, OL, mm, perimeter, OP, mm, and surface, OS, mm^2), through the getMeasurements function. Proper package functions were applied for the extraction, and subsequent adjusting, of Wavelet and Fourier coefficients, to assess the allometric relationships between fish lengths and otolith shapes. Wavelet coefficients were used to provide the comparison between the mean *sagittae* shape of the analyzed populations. The reconstruction's quality was estimated analyzing the deviation of the coefficient's reconstruction from the otolith outline (S1 Fig). Finally, a g-plots R package's specific function was used to investigate how the position along the outline can influence the wavelet coefficients variation (S2 Fig).

Otoliths measurements performed with shape R were used to calculate several indexes. The *sagittae* length increase, related to the total fish length, was evaluated assessing otolith length to total fish length ratio (OL/TL); while, according to literature [111–116], several shape indexes were used to evaluate intra and inter specific variability of *sagittae* shape: roundness ($Ro = 4OS/\pi OL^2$), form factor ($FF = 4\pi OS/OP^2$), aspect ratio (AR = OW/OL%), circularity ($C = OP^2/OS$), rectangularity (Re = OS/[OL×OW]) and ellipticity (E = (OL–OW)/(OL+OW)).

2.5 Statistical analysis

Length frequency distributions of individuals from the two sampling areas were compared using the Kolmogorov–Smirnov two-sample test.

The von Bertalanffy growth model was fitted to the estimated age-length dataset using a non-linear least-square procedure of a Gauss–Newton algorithm. The von Bertalanffy growth parameters ($L\infty$, K and t0) were calculated for both fish populations sampled in the Messina's Strait and Split area and compared by the multivariate Hotelling's T2-test. The growth performance index ($\Phi' = 2 \log L\infty + \log K$) was then calculated to compare the different populations of the black scorpionfish throughout its distribution range.

Univariate and multivariate statistical methods were applied to conduct investigations on fish parameters and *sagittae* features of specimens from Messina using Prism V.8.2.1 (Graph- pad Software Ltd., La Jolla, CA 92037, USA), R vegan package V.2.5, and PAST V.4. *Sagittae* morphometric variations between the different size classes investigated were detected using a one-way analysis of variance (one-way ANOVA) or Kruskal–Wallis one-way ANOVA, followed by Tukey or Dunn's post-hot test respectively. A Linear Discriminant Analysis (LDA) was conducted to obtain an overview of the differences in otolith parameters between the size classes examined Additionally, the correlation between the measured parameters and fish body weight (BW) and total length (TL) was tested using the Spearman correlation analysis.

To explore the variation of otolith contours between specimens the shape indices were extrapolated and analysed through an ANOVA-like permutation test and a Linear Discriminant Analysis (LDA) to obtain an overview of the differences in otolith shape between the size classes examined. The significance level of p-value was set at <0.05.

Univariate and multivariate statistical methods were applied to conduct investigations on fish parameters and *sagittae* features of specimens from Split using Prism V.8.2.1 (Graph- pad Software Ltd., La Jolla, CA 92037, USA), R vegan package V.2.5, and PAST V.4. *Sagittae* morphometric variations between the different size classes investigated were detected using a one-way analysis of variance (one-way ANOVA) or Kruskal–Wallis one-way ANOVA, followed by Tukey or Dunn's post-hot test respectively. A Linear Discriminant Analysis (LDA) was conducted to obtain an overview of the differences in otolith parameters between the size classes examined Additionally, the correlation between the measured parameters and fish body weight (BW) and total length (TL) was tested using the Spearman correlation analysis.

To explore the variation of otolith contours between specimens the shape indices were extrapolated and analysed through an ANOVA-like permutation test and a Linear Discriminant Analysis (LDA) to obtain an overview of the differences in otolith shape between the size classes examined. The significance level of p-value was set at < 0.05.

A one-way analysis of variance, or a corresponding non-parametric test in case of non-homogeneity of the data, were used to verify the existence of any differences in the *sagittae* extracted from Messina and Split specimens, using the origin site of the samples as the only independent factor. For a more detailed description of the two populations examined, a Mann Whitney test was used to explore the variability of individual otolith morphometric parameter, within each size class, between the sampling sites identified in the current study. P value significance was set at <0.05. Additionally, to obtain an overview of the *sagittae* characteristics of the two populations under examination, a PCA was applied to the dataset.

Finally, to investigate the variation of otolith contours between specimens, the shape indices were extrapolated and analysed through an ANOVA-like permutation test and a Principal Component Analysis (PCA) to obtain an overview of the differences in otolith shape in individuals from Messina and from Split.

3. RESULTS

The 45 specimens from Messina showed a TL ranging from 6.5 to 23 cm, with a Mean TL ± SD of 12.61 ± 0.69. Concerning Split area, specimens showed a TL ranging from 11.2 to 24.1 cm and a Mean TL ± SD of 14.71 ± 0.41 cm (Table 1). Length-frequency distributions were significantly different between the two sampling areas (Kolmogorov–Smirnov test; $P < 0.001$).

Table 1. Number of analyzed *S. porcus* specimens, total length (TL) range and mean, with standard deviation (SD), from Messina and Split.

	Messina	Split
Number	45	45
TL range (cm)	6.5 - 23	11.2 – 24.1
Mean TL ± SD	12.61 ± 0.69	14.71 ± 0.41

3.1 Growth rates and age structure

Age counts were successfully provided for all the otoliths from Messina and Split, with no sample discarded. The age-length composition, provided for both the studied area, in Table 2, showed 3 to 5 years old as the main estimated ages (57.77 %) for the Messina specimens, with a maximum age of 5 years. In Split area, the larger part of the specimens was between 5 and 8 years old (75.57 %), with a maximum age of 8 years.

Table 2. Age-length keys of *S. porcus* specimens from Messina and Split area

	Messina					Split						
TL (cm)	1	2	3	4	5	2	3	4	5	6	7	8
7	7											
8	6											
9	5											
10												
11			1					2				
12			1			1	4	3		1		

13			2						5	1		
14		1	6						1	3		
15			2					1		7	1	
16			3	1						3	3	
17			5							2	1	
18												
19				1					1		1	2
20					1							
21												1
22					1							
23			2									
24											1	
N	18	1	22	2	2	1	4	6	7	17	7	3
%	40	2.22	48.89	4.44	4.44	2.22	8.89	13.33	15.56	37.78	15.56	6.67

The von Bertalanffy growth curves were fitted to age-length dataset, estimated for individuals from the Messina Strait and Split area (Figure 2). Estimated parameters for *Scorpaena porcus* from the Messina Strait and Split area were L_∞ = 28.78 cm, K = 0.22 year^{-1}, t_0 = -0.42 year (R^2 = 0.89) and L_∞ = 41.04 cm, K = 0.06 year^{-1}, t_0 = -2.45 year (R^2 = 0.73), respectively. The growth performance index (Φ') was 2.26 for the fish from the Messina Strait and 2.00 for the fish from the Split area.

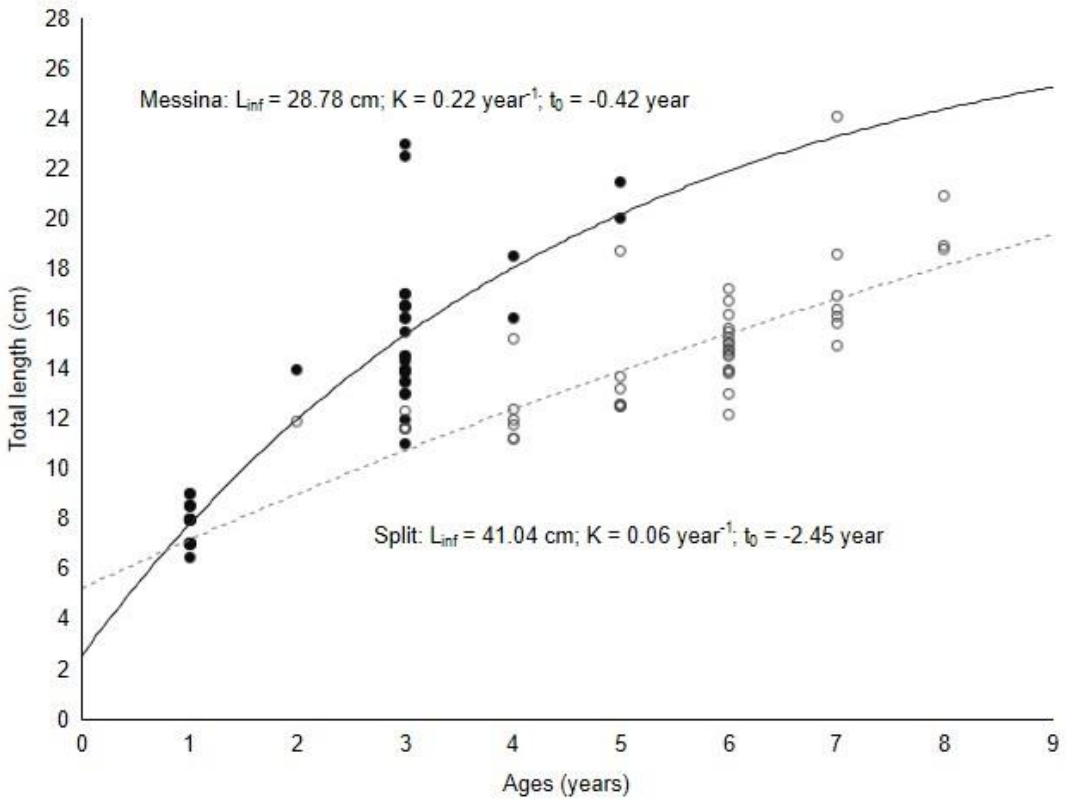

Figure 2. Fitted von Bertalanffy growth curve for *S. porcus* individual from Messina and Split

The Hotelling's T^2-test indicated that the von Bertalanffy growth curves differed significantly between the two tested populations ($T^2 = 2741.77 > T^2_{0\ (0.05,\ 3,86)} = 12.20$). The L_∞ value was higher in fish from the Split area and the K value was higher in fish from the Messina Strait. Therefore, considering the growth coefficient, fish from the Messina Strait grew faster than fish from the Split area. Statistical difference in length-at-age data (Table 3) derived from the von Bertalanffy growth curves was observed between the two populations (t-test for paired comparison, P = 0.025).

Table 3. Length-at-age's estimates of *S. porcus* specimens from Messina and Split

Age (Years)	Length-at-Age (cm)	
	Messina	Split
1	7.77	-
2	14	11.9
3	15.34	11.77
4	17.25	12.3
5	20.75	13.67
6	-	14.82
7	-	17.54
8	-	19.53

3.2 Morphometric and Shape analysis

Following the terminology used by Tuset, Nolf and Assis [37,76,117], studied specimens showed an overall morphology of *sagittae* characterized by an oblong to lanceolate outline, with serrate to crenate margins. The anterior region was peaked, with *rostrum*, *antirostrum* and *excisura ostii*, that, together with the notch tilt angle, changed between the two populations (Figure 3 a-f). The posterior region was oblique to irregular, and the *sulcus acusticus* was heterosulcoid, ostial and median.

In Table 4 and 5 are provided the morphometric mean values for the two investigated populations, with the minimum and maximum range, divided in the three size classes.

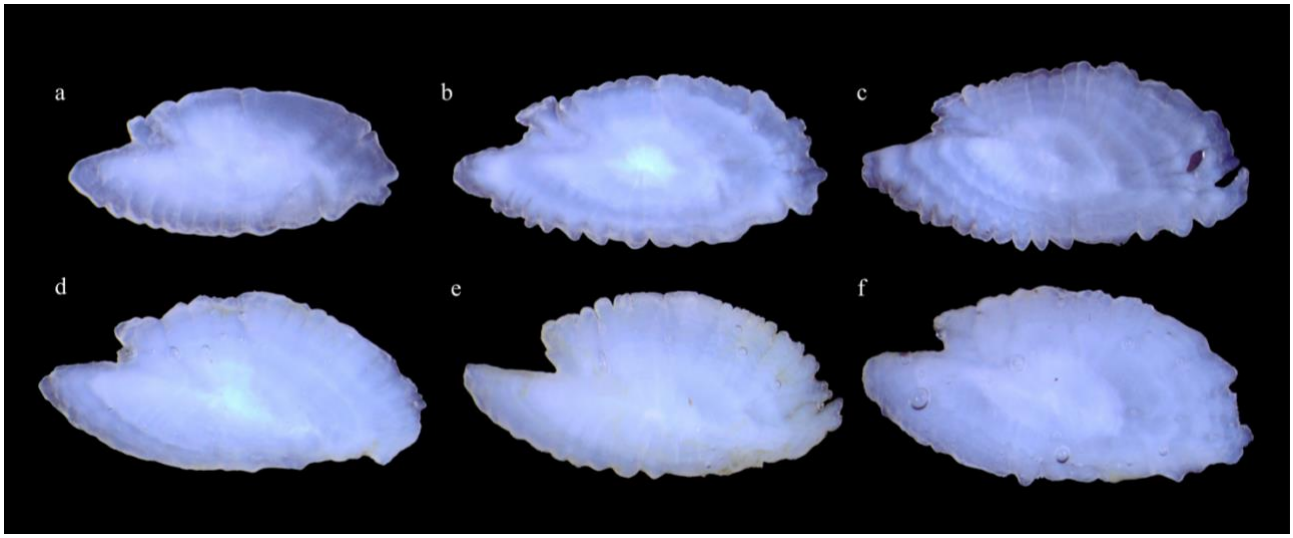

Figure 3. Stereoscope images of the medial view of the *sagittae* belonging to specimens from Messina (a-c) and Split (d-f)

Table 4. Morphometric mean values of left *sagittae* of *S. porcus* individuals from Messina, with standard deviation (SD), minimum (Min.) and maximum (Max.) range, for the three investigated size classes: OL (otolith length), OW (otolith width), OP (otolith perimeter), OS (otolith surface), OL/TL (the ratio of otolith length to total fish length), C (circularity), Re (rectangularity), E (ellipticity), AR (aspect ratio), FF (form factor), Ro (roundness).

	CLASS I			**CLASS II**			**CLASS III**		
	Mean	**d. st.**	**Min. – Max.**	**Mean**	**d. st.**	**Min. – Max.**	**Mean**	**d. st.**	**Min. – Max.**
OL	3.89	0.33	3.35 – 4.77	6.18	0.51	5.37 – 7.03	7.5	0.68	6.86 – 8.36
OW	1.71	0.12	1.52 – 2.04	2.45	0.17	2.12 – 2.86	3.01	0.35	2.57 – 3.54
OP	10.37	0.92	8.74 – 12.49	17.19	1.4	15.21 – 20.18	22.05	3.06	18.23 – 25.65
OS	4.6	0.79	3.59 – 6.9	10.53	1.41	8.49 – 13.1	22.05	3.11	12.33 – 20.49
OL / TL	4.92	0.31	4.33 – 5.45	4.22	0.58	3.42 – 5.52	3.59	0.51	3 – 4.03
C	23.52	1.46	21.3 – 27.1	28.19	1.87	25.59 – 32.62	30.59	3.1	26.98 – 34.93
Re	0.69	1.86	0.65 – 0.73	0.69	0.01	0.66 – 0.71	0.7	0.01	0.69 – 0.72
E	0.39	0.02	0.36 – 0.42	0.43	0.03	0.38 – 0.49	0.43	0.03	0.38 – 0.46
AR	0.44	1.67	0.41 – 0.47	0.4	0.03	0.34 – 0.45	0.4	0.03	0.37 – 0.45
FF	0.54	0.03	0.46 – 0.59	0.45	0.03	0.38 – 0.49	0.41	0.04	0.36 – 0.47
Ro	0.38	0.01	0.36 – 0.41	0.35	0.02	0.30 – 0.40	0.36	0.03	0.33 – 0.4

Table 5. Morphometric mean values of left *sagittae* of *S. porcus* individuals from Split, with standard deviation (SD), minimum (Min.) and maximum (Max.) range, for the three investigated size classes: OL (otolith length), OW (otolith width), OP (otolith perimeter), OS (otolith surface), OL/TL (the ratio of otolith length to total fish length), C (circularity), Re (rectangularity), E (ellipticity), AR (aspect ratio), FF (form factor), Ro (roundness)

	CLASS I			**CLASS II**			**CLASS III**		
	Mean	**d. st.**	**Min. – Max.**	**Mean**	**d. st.**	**Min. – Max.**	**Mean**	**d. st.**	**Min. – Max.**
OL	5.56	0.59	4.94 – 6.7	6.33	0.44	5.45 – 7.27	8.03	0.68	6.68 – 8.55
OW	2.42	0.2	2.15 – 2.69	2.83	0.25	2.37 – 3.37	3.32	0.23	3.02 – 3.65
OP	15.45	1.56	13.98 – 18.48	18.48	1.49	15.32 – 20.67	23.75	2.88	18.84 – 27.03
OS	9.33	1.7	7.69 – 12.42	12.34	1.86	9.43 – 16.63	18.44	3.14	14.32 – 23.17
OL / TL	4.82	0.62	41.83 – 59.83	4.42	0.44	3.37 – 5.42	4.04	0.4	3.54 – 4.42
C	25.76	1.62	23.06 – 27.58	27.96	2.86	22.68 – 33.3	30.96	5.58	24.78 – 40.85
Re	0.69	0.005	0.68 – 0.7	0.68	0.02	0.64 – 0.72	0.69	0.04	0.64 – 0.74
E	0.39	0.02	0.36 – 0.43	0.38	0.03	0.32 – 0.46	0.41	0.02	0.38 – 0.45
AR	0.44	0.03	0.4 – 0.47	0.45	0.03	0.37 – 0.51	0.41	0.02	0.38 – 0.45
FF	0.49	0.03	0.46 – 0.54	0.44	0.08	0.12 – 0.55	0.42	0.07	0.31 – 0.51
Ro	0.38	0.02	0.35 – 0.41	0.39	0.02	0.34 – 0.45	0.36	0.04	0.32 – 0.41

Sagittae belonging to Messina specimens showed an oblong shape, with an enhanced margins serration. The *rostrum* and the *antirostrum* were short, with an arrow *excisura ostii*, a not acute notch, and an irregular posterior margin (Figure 4 a-c). Concerning the intra specific differences among size classes, morphometrical analyses showed an enhanced variability, confirmed also by the mean otoliths' shapes (Figure 4 d). *Sagittae* of specimens belonging to Size Class I showed a most circular contour, then the other classes. Also, the posterior region showed a peculiar organization, with a most oblique margin than the other size classes. In the Size Class II, the contour was less circular than the Class I, with most irregular posterior margin and less acute notch of *excisura*. The Size Class III showed a very different shape, with an enhanced ellipticity (as highlighted by the highest E value among size classes: 0.41 ± 0.02 mm, see Table 4) resulting in a less wide and longer *sagitta* than the other size classes.

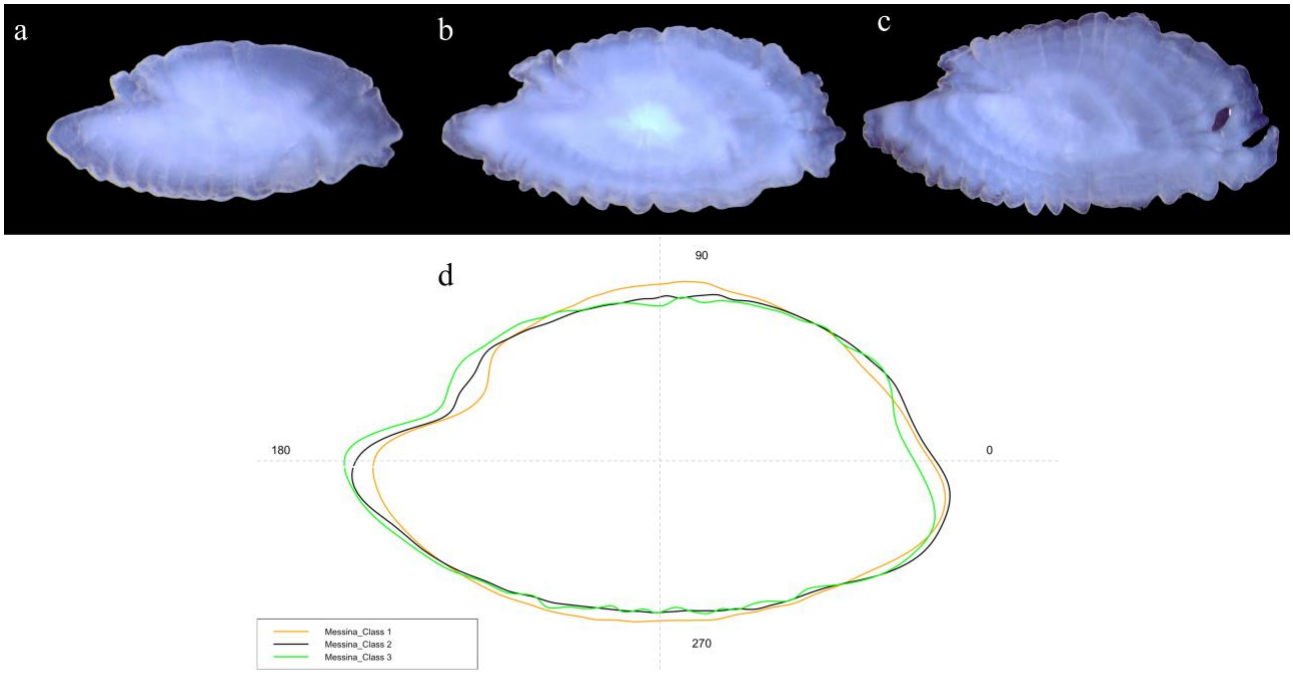

Figure 4. Stereoscope images of the medial view of the *sagittae* belonging to specimens from Messina, for the three investigated size classes (a: Class I, b: Class II, c: Class III), with their mean otoliths shape (d)

Overall, the specimens examined showed significant variations in total length and body weight between the size classes considered in the study. In particular, the Dunn's test highlighted variations in the total length of the specimens belonging to the three size classes and variations in body weight, which essentially concerned Class I and Class II, and then also Class I and Class III ($p<0.05$).

The results of the variations observed for the individual parameters of the otoliths extracted from each size class are reported in Table 6.

Table 6 Dunn's post hoc test results obtained through the *sagittae* parameters comparison between samples from Class I, II and III, belonging to Messina population. P value legend: (ns), P>0.05, not significant; (*), P<0.05, significant.

	Comparison		
	I *vs* II	**I *vs* III**	**II *vs* III**
Sagittae parameters	p value	p value	p value
OS	<0.001*	<0.001*	0.167ns
OL	<0.001*	<0.001*	0.182ns
OW	<0.001*	<0.001*	0.198ns
OP	<0.001*	<0.001*	0.216ns
Ro	<0.001*	0.009*	0.998ns
FF	<0.001*	<0.001*	0.972ns
E	<0.001*	0.020*	0.153ns

P^2/A	<0.001*	<0.001*	0.972ns
Re	0.187ns	0.187ns	0.187ns
AR	<0.001*	0.007*	0.911ns
OL/TL	<0.001*	<0.001*	0.028*

LDA confirmed the results obtained by univariate analysis (Figure 5), explaining the main differences observed between the classes I vs II and I vs III.

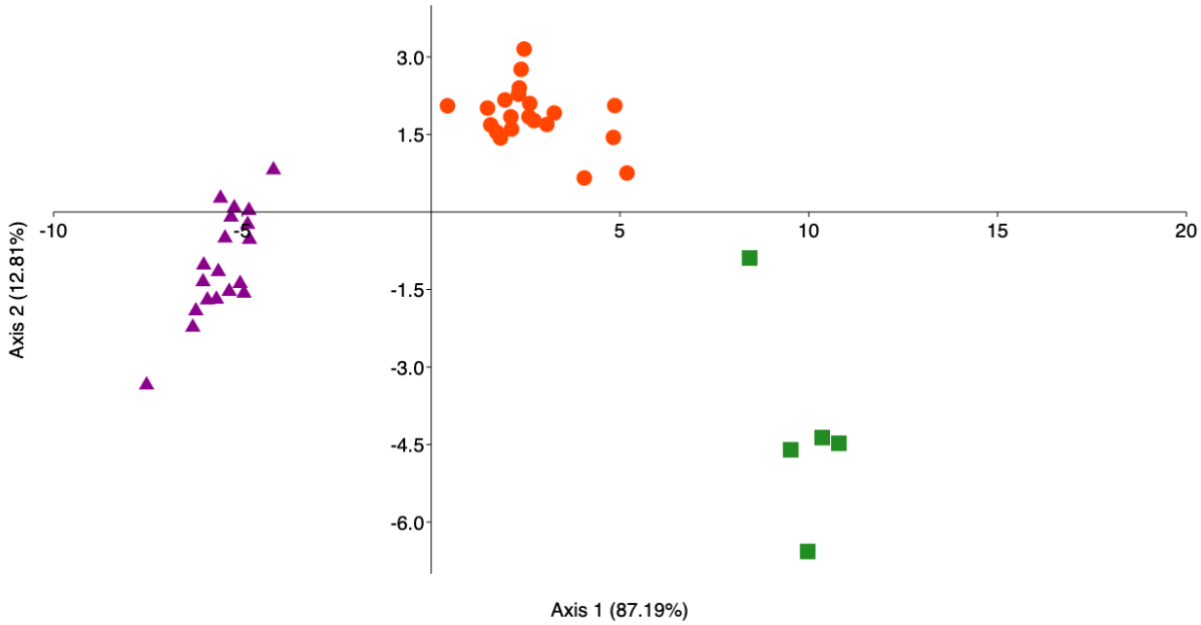

Figure 5. Linear discriminant analysis (LDA) plot between the specimens belonging to size classes I, II and III, calculated on *sagittae* parameters of Messina population.

All *sagittae* measurements showed significant correlation with specimen parameters TL and BW. Results of Spearman correlation analysis are reported in Table 7.

Table 7 Spearman correlation results for Messina specimens

	Spearman r		
	r value	**95% confidence interval**	**P value**
Total length (mm) vs OS	0,8702	0,7709 to 0,9282	<0,0001
Total length (mm) vs OL	0,8751	0,7790 to 0,9310	<0,0001

Total length (mm) vs OW	0,8624	0,7578 to 0,9237	<0,0001
Total length (mm) vs OP	0,8668	0,7653 to 0,9263	<0,0001
Total length (mm) vs Ro	0,6035	0,3689 to 0,7657	<0,0001
Total length (mm) vs FF	-0,778	-0,8744 to -0,6223	<0,0001
Total length (mm) vs E	0,613	0,3829 to 0,7724	<0,0001
Total length (mm) vs P^2/A	0,778	0,6223 to 0,8744	<0,0001
Total length (mm) vs Re	0,3596	0,06494 to 0,5965	0,0153
Total length (mm) vs AR	-0,6137	-0,7724 to -0,3829	<0,0001
Total length (mm) vs OL/TL	-0,8616	-0,9233 to -0,7566	<0,0001
Body weight (g) vs OS	0,8542	0,7442 to 0,9190	<0,0001
Body weight (g) vs OL	0,8583	0,7510 to 0,9214	<0,0001
Body weight (g) vs OW	0,8414	0,7234 to 0,9117	<0,0001
Body weight (g) vs OP	0,8526	0,7416 to 0,9181	<0,0001
Body weight (g) vs Ro	0,6107	0,3788 to 0,7704	<0,0001
Body weight (g) vs FF	-0,7635	-0,8658 to -0,6000	<0,0001
Body weight (g) vs E	0,6216	0,3938 to 0,7775	<0,0001

Body weight (g) vs P^2/A	0,7635	0,6000 to 0,8658	<0,0001
Body weight (g) vs Re	0,3634	0,06929 to 0,5994	0,0141
Body weight (g) vs AR	-0,6216	-0,7775 to -0,3938	<0,0001
Body weight (g) vs OL/TL	-0,8639	-0,9246 to -0,7604	<0,0001

	Spearman r		
	r value	**95% confidence interval**	**P value**
Total length (mm) vs OS	0,8702	0,7709 to 0,9282	<0,0001
Total length (mm) vs OL	0,8751	0,7790 to 0,9310	<0,0001
Total length (mm) vs OW	0,8624	0,7578 to 0,9237	<0,0001
Total length (mm) vs OP	0,8668	0,7653 to 0,9263	<0,0001
Total length (mm) vs Ro	0,6035	0,3689 to 0,7657	<0,0001
Total length (mm) vs FF	-0,778	-0,8744 to -0,6223	<0,0001
Total length (mm) vs E	0,8762	0,7810 to 0,9316	<0,0001
Total length (mm) vs P^2/A	0,778	0,6223 to 0,8744	<0,0001
Total length (mm) vs Re	0,3596	0,06494 to 0,5965	0,0153
Total length (mm) vs AR	-0,6137	-0,7724 to -0,3829	<0,0001

Total length (mm) vs OL/TL	-0,8616	-0,9233 to -0,7566	<0,0001
Body weight (g) vs OS	0,8542	0,7442 to 0,9190	<0,0001
Body weight (g) vs OL	0,8583	0,7510 to 0,9214	<0,0001
Body weight (g) vs OW	0,8414	0,7234 to 0,9117	<0,0001
Body weight (g) vs OP	0,8526	0,7416 to 0,9181	<0,0001
Body weight (g) vs Ro	0,6107	0,3788 to 0,7704	<0,0001
Body weight (g) vs FF	-0,7635	-0,8658 to -0,6000	<0,0001
Body weight (g) vs E	0,859	0,7523 to 0,9218	<0,0001
Body weight (g) vs P^2/A	0,7635	0,6000 to 0,8658	<0,0001
Body weight (g) vs Re	0,3634	0,06929 to 0,5994	0,0141
Body weight (g) vs AR	-0,6216	-0,7775 to -0,3938	<0,0001
Body weight (g) vs OL/TL	-0,8639	-0,9246 to -0,7604	<0,0001

The mean shape of otoliths differed significantly between the 3 size classes investigated ($p < 0.001$). Marked differences in otolith shape have also been confirmed by LDA. From the LDA plot we can observe that the three size classes were quite well separated (Figure 6).

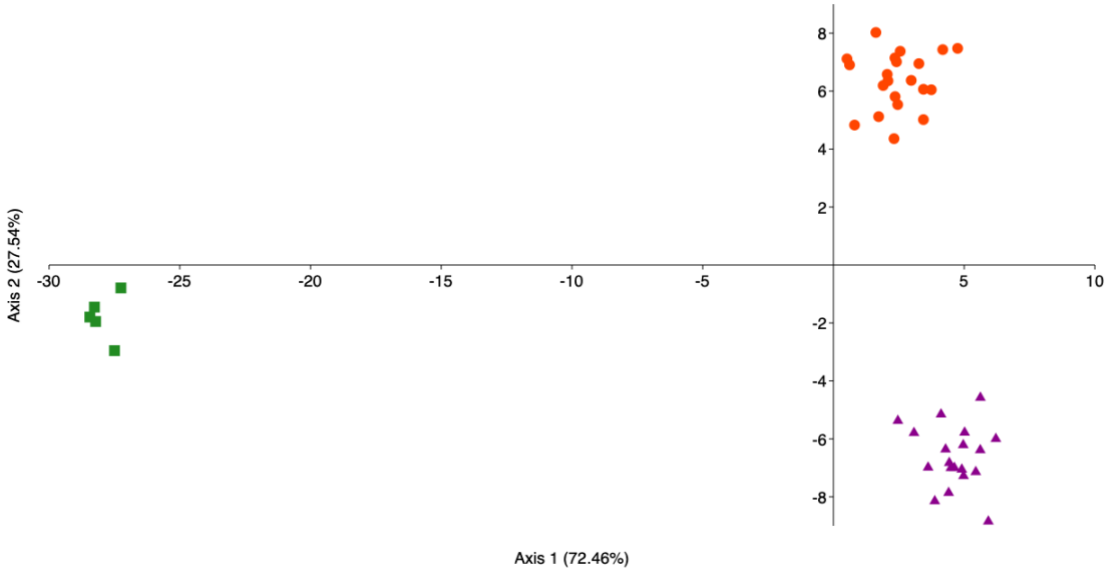

Figure 6 Linear discriminant analysis (LDA) plot between the Messina's specimens belonging to size classes I, II and III, calculated on calculated on elliptic Fourier descriptors.

Concerning *sagittae* belonging to Split specimens, they showed a lanceolate contour, with a marked irregularity of margins. The *rostrum* and *antirostrum* were long, with a wide *excisura* a very acute notch (Figure 7 a-c). Concerning the intra specific differences among size classes, shape analysis showed a general uniform shape (Figure 7 d). The Class I was characterized by most enhanced circular contour than the other classes, with an oblique posterior margin and a not acute notch. In the Class II the notch became more acute than the first Class, and the circular shape started to become flat. In the Class III the *sagittae* were more elliptic than the other classes, as highlighted by the highest E value among size classes (0.41 ± 0.02 mm, see Table 5), with an enhanced length and a reduced width.

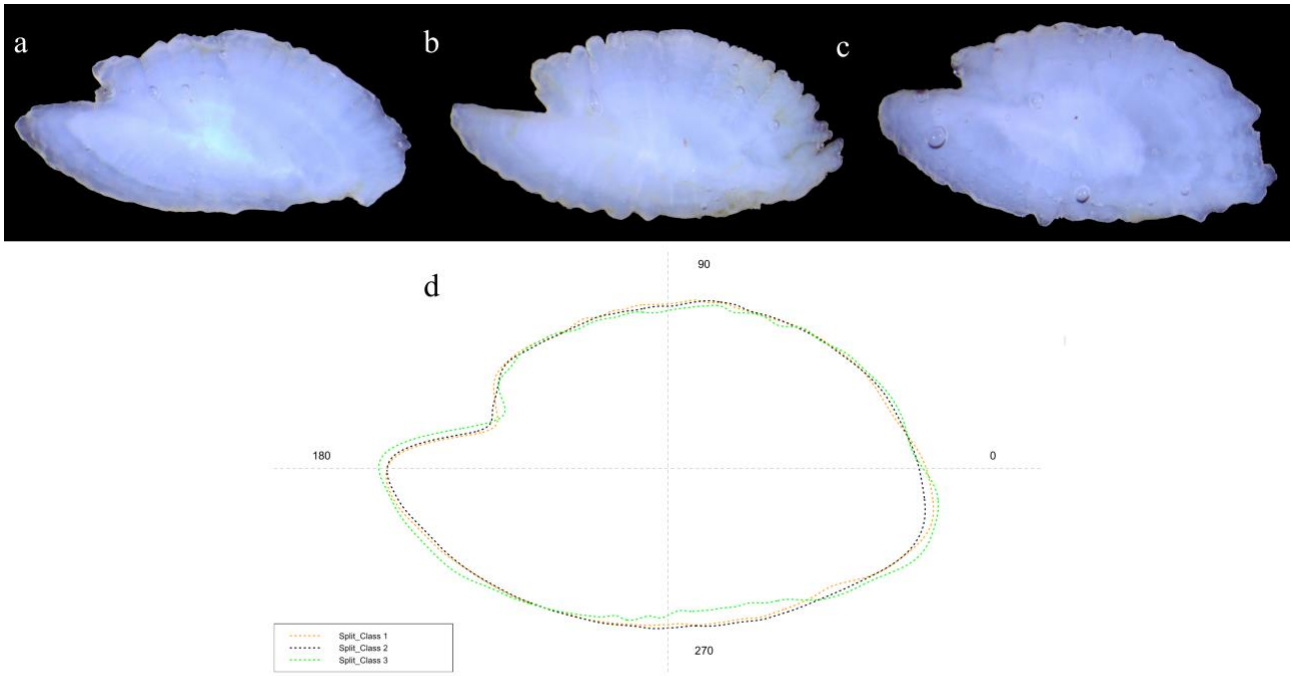

Figure 7. Stereoscope images of the medial view of the *sagittae* belonging to specimens from Split, for the three investigated size classes (a: Class I, b: Class II, c: Class III), with their mean otoliths shape (d)

The specimens examined showed significant variations in total length and body weight between all the three size classes investigated in the study ($p<0.05$).

The results of the variations observed for the individual parameters of the otoliths extracted from each size class are reported in Table 8.

Table 8. Dunn's post hoc test results obtained through the *sagittae* parameters comparison between samples, belonging to Split population, from Class I, II and III. P value legend: (ns), P>0.05, not significant; (*), P<0.05, significant.

	Comparison		
	I *vs* II	**I *vs* III**	**II *vs* III**
Sagittae parameters	p value	p value	p value
OS	0.003*	<0.001*	<0.001*
OL	0.002*	<0.001*	<0.001*
OW	<0.001*	<0.001*	<0.001*
OP	<0.001*	<0.001*	<0.001*
Ro	0.716ns	0.695ns	0.292 ns
FF	0.205ns	0.026*	0.196ns
E	0.999 ns	0.471 ns	<0.029*
P^2/A	0.236ns	0.015*	0.097ns
Re	0.640ns	0.640ns	0.640ns
AR	0.618ns	0.330ns	0.028*
OL/TL	0.121ns	0.011*	0.150*

LDA confirmed the results obtained by univariate analysis (Figure 8), explaining the main differences observed between the size.

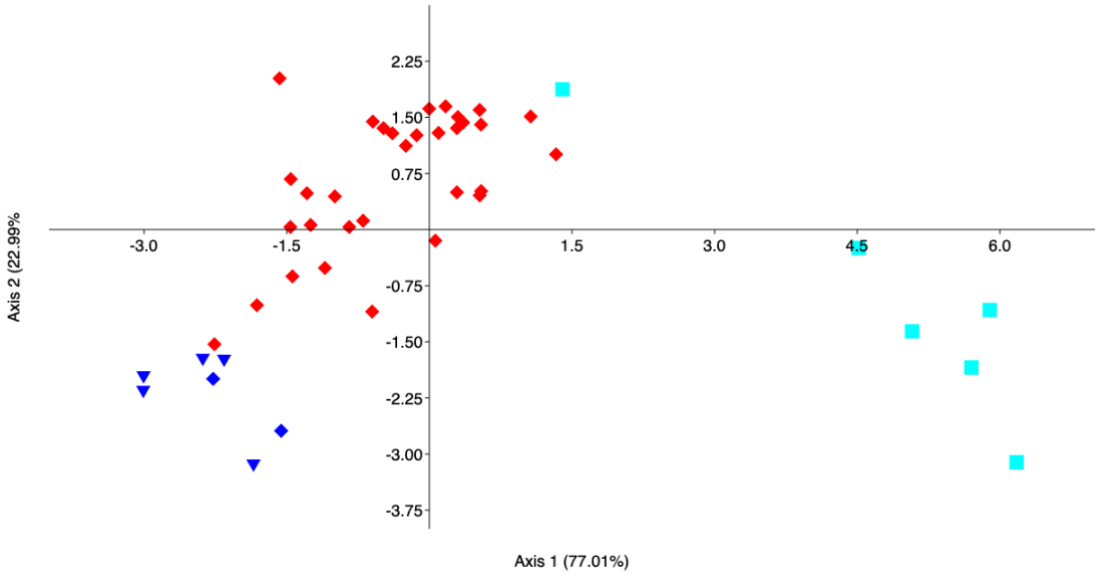

Figure 8. Linear discriminant analysis (LDA) plot between the specimens belonging to size classes I, II and III, calculated on *sagittae* parameters from Split population.

Almost all *sagittae* measurements showed significant correlation with specimen parameters TL and BW. Results of Spearman correlation analysis are reported in Table 9.

Table 9. Spearman correlation results for Split population

	Spearman Correlation		
	r	**95% confidence interval**	**P value**
Total Length (mm) vs OS	0,7055	0,5131 to 0,8305	<0,0001
Total Length (mm) vs OL	0,6988	0,5033 to 0,8263	<0,0001
Total Length (mm) vs OW	0,6053	0,3715 to 0,7670	<0,0001

Total Length (mm) vs OP	0,6709	0,4629 to 0,8089	<0,0001
Total Length (mm) vs Ro	-0,1929	-0,4674 to 0,1155	0,2041
Total Length (mm) vs FF	-0,2544	-0,5165 to 0,05119	0,0917
Total Length (mm) vs E	0,3044	0,0030 to 0,5551	0,0420
Total Length (mm) vs P^2/A	0,2544	-0,05119 to 0,5165	0,0917
Total Length (mm) vs Re	0,06491	-0,2415 to 0,3595	0,6719
Total Length (mm) vs AR	-0,3044	-0,5551 to -0,003034	0,042
Total Length (mm) vs OL/TL	-0,7122	-0,8346 to -0,5229	<0,0001
Body weight (g) vs OS	0,7048	0,5119 to 0,8300	<0,0001
Body weight (g) vs OL	0,7072	0,5154 to 0,8315	<0,0001
Body weight (g) vs OW	0,6043	0,3701 to 0,7663	<0,0001
Body weight (g) vs OP	0,6878	0,4873 to 0,8195	<0,0001

Body weight (g) vs Ro	-0,2315	-0,4984 to 0,0754	0,1260
Body weight (g) vs FF	-0,306	-0,5563 to -0,004762	0,0409
Body weight (g) vs E	0,3225	0,0230 to 0,5688	0.0307
Body weight (g) vs P^2/A	0,306	0,004762 to 0,5563	0,0409
Body weight (g) vs Re	0,03966	-0,2652 to 0,3373	0,7959
Body weight (g) vs AR	-0,3225	-0,5688 to -0,02303	0,0307
Body weight (g) vs OL/TL	-0,6734	-0,8105 to -0,4665	<0,0001

The mean shape of otoliths differed significantly between the 3 size classes investigated ($p < 0.001$). Marked differences in otolith shape have also been confirmed by LDA. From the LDA plot we can observe that the three size classes were quite well separated (Figure 9).

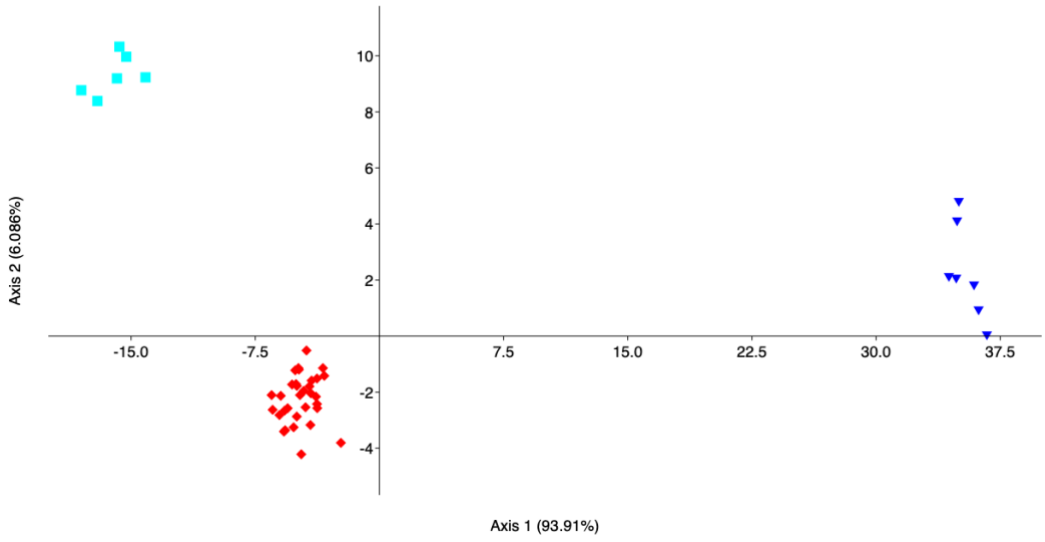

Figure 9. Linear discriminant analysis (LDA) plot between the specimens belonging to size classes I, II and III, from Split calculated on elliptic Fourier descriptors.

3.3 Inter-population differences between sagittae features

Overall, the two populations examined prove to be intimately different both for fish parameters and *sagittae* features (P<0.05), as well confirmed by PCA analysis (PC1 96.10%; PC2 3.51%) (Figure 10).

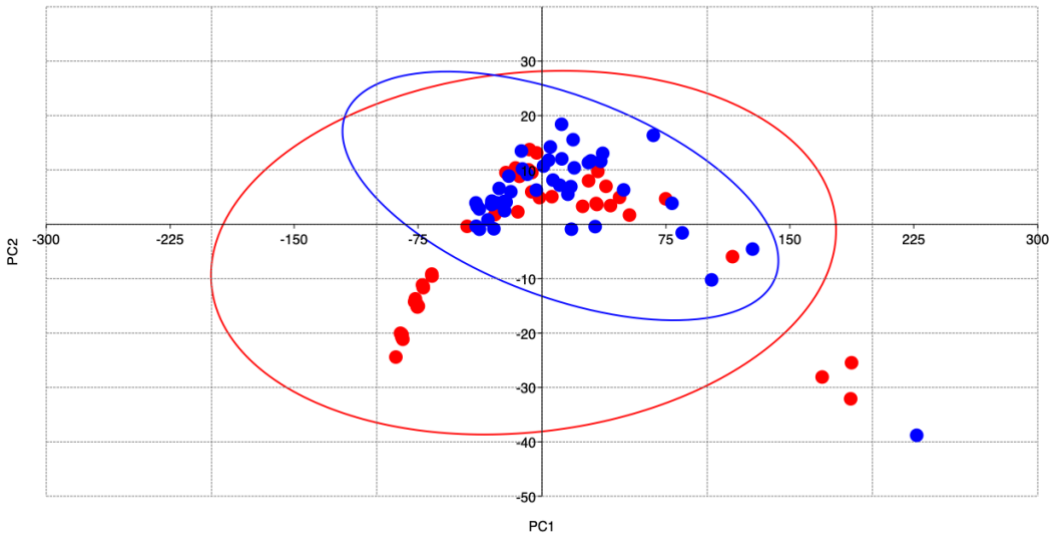

Figure 10. Principal Component Analysis showing fish and *sagittae* features differences between the sampling sites: Messina (red dots) and Split (blue dots)

The results obtained through the Mann Whitney test are reported in Table 10.

Table 10. Mann Whitney test results obtained for otolith morphometric parameters comparison between sampling sites, Strait of Messina, and Split. P value legend: >0.05, not significant (ns); 0.03*, moderately significant; 0.002 **, significant; 0.001 *** highly significant.

	Messina *vs* Split Class I	**Messina *vs* Split Class II**	**Messina *vs* Split Class III**
Sagittae parameters	P value	P value	P value
TL (mm)	<0.0001***	0.3982 ns	0.5368 ns
BW (g)	<0.0001***	0.2002 ns	0.4286 ns
OS	<0.0001***	0.0008***	0.3290 ns
OL	<0.0001***	0.2506 ns	0.2468 ns
OW	<0.0001***	<0.0001***	0.1255 ns
OP	<0.0001***	0.0019***	0.4286 ns
Ro	<0.0001***	<0.0001***	0.0043**
FF	0.0056*	0.8218 ns	0.9307 ns

E	0.8656 ^{ns}	<0.0001***	0.5368 ^{ns}
P^2/A	0.0056*	0.8218 ^{ns}	0.9307 ^{ns}
Re	0.3339 ^{ns}	0.0646 ^{ns}	0.7922 ^{ns}
AR	0.8656 ^{ns}	<0.0001***	0.5368 ^{ns}
OL/TL	0.3002 ^{ns}	0.108 ^{ns}	0.1255 ^{ns}

It is easy to see how the major differences concern size classes I and II. Therefore, it is plausible that the dissimilarities highlighted by the LDA (Figure 11) are to be attributed to the size classes of the specimens.

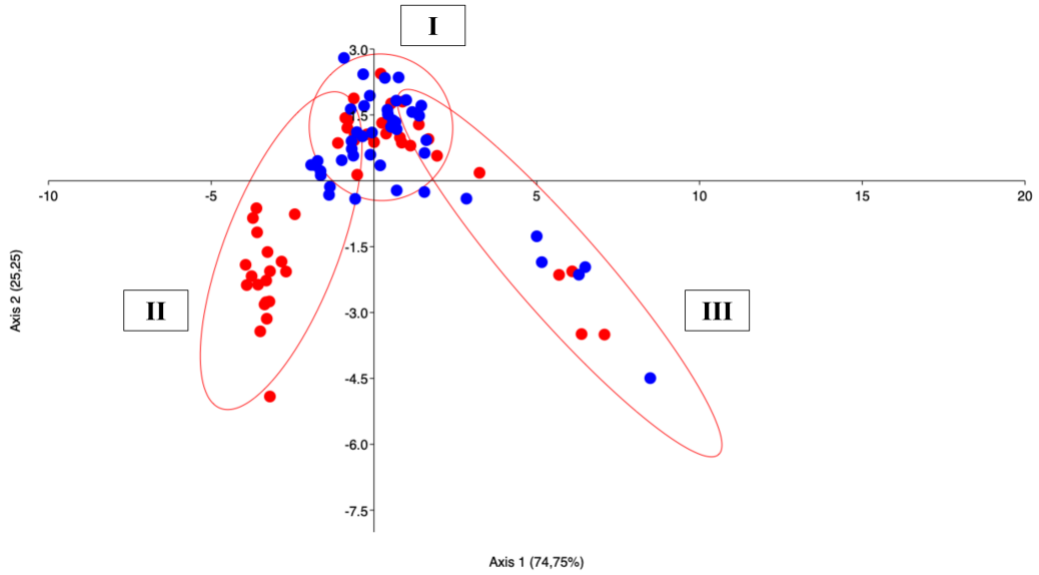

Figure 11. Linear Discriminant Analysis (LDA) between morphometric parameters of the investigated populations for the three investigated size classes.

The analysis of the *sagittae* contours of the two populations examined showed a strong variability between the specimens of class I (p=0.008), class II (p=0.001) and class III (p=0.02). Results of PCA and mean otoliths shapes confirmed the differences observed for each class between the sampling sites, showing a variance of 24.29% (PC1) and 17.16% (PC2) for Class I, 40.32% (PC1) and 18.21% (PC2) for Class II, and 44.37% (PC1) and 18.71% (PC2) for Class III (Figure 12 a-c).

In Figure 12 d-f is provided a comparison of the mean otoliths' contours for the three investigate size classes. Specimens belonging to size Class I showed an enhanced variability concerning the *excisura ostii* and dorsal and ventral margins, more irregular in Split than Messina one. Specimens from Class II showed visible inter-population differences regarding *rostrum* and overall mean contour, oval in individuals from Split and elliptical in those from Messina. In the Class III, the differences detected for the second size class were confirmed, with most marked *excisura ostii* showed by Split specimens

than Messina ones, which reported a less marked irregularity of the margins, a shorter *rostrum* and a less pointed *antirostrum*.

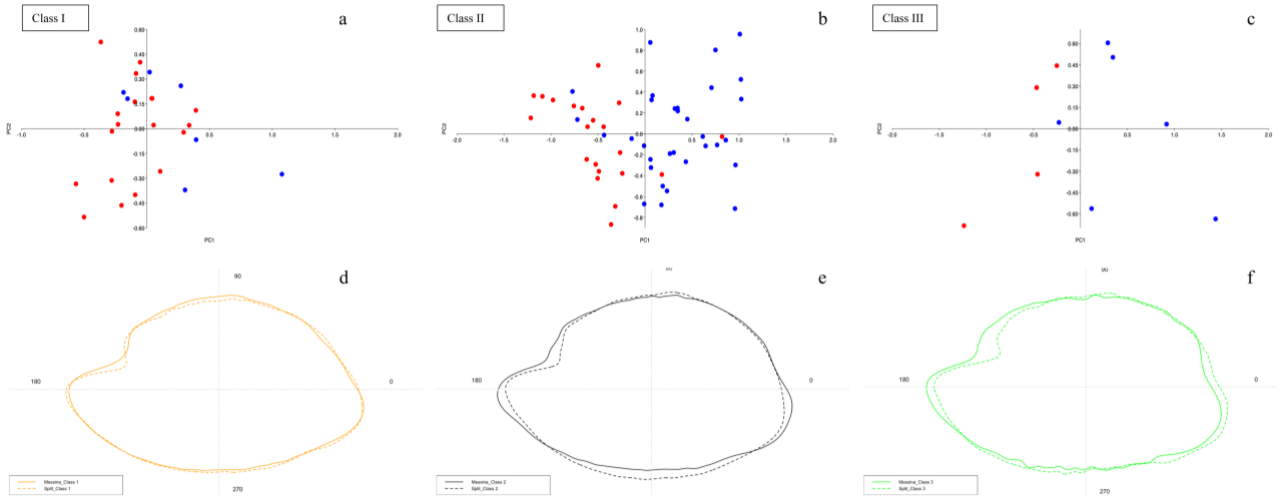

Figure 12. Results of PCA performed on Wavelet coefficient obtained by *sagittae* contours of specimens collected from Messina (red dots) and Split (blue dots). Results are reported for Class I, II and III, figures a, b, and c respectively. Wavelet coefficient variance for each size classes investigated is expressed as percentage. Comparison of the mean otoliths shapes from the two populations is provided in figures d to f, respectively for Class I, II and III

The shape analysis performed on the total interclass samples showed mean *sagittae* shapes clearly different between the two analyzed populations (Figure 13). The main differences were detected in the *rostrum* organization (longer and more pointed in Split population than in the Messina one), in the *excisura ostii* (deeper in Split population than in the Messina one), in the *antirostrum* organization (more prominent and pointed in Split population than in the Messina one), and in the overall *sagittae* shape, oval in Split specimens and elliptical in Messina ones.

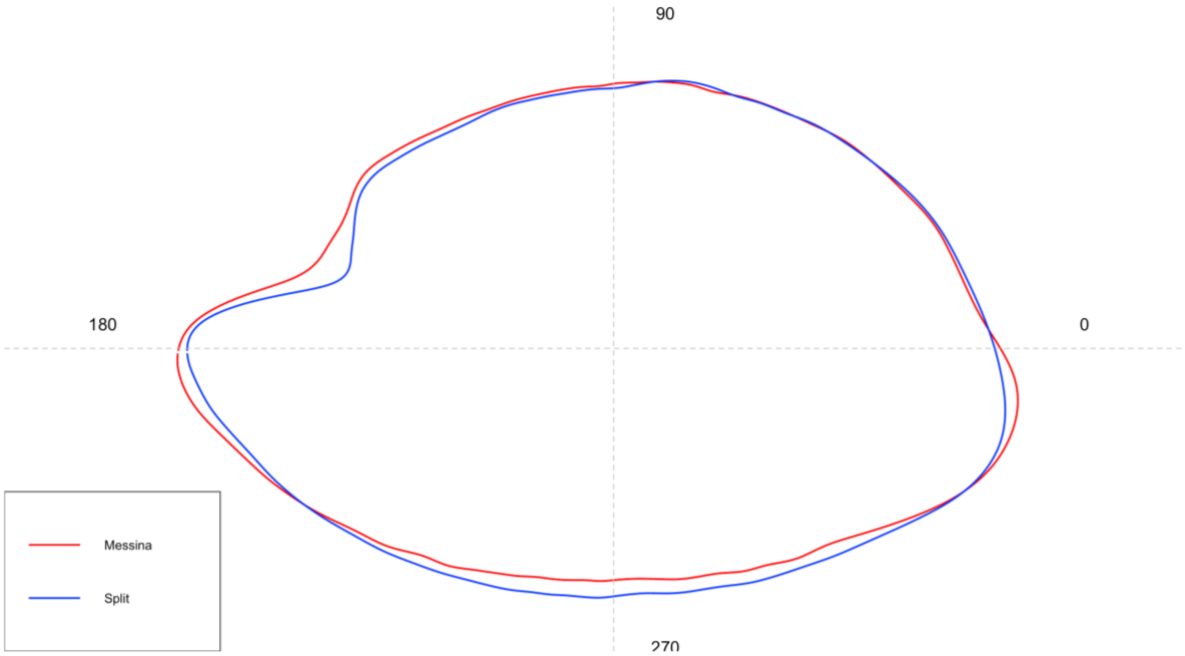

Figure 13. Mean shape of *sagittae* contours of the investigated *S. porcus* population.

3.4 Stomach content analysis

The analysis of the 49 sampled stomachs (9 empty stomachs, with a Vacuity Index of 4.9) have shown a total of 80 preys, belonging to 29 taxa. As reported in Table 11, Crustacea and Osteichthyes were the major taxa with the highest number of preys, with also the highest values of IRI %. The infraorder Brachyura was the taxon which showed the highest IRI % value (IRI % = 32.81), followed by the species, belonging to the infraorder Brachuyra, *Pachygrapsus marmoratus* (Fabricius, 1787) (IRI % = 27.59), that was the taxon with the highest relative abundance (N % = 18.75) among the preys. The order Amphipoda (IRI % = 10.74) and the species *Xantho pilipes* (A. Milne-Edwards, 1867) (IRI % = 9.86), belonging to the infraorder Brachuyra, were the other two most relevant taxa for relative importance. Concerning the Osteichthyes preys, those belonging to the species *Chelon auratus* (Risso, 1810) (IRI % = 3.24) and *Thalassoma pavo* (Linnaeus, 1758) (IRI % = 2.36) were the most relevant preys, with the genus *Parablennius* as taxon with the highest relative abundance value (N % = 2.50). Concerning the class Polychaeta, it was the major taxa with the less relative importance (IRI % = 0.15).

Table 11. Diet composition of *S. porcus* individuals with %N (relative abundance), %W (percentage in biomass), %F (frequency of occurrence), IRI (index of relative importance) and %IRI (index of relative importance expressed as percentage) expressed for each prey items.

TAXA	N%	W%	F%	IRI	IRI%
Polychaeta	1,25	0,04	1,59	2,044	0,15
Total Polychaeta	**1,25**	**0,04**	**1,59**	**2,044**	**0,15**
Xantho pilipes	6,25	14,39	6,35	131,036	9,86
Brachinotus sexdentatus	1,25	1,74	1,59	4,742	0,36
Pachygrapsus marmoratus	18,75	14,24	11,11	366,524	27,59
Pachygrapsus sp	1,25	2,11	1,59	5,341	0,40
Inachus dorsettensis	1,25	0,30	1,59	2,464	0,19
Percnon gibbesi	1,25	1,74	1,59	4,742	0,36
Brachyura	16,25	4,87	20,63	435,843	32,81
Palemon sp	3,75	1,02	4,76	22,7	1,71
Lysmata sp	1,25	0,38	1,59	2,58	0,19
Athanas nitescens	1,25	0,04	1,59	2,0	0,15
Palaemon elegans	1,25	0,26	1,59	2,40	0,18
Dendrobranchiata	6,25	0,94	7,94	57,10	4,30
Decapoda n.d.	1,25	0,04	1,59	2,04	0,15
Total Decapoda	**61,25**	**42,07**	**63,49**	**1039,57**	**78,26**
Lysianassa sp	1,25	0,04	1,59	2,04	0,15
Dexamine spinosa	1,25	0,04	1,59	2,0	0,15
Microdeutopus sp	1,25	0,04	1,59	2,04	0,15
Amphipoda	12,50	0,34	11,11	142,67	10,74
Dynamenella sp	1,25	0,04	1,59	2,04	0,15
Sphaeroma sp	7,50	0,68	3,17	25,97	1,95
Isopoda	1,25	0,11	1,59	2,16	0,16
Total Peracarida	**26,25**	**1,28**	**22,22**	**178,97**	**13,47**
Crustacea n.d	1,25	0,08	1,59	2,10	0,16
Total Crustacea	**88,75**	**43,43**	**87,30**	**1220,65**	**91,90**
Chelon auratus	1,25	25,83	1,59	42,99	3,24
Tripterygion delaisi	1,25	0,08	1,59	2,10	0,16
Gobius sp	1,25	4,34	1,59	8,88	0,67
Gobius incognitus	1,25	6,34	1,59	12,05	0,91
Thalassoma pavo	1,25	18,50	1,59	31,36	2,36
Parablennius sp	2,50	0,83	1,59	5,29	0,40
Osteichtyes n.d.	1,25	0,60	1,59	2,94	0,22
Total Osteichtyes	**10,00**	**56,53**	**11,11**	**105,61**	**7,95**

DISCUSSION

Data obtained have shown an enhanced inter population variability concerning *S. porcus* from the two studied areas. The differences mainly involved the growth dynamics, age structure and *sagittae* features. While, concerning diet composition, results showed a similarity between the feeding habits of the studied species in the two areas, especially regarding the major taxa of the main preys. The maximum age estimated was higher in Split (8) than in Messina (5), with the von Bertalanffy growth curves which have shown K parameters higher in Messina, and L_{∞} parameters higher in Split. The age structures were very different, with the population of Messina that was mainly composed by specimens belonging to the third age class (3), with length-at-age values significantly higher than those showed by Split specimens. All these data indicated a faster growth rate of the studied species in the Strait of Messina than in Split area, as also highlighted by the growth performance index, that was higher for Messina population. These data have confirmed the high degree of populations separation in *S. porcus*, as also highlighted by the different growth parameters and age structures reported by results from others geographical area [6,13,17,18,20]. This heterogeneity is common in low range benthic species with a high site fidelity, as *S. porcus*, in which biological traits often responds to local environmental conditions [28]. Concerning the variation in growth rates between the two studied populations, this could be related to the different oceanographic and environmental conditions of the sampling areas. The Strait of Messina represents a singularity inside the Mediterranean Sea, with a unique hydrographic regime and a peculiar seawater masses chemistry [93,99]. The intense hydro-dynamism, together with the massive presence of "upwelling" events, make this area an "Atlantic Island" inside the Mediterranean basin, with oxygen concentrations, nutrients, and temperature similar to those reported for the Atlantic Ocean [100,118]. Otherwise, the Adriatic Sea generally shows a pronounced seasonality and an enhanced longitudinal gradient in dissolved oxygen, temperature, nutrients, salinity, and chlorophyll a [119], with urbane discharges, aeolian inputs, underground waters and surface runoff representing the main nutrients sources. In surface layers, nutrients exhibit a progressive decline in concentration, and in the middle and southern Adriatic, an amplitude seasonality decrease [120]. According to literature, different oceanographic features can influence the growth dynamics of species, resulting in a faster growth in populations inhabiting cold and productive water masses, than those from less productive and warm ones [121]. In addition to the oceanographic differences between the water masses, also the environmental conditions experienced by the studied populations in the two different habitats were completely different. Specimens from Messina were sampled in the tidal ponds present in the beach rock

formations, with reduced depth and large variations, also daily, of both biotic and abiotic conditions, related to tidal cycles and storms [96]. This represents an "extreme" environment, and it is considered a perfect case of study to explore the behavioral, physiological and morphological adaptations of marine species to peculiar hydrographic and ecological conditions [93,96,122]. Tidal pools are a shelter from the intense hydro-dynamism affecting the area, a nursery area and a perfect hunting ground for many predators, *S. porcus* included. Conversely, the biotope of the coastal waters near Split is the classical environment inhabited by the studied species, and other scorpaenids, in the Mediterranean Sea. It is characterized by depths ranging from 10 and 40 m, the presence of rocky bottoms covered by algae, sandy bottoms, and patches of *P. oceanica.* Specimens for Split area here analyzed were sampled at an average depth of 20 m, very different from that of the tidal ponds of the Messina's beachrock formations. According to literature [7,123,124], these differences in biotic and abiotic environmental conditions between the two studied areas could drive the inter populations growth dynamics variations showed by results.

It well known as temperature can influence the metabolism, and consequently the growth rates, of several teleost species [125–127], but also food availability and quality can shape them [123,128].

Results from the stomach content analysis on specimens sampled in Messina showed a high selectivity for decapods preys, as assessed also for other Scorpaenidae species from other geographical areas [7–10,129]. The high relevance of brachyuran decapods (e.g., *X. pilipes, P. marmoratus,* Brachyura) reported by results was also in line with literature data on the studied species from others geographical areas, but some differences regarding the contribution of teleost fishes, peracarids crustaceans and mollusks were detected. The differences in feeding habits with *S. porcus* population from Split mainly consisted in the completely absence of Mollusks and Anomura from the diet of Messina's species. According to literature [7], these preys' items represent an important source of food for Split population, together with teleost fishes and Caridea decapods, that showed a reduced occurrence in Messina specimens. Concerning peracarids crustaceans (e.g., Amphipoda and Isopoda), they were well represented in the stomach content from Messina, but they are very marginal in the diet composition from Split area. This variability in peracarids preys could be strictly related to the biocenosis present in the tidal pools of the beachrock formations of Messina, rich in Amphipods and Isopods (being the perfect habitats for them [130]). Indeed, the presence of these crustaceans in the diet of this Scorpaenidae species has been reported also from other similar formations present in Spain (Gulf of Cadiz) [10]. These feeding habits differences at inter population level have confirmed the role of generalist and opportunistic feeder of the studied species, capable to adapt its diet to the preys' availability of the different areas. This is an essential feature which allowed this species to inhabit a wide range of Mediterranean areas and habitats. Further analyses on a wider temporal scale are

required to better reconstruct the feeding habits and diet composition of *S. porcus* during the entire year in the tidal ponds of the Strait of Messina. This is essential to understand how much diet variations, added to the other genetic and environmental features, can allow to the differences in growth rates between the two populations highlighted by results.

Fish growth dynamic and metabolism, such as biotic and abiotic habitat features, can also influence otoliths growth and, consequently, their morphometry and shape [131]. Lifestyle, diet composition, food quality and feeding fitness have a role in otoliths' morphology, shape, growth patterns and physiology [36,132,133]. According to literature [73,134–137], otoliths shape and morphometry are influenced by water temperature, depth (e.g., size of otoliths increase with greater depths and warmer water masses), genetic and lifestyle of the species (e.g., epipelagic species show smaller and more elongated *sagittae* than benthic ones). Thanks to this high sensitivity to environmental conditions, otoliths (especially *sagittae*) have become an essential tool in fish stocks assessment and populations discrimination. This was confirmed by results on *S. porcus* inter population analysis on *sagittae.* The overall morphology and shape of both the populations were in line with data from literature, with several differences in morphometry. Tuset et al. [76] reported rectangularity and circularity values, for specimens from western and central Mediterranean Sea, different from those of both the analyzed populations; while Yedier et al. [138] reported, from the Black Sea, Aegean Sea and Sea of Marmora, different shape indices values, e.g., roundness, ellipticity and aspect ratio. This shape heterogeneity of *sagittae* was also evident comparing Split and Messina populations. As highlighted by the overall contours and the statistical analysis on the morphometrical parameters between the two populations, specimens from Split showed wider, double picked (with an enhanced *antirostrum*) more circular *sagittae*, than those from Messina. Otherwise, these last showed more lanceolate, larger, with a most marked *rostrum, sagittae*, with higher otolith surface values and a more elliptical than circular shape. Several factors could have induced these differences, being otoliths under a double control of genetic and environment, and sensitive to variation in physiological and metabolic individuals' conditions. According to Vignon and Morat [89], different environmental factors can reshape the overall *sagittae* outlines, while genetic variations at intra-specific level, related to long time separation between the populations, only influence the shape of the otoliths locally (mainly at *rostrum* and *antirostrum* level). Concerning the environmental conditions experienced by the two populations, one of the most evident differences between the two sampling areas was the depth range, significantly higher in Split than in Messina. Indeed, it is widely reported how species and populations inhabiting deeper habitats show wider, more circular *sagittae* than those from shallower ones [135,136,139]. This finding is in line with results, which showed also most lanceolate *sagittae* in specimens from Messina, inhabiting a very shallow environment. The sound scape can be another factor that can strongly influence the

otolith morphology and development. Indeed, according to the sensory drive hypothesis postulated by Endler [140,141] there is a coevolution between detected signals and sensory systems, with the speciation that may be strongly influenced by the diversification of the organisms' sensory interactions and environment. This is strongly evident in deep species and in species that use sound to communicate (as rockfishes [142]), The soundscapes experienced by individuals drive a selection on the form-function of the fishes' auditory system, with species or group of individuals sharing a similar surrounding soundscape that could express a inner ears' phenotypic similarity, expressed by otolith morphology and shape [92,143]. This could be also the case of the two analyzed *S. porcus* populations, with the differences related to the soundscapes of the two different studied area that may have also influenced the detected *sagittae* variability in morphology, morphometry and shaèe. Also metabolic rate and somatic growth can influence otolith features, such as morphometry, size and shape [36,52]. Messina population showed a faster growth than the Split one, which could be related to several environmental factors, such as the most enhanced availability of food in the tidal ponds habitats [130], which could result in a major food intake. It is not clear the relation between somatic growth, metabolic rate, food intake and otoliths size and growth, also because a faster fish growth and a most enhanced food intake not always results in larger otoliths [131,144]. Concerning the differences among the size classes at inter population level, statistical analysis highlighted significant shape differences between the three size classes, while size Classes III were the only with no significant differences in morphometry between the two populations. This could be related to the life habits of the specimens from Messina, which could pass more time inside the tidal ponds of the beachrock formations during the first part of their life, searching for shelter and a good hunting ground, as reported for other teleost species in the area [93,96]. Indeed, tidal pools are recognized worldwide as an important nursery area for several teleost families, that in these environments can found shelter from predators and an increased preys availability [130,145,146]. This could explain the more significant morphometrical differences at inter population level between the size classes I and II than the third. According to literature, otoliths shape and morphometry are under the control of both genetic and environmental influences [147]. The environment can strongly shape the sensory organs, as also highlighted by the sensory drive hypothesis, tested by Tuset et al. [137] on the *sagittae* of others Scorpaenidae species (*Sebastes spp*). Specimens belonging to the first and the second size classes could be more influenced by the beachrock's tidal ponds than the third, spending more time in these habitats. Getting larger, *S. porcus* individuals could, conversely, spend more time in the nearshore coastal waters (reentering in the tidal pounds searching for food, as reported for several transient species inhabiting these environments worldwide [130]), with biotopes and depths like those present in the Split area. This could also explain the absence of significant intra population differences

between the three sizes classes in shape indices of individuals from Split, highlighted by Dunn's post hoc test at intra population level. Otherwise, the Messina specimens were characterized by a most enhanced variability in morphometrical parameters, especially between the first and the other size classes, than Split ones, which showed an enhanced morphometric stability between the three classes.

CONCLUSION

Assess and explore the variations in ecomorphological features and population parameters at inter population level is essential for both conservation porpoises (being morphological features, such as those related to otoliths, and population dynamics widely used in stock assessment) and ecological studies. The eco-morphological adaptation of species to different habitats and environmental features is the basis of the phenotypic plasticity (i.e., the capability to express different phenotypes as a result of different environmental factors) [148]. This becomes an essential concept for the identification of the marine fishes' populations, being assumed that each population, living under peculiar environmental conditions, can display specific phenotypes under the regulation of genetic and/or environmental mechanisms [149–151]. This process, being also the basis of the stock's differentiation, assumes a relevant importance in the conservation of fishery resources and in the maintenance of marine ecosystems well-being. The detection of phenotypic features (e.g., body shape, growth parameters, otoliths microstructure and shape) is widely used for the stock assessment, together with the populations' parameters and life history patterns (e.g., age structure, length at age distribution, length frequency distribution, sex ratio), and it is also involved in the fishing pressure monitoring [32,152–154]. For all these reasons, it is essentials to improve the knowledge base on the population structure of the marine teleost species, especially those with a high ecological and commercial value, exploring the relations between the inter population variability in eco-morphology, population dynamics and the environment.

Concerning the studied species, further analyses are required to knowledge the direct influence of the environment on the inter population differences regarding *sagittae* features and somatic growth dynamics. It will be essential to add phylogenetic analysis to understand how much the detected inter population differences could be influenced by genetic and/or environmental factors. The dual regulation, both genetically and environmentally related, of otoliths shape and growth is still widely recognized, especially at inter specific level [136,155]. At intra specific level, in the context of the stock discrimination, it is not clear the relative influence of genetic/environment on otoliths shape, morphometry and morphology [156]. Vignon and Morat [89] have confirmed the dual regulation of otoliths also at intra population level, investigating *Lutjanus kasmira* (Forsskål, 1775) specimens

intentionally introduced in a Hawaiian islands from the French Polynesia. The detected differences between Messina and Split populations have involved both the overall *sagittae* outlines and the local otoliths shape, suggesting, also for the studied specimens, the influence of both contrasting environmental factors and inter population genetics variations, related to long time separation. The overall shape differences could highlight the influence of the depth (very different between the two sampling areas), while the faster somatic growth rate detected in Messina population could assessed the influence of oceanographic features on fish metabolism and growth dynamics (with a faster growth reported in the population from the Strait of Messina area, characterized by cold and productive waters). Concerning diet composition, further analysis on feeding habits of specimens from Messina, exploring the seasonal composition of diet and metabolic rates, are required to deepen the knowledge on the influence of diet composition, food intake and metabolism on somatic growth and otoliths features.

In conclusion, present paper assessed both the reliability of *S. porcus* as model species to explore the eco-morphological variability of otoliths and population dynamics plasticity, and the reliability of otoliths shape and morphometric analysis for the populations' discrimination in the studied species. The low home-range distribution of this benthic species, its heterogeneity in growth somatic patterns and feeding habits related to different environments, added to the high inter population variability of *sagittae* in shape and morphometry reported by results, make *S. porcus* perfect to explore the influence of different environmental conditions on teleost species. Populations inhabiting the tidal ponds of the beachrock formations could be a perfect case of study to understand how teleost species can adapt to extreme environmental conditions and peculiar habitat features. Future analysis on populations dynamics and seasonal distribution of the studied species in this peculiar environment are required, to understand at all the ecology of this species and its life habits in these habitats. Moreover, it will be also essential to provide valuable data about the species composition and ecological inter specific dynamics existing in tidal pounds, recognized worldwide as fundamental nursery areas and feeding grounds for several marine species, and, consequently, as important biocenosis for the well-being and the conservation of the marine biodiversity.

BIBLIOGRAPHY

1. Nelson, J.S.; Grande, T.C.; Wilson, M.V.H. *Fishes of the World: Fifth Edition*; 2016; ISBN 9781119174844.
2. Fricke, R.; Golani, D.; Appelbaum-Golani, B.; Zajonz, U. Scorpaena decemradiata new species (Teleostei: Scorpaenidae) from the gulf of aqaba, northern red sea, a species distinct

from scorpaena porcus. *Sci. Mar.* **2018**, *82*, 169–184, doi:10.3989/scimar.04824.17A.

3. Wheeler, A.; Whitehead, P.J.P.; Bauchot, M.-L.; Hureau, J.-C.; Nielsen, J.; Tortonese, E. Fishes of the North-Eastern Atlantic and the Mediterranean. Vol. 1. *Copeia* **1986**, *1986*, 266, doi:10.2307/1444931.
4. Mahé, K.; Goascoz, N.; Dufour, J.L.; Iglesias, S.P.; Tetard, A. Black scorpionfish Scorpaena porcus (Scorpaenidae): A first record in the eastern English Channel. *Mar. Biodivers. Rec.* **2014**, *7*, e6, doi:10.1017/S1755267214000037.
5. Poutiers, J.M. FICHES FAO D'IDENTIFICATION DES ESPECES POUR LES BESOINS DE LA PECHE. MEDITERRANEE ET MER NOIRE ZONE DE PECHE 37 Révision 1 Volume 1 VEGETAUX ET INVERTEBRES. *Vertebres* **1987**, *2*.
6. Pashkov, A.N.; Shevchenko, N.F.; Oven, L.S.; Giragosov, V.E.; Kruglov, M.V. Distribution, numbers and principal population indexes of Scorpaena porcus under anthropogenic pollution of the Black Sea. *J. Ichthyol.* **1999**, *39*, 634–641.
7. Ferri, J.; Matić-Skoko, S. The spatial heterogeneity of the black scorpionfish, scorpaena porcus (Scorpaenidae): Differences in length, dietary and age compositions. *Appl. Sci.* **2021**, *11*, 11919, doi:10.3390/app112411919.
8. Aydin, M.; Mazlum, R.E. Feeding ecology of black scorpion fish (Scorpaena porcus Linnaeus, 1758) in SE Black Sea region, (Ordu) Turkey. *J. Mar. Biol. Assoc. United Kingdom* **2020**, *100*, 435–444, doi:10.1017/S002531542000020X.
9. Başçïnar, N.S.; Sağlam, H. Feeding habits of black scorpion fish scorpaena porcus, in the South-Eastern Black Sea. *Turkish J. Fish. Aquat. Sci.* **2009**, *9*, 99–103.
10. Compaire, J.C.; Casademont, P.; Cabrera, R.; Gómez-Cama, C.; Soriguer, M.C. Feeding of Scorpaena porcus (Scorpaenidae) in intertidal rock pools in the Gulf of Cadiz (NE Atlantic). *J. Mar. Biol. Assoc. United Kingdom* **2018**, *98*, 845–853, doi:10.1017/S0025315417000030.
11. Demirhan, S.A.; Can, M.F. Age, growth and food composition of Scorpaena porcus (Linnaeus, 1758) in the southeastern Black Sea. *J. Appl. Ichthyol.* **2009**, *25*, 215–218, doi:10.1111/j.1439-0426.2009.01217.x.
12. Rosca, I.; Arteni, O. Feeding ecology of black scorpionfish (Scorpaena porcus Linnaeus, 1758) from the Romanian Black Sea (Agigea-Eforie Nord area). *ABAH Bioflux* **2010**, *2*, 39–46.
13. Kutsyn, D.N.; Skuratovskaya, E.N.; Chesnokova, I.I. Body Size, Age Structure, Growth, and Maturation of Black Scorpionfish Scorpaena porcus (Scorpaenidae) from Southwestern Crimea (Black Sea). *J. Ichthyol.* **2019**, *59*, 864–869, doi:10.1134/S0032945219060067.
14. La Mesa, M.; Scarcella, G.; Grati, F.; Fabi, G. Age and growth of the black scorpionfish,

Scorpaena porcus (Pisces: Scorpaenidae) from artificial structures and natural reefs in the Adriatic Sea. *Sci. Mar.* **2010**, *74*, 677–685, doi:10.3989/scimar.2010.74n4677.

15. Bradai, M.N.; Bouain, A. Age et croissance de Scorpaena porcus et Scorpaena scrofa du golfe de Gábes. *Oebalia* **1988**, *15*, 13–38.
16. Unsal, N.; Oral, M. An investigation on the Growth and Reproduction Characteristics of the Black Scorpionfish in the Sea of Marmara. *Turkish J. Zool.* **1994**, *20*, 303–308.
17. Sahin, C.; Erbay, M.; Kalayci, F.; Ceylan, Y.; Yesilcicek, T. Life-history traits of the Black Scorpionfish (Scorpaena porcus) in southeastern Black Sea. *Turkish J. Fish. Aquat. Sci.* **2019**, *19*, 571–584, doi:10.4194/1303-2712-v19_7_04.
18. Jardas, I.; Pallaoro, A. Age and growth of black scorpionfish, Scorpaena porcus L., 1758 in the Adriatic Sea. *Rapp. la Comm. Int. pour Mer Méditerranean* **1992**, *33*, 296.
19. Ferri, J.; Stagličić, N.; Matić-Skoko, S. The black scorpionfish, Scorpaena porcus (Scorpaenidae): Could it serve as reliable indicator of Mediterranean coastal communities' health? *Ecol. Indic.* **2012**, *18*, 25–30, doi:10.1016/j.ecolind.2011.11.004.
20. Kuzminova, N.; Rudneva, I.; Salekhova, L.; Shevchenko, N.; Oven, L. State of black scorpionfish (Scorpaena porcus Linnaeus, 1758) inhabited coastal area of Sevastopol region (Black sea) in 1998-2008. *Turkish J. Fish. Aquat. Sci.* **2011**, *11*, 101–111.
21. Medinets, S.; Medinets, V. Results of investigations of atmospheric pollutants fluxes in zmeiny island in western part of the black sea in 2003-2007 years. *J. Environ. Prot. Ecol.* **2010**, *11*, 1030–1036.
22. Rudneva, I.I.; Shevchenko, N.F.; Zalevskaya, I.N.; Zherko, N. V. Biomonitoring of the coastal waters of the Black Sea. *Water Resour.* **2005**, *32*, 215–222, doi:10.1007/s11268-005-0028-x.
23. Oven, L.S.; Rudneva, I.I.; Shevchenko, N.F. Responses of Scorpaena porcus(Scorpaenidae) to Anthropogenic Impact. *J. Ichthyol.* **2000**, *40*, 70–73.
24. JARDAS, I. Review of long-term changes in trammel bottom set catches, crustacean, cephalopoda and fish communities along the eastern Adriatic (Croatian) coastal area. *Acta Adriat.* **1999**, *40*, 67–78.
25. Jardas, I.; Pallaoro, A.; Kraljević, M.; Dulćić, J.; Cetinić, P. Long-term changes in biodiversity of the coastal area of the eastern Adriatic: Fish, crustaceam and cephalopoda communities. *Period. Biol.* **1998**, *100*, 19–28.
26. Stagličić, N.; Matić-Skoko, S.; Pallaoro, A.; Grgičević, R.; Kraljević, M.; Tutman, P.; Dragičević, B.; Dulčić, J. Long-term trends in the structure of eastern Adriatic littoral fish assemblages: Consequences for fisheries management. *Estuar. Coast. Shelf Sci.* **2011**, *94*,

263–271, doi:10.1016/j.ecss.2011.07.005.

27. Forcada, A.; Valle, C.; Bonhomme, P.; Criquet, G.; Cadiou, G.; Lenfant, P.; José, L.S.L. Effects of habitat on spillover from marine protected areas to artisanal fisheries. *Mar. Ecol. Prog. Ser.* **2009**, *379*, 197–211, doi:10.3354/meps07892.
28. Özgül, A.; Lök, A.; Tansel Tanrıkul, T.; Alós, J. Home range and residency of Scorpaena porcus and Scorpaena scrofa in artificial reefs revealed by fine-scale acoustic tracking. *Fish. Res.* **2019**, *210*, 22–30, doi:10.1016/j.fishres.2018.10.008.
29. Goñi, R.; Adlerstein, S.; Alvarez-Berastegui, D.; Forcada, A.; Reñones, O.; Criquet, G.; Polti, S.; Cadiou, G.; Valle, C.; Lenfant, P.; et al. Spillover from six western Mediterranean marine protected areas: Evidence from artisanal fisheries. *Mar. Ecol. Prog. Ser.* **2008**, *366*, 159–174, doi:10.3354/meps07532.
30. García-Rodríguez, M.; Fernández, Á.M.; Esteban, A. Characterisation, analysis and catch rates of the small-scale fisheries of the Alicante Gulf (SE Spain) over a 10 years time series. *Fish. Res.* **2006**, *77*, 226–238, doi:10.1016/j.fishres.2005.09.002.
31. Forcada Almarcha, A.; J.T. Bayle Sempere, J.L.S. lizaso Evaluación de las áreas marinas protegidas y su efecto en pesquerías artesanales del Mediterráneo Occidental. *Dep. Ciencias del Mar y Biol. Apl.* 2007, 402 pp.
32. Perdichizzi, A.; D'Iglio, C.; Giordano, D.; Profeta, A.; Ragonese, S.; Rinelli, P. Comparing life-history traits in two contiguous stocks of the deep-water rose shrimp Parapenaeus longirostris (H. Lucas, 1846) (Crustacea: Decapoda) in the Southern Tyrrhenian Sea (Central Mediterranean Sea). *Fish. Res.* **2022**, *248*, 106206, doi:10.1016/j.fishres.2021.106206.
33. Cochrane, K. (ed. . *A fishery manager's guidebook – Management measures and their application. FAO Fisheries Technical Paper No. 424.*; Food & Agriculture Org., 2002; ISBN 9251047731.
34. Charles, A.T. *Sustainable Fishery Systems. Fish and aquatic resources series*; vol 10.; Blackwell Science, Ltd., 2001; ISBN 9780632057757.
35. Dimech, M.; Kaiser, M.J.; Ragonese, S.; Schembri, P.J. Ecosystem effects of fishing on the continental slope in the Central Mediterranean Sea. *Mar. Ecol. Prog. Ser.* **2012**, *449*, 41–54, doi:10.3354/meps09475.
36. Schulz-Mirbach, T.; Ladich, F.; Plath, M.; Heß, M. Enigmatic ear stones: what we know about the functional role and evolution of fish otoliths. *Biol. Rev.* **2019**, *94*, 457–482, doi:10.1111/brv.12463.
37. Nolf, D. *Otolithi Piscium. Handbook of Paleoichthyology, Vol. 10.*; Fischer, G., Ed.; Stuttgart, New York, 1985;

38. Platt, C.; Popper, A.N. Fine Structure and Function of the Ear. In; 1981; pp. 3–38.
39. Popper, A.N.; Lu, Z. Structure-function relationships in fish otolith organs. *Fish. Res.* **2000**, *46*, 15–25, doi:10.1016/S0165-7836(00)00129-6.
40. Clack, J.A.; Anderson, J.S. Early Tetrapods: Experimenting with Form and Function. In; Clack, J.A., Fay, R.R., Popper, A.N., Eds.; Springer International Publishing: Cham, 2016; pp. 71–105 ISBN 978-3-319-46661-3.
41. Popper, A.N.; Fay, R.R. Rethinking sound detection by fishes. *Hear. Res.* **2011**, *273*, 25–36, doi:10.1016/j.heares.2009.12.023.
42. Fay, R.R.; Popper, A.N. Acoustic stimulation of the ear of the goldfish (Carassius auratus). *J. Exp. Biol.* **1974**, *61*, 243–260, doi:10.1242/jeb.61.1.243.
43. Popper, A.N.; Fay, R.R.; Platt, C.; Sand, O. Sound Detection Mechanisms and Capabilities of Teleost Fishes. *Sens. Process. Aquat. Environ.* **2008**, 3–38, doi:10.1007/978-0-387-22628-6_1.
44. Popper, A.N.; Pay, R.R. Sound detection and processing by fish: Critical review and major research questions. *Brain. Behav. Evol.* **1993**, *41*, 14–38, doi:10.1159/000113821.
45. Lu, Z.; Xu, Z. Effects of saccular otolith removal on hearing sensitivity of the sleeper goby (Dormitator latifrons). *J. Comp. Physiol. A Neuroethol. Sensory, Neural, Behav. Physiol.* **2002**, *188*, 595–602, doi:10.1007/s00359-002-0334-6.
46. Lu, Z.; Xu, Z.; Buchser, W.J. Acoustic response properties of lagenar nerve fibers in the sleeper goby, Dormitator latifrons. *J. Comp. Physiol. A Neuroethol. Sensory, Neural, Behav. Physiol.* **2003**, *189*, 889–905, doi:10.1007/s00359-003-0462-7.
47. Lu, Z.; Xu, Z.; Buchser, W.J. Frequency coding of particle motion by saccular afferents of a teleost fish. *J. Exp. Biol.* **2010**, *213*, 1591–1601, doi:10.1242/jeb.038836.
48. Edds-Walton, P.L. What the toadfish ear tells the toadfish brain about sound. *Adv. Exp. Med. Biol.* **2016**, *877*, 197–226, doi:10.1007/978-3-319-21059-9_10.
49. Lu, Z.; Song, J.; Popper, A.N. Encoding of acoustic directional information by saccular afferents of the sleeper goby, Dormitator latifrons. *J. Comp. Physiol. - A Sensory, Neural, Behav. Physiol.* **1998**, *182*, 805–815, doi:10.1007/s003590050225.
50. Braun, C.B.; Grande, T. Evolution of Peripheral Mechanisms for the Enhancement of Sound Reception. *Fish Bioacoustics* **2008**, 99–144, doi:10.1007/978-0-387-73029-5_4.
51. Fay, R.R.; Edds-Walton, P.L. Diversity in frequency response properties of saccular afferents of the toadfish, Opsanus tau. *Hear. Res.* **1997**, *113*, 235–246, doi:10.1016/S0378-5955(97)00148-2.
52. Popper, A.N.; Ramcharitar, J.; Campana, S.E. Why otoliths? Insights from inner ear

physiology and fisheries biology. *Mar. Freshw. Res.* **2005**, *56*, 497–504, doi:10.1071/MF04267.

53. Thomas, O.R.B.; Swearer, S.E. Otolith biochemistry—a review. *Rev. Fish. Sci. Aquac.* **2019**, *27*, 458–489.
54. Assis, C.A. The lagenar otoliths of teleosts: Their morphology and its application in species identification, phylogeny and systematics. *J. Fish Biol.* **2003**, *62*, 1268–1295, doi:10.1046/j.1095-8649.2003.00106.x.
55. Assis, C.A. The utricular otoliths, lapilli, of teleosts: Their morphology and relevance for species identification and systematics studies. *Sci. Mar.* **2005**, *69*, 259–273, doi:10.3989/scimar.2005.69n2259.
56. Ladich, F.; Schulz-Mirbach, T. Diversity in fish auditory systems: One of the riddles of sensory biology. *Front. Ecol. Evol.* **2016**, *4*, 28, doi:10.3389/fevo.2016.00028.
57. Newman, S.J.; Dunk, I.J. Growth, age validation, mortality, and other population characteristics of the red emperor snapper, Lutjanus sebae (Cuvier, 1828), off the Kimberley coast of north-western Australia. *Estuar. Coast. Shelf Sci.* **2002**, doi:10.1006/ecss.2001.0887.
58. Velasco, E.M.; Jiménez-Tenorio, N.; Del Arbol, J.; Bruzón, M.A.; Baro, J.; Sobrino, I. Age, growth and reproduction of the axillary seabream, Pagellus acarne, in the Atlantic and Mediterranean waters off southern Spain. *J. Mar. Biol. Assoc. United Kingdom* **2011**, *91*, 1243–1253, doi:10.1017/S0025315410000305.
59. Hüssy, K.; Limburg, K.E.; de Pontual, H.; Thomas, O.R.B.; Cook, P.K.; Heimbrand, Y.; Blass, M.; Sturrock, A.M. Trace Element Patterns in Otoliths: The Role of Biomineralization. *Rev. Fish. Sci. Aquac.* **2021**, *29*, 445–477, doi:10.1080/23308249.2020.1760204.
60. Sturrock, A.M.; Trueman, C.N.; Darnaude, A.M.; Hunter, E. Can otolith elemental chemistry retrospectively track migrations in fully marine fishes? *J. Fish Biol.* **2012**, *81*, 766–795, doi:10.1111/j.1095-8649.2012.03372.x.
61. Elsdon, T.S.; Wells, B.K.; Campana, S.E.; Gillanders, B.M.; Jones, C.M.; Limburg, K.E.; Secor, D.H.; Thorrold, S.R.; Walther, B.D. Otolith chemistry to describe movements and life-history parameters of fishes: Hypotheses, assumptions, limitations and inferences. In *Oceanography and Marine Biology*; CRC Press, 2008; Vol. 46, pp. 297–330 ISBN 0429137257.
62. Schroeder, R.; Avigliano, E.; Volpedo, A. V; Fortunato, R.C.; Barrulas, P.; Daros, F.A.; Schwingel, P.R.; Dias, M.C.; Correia, A.T. Lebranche mullet Mugil liza population structure and connectivity patterns in the southwest Altantic ocean using a multidisciplinary approach.

Estuar. Coast. Shelf Sci. **2023**, *288*, 108368.

63. Maciel, T.R.; Avigliano, E.; Carvalho, B.M. de; Miller, N.; Vianna, M. Population structure and habitat connectivity of Genidens genidens (Siluriformes) in tropical and subtropical coasts from Southwestern Atlantic. *Estuar. Coast. Shelf Sci.* **2020**, *242*, 106839, doi:10.1016/j.ecss.2020.106839.
64. Avigliano, E.; Carvalho, B.; Velasco, G.; Tripodi, P.; Vianna, M.; Volpedo, A.V. Nursery areas and connectivity of the adults anadromous catfish (Genidens barbus) revealed by otolith-core microchemistry in the south-western Atlantic Ocean. *Mar. Freshw. Res.* **2017**, *68*, 931–940, doi:10.1071/MF16058.
65. Rogers, T.A.; Fowler, A.J.; Steer, M.A.; Gillanders, B.M. Discriminating Natal Source Populations of a Temperate Marine Fish Using Larval Otolith Chemistry. *Front. Mar. Sci.* **2019**, *6*, 711, doi:10.3389/fmars.2019.00711.
66. McMahon, K.W.; Fogel, M.L.; Johnson, B.J.; Houghton, L.A.; Thorrold, S.R. A new method to reconstruct fish diet and movement patterns from δ 13C values in otolith amino acids. *Can. J. Fish. Aquat. Sci.* **2011**, *68*, 1330–1340, doi:10.1139/f2011-070.
67. Radtke, R.L.; Showers, W.; Moksness, E.; Lenz, P. Environmental information stored in otoliths: Insights from stable isotopes. *Mar. Biol.* **1996**, *127*, 161–170, doi:10.1007/BF00993656.
68. Correia, A.T.; Moura, A.; Triay-Portella, R.; Santos, P.T.; Pinto, E.; Almeida, A.A.; Sial, A.N.; Muniz, A.A. Population structure of the chub mackerel (Scomber colias) in the NE Atlantic inferred from otolith elemental and isotopic signatures. *Fish. Res.* **2021**, *234*, 105785.
69. D'Iglio, C.; Albano, M.; Famulari, S.; Savoca, S.; Panarello, G.; Di Paola, D.; Perdichizzi, A.; Rinelli, P.; Lanteri, G.; Spanò, N.; et al. Intra- and interspecific variability among congeneric Pagellus otoliths. *Sci. Rep.* **2021**, *11*, 16315, doi:10.1038/s41598-021-95814-w.
70. D'iglio, C.; Natale, S.; Albano, M.; Savoca, S.; Famulari, S.; Gervasi, C.; Lanteri, G.; Panarello, G.; Spanò, N.; Capillo, G. Otolith Analyses Highlight Morpho-Functional Differences of Three Species of Mullet (Mugilidae) from Transitional Water. *Sustain.* 2022, *14*.
71. Jaramilo, A.M.; Tombari, A.D.; Benedito Dura, V.; Eugeni Rodrigo, M.; Volpedo, A. V. Otolith eco-morphological patterns of benthic fishes from the coast of Valencia (Spain). *Thalassas* **2014**, *30*, 57–66.
72. Zhuang, L.; Ye, Z.; Zhang, C. Application of otolith shape analysis to species separation in Sebastes spp. from the Bohai Sea and the Yellow Sea, northwest Pacific. *Environ. Biol.*

Fishes **2015**, *98*, 547–558, doi:10.1007/s10641-014-0286-z.

73. Volpedo, A. V.; Tombari, A.D.; Echeverría, D.D. Eco-morphological patterns of the sagitta of Antarctic fish. *Polar Biol.* **2008**, *31*, 635–640, doi:10.1007/s00300-007-0400-1.
74. D'Iglio, C.; Famulari, S.; Albano, M.; Carnevale, A.; Di Fresco, D.; Costanzo, M.; Lanteri, G.; Spanò, N.; Savoca, S.; Capillo, G. Intraspecific variability of the saccular and utricular otoliths of the hatchetfish Argyropelecus hemigymnus (Cocco, 1829) from the Strait of Messina (Central Mediterranean Sea). *PLoS One* **2023**, *18*, 1–31, doi:10.1371/journal.pone.0281621.
75. Lombarte, A.; Miletić, M.; Kovačić, M.; Otero-Ferrer, J.L.; Tuset, V.M. Identifying sagittal otoliths of Mediterranean Sea gobies: variability among phylogenetic lineages. *J. Fish Biol.* **2018**, *92*, 1768–1787, doi:10.1111/jfb.13615.
76. Tuset, V.M.; Lombarte, A.; Assis, C.A. Otolith atlas for the western Mediterranean, north and central eastern Atlantic. *Sci. Mar.* **2008**, *72*, 7–198.
77. Campana, S.E. *Photographic Atlas of Fish Otoliths of the Northwest Atlantic Ocean*; NRC Research Press, 2004; ISBN 0660191083.
78. Kasapoglu, N.; Duzgunes, E. Otolith atlas for the black sea. *J. Environ. Prot. Ecol.* **2015**, *16*, 133–144.
79. Smale, M.J.; Watson, G.; Hecht, T. Otolith atlas of Southern African marine fishes. *Ichthyol. Monogr. J.L.B. Smith Inst. Ichthyol.* **1995**, *1*.
80. Nolf, D. Studies on fossil otoliths - The state of the art. *Recent Dev. Fish Otolith Res.* **1995**, *19*, 513–544.
81. Girone, A.; Nolf, D.; Cappetta, H. Pleistocene fish otoliths from the Mediterranean Basin: a synthesis. *Geobios* **2006**, *39*, 651–671, doi:10.1016/j.geobios.2005.05.004.
82. Lin, C.H.; Girone, A.; Nolf, D. Fish otolith assemblages from Recent NE Atlantic sea bottoms: A comparative study of palaeoecology. *Palaeogeogr. Palaeoclimatol. Palaeoecol.* **2016**, *446*, 98–107, doi:10.1016/j.palaeo.2016.01.022.
83. D'Iglio, C.; Famulari, S.; Albano, M.; Giordano, D.; Rinelli, P.; Capillo, G.; Spanò, N.; Savoca, S. Time-Scale Analysis of Prey Preferences and Ontogenetic Shift in the Diet of European Hake Merluccius merluccius (Linnaeus, 1758) in Southern and Central Tyrrhenian Sea. *Fishes* **2022**, *7*, doi:10.3390/fishes7040167.
84. D'Iglio, C.; Porcino, N.; Savoca, S.; Profeta, A.; Perdichizzi, A.; Armeli Minicante, E.; Salvati, D.; Soraci, F.; Rinelli, P.; Giordano, D. Ontogenetic shift and feeding habits of the European hake (Merluccius merluccius L., 1758) in Central and Southern Tyrrhenian Sea (Western Mediterranean Sea): A comparison between past and present data . *Ecol. Evol.*

2022, *12*, e8634, doi:10.1002/ece3.8634.

85. Neves, J.; Silva, A.A.; Moreno, A.; Veríssimo, A.; Santos, A.M.; Garrido, S. Population structure of the European sardine Sardina pilchardus from Atlantic and Mediterranean waters based on otolith shape analysis. *Fish. Res.* **2021**, *243*, 106050, doi:10.1016/j.fishres.2021.106050.
86. Higgins, R.; Isidro, E.; Menezes, G.; Correia, A. Otolith elemental signatures indicate population separation in deep-sea rockfish, Helicolenus dactylopterus and Pontinus kuhlii, from the Azores. *J. Sea Res.* **2013**, *83*, 202–208, doi:10.1016/j.seares.2013.05.014.
87. Benzinou, A.; Carbini, S.; Nasreddine, K.; Elleboode, R.; Mahé, K. Discriminating stocks of striped red mullet (Mullus surmuletus) in the Northwest European seas using three automatic shape classification methods. *Fish. Res.* **2013**, *143*, 153–160, doi:10.1016/j.fishres.2013.01.015.
88. Muniz, A.A.; Moura, A.; Triay-Portella, R.; Moreira, C.; Santos, P.T.; Correia, A.T. Population structure of the chub mackerel (Scomber colias) in the North-east Atlantic inferred from otolith shape and body morphometrics. *Mar. Freshw. Res.* **2021**, *72*, 341–352, doi:10.1071/MF19389.
89. Vignon, M.; Morat, F. Environmental and genetic determinant of otolith shape revealed by a non-indigenous tropical fish. *Mar. Ecol. Prog. Ser.* **2010**, *411*, 231–241, doi:10.3354/meps08651.
90. Schulz-Mirbach, T.; Ladich, F.; Riesch, R.; Plath, M. Otolith morphology and hearing abilities in cave- and surface-dwelling ecotypes of the Atlantic molly, Poecilia mexicana (Teleostei: Poeciliidae). *Hear. Res.* **2010**, *267*, 137–148, doi:10.1016/j.heares.2010.04.001.
91. Abaad, M.; Tuset, V.M.; Montero, D.; Lombarte, A.; Otero-Ferrer, J.L.; Haroun, R. Phenotypic plasticity in wild marine fishes associated with fish-cage aquaculture. *Hydrobiologia* **2016**, *765*, 343–358, doi:10.1007/s10750-015-2428-5.
92. Bose, A.P.H.; Zimmermann, H.; Winkler, G.; Kaufmann, A.; Strohmeier, T.; Koblmüller, S.; Sefc, K.M. Congruent geographic variation in saccular otolith shape across multiple species of African cichlids. *Sci. Rep.* **2020**, *10*, 1–14, doi:10.1038/s41598-020-69701-9.
93. Savoca, S.; Grifó, G.; Panarello, G.; Albano, M.; Giacobbe, S.; Capillo, G.; Spanó, N.; Consolo, G. Modelling prey-predator interactions in Messina beachrock pools. *Ecol. Modell.* **2020**, *434*, doi:10.1016/j.ecolmodel.2020.109206.
94. Spanò, N.; Domenico, E. De Biodiversity in Central Mediterranean Sea. *Mediterr. Identities - Environ. Soc. Cult.* **2017**, *6*, 129–148, doi:10.5772/intechopen.68942.
95. Ingrosso, G.; Abbiati, M.; Badalamenti, F.; Bavestrello, G.; Belmonte, G.; Cannas, R.;

Benedetti-Cecchi, L.; Bertolino, M.; Bevilacqua, S.; Bianchi, C.N.; et al. Mediterranean Bioconstructions Along the Italian Coast. *Adv. Mar. Biol.* **2018**, *79*, 61–136, doi:10.1016/bs.amb.2018.05.001.

96. Capillo, G.; Panarello, G.; Savoca, S.; Sanfilippo, M.; Albano, M.; Volsi, R.L.; Consolo, G.; Spanò, N. Intertidal ponds of messina's beachrock faunal assemblage, evaluation of ecosystem dynamics and communities' interactions. *AAPP Atti della Accad. Peloritana dei Pericolanti, Cl. di Sci. Fis. Mat. e Nat.* **2018**, *96*, A41–A416, doi:10.1478/AAPP.96S3A4.
97. Gravem, S.A.; Morgan, S.G. Shifts in intertidal zonation and refuge use by prey after mass mortalities of two predators. *Ecology* **2017**, *98*, 1006–1015, doi:10.1002/ecy.1672.
98. Longhitano, S.G. Between Scylla and Charybdis (part 2): The sedimentary dynamics of the ancient, Early Pleistocene Messina Strait (central Mediterranean) based on its modern analogue. *Earth-Science Rev.* **2018**, *179*, 248–286, doi:10.1016/j.earscirev.2018.01.017.
99. Cucco, A.; Quattrocchi, G.; Olita, A.; Fazioli, L.; Ribotti, A.; Sinerchia, M.; Tedesco, C.; Sorgente, R. Hydrodynamic modelling of coastal seas: The role of tidal dynamics in the Messina Strait, Western Mediterranean Sea. *Nat. Hazards Earth Syst. Sci.* **2016**, *16*, 1553–1569, doi:10.5194/nhess-16-1553-2016.
100. De Domenico, E. Caratteristiche fisiche e chimiche delle acque nello Stretto di Messina. *Doc. Trav. IGAL* **1987**, *11*, 225–235.
101. Nikolić, V.; Žuljević, A.; Mangialajo, L.; Antolić, B.; Kušpilić, G.; Ballesteros, E. Cartography of littoral rocky-shore communities (CARLIT) as a tool for ecological quality assessment of coastal waters in the Eastern Adriatic Sea. *Ecol. Indic.* **2013**, *34*, 87–93, doi:10.1016/j.ecolind.2013.04.021.
102. Institute of Oceanography and Fisheries Database and indicators of the state of the marine environment, mariculture and fisheries Available online: http://baltazar.izor.hr/azopub/bobazi.
103. Zorica, B.; Čikeš Keč, V.; Pešić, A.; Gvozdenović, S.; Kolitari, J.; Mandić, M. Spatiotemporal distribution of anchovy early life stages in the eastern part of the Adriatic Sea in relation to some oceanographic features. *J. Mar. Biol. Assoc. United Kingdom* **2019**, *99*, 1205–1211, doi:10.1017/S0025315418001145.
104. Orlić, M.; Dadić, V.; Grbec, B.; Leder, N.; Marki, A.; Matić, F.; Mihanović, H.; Beg Paklar, G.; Pasarić, M.; Pasarić, Z. Wintertime buoyancy forcing, changing seawater properties, and two different circulation systems produced in the Adriatic. *J. Geophys. Res. Ocean.* **2006**, *111*.
105. Vilibić, I.; Orlić, M. Least-squares tracer analysis of water masses in the South Adriatic

(1967-1990). *Deep. Res. Part I Oceanogr. Res. Pap.* **2001**, *48*, 2297–2330, doi:10.1016/S0967-0637(01)00014-0.

106. Hyslop, E.J. Stomach contents analysis—a review of methods and their application. *J. Fish Biol.* **1980**, *17*, 411–429, doi:10.1111/j.1095-8649.1980.tb02775.x.
107. Cortés, E. A critical review of methods of studying fish feeding based on analysis of stomach contents: Application to elasmobranch fishes. In Proceedings of the Canadian Journal of Fisheries and Aquatic Sciences; 1997.
108. D'Iglio, C.; Albano, M.; Tiralongo, F.; Famulari, S.; Rinelli, P.; Savoca, S.; Spanò, N.; Capillo, G. Biological and Ecological Aspects of the Blackmouth Catshark (Galeus melastomus Rafinesque, 1810) in the Southern Tyrrhenian Sea. *J. Mar. Sci. Eng.* **2021**, *9*, 967, doi:10.3390/jmse9090967.
109. D'Iglio, C.; Porcino, N.; Savoca, S.; Profeta, A.; Perdichizzi, A.; Armeli, E.; Davide, M.; Francesco, S.; Rinelli, P.; Giordano, D. Ontogenetic shift and feeding habits of the European hake (Merluccius merluccius L ., 1758) in Central and Southern Tyrrhenian Sea (Western Mediterranean Sea): A comparison between past and present data. *Ecol. Evol.* **2022**, *12*, doi:10.1002/ece3.8634.
110. Libungan, L.A.; Pálsson, S. ShapeR: An R package to study otolith shape variation among fish populations. *PLoS One* **2015**, *10*, 1–12, doi:10.1371/journal.pone.0121102.
111. Jawad, L.A.; Sabatino, G.; Ibáñez, A.L.; Andaloro, F.; Battaglia, P. Morphology and ontogenetic changes in otoliths of the mesopelagic fishes Ceratoscopelus maderensis (Myctophidae), Vinciguerria attenuata and V. poweriae (Phosichthyidae) from the Strait of Messina (Mediterranean Sea). *Acta Zool.* **2018**, doi:10.1111/azo.12197.
112. Pavlov, D.A. Otolith Morphology and Relationships of Several Fish Species of the Suborder Scorpaenoidei. *J. Ichthyol.* **2021**, *61*, 33–47, doi:10.1134/S0032945221010100.
113. Pavlov, D.A. Differentiation of three species of the genus Upeneus (Mullidae) based on otolith shape analysis. *J. Ichthyol.* **2016**, *56*, 37–51, doi:10.1134/S0032945216010094.
114. Tuset, V.M.; Farré, M.; Otero-Ferrer, J.L.; Vilar, A.; Morales-Nin, B.; Lombarte, A. Testing otolith morphology for measuring marine fish biodiversity. *Mar. Freshw. Res.* **2016**, *67*, 1037–1048, doi:10.1071/MF15052.
115. Tuset, V.M.; Lozano, I.J.; GonzÍez, J.A.; Pertusa, J.F.; García-Díaz, M.M. Shape indices to identify regional differences in otolith morphology of comber, Serranus cabrilla (L., 1758). *J. Appl. Ichthyol.* **2003**, *19*, 88–93, doi:10.1046/j.1439-0426.2003.00344.x.
116. Tuset, V.M.; Lombarte, A.; González, J.A.; Pertusa, J.F.; Lorente, M.J. Comparative morphology of the sagittal otolith in Serranus spp. *J. Fish Biol.* **2003**, *63*, 1491–1504,

doi:10.1111/j.1095-8649.2003.00262.x.

117. Assis, C.A. Estudo morfológico dos otólitos sagitta, asteriscus e lapillus de Teleóstei (Actinopterygii, Teleostei) de Portugal continental. Sua aplicação em estudos de filogenia, sistematica e ecologia. *Ecologia* 2000, 1005.
118. Cortese, G.; De Domenico, E. Some considerations on the levantine intermediate water distribution in the Straits of Messina. *Boll. Ocean. Teor. Appl* **1990**, *8*, 197–207.
119. Lipizer, M.; Partescano, E.; Rabitti, A.; Giorgetti, A.; Crise, A. Qualified temperature, salinity and dissolved oxygen climatologies in a changing Adriatic Sea. *Ocean Sci.* **2014**, *10*, 771–797, doi:10.5194/os-10-771-2014.
120. Solidoro, C.; Bastianini, M.; Bandelj, V.; Codermatz, R.; Cossarini, G.; Canu, D.M.; Ravagnan, E.; Salon, S.; Trevisani, S. Current state, scales of variability, and trends of biogeochemical properties in the northern Adriatic Sea. *J. Geophys. Res. Ocean.* **2009**, *114*, doi:10.1029/2008JC004838.
121. Kikuchi, E.; Cardoso, L.G.; Canel, D.; Timi, J.T.; Haimovici, M. Using growth rates and otolith shape to identify the population structure of Umbrina canosai (Sciaenidae) from the Southwestern Atlantic. *Mar. Biol. Res.* **2021**, *17*, 272–285, doi:10.1080/17451000.2021.1938131.
122. Gomes, P.B.; Belém, M.J. da C.; Schlenz, E. Distribution, abundance and adaptations of three species of Actiniidae (Cnidaria, Actiniaria) on an intertidal beach rock in Cameiros beach, Pemambuco, Brazil. *Misc. Zool.* **1998**, *21*, 65–72.
123. Bacha, M.; Moali, A.; Benmansour, N.E.; Brylinski, J.M.; Mahé, K.; Amara, R. Relationships between age, growth, diet and environmental parameters for anchovy (Engraulis encrasicolus L.) in the Bay of Bénisaf (SW Mediterranean, west Algerian coast). *Cybium* **2010**, *34*, 47–57.
124. Lek, E.; Fairclough, D. V.; Hall, N.G.; Hesp, S.A.; Potter, I.C. Do the maximum sizes, ages and patterns of growth of three reef-dwelling labrid species at two latitudes differ in a manner conforming to the metabolic theory of ecology? *J. Fish Biol.* **2012**, *81*, 1936–1962, doi:10.1111/j.1095-8649.2012.03446.x.
125. Atkinson, D. Temperature and Organism Size—A Biological Law for Ectotherms? *Adv. Ecol. Res.* **1994**, *25*, 1–58, doi:10.1016/S0065-2504(08)60212-3.
126. Kozłowski, J.; Czarnołęski, M.; Dańko, M. Can optimal resource allocation models explain why ectotherms grow larger in cold? *Integr. Comp. Biol.* **2004**, *44*, 480–493, doi:10.1093/icb/44.6.480.
127. Jobling, M. Temperature and growth: modulation of growth rate via temperature change.

Glob. Warm. **2011**, 225–254, doi:10.1017/cbo9780511983375.010.

128. Mommsen, T.P. Growth and metabolism. *Physiol. fishes* **1998**, *2*, 65–97.
129. Harmelin-Vivien, M.L.; Kaim-Malka, R.A.; Ledoyer, M.; Jacob-Abraham, S.S. Food partitioning among scorpaenid fishes in Mediterranean seagrass beds. *J. Fish Biol.* **1989**, *34*, 715–734, doi:10.1111/j.1095-8649.1989.tb03352.x.
130. Dias, M.A.D. Tidal pools as nursery areas for marine fish larvae and juveniles – habitat use and trophic ecology. *Mestr. em Ecol. Mar.* 2013, 1–92.
131. Grønkjær, P. Otoliths as individual indicators: A reappraisal of the link between fish physiology and otolith characteristics. *Mar. Freshw. Res.* **2016**, *67*, 881–888, doi:10.1071/MF15155.
132. Popper, A.N.; Lu, Z. Structure-function relationships in fish otolith organs. *Fish. Res.* **2000**, *46*, 15–25, doi:10.1016/S0165-7836(00)00129-6.
133. Popper, A.N.; Schilt, C.R. Hearing and Acoustic Behavior: Basic and Applied Considerations. *Fish Bioacoustics* **2008**, 17–48, doi:10.1007/978-0-387-73029-5_2.
134. Lombarte, A.; Palmer, M.; Matallanas, J.; Gómez-Zurita, J.; Morales-Nin, B. Ecomorphological trends and phylogenetic inertia of otolith sagittae in Nototheniidae. *Environ. Biol. Fishes* **2010**, *89*, 607–618, doi:10.1007/s10641-010-9673-2.
135. Lombarte, A.; Cruz, A. Otolith size trends in marine fish communities from different depth strata. *J. Fish Biol.* **2007**, *71*, 53–76, doi:10.1111/j.1095-8649.2007.01465.x.
136. Lombarte, A.; Lleonart, J. Otolith size changes related with body growth, habitat depth and temperature. *Environ. Biol. Fishes* **1993**, *37*, 297–306, doi:10.1007/BF00004637.
137. Tuset, V.M.; Imondi, R.; Aguado, G.; Otero-Ferrer, J.L.; Santschi, L.; Lombarte, A.; Love, M. Otolith patterns of rockfishes from the northeastern pacific. *J. Morphol.* **2015**, *276*, 458–469, doi:10.1002/jmor.20353.
138. YediEr, S.; Bostanci, D. Morphologic and morphometric comparisons of Sagittal otoliths of five Scorpaena species in the Sea of Marmara, Mediterranean Sea, Aegean Sea and Black Sea. *Cah. Biol. Mar.* **2021**, *62*, 357–369, doi:10.21411/CBM.A.6B8915B2.
139. Monteiro, L.R.; Di Beneditto, A.P.M.; Guillermo, L.H.; Rivera, L.A. Allometric changes and shape differentiation of sagitta otoliths in sciaenid fishes. *Fish. Res.* **2005**, *74*, 288–299, doi:10.1016/j.fishres.2005.03.002.
140. Endler, J.A. Signals, signal conditions, and the direction of evolution. *Am. Nat.* **1992**, *139*, S125–S153, doi:10.1086/285308.
141. Endler, J.A. Some general comments on the evolution and design of animal communication systems. *Philos. Trans. - R. Soc. London, B* **1993**, *340*, 215–225, doi:10.1098/rstb.1993.0060.

142. Tuset, V.M.; Otero-Ferrer, J.L.; Gómez-Zurita, J.; Venerus, L.A.; Stransky, C.; Imondi, R.; Orlov, A.M.; Ye, Z.; Santschi, L.; Afanasiev, P.K.; et al. Otolith shape lends support to the sensory drive hypothesis in rockfishes. *J. Evol. Biol.* **2016**, *29*, 2083–2097, doi:10.1111/jeb.12932.
143. Chapuis, L.; Yopak, K.E.; Radford, C.A. From the morphospace to the soundscape: Exploring the diversity and functional morphology of the fish inner ear, with a focus on elasmobranchs. *J. Acoust. Soc. Am.* **2023**, *154*, 1526–1538, doi:10.1121/10.0020850.
144. Hoff, G.R.; Fuiman, L.A. Morphometry and composition of red drum otoliths: Changes associated with temperature, somatic growth rate, and age. *Comp. Biochem. Physiol. -- Part A Physiol.* **1993**, *106*, 209–219, doi:10.1016/0300-9629(93)90502-U.
145. Mendonça, V.; Flores, A.A.V.; Silva, A.C.F.; Vinagre, C. Do marine fish juveniles use intertidal tide pools as feeding grounds? *Estuar. Coast. Shelf Sci.* **2019**, *225*, 106255, doi:10.1016/j.ecss.2019.106255.
146. Dias, M.; Roma, J.; Fonseca, C.; Pinto, M.; Cabral, H.N.; Silva, A.; Vinagre, C. Intertidal pools as alternative nursery habitats for coastal fishes. *Mar. Biol. Res.* **2016**, *12*, 331–344, doi:10.1080/17451000.2016.1143106.
147. Cardinale, M.; Doering-Arjes, P.; Kastowsky, M.; Mosegaard, H. Effects of sex, stock, and environment on the shape of known-age Atlantic cod (Gadus morhua) otoliths. *Can. J. Fish. Aquat. Sci.* **2004**, *61*, 158–167, doi:10.1139/f03-151.
148. Via, S.; Gomulkiewicz, R.; De Jong, G.; Scheiner, S.M.; Schlichting, C.D.; Van Tienderen, P.H. Adaptive phenotypic plasticity: consensus and controversy. *Trends Ecol. Evol.* **1995**, *10*, 212–217, doi:10.1016/S0169-5347(00)89061-8.
149. Grabowski, T.B.; Young, S.P.; Libungan, L.A.; Steinarsson, A.; Marteinsdóttir, G. Evidence of phenotypic plasticity and local adaption in metabolic rates between components of the Icelandic cod (gadus morhua l.) stock. *Environ. Biol. Fishes* **2009**, *86*, 361–370, doi:10.1007/s10641-009-9534-z.
150. Berg, F.; Almeland, O.W.; Skadal, J.; Slotte, A.; Andersson, L.; Folkvord, A. Genetic factors have a major effect on growth, number of vertebrae and otolith shape in Atlantic herring (Clupea harengus). *PLoS One* **2018**, *13*, e0190995, doi:10.1371/journal.pone.0190995.
151. Swain, D.P.; Foote, C.J. Stocks and chameleons: The use of phenotypic variation in stock identification. *Fish. Res.* **1999**, *43*, 113–128, doi:10.1016/S0165-7836(99)00069-7.
152. Hilborn, C.R.; Walters, J. *Quantitative Fisheries Stock Assessment: Choice, Dynamics and Uncertainty*; Springer Science & Business Media, 1992; Vol. 67; ISBN 1461535980.
153. Gayanilo, F.C.; Sparre, F.; Pauly, D.; Gayanilo, F.C.Jr.; Sparre, P.; Pauly, D. FAO-ICLARM

Stock Assessment Tools II (FiSAT II). Revised version. User's guide. *FAO Comput. Inf. Ser.* **2005**.

154. Soeth, M.; Daros, F.A.; Correia, A.T.; Fabré, N.N.; Medeiros, R.; Feitosa, C.V.; de Sousa Duarte, O.; Lenz, T.M.; Spach, H.L. Otolith phenotypic variation as an indicator of stock structure of Scomberomorus brasiliensis from the southwestern Atlantic Ocean. *Fish. Res.* **2022**, *252*, 106357, doi:10.1016/j.fishres.2022.106357.
155. Lombarte, A.; Castellon, A. Interspecific and intraspecific otolith variability in the genus Merluccius as determined by image analysis. *Can. J. Zool.* **1991**, *69*, 2442–2449, doi:10.1139/z91-343.
156. Burke, N.; Brophy, D.; King, P.A. Shape analysis of otolith annuli in Atlantic herring (Clupea harengus); a new method for tracking fish populations. *Fish. Res.* **2008**, *91*, 133–143, doi:10.1016/j.fishres.2007.11.013.

4. DISCUSSION

Present thesis aimed to analyze the functional morphology of otoliths, exploring their intra and inter specific variability in several Mediterranean teleost species, characterized by different life habits, biology traits, and distribution range. Despite the large amount of information that otoliths provided through morphometrical, morphological, shape and SEM analysis, these were not enough to assess direct correlation to the environmental conditions experienced by specimens. Indeed, as stated in the Introduction chapter, several factors can influence otoliths' features, added to their somatic growth, chemical composition, and interaction with the inner ears' components. These factors include physiochemical conditions of the water masses, genetic and life habits of the different species, their trophic ecology and diet composition, and many others. For this reason, further analyses are required to confirm and found direct correlations that could explain at all the functional morphology of the otoliths. This can be essential to improve the knowledge base on the teleost inner ear, which play a fundamental role in the interaction between marine species and habitats.

4.1 The inter-specific differences between phylogenetically close species and the reliability of sagittae for cryptic species and genus identification.

Concerning the first three cases of study, the comparison among phylogenetically close species confirmed the strong influence of genetics on *sagittae* development, morphology, and shape. Indeed, results showed, in all the investigated teleost families, a pattern of similarity in mean shape and morphometrical parameters between congeneric species (e.g., *Nezumia* genus, *Chelon* genus), or species belonging to phylogenetically close genus (e.g., *Coelorhynchis* sp and *Coryphaenoides* sp, *Chelon* sp and *Oedalechilus* sp). According to Schulz-Mirbach et al. [1], several authors have related the extremely wide range of different sizes, shapes and morphologies, showed by otoliths, to the functionalization of duplicated genes [2,3], derived by teleost-specific whole-genome duplication event (TGD) [4,5] and to the vertebrate-specific whole-genome duplication [6]. This hypothesis may provide a genetic explanation to the taxon-specific shapes of otoliths, *sulcus acusticus* and *fossa acustica,* with TGD that could has provided the genomic base for their massive diversification, driven by the wide range of selective forces experienced by the different teleost species in their countless different habitats (e.g., differences in eco-acoustical habitats conditions, water pressure, permanent darkness conditions) [7,8]. Data from the first case of study could be in line with this thesis. Indeed, results showed differences in morphometrical and shape features of *sagittae,* despite the genetic closeness of the congeneric analyzed *Pagellus* species. This variability may be related to the

differences in the environmental conditions related to the differences in exploited habitats and life habits between the species. Several habitats' features can indeed influence the *sagittae*, as also highlighted by Tuset et al. [9]. They have found significant relationships between morphology, ecology, habitats features, and otoliths shape in several congeneric rockfishes' species (*Sebastes* sp), some of them detected also in *Pagellus* species. For instance, the oblong-fusiform *sagittae* shape detected in long body rockfishes, characterized by an active lifestyle, a dull coloration and more pelagic life habits, deeply different from the more elliptic otoliths shape detected in bottom-dwelling sedentary species, characterized by a deep body and bright colors pattern. This relation between ecology, morphology, and otoliths shape has been also detected in *P. acarne, P. bogaraveo* and *P. erythrinus.* Specimens belonging to this last species (characterized by a strictly benthic lifestyle) showed the widest *sagitta* among them, with the most circular shape and the shortest *rostrum*, while *P. acarne* specimens, which is the species with a most pelagic lifestyle (also characterized by a planktivorous feeding habits) showed an elongated *sagitta,* with the longest *rostrum*. Concerning *P. bogaraveo*, the species with the largest *sagitta* and the deepest distribution among them, it could has reflected the influence of depth on otoliths. Indeed, according to Lombarte et al. [10,11] that analyzed sagittal otoliths morphology and morphometry of different species characterized by different depth distributions, the size of *sagittae* increases with depth, except for the abyssal communities. Indeed, at depths between 1000 and 2000 m, species show a decrease in otoliths size. This was confirmed also by the results from the third case of study, in which species belonging to *Nezumia* genus (inhabiting also the abyssal depths) were characterized by smaller *sagittae* than *C. coelorhynchus* and *C. guentheri* (mainly distributed between 400 and 500 m of depth). Moreover, the most significant different size, shape, and morphometry of *sagittae* among the analyzed Macrourids *sagittae,* were detected in *H. italicus,* confirming once again the strong relation between life habits, environmental conditions, and otoliths features. Indeed, the glass head grenadier is a species characterized by pelagic habits, with a diet mainly composed of planktonic and pelagic crustaceans, strongly different form the benthic lifestyle reported for the other investigated grenadiers' species. As reported also for Nototheniidae species [12], species characterized by a strictly benthic life habits show significantly larger *sagittae* than those of pelagic species, with the strong influence of phylogenetic inertia. According to Schwarzans et al. and Tuset et al. [13,14], the morphology of body and otoliths can give a picture of the evolutionary divergence and niche partitioning within a genus or a family. Information provided by otoliths can confirm the trophic and functional niche partitioning, being functional traits often resulted by sensory based differences [15], with an often respected correspondence between otoliths morphology and neurocranium/head shape [16,17]. The detected differences and similarities between *sagittae* of the investigated Macrourids species reflected the existence of different niche

dimensions, essential for the coexistence and habitats substitution of sympatric morphologically close species [18]. All the Mediterranean grenadiers' species are generalist feeders [19], a common adaptation in bathyal and abyssal teleost to the low-productivity of deep environments [20]. The combination of different depth distributions and feeding habits allow to maintain their ecological segregation [21], with the differences in head and body morphology deeply correlated to their different feeding habits and foraging tactics [22]. According to results from the third case of study, the three *sagittae* morphotypes (*Coelorhynchus*/*Coryphaenoides* morphotype, *Nezumia* sp morphotype and *H. italicus* morphotype), highlighted by the significant differences in mean shape and morphometry, and characterized by a common general morphometry and shape of *sagittae* inside each morphotype, have followed, according to literature, the ecological segregation among Macrourids provided by the combination of the different depth distributions and feeding habits of species [18,21,22]. Specimens belonging to *Coelorhynchus*/*Coryphaenoides* morphotype share the same feeding habits and depth distribution, such as specimens belonging to *Nezumia* sp morphotype. Conversely, specimens belonging to *Coelorhynchus*/*Coryphaenoides* morphotype share with those belonging to *Nezumia* sp morphotype a common feeding habit (being all of them benthic predators) with a very different depth distribution. Both morphotypes were strongly separated from *H. italicus* morphotype. This reflects the high degree of niche separation between *H. italicus* and the others Macrourids species. Indeed, *H. italicus* specimens are characterized by a wide depth distribution (until 1200 m), a strictly pelagic/planktivorous feeding habits and a bathypelagic life habit, strongly different from that of the other studied grenadiers' species.

Data from the second and the third cases of study have also confirmed the reliability of *sagittae* for species discrimination in cryptic taxonomic groups. Indeed, mean shape and morphometry of sagittal otoliths have been widely applied for species and genus identification in several teleost families and genus characterized by a challenging species discrimination. This is the case of *Scomberomorus* genus [23], in which otoliths morphometries have been used for species discrimination; or the *Lutjanus* genus [24] and Gobiidae family [25], in which mean otoliths shape have been provided by shape analysis for species identification. In the second case of study, data from shape and morphometry of the three investigated Mugilidae species showed the effectiveness of *sagittae* morphometrical and mean shape features to discriminate between different genus and even species. Indeed, the classic taxonomic identification applied to species belonging to this family is often difficult, being these characterized by a high morphological similarity [26]. This is also the case of the Macrouridae species analyzed in the third case of study, in which morphological differences are not always the easier way for species identification [27]. Here otoliths morphometrical and shape analysis have proved to give reliable diagnostic characters, useful to distinguish between genus and, as in *H. italicus,* even species.

Indeed, it has been widely reported in several teleost groups as interspecific otoliths differences inside a family or a genus can follow the phylogenetic lineages defined through molecular techniques [25,28]. This was proved by the most enhanced differences detected by results between phylogenetically distant genus or species (such as between *Chelon* and *Oedalechilus* genus*, H. italicus* and the other grenadiers' species), most clearly visible, and, consequently, most suitable for taxonomic identification. Concerning the most phylogenetically close taxonomic groups, the differences in otoliths' shape and morphometry often became less evident, making difficult, as in the case of *N. sclelorhynchus* and *N. aequalis,* a correct species identification only through otoliths features. This proves the strong genetic control affecting otoliths development. But in other cases, such within *Pagellus* genus, or among *H. italicus* and the other grenadiers investigated species, despite the phylogenetic closeness, otoliths analysis provided enough information useful for species identification, as also reported, according to literature, for the *Lutjanus* genus [24]. This may be related to the influence on otoliths development and, consequently, on inter specific differences of ecological, ontogenetic, and environmental factors. A correct species discrimination is essential for a correct biodiversity and species abundance evaluation, especially for the main harvested and ecologically relevant teleost species, such as those belonging to the Macrouridae and Mugiliidae families. The accuracy of fisheries sampling programs and, consequently, of the entire management design, can be strongly affected by an incorrect species identification. Indeed, species discrimination can influence data regarding catch and landings by vessels, the collection of biological data, the reconstruction of marine biocenosis from catch provided by scientific surveys. For this reason, improved the knowledge on the application of *sagittae* shape and morphometry for species identification, especially in the most challenging and time-consuming teleost groups, can be important to provide a reliable and relatively easy tool to confirm species identification, together with molecular and morphological data.

4.2 The otoliths' intra-specific variability: size related variations and directional bilateral asymmetry in the three otoliths' pairs.

Concerning the fourth and the fifth cases of study, the analysis of the intra specific variability of the three otoliths pairs, from two species with marked different life habits, ecology, and life history traits, revealed for both the strong relation between the fish length and otoliths' shape and morphometry. This variability was especially enhanced in *A. hemigymnus* specimens from the Strait of Messina, for both *sagittae* and *lapilli,* also showing a significant difference between left and right otoliths pairs. In *B. belone* specimens from the fifth case of study, the variability between size classes was significantly

evident in *sagittae*, while, concerning *lapilli* and *asterisci*, the lack of representative samples numbers from all the investigated size classes made it impossible to assess it in. Conversely, it was analyzed the presence of directional bilateral asymmetry, with the absence of significant differences between left and right otoliths in all the three otoliths' pairs. A strong intra specific size-related *sagittae* variability was also detected in the three studied *Pagellus* species from the first case of study, with a slight variability between otoliths pairs in *P. acarne* and *P. erythrinus.* The differences in morphometry and mean shape of *sagittae* between size classes could be related, in both the investigated species, to changes in life habits, exploited habitats, biology and environmental conditions experienced by specimens during the growth process. Indeed, it is widely reported, in several teleost species form different marine domains, an often radical variation in feeding ground, diet composition, depth distribution and habitat use between ontogenetic, maturity stages, and size classes [29–35]. Concerning *A. hemigymnus*, bathy-pelagic teleost species show evident differences in feeding patterns and depth distributions during their life time [33,36]. Additionally, especially in the studied area from the fourth case of the study, they perform wide trophic movements, following preys' diel vertical migrations, during their adult stages, as confirmed by studies on their vertical distribution and abundance [37–39]. This ontogenetic shift in habitat preferences and feeding habits, added to the vertical migration performed by larger specimens, can deeply influence otoliths features, allowing to the intra specific size related differences showed by results. Concerning pelagic species, for many of them (*B. belone* included) [34,40–42], it is reported a shift from nearshore to offshore waters between small and large specimens, with also marked trophic differences in diet composition and feeding habits. All these differences in the experienced environmental conditions between juvenile and adults, and the reported life habits and behaviors between small and large specimens, could have allowed to the large variability in shape and morphometry detected between otoliths' belonging to different size classes.

The asymmetry between otoliths sides is a diffused features characterizing several teleost groups and populations. It is often linked to stress conditions and environmental heterogeneity (as in the case of fluctuating asymmetry), or to the significant greater development of an inner ear side than the other within a population (directional asymmetry) [43]. The differences between left and right otoliths inside a population can strongly influence the stock assessment, being mean otoliths shape a widely used tool to assess different stocks of a species. For this reason, it is important to detect the presence of differences related to shape and morphometry between otoliths sides inside the several teleost populations, especially in species with a high commercial value, being more sensitive to fisheries activities and stocks depletion. Moreover the fluctuation of bilateral asymmetry in otoliths can be directly used to discriminate among populations, being a phenotypic or genetic marker that can

change geographically, as also reported for many other calcified and skeleton structures [44–47]. The presence of directional bilateral asymmetry, fluctuating asymmetry and sexual dimorphism in otoliths has been evaluated in studied species from the first five cases of study. *P. erithrynus* specimens showed slightly differences in shape indexes between left and right *sagittae,* while in *A. hemigymnus* it was highlighted the presence of significant differences in mean otoliths shape between *sagittae*, except in class II, and between *lapilli* pairs only in size class IV. Conversely, *C. labrosus* and *N. sclerorhynchus* specimens were characterized by differences only regarding morphometry of *sulcus acusticus* between *sagittae* sides. The fluctuating directional asymmetry detected in *C. labrosus* and *N. sclerorhynchus* could be related to the ecology of the species and to the peculiarity of the sampling areas, being the first time in which this variation between otoliths side has been detected for these species. This is widely evident especially for *C. labrosus,* being the analyzed specimens sampled in a peculiar brackish environment (the Ganzirri lagoon) characterized by wide seasonal fluctuation of several environmental parameters and productivity [48–50]. Further analysis on the *N. sclerorhynchus* life habits from the studied area are required to understand the possible correlation between its ecology and the fluctuating asymmetry detected by results. Indeed, *sulcus acusticus* is important to analyze the teleost's hearing mechanism, being this strictly related to the physical interaction between *macula* and *sagitta* (see Introduction chapter). It assumes a high ecomorphological value, being widely used for inter specific and inter population studies, and also to investigate communication behavior in sound producing species [51–56]. Further comparisons of data from different *N. sclerorhynchus* populations will be interesting to understand if the differences detected between *sulcus acusticus* morphometries can be a useful tool for population discrimination in this species. The variability of directional asymmetry detected in *sagittae* and *lapilli* between the analyzed size classes of *A. hemigymnus* could depend on the heterogeneity of the sampling area (the Strait of Messina) and the large vertical migration performed by adult specimens. It is widely reported how the Strait of Messina is a peculiar environment characterized by a strong tidal current regime, which change in direction and intensity following moon phases, influenced by winds, particularly strong in the area [57,58]. This heterogeneity, added to the differences in migratory behavior between small and large specimens, could have allowed to the differences in shape detected between left and right sagittal and utricular otoliths especially in large individuals.

Go beyond sagittal otoliths: what we can find out about lapilli and asterisci?

Data from the fourth and fifth cases of study represented the first accurate description of morphology, morphometry, and shape of *lapilli* and *asterisci* from the studied species in the Mediterranean Sea,

also assessing for the first time their intra specific variability related to fish size and otoliths' side. Results showed different patterns of variability between the two different studied species. *Lapilli* and *asterisci* belonging to *B. belone* presented a stable symmetry between the two otoliths pairs, differently to the *lapilli* belonging to *A. hemigymnus.* It is hard to find some correlation between these different degrees of intra specific variability, the ecology and the environmental conditions experienced by the species, being literature on utricular and lagenar otoliths of marine teleost fragmentary and limited. Moreover, data regarding Mediterranean species are almost completely absent. Indeed, for several decades these otoliths pairs have been considered, in non-otophysan teleost, without any taxonomic or ecomorphological value, and with a lower intra specific and inter specific variability if compared to the widely studied sagittal otoliths [59]. This is also related to their very small dimensions and enhanced fragility, which make their extraction and processing challenging and time consuming.

Only recently scientific community has started to analyze all the three otoliths' pairs for several scientific aims. Millet et al [60] have compared the several calcified structures for age estimation in *Xiphias gladius* Linnaeus, 1758, assessing the sections reading of the three otoliths pairs as the most reliable methods. In five commercially important flying fishes' species from Taiwan, *asterisci* have proven to be the most reliable and simple otoliths for age reading, enabling researchers to avoid challenging processing procedures to obtain accurate growth parameters [61]. In Anguilliformes species from Taiwan, it has been stated that *lapilli* are characterized by a regular morphology, while *asterisci* show a high specie-specific morphology, useful for species identification [62]. Schulz-Mirbach et al. [63–65] have widely investigated the intra and inter specific variability of *lapilli* and *asterisci* in several species belonging to the non-otophysan freshwater genus *Poecilia*, dispelling the myth of their inaccuracy for ecomorphological, inter populations and taxonomic studies. Assis et al. [66–68] have described the morphology and gross morphometry of several marine teleost species from the Portuguese waters, confirming their inter and intra specific variability. Concerning their microchemical composition, it is widely used to asses migratory behavior and physiochemical features of water masses inhabited by individuals [69]. Recent common garden experiments, performed on *B. belone* larvae [70] have shown how also *lapilli* could be strongly influenced by environmental conditions (increase of pCO_2 related to Ocean acidification), increasing in size in global warming and ocean acidification future scenarios. According to literature, this finding, added to an enhanced calcite deposition rate, has been also confirmed in several other species, as white sea bass, sole, Atlantic cod, and gilthead sea bream [71–74]. Concerning freshwater teleost, in several species (especially in otophysan ones, in which lagenar and utricular otoliths are larger than sagittal otoliths, and, for this reason, most commonly used for scientific investigations) *lapilli* and *asterisci*

are widely and long been used thanks to their high inter and intra specific variability and enhanced phenotypic plasticity, which made them a useful tool for ecomorphological studies [64,75–79].
Concerning the cases of study on *A. hemigymnus* and *B. belone,* they confirmed the inter specific variability of both utricular and lagenar otoliths in morphology, morphometry, shape and intra population relation with fish size and side. Moreover, comparing morphometrical and morphological data obtained by results, to the literature data from other geographical areas provided by Assis on the studied species [66–68], it was also possible to confirm the presence of an inter population variability also in *lapilli* and *asterisci.* These inter and intra specific variability could reflect a plasticity to environmental conditions and life habits, so different between the two investigated species, but also a high relation to genetic, as widely stated for the entire inner ear and *sagittae* (see Introduction chapter). According to the wide literature recently provided by several authors [61–64,71,73,75,78,80], the strong sensitivity to habitats features and life habits, the strictly relation to somatic growth, the deep connection to the phylogenetic relationships among species, the influences of physiochemical characteristics of water masses, can all together influence the intra and inter specific differences reported by results. Data on *asterisci* and *lapilli* from different populations of the studied species, and different species with other life habits and from other exploited habitats, can give new and useful information on the dynamics allowing to the variability of these poorly understood otoliths pairs. This is essential to improve the knowledge base on the functioning, development, intra and inter specific relationships, and ecomorphological features of all the three otoliths pairs in order to understand at all the functioning of teleost inner ear, and to discover new information and data which *lapilli* and *asterisci* can provide on eco morphology, life history and evolution of marine teleost species [65,67,68,81].

4.3 The inter-population differences and the eco-morphological adaptation revealed by sagittae, somatic growth rates and feeding habits: the S. porcus case of study.

Data from the last case of study, regarding two populations of *S. porcus* from two totally different habitats, confirmed the high degree of ecomorphological plasticity of *sagittae* and their reliability for populations discrimination. The geographical variability in morphometry and morphology of *sagittae* was widely showed also by the investigated species from the other cases of study. Indeed, several differences have been reported on morphometric and shape indexes, together with morphological variations, compared to literature data from different geographical areas. This confirmed once again the strong environmental and genetic plasticity of *sagittae*, able to reflect the degree of isolation between populations in marine bony fishes [1,82,83]. Further analysis comparing data on mean shape,

morphometry, and morphology of *sagittae* from different geographical area of the species investigated in the present thesis are required to confirm these inter populations variability. It is also essential to elucidate the relationships between differences in sagittal otoliths features and those regarding life habits, environmental conditions, and genetic segregation at inter population level. This is important to deepen the knowledge on the mechanisms allowing to this *sagittae* variability between different geographical area and habitats, for both, conservation porpoises (being these variations at the base of stock and populations differentiation) and ecomorphological meanings.

Concerning results on *S. porcus,* the detected inter population differences in somatic growth rates, age structures and *sagittae* features highlighted the high degree of isolation between the specimens from Split area and those from the tidal ponds occurring in the "beach rock" formations of the Strait of Messina. These represent two totally different environments for biotic and abiotic conditions, as also for their ecological features. The biotope of the sampling area near Split is characterized by a depth ranging from 10 to 40 m (specimens were sampled at an average depth of 20 m), the presence of rocky substrata and photophilic algae, with patches of sand and *Posidonia oceanica* (Delile, 1813) seagrass beds. From an oceanographic point of view, Adriatic Sea is characterized by an enhanced seasonality and longitudinal gradient regarding dissolved oxygen, temperature, nutrients, salinity, and chlorophyll-a, with the main nutrient sources represented by aeolian inputs, urbane discharges, surface runoff and underground waters [84,85]. Conversely, the Strait of Messina is a highly productive area, characterized by an intense hydro-dynamism and a massive occurrence of upwelling events that makes the water masses of this area similar, from a physiochemical point of view (e.g., temperature, nutrients, dissolved oxygen), to the Atlantic Ocean [57,86,87]. Moreover, the tidal pounds represent an extreme environment, characterized by habitats' peculiarities as a reduced depths (specimens were sampled from 0.2 to 0.4 m of depth) and an enhanced fluctuation of biotic and abiotic conditions, due to the highly sensitiveness to tidal cycles and storms [86,88]. In the Strait of Messina ecosystems, tidal pools occurring in the beach rock formations are an essential shelter from the intense tidal currents regime affecting the area, a nursery area for several species and an important feeding ground for several predators, as also reported in similar habitats from different geographical area [88–91]. These habitats differences between the two sampling area have been widely reflected by the analyzed somatic growth rates, age structures and *sagittae* features of the two populations. Indeed, *S. porcus* specimens from the Strait of Messina area showed the fastest growth rate, the highest length at age values and the highest growth performance index, confirming the faster growth of teleost species in cold and productive water masses widely reported in literature [92–95]. Added to these abiotic factors, also food availability and diet composition can strongly influence metabolic and somatic growth rates [96,97]. Preliminary results from the diet composition of the studied species

from Messina revealed a diet composition in line with literature data regarding the major taxa of the main preys, with several differences related to the contribution of teleost fishes, peracarids crustaceans and mollusks reflecting the preys availability in the tidal pools habitats [98–101].

The differences in somatic growth rates, feeding habits and environmental conditions experienced by the two different populations were widely reflected by *sagittae.* Indeed, their morphology, morphometry and mean shape were deeply different between specimens belonging to the two different sampling area. The detected differences involved the mean otoliths' shape (more circular in Split population than Messina one, which showed most lanceolate *sagittae*), the morphometry (Messina population showed larger *sagittae*, with higher surface values, than Split one, showing wider sagittal otoliths) and general morphology (Split *sagittae* were double picked, with an most enhanced *antirostrum* and a smaller *rostrum* than Messina ones). These differences are in line with literature, reporting wider and most circular *sagittae* in species and individuals inhabiting deeper environments than those from shallower ones [10,11,102]. Moreover, the detected differences regarding *rostrum* and *antirostrum* could be related to the genetic variability which has been allowed by the long time separation between the two population, while the overall different outlines of *sagittae* could have been influenced by the different environmental conditions between habitats [103].

These findings have confirmed once again the reliability of *sagittae* for populations' discrimination, being sagittal otoliths so sensitive to both genetic and environmental variability experienced by different specimens from different habitats and geographical areas. This sensitiveness is the base of the eco morphological adaptation of different species and populations to different habitat pressures, under a strong genetic control. Understand this process is essential to find the direct relation between the inner ear development and the differentiation in teleost fishes of different ecotypes and phenotypes under the environmental and genetic pressure. This is essential to increase the knowledge base on populations and stocks differentiation, and, consequently, to find better and improved management and conservative actions, especially regarding species with high commercial and ecological value.

Concerning the studied populations of *S. porcus,* further analyses are required to understand at all the role of feeding habits and genetic in the detected inter population differences. Indeed, adding data on the seasonal diet composition and genetic isolation between specimens from the two studied habitats, it could be possible to find direct relationships between otoliths development, somatic growth rate and environmental conditions, adding new essential pieces to the comprehension of the morphological adaptation of sensory organ to different environmental pressures.

4.4 How can otoliths reveal about feeding habits and diet composition of teleost groups? Explore the connection between trophic ecology and eco-morphology.

As stated in the Introduction chapter of the present thesis, otoliths development, growth and shape are deeply influenced by food intake, feeding rates and diet composition. Thanks to this close connection, otoliths are widely used as a tool to investigate teleost's trophic ecology, applying several techniques, such as stable carbon and nitrogen isotopes analysis [104,105]. Indeed, the matrix which embed $CaCO_3$ in otoliths is composed of organic material, primary proteins [106]. This represents a valuable, and often underestimated, archive of carbon and nitrogen widely suitable for stable isotopes analyses. Moreover, the metabolic inertia, the continuous deposition of new organic and inorganic materials during otoliths growth, and their connection with somatic growth rates, make them perfect to understand the temporal variations in diet and trophic structure of specimens, and how these can be related to growth rates' changes. Also their morphology, morphometry and mean shape can reveal several information on fish ecology, such as feeding habits, habitats use and resources exploitation in different teleost groups [107,108]. The connection between otoliths morphology and shape, and life habits and environmental history experienced by species, has to be searched in the functions carried out by them, as water column positioning, sound detection and acceleration notion [109,110]. Indeed, according to Schulz-Mirbach et al. [1], the different shape and mass of otoliths could be related to the different auditory functions of teleost. For this reason, the different shape and morphology of otoliths, in the several fishes' species and groups, may reflect several aspects of their ecology, under a strong genetic control, such as movement dynamics, depth preferences, substrate type, ontogenetic shifts, feeding habits and environmental conditions [111–113]. Despite this, it is hard to find otoliths patterns which can directly reflect the feeding history of species and populations, due to the multiple and complex processes influencing otoliths shape, growth and morphology [114]. Indeed, factors influencing feeding ecology of teleost species, such as depth and substrate type preferences, can also affect otoliths features [115], making difficult to find direct link between otoliths morphological patterns and feeding ecology. Detect these patterns could develop new approaches for functional ecology, essentials to reveal the several dimensions of species niche, assessing the relationships between morphological variations and organisms' ecological performances [28,116,117]. This assumes a valuable relevance especially for species and geographical regions in which investigate feeding ecology is challenging due to high diversity of consumed prey items and niche differenciation within and among species [111].

According to literature [9,112,118,119], all the investigated species from present thesis showed a *sagittae* morphology and mean shape in line with their trophic and spatial niche, also reflecting the morphological adaptation of teleost to exploited habitats (as in *S. porcus* and *Pagellus* species) and the niche partitioning among sympatric phylogenetically and morphologically close species (as in

Macrouridae species). Moreover, the last case of study investigated the relation between somatic growth rates, *sagittae* shape and morphological differences and feeding habits, assessing the deep interpopulation variations for all these factors, resulting in a high degree of differentiation between *sagittae* of specimens from the two studied areas. Further analyses are required to assess the direct link between trophic ecology and *sagittae* morphology. It shall be necessary to provide wide data about the environmental conditions, the feeding niche, the diet composition and the genetic differences between populations and different species. This is essential to improve the knowledge base on otoliths eco-morphology and how this can be influenced by trophic history and foraging habits in the different teleost groups.

CONCLUSION

Improve the knowledge base on the phenotypic plasticity of teleost species is essential to understand the process allowing to the populations' differentiation, being assumed that different species or populations of the same species can display specific phenotypes under the regulation of both genetic and environmental pressure [82,120,121]. Indeed, for phenotypic plasticity is meant the capability to express different phenotypes as a result of the different environmental pressures, under genetic control [122]. The eco-morphological adaptation to different habitats and environmental conditions is the process at the base of phenotypic plasticity. For this reason, deepen the knowledge on the mechanisms and dynamics regulating and promoting the morphological adaptation, which allowed the different teleost species to colonize all the marine habitats worldwide, and the different teleost groups to differentiate in genetically isolated populations under the different environmental pressures experienced in the different habitats, is essential to investigate teleost evolution, biodiversity, and ecology, and to define useful characters for populations discrimination. This assumes a high value for ecosystems conservation, being morphological features, such as those related to otoliths, population dynamics and life histories widely used in stock assessment for fisheries resources conservation and fishing pressure monitoring [123–125].

Results provided by the six cases of study, investigated from the Chapter II to Chapter VII of present thesis, have explored the diversity in morphology, mean shape, and morphometry of several Mediterranean teleost species, characterized by different life habits, habitat preferences and phylogenetic relationships. They were also described the inter and intra specific variability occurring between and within the different species, also providing, for the first time, data on the mean *sagittae* shape from shape analysis for many of them (such as

Macrouridae species, *A. hemigymnus, B. belone* and *S. porcus*). Moreover, for the first time in the Mediterranean Sea, it was provided an accurate description, with data from shape and morphometric analyses, also analyzing their intra specific variability, of *lapilli* and *asterisci* belonging to *A. hemigymnus* and *B. belone* specimens. Thanks to these data it was analyzed also the intra and inter specific variability of the less studied utricular and lagenar otoliths in the studied species, assessing the needing to get new and valuable information about their ecomorphological value in non-otophysan teleost species. Finally, it was also confirmed the reliability for populations discrimination of *sagittae* in *S. porcus,* a low-range benthic species, common in all the Mediterranean coastal ecosystems. Results from inter population analysis provided evidence on the high plasticity in sagittal otoliths features, feeding habits and somatic growth rates under different environmental pressures, experienced by specimens from two totally different habitats.

All these data have opened new scenarios for future studies on the eco-morphology of the three otolith pairs from marine teleost species, to better understand the inner ear functioning and to detect the mechanisms of population differentiation and speciation processes. Further analysis applying new techniques (as stable isotopes and microchemical analyses) are required to understand the relationships between trophic ecology, life habits and otoliths features in the different teleost groups. This will improve our ability to read and extract all the information about species ecology, life history, phylogenetic relationships and evolutionary patterns stored inside the otoliths, especially regarding the less-known taxonomic groups. Thanks to otoliths, and future advances in otoliths science, it will be possible to understand several aspects of species ecology, difficult to explore directly, or evolution, being inner ear the sensory organ which allowed teleost to colonize all the marine habitats. This will increase our knowledge about the ecological relationships and niche partitioning in marine communities, the dynamics of populations discrimination and the connection between phylogenetic and morphological differentiation. All these improvements are necessary for both scientific and conservation porpoises, being the marine ecosystem under a constantly growing pressure due to the anthropogenetic impacts (such as those related to fisheries activities and pollution) and the climate change scenarios.

BIBLIOGRAPHY

1. Schulz-Mirbach, T.; Ladich, F.; Plath, M.; Heß, M. Enigmatic ear stones: what we know about the functional role and evolution of fish otoliths. *Biol. Rev.* **2019**, *94*, 457–482, doi:10.1111/brv.12463.
2. Schartl, M.; Walter, R.B.; Shen, Y.; Garcia, T.; Catchen, J.; Amores, A.; Braasch, I.; Chalopin,

D.; Volff, J.N.; Lesch, K.P.; et al. The genome of the platyfish, Xiphophorus maculatus, provides insights into evolutionary adaptation and several complex traits. *Nat. Genet.* **2013**, *45*, 567–572, doi:10.1038/ng.2604.

3. Jovelin, R.; He, X.; Amores, A.; Yan, Y.L.; Shi, R.; Qin, B.; Roe, B.; Cresko, W.A.; Postlethwait, J.H. Duplication and divergence of fgf8 functions in teleost development and evolution. *J. Exp. Zool. Part B Mol. Dev. Evol.* **2007**, *308*, 730–743, doi:10.1002/jez.b.21193.
4. Glasauer, S.M.K.; Neuhauss, S.C.F. Whole-genome duplication in teleost fishes and its evolutionary consequences. *Mol. Genet. Genomics* **2014**, *289*, 1045–1060, doi:10.1007/s00438-014-0889-2.
5. Braasch, I.; Postlethwait, J.H. Polyploidy in fish and the teleost genome duplication. In *Polyploidy and Genome Evolution*; Springer, 2012; Vol. 9783642314, pp. 341–383 ISBN 9783642314421.
6. Smith, J.J.; Keinath, M.C. The sea lamprey meiotic map improves resolution of ancient vertebrate genome duplications. *Genome Res.* **2015**, *25*, 1081–1090, doi:10.1101/gr.184135.114.
7. Ladich, F.; Schulz-Mirbach, T. Diversity in fish auditory systems: One of the riddles of sensory biology. *Front. Ecol. Evol.* **2016**, *4*, doi:10.3389/fevo.2016.00028.
8. Ladich, F. Diversity in Hearing in Fishes: Ecoacoustical, Communicative, and Developmental Constraints. *Insights from Comp. Hear. Res.* **2013**, 289–321, doi:10.1007/2506_2013_26.
9. Tuset, V.M.; Imondi, R.; Aguado, G.; Otero-Ferrer, J.L.; Santschi, L.; Lombarte, A.; Love, M. Otolith patterns of rockfishes from the northeastern pacific. *J. Morphol.* **2015**, *276*, 458–469, doi:10.1002/jmor.20353.
10. Lombarte, A.; Cruz, A. Otolith size trends in marine fish communities from different depth strata. *J. Fish Biol.* **2007**, *71*, 53–76, doi:10.1111/j.1095-8649.2007.01465.x.
11. Lombarte, A.; Lleonart, J. Otolith size changes related with body growth, habitat depth and temperature. *Environ. Biol. Fishes* **1993**, *37*, 297–306, doi:10.1007/BF00004637.
12. Lombarte, A.; Palmer, M.; Matallanas, J.; Gómez-Zurita, J.; Morales-Nin, B. Ecomorphological trends and phylogenetic inertia of otolith sagittae in Nototheniidae. *Environ. Biol. Fishes* **2010**, *89*, 607–618, doi:10.1007/s10641-010-9673-2.
13. Schwarzhans, W. A comparative morphological study of the recent otoliths of the genera Diaphus, Idiolychnus and Lobianchia (Myctophidae). *Palaeo Ichthyol.* **2013**, *13*, 41–82.
14. Tuset, V.M.; Olivar, M.P.; Otero-Ferrer, J.L.; López-Pérez, C.; Hulley, P.A.; Lombarte, A. Morpho-functional diversity in Diaphus spp. (Pisces: Myctophidae) from the central Atlantic Ocean: Ecological and evolutionary implications. *Deep. Res. Part I Oceanogr. Res. Pap.* **2018**,

138, 46–59, doi:10.1016/j.dsr.2018.07.005.

15. Falk, J.J.; Ter Hofstede, H.M.; Jones, P.L.; Dixon, M.M.; Faure, P.A.; Kalko, E.K.V.; Page, R.A. Sensory-based niche partitioning in a multiple predator-multiple prey community. *Proc. R. Soc. B Biol. Sci.* **2015**, *282*, 20150520, doi:10.1098/rspb.2015.0520.
16. Schwarzhans, W. Head and otolith morphology of the genera Hymenocephalus, Hymenogadus and Spicomacrurus (Macrouridae), with the description of three new species. *Zootaxa* **2014**, *3888*, 1–73, doi:10.11646/zootaxa.3888.1.1.
17. Kéver, L.; Colleye, O.; Herrel, A.; Romans, P.; Parmentier, E. Hearing capacities and otolith size in two ophidiiform species (Ophidion rochei and Carapus acus). *J. Exp. Biol.* **2014**, *217*, 2517–2525, doi:10.1242/jeb.105254.
18. García-Ruiz, C.; Hidalgo, M.; Carpentieri, P.; Fernandez-Arcaya, U.; Gaudio, P.; González, M.; Jadaud, A.; Mulas, A.; Peristeraki, P.; Rueda, J.L.; et al. Spatio-temporal patterns of macrourid fish species in the northern Mediterranean sea. *Sci. Mar.* **2019**, *83*, 117–127, doi:10.3989/scimar.04889.11A.
19. Macpherson Mayol, E. Estudio sobre relaciones tróficas en peces bentónicos de la costa catalana. *PhD Thesis* **1979**, 379 pp. (220+150 de tablas).
20. Madurell, T.; Cartes, J.E. Trophic relationships and food consumption of slope dwelling macrourids from the bathyal Ionian Sea (eastern Mediterranean). *Mar. Biol.* **2006**, *148*, 1325–1338, doi:10.1007/s00227-005-0158-3.
21. Carrassón, M.; Matallanas, J. Diets of deep-sea macrourid fishes in the western Mediterranean. *Mar. Ecol. Prog. Ser.* **2002**, *234*, 215–228, doi:10.3354/meps234215.
22. Mauchline, J.; Gordon, J.D.M. Diets and bathymetric distributions of the macrourid fish of the Rockall Trough, northeastern Atlantic Ocean. *Mar. Biol.* **1984**, *81*, 107–121, doi:10.1007/BF00393109.
23. Zischke, M.T.; Litherland, L.; Tilyard, B.R.; Stratford, N.J.; Jones, E.L.; Wang, Y.G. Otolith morphology of four mackerel species (Scomberomorus spp.) in Australia: Species differentiation and prediction for fisheries monitoring and assessment. *Fish. Res.* **2016**, *176*, 39–47, doi:10.1016/j.fishres.2015.12.003.
24. Sadighzadeh, Z.; Tuset, V.M.; Valinassab, T.; Dadpour, M.R.; Lombarte, A. Comparison of different otolith shape descriptors and morphometrics for the identification of closely related species of Lutjanus spp. from the Persian Gulf. *Mar. Biol. Res.* **2012**, *8*, 802–814, doi:10.1080/17451000.2012.692163.
25. Lombarte, A.; Miletić, M.; Kovačić, M.; Otero-Ferrer, J.L.; Tuset, V.M. Identifying sagittal otoliths of Mediterranean Sea gobies: variability among phylogenetic lineages. *J. Fish Biol.*

2018, *92*, 1768–1787, doi:10.1111/jfb.13615.

26. Whitfield, A.K. Ecological Role of Mugilidae in the Coastal Zone. *Biol. Ecol. Cult. Grey Mullets* **2015**, 334–358, doi:10.1201/b19927-17.
27. Moore, B.R.; Parker, S.J.; Pinkerton, M.H. Otolith shape as a tool for species identification of the grenadiers Macrourus caml and M. whitsoni. *Fish. Res.* **2022**, *253*, 106370.
28. Tuset, V.M.; Otero-Ferrer, J.L.; Gómez-Zurita, J.; Venerus, L.A.; Stransky, C.; Imondi, R.; Orlov, A.M.; Ye, Z.; Santschi, L.; Afanasiev, P.K.; et al. Otolith shape lends support to the sensory drive hypothesis in rockfishes. *J. Evol. Biol.* **2016**, *29*, 2083–2097, doi:10.1111/jeb.12932.
29. Arneri, E.; Morales-Nin, B. Aspects of the early life history of European hake from the central Adriatic. *J. Fish Biol.* **2000**, *56*, 1368–1380, doi:10.1006/jfbi.2000.1255.
30. Carrozzi, V.; Di Lorenzo, M.; Massi, D.; Titone, A.; Ardizzone, G.; Colloca, F. Prey preferences and ontogenetic diet shift of European hake Merluccius merluccius (Linnaeus, 1758) in the central Mediterranean Sea. *Reg. Stud. Mar. Sci.* **2019**, doi:10.1016/j.rsma.2018.100440.
31. D'Iglio, C.; Porcino, N.; Savoca, S.; Profeta, A.; Perdichizzi, A.; Armeli, E.; Davide, M.; Francesco, S.; Rinelli, P.; Giordano, D. Ontogenetic shift and feeding habits of the European hake (Merluccius merluccius L ., 1758) in Central and Southern Tyrrhenian Sea (Western Mediterranean Sea): A comparison between past and present data. *Ecol. Evol.* **2022**, *12*, doi:10.1002/ece3.8634.
32. ORSI RELINI, L.; CAPPANERA, M.; FIORENTINO, F. Spatial-temporal distribution and growth of Merluccius merluccius recruits in the Ligurian sea. Observations on the O group. *Cybium (Paris)* **1989**, *13*, 263–270.
33. Contreras, T.; Olivar, M.P.; Bernal, A.; Sabatés, A. Comparative feeding patterns of early stages of mesopelagic fishes with vertical habitat partitioning. *Mar. Biol.* **2015**, *162*, 2265–2277, doi:10.1007/s00227-015-2749-y.
34. Lin, C.H.; Lin, J.S.; Chen, K.S.; Chen, M.H.; Chen, C.Y.; Chang, C.W. Feeding Habits of Bigeye Tuna (Thunnus obesus) in the Western Indian Ocean Reveal a Size-Related Shift in Its Fine-Scale Piscivorous Diet. *Front. Mar. Sci.* **2020**, *7*, 582571, doi:10.3389/fmars.2020.582571.
35. Cotton, C.F.; Grubbs, R.D. Biology of deep-water chondrichthyans: Introduction. *Deep. Res. Part II Top. Stud. Oceanogr.* 2015.
36. Olivar, M.P.; Sabatés, A.; Alemany, F.; Balbín, R.; de Puelles, M.L.F.; Torres, A.P. Diel-depth distributions of fish larvae off the Balearic Islands (western Mediterranean) under two

environmental scenarios. *J. Mar. Syst.* **2014**, *138*, 127–138.

37. Granata, A.; Brancato, G.; Sidoti, O.; Guglielmo, L. Energy Flux in the South Tyrrhenian Deep-sea Ecosystem: Role of Mesopelagic Fishes and Squids. In *Mediterranean Ecosystems*; Springer, 2001; pp. 197–207.
38. Guglielmo, L.; Marabello, F.; Vanucci, S. The role of the mesopelagic fishes in the pelagic food web of the Strait of Messina. *Straits Messin. Ecosyst. Proc. Symp. Messin.* **1995**, 223–246.
39. Olivar, M.P.; Bernal, A.; Molí, B.; Peña, M.; Balbín, R.; Castellón, A.; Miquel, J.; Massutí, E. Vertical distribution, diversity and assemblages of mesopelagic fishes in the western Mediterranean. *Deep. Res. Part I Oceanogr. Res. Pap.* **2012**, *62*, 53–69, doi:10.1016/j.dsr.2011.12.014.
40. Griffiths, S.P.; Kuhnert, P.M.; Fry, G.F.; Manson, F.J. Temporal and size-related variation in the diet, consumption rate, and daily ration of mackerel tuna (euthynnus affinis) in neritic waters of eastern Australia. *ICES J. Mar. Sci.* **2009**, *66*, 720–733, doi:10.1093/icesjms/fsp065.
41. Dorman, J.A. Investigations into the biology of the garfish, Belone belone (L.), in Swedish waters. *J. Fish Biol.* **1991**, *39*, 59–69, doi:10.1111/j.1095-8649.1991.tb04341.x.
42. Dorman, J.A. Diet of the garfish, Belone belone (L.), from Courtmacsherry Bay, Ireland. *J. Fish Biol.* **1988**, *33*, 339–346, doi:10.1111/j.1095-8649.1988.tb05476.x.
43. Mahé, K.; MacKenzie, K.; Ider, D.; Massaro, A.; Hamed, O.; Jurado-Ruzafa, A.; Gonçalves, P.; Anastasopoulou, A.; Jadaud, A.; Mytilineou, C.; et al. Directional Bilateral Asymmetry in Fish Otolith: A Potential Tool to Evaluate Stock Boundaries? *Symmetry (Basel).* **2021**, *13*, 987, doi:10.3390/sym13060987.
44. Sherratt, E.; Serb, J.M.; Adams, D.C. Rates of morphological evolution, asymmetry and morphological integration of shell shape in scallops. *BMC Evol. Biol.* **2017**, *17*, 248, doi:10.1186/s12862-017-1098-5.
45. Stewart, T.A.; Albertson, R.C. Evolution of a unique predatory feeding apparatus: Functional anatomy, development and a genetic locus for jaw laterality in Lake Tanganyika scale-eating cichlids. *BMC Biol.* **2010**, *8*, 1–11, doi:10.1186/1741-7007-8-8.
46. Hata, H.; Yasugi, M.; Takeuchi, Y.; Takahashi, S.; Hori, M. Measuring and evaluating morphological asymmetry in fish: Distinct lateral dimorphism in the jaws of scale-eating cichlids. *Ecol. Evol.* **2013**, *3*, 4641–4647, doi:10.1002/ece3.849.
47. Leung, C.; Duclos, K.K.; Grünbaum, T.; Cloutier, R.; Angers, B. Asymmetry in dentition and shape of pharyngeal arches in the clonal fish Chrosomus eos-neogaeus: Phenotypic plasticity and developmental instability. *PLoS One* **2017**, *12*, e0174235,

doi:10.1371/journal.pone.0174235.

48. Manganaro, A.; Pulicanò, G.; Sanfilippo, M. Temporal evolution of the area of Capo Peloro (Sicily, Italy) from pristine site into urbanized area. *Transitional Waters Bull.* **2011**, *5*, 23–31, doi:10.1285/i1825229Xv5n1p23.
49. Marilena Sanfilippo La componente organica del seston nel lago di Ganzirri: qualità e valore nutrizionale come risorsa ambientale, University of Messina, 2000.
50. Spanò, N.; Di Paola, D.; Albano, M.; Manganaro, A.; Sanfilippo, M.; D'Iglio, C.; Capillo, G.; Savoca, S. Growth performance and bioremediation potential of Gracilaria gracilis (Steentoft, L.M. Irvine & Farnham, 1995). *Int. J. Environ. Stud.* **2021**, 1–13, doi:10.1080/00207233.2021.1954775.
51. Chollet-Villalpando, J.G.; García-Rodríguez, F.J.; De Luna, E.; De La Cruz-Agüero, J. Geometric morphometrics for the analysis of character variation in size and shape of the sulcus acusticus of sagittae otolith in species of Gerreidae (Teleostei: Perciformes). *Mar. Biodivers.* **2019**, *49*, 2323–2332, doi:10.1007/s12526-019-00970-y.
52. Verocai, J.E.; Cabrera, F.; Lombarte, A.; Norbis, W. Form function of sulcus acusticus of the sagittal otolith in seven Sciaenidae (Acanthuriformes) species using geometric morphometrics (southwestern Atlantic). *J. Fish Biol.* **2023**, doi:10.1111/jfb.15521.
53. Çiçek, E.; Avşar, D.; Yeldan, H.; Manaşirli, M. Comparative morphology of the sagittal otolith of mullet species (Mugilidae) from the Iskenderun Bay , north-eastern Mediterranean. *Acta Biol. Turc.* **2020**, *33*, 219–226.
54. Granados-Amores, E.; Granados-Amores, J.; Zavala-Leal, O.I.; Flores-Ortega, J.R. Geometric morphometrics in the sulcus acusticus of the sagittae otolith as tool to discriminate species of the genus Centropomus (Centropomidae: Perciformes) from the southeastern Gulf of California. *Mar. Biodivers.* **2020**, *50*, 1–7, doi:10.1007/s12526-019-01030-1.
55. Torres, G.J.; Lombarte, A.; Morales-Nin, B. Variability of the sulcus acusticus in the sagittal otolith of the genus Merluccius (Merlucciidae). *Fish. Res.* **2000**, *46*, 5–13, doi:10.1016/S0165-7836(00)00128-4.
56. Montanini, S.; Stagioni, M.; Valdrè, G.; Tommasini, S.; Vallisneri, M. Intra-specific and inter-specific variability of the sulcus acusticus of sagittal otoliths in two gurnard species (Scorpaeniformes, Triglidae). *Fish. Res.* **2015**, *161*, 93–101, doi:10.1016/j.fishres.2014.07.003.
57. De Domenico, E. Caratteristiche fisiche e chimiche delle acque nello Stretto di Messina. *Doc. Trav. IGAL* **1987**, *11*, 225–235.
58. Battaglia, P.; Ammendolia, G.; Cavallaro, M.; Consoli, P.; Esposito, V.; Malara, D.; Rao, I.; Romeo, T.; Andaloro, F. Influence of lunar phases, winds and seasonality on the stranding of

mesopelagic fish in the Strait of Messina (Central Mediterranean Sea). *Mar. Ecol.* **2017**, *38*, e12459, doi:10.1111/maec.12459.

59. Nolf, D. *Otolithi Piscium. Handbook of Paleoichthyology, Vol. 10.*; Fischer, G., Ed.; Stuttgart, New York, 1985;
60. Millot, R.; Vanalderweireldt, L.; Finelli, L.; Durieux, E.D.H. Age estimates derived from hard parts of swordfish Xiphias gladius from the north-western Mediterranean Sea . *J. Fish Biol.* **2023**, doi:10.1111/jfb.15558.
61. Chang, S.K.; Yuan, T.L.; Hoyle, S.D.; Farley, J.H.; Shiao, J.C. Growth Parameters and Spawning Season Estimation of Four Important Flyingfishes in the Kuroshio Current Off Taiwan and Implications From Comparisons With Global Studies. *Front. Mar. Sci.* **2022**, *8*, 747382, doi:10.3389/fmars.2021.747382.
62. Chulin, A.K.; Chen, H.M. Comparative morphological study of otoliths in Taiwanese anguilliformes fishes. *J. Mar. Sci. Technol.* **2013**, *21*, 77–85, doi:10.6119/JMST-013-1220-3.
63. Schulz-Mirbach, T.; Ladich, F.; Riesch, R.; Plath, M. Otolith morphology and hearing abilities in cave- and surface-dwelling ecotypes of the Atlantic molly, Poecilia mexicana (Teleostei: Poeciliidae). *Hear. Res.* **2010**, *267*, 137–148, doi:10.1016/j.heares.2010.04.001.
64. Schulz-Mirbach, T.; Riesch, R.; García de León, F.J.; Plath, M. Effects of extreme habitat conditions on otolith morphology - a case study on extremophile livebearing fishes (Poecilia mexicana, P. sulphuraria). *Zoology* **2011**, *114*, 321–334, doi:10.1016/j.zool.2011.07.004.
65. Schulz-Mirbach, T.; Plath, M. All good things come in threes–species delimitation through shape analysis of saccular, lagenar and utricular otoliths. *Mar. Freshw. Res.* **2012**, *63*, 934–940.
66. Assis, C.A. Estudo morfológico dos otólitos sagitta, asteriscus e lapillus de Teleóstei (Actinopterygii, Teleostei) de Portugal continental. Sua aplicação em estudos de filogenia, sistematica e ecologia. *Ecologia* 2000, 1005.
67. Assis, C.A. The lagenar otoliths of teleosts: Their morphology and its application in species identification, phylogeny and systematics. *J. Fish Biol.* **2003**, *62*, 1268–1295, doi:10.1046/j.1095-8649.2003.00106.x.
68. Assis, C.A. The utricular otoliths, lapilli, of teleosts: Their morphology and relevance for species identification and systematics studies. *Sci. Mar.* **2005**, *69*, 259–273, doi:10.3989/scimar.2005.69n2259.
69. Chesney, E.J.; McKee, B.M.; Blanchard, T.; Chan, L.H. Chemistry of otoliths from juvenile menhaden Brevoortia patronus: Evaluating strontium, strontium:calcium and strontium isotope ratios as environmental indicators. *Mar. Ecol. Prog. Ser.* **1998**, *171*, 261–273,

doi:10.3354/meps171261.

70. Alter, K.; Peck, M.A. Ocean acidification but not elevated spring warming threatens a European seas predator. *Sci. Total Environ.* **2021**, *782*, 146926, doi:10.1016/j.scitotenv.2021.146926.
71. Coll-Lladó, C.; Giebichenstein, J.; Webb, P.B.; Bridges, C.R.; De La Serrana, D.G. Ocean acidification promotes otolith growth and calcite deposition in gilthead sea bream (Sparus aurata) larvae. *Sci. Rep.* **2018**, *8*, 8384, doi:10.1038/s41598-018-26026-y.
72. Faria, A.M.; Filipe, S.; Lopes, A.F.; Oliveira, A.P.; Gonçalves, E.J.; Ribeiro, L. Effects of high pCO2 on early life development of pelagic spawning marine fish. *Mar. Freshw. Res.* **2017**, *68*, 2106–2114, doi:10.1071/MF16385.
73. Shen, S.G.; Chen, F.; Schoppik, D.E.; Checkley, D.M. Otolith size and the vestibulo-ocular reflex of larvae of white seabass Atractoscion nobilis at high pCO2. *Mar. Ecol. Prog. Ser.* **2016**, *553*, 173–182, doi:10.3354/meps11791.
74. Pimentel, M.S.; Faleiro, F.; Marques, T.; Bispo, R.; Dionísio, G.; Faria, A.M.; Machado, J.; Peck, M.A.; Pörtner, H.; Pousão-Ferreira, P.; et al. Foraging behaviour, swimming performance and malformations of early stages of commercially important fishes under ocean acidification and warming. *Clim. Change* **2016**, *137*, 495–509, doi:10.1007/s10584-016-1682-5.
75. da Costa, R.M.R.; Fabré, N.N.; Amadio, S.A.; Tuset, V.M. Plasticity in the shape and growth pattern of asteriscus otolith of black prochilodus prochilodus nigricans (Teleostei: Characiformes: Prochilodontidae) freshwater neotropical migratory fish. *Neotrop. Ichthyol.* **2018**, *16*, doi:10.1590/1982-0224-20180051.
76. Avigliano, E.; Fortunato, R.C.; Biolé, F.; Domanico, A.; De Simone, S.; Neiff, J.J.; Volpedo, A. V. Identification of nurseries areas of juvenile prochilodus lineatus (Valenciennes, 1836) (characiformes: Prochilodontidae) by scale and otolith morphometry and microchemistry. *Neotrop. Ichthyol.* **2016**, *14*, doi:10.1590/1982-0224-20160005.
77. Teimori, A.; Schulz-Mirbach, T.; Esmaeili, H.R.; Reichenbacher, B. Geographical differentiation of Aphanius dispar (Teleostei: Cyprinodontidae) from Southern Iran. *J. Zool. Syst. Evol. Res.* **2012**, *50*, 289–304, doi:10.1111/j.1439-0469.2012.00667.x.
78. Hoff, G.R.; Logan, D.J.; Markle, D.F. Notes: Otolith Morphology and Increment Validation in Young Lost River and Shortnose Suckers. *Trans. Am. Fish. Soc.* **1997**, *126*, 488–494, doi:10.1577/1548-8659(1997)126<0488:nomaiv>2.3.co;2.
79. Volpedo, A. V.; Fuchs, D. V. Ecomorphological patterns of the lapilli of Paranoplatense Siluriforms (South America). *Fish. Res.* **2010**, *102*, 160–165,

doi:10.1016/j.fishres.2009.11.007.

80. Schulz-Mirbach, T.; Stransky, C.; Schlickeisen, J.; Reichenbacher, B. Differences in otolith morphologies between surface- and cave-dwelling populations of Poecilia mexicana (Teleostei, Poeciliidae) reflect adaptations to life in an extreme habitat. *Evol. Ecol. Res.* **2008**, *10*, 537–558.
81. Schulz-Mirbach, T.; Ladich, F.; Mittone, A.; Olbinado, M.; Bravin, A.; Maiditsch, I.P.; Melzer, R.R.; Krysl, P.; Heß, M. Auditory chain reaction: Effects of sound pressure and particle motion on auditory structures in fishes. *PLoS One* **2020**, *15*, e0230578, doi:10.1371/journal.pone.0230578.
82. Berg, F.; Almeland, O.W.; Skadal, J.; Slotte, A.; Andersson, L.; Folkvord, A. Genetic factors have a major effect on growth, number of vertebrae and otolith shape in Atlantic herring (Clupea harengus). *PLoS One* **2018**, *13*, e0190995, doi:10.1371/journal.pone.0190995.
83. Bose, A.P.H.; Zimmermann, H.; Winkler, G.; Kaufmann, A.; Strohmeier, T.; Koblmüller, S.; Sefc, K.M. Congruent geographic variation in saccular otolith shape across multiple species of African cichlids. *Sci. Rep.* **2020**, *10*, 1–14, doi:10.1038/s41598-020-69701-9.
84. Lipizer, M.; Partescano, E.; Rabitti, A.; Giorgetti, A.; Crise, A. Qualified temperature, salinity and dissolved oxygen climatologies in a changing Adriatic Sea. *Ocean Sci.* **2014**, *10*, 771–797, doi:10.5194/os-10-771-2014.
85. Solidoro, C.; Bastianini, M.; Bandelj, V.; Codermatz, R.; Cossarini, G.; Canu, D.M.; Ravagnan, E.; Salon, S.; Trevisani, S. Current state, scales of variability, and trends of biogeochemical properties in the northern Adriatic Sea. *J. Geophys. Res. Ocean.* **2009**, *114*, doi:10.1029/2008JC004838.
86. Savoca, S.; Grifó, G.; Panarello, G.; Albano, M.; Giacobbe, S.; Capillo, G.; Spanó, N.; Consolo, G. Modelling prey-predator interactions in Messina beachrock pools. *Ecol. Modell.* **2020**, *434*, doi:10.1016/j.ecolmodel.2020.109206.
87. Cortese, G.; De Domenico, E. Some considerations on the levantine intermediate water distribution in the Straits of Messina. *Boll. Ocean. Teor. Appl* **1990**, *8*, 197–207.
88. Capillo, G.; Panarello, G.; Savoca, S.; Sanfilippo, M.; Albano, M.; Volsi, R.L.; Consolo, G.; Spanò, N. Intertidal ponds of messina's beachrock faunal assemblage, evaluation of ecosystem dynamics and communities' interactions. *AAPP Atti della Accad. Peloritana dei Pericolanti, Cl. di Sci. Fis. Mat. e Nat.* **2018**, *96*, A41–A416, doi:10.1478/AAPP.96S3A4.
89. Gomes, P.B.; Belém, M.J. da C.; Schlenz, E. Distribution, abundance and adaptations of three species of Actiniidae (Cnidaria, Actiniaria) on an intertidal beach rock in Cameiros beach, Pemambuco, Brazil. *Misc. Zool.* **1998**, *21*, 65–72.

90. Mendonça, V.; Flores, A.A.V.; Silva, A.C.F.; Vinagre, C. Do marine fish juveniles use intertidal tide pools as feeding grounds? *Estuar. Coast. Shelf Sci.* **2019**, *225*, 106255, doi:10.1016/j.ecss.2019.106255.
91. Dias, M.; Roma, J.; Fonseca, C.; Pinto, M.; Cabral, H.N.; Silva, A.; Vinagre, C. Intertidal pools as alternative nursery habitats for coastal fishes. *Mar. Biol. Res.* **2016**, *12*, 331–344, doi:10.1080/17451000.2016.1143106.
92. Kikuchi, E.; Cardoso, L.G.; Canel, D.; Timi, J.T.; Haimovici, M. Using growth rates and otolith shape to identify the population structure of Umbrina canosai (Sciaenidae) from the Southwestern Atlantic. *Mar. Biol. Res.* **2021**, *17*, 272–285, doi:10.1080/17451000.2021.1938131.
93. Atkinson, D. Temperature and Organism Size—A Biological Law for Ectotherms? *Adv. Ecol. Res.* **1994**, *25*, 1–58, doi:10.1016/S0065-2504(08)60212-3.
94. Kozłowski, J.; Czarnołęski, M.; Dańko, M. Can optimal resource allocation models explain why ectotherms grow larger in cold? *Integr. Comp. Biol.* **2004**, *44*, 480–493, doi:10.1093/icb/44.6.480.
95. Jobling, M. Temperature and growth: modulation of growth rate via temperature change. *Glob. Warm.* **2011**, 225–254, doi:10.1017/cbo9780511983375.010.
96. Bacha, M.; Moali, A.; Benmansour, N.E.; Brylinski, J.M.; Mahé, K.; Amara, R. Relationships between age, growth, diet and environmental parameters for anchovy (Engraulis encrasicolus L.) in the Bay of Bénisaf (SW Mediterranean, west Algerian coast). *Cybium* **2010**, *34*, 47–57.
97. Mommsen, T.P. Growth and metabolism. *Physiol. fishes* **1998**, *2*, 65–97.
98. Ferri, J.; Matić-Skoko, S. The spatial heterogeneity of the black scorpionfish, scorpaena porcus (Scorpaenidae): Differences in length, dietary and age compositions. *Appl. Sci.* **2021**, *11*, 11919, doi:10.3390/app112411919.
99. Harmelin-Vivien, M.L.; Kaim-Malka, R.A.; Ledoyer, M.; Jacob-Abraham, S.S. Food partitioning among scorpaenid fishes in Mediterranean seagrass beds. *J. Fish Biol.* **1989**, *34*, 715–734, doi:10.1111/j.1095-8649.1989.tb03352.x.
100. Başçïnar, N.S.; Sağlam, H. Feeding habits of black scorpion fish scorpaena porcus, in the South-Eastern Black Sea. *Turkish J. Fish. Aquat. Sci.* **2009**, *9*, 99–103.
101. Compaire, J.C.; Casademont, P.; Cabrera, R.; Gómez-Cama, C.; Soriguer, M.C. Feeding of Scorpaena porcus (Scorpaenidae) in intertidal rock pools in the Gulf of Cadiz (NE Atlantic). *J. Mar. Biol. Assoc. United Kingdom* **2018**, *98*, 845–853, doi:10.1017/S0025315417000030.
102. Monteiro, L.R.; Di Beneditto, A.P.M.; Guillermo, L.H.; Rivera, L.A. Allometric changes and shape differentiation of sagitta otoliths in sciaenid fishes. *Fish. Res.* **2005**, *74*, 288–299,

doi:10.1016/j.fishres.2005.03.002.

103. Vignon, M.; Morat, F. Environmental and genetic determinant of otolith shape revealed by a non-indigenous tropical fish. *Mar. Ecol. Prog. Ser.* **2010**, *411*, 231–241, doi:10.3354/meps08651.
104. Grønkjær, P.; Pedersen, J.B.; Ankjærø, T.T.; Kjeldsen, H.; Heinemeier, J.; Steingrund, P.; Nielsen, J.M.; Christensen, J.T. Stable N and C isotopes in the organic matrix of fish otoliths: Validation of a new approach for studying spatial and temporal changes in the trophic structure of aquatic ecosystems. *Can. J. Fish. Aquat. Sci.* **2013**, *70*, 143–146, doi:10.1139/cjfas-2012-0386.
105. Rowell, K.; Dettman, D.L.; Dietz, R. Nitrogen isotopes in otoliths reconstruct ancient trophic position. *Environ. Biol. Fishes* **2010**, *89*, 415–425, doi:10.1007/s10641-010-9687-9.
106. Hüssy, K.; Mosegaard, H.; Jessen, F. Effect of age and temperature on amino acid composition and the content of different protein types of juvenile Atlantic cod (Gadus morhua) otoliths. *Can. J. Fish. Aquat. Sci.* **2004**, *61*, 1012–1020, doi:10.1139/F04-037.
107. Nonogaki, H.; Nelson, J.A.; Patterson, W.P. Dietary histories of herbivorous loricariid catfishes: Evidence from δ13C values of otoliths. *Environ. Biol. Fishes* **2007**, *78*, 13–21, doi:10.1007/s10641-006-9074-8.
108. Aguirre, H.; Lombarte, A. Ecomorphological comparisons of sagittae in Mullus barbatus and M. surmuletus. *J. Fish Biol.* **1999**, *55*, 105–114, doi:10.1006/jfbi.1999.0974.
109. Fay, R.R.; Popper, A.N. Modes of stimulation of the teleost ear. *J. Exp. Biol.* **1975**, *62*, 379–387, doi:10.1242/jeb.62.2.379.
110. Popper, A.N.; Lu, Z. Structure-function relationships in fish otolith organs. *Fish. Res.* **2000**, *46*, 15–25, doi:10.1016/S0165-7836(00)00129-6.
111. Assis, I.O.; da Silva, V.E.L.; Souto-Vieira, D.; Lozano, A.P.; Volpedo, A. V.; Fabré, N.N. Ecomorphological patterns in otoliths of tropical fishes: assessing trophic groups and depth strata preference by shape. *Environ. Biol. Fishes* **2020**, *103*, 349–361, doi:10.1007/s10641-020-00961-0.
112. Volpedo, A. V.; Tombari, A.D.; Echeverría, D.D. Eco-morphological patterns of the sagitta of Antarctic fish. *Polar Biol.* **2008**, *31*, 635–640, doi:10.1007/s00300-007-0400-1.
113. Volpedo, A.; Diana Echeverría, D. Ecomorphological patterns of the sagitta in fish on the continental shelf off Argentine. *Fish. Res.* **2003**, *60*, 551–560, doi:10.1016/S0165-7836(02)00170-4.
114. Gagliano, M.; McCormick, M.I. Feeding history influences otolith shape in tropical fish. *Mar. Ecol. Prog. Ser.* **2004**, *278*, 291–296, doi:10.3354/meps278291.

115. Allen, L.G.; Pondella, D.J.; Horn, M.H. *Ecology of marine fishes: California and adjacent waters*; Univ of California Press, 2006; ISBN 0520246535.
116. Tuset, V.M.; Farré, M.; Otero-Ferrer, J.L.; Vilar, A.; Morales-Nin, B.; Lombarte, A. Testing otolith morphology for measuring marine fish biodiversity. *Mar. Freshw. Res.* **2016**, *67*, 1037–1048, doi:10.1071/MF15052.
117. Abaad, M.; Tuset, V.M.; Montero, D.; Lombarte, A.; Otero-Ferrer, J.L.; Haroun, R. Phenotypic plasticity in wild marine fishes associated with fish-cage aquaculture. *Hydrobiologia* **2016**, *765*, 343–358, doi:10.1007/s10750-015-2428-5.
118. Jaramilo, A.M.; Tombari, A.D.; Benedito Dura, V.; Eugeni Rodrigo, M.; Volpedo, A. V. Otolith eco-morphological patterns of benthic fishes from the coast of Valencia (Spain). *Thalassas* **2014**, *30*, 57–66.
119. Mille, T.; Mahé, K.; Cachera, M.; Villanueva, M.C.; De Pontual, H.; Ernande, B. Diet is correlated with otolith shape in marine fish. *Mar. Ecol. Prog. Ser.* **2016**, *555*, 167–184, doi:10.3354/meps11784.
120. Swain, D.P.; Foote, C.J. Stocks and chameleons: The use of phenotypic variation in stock identification. *Fish. Res.* **1999**, *43*, 113–128, doi:10.1016/S0165-7836(99)00069-7.
121. Grabowski, T.B.; Young, S.P.; Libungan, L.A.; Steinarsson, A.; Marteinsdóttir, G. Evidence of phenotypic plasticity and local adaption in metabolic rates between components of the Icelandic cod (gadus morhua l.) stock. *Environ. Biol. Fishes* **2009**, *86*, 361–370, doi:10.1007/s10641-009-9534-z.
122. Via, S.; Gomulkiewicz, R.; De Jong, G.; Scheiner, S.M.; Schlichting, C.D.; Van Tienderen, P.H. Adaptive phenotypic plasticity: consensus and controversy. *Trends Ecol. Evol.* **1995**, *10*, 212–217, doi:10.1016/S0169-5347(00)89061-8.
123. Lleonart, J.; Maynou, F. Fish stock assessments in the Mediterranean: State of the art. *Sci. Mar.* **2003**, doi:10.3989/scimar.2003.67s137.
124. Parrish, B.B.; Gullard, J.A. Manual of Methods for Fish Stock Assessment. Part I. Fish Population Analysis. *J. Appl. Ecol.* **1971**, *8*, 616, doi:10.2307/2402904.
125. Stransky, C.; Murta, A.G.; Schlickeisen, J.; Zimmermann, C. Otolith shape analysis as a tool for stock separation of horse mackerel (Trachurus trachurus) in the Northeast Atlantic and Mediterranean. *Fish. Res.* **2008**, *89*, 159–166, doi:10.1016/j.fishres.2007.09.017.